The design and development of steric stabilisers for bicontinuous cubic lyotropic liquid crystalline nanostructured particles for drug delivery systems

A thesis submitted to Monash University in fulfilment of the requirements for the degree

of Doctor of Philosophy

Josephine Yin Tse Chong, BAnVetBioSci (Hons)

CSIRO Material Science and Engineering,

Commonwealth Scientific and Industrial Research Organisation (CSIRO),

Clayton, Victoria, Australia

Drug Delivery, Disposition and Dynamics,

Monash Institute of Pharmaceutical Sciences

Parkville, Victoria, Australia

July 2014

ADDENDUM

p 4 table 1: delete table and replace with:

	Increasing the CPP	**Decreasing the CPP**
a	❖ Larger polar groups (non-ionics) ❖ Low temperature (ethylene oxide (EO) surfactants) ❖ Charged polar group ❖ No salt present (ionics)	❖ Smaller polar groups (non-ionics) ❖ High temperature (ethylene oxide (EO) surfactants) ❖ Presence of salt (ionics)
l	❖ Long hydrocarbon chains	❖ Short hydrocarbon chains
v	❖ Double-chain surfactants ❖ Branched hydrophobic chains ❖ Increase temperature affecting chain splay	❖ Linear single-chain surfactants

p 50 table 1: Add unit "(°C)" below "Cloud point" column labels

p 54 fig 8: Add "Pn3m" label to lower identified region in figure

p 87: Comment: The proposed method assumes particles that are well-dispersed will obscure the fluorescein's emission and reduce the signal. This requires the particles to be sufficiently small and low density to not separate out by sedimentation.

P 116 line 45: delete:

"This confirms that an essentially random copolymer structure can be as effective as an ABA triblock copolymer to provide steric stabilization for lyotropic liquid crystalline nanostructured particles. It is felt that the PEG-PHYT copolymers behave as block systems rather than random copolymers due to their amphiphilic nature. This type of behavior, displayed by random copolymers, has also been reported before for random polymers with varying hydrophilic and lipophilic characteristics.[57]"

and read:

"This confirms that even random amphiphilic copolymer structures are able to sterically stabilize lyotropic liquid crystalline nanostructured particles. Although random amphiphilic copolymers have not been reported as steric stabilizers, they have been reported to have self-assembly behavior similar to block systems.[57]"

Contents

List of abbreviations

20:5, EPA	cis-5,8,11,14,17-eicosapentaenoic acid
AIBN	2,2'-azobis(isobutyronitrile)
ASA	Accelerated Stability Assay
ATRP	Atom Transfer Radical Polymerisation
β-XP	1-*O*-(5,9,13,17-tetramethyloctadecyl)-β-D-xylopyranoside
BPS-05	Polyethoxylated (5) phytosterols
BPS-30	Polyethoxylated (30) phytosterols
CAC	Critical Aggregation Concentration
CAPSUL-E	n–octenyl succinic anhydride (OSA)-modified starch
CCD	Charge-Coupled Device
CMC	Critical Micelle Concentration
CPLM	Cross-polarised Light Microscopy
Cremophor® EL	Polyethoxylated castor oil
Cryo-TEM	Cryo-Transmission Electron Microscopy
DDP	1,3-didodecyloxy-propane-2-ol
DDP(EO)	1,3-didodecyloxy-propane-2-ol-PEG
DDGG	1,3-didodecyloxy-2-glycidyl-glycerol
DDGG-(EO)	1,3-didodecyloxy-2-glycidyl-glycerol-PEG
DDGG-(EO)-DDGG	1,3-didodecyloxy-2-glycidyl-glycerol-(PEG)-1,3-didodecyloxy-2-glycidyl-glycerol
DEPE	Dielaidoylphosphatidylethanolamine
DGMO	Diglycerol monooleate
Dimodan U/J	96% monoglyceride mixture: 62% linoleate and 25% oleate
DLS	Dynamic Light Scattering
DMPE	1,2-dimyristoyl-sn-glycero-3-phosphoethanolamine
DMPE-PEG	PEGylated 1,2-dimyristoyl-*sn*-glycero-3-phosphoethanolamine
DOPE	1,2-dioleyl-sn-glycero-3-phosphoethanolamine
DOPE-PEG	PEGylated 1,2-Dioleoylphosphatidylethanolamine
DPPS	Dipalmitoyl phosphatidylserine
DSPE	1,2-distearoyl-sn-glycero-3-phosphatidylethanolamine
DSPE-PEG	PEGylated 1,2-distearorylphosphatidylethanolamine
EPHP	*N*-ethylpiperidine hypophosphite
EPR	Enhanced Permeability and Retention
EROCO C22	1-*O*-(5,9,13,17-Tetramethyloctadecanoyl)erythritol
F127	Pluronic®F127 (PEO_{100}-PPO_{65}- PEO_{100})
FFT	Fast Fourier Transform
ΔG_{agg}	Gibbs free energy of aggregation
GDO	Glycerol dioleate
GME	1-glycerol monooleyl ether
GMO	Glycerol monooleate
GPC	Gel Permeation Chromatography
H_1	Hexagonal phase
H_2	Inverse hexagonal phase
HB	3-hydroxybutyrate
HFarnesyl$(EO)_n$	Hexahydrofarnesyl ethylene oxide surfactant
HI-CAP100	n–octenyl succinic anhydride (OSA)-modified starch
HMEHEC	Hydrophobically modified ethyl hydroxyethyl cellulose
^{1}H NMR	Proton Nuclear Magnetic Resonance
HPMCAS	Hydroxypropyl methyl cellulose acetate succinate
HTP	High-Throughput
HV	3-hydroxyvalerate
I_1	Discrete micellar cubic phase

I_2	Inverse/reverse discrete micellar cubic phase
Ia3d	Schoen gyroid crystallographic space group symmetry
IDL	Interface Definition Language
Im3m	Primitive cubic crystallographic space group symmetry
IPMS	Infinite Periodic Minimal Surfaces
L_α	Lamellar phase
Laponite XLG	Clay nanoparticles
LCST	Lower Critical Solution Temperature
MLO	Monolinolein
MO-PEG	PEGylated monoolein
MPS	Mononuclear Phagocyte System
MW	Molecular Weight
MWCO	Molecular Weight Cut Off
Myrj®	Polyethoxylated stearate/PEG-stearate
Myrj®52	PEG_{40}-stearate
Myrj®59	PEG_{100}-stearate
MYS-10 V	PEG_{10}-stearate
MYS-25 V	PEG_{25}-stearate
MYS-45 V	PEG_{45}-stearate
MYS-55 V	PEG_{55}-stearate
Myverol™ 18-99 K	Monoacylglycerol
NMP	Nitroxide-Mediated Free Radical Polymerisation
NMR	Nuclear Magnetic Resonance
PBS	Phosphate Buffered Saline
PCS	Photon Correlation Spectroscopy
PDI	Polydispersity Index
PEO/PEG/EO	Poly(ethylene oxide)/Poly(ethylene glycol)/ethylene oxide
PEG-lipid	PEGylated lipid
PEG-PHYT	PEGylated-phytanyl copolymer
PEO-PPO-PEO/ PEG-PPO-PEG	Poloxamer™/Pluronic® – a triblock copolymer consisting of poly(propylene oxide) and poly(ethylene oxide)/poly(ethylene glycol)
PHV	Poly(hydroxyvaleric acid)
Phytanyl$(EO)_n$	Phytanyl ethylene oxide surfactant
Pluronic®	Poloxamer™– a triblock copolymer consisting of poly(propylene oxide) and poly(ethylene oxide)/poly(ethylene glycol)
Pn3m	Schwartz diamond crystallographic space group symmetry
PNIPAM	Poly(*N*-isopropylacrylamide)
P(ODA)	Poly(octadecyl acrylate)
P(ODA)-b-P(PEGA-OMe)	Poly(octadecyl acrylate)-*block*-poly(poly(ethylene glycol) methyl ether acrylate)
P(PEGA-OMe)	Poly(poly(ethylene glycol) methyl ether acrylate)
PPO/PO	Poly(propylene oxide)/propylene oxide
RAFT	Reversible Addition-Fragmentation chain Transfer polymerisation
RCF	Relative Centrifugal Force
ROMP	Ring-Opening Metathesis Polymerisation
ROP	Ring-Opening Polymerisation
RPM	Revolutions Per Minute
RYLO MG 90	Glycerol monooleate; 98.1 wt% monoglyceride
SA	Succinic anhydride
SAXS	Small Angle X-ray Scattering
Sm	Smectic
Soy PE	L-α-phosphatidylethanolamine
SPC	Soy phosphatidyl choline
TEM	Transmission Electron Microscopy
Tetronic®	Poloxamine™ – a tetrafunctional polyethylene glycol-polypropylene oxide

	ethylenediamine block copolymer
Tween®20	Polysorbate 20 - polyoxyethylene (20) sorbitan monolaurate
Tween®40	Polysorbate 40 - polyoxyethylene (20) sorbitan monopalmitate
Tween®60	Polysorbate 60 - polyoxyethylene (20) sorbitan monostearate
Tween®80	Polysorbate 80 - polyoxyethylene (20) sorbitan monooleate
Tween®85	Polysorbate 85 - polyoxyethylene (20) sorbitan trioleate
V_1/Q_1	Bicontinuous cubic phase
V_2/Q_2	Inverse/reverse bicontinuous cubic phase
V_2^D/Q_2^D	Schwartz diamond cubic phase with crystallographic space group symmetry *Pn3m*
V_2^G/Q_2^G	Schoen gyroid cubic phase with crystallographic space group symmetry *Ia3d*
V_2^P/Q_2^P	Primitive cubic phase with crystallographic space group symmetry *Im3m*
Vazo™88	1,1'-azobis(cyclohexanecarbonitrile)
Vitamin E	D-alpha-tocopheryl
Vitamin E TPGS	D-alpha-tocopheryl PEO_{1000} succinate
WAXS	Wide Angle X-ray Scattering
wt % or % w/w	Weight percent or percent weight per weight

Abstract

Lyotropic liquid crystalline nanostructured particles, such as cubosomes, have been growing in popularity as drug delivery systems in the last few years. These systems require steric stabilisers to maintain colloidal stability in an aqueous medium. Therefore, it is important to investigate the effectiveness of steric stabilisers stabilising nonlamellar liquid crystalline nanostructured particles in order to understand the structure-property relationships which are important for developing more effective steric stabilisers.

In this project, high throughput sample preparation and batch screening techniques were used for investigating steric stabilisers for cubosomes, with a focus on stabilising nonlamellar liquid crystalline dispersions of phytantriol and monoolein. New steric stabilisers were thereupon identified from pre-existing and novel steric stabiliser classes. The motive for screening steric stabilisers was to ultimately develop effective, stable, targeted systems. However, a lack of knowledge on the effectiveness of alternative steric stabiliser compared to the 'gold-standard' steric stabiliser, Pluronic®F127, highlighted the need for an efficient, high throughput stability assay.

A high throughput technique, an accelerated stability assay (ASA) for assessing the effectiveness of steric stabilisers at maintaining colloidal stability of cubosomes was consequently developed and validated. This technique proved to be useful as it allowed for the performance of different steric stabilisers to be quantitatively compared between each other and especially against frequently used Pluronic®F127. Henceforth, several alternative commercially-available steric stabilisers were identified to have equivalent and/or superior steric stabilising effectiveness as Pluronic®F127.

Subsequent to the development of the ASA, two series of custom steric stabilisers were synthesised with varying sizes of their hydrophobic and hydrophilic domains. The first stabiliser series was a PEGylated-lipid copolymer prepared using a high throughput combinatorial one-pot reaction approach. The polymers in the series had a range of structural variables, such as poly(ethylene glycol) (PEG) or lipid (i.e. phytantriol) molar ratio content and PEG length. This enabled the identification of key design parameters to utilise in a more controlled synthetic approach with potential for eventual functionalisation for targeting purposes.

Using the controlled RAFT approach, a second stabiliser series containing a PEGylated amphiphilic brush copolymer, with a di-block copolymer structure was prepared. Despite the large differences in structure from known steric stabilisers, some of the stabilisers synthesised from either copolymer series provided effective colloidal stability for cubosomes comparable to that provided by Pluronic®F127. Furthermore the retention of the internal structure of the bulk phase was also conserved in the cubosomes stabilised using the synthesised copolymers.

The steric stabilisers and techniques developed in this project are likely to be valuable tools for prospective, custom steric stabiliser designs, as well as in the specific study of steric stabilisation of nonlamellar liquid crystalline nanostructured particles or other colloidal systems.

Declaration

In accordance with Monash University Doctorate Regulation 17/Doctor of Philosophy and Master of Philosophy (MPhil) regulations the following declarations are made:

I hereby declare that this thesis contains no material which has been accepted for the award of any other degree or diploma at any university or equivalent institution and that, to the best of my knowledge and belief, this thesis contains no material previously published or written by another person, except where due reference is made in the text of the thesis.

This thesis includes 3 original papers published in peer reviewed journals and 3 (submitted) unpublished publications. The core theme of the thesis is the investigation and development of steric stabilisers for cubic lyotropic liquid crystalline nanostructured particles for drug delivery systems. The ideas, development and writing up of all the papers in the thesis were the principle responsibility of myself, the candidate, working within the theme of Drug Delivery, Disposition and Dynamics, and within the division of CSIRO Materials Science and Engineering under the supervision of (Professor) Dr Ben J. Boyd and (Professor) Dr Calum J. Drummond.

The inclusion of co-authors reflects the fact that the work came from active collaboration between researchers and acknowledges input into team-based research.

In the case of Chapters 2-6 my contribution to the work involved the following:

Thesis chapter	Publication title	Publication status	Nature and extent of candidate's contribution
2	Steric Stabilisation of Self-Assembled Cubic Lyotropic Liquid Crystalline Nanoparticles: High Throughput Evaluation of Triblock Polyethylene oxide-Polypropylene oxide-Polyethylene oxide Copolymers	Published	Research design, performance of data collection and analysis, manuscript preparation
3	High-Throughput Discovery of Novel Steric Stabilisers for Cubic Lyotropic Liquid Crystal Nanoparticle Dispersions	Published	Research design, performance of data collection and analysis, manuscript preparation
4	Accelerated Stability Assay (ASA) for Colloidal Systems	Published	Research design, development of methods, performance of data collection and analysis, manuscript preparation
5	Novel steric stabilisers for lyotropic liquid crystalline nanoparticles: Pegylated-phytanyl copolymers	Submitted	Research design, polymer synthesis and analysis, performance of data collection and analysis, manuscript preparation
6.1	RAFT preparation and aqueous self-assembly of amphiphilic poly(octadecyl acrylate)-*block*-poly(poly(ethylene glycol) methyl ether acrylate) copolymers	Submitted	Research design, polymer synthesis and analysis, performance of data collection and analysis, manuscript preparation
6.2	Novel RAFT amphiphilic brush copolymer steric stabilisers for cubosomes: Poly(octadecyl acrylate)-*block*-poly(polyethylene glycol methyl ether acrylate)	Submitted	Research design, performance of data collection and analysis, manuscript preparation

Chapters 2-6 appear in the format in which they were published in peer-reviewed journals, and are not renumbered/reformatted.

Signed: 

Date: 10.07.2014

x

List of publications

Thesis chapters

Chong JYT, Mulet X, Waddington LJ, Boyd BJ, Drummond CJ, *Steric stabilisation of self-assembled cubic lyotropic liquid crystalline nanoparticles: high throughput evaluation of triblock polyethylene oxide-polypropylene oxide-polyethylene oxide copolymers.* Soft Matter, 2011. **7**(10): p. 4768-4777.

Chong JYT, Mulet X, Waddington LJ, Boyd BJ, Drummond CJ, *High-throughput discovery of novel steric stabilisers for cubic lyotropic liquid crystal nanoparticle dispersions.* Langmuir: the ACS journal of surfaces and colloids*,* 2012. **28** (25): p. 9223-9232.

Chong JYT, Mulet X, Boyd BJ, Drummond CJ, *Accelerated stability assay (ASA) for colloidal systems*. ACS Combinatorial Science, 2014. **16**(5): p. 205-210.

Chong JYT, Mulet X, Keddie D, Waddington L, Mudie ST, Boyd BJ, Drummond CJ, *Novel steric stabilisers for lyotropic liquid crystalline nanoparticles: PEGlated-phytanyl copolymers.* (SUBMITTED to Langmuir on 17.4.2014)

Chong JYT, Keddie D, Postma A, Mulet X, Boyd BJ, Drummond CJ, *RAFT preparation and the aqueous self-assembly of amphiphilic poly(octadecyl acrylate)-block-poly(polyethylene glycol methyl ether acrylate copolymers*. (SUBMITTED to Colloid and Polymer Science on 23.5.2014)

Chong JYT, Mulet X, Postma A, Keddie D, Waddington LJ, Boyd BJ, Drummond CJ, *Novel RAFT amphiphilic brush copolymer steric stabilisers for cubosomes: Poly(octadecyl acrylate)-block-poly(polyethylene glycol methyl ether acrylate)*. (SUBMITTED to Soft Matter on 15.5.2014).

Additional publications

Fong C, Weerawardena A, Sagnella SM, Mulet X, Krodkiewska I, Chong J, Drummond CJ, *Monodisperse Nonionic Isoprenoid-Type Hexahydrofarnesyl Ethylene Oxide Surfactants: High Throughput Lyotropic Liquid Crystalline Phase Determination.* Langmuir, 2011. **27**(6): p. 2317-2326.

Tilley AJ, Dong YD, Chong JYT, Hanley T, Nigel K, Drummond CJ, Boyd BJ, *Transfer of lipid between triglyceride dispersions and lyotropic liquid crystal nanostructured particles using time-resolved SAXS.* Soft Matter, 2012. **8**(20): p. 5696-5708.

Acknowledgements

First and foremost I would like to sincerely thank my supervisors, Prof. Calum J. Drummond (CSIRO and RMIT) and Prof. Ben J. Boyd (Monash University) for their advice, support and guidance throughout my project. Not only do I get the great fortune of gaining access to their leadership and shared cumulative wealth of extensive specialist knowledge in colloidal and material science, but I also get to share the unique experience of being co-supervised by one of my PhD supervisor's former PhD supervisor. And although that might make a great tongue-twister, that's also just ridiculously special!

Massive thanks to Dr Xavier Mulet for being an inspiring mentor and whose continuous support, encouragement and advice have been nothing short than awesome. I would also like to thank the many collaborators I worked with throughout my candidature for their technical guidance and support, particularly Dr Almar Postma and Dr Daniel Keddie for RAFT polymerisation; Lynne Waddington for cryo-TEM; and Dr Nigel Kirby, Dr Stephen Mudie and Dr Adrian Hawley for SAXS at the Australian Synchrotron.

I would also like to thank members of the Drummond research group: Dr Celesta Fong, Dr Charlotte Conn, Dr George Feast, Dr Tamar Greaves, Dr Danielle Kennedy, Dr Irena Krodkiewska, Dr Asoka Weerawardeena, Dr Ben Muir, Dr Chantelle Driever, Dr Nic Tse; and members of the Boyd research group: Dr Wye Khay Fong, Dr Adam Tilley, Dr Aurelia Dong, Dr Charlie Dong, Dr Stephanie Wallace, Dr Tri-Hung Nguyen and Danielle Senyschyn, for their warm friendships and support over the years.

My tenure on this project would not have been possible without the financial support of CSIRO PhD studentship. I would also like to thank the organisers of the Cheiron School, Spring-8, Japan, which include AOFSRR (Asia-Oceania Forum for Synchrotron Radiation Research), RIKEN (Institute of Physical and Chemical Research), JASRI (Japan Synchrotron Radiation Research Institute) and KEK (The High Energy Accelerator Research Organization), for the synchrotron summer school scholarship, giving me the opportunity to travel to Japan and learn more about synchrotron beamlines.

To my big brother, Christopher Keat Yong Chong, and his beautiful wife, Wikanya Amornsak, thank you for your continuous love and support throughout the years. Your company and reassuring words always help me get through the day (and some long late nights).

All that I am, or hope to be, I owe to my darling parents, Yook Mooi Chong and Seh Keow Chong. If I could reach up and hold a star for every time you have made me smile (especially during rough times), the entire evening sky would be in the palm of my hand. This doctorate is as much yours, as it is mine. Thank you for always believing in me; even though it cost you (a few) white hairs. I love you dearly. You gave me the world and as a token of appreciation I would like to share with you mine; I hereby dedicate this thesis/doctorate to you!

It has long been an axiom of mine that the little things are infinitely the most important.

Sir Arthur Conan Doyle

Chapter 1

Introduction

1.1 Cubosomes and the formation of cubic lyotropic liquid crystalline phases

Cubosomes are lipid-based particles, typically approximately 200 nm in diameter, which can be formed by dispersing mesophases that possess a minimal surface-shaped infinite lipid bilayer in excess water. The first observation of a cubic phase in lipid-water systems was reported by Luzzati *et al.* in 1960.[1] This was the cubic phase (Q^{230}, crystallographic space group symmetry *Ia3d*) and its internal structure was confirmed in 1967.[2-3] Since then six other cubic phases have been discovered; Q^{224} (crystallographic space group symmetry *Pn3m*)[4-5], Q^{229} (crystallographic space group symmetry *Im3m*)[6-8], Q^{225} (crystallographic space group symmetry *Fm3m*)[9], Q^{223} (crystallographic space group symmetry *Pm3n*)[4, 10], Q^{227} (crystallographic space group symmetry *Fd3m*)[7, 11-14] and Q^{212} (crystallographic space group symmetry $P4_332$)[7]. Recently a new lyotropic liquid crystalline phase was reported based on a 3D hexagonal close-packed arrangement of inverse micelles, of space group $P6_3lmmc$.[15] These cubic phases may be classified as bicontinuous cubic phases, with the exception of Q^{223} and Q^{227}, which are discontinuous or discrete micellar cubic phases. The cubic phase is often symbolised using a 'Q' or 'V' annotation in the literature.

Bicontinuous cubic phases have an internal structure based on periodic minimal surfaces. [16-18] In the bicontinuous cubic phase lipid bilayers are arranged in periodic three dimensional cubic lattice structures. By mapping the bilayers onto the surface of infinite periodic minimal surfaces, the mean curvature at any point on the surface is zero. The mean curvature H is defined as $½(K_1 + K_2)$, in which K_1 and K_2 are two principle curvatures. A minimal surface is a surface with H=0 at all points, so that every point on the surface is a balanced saddle point. There are three types of inverse cubic phases identified in lipid systems, which are based on the Schwartz diamond (D) and primitive (P) and on the Schoen gyroid (G) minimal surfaces (Figure 1).[16-18] The Q^{224}, Q^{229} and Q^{230} cubic phases are denoted by their crystallographic space group symmetry, which are *Pn3m, Im3m* and *Ia3d* respectively. The size of the two distinct interpenetrating aqueous water channels in these space group symmetries are a function of the surfactant or amphiphilic lipid composition and the space group, and can range from 4 to 20 nm in diameter which is sufficiently large to accommodate certain water-soluble compounds.[17, 19] The amount of water accommodated in the cubic phases as well as the size of the water channels increases from G to D to P minimal surface phases.[17]

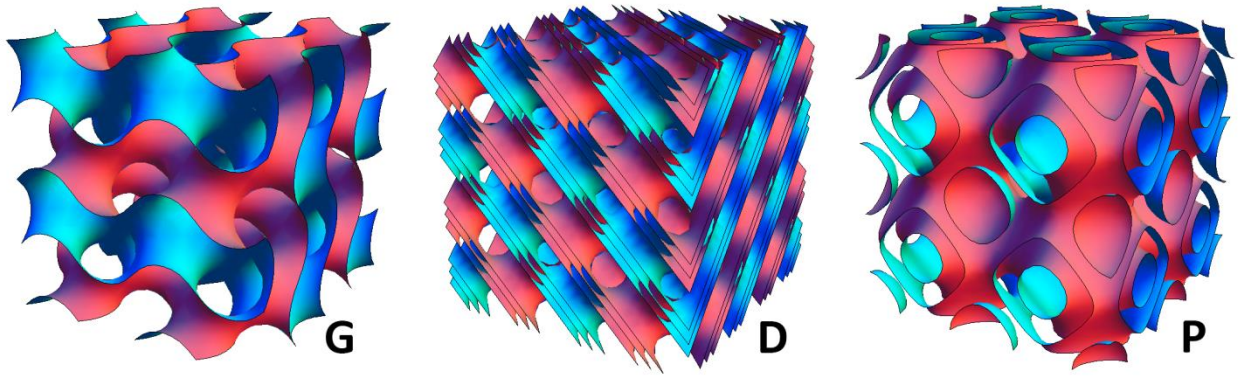

Figure 1. Minimal surfaces of the Schoen gyroid (G), Schwartz diamond (D) and Schwartz primitive (P). Images were generated using Mathematica V.9, based on equations obtained from[20]

Cubic phases are typically prepared using lipids. Lipids are often amphiphilic, which means that they are partly hydrophilic and partly hydrophobic. Usually the hydrophilic portion is depicted as a 'head', whilst the hydrophobic portion as the 'tail' in illustrations. Some surfactants or amphiphilic lipid-water systems are known to form a variety of different lyotropic liquid crystalline phases. Lyotropic liquid crystals are often termed 'mesophases', representing intermediate states of matter between an isotropic liquid and a solid crystal. The formation of different geometries and their resultant structures that are representative of various mesophases can be understood using the critical packing parameter (CPP) concept.[21] CPP is often defined using equation [1]:

$$CPP = \frac{v}{a \cdot l} \quad [1]$$

where v is the volume of the hydrophobic tail(s), a is the polar headgroup area, and l is the length of the hydrophobic chain of the surfactant. The lamellar phase has a structure with no interfacial curvature (i.e. CPP = 1) because under the CPP concept the surfactants/or amphiphilic lipids occupy an apparently cylindrical space (Figure 2).

The remaining mesophases can be classified under two categories subdivided into two topologically distinct regions; type 1/I ('normal' or oil-in-water) or type 2/II ('reverse' or water-in-oil).[22] Type 1 mesophases, which include discrete micellar cubic, hexagonal and bicontinuous cubic phases, are composed of surfactants/or amphiphilic lipids that have an overall geometry that occupy an apparently cone shape space (Figure 2), whereby CPP < 1. This conical geometry consequently results in the formation of spheres and cylindrical rods, which have their hydrophilic heads in contact with the water.

In contrast, type 2 mesophases, which include reverse discrete micellar cubic, reverse hexagonal and reverse bicontinuous cubic phases, are composed of surfactants/or amphiphilic lipids which have an overall geometry that occupy an inverse cone shape space (Figure 2), whereby CPP > 1. This geometry results in the formation of inverse spheres and cylindrical rods, that have their hydrophobic tails in contact with the

solvent (Figure 2). Factors effecting v (volume of the hydrophobic tail(s)), a (polar headgroup area) and l (length of the hydrophobic chain of the surfactant) are summarised in Table 1.[23]

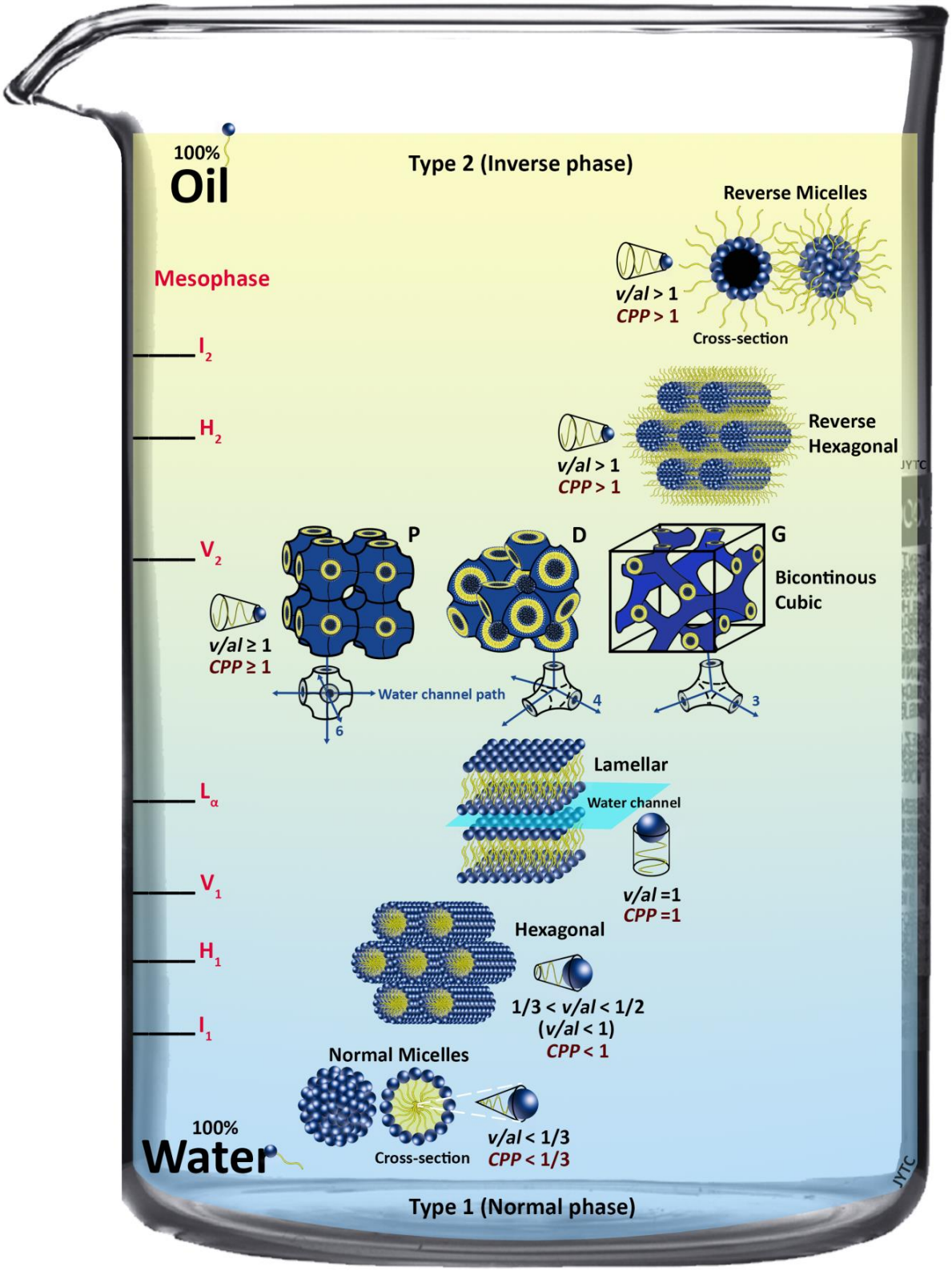

Figure 2. An illustration of the main types of liquid crystal phases depending on the interface curvature (molecular shape or concentration in water). The mesophases are denoted as I_1, I_2 (discrete micellar cubic phase), H_1, H_2 (hexagonal phase), V_1, V_2 (bicontinuous cubic phase) and L_α (lamellar phase)

Table 1. Factors that influence the critical packing parameter (CPP), where a is the polar headgroup area, l is the length of the hydrophobic chain of the surfactant and v is the volume of the hydrophobic tail(s)

	Increasing the CPP	Decreasing the CPP
a	❖ Larger polar groups (non-ionics) ❖ Low temperature (EO surfactants) ❖ Charged polar group ❖ No salt present (ionics)	❖ Smaller polar groups (non-ionics) ❖ High temperature (EO surfactants) ❖ Presence of salt (ionics)
l	❖ Long hydrocarbon chains	❖ Short hydrocarbon chains
v	❖ Double-chain surfactants ❖ Branched hydrophobic chains ❖ Increase temperature affecting chain splay	❖ Linear single-chain surfactants

In lyotropic liquid crystal phases the solvent concentration is an extra variable that can dictate the self-assembly behaviour.[24] In contrast, thermotropic liquid crystal phase transitions are dependent on temperature and pressure.[24] The order/sequence of self assembly phases that are typically observed as the surfactant/lipid concentration increases in an amphiphilic lipid/water system are micelles, micellar cubic, hexagonal, bicontinuous cubic, lamellar and their respective reverse phases, which are illustrated in Figure 2.[25-27]

Materials which have been reported to form cubic phase systems have been listed by Fontell in 1990.[28] These materials include anionic and cationic "soaps", zwitterionic and nonionic surfactants and amphiphilic lipids of biological origin, such as monoglycerides, sphingolipids and phospholipids, and also galactolipids, glycolipids and tetra ether lipids.[28] Since then reviews have reported that inverse bicontinuous cubic phases have been observed for many different types of lipids, including monoacylglycerides, glycolipids, urea and urea-like amphiphiles and mono-ethanolamides.[29-31] The amphiphilic lipids most commonly used in lipid liquid crystal research have been glycerol monooleate (GMO), a food emulsifier, and phytantriol, a cosmetic ingredient (Figure 3) due to their low cost, ease of availability and potential biocompatibility based on their history of use in other fields.

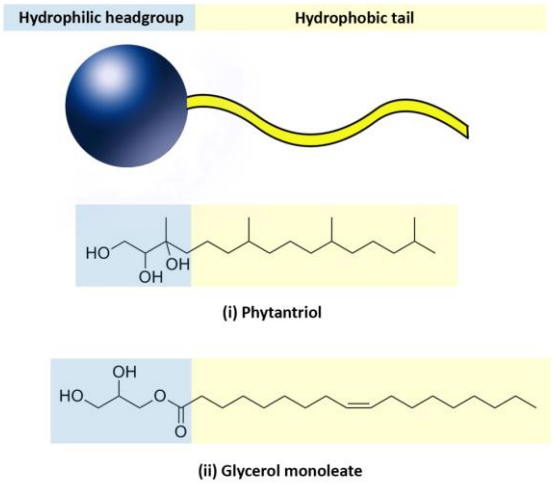

Figure 3. The chemical structures of amphiphilic lipids (i) Phytantriol and (ii) Glycerol monoleate

1.2 Cubosomes and their relevance for drug delivery

The aforementioned lyotropic liquid crystal systems are thermodynamically stable and so can be dispersed into smaller particles that retain the complex internal nanostructure in the presence of a stabiliser. Dispersions of these bulk 'parent' phases have been given the suffix '-osome'. For example, dispersions from the lamellar, hexagonal and cubic phases are known as 'liposomes', 'hexosomes' and 'cubosomes' respectively. Lyotropic liquid crystalline nanostructured particles have been explored for their potential as drug delivery systems. These dispersed drug delivery systems typically consist of the lipid matrix and a steric stabiliser, which provides the dispersion with varying degrees of colloidal stability depending on the lipid/stabiliser combination and concentrations. Liposomes, dispersed particles based on the lamellar lyotropic liquid crystalline structure, have been extensively utilised as drug delivery vehicles with twelve clinically-approved liposomal drug formulations currently on the market and twenty-two liposomal drugs undergoing clinical trials.[32-33] Particles based on other lyotropic liquid crystalline structures such as cubosomes (inverse bicontinuous cubic phase, Figure 4) and hexosomes (inverse hexagonal phase) are also being developed as potential drug delivery systems.[34-35]

The key advantages of these nanostructured particles compared to liposomes, include their complex internal structure with potential for controllable release and their increased lipid volume fraction per particle, which provides a large lipophilic area for containing poorly water-soluble lipophilic therapeutics.[36-37] The liquid crystalline structure and dimensions of the phase, specifically the water channels, determine the release rate of drugs from within the liquid crystal phase.[38-39] The phases can accommodate molecules of varying properties.[40-41] A recent study by Zabara and Mezzenga reported the controlled release of encapsulated protein within Q^{224} cubic nanostructured particles by doping the mesophase with a hydration-modulating agent that causes an increase in the diameter of the water channels.[42] In a similar manner the swelling of the aqueous domain can also be manipulated with polysaccharides, as illustrated by Mezzenga *et al*.[43] The possibility of controlled drug release from nonlamellar liquid crystalline systems is one of the main attractive features for using these systems for drug delivery. Examples of therapeutics which have been incorporated into cubosomes for investigating their potential as drug delivery systems are listed in Table 2. Cubosomes have been studied for administration via the ocular, dermal, intrademal, mucosal, intranasal, oral, precutaneous, intraperitoneal, intratympanic and intravenous routes, as presented in Table 2. In addition, studies have also been performed on the interaction of nanostructured particles with model and cell membranes[44] and blood components[45], for their biocompatibility within the body as effective drug delivery systems.

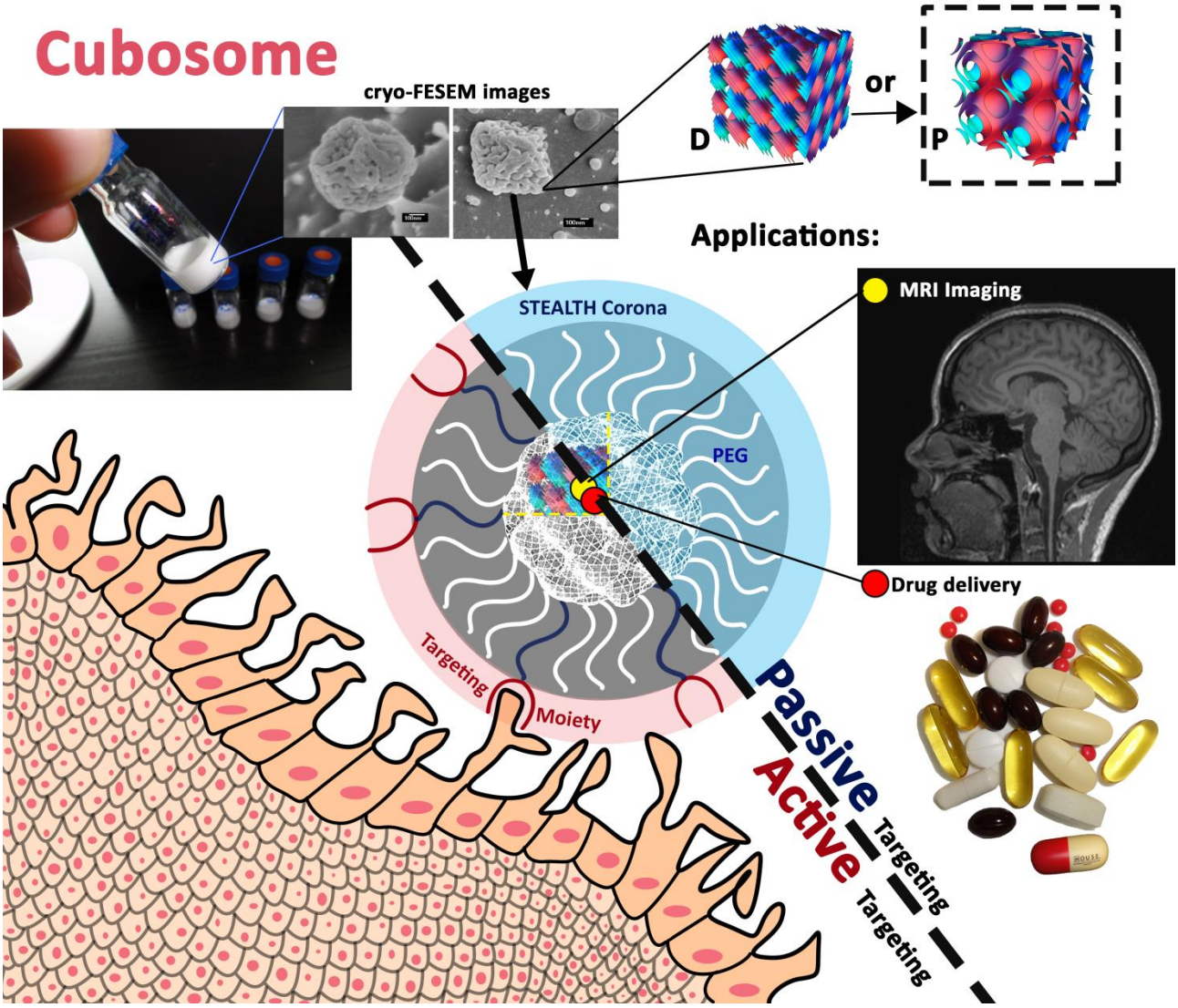

Figure 4. An illustration of the particle morphology and application of the cubosome. The cryo-FESEM images display the 3D particle morphology of cubosomes and are adapted from Rizwan *et al.*[46]

Recent reviews by Rizwan *et al*[47] and Conn and Drummond[31], have collected examples where lyotropic liquid crystalline nanostructured particles accommodate biologically active molecules such as vitamins, enzymes, and other proteins, as well as crystallizing membrane proteins, which have important application for membrane protein crystallisation, biosensors, biofuel applications, as well as in drug delivery. Owing to the high surface area of the internal mesophase structure (up to 400m^2/g) and the large pore size (about 20 nm when fully swollen),[48] the cubic phase can be used to incorporate typical globular proteins, which have similar dimensions to the water channels in the bicontinuous cubic phases.[49]

In other recent developments, cubosomes are also being investigated for containment of contrasting agents for medical imaging applications[50-52], and capabilities as a cell-free bio-sensing platform[53]. Apart from drug delivery and biomedical applications, the use and application of lyotropic liquid crystalline nanostructured particles is also relevant within the food industry (e.g. solubilisation of food bioactives within lyotropic liquid crystalline mesophases) [54-55] and agriculture industry (e.g. delivery of plant

agrochemicals) [56]. Therefore any research into the colloidal stability and retention of internal structure of nanostructured particles would be highly relevant to many fields.

Table 2. A table listing examples of the therapeutics and lipid composition of drug-loaded cubosomes as drug nanocarriers

Bioactive molecule (peptide, drug)	Matrix constituent	Stabiliser	Administration route (if applicable)	Ref.
hinokitiol	Glyceryl monooleate	Pluronic®F127	Dermal	57
soluble extracts of Korean barberry	Glyceryl monooleate	Pluronic®F127	Dermal	58
Herbal extracts (obtained from *Poria cocos*, *Thuja orientalis*, *Espinosilla*, *Lycium chinense Mill*, *Coix lacryma-jobi* and *Polygonum multiflorum Thunberg*)	Glyceryl monooleate	Pluronic®F127	Skin (For hair regrowth)	59
saponin adjuvant Quil A and monophosphoryl lipid A	Phytantriol	Pluronic®F127	*In vitro* (skin)	60
triclosan	Glyceryl monooleate	Pluronic®F127	*In vitro* (skin)	61
KIOM-MA-128 (water-soluble extract)	Glyceryl monooleate	Pluronic®F127	*In vitro* (skin)	62
tacrolimus	Glyceryl monooleate	Pluronic®F127	Intradermal	63
clotrimazole	Glyceryl monooleate	Pluronic®F127	Mucosal	64
dexamethasone	Glyceryl monooleate	Pluronic®F127	Ocular	65
flurbiprofen	Glyceryl monooleate	Pluronic®F127	Ocular	66
cyclosporine A	Glyceryl monooleate	Pluronic®F127	Ocular	67
5-FC oleyl carbamate (Pro drug)	5-FC oleyl carbamate	Pluronic®F127	Oral	68
amphotericin B	Phytantriol	Pluronic®F127	Oral	69-70
cinnarizine	Phytantriol or Glyceryl monooleate	Pluronic®F127	Oral	71
cyclosporine A	Glyceryl monooleate	Pluronic®F127	Oral	72
ibuprofen	Phytantriol	Pluronic®F127	Oral	73
insulin	Glyceryl monooleate	Pluronic®F127	Oral	74
20(S)-protopanaxadiol/piperine	Glyceryl monooleate	Pluronic®F127	Oral	75-76
simvastatin	Glyceryl monooleate	Pluronic®F127	Oral	77
omapatrilat	Glyceryl monooleate	Pluronic®F127	Oral	78
omapatrilat	Glyceryl monooleate	Pluronic®F68	Oral	78
paclitaxel	Soy phosphatidylcholine/ glycerol dioleate	Polysorbate 80	Oral	79
baicalin/KiOM-C	Glyceryl monooleate	Pluronic®F127	*In vitro* (Small intestine adsorption)	80
S-164 (water-soluble extract)	Glyceryl monooleate	Pluronic®F127	*In vitro* (Small intestine adsorption)	81
odorranalectin/streptavidin	Glyceryl monooleate	Pluronic®F127	Intranasal	82
indomethacin	Glyceryl monooleate	Pluronic®F127	Precutaneous	83
bromocriptine	Glyceryl monooleate	Pluronic®F127	Intraperitoneal	84
adjuvants imiquimod and monophosphoryl lipid A	Phytantriol	Pluronic®F127	Intravenous	85
fluorescein isothiocyanate-ovalbumin/ Quil A®	Phytantriol	Pluronic®F127	Intravenous	86
paclitaxel	Glyceryl monooleate	Pluronic®F127/ $mPEG_{2K}DSPE$	Intravenous	87
propofol	Soy phosphatidylcholine/ Glycerol dioleate	Polysorbate 80	Intravenous	88
somatostatin	Soy phosphatidylcholine/ Glycerol dioleate	Polysorbate 80	Intravenous	89
earthworm fibrinolytic enzyme (protein)	Glyceryl monooleate/Propylene glycol	Pluronic®F127	Intratympanic	90
ovalbumin	Phytantriol or Glyceryl monooleate	Pluronic®F127		91
α-chymotrypsinogen A (Protein)	Glyceryl monooleate	MO-PEG_{2000}, [poly(ethylene glycol) monooleate]		92
annexin V (Protein)	Phytantriol	Pluronic®F127		93
curcumin	Glyceryl monooleate	Pluronic®F127		94

Continued on page 8

Continued from page 7

Bioactive molecule (peptide, drug)	Matrix constituent	Stabiliser	Administration route (if applicable)	Ref.
quercetin	Glyceryl monooleate	Pluronic®F108		95
dacarbazine	Glyceryl monooleate	Pluronic®F127		96-98
carbamazepine (CBZ) coenzyme Q10 (CoQ10) cholesterol (Chl) (Sterol) phytosterols (PSs, plant sterols) diazepam griseofulvin propofol rifampicin	Glyceryl monooleate Myverol™ 18-99	Pluronic®F127 Pluronic®F127		99 100
50-deoxy-5-fluoro-N4-(phytanyloxycarbonyl) cytidine (Phytanyl Pro-Drug Analogue of Capecitabine)	50-deoxy-5-fluoro-N4-(phytanyloxycarbonyl) cytidine	Pluronic®F127		101
hydrocortisone	Phytantriol	Pluronic®F127		36
atropine	Phytantriol	Pluronic®F127		36
transretinol	Phytantriol	Pluronic®F127		36
diazepam	Phytantriol	Pluronic®F127		36
prednisolone	Phytantriol	Pluronic®F127		36
dexamethasone	Phytantriol	Pluronic®F127		36
progesterone	Phytantriol	Pluronic®F127		36
haloperidol	Phytantriol	Pluronic®F127		36
levofloxacin	Phytantriol	Pluronic®F127		36
indometacin	Phytantriol	Pluronic®F127		36
hydrocortisone	Myverol™ 18-99 K	Pluronic®F127		36
atropine	Myverol™ 18-99 K	Pluronic®F127		36
transretinol	Myverol™ 18-99 K	Pluronic®F127		36
diazepam	Myverol™ 18-99 K	Pluronic®F127		36
prednisolone	Myverol™ 18-99 K	Pluronic®F127		36
dexamethasone	Myverol™ 18-99 K	Pluronic®F127		36
progesterone	Myverol™ 18-99 K	Pluronic®F127		36
haloperidol	Myverol™ 18-99 K	Pluronic®F127		36
levofloxacin	Myverol™ 18-99 K	Pluronic®F127		36
indometacin	Myverol™ 18-99 K	Pluronic®F127		36
DOPURu (amphiphilic ruthenium-based molecule)	1,2-dioleoyl-sn-glycero-3-phosphocholine (DOPC) and 1,2- dioleoyl-sn-glycero-3-phosphoethanolamine (DOPE)			102

1.3 Steric Stabilisation of Cubosomes

Although the internal mesophase of lyotropic liquid crystalline particles are thermodynamically stable, cubosomes are often less stable than regular emulsions in an aqueous solution and often employ a steric stabiliser to retain colloidal stability.[103] The van der Waals forces driving flocculation, coalescence and creaming of typical oil/water emulsion systems are also a factor in the colloidal stability of cubosome dispersions. An ideal stabiliser for cubosomes prevents unfavourable interaction between the hydrophobic domains on encounter between particles, without causing disruption to the inner cubic structure, providing a steric and/or electrostatic repulsive barrier between approaching particles. Therefore stabilisers are considered an essential component in liquid crystalline nanostructured particle preparation. A further element of consideration for cubosomes is their high internal interfacial area which may lead to stabiliser sequestration within the liquid crystalline nanostructure, which will reduce its contribution to colloidal stability.[104] Although a charged stabiliser can be applied to provide an electrostatic barrier to the flocculation of cubosomes, it is more common to utilise a steric stabiliser, as charged surfactant molecules have a high propensity to disrupt the internal phase structure of cubosomes.[105] Charged nanostructured particles, such as negatively charged liposomes, have also been reported to have a shorter half-life in the blood than neutral liposomes[106-107] and positively charged liposomes were found to be toxic and thus quickly removed from circulation[108]. It was reported that the surface charge (i.e. positive or negative) is a key determinant in complement-system activation by liposomes for both human and guinea-pig serum.[109-110] The main focus in this thesis is on the steric stabilisation of cubosomes and although the steric stabilisers listed may also be applicable to hexosomes their systems will not be addressed.

Stealth and steric hindrance are provided by polymers that have been reported to confer repellency to surfaces, which share a number of properties, such as hydrophilicity, presence of hydrogen bond acceptors but absence of hydrogen bond donors, and electrical neutrality.[111-112] Polyethylene glycol (PEG) also known as polyethylene oxide (PEO) fits this profile, being an uncharged, hydrophilic polymer that is soluble in water. Due to its low toxicity and immunogenicity, PEG is considered to be the chemical moiety that yields the most effective steric repulsion barrier while improving the pharmacokinetics and pharmacodynamics of nanoscale drug delivery systems (e.g. stealth liposomes).[113-115] PEG has been shown to be able to form a stealth corona around liposomes, significantly reducing the rapid uptake of intravenously injected particulate drug carriers by cells of the mononuclear phagocyte system (MPS).[116-117] It has been demonstrated theoretically[118-121] and experimentally[122-127] that protein repellence of PEG coatings depends on both chain length and chain density which jointly determine the thickness of the adlayer.[111]

Steric stabilisation of nanostructured particles is also highly dependent on the amount of stabiliser within the dispersion (i.e. stabiliser concentration). Low stabiliser surface coverage often results in a ‘mushroom’ surface conformation of the stabiliser on the surface of the particle (Figure 5). Increasing the density of PEG chains on the surface of the particle often results in a ‘brush’ conformation of the stabilising

polymer, which is more effective in stabilisation and protein repellence. However, little is currently known on the optimal stabiliser concentration range for preparation of cubosome dispersions, although 10% w/w is the standard concentration often used in their preparation, as it produces an aggregate free dispersion.[128] Besides PEG length and concentration, it was also established by Thies in 1976, that stabiliser composition/structure and establishing a favourable balance between the anchoring unit (i.e. hydrophobic head) and extending unit (i.e. hydrophilic tail) was as equally important in achieving optimum stability performance when using copolymers as steric stabilisers.[129] This highlights the importance of assessing various copolymer structures as stabilisers for liquid crystalline nanostructured particles, as it is possible that better copolymer structure configurations which will enable more effective stabilisation have not yet been explored.

Accordingly, steric hindrance and provision of stealth onto a nanostructured particle is also dependent on the concentration of steric stabiliser applied and the PEG length in the steric stabiliser (Figure 5). In 1954, Heller and Pugh found that increasing the PEG length and concentration on their gold sols increased their stability.[130] This was later confirmed by Lee *et al.* in 1989, using a range of poloxamers™ (Pluronic®L63, P65, P105, F68, F88, F108) and poloxamine™ (Tetronic® 908), with increasing hydrophilic PEG chain lengths on polystyrene beads. Whereby it was also found that increasing the PEG length also increased the stability of the beads, with Pluronic®F108 and Tetronic® 908 being the best stabilisers from the series.[131] Pluronic®F108 was also used on polystyrene beads in 1998 achieving similar stability results.[132] Short PEG lengths on steric stabilisers may be unfavourable because there is not much distance created between neighbouring particles if the PEG chain is too short and thus a higher occurrence of aggregation may proceed. For this reason typically the longer the PEG chain (e.g. Pluronic®F108) the better its effectiveness at providing stabilisation to a hydrophobic particle. However, it may also be detrimental to have a PEG chain which is too long as bridging of multiple particles by the same stabiliser may occur, increasing the incidence of aggregation within the system. Whilst PEG is regarded as an ideal hydrophilic domain for steric stabilisers for lyotropic liquid crystalline nanostructured particles, little is known about the ideal PEG chain length for establishing maximum steric stabilisation effectiveness onto cubosomes.

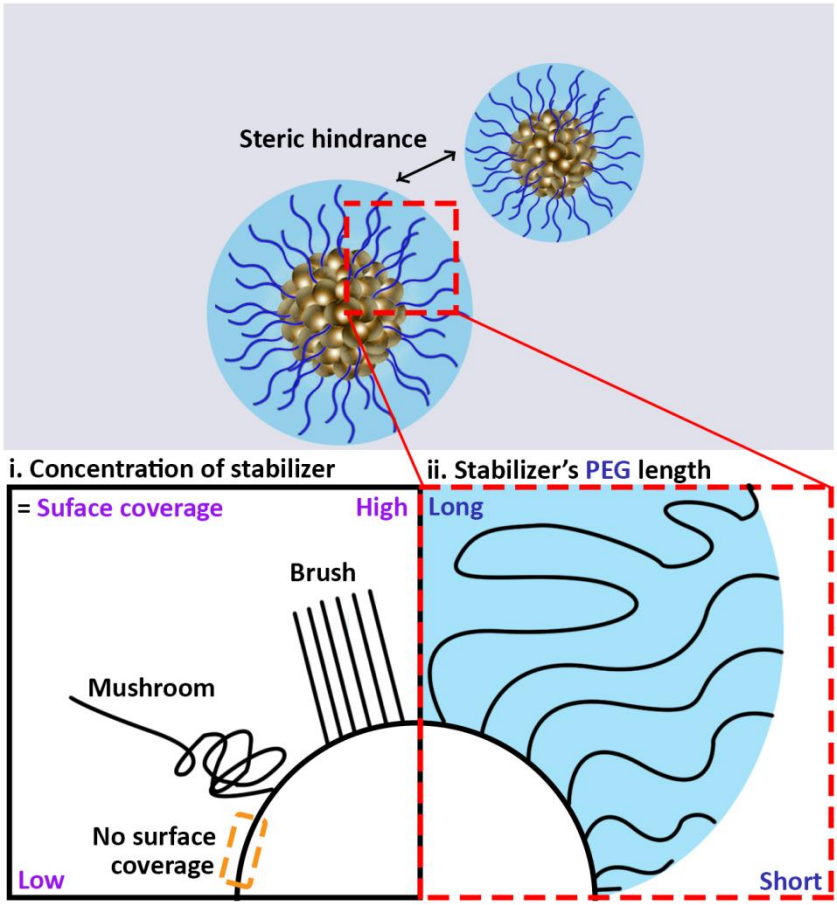

Figure 5. An illustration of some of the factors affecting steric hindrance between nanostructured particles: (i) the concentration of steric stabiliser used and (ii) PEG length in steric stabiliser

1.3.1 Classes of Cubosome Steric Stabilisers

The steric stabilisers which have been reported in the literature for preparing cubosome dispersions have been categorized into three groups: (i) Amphiphilic block copolymers (i.e. poloxamer™ and poloxamine™), (ii) PEGylated-lipids (e.g. GMO-PEG, vitamin E TPGS, Tween®, DMPE-PEG, DOPE-PEG, DSPE-PEG) and (iii) Alternative steric stabilisers (i.e. bile salts, protein, polysaccharide polymers, vitamin and nanoparticles). These are summarised in Table 3.1, 3.2 and 3.3 and are described in more detail below.

Table 3.1. A table listing amphiphilic block copolymer steric stabilisers for cubosomes reported in the general literature

Stabiliser	Lipid Matrix constituent	Space group of inner structure	Ref.
POLOXAMER™			
Pluronic®F127	phytantriol	Pn3m (Q^{224})	36, 46, 52-53, 60, 69-71, 73, 85-86, 91, 93, 104, 133-141
Pluronic®F127	phytantriol/dipalmitoyl phosphatidylserine (DPPS)	Pn3m (Q^{224}) or Im3m (Q^{229})	138
Pluronic®F127	1-*O*-(5,9,13,17-tetramethyloctadecanoyl)erythritol (EROCO C22)	Pn3m (Q^{224}) and Im3m (Q^{229})	142
Pluronic®F127	1-*O*-(5,9,13,17-tetramethyloctadecyl)-β-D-xylopyranoside (β-XP)	Pn3m (Q^{224}) and Im3m (Q^{229})	142-144
Pluronic®F127	The glycolipid 1-O-phytanyl-β-d-xyloside(β-XP)	Pn3m (Q^{224}) and Im3m (Q^{229})	144
Pluronic®F127	5-FC oleyl carbamate	Pn3m (Q^{224}) and Ia3d (Q^{230})	68
Pluronic®F127	50-deoxy-5-fluoro-N4-(phytanyloxycarbonyl) cytidine	Pn3m (Q^{224}) and Ia3d (Q^{230})	101
Pluronic®F127	monolinolein (MLO)	Pn3m (Q^{224}) at 25°C	145
Pluronic®F127	monolinolein (MLO)/oil	Pn3m (Q^{224})	146-149
		Fd3m (Q^{227})	146-149
Pluronic®F127	monolinolein (MLO)/diglycerol monooleate(DGMO) or soybean PC/oil	Pn3m (Q^{224}) or Im3m (Q^{229})	150
Pluronic®F127	monoelaidin	Im3m (Q^{229})	151
Pluronic®F127	Myverol™ 18-99 K	Pn3m (Q^{224}) or Im3m (Q^{229})	36, 52, 100, 136, 152
Pluronic®F127	RYLO MG19	Pn3m (Q^{224}) and Im3m (Q^{229})	98, 152
Pluronic®F127	glyceryl monooleate	Pn3m (Q^{224}) or Im3m (Q^{229})	44, 55, 57-59, 61-67, 71-72, 74-78, 80-84, 91, 94, 96-99, 103, 136, 139, 151, 153-168
Pluronic®F127	glyceryl monooleate/propylene glycol	Pn3m (Q^{224}) and Im3m (Q^{229})	90
Pluronic®F127	glyceryl monooleate/soya phospholipids	Im3m (Q^{229})	169
Pluronic®F127	glyceryl monooleate/oil	Im3m (Q^{229})	170
		Fd3m (Q^{227})	170
Pluronic®F127	glyceryl monooleate/1-glycerol monooleyl ether (GME)	Pn3m (Q^{224}), Im3m (Q^{229})	171
Pluronic®F127	Dimodan U/J (96% monoglycerides: 62% linoleate and 25% oleate)/tetradecane (oil)	Pn3m (Q^{224}) and Im3m (Q^{229})	172
Pluronic®F127	Dimodan U/J (96% monoglycerides: 62% linoleate and 25% oleate)	Pn3m (Q^{224}) and Im3m (Q^{229})	173-174
Pluronic®F127/mPEG$_{2K}$DSPE	glyceryl monooleate	Im3m (Q^{229})	87
Pluronic®F127/*β*-casein mixture	phytantriol	Pn3m (Q^{224})	136
Pluronic®F68	glyceryl monooleate	Cubosome	78
Pluronic®F68	Myverol™ 18-99 K	Cubosome	128
Pluronic®F108 *	glyceryl monooleate	Pn3m (Q^{224})	95
POLAXAMINE™			
Poloxamine™ 908	Myverol™ 18-99 K	Cubosome	128
Poloxamine™ 908/Pluronic® F127 combinations	Myverol™ 18-99 K	Cubosome	128

**Note this stabiliser was used post publication of Chapter 2 in thesis*

Table 3.2. A table listing PEGylated-lipid copolymer steric stabilisers for cubosomes reported in the general literature

Stabiliser			Lipid Matrix constituent	Space group of inner structure	Ref.
PEG-LIPID	**PEG Mw**	**PEG units**			
1,2-dimyristoyl-*sn*-glycero-3-phosphoethanolamine-*N*-PEG ($DMPE\text{-}PEG_{550}$)	550	12	dielaidoylphosphatidylethanolamine (DEPE)	Im3m (Q^{229})	175-176
PEGylated monoolein ($MO\text{-}PEG_{660}$)	660	15	1,2-dioleoylphosphatidylethanolamine (DOPE)	Q^{230} (Ia3d), Q^{224} (Pn3m)	177
1,2-distearorylphosphatidylethanolamine-PEG, ($DSPE\text{-}PEG_{750}$)	750	17	1,2-dioleoylphosphatidylethanolamine (DOPE)	Cubosome	178
Polyoxyethylene (20) sorbitan monopalmitate (Tween®40)	900	20	Myverol™ 18-99 K	Cubosome	128
Polyoxyethylene (20) sorbitan monooleate (Tween®80)	900	20	glyceryl monooleate	Cubosome	44
Polyoxyethylene (20) sorbitan monooleate (Tween®80)	900	20	soy phosphatidylcholine/ glycerol dioleate	Cubosome	79, 88-89
Polyoxyethylene (20) sorbitan monooleate (Tween®80)	900	20	soy PE (L-α-phosphatidylethanolamine)	Cubosome	35
D-alpha-tocopheryl PEO_{1000} succinate (Vitamin E TPGS)	1000	22	phytantriol	Im3m (Q^{229})	35
1,3-didodecyloxy-propane-2-ol-PEG ($DDP(EO)_{30}$)	1340	30	GMO (RYLO MG 90)	Ia3d (Q^{230})	179
1,2-dioleoylphosphatidylethanolamine-PEG (DOPE-PEG)	2000	45	glyceryl monooleate and cis-5,8,11,14,17-eicosapentaenoic acid (20:5, EPA)	Cubosome	180
PEGylated monoolein ($MO\text{-}PEG_{2000}$)	2000	45	glyceryl monooleate	Pn3m (Q^{224}) or Im3m (Q^{229})	92
1,2-distearorylphosphatidylethanolamine-PEG ($DSPE\text{-}PEG_{2000}$)	2000	45	1,2-dioleoylphosphatidylethanolamine (DOPE)	Cubosome	178, 181
1,2-distearorylphosphatidylethanolamine-PEG ($DSPE\text{-}PEG_{2000}$)	2000	45	soy phosphatidyl choline (SPC) and glycerol dioleate (GDO)	Cubosome	181
1,3-didodecyloxy-propane-2-ol-PEG ($DDP\text{-}(EO)_{52}$)	2309	52	GMO (RYLO MG 90)	Im3m (Q^{229}), Ia3d (Q^{230}) (coexisting with L_3 phase)	179, 182
1,3-didodecyloxy-propane-2-ol-PEG ($DDP\text{-}(EO)_{92}$)	4071	92	GMO (RYLO MG 90)	Im3m (Q^{229}), Ia3d (Q^{230}) (coexisting with L_3 phase)	179, 182
1,3-didodecyloxy-2-glycidyl-glycerol-PEG ($DDGG_4\text{-}(EO)_{114}$)	5040	114	GMO (RYLO MG 90)	Im3m (Q^{229}), Ia3d (Q^{230}) (coexisting with L_3 phase)	179, 182
1,3-didodecyloxy-2-glycidyl-glycerol-PEG-1,3-didodecyloxy-2-glycidyl-glycerol ($DDGG_2\text{-}(EO)_{136}\text{-}DDGG_2$)	6009	136	GMO (RYLO MG 90)	Im3m (Q^{229}), Ia3d (Q^{230}) (coexisting with L_3 phase)	179, 182
PEG-based copolymers bearing lipid-mimetic anchors			glyceryl monooleate/sodium cholate	Cubosome (coexisting with L_3 phase)	183

Table 3.3. A table listing alternative steric stabilisers for cubosomes reported in the general literature

Stabiliser	Lipid Matrix constituent	Space group of inner structure	Ref.
CASEIN			
β-casein	glyceryl monooleate	Pn3m (Q^{224})	136
casein	Myverol™ 18-99 K	Cubosome	128
ALBUMIN			
albumin	Myverol™ 18-99 K	Cubosome	128
MODIFIED CELLULOSE			
hydroxypropyl methyl cellulose acetate succinate (HPMCAS)	glyceryl monooleate	Pn3m (Q^{224})	142
hydroxypropyl methyl cellulose acetate succinate (HPMCAS)	1-*O*-(5,9,13,17-tetramethyloctadecanoyl)erythritol (EROCO C22)	Pn3m (Q^{224})	142
hydroxypropyl methyl cellulose acetate succinate (HPMCAS)	1-*O*-(5,9,13,17-tetramethyloctadecyl)-β-D-xylopyranoside (β-XP)	Pn3m (Q^{224})	142
MODIFIED STARCH			
HI-CAP100 (hydrophobically modified with octenyl succinate groups)	glyceryl monooleate	Cubosome	184
CAPSUL-E (hydrophobically modified with octenyl succinate groups)	glyceryl monooleate	Cubosome	184
dextran	glyceryl monooleate	Cubosome	184
LAPONITE			
Laponite XLG	phytantriol	Pn3m (Q^{224})	135
Laponite XLG	Dimodan U/J (96% monoglycerides: 62% linoleate and 25% oleate)	Pn3m (Q^{224})	173
Laponite XLG	Dimodan U/J (96% monoglycerides: 62% linoleate and 25% oleate)/Tetradecane (oil)	Pn3m (Q^{224})	172
SILICA NANOPARTICLES			
Silica nanoparticles	phytantriol/tetradecane (oil)	Pn3m (Q^{224})	185
NO STABILISER			
	1,2-dioleoyl-sn-glycero-3-phosphocholine (DOPC) and 1,2- dioleoyl-sn-glycero-3-phosphoethanolamine (DOPE)	Im3m (Q^{229})	102
	glyceryl monooleate/*cis*-5,8,11,14,17-eicosapentaenoic acid/1,2-dioleyl-*sn*-glycero-3-phosphoethanolamine-*N*-[methoxy(poly(ethylene glycol))-2000] (DOPE-PEG_{2000})	Cubosome	180

1.3.1.1 Amphiphilic Block Copolymers

Two classes of amphiphilic block copolymers have been reported as steric stabilisers for cubosomes to date. These are the poloxamer™ and poloxamine™.

1.3.1.1.1 Poloxamer™

i. Poloxamer™ 407/Pluronic®F127

By far the most widely and frequently used steric stabiliser for cubosomes is poloxamer™ 407 (also known as Pluronic®F127), a nonionic triblock copolymer composed of polyethylene glycol (PEG) and polypropylene oxide (PPO): $PEG_{100}PPO_{65}PEG_{100}$, with a molecular weight of approximately 12600 Da (Figure 6). Pluronic®F127 is a non-ionic detergent that is used widely in pharmaceutical formulations and personal care products. In liquid crystalline dispersions, Pluronic®F127 acts as a steric stabiliser through the incorporation or adsorption of its hydrophobic PPO block onto the surface of the nanostructured particle.

Whilst the PPO domain/block acts as an 'anchor' to the particle, the hydrophilic PEG chains/block extends to cover the surface, providing steric shielding and stabilising the colloidal particles in aqueous solutions.[186]

Pluronic®F127 has been employed to stabilise cubosome dispersions in various lipid systems, including GMO, glycerol monolinoleate and phytantriol. The GMO system has been the most extensively studied. At low stabiliser concentrations (<4 % w/w vs. GMO), Pluronic®F127 stabilised GMO dispersions form Q^{224} cubosomes with *Pn3m* space group symmetry, whilst at higher stabiliser concentrations (i.e. 7.4 or 10 % w/w vs. GMO), Q^{229} cubosomes with *Im3m* space group symmetry are formed.[154] Although using low stabiliser concentrations of Pluronic®F127 can produce Q^{224} cubosomes, the overall quality of the dispersed sample is poor with aggregates present. Therefore higher stabiliser concentrations (i.e. 10% w/w vs. lipid) are typically employed in cubosome preparation, as they establish dispersions that are aggregate-free.

It is important to preserve the *Pn3m* space group symmetry within GMO cubosomes because not only does the change to an *Im3m* space group symmetry indicate a disruption and destabilisation of the liquid crystal system, but the release rate of encapsulated drugs from a cubic phase system with an *Im3m* space group symmetry is much faster than it is for one with a *Pn3m* space group symmetry.[38]

In contrast to the case of GMO, using similar high Pluronic®F127 concentrations with either glycerol monolinoleate[145] and phytantriol[133] as the main lipid, results in retention of the *Pn3m* diamond bicontinuous cubic phase within their dispersions. The Pluronic®F127 content was as high as 33% relative to lipid in some of the phytantriol dispersions in water.[133] Mixed Q^{229} and Q^{224} cubosome dispersions can also be obtained from a cubic phase-forming lipid, 1-*O*-(5,9,13,17-tetramethyloctadecyl)-β-D-xylopyranoside (β-XP) system that used 5.1% w/w Pluronic®F127.[143] Similarly mixed phases were also observed from a ternary system composed of pine needle oil monoglycerides (89.5 wt% GMO), Pluronic® F127 and water, whereby an extended inverted cubic-phase field in which four different cubic structures (Q^{230} (Gyroid periodic minimal surface), Q^{224} (Diamond periodic minimal surface), Q^{229} (Primitive periodic minimal surface) and Q^{229} (Neovius' periodic minimal surface) were detected by X-ray diffraction.[168]

ii. Poloxamer™ 188/Pluronic®F68

Pluronic®F68: $PEG_{76}PPO_{29}PEG_{76}$ (Figure 6) is another poloxamer™ amphiphile which has been used to sterically stabilise cubosomes. It is shorter than Pluronic®F127 with a molecular weight of approximately 8400 Da. Tamayo-Esquivel *et al.* and Boyd *et al.* reported cubic nanostructured particles from aqueous dispersions based on glyceryl monooleate (GMO-Pluronic®F68-water system) employing Pluronic®F68, as a steric stabilising agent.[78, 128]

1.3.1.1.2 Poloxamine™

i. Poloxamine™ 908/Tetronic®908

Poloxamine™ 908, also known as Tetronic®908, is a tetrafunctional polyethylene glycol-polypropylene oxide ethylenediamine block copolymer (Figure 6). Boyd *et al.* reported stabilising aqueous dispersions of Myverol™ 18-99 K in water, using poloxamine™ 908, as a steric stabilising agent.[128] Aqueous dispersions of Myverol™ 18-99 K in water were also achieved using a combination of poloxamer™ 407 and poloxamine™ 908, as stabilising agents.[128]

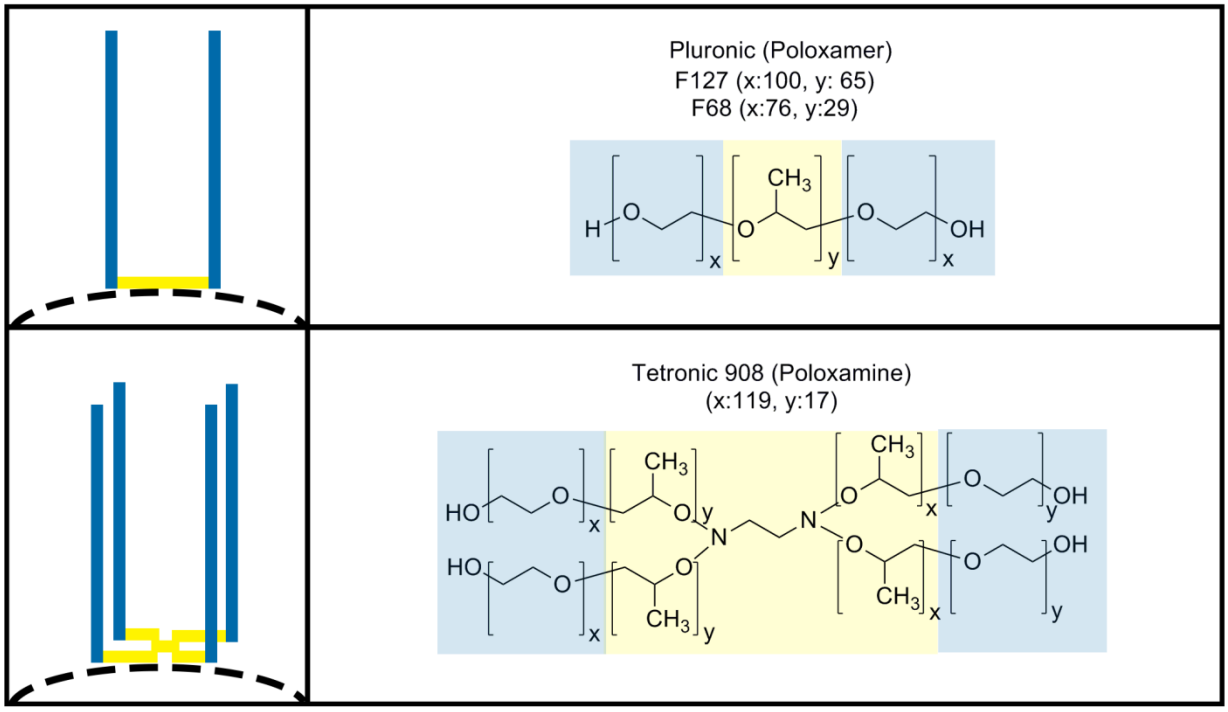

Figure 6. The chemical structures of stabilisers Pluronic® and Tetronic®. The blue shading indicates the hydrophilic domain, whilst the yellow shading indicates the hydrophobic domain. A graphic illustration of the stabiliser structure is shown on the left hand side, with the dashed line representative of the surface of a nanostructured particle.

1.3.1.2 PEGylated-lipids

In addition to commercially available block copolymer stabilisers, PEGylated-lipids (i.e. PEG-lipids) have also been reported to sterically stabilise inverse bicontinuous cubic phase particles. To date only a few PEGylated-lipids have been published to be stabilisers for cubic lyotropic liquid crystalline nanostructured particle dispersions (Figure 7).[35, 92, 175-183]

The **lipid anchors** of these PEGylated lipids include:

i. Glycerol monooleate (GMO)

Johnsson *et al.* reported cubic nanostructured particles from aqueous dispersions of dioleoylphosphatidylethanolamine (DOPE) with PEG-lipid, PEGylated monoolein (MO-PEG_{660}) as a steric stabilising agent.[177] These cubosomes were identified with cubic phase Q^{230}, with *Ia3d* space group and cubic phase Q^{224}, with *Pn3m* space group symmetry.

Using a PEGylated monoolein (MO-PEG_{2000}) with a longer PEG chain as a steric stabilising agent, Angelov *et al.* reported cubic nanostructured particles from aqueous dispersions of glyceryl monooleate in water.[92] These cubosomes were identified with cubic phase Q^{229}, with *Im3m* space group and cubic phase Q^{224}, with *Pn3m* space group symmetry.

ii. Sorbitan monooleate and Sorbitan monopalmitate

Polyoxyethylene (20) sorbitan monooleate, otherwise known as polysorbate 80 and Tween®80, is a commercially available PEGylated lipid which has been reported to stabilise cubosomes (Figure 5). Polysorbate 80 is a solubilizing agent ubiquitously used in nutritives, creams, ointments, lotions, and multiple medical preparations (e.g., vitamin oils, vaccines, and anticancer agents) and as an additive in tablets. Barauskas *et al.* reported cubic nanostructured particles from aqueous dispersions of glyceryl monooleate (GMO-Tween®80-water system) with Tween®80, as a steric stabilising agent.[44] Cubosomes have also been prepared using soy phosphatidylcholine and glycerol dioleate in water, sterically stabilised with Tween®80.[79, 88-89] Barauskas et al. have also stabilised cubic nanostructured particles from aqueous dispersions of soy PE (L-α-phosphatidylethanolamine) (Soy PE-Tween®80-water system) using Tween®80.[35]

It is interesting to note that Boyd *et al.* observed immediate phase separation when using polysorbate 80 to stabilise dispersions of Myverol™ 18-99K, using 10% w/w solution of stabiliser.[128] Although polysorbate 80 was successfully used to stabilise GMO cubosomes, Myverol™ is a mixture of monoglycerides, and it is possible the impurities influence the effect of the polysorbate stabiliser. Boyd *et al.* have also assessed other polysorbates for their effectiveness at stabilising Myverol™ dispersions. These were polysorbate 20 (polyoxyethylene (20) sorbitan monolaurate), polysorbate 40 (polyoxyethylene (20) sorbitan monopalmitate) and polysorbate 60 (polyoxyethylene (20) sorbitan monostearate), which are commercially known as Tween®20, 40 and 60 respectively.[128]

Similar to polysorbate 80, it was found that polysorbate 20 and 60 stabilised Myverol™ systems in water displayed immediate phase separation. Only polysorbate 40 (Figure 5) was found to produce a coarse dispersion of Myverol™ in water. This indicates the importance of the lipophilic domain length of

a polysorbate stabiliser and that a minimum hydrocarbon chain length (e.g. C_{15}) is required to sufficiently anchor the stabiliser to the nanostructured particles and effectively stabilise these systems.

iii. D-alpha-tocopheryl (vitamin E)

Barauskas *et al.* reported cubic nanostructured particles from aqueous dispersions of phytantriol in water, with D-alpha-tocopheryl PEO_{1000} succinate (vitamin E TPGS) as the steric stabiliser.[35] Cubosomes were identified with cubic phase Q^{229}, with *Im3m* space group symmetry.

iv. Phospholipids (DOPE, DSPE and DMPE)

The use of PEGylated-phospholipids as a steric stabiliser for cubic nanostructured particles was reported by Angelov *et al.* [180], Johnsson and Edwards[178], Zeng *et al.* [181] and Koynova *et al.*[175-176]. Angelov *et al.* reported cubic nanostructured particles from aqueous dispersions of glyceryl monooleate and cis-5,8,11,14,17-eicosapentaenoic acid (20:5, EPA) in water, with 1,2-Dioleoylphosphatidylethanolamine-PEG (DOPE-PEG_{2000}) as the steric stabiliser.[180]

Johnsson and Edwards reported cubic nanostructured particles from aqueous dispersions of dioleophosphatidylethanolamine (DOPE)-PEG-derivatized phospholipids (PEG-lipid-water systems) with PEG-lipids (1,2-distearorylphosphatidylethanolamine-PEG, (DSPE-PEG_{750} or DSPE-PEG_{2000})) as a steric stabilising agent.[178] Zeng *et al.* also used DSPE-PEG_{2000} as a stabilising agent for forming cubic nanostructured particles from aqueous dispersions of soy phosphatidyl choline (SPC) and glycerol dioleate (GDO).[181]

Koynova *et al.* reported cubic nanostructured particles from aqueous dispersions of dielaidoylphosphatidylethanolamine (DEPE) with PEG-lipid, PEGylated 1,2-dimyristoyl-*sn*-glycero-3-phosphoethanolamine (DMPE-PEG_{550}) as a steric stabilising agent.[175-176] Cubosomes were identified with cubic phase Q^{229}, with *Im3m* space group symmetry.

v. 1,3-didodecyloxy-propane-2-ol (DDP)

Rangelov *et al.* reported cubic nanostructured particles from aqueous dispersions of glyceryl monooleate (RYLO MG 90) in water, with 1,3-didodecyloxy-propane-2-ol-PEG ($DDP(EO)_{30}$) as the steric stabiliser.[179] Cubosomes were identified with cubic phase Q^{230}, with *Ia3d* space group symmetry.

These findings were further supported by both Almgren *et al.* and Rangelov *et al.* whom reported cubic nanostructured particles from aqueous dispersions of glyceryl monooleate (RYLO MG 90) in water, using 1,3-didodecyloxy-propane-2-ol-PEG ($DDP(EO)_{52}$ or $DDP(EO)_{92}$) as the steric stabiliser.[179, 182] These cubosomes were also identified with cubic phase Q^{230}, with *Ia3d* space group but an additional cubic phase Q^{229}, with *Im3m* space group symmetry was also detected.

vi. 1,3-didodecyloxy-2-glycidyl-glycerol (DDGG)

Almgren *et al.*[182] and Rangelov *et al.*[179] also reported cubic nanostructured particles from aqueous dispersions of glyceryl monooleate (RYLO MG 90) in water, with 1,3-didodecyloxy-2-glycidyl-glycerol-PEG ($DDGG_4$-$(EO)_{114}$) as the steric stabiliser. They also used PEG-lipid with a triblock copolymer structure, where the lipids were located on both terminal ends of the PEG domain ($DDGG_2$-$(EO)_{136}$-$DDGG_2$).[179, 182] Cubosomes formed were identified with cubic phase Q^{230}, with *Ia3d* space group and cubic phase Q^{229}, with *Im3m* space group symmetry.

Although several PEG-lipid stabilisers with different PEG lengths have been identified, the most frequently used PEG length in PEG-lipid stabilisers is 45 PEG units (i.e. PEG2000).[92, 178, 180-181] The use of PEG2000 was based on liposome stabilisation, whereby use of PEG2000 hindered aggregation of lipid nanostructured particles under physiological conditions.[92, 187-189] However, the shortest and longest PEG-lipid stabilisers' PEG chain lengths that have been reported are 10 PEG units on average (i.e. PEG550)[175-176] and 136 PEG units on average (i.e. PEG6000)[179, 182] respectively.

These PEG-lipids have mainly been used to stabilise dispersions of glycerol monooleate, resulting in Q^{229} cubic phase dispersions, with an *Im3m* space group. However, other lipid dispersions stabilised using PEG-lipids as steric stabilisers include: dielaidoylphosphatidylethanolamine (DEPE), dioleoylphosphatidylethanolamine (DOPE) and a mixture of soy phosphatidyl choline (SPC) and glycerol dioleate (GDO). Only one PEG-lipid has been reported to stabilise phytantriol dispersions in water, namely D-alpha-tocopheryl poly(ethylene glycol) 1000 succinate (vitamin E TPGS), which was used at around 10% w/w stabiliser concentration. This resulted in a primitive cubic phase dispersion, with an *Im3m* space group.[35]

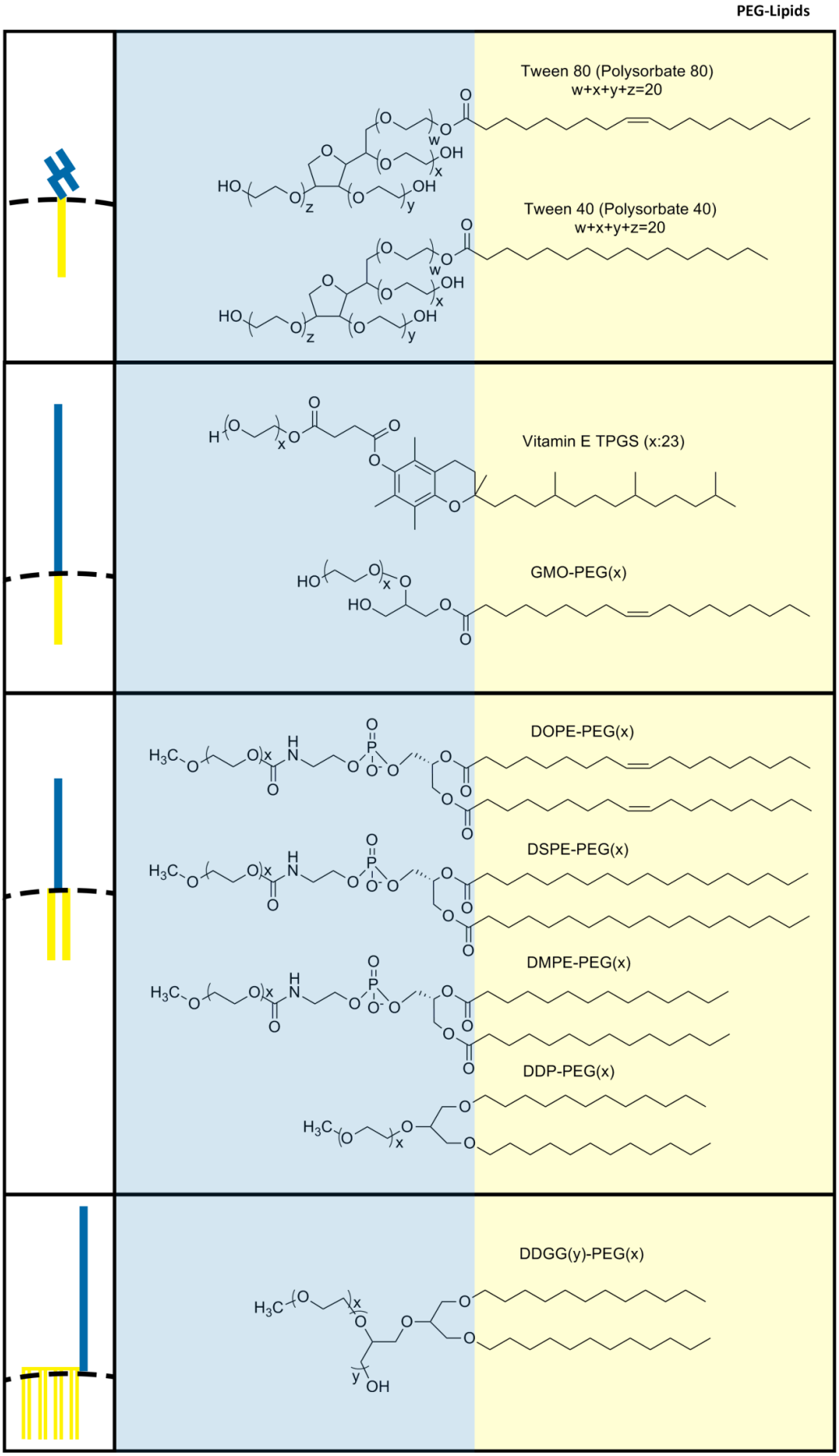

Figure 7. The chemical structures of PEG-lipid stabilisers. The blue shading indicates the hydrophilic domain and the yellow shading indicates the hydrophobic domain. A graphic illustration of the stabiliser structure is shown on the left hand side, with the dashed line representative of the nanostructured particle's surface.

1.3.1.3 Alternative Steric Stabilisers

In addition to amphiphilic block copolymers and PEGylated lipids, other amphiphilic stabilising agents have also been reported for cubosomes, including bile salts, amphiphilic proteins (i.e. casein and albumin), modified polysaccharide polymers (i.e. modified cellulose and starch), poly(vinyl) alcohol and nanoparticles (i.e. silica and clay nanoparticles).

1.3.1.3.1 Bile salts

The first fragmented bilayer cubic-phase structure was observed in 1979.[190] The cubic phase formed from a monoglyceride-water mixture was dispersed in the presence of micellar solutions of bile salts.[103, 183, 191] The cubic phase was stabilised by the formation of a lamellar envelope composed of bile salt and monoglycerides shielding the inner cubic structure.

1.3.1.3.2 Amphiphilic Protein

i. β-casein

β-casein is an amphiphilic protein and a very effective emulsifier and so was employed as a stabiliser in a disperse monoglyceride-water cubic phase. Here, the protein is believed to partition into the outer layer of the lipid, making it more hydrophilic and therefore easy to disperse.[136, 192]

ii. albumin

Albumin is a ubiquitous protein which is soluble in water and can be found in egg white, milk and blood serum. Boyd *et al.* briefly reported coarse dispersions of Myverol™ 18-99 K in water using albumin as a steric stabiliser.[128]

1.3.1.3.3 Modified Polysaccharide Polymers

i. Hydrophobically modified ethyl hydroxyethyl cellulose (HMEHEC) (Modified cellulose)

Almgren *et al.* applied hydrophobically modified ethyl hydroxyethyl cellulose (HMEHEC) to the GMO-based cubic phase.[193] Although cubosomes were formed, HMEHEC polymers do not make successful cubosome stabilisers as they were observed to have interacted so strongly with lipids that shortly after dispersion of the sample, the internal nanostructure of the cubosome transformed into lamellar and reversed hexagonal phase.

ii. Hydroxypropyl methyl cellulose acetate succinate (HPMCAS) (Modified cellulose)

Uyama *et al.* reported cubic nanostructured particles from aqueous dispersions of three lipids: (i) glyceryl monooleate, (ii) 1-*O*-(5,9,13,17-tetramethyloctadecanoyl)erythritol (EROCO C22), and (iii) 1-*O*-

(5,9,13,17-tetramethyloctadecyl)-β-D-xylopyranoside (β-XP), using hydroxypropyl methyl cellulose acetate succinate (HPMCAS) as a stabilising agent.[142] The cubosomes formed were identified to have cubic phase Q^{224}, with *Pn3m* space group symmetry. The motivation for using modified cellulose was because cellulose products are widely used in the cosmetics, food, and pharmaceutical industries, such as in eye drops and inhalants. HPMCAS is a commercially available generic coating agent and widely used in dry coating or solid dispersion systems[194-196], and demonstrated by Uyama *et al.* to be applicable as a stabiliser for cubosomes, which allows for sufficient dispersion stability without any internal structure modification.[142]

iii. HI-CAP100, CAPSUL-E, dextran (modified starch)

Spicer *et al.* presented a pseudoternary phase diagram of GMO with hydrophobically modified starch in water and prepared cubosomes by the rehydration of spray-dried starch-GMO mixtures.[184] In that system, starch was mixed 3-fold higher than the weight of GMO, and the particle size was 600 nm on average.

1.3.1.3.4 Amphiphilic poly(vinyl) alcohol

Poly(vinyl) alcohol is a water soluble synthetic polymer which has been used in papermaking and textiles. Tamayo-Esquivel *et al.* has reported using poly(vinyl) alcohol to stabilise aqueous GMO dispersions, resulting in sub-200 nm particles.[78]

1.3.1.3.5 Nanoparticles

i. Laponite XLG (clay nanoparticles)

Muller *et al.* and Salonen *et al.* have reported cubic nanostructured particles from aqueous dispersions of two lipids: (i) phytantriol [135] and (ii) Dimodan U/J (consisting of 96% monoglycerides, which contain 62% linoleate and 25% oleate), with[172] and without[173] tetradecane (oil) in water, using Laponite XLG (clay nanoparticles) as the steric stabiliser. The cubosomes formed were identified with cubic phase Q^{224}, with *Pn3m* space group symmetry.

ii. Silica (silica nanoparticles)

Salonen *et al.* have reported cubic nanostructured particles from aqueous dispersions of phytantriol and tetradecane (oil) in water, using silica nanoparticles as the steric stabilising agent.[185] The cubosomes formed were identified with cubic phase Q^{224}, with *Pn3m* space group symmetry.

1.4 Cubosome Preparation and Characterisation Techniques

1.4.1 Cubosome Preparation

For the preparation of any cubosome dispersion there are three main components which are required, which have already been outlined; these are the (i) lipid, (ii) steric stabiliser and (iii) an aqueous solution, which is typically water or a buffer system. Boyd *et al.* and Guo *et al.* have extensively reviewed and listed established preparation methodologies used for producing cubosome dispersion.[128, 197] In summary, there are two main approaches which are typically used to produce cubosome dispersions:

i. **Top-down approach**

This approach requires an extreme viscous bulk phase to be prepared by mixing structure-forming lipids with stabilisers, and the resultant mixture is subsequently dispersed into the aqueous solution by sonication. The high energy created by sonication can also be produced by high-pressure homogenisation and shearing. Since the report of this approach by Ljusberg-Wahren in 1996,[198] high-pressure homogenisation and sonication are still the most frequently used techniques in the preparation of cubosomes.[128, 197] This is probably because it is a rapid method for forming more uniform and refined dispersions with particle size below 200 nm. The small dispersion particle size is beneficial for use in intravenous applications and also suitable for sterilisation by filtration.[128] However, it has been stated that the cubosomes prepared using this top-down approach are almost always observed to coexist with vesicles (dispersed nanoparticles of lamellar liquid crystalline phase) or vesicle-like structures, which may complicate understanding the influence of cubosomes in these mixtures.[197]

In order to widen the application of cubosomes in the pharmaceutical field for the preparation of oral solid formulations and inhalants, a spray drying technique was implemented. Although spray drying is not a method of producing cubosomes, it is useful in providing a convenient powder form/template that re-forms cubosomes on exposure to water. This method was originally proposed and investigated by Spicer *et al.* whereby a powder precursor could be prepared through drying a pre-dispersed aqueous solution that consisted of (i) GMO, hydrophobically modified starch and water, or (ii) GMO, dextran, ethanol and water, and then the colloidally stable dispersions of nanostructured cubosomes could be recreated by hydrating the precursors.[184] Shah *et al.* also successfully re-formed GMO-based cubosomes using the spray drying method.[199] The precursor was proven to have more effective and prolonged anti-inflammatory and analgesic activity than pure drug when administered perorally, however the residual solvent content and consequently *in vivo* toxicity is still a problem with this technique.[197]

ii. **Bottom-up approach**

The bottom-up approach is one in which a single phase solution is diluted into a two phase regime of cubosomes coexisting with an excess aqueous phase. An advantage of this method compared to the top-down approach is that it requires less energy input to generate dispersions. The key factor in the bottom-up approach is the presence of a hydrotrope (e.g. chloroform), which is miscible with water-insoluble lipids to create single phase liquid precursors and prevent the formation of liquid crystals at high concentration. Selecting the dilution trajectory requires a knowledge of the ternary phase diagram (lipid-water-hydrotrope).[197] This approach also may result in cubosomes coexisting with vesicles and vesicle-like structures.

1.4.2 Cubosome Characterisation Techniques

In order to verify that the dispersion prepared using the desired preparation technique are indeed 'cubosomes', characterisation techniques, such as visual assessment, dynamic light scattering, cross-polarized light microscopy, small angle X-ray scattering and cryo-transmission electron microscopy are employed. These techniques are described in greater detail below. Although these may not be the only characterisation techniques used for cubosome analysis, these are the major techniques utilised in this project and in the literature to date. These techniques have been well established and used with great success in distinguishing different aspects of the lyotropic liquid crystalline nanostructured particle, such as particle size and lyotropic liquid crystal phase/nanostructure type.

1.4.2.1 Visual Assessment

A visual assessment can be done on cubosome dispersions to indicate the quality of the dispersed sample in terms of colloidal stability. This is a useful and efficient technique to initially determine and rank the effectiveness of steric stabilisers to produce dispersions. However, only Boyd *et al.* has reported the relative performance of steric stabilisers in a nanostructured dispersion using technique visual ranking in combination with particle size measurements.[128] A scoring system was implemented with '–' indicating immediate phase separation and '++++' indicating excellent stability. The stabilisers which produced high scores were (i) Pluronic®F127 with '++++' score, (ii) Poloxamine™ 908 with '+++' score and (iii) Pluronic®F127/Poloxamine™ 908 combinations with '+++' score. The evident lack in use of this simple technique may be due to the vast majority of cubosome research using a single stabiliser Pluronic®F127, and therefore do not require these dispersions to be scored in a visual assessment.

1.4.2.2 LUMiFuge® – Stability Analyser Instrument

Quantifying the stability of dispersions (i.e. cubosome and hexosome dispersions) has only been reported twice using a stability analyser, the LUMiFuge®, which is a specialist instrument designed to

quantify stability principally for emulsion or other colloidal systems.[200-201] The stability of the dispersion is quantified by using a microprocessor-controlled analytical centrifuge that detects demixing phenomena (e.g. floating and clarification) of the dispersed systems during centrifugation over the whole sample length. Although it may reliably allow the comparison of stability of dispersions and thus become an effective indicator of the effectiveness of steric stabilisers, it is a low throughput technique, as it only allows single sample analysis at any one time.

1.4.2.3 Dynamic Light Scattering (DLS)

Dynamic light scattering (DLS) is a characterisation technique used for the measurement of particle size and polydispersity of the distribution for liquid crystalline particle dispersions. The DLS technique most extensively utilised in particle characterisation of liquid crystalline particle dispersions is photon correlation spectroscopy (PCS), as it has the ability to measure translational diffusion of particles in the range from 1 to 1000 nm. PCS is based on the fact that the intensity of light scattered from a dispersion of particles into a given scattering angle is the result of interference on the surface of a square-law detector between light scattered from different particles in the medium.[202] As particles in solution exhibit Brownian motion their positions within the solution fluctuate, which leads to fluctuations of the scattered intensity. These scattered intensity fluctuations occur on a time scale that take a particle to move a significant fraction of the wavelength of light. The scattered intensity is a stochastic signal as it reflects the thermal (Brownian) motion of the particles. Thus, in order to extract useful information from the signal, its time correlation function is calculated using an autocorrelator, which allows for rapid real-time calculation of the scattered intensity time correlation function.[202]

In DLS, light from a laser is focused on a sample and the light scattered at a given scattering angle is collected by a square law detector, a photomultiplier or an avalanche photodiode. The output of the photomultiplier is then digitalised by a photon counting system and the output is sent to an autocorrelator. Fiber optic guides are often used for precision deliverance of the light to the sample and for the collection of the scattered light back to the detector.[203] In DLS, the particle size of a spherical particle is derived from the Stokes-Einstein relation/equation [2], as it relates the translational self-diffusion coefficient (*D*) to the particle radius R.[202]

$$D = \frac{k_B T}{6\pi\eta R} \quad [2]$$

where k_B is Boltzmann's constant, T the absolute temperature and η is the viscosity of the suspending medium.

In addition to measuring particle size and their distribution, DLS can also be useful for determining the critical aggregation concentration (CAC) of amphiphilic material. This is done by measuring the changes in

the scattered light intensity detected during DLS, as the intensity of backscattered light is comparable to that of the solvent when a solution is absence of aggregates, and therefore intensities which are greater than that detected from the solvent indicates the presence of aggregates.[204] This intensity of backscattered light subsequently increases with increasing aggregate concentrations.

1.4.2.4 Cross-polarised Light Microscopy (CPLM)

Cross-polarized light microscopy (CPLM) can be used to determine the type of lyotropic liquid crystalline phase that may be present in nanostructured particle dispersions. This is based on the assumption that the phase behaviour of the bulk material will be the same as that of the dispersed particles. Consequently investigating the liquid crystalline behaviour of the bulk nondispersed material in excess water using CPLM has become a popular characterisation technique, as it is a cheap, rapid, and reliable method for preliminary phase determination, and can be conducted with increasing temperature to determine thermal stability of phase structures.[205] In conducting CPLM measurements, the lipid used for producing the nonlamellar liquid crystalline dispersions is compressed to a thin film between a microscope slide and a coverslip, and an excess of water is applied to the edge of the slides to observe lipid-water interface interactions. The interface is viewed under a microscope equipped with a polariser and an analyser.

Phase identity is indicated by (i) whether the lipid material exhibits birefringence, (ii) the type of optical textures exhibited by the birefringence, and/or (iii) the viscosity of the lipid material. The presence of birefringence indicates the presence of lamellar or inverse hexagonal phase (Figure 8). The characteristic optical textures within the birefringence allow discrimination between lamellar phase and hexagonal phase.[206-207] An optically isotropic appearance indicates the presence of cubic phase or inverse micellar phase. The viscosity of the material at the interface with excess water discriminates between the cubic and inverse micellar phases. High viscosity of the cubic phase imparts a structured appearance to the interface, whereas the low viscosity of the micellar phase results in an effectively flat, contracted interface.[128]

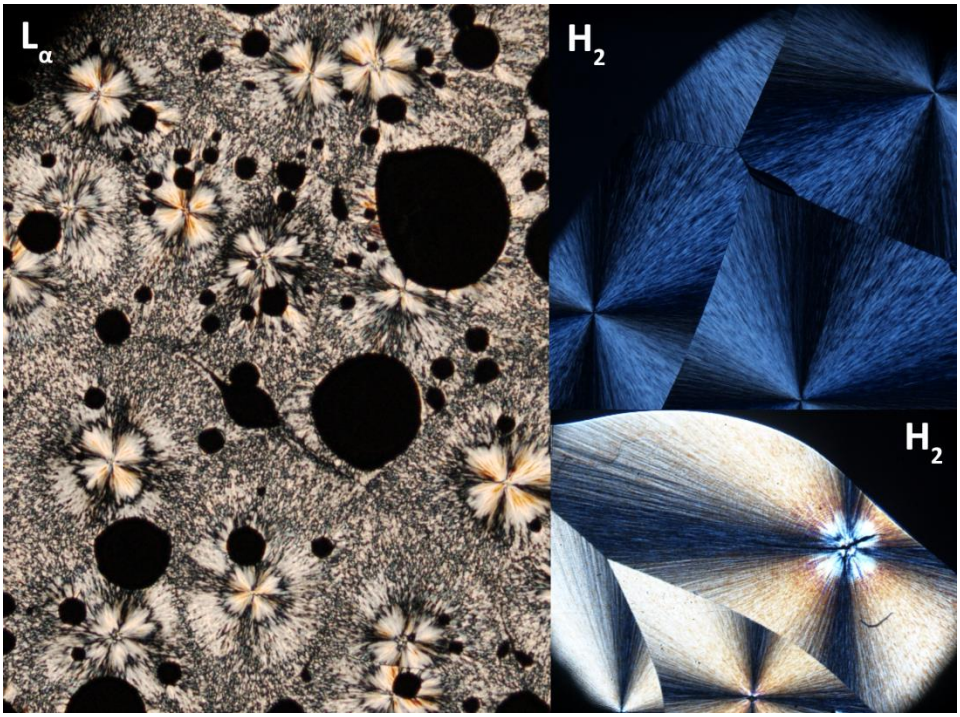

Figure 8. Birefringence material under CPLM displaying examples of lamellar (L_α) and hexagonal (H_2) optical textures

The use of a hot stage in conjunction with CPLM allows for the approximate boundaries between phases in excess water to be determined with increasing temperature. However, caution should be taken in using CPLM as a definitive guide to phase-structure determination in dispersed systems, as coexisting regions are difficult to determine, and phase transition temperatures seen in CPLM from using the bulk nondispersed material are not always reflected in that of the dispersed samples.[128] For example, although a hexagonal (H_2) phase is observed for the bulk phytantriol/water system during CPLM analysis, a H_2 phase is not observed for the dispersed system during small angle X-ray scattering.[133] Thus, even though CPLM is a useful guide to phase-identification and phase-transition regimes, it should always be used in conjunction with a secondary technique, most often small angle X-ray scattering (SAXS), to definitively obtain the lyotropic liquid crystalline phase type of the nanostructure of the dispersed particles.

1.4.2.5 Small Angle X-ray Scattering (SAXS)

Small angle X-ray scattering (SAXS) is the key technique employed to identify the type of lyotropic liquid crystalline phase present within a nanostructured particle dispersion (Figure 9.1). SAXS experiments involve probing the lyotropic liquid crystal structure with a well-collimated X-ray beam of wavelength λ through a sample and measuring with variation of the intensity of scattered X-rays as a function of the scattering angle θ. The incoming waves are reflected at parallel lattice planes defined by the particular structure (e.g. cubosome) present. The scattering angle is often expressed as the scattering vector q, as shown in the following equation [3]:

$$q = \frac{4\pi}{\lambda}\sin\frac{\theta}{2} \quad [3]$$

The scattering intensity is most often expressed as a function of q. Intensity vs. q plots (examples in Figure 9.2) are used to identify different mesophases, as the spacings corresponding to the peaks, which are a consequence of reflection planes present in the sample, are characteristic to different liquid crystal geometries.[208] The absolute q values for the reflections allow the determination of the liquid crystal structure present and the dimensions of the repeat unit for that particular nanostructure. Hyde has provided a collation of the expected ratios of q values for different liquid crystal geometries/mesophases (Table 16.1 in Hyde, 2001).[208]

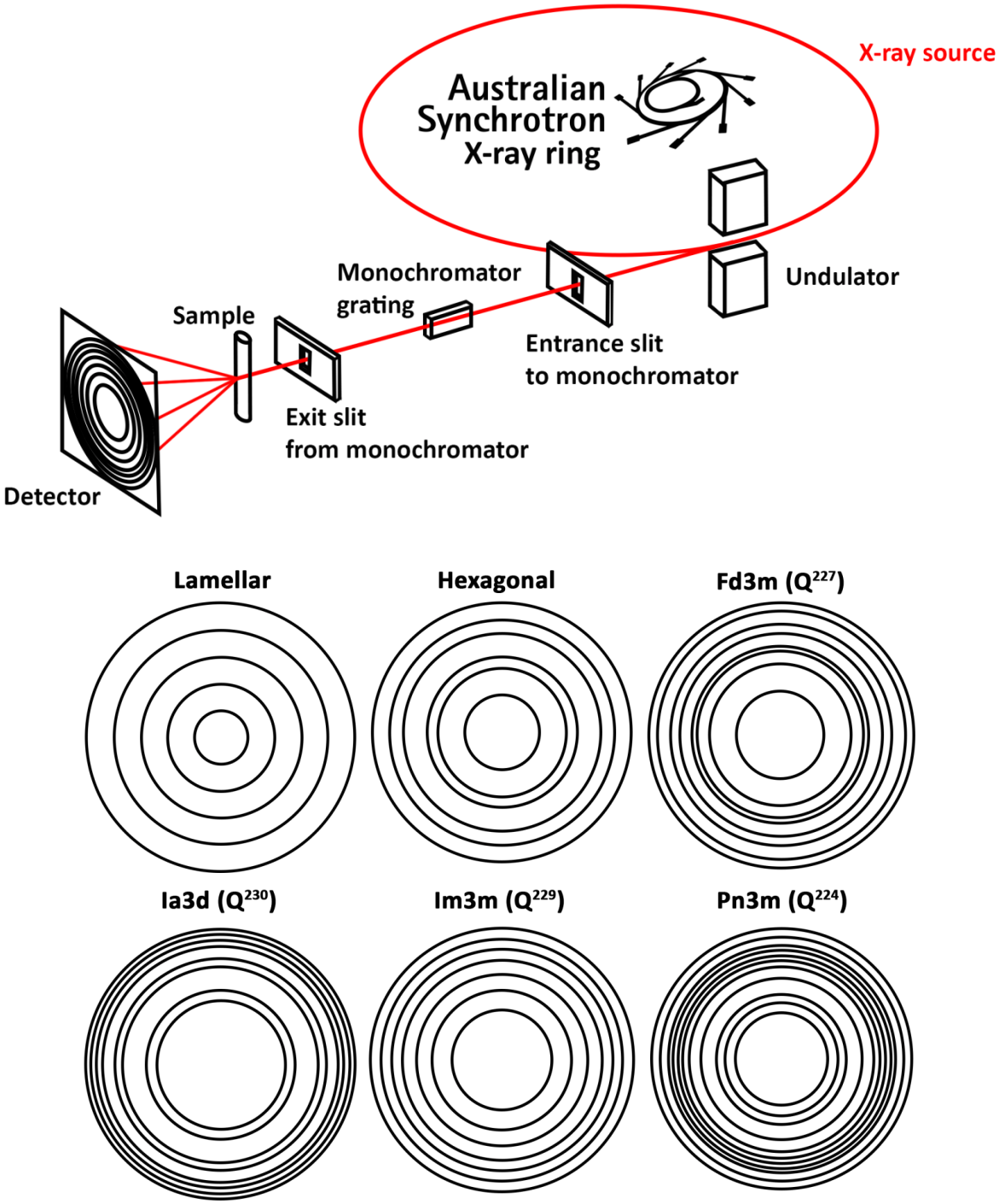

Figure 9.1 A diagram of the SAXS instrument set up using a synchrotron X-ray source and a schematic of the detector view for different mesophase structures

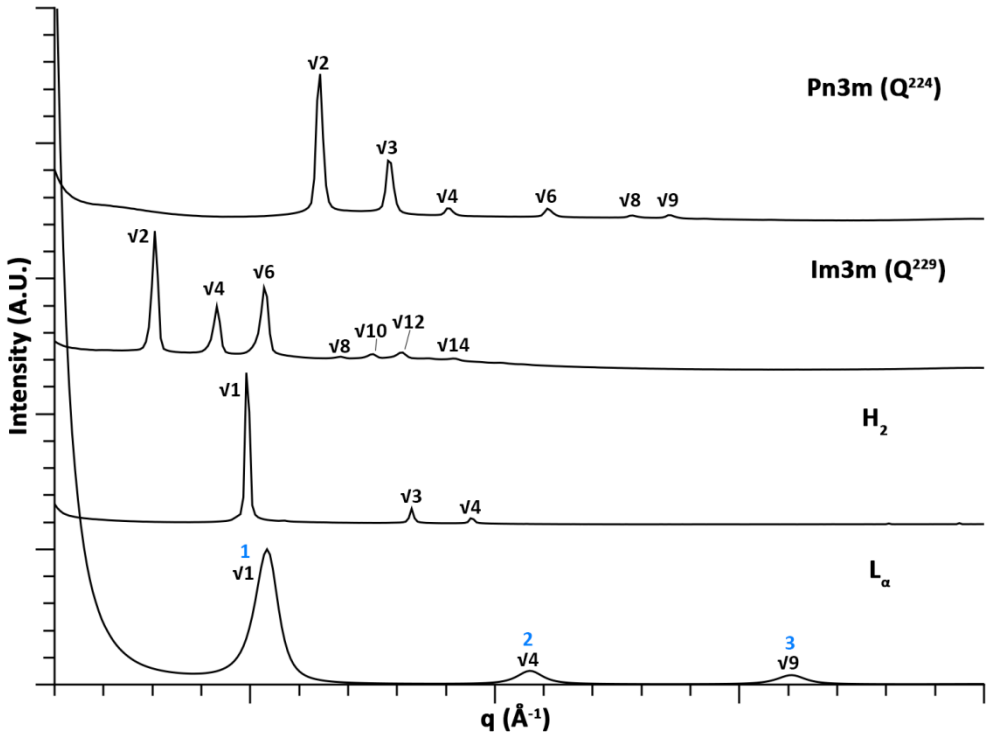

Figure 9.2 Intensity vs. *q* plots for commonly encountered mesophases obtained using SAXS. The number above peaks refer to the Miller indices (h, k, l) used to identify the phase type, space group and lattice dimensions

The peak ratios, or observed reciprocal spacings between allowed (reciprocal) lattice Bragg reflections, refer to the Miller indices (h, k, l) that are used to identify the phase type, space group and lattice dimensions. Of most interest in this context are the bicontinuous cubic phases, inverse hexagonal phase, and inverse micellar geometries, for which the typical scattering patterns are illustrated in Figure 9.1 and 9.2. For cubosome systems, only the bicontinuous cubic phases that exist in equilibrium with excess water are expected to be found, consequently the only patterns likely to be observed correspond to either the primitive *Im3m* space group symmetry or the diamond *Pn3m* space group symmetry.[128] The gyroid (*Ia3d*) geometry would not be expected in dispersed cubosome systems, as it exists at lower water content than the primitive or diamond phase; however, this is not always the case in non-equilibrium situations.[128]

SAXS has been extensively used as the primary characterisation technique to investigate the internal nanostructure of liquid crystalline dispersions.[35, 133, 153-154, 159-160, 162, 169, 177, 209] The use of synchrotron sources for doing SAXS on cubosome systems, especially to follow kinetic processes or for high throughput evaluation of structure has been gaining popularity over conventional laboratory SAXS instruments. This is attributed to the higher intensity of the X-rays produced from synchrotron sources. The higher intensity of X-rays from the synchrotron source allows faster data acquisition over conventional laboratory SAXS instruments.[128]

1.4.2.6 Cryo-Transmission Electron Microscopy (Cryo-TEM)

Cryo-transmission electron microscopy (cryo-TEM) is employed to obtain a direct visualisation of nonlamellar liquid crystalline particles, such as cubosomes, trapped in their native state in an aqueous environment. As nonlamellar liquid crystalline particles can only exist in an aqueous environment, the retention of internal water at equilibrium or excess levels is necessary to ensure the morphology of the nanostructured particle is representative of that in the fully hydrated state. The preservation of the internal nanostructure of the liquid crystalline dispersion can be achieved by vitrifying the nanostructured particles within a thin film of the aqueous sample on a transmission grid, and imaging under frozen conditions and under vacuum. As such, cryo-TEM is frequently used to obtain images of cubosome and hexosome dispersions. These images are often presented in which the square faceting of cubosomes (Figure 10) and hexagonal faceting of hexosomes is apparent.[35, 134, 154, 160, 177, 179, 193, 210-213] In addition to capturing images of nonlamellar liquid crystal particles, cryo-TEM has also been applied to many biological specimens and other self-assembled synthetic materials, such as liposomes.[214-216]

Cubosomes are often found to have co-existing vesicle structures present, frequently seen attached to the corners of the nanostructured particles (Figure 10). These co-existing vehicles have been postulated to stabilise the vertices of the cubic structure. These vesicles are also proposed to possibly be the precursors of cubosomes during the kinetic formation of the particles, which is highly plausible considering that the lamellar phase region must be transversed by the system with increasing hydration to reach the excess water boundary in the equilibrated dispersion.[128, 159] A lower apparent proportion of vesicle structures within liquid crystalline dispersions can be achieved by autoclaving the cubosome.[160]

In addition to the morphological information, further insight on the internal nanostructure of the non-lamellar liquid crystalline nanostructured particles can also be obtained from cryo-TEM imaging, using the Fast Fourier Transform (FFT) of images. The FFT of images can reveal the orientation of the crystallographic planes of the nanostructure, allowing differentiation between different cubic and hexagonal phase structures.[212, 216] The use of a tilt stage also allows visualisation of different planes from a single structure[35, 212], making cryo-TEM both a powerful tool for investigation of morphology and internal structure. However, cryo-TEM is not suitable for studying dynamic changes in particle morphology or structure over time (i.e. on relatively short time frames). It should also be noted that cryo-TEM images do not necessarily provide a true representation of the average appearance of the dispersion being sampled, as only a small fraction of the sample is observed under the TEM stage and is therefore subject to some subjectivity by the microscopist.

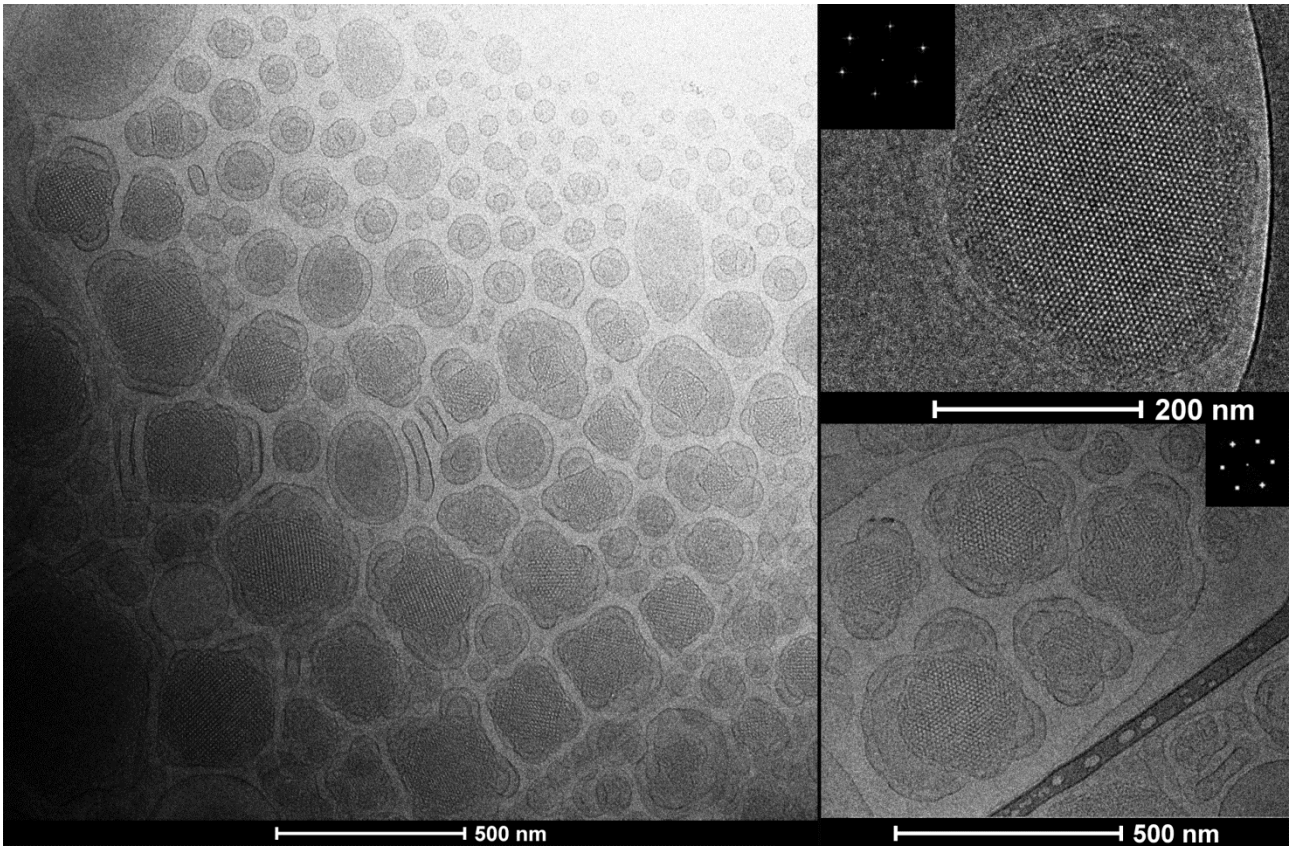

Figure 10 Examples of cryo-TEM images with some reciprocal FFT of cubosome dispersions in water

1.5 Current 'Gaps in knowledge' regarding Steric Stabilisers for Cubosomes

It is clear from the earlier discussion that steric stabilisation is an important issue to be addressed in the cubosome research field, and that there are currently 'gaps' in understanding around this topic as outlined below:

1.5.1 The list of known steric stabilisers is limited

The current list of steric stabilisers for cubosomes is relatively small and limited to a few classes of steric stabilisers. This limits potential progression of these materials into viable products by reducing the available formulation space. Despite the applicability of the possible classes of steric stabilisers for cubosomes, there is an overwhelming reliance and frequency of use with one particular steric stabiliser, Pluronic®F127. Pluronic®F127 is currently the main steric stabiliser for cubosome preparation of drug encapsulated cubosomes for drug delivery applications. This may be in part use to a lack of systematic approach to understanding the structure-performance relationships dictating the colloidal stability for these relatively complex self-assembled particles.

Although Pluronic®F127 is an established and effective steric stabiliser for cubosomes, some issues have been raised regarding its use, both practically and physiochemically. Pluronic®F127 has been said to be a skin or eye irritant and may be hazardous in the case or ingestion or inhalation. Physiochemically, Pluronic®F127 is thought to adsorb onto the particle surface[104] however, this polymer has been shown to

affect the internal structure of GMO based cubosomes, inducing a transition from the parent *Pn3m* to *Im3m* space group.[153-154, 162, 168] In addition, the cubic phase is transformed to a lamellar phase (vesicles) at high Pluronic®F127 concentrations.[168] Thus there is generally a need to identify alternative steric stabilisers, both commercially available and custom synthesised, which in turn requires establishment of structure-property relationships to inform rational selection and design respectively.

1.5.2 The effectiveness of steric stabilisers for cubosomes has not been quantified

The establishment of structure-property relationships requires the screening of structural variables and their impact on performance in terms of colloidal stability. Only one technique has been reported to quantifiably assess the effectiveness of steric stabilisers of nanostructured particles (i.e. hexosomes), which is by using LUMiFuge® as described above. This is a single-sample specialist analysis instrument and is not an effective technique for batch screening of many steric stabilisers. Consequently, the high throughput characterisation of the cubosome dispersion stability as an indicator of the steric stabiliser effectiveness has not yet been conducted. Hence there is a lack of high throughput quantifiable techniques for the assessment of the effectiveness of performance of steric stabilisers for stabilising cubosome dispersions. Consequently, the relative effectiveness of listed/known steric stabilisers compared to the most commonly used Pluronic®F127 is unknown. Hence there is little rational basis for selection of one stabiliser over another.

In order to address this gap in knowledge, techniques for the assessment of steric stabilisation of lipidic dispersions that are easily accessible and applicable for the batch processing of samples need to be developed.

1.5.3 The structural variables such as PEG chain length for providing effective steric hindrance for colloidal stability in cubosome formulations is unknown

The PEG length required to provide effective steric stabilisation for liposomes is 45 PEG units (i.e. PEG molecular weight of 2000).[187-189] Whilst PEG is regarded as the ideal hydrophilic domain for steric stabilisers for lyotropic liquid crystalline nanostructured particles, such as cubosomes, little is actually known regarding the ideal PEG chain length for establishing maximum steric stabilisation and colloidal stability. In addition, there is also a need to determine optimal steric stabiliser concentration. To date, the most commonly used steric stabiliser concentration is 10% w/w with respect to the lipid. The stabiliser concentration can relate to the surface coverage of steric stabilisers, which if too sparse can result in 'gaps' in coverage of the surface, whilst if too high it can also be unfavourable, as this can cause aggregation of excess steric stabiliser in the solution.

Studies into steric stabilisers with systematically varying structural variables will allow for the determination of structure-performance relationships, and which will lead to selection of stabilisers that provide optimal steric stabilisation.

1.5.4 There have not been any functionalisable steric stabilisers reported and therefore active drug targeting for cubosome systems has not been explored

Liposomes have been reported with functional targeting moieties conjugated to the terminal end of PEG, rendering them suitable for active drug targeting application.[217-221] However, current steric stabilisers reported for cubosomes have not been modified with targeting capabilities and as such exploration into active targeting cubosome drug delivery systems is still unknown.

Be that as it may, controlled polymerisation techniques, such as reversible addition-fragmentation chain transfer (RAFT)[222-223], facilitate the possibility of developing functionalised steric stabilisers with antibody or antibody fragment conjugation for active targeting functionalities.

1.6 Project Hypotheses

It is envisaged that investigating the structure-performance relationships of different aspects of steric stabilisation of nonlamellar liquid crystalline nanostructured particles will allow/enhance the development of more effective novel steric stabilisers for these systems. These aspects include different hydrophilic and hydrophobic domain lengths, stabiliser concentration and stabiliser structure design. The overriding hypotheses governing this thesis with these points in mind are:

1. That within the poloxamer™ series, the prevailing assumption that Pluronic®F127 is the most effective stabiliser is false, and that other potentially more effective stabilisers for cubosomes exist for both phytantriol and GMO dispersed systems, which are able to retain the internal structure of the native/parent/bulk phase in both systems.
2. That steric stabilisers for cubosomes that are more effective than poloxamers™ exist in other classes of non-ionic surfactants that can be discovered using high throughput approaches and that the effectiveness of a steric stabiliser for cubosomes does not always indicate the retention of the internal structure of the parent/bulk phase.
3. That the design principles for colloidal stabilisers for cubosomes identified from studying existing non-ionic surfactants can be used to design novel effective custom amphiphilic copolymers. Such designer stabilisers will be as effective as small molecule surfactant-based stabilisers and poloxamers™.

1.7 Project Aims

In order to prove or disprove the hypotheses and address the 'gaps in knowledge' in steric stabilisation of cubosomes, this thesis accomplishes the following specific aims:

i. To develop a high throughput means to quantify colloidal stabiliser effectiveness for cubosomes. This will allow for a more effective screening process than single sample analysis, leading to faster screening of effectiveness of steric stabilisers, and thereby efficient discovery of structure-performance relationships.

ii. To utilise high throughput approaches to identify structure-performance relationships for polymers within known steric stabiliser classes for cubosomes (i.e. poloxamer™/Pluronic® copolymers series) to identify new steric stabilisers for cubosomes within those classes. The impact of the stabiliser on the internal phase structure of the particles and particle morphology will also be determined.

iii. To utilise high throughput approaches to identify structure-performance relationships for non-ionic amphiphilic compounds from other commercially available classes that have potential to be novel steric stabilisers for cubosomes. The impact of the stabiliser on the internal phase structure of the particles and particle morphology will also be determined.

iv. To utilise the design principles determined from the above aims to develop a series of custom steric stabilisers based on a random amphiphilic copolymer structure. The copolymers will be synthesised varying in structural variables (PEG, lipid content), and their impact on colloidal stability and internal structure of cubosomes will be determined.

v. To utilise the design principles from aim iii to selectively synthesise highly controlled structured amphiphilic polymers using RAFT approaches to provide highly effective and potentially functionalisable steric stabilisers for cubosomes.

References

1. Luzzati, V.; Mustacchi, H.; Skoulios, A.; Husson, F. La structure des colloïdes d'association. I. Les phases liquide–cristallines des systèmes amphiphile–eau. *Acta Crystallogr.* **1960,** *13* (8), 660-667.
2. Luzzati, V.; Spegt, P. A. Polymorphism of lipids *Nature* **1967,** *215* (5102), 701-&.
3. Luzzati, V.; Tardieu, A.; Gulikkrz.T; Rivas, E.; Reisshus.F. Structure of cubic phases of lipid-water systems *Nature* **1968,** *220* (5166), 485-&.
4. Tardieu, A.; Luzzati, V. Polymorphism of lipids: A novel cubic phase - A cage-like network of rods with enclosed spherical micelles *Biochim. Biophys. Acta* **1970,** *219* (1), 11-&.
5. Longley, W.; McIntosh, T. J. A bicontinuous tetrahedral structure in a liquid-crystalline lipid *Nature* **1983,** *303* (5918), 612-614.
6. Caffrey, M. Kinetics and mechanism of transitions involving the lamellar, cubic, inverted hexagonal and fluid isotropic phases of hydrated monoacylglycerides monitored by time-resolved x-ray diffraction. *Biochemistry* **1987,** *26* (20), 6349-6363.
7. Mariani, P.; Luzzati, V.; Delacroix, H. Cubic phases of lipid-containing systems: Structure analysis and biological implications. *J. Mol. Biol.* **1988,** *204* (1), 165-189.
8. Maddaford, P. J.; Toprakcioglu, C. Structure of cubic phases in the ternary system didodecyldimethylammonium bromide/water/hydrocarbon. *Langmuir* **1993,** *9* (11), 2868-2878.

9. Diat, O.; Porte, G.; Berret, J.-F. Orientation and twins separation in a micellar cubic crystal under oscillating shear. *Phys. Rev. B* **1996,** *54* (21), 14869-14872.
10. Balmbra, R. R.; Clunie, J. S.; Goodman, J. F. Cubic mesomorphic phases *Nature* **1969,** *222* (5199), 1159-&.
11. Luzzati, V.; Vargas, R.; Gulik, A.; Mariani, P.; Seddon, J. M.; Rivas, E. Lipid polymorphism: a correction. The structure of the cubic phase of extinction symbol Fd--consists of two types of disjointed reverse micelles embedded in a three-dimensional hydrocarbon matrix. *Biochemistry* **1992,** *31* (1), 279-285.
12. Mariani, P.; Rivas, E.; Luzzati, V.; Delacroix, H. Polymorphism of a lipid extract from Pseudomonas fluorescens: structure analysis of a hexagonal phase and of a novel cubic phase of extinction symbol Fd. *Biochemistry* **1990,** *29* (29), 6799-6810.
13. Charvolin, J.; Sadoc, J. F. Periodic-systems of fustrated fluid films and micellar cubic structures in liquid crystals *J. Phys.* **1988,** *49* (3), 521-526.
14. Delacroix, H.; Gulik-Krzywicki, T.; Seddon, J. M. Freeze fracture electron microscopy of lyotropic lipid systems: Quantitative analysis of the inverse micellar cubic phase of space group Fd3m (Q227). *J. Mol. Biol.* **1996,** *258* (1), 88-103.
15. Shearman, G. C.; Tyler, A. I. I.; Brooks, N. J.; Templer, R. H.; Ces, O.; Law, R. V.; Seddon, J. M. A 3-D Hexagonal Inverse Micellar Lyotropic Phase. *J. Am. Chem. Soc.* **2009,** *131* (5), 1678-1679.
16. Schwarz, H. A. *Gesammelte matematische Abhandlung*; Springer-Verlag: Berlin, 1890; Vol. 1.
17. Schoen, A. H. Infinite periodic minimal surfaces without self-intersections. In *NASA Tech, Note, TD-5541*; National Technical Information Service Document N70-29782: Springfield, 1970.
18. Scriven, L. E. Equilibrium bicontinuous structure *Nature* **1976,** *263* (5573), 123-125.
19. Yang, D.; Armitage, B.; Marder, S. R. Cubic liquid-crystalline nanoparticles. *Angew. Chem. Int. Edit.* **2004,** *43* (34), 4402-4409.
20. Enlow, J. D. Mathematical Modelling of Surfactant Liquid Crystal X-ray Diffraction. Doctor of Philosophy, University of Otago 11.12.2002 2001.
21. Israelachvili, J. N.; Mitchell, D. J.; Ninham, B. W. Theory of self-assembly of lipid bilayers and vesicles. *Biochim. Biophys. Acta* **1977,** *470* (2), 185-201.
22. Luzzati, V.; Tardieu, A. Lipid phases - Structure and structural transitions *Annu. Rev. Phys. Chem.* **1974,** *25*, 79-94.
23. Malmsten, M. *Surfactants and polymers in drug delivery* Marcel Dekker: New York, 2002; Vol. 122. p 368.
24. Figueiredo Neto, A. M.; Salinas, S. R. A. *The physics of lyotropic liquid crystals: Phase transitions and structural properties*; Oxford University Press: New York, 2005.
25. Winsor, P. A. Binary and multicomponent solutions of amphiphilic compounds. Solubilization and the formation, structure, and theoretical significance of liquid crystalline solutions. *Chem. Rev.* **1968,** *68* (1), 1-40.
26. Tiddy, G. J. T. Surfactant-water liquid crystal phases. *Phys. Rep.* **1980,** *57* (1), 1-46.
27. Charvolin, J. Crystals of interfaces - The cubic phases of amphiphile water-systems *J. Phys.* **1985,** *46* (C3), 173-190.
28. Fontell, K. Cubic phases in surfactant and surfactant-like lipid systems. *Colloid Polym. Sci.* **1990,** *268* (3), 264-285.
29. Fong, C.; Le, T.; Drummond, C. J. Lyotropic liquid crystal engineering-ordered nanostructured small molecule amphiphile self-assembly materials by design. *Chem. Soc. Rev.* **2012,** *41* (3), 1297-1322.
30. Kaasgaard, T.; Drummond, C. J. Ordered 2-D and 3-D nanostructured amphiphile self-assembly materials stable in excess solvent. *Phys. Chem. Chem. Phys.* **2006,** *8* (43), 4957-4975.
31. Conn, C. E.; Drummond, C. J. Nanostructured bicontinuous cubic lipid self-assembly materials as matrices for protein encapsulation. *Soft Matter* **2013,** *9* (13), 3449-3464.
32. Chang, H.-I.; Yeh, M.-K. Clinical development of liposome-based drugs: Formulation, characterization, and therapeutic efficacy. *Int. J. Nanomed.* **2012,** *7*, 49-60.
33. Zhang, J.-X.; Wang, K.; Mao, Z.-F.; Fan, X.; Jiang, D.-L.; Chen, M.; Cui, L.; Sun, K.; Dang, S.-C. Application of liposomes in drug development - Focus on gastroenterological targets. *Int. J. Nanomed.* **2013,** *8*, 1325-1334.

34. Yaghmur, A.; Glatter, O. Characterization and potential applications of nanostructured aqueous dispersions. *Adv. Colloid Interfac.* **2009,** *147–148* (0), 333-342.
35. Barauskas, J.; Johnsson, M.; Tiberg, F. Self-assembled lipid superstructures: Beyond vesicles and liposomes. *Nano Lett.* **2005,** *5* (8), 1615-1619.
36. Mulet, X.; Kennedy, D. F.; Conn, C. E.; Hawley, A.; Drummond, C. J. High throughput preparation and characterisation of amphiphilic nanostructured nanoparticulate drug delivery vehicles. *Int. J. Pharm.* **2010,** *395* (1-2), 290-297.
37. Fong, W.-K.; Hanley, T. L.; Thierry, B.; Kirby, N.; Waddington, L. J.; Boyd, B. J. Controlling the nanostructure of gold nanorod-lyotropic liquid-crystalline hybrid materials using near-infrared laser irradiation. *Langmuir* **2012,** *28* (40), 14450-14460.
38. Lee, K. W. Y.; Nguyen, T.-H.; Hanley, T.; Boyd, B. J. Nanostructure of liquid crystalline matrix determines in vitro sustained release and in vivo oral absorption kinetics for hydrophilic model drugs. **2009,** *365* (1–2), 190-199.
39. Negrini, R.; Mezzenga, R. Diffusion, Molecular Separation, and Drug Delivery from Lipid Mesophases with Tunable Water Channels. **2012,** *28* (47), 16455-16462.
40. Clogston, J.; Craciun, G.; Hart, D. J.; Caffrey, M. Controlling release from the lipidic cubic phase by selective alkylation. **2005,** *102* (2), 441-461.
41. Clogston, J.; Caffrey, M. Controlling release from the lipidic cubic phase. Amino acids, peptides, proteins and nucleic acids. **2005,** *107* (1), 97-111.
42. Zabara, A.; Mezzenga, R. Modulating the crystal size and morphology of in meso-crystallized lysozyme by precisely controlling the water channel size of the hosting mesophase. **2013,** *9* (4), 1010-1014.
43. Mezzenga, R.; Grigorov, M.; Zhang, Z. D.; Servais, C.; Sagalowicz, L.; Romoscanu, A. I.; Khanna, V.; Meyer, C. Polysaccharide-induced order-to-order transitions in lyotropic liquid crystals. **2005,** *21* (14), 6165-6169.
44. Barauskas, J.; Cervin, C.; Jankunec, M.; Špandyreva, M.; Ribokaitė, K.; Tiberg, F.; Johnsson, M. Interactions of lipid-based liquid crystalline nanoparticles with model and cell membranes. *Int. J. Pharm.* **2010,** *391* (1–2), 284-291.
45. Bode, J. C.; Kuntsche, J.; Funari, S. S.; Bunjes, H. Interaction of dispersed cubic phases with blood components. *Int. J. Pharm.* **2013,** *448* (1), 87-95.
46. Rizwan, S. B.; Dong, Y. D.; Boyd, B. J.; Rades, T.; Hook, S. Characterisation of bicontinuous cubic liquid crystalline systems of phytantriol and water using cryo field emission scanning electron microscopy (cryo FESEM). *Micron* **2007,** *38* (5), 478-485.
47. Rizwan, S. B.; Boyd, B. J.; Rades, T.; Hook, S. Bicontinuous cubic liquid crystals as sustained delivery systems for peptides and proteins. *Expert Opin. Drug Del.* **2010,** *7* (10), 1133-1144.
48. Wyatt, D.; Dorschel, D. Cubic-phase delivery system composed of glyceryl monooleate and water for sustained release of water-soluble drugs. *Pharm. Tech.* **1992,** *16*, 116-30.
49. Larsson, K.; Tiberg, F. Periodic minimal surface structures in bicontinuous lipid–water phases and nanoparticles. *Curr. Opin. Colloid In.* **2005,** *9* (6), 365-369.
50. Mulet, X.; Boyd, B. J.; Drummond, C. J. Advances in drug delivery and medical imaging using colloidal lyotropic liquid crystalline dispersions. *J. Colloid Interf. Sci.* **2013,** *393* (0), 1-20.
51. Liu, G. Z.; Conn, C. E.; Waddington, L. J.; Mudie, S. T.; Drummond, C. J. Colloidal amphiphile self-assembly particles composed of gadolinium oleate and myverol: Evaluation as contrast agents for magnetic resonance imaging. *Langmuir* **2010,** *26* (4), 2383-2391.
52. Muir, B. W.; Acharya, D. P.; Kennedy, D. F.; Mulet, X.; Evans, R. A.; Pereira, S. M.; Wark, K. L.; Boyd, B. J.; Nguyen, T. H.; Hinton, T. M.; Waddington, L. J.; Kirby, N.; Wright, D. K.; Wang, H. X.; Egan, G. E.; Moffat, B. A. Metal-free and MRI visible theranostic lyotropic liquid crystal nitroxide-based nanoparticles. *Biomaterials* **2012,** *33* (9), 2723-2733.
53. Fraser, S. J.; Dawson, R. M.; Waddington, L. J.; Muir, B. W.; Mulet, X.; Hartley, P. G.; Separovic, F.; Polyzos, A. Development of cubosomes as a cell-free biosensing platform. *Aust. J. Chem.* **2011,** *64* (1), 46-53.
54. Amar-Yuli, I.; Libster, D.; Aserin, A.; Garti, N. Solubilization of food bioactives within lyotropic liquid crystalline mesophases. *Curr. Opin. Colloid In.* **2009,** *14* (1), 21-32.

55. Larsson, K. Lyotropic liquid crystals and their dispersions relevant in foods. *Curr. Opin. Colloid In.* **2009,** *14* (1), 16-20.
56. Nadiminti, P. P.; Dong, Y. D.; Sayer, C.; Hay, P.; Rookes, J. E.; Boyd, B. J.; Cahill, D. M. Nanostructured liquid crystalline particles as an alternative delivery vehicle for plant agrochemicals. *ACS Appl. Mater. Interfaces* **2013,** *5* (5), 1818-1826.
57. Kwon, T. K.; Kim, J.-C. Preparation and in vitro skin permeation of cubosomes containing Hinokitiol. *J. Disper. Sci. Technol.* **2010,** *31* (7), 1004-1009.
58. Kwon, T.; Lee, H.; Kim, J.; Shin, W.; Park, S.; Kim, J.-C. In vitro skin permeation of cubosomes containing water soluble extracts of Korean barberry. *Colloid J.* **2010,** *72* (2), 205-210.
59. Seo, S. R.; Kang, G.; Ha, J. W.; Kim, J.-C. In vivo hair growth-promoting efficacies of herbal extracts and their cubosomal suspensions. *J. Ind. Eng. Chem.* **2013,** *19* (4), 1331-1339.
60. Rattanapak, T.; Young, K.; Rades, T.; Hook, S. Comparative study of liposomes, transfersomes, ethosomes and cubosomes for transcutaneous immunisation: characterisation and in vitro skin penetration. *J. Pharm. Pharmacol.* **2012,** *64* (11), 1560-1569.
61. Kwon, T. K.; Hong, S. K.; Kim, J. C. In vitro skin permeation of cubosomes containing triclosan. *J. Ind. Eng. Chem.* **2012,** *18* (1), 563-567.
62. Hong, S. K.; Ma, J. Y.; Kim, J.-C. In vitro skin permeation enhancement of KIOM-MA-128 by monoolein cubosomes. *J. Disper. Sci. Technol.* **2012,** *33* (10), 1503-1508.
63. Thapa, R. K.; Baskaran, R.; Madheswaran, T.; Kim, J. O.; Yong, C. S.; Yoo, B. K. Preparation, characterization, and release study of Tacrolimus-loaded liquid crystalline nanoparticles. *J. Disper. Sci. Technol.* **2013,** *34* (1), 72-77.
64. Esposito, E.; Ravani, L.; Contado, C.; Costenaro, A.; Drechsler, M.; Rossi, D.; Menegatti, E.; Grandini, A.; Cortesi, R. Clotrimazole nanoparticle gel for mucosal administration. *Mater. Sci. Eng. C* **2013,** *33* (1), 411-418.
65. Gan, L.; Han, S.; Shen, J.; Zhu, J.; Zhu, C.; Zhang, X.; Gan, Y. Self-assembled liquid crystalline nanoparticles as a novel ophthalmic delivery system for dexamethasone: Improving preocular retention and ocular bioavailability. *Int. J. Pharm.* **2010,** *396* (1–2), 179-187.
66. Han, S.; Shen, J.-q.; Gan, Y.; Geng, H.-m.; Zhang, X.-x.; Zhu, C.-l.; Gan, L. Novel vehicle based on cubosomes for ophthalmic delivery of flurbiprofen with low irritancy and high bioavailability. *Acta Pharmacol. Sin.* **2010,** *31* (8), 990-998.
67. Chen, Y.; Lu, Y.; Zhong, Y.; Wang, Q.; Wu, W.; Gao, S. Ocular delivery of cyclosporine A based on glyceryl monooleate/poloxamer 407 liquid crystalline nanoparticles: preparation, characterization, in vitro corneal penetration and ocular irritation. *J. Drug Target.* **2012,** *20* (10), 856-863.
68. Gong, X.; Moghaddam, M. J.; Sagnella, S. M.; Conn, C. E.; Mulet, X.; Danon, S. J.; Waddington, L. J.; Drummond, C. J. Nanostructured self-assembly materials from neat and aqueous solutions of C18 lipid pro-drug analogues of Capecitabine-a chemotherapy agent. Focus on nanoparticulate cubosomes (TM) of the oleyl analogue. *Soft Matter* **2011,** *7* (12), 5764-5776.
69. Yang, Z.; Peng, X.; Tan, Y.; Chen, M.; Zhu, X.; Feng, M.; Xu, Y.; Wu, C. Optimization of the preparation process for an oral phytantriol-based Amphotericin B cubosomes. *J. Nanomater.* **2011**.
70. Yang, Z.; Tan, Y.; Chen, M.; Dian, L.; Shan, Z.; Peng, X.; Wu, C. Development of Amphotericin B-loaded cubosomes through the SolEmuls technology for enhancing the oral bioavailability. *AAPS PharmSciTech* **2012,** *13* (4), 1483-1491.
71. Nguyen, T.-H.; Hanley, T.; Porter, C. J. H.; Boyd, B. J. Nanostructured liquid crystalline particles provide long duration sustained-release effect for a poorly water soluble drug after oral administration. *J. Control. Release* **2011,** *153* (2), 180-186.
72. Lai, J.; Lu, Y.; Yin, Z. N.; Hu, F. Q.; Wu, W. Pharmacokinetics and enhanced oral bioavailability in beagle dogs of cyclosporine A encapsulated in glyceryl monooleate/poloxamer 407 cubic nanoparticles. *Int. J. Nanomed.* **2010,** *5*, 13-23.
73. Dian, L.; Yang, Z.; Li, F.; Wang, Z.; Pan, X.; Peng, X.; Huang, X.; Guo, Z.; Quan, G.; Shi, X.; Chen, B.; Li, G.; Wu, C. Cubic phase nanoparticles for sustained release of ibuprofen: formulation, characterization, and enhanced bioavailability study. *Int. J. Nanomed.* **2013,** *8*, 845-854.
74. Chung, H.; Kim, J.; Um, J. Y.; Kwon, I. C.; Jeong, S. Y. Self-assembled "nanocubicle" as a carrier for peroral insulin delivery. *Diabetologia* **2002,** *45* (3), 448-451.

75. Jin, X.; Zhang, Z.-h.; Li, S.-l.; Sun, E.; Tan, X.-b.; Song, J.; Jia, X.-b. A nanostructured liquid crystalline formulation of 20(S)-protopanaxadiol with improved oral absorption. *Fitoterapia* **2013,** *84*, 64-71.
76. Jin, X.; Zhang, Z.-H.; Sun, E.; Tan, X.-B.; Li, S.-L.; Cheng, X.-D.; You, M.; Jia, X.-B. Enhanced oral absorption of 20(S)-protopanaxadiol by self-assembled liquid crystalline nanoparticles containing piperine: in vitro and in vivo studies. *Int. J. Nanomed.* **2013,** *8*, 641-52.
77. Lai, J.; Chen, J.; Lu, Y.; Sun, J.; Hu, F.; Yin, Z.; Wu, W. Glyceryl monooleate/poloxamer 407 cubic nanoparticles as oral drug delivery systems: I. In vitro evaluation and enhanced oral bioavailability of the poorly water-soluble drug Simvastatin. *AAPS PharmSciTech* **2009,** *10* (3), 960-966.
78. Tamayo-Esquivel, D.; Ganem-Quintanar, A.; Martinez, A. L.; Navarrete-Rodriguez, M.; Rodriguez-Romo, S.; Quintanar-Guerrero, D. Evaluation of the enhanced oral effect of omapatrilat-monolein nanoparticles prepared by the emulsification-diffusion method. *J. Nanosci. Nanotechno.* **2006,** *6* (9-10), 3134-3138.
79. Zeng, N.; Gao, X.; Hu, Q.; Song, Q.; Xia, H.; Liu, Z.; Gu, G.; Jiang, M.; Pang, Z.; Chen, H.; Chen, J.; Fang, L. Lipid-based liquid crystalline nanoparticles as oral drug delivery vehicles for poorly water-soluble drugs: cellular interaction and in vivo absorption. *Int. J. Nanomed.* **2012,** *7*, 3703-3718.
80. Hong, S. K.; Ma, J. Y.; Kim, J.-C. Preparation and characterization of cubosomal KIOM-C suspension and investigation on in vitro small intestinal absorption of Baicalin. *J. Disper. Sci. Technol.* **2013,** *34* (2), 252-258.
81. Hong, S. K.; Ma, J. Y.; Kim, J.-C. In vitro small intestinal absorption enhancement of S-164 by monoolein cubic phase nanoparticles. *J. Disper. Sci. Technol.* **2013,** *34* (4), 511-515.
82. Wu, H.; Li, J.; Zhang, Q.; Yan, X.; Guo, L.; Gao, X.; Qiu, M.; Jiang, X.; Lai, R.; Chen, H. A novel small Odorranalectin-bearing cubosomes: Preparation, brain delivery and pharmacodynamic study on amyloid-beta(25-35)-treated rats following intranasal administration. *Eur. J. Pharm. Biopharm.* **2012,** *80* (2), 368-378.
83. Esposito, E.; Cortesi, R.; Drechsler, M.; Paccamiccio, L.; Mariani, P.; Contado, C.; Stellin, E.; Menegatti, E.; Bonina, F.; Puglia, C. Cubosome dispersions as delivery systems for percutaneous administration of indomethacin. *Pharm. Res.* **2005,** *22* (12), 2163-2173.
84. Esposito, E.; Mariani, P.; Ravani, L.; Contado, C.; Volta, M.; Bido, S.; Drechsler, M.; Mazzoni, S.; Menegatti, E.; Morari, M.; Cortesi, R. Nanoparticulate lipid dispersions for bromocriptine delivery: Characterization and in vivo study. *Eur. J. Pharm. Biopharm.* **2012,** *80* (2), 306-314.
85. Rizwan, S. B.; McBurney, W. T.; Young, K.; Hanley, T.; Boyd, B. J.; Rades, T.; Hook, S. Cubosomes containing the adjuvants imiquimod and monophosphoryl lipid A stimulate robust cellular and humoral immune responses. *J. Control. Release* **2013,** *165* (1), 16-21.
86. Gordon, S.; Young, K.; Wilson, R.; Rizwan, S.; Kemp, R.; Rades, T.; Hook, S. Chitosan hydrogels containing liposomes and cubosomes as particulate sustained release vaccine delivery systems. *J. Liposome Res.* **2012,** *22* (3), 193-204.
87. Jain, V.; Swarnakar, N. K.; Mishra, P. R.; Verma, A.; Kaul, A.; Mishra, A. K.; Jain, N. K. Paclitaxel loaded PEGylated gleceryl monooleate based nanoparticulate carriers in chemotherapy. *Biomaterials* **2012,** *33* (29), 7206-7220.
88. Johnsson, M.; Barauskas, J.; Norlin, A.; Tiberg, F. Physicochemical and drug delivery aspects of lipid-based liquid crystalline nanoparticles: A case study of intravenously administered propofol. *J. Nanosci. Nanotechno.* **2006,** *6* (9-10), 3017-3024.
89. Cervin, C.; Vandoolaeghe, P.; Nistor, C.; Tiberg, F.; Johnsson, M. A combined in vitro and in vivo study on the interactions between somatostatin and lipid-based liquid crystalline drug carriers and bilayers. *Eur. J. Pharm. Sci.* **2009,** *36* (4–5), 377-385.
90. Liu, H.; Wang, Y.; Wang, Q.; Li, Z.; Zhou, Y.; Zhang, Y.; Li, S. Protein-bearing cubosomes prepared by liquid precursor dilution: Inner ear delivery and pharmacokinetic study following intratympanic administration. *J. Biomed. Nanotechnol.* **2013,** *9* (10), 1784-1793.
91. Rizwan, S. B.; Assmus, D.; Boehnke, A.; Hanley, T.; Boyd, B. J.; Rades, T.; Hook, S. Preparation of phytantriol cubosomes by solvent precursor dilution for the delivery of protein vaccines. *Eur. J. Pharm. Biopharm.* **2011,** *79* (1), 15-22.
92. Angelov, B.; Angelova, A.; Papahadjopoulos-Sternberg, B.; Hoffmann, S. V.; Nicolas, V.; Lesieur, S. Protein-containing PEGylated cubosomic particles: Freeze-fracture electron microscopy and synchrotron radiation circular dichroism study. *J. Phys. Chem. B* **2012,** *116* (26), 7676-7686.

93. Shen, H.-H.; Lake, V.; Le Brun, A. P.; James, M.; Duff, A. P.; Peng, Y.; McLean, K. M.; Hartley, P. G. Targeted detection of phosphatidylserine in biomimetic membranes and invitro cell systems using annexin V-containing cubosomes. *Biomaterials* **2013,** *34* (33), 8361-9.
94. Esposito, E.; Ravani, L.; Mariani, P.; Contado, C.; Drechsler, M.; Puglia, C.; Cortesi, R. Curcumin containing monoolein aqueous dispersions: A preformulative study. *Mater. Sci. Eng. C* **2013,** *33* (8), 4923-34.
95. Murgia, S.; Bonacchi, S.; Falch, A. M.; Lampis, S.; Lippolis, V.; Meli, V.; Monduzzi, M.; Prodi, L.; Schmidt, J.; Talmon, Y.; Caltagirone, C. Drug-loaded fluorescent cubosomes: Versatile nanoparticles for potential theranostic applications. *Langmuir* **2013,** *29* (22), 6673-6679.
96. Bei, D.; Marszalek, J.; Youan, B. B. C. Formulation of Dacarbazine-loaded cubosomes-Part I: Influence of formulation variables. *AAPS PharmSciTech* **2009,** *10* (3), 1032-1039.
97. Bei, D.; Marszalek, J.; Youan, B. B. C. Formulation of Dacarbazine-loaded cubosomes-Part II: Influence of process parameters. *AAPS PharmSciTech* **2009,** *10* (3), 1040-1047.
98. Bei, D.; Zhang, T.; Murowchick, J. B.; Youan, B. B. C. Formulation of Dacarbazine-loaded cubosomes. Part III. Physicochemical characterization. *AAPS PharmSciTech* **2010,** *11* (3), 1243-1249.
99. Efrat, R.; Kesselman, E.; Aserin, A.; Garti, N.; Danino, D. Solubilization of hydrophobic guest molecules in the monoolein discontinuous Q(L) cubic mesophase and its soft nanoparticles. *Langmuir* **2009,** *25* (3), 1316-1326.
100. Boyd, B. J. Characterisation of drug release from cubosomes using the pressure ultrafiltration method. *Int. J. Pharm.* **2003,** *260* (2), 239-247.
101. Gong, X.; Moghaddam, M. J.; Sagnella, S. M.; Conn, C. E.; Danon, S. J.; Waddington, L. J.; Drummond, C. J. Lyotropic liquid crystalline self-assembly material behavior and nanoparticulate dispersions of a phytanyl pro-drug analogue of Capecitabine-A chemotherapy agent. *ACS Appl. Mater. Interfaces* **2011,** *3* (5), 1552-1561.
102. Mangiapia, G.; Vaccaro, M.; D'Errico, G.; Frielinghaus, H.; Radulescu, A.; Pipich, V.; Carnerup, A. M.; Paduano, L. Cubosomes for ruthenium complex delivery: formulation and characterization. *Soft Matter* **2011,** *7* (22), 10577-10580.
103. Larsson, K. Cubic lipid-water phases - Structures and biomembrane aspects *J. Phys. Chem.* **1989,** *93* (21), 7304-7314.
104. Tilley, A. J.; Drummond, C. J.; Boyd, B. J. Disposition and association of the steric stabilizer Pluronic (R) F127 in lyotropic liquid crystalline nanostructured particle dispersions. *J. Colloid Interf. Sci.* **2013,** *392*, 288-296.
105. Lindell, K.; Engblom, J.; Engström, S.; Jonströmer, M.; Carlsson, A. Influence of a charged phospholipid on the release pattern of timolol maleate from cubic liquid crystalline phases. In *The Colloid Science of Lipids*, Lindman, B.; Ninham, B. W., Eds.; Steinkopff, 1998; Vol. 108, pp 111-118.
106. Nishikawa, K.; Arai, H.; Inoue, K. Scavenger receptor-mediated uptake and metabolism of lipid vesicles containing acidic phospholipids by mouse peritoneal macrophages. *J. Biol. Chem.* **1990,** *265* (9), 5226-5231.
107. Funato, K.; Yoda, R.; Kiwada, H. Contribution of complement system on destabilization of liposomes composed of hydrogenated egg phosphatidylcholine in rat fresh plasma. *BBA - Biomembranes* **1992,** *1103* (2), 198-204.
108. Senior, J. Fate and behavior of liposomes in vivo: a review of controlling factors. *Crit. Rev. Ther. Drug Carrier Syst.* **1987,** *3* (2), 123-193.
109. Chonn, A.; Cullis, P.; Devine, D. The role of surface charge in the activation of the classical and alternative pathways of complement by liposomes. *J. Immunol.* **1991,** *146* (12), 4234-4241.
110. Immordino, M. L.; Dosio, F.; Cattel, L. Stealth liposomes: review of the basic science, rationale, and clinical applications, existing and potential. *Int. J. Nanomed.* **2006,** *1* (3), 297-315.
111. Wattendorf, U.; Merkle, H. P. PEGylation as a tool for the biomedical engineering of surface modified microparticles. *J. Pharm. Sci.* **2008,** *97* (11), 4655-4669.
112. Ostuni, E.; Chapman, R. G.; Holmlin, R. E.; Takayama, S.; Whitesides, G. M. A survey of structure−property relationships of surfaces that resist the adsorption of protein. *Langmuir* **2001,** *17* (18), 5605-5620.
113. Harris, J. M.; Martin, N.; Modi, M. Pegylation. *Clin. Pharmacokinet.* **2001,** *40* (7), 539-551.

114. Harris, J. M.; Chess, R. B. Effect of pegylation on pharmaceuticals. *Nat. Rev. Drug Discov.* **2003,** *2* (3), 214-221.
115. Torchilin, V. P. Immunoliposomes and PEGylated immunoliposomes: Possible use for targeted delivery of imaging agents. *ImmunoMethods* **1994,** *4* (3), 244-258.
116. Klibanov, A. L.; Maruyama, K.; Torchilin, V. P.; Huang, L. Amphipathic polyethyleneglycols effectively prolong the circulation time of liposomes. *FEBS Lett.* **1990,** *268* (1), 235-237.
117. Gref, R.; Luck, M.; Quellec, P.; Marchand, M.; Dellacherie, E.; Harnisch, S.; Blunk, T.; Muller, R. H. 'Stealth' corona-core nanoparticles surface modified by polyethylene glycol (PEG): Influences of the corona (PEG chain length and surface density) and of the core composition on phagocytic uptake and plasma protein adsorption. *Colloid Surface B* **2000,** *18* (3-4), 301-313.
118. Morra, M. On the molecular basis of fouling resistance. *J. Biomat. Sci-Polym. E.* **2000,** *11* (6), 547-569.
119. Jeon, S. I.; Andrade, J. D. Protein-surface interactions in the presence of polyethylene oxide: II. Effect of protein size. *J. Colloid Interf. Sci.* **1991,** *142* (1), 159-166.
120. Jeon, S. I.; Lee, J. H.; Andrade, J. D.; De Gennes, P. G. Protein-surface interactions in the presence of polyethylene oxide: I. Simplified theory. *J. Colloid Interf. Sci.* **1991,** *142* (1), 149-158.
121. Halperin, A. Polymer brushes that resist adsorption of model proteins: Design parameters. *Langmuir* **1999,** *15* (7), 2525-2533.
122. Zhu, B.; Eurell, T.; Gunawan, R.; Leckband, D. Chain-length dependence of the protein and cell resistance of oligo(ethylene glycol)-terminated self-assembled monolayers on gold. *J. Biomed. Mater. Res.* **2001,** *56* (3), 406-416.
123. Prime, K. L.; Whitesides, G. M. Adsorption of proteins onto surfaces containing end-attached oligo(ethylene oxide): a model system using self-assembled monolayers. *J. Am. Chem. Soc.* **1993,** *115* (23), 10714-10721.
124. McPherson, T.; Kidane, A.; Szleifer, I.; Park, K. Prevention of protein adsorption by tethered poly(ethylene oxide) layers: Experiments and single-chain mean-field analysis. *Langmuir* **1998,** *14* (1), 176-186.
125. Malmsten, M.; Emoto, K.; Van Alstine, J. M. Effect of chain density on inhibition of protein adsorption by poly(ethylene glycol) based coatings. *J. Colloid Interf. Sci.* **1998,** *202* (2), 507-517.
126. Kingshott, P.; Thissen, H.; Griesser, H. J. Effects of cloud-point grafting, chain length, and density of PEG layers on competitive adsorption of ocular proteins. *Biomaterials* **2002,** *23* (9), 2043-2056.
127. Pasche, S.; De Paul, S. M.; Vörös, J.; Spencer, N. D.; Textor, M. Poly(l-lysine)-graft-poly(ethylene glycol) Assembled Monolayers on Niobium Oxide Surfaces: A Quantitative Study of the Influence of Polymer Interfacial Architecture on Resistance to Protein Adsorption by ToF-SIMS and in Situ OWLS. *Langmuir* **2003,** *19* (22), 9216-9225.
128. Boyd, B. J.; Dong, Y. D.; Rades, T. Nonlamellar liquid crystalline nanostructured particles: advances in materials and structure determination. *J. Liposome Res.* **2009,** *19* (1), 12-28.
129. Thies, C. Adsorption of styrene/butadiene copolymers and stabilization of silica dispersed in perchloroethylene. *J. Colloid Interf. Sci.* **1976,** *54* (1), 13-21.
130. Heller, W.; Pugh, T. L. "Steric protection" of hydrophobic colloidal particles by adsorption of flexible macromolecules. *J. Chem. Phys.* **1954,** *22* (10), 1778-1778.
131. Lee, J.; Martic, P. A.; Tan, J. S. Protein adsorption on pluronic copolymer-coated polystyrene particles. *J. Colloid Interf. Sci.* **1989,** *131* (1), 252-266.
132. Neff, J. A.; Caldwell, K. D.; Tresco, P. A. A novel method for surface modification to promote cell attachment to hydrophobic substrates. *J. Biomed. Mater. Res.* **1998,** *40* (4), 511-519.
133. Dong, Y.-D.; Larson, I.; Hanley, T.; Boyd, B. J. Bulk and dispersed aqueous phase behavior of phytantriol: Effect of vitamin E acetate and F127 polymer on liquid crystal nanostructure. *Langmuir* **2006,** *22* (23), 9512-9518.
134. Boyd, B. J.; Rizwan, S. B.; Dong, Y.-D.; Hook, S.; Rades, T. Self-assembled geometric liquid-crystalline nanoparticles imaged in three dimensions: Hexosomes are not necessarily flat hexagonal prisms. *Langmuir* **2007,** *23* (25), 12461-12464.
135. Muller, F.; Salonen, A.; Glatter, O. Phase behavior of Phytantriol/water bicontinuous cubic Pn3m cubosomes stabilized by Laponite disc-like particles. *J. Colloid Interf. Sci.* **2010,** *342* (2), 392-398.

136. Zhai, J.; Waddington, L.; Wooster, T. J.; Aguilar, M.-I.; Boyd, B. J. Revisiting β-Casein as a stabilizer for lipid liquid crystalline nanostructured particles. *Langmuir* **2011,** *27* (24), 14757-14766.
137. Kojarunchitt, T.; Hook, S.; Rizwan, S.; Rades, T.; Baldursdottir, S. Development and characterisation of modified poloxamer 407 thermoresponsive depot systems containing cubosomes. *Int. J. Pharm.* **2011,** *408* (1-2), 20-26.
138. Shen, H. H.; Crowston, J. G.; Huber, F.; Saubern, S.; McLean, K. M.; Hartley, P. G. The influence of dipalmitoyl phosphatidylserine on phase behaviour of and cellular response to lyotropic liquid crystalline dispersions. *Biomaterials* **2010,** *31* (36), 9473-9481.
139. Conn, C. E.; Mulet, X.; Moghaddam, M. J.; Darmanin, C.; Waddington, L. J.; Sagnella, S. M.; Kirby, N.; Varghese, J. N.; Drummond, C. J. Enhanced uptake of an integral membrane protein, the Dopamine D2L receptor, by cubic nanostructured lipid nanoparticles doped with Ni(II) chelated EDTA amphiphiles. *Soft Matter* **2011,** *7* (2), 567-578.
140. Shen, H. H.; Hartley, P. G.; James, M.; Nelson, A.; Defendi, H.; McLean, K. M. The interaction of cubosomes with supported phospholipid bilayers using neutron reflectometry and QCM-D. *Soft Matter* **2011,** *7* (18), 8041-8049.
141. Fraser, S. J.; Mulet, X.; Martin, L.; Praporski, S.; Mechler, A.; Hartley, P. G.; Polyzos, A.; Separovic, F. Surface immobilization of bio-functionalized cubosomes: Sensing of proteins by quartz crystal microbalance. *Langmuir* **2012,** *28* (1), 620-627.
142. Uyama, M.; Nakano, M.; Yamashita, J.; Handa, T. Useful modified cellulose polymers as new emulsifiers of cubosomes. *Langmuir* **2009,** *25* (8), 4336-4338.
143. Abraham, T.; Hato, M.; Hirai, M. Glycolipid based cubic nanoparticles: preparation and structural aspects. *Colloid Surface B* **2004,** *35* (2), 107-118.
144. Abraham, T.; Hato, M.; Hirai, M. Polymer-dispersed bicontinuous cubic glycolipid nanoparticles. *Biotechnol. Progr.* **2005,** *21* (1), 255-262.
145. de Campo, L.; Yaghmur, A.; Sagalowicz, L.; Leser, M. E.; Watzke, H.; Glatter, O. Reversible phase transitions in emulsified nanostructured lipid systems. *Langmuir* **2004,** *20* (13), 5254-5261.
146. Yaghmur, A.; de Campo, L.; Salentinig, S.; Sagalowicz, L.; Leser, M. E.; Glatter, O. Oil-loaded monolinolein-based particles with confined inverse discontinuous cubic structure (Fd3m). *Langmuir* **2005,** *22* (2), 517-521.
147. Yaghmur, A.; de Campo, L.; Sagalowicz, L.; Leser, M. E.; Glatter, O. Emulsified microemulsions and oil-containing liquid crystalline phases. *Langmuir* **2004,** *21* (2), 569-577.
148. Salonen, A.; Guillot, S.; Glatter, O. Determination of water content in internally self-assembled monoglyceride-based dispersions from the bulk phase. *Langmuir* **2007,** *23* (18), 9151-9154.
149. Guillot, S.; Moitzi, C.; Salentinig, S.; Sagalowicz, L.; Leser, M. E.; Glatter, O. Direct and indirect thermal transitions from hexosomes to emulsified micro-emulsions in oil-loaded monoglyceride-based particles. *Colloid Surface A* **2006,** *291* (1–3), 78-84.
150. Yaghmur, A.; de Campo, L.; Sagalowicz, L.; Leser, M. E.; Glatter, O. Control of the internal structure of MLO-based isasomes by the addition of diglycerol monooleate and soybean phosphatidylcholine. *Langmuir* **2006,** *22* (24), 9919-9927.
151. Yaghmur, A.; Laggner, P.; Almgren, M.; Rappolt, M. Self-assembly in monoelaidin aqueous dispersions: Direct vesicles to cubosomes transition. *PLoS One* **2008,** *3* (11).
152. Esposito, E.; Eblovi, N.; Rasi, S.; Drechsler, M.; Gregorio, G.; Menegatti, E.; Cortesi, R. Lipid-based supramolecular systems for topical application: A preformulatory study. *AAPS PharmSci* **2003,** *5* (4), 62-76.
153. Gustafsson, J.; LjusbergWahren, H.; Almgren, M.; Larsson, K. Cubic lipid-water phase dispersed into submicron particles. *Langmuir* **1996,** *12* (20), 4611-4613.
154. Gustafsson, J.; Ljusberg-Wahren, H.; Almgren, M.; Larsson, K. Submicron particles of reversed lipid phases in water stabilized by a nonionic amphiphilic polymer. *Langmuir* **1997,** *13* (26), 6964-6971.
155. Larsson, K. Colloidal dispersions of ordered lipid-water phases *J. Disper. Sci. Technol.* **1999,** *20* (1-2), 27-34.
156. Larsson, K. Aqueous dispersions of cubic lipid–water phases. *Curr. Opin. Colloid In.* **2000,** *5* (1–2), 64-69.
157. Larsson, K. Bicontinuous cubic lipid-water particles and cubosomal dispersions. In *Studies in Surface Science and Catalysis*, Osamu, T., Ed.; Elsevier, 2004; Vol. Volume 148, pp 41-51.

158. Neto, C.; Aloisi, G.; Baglioni, P.; Larsson, K. Imaging soft matter with the atomic force microscope: Cubosomes and Hexosomes. *J. Phys. Chem. B* **1999,** *103* (19), 3896-3899.
159. Spicer, P. T.; Hayden, K. L.; Lynch, M. L.; Ofori-Boateng, A.; Burns, J. L. Novel process for producing cubic liquid crystalline nanoparticles (Cubosomes). *Langmuir* **2001,** *17* (19), 5748-5756.
160. Barauskas, J.; Johnsson, M.; Johnson, F.; Tiberg, F. Cubic phase nanoparticles (Cubosome): Principles for controlling size, structure, and stability. *Langmuir* **2005,** *21* (6), 2569-2577.
161. Monduzzi, M.; Ljusberg-Wahren, H.; Larsson, K. A 13C NMR study of aqueous dispersions of reversed lipid phases. *Langmuir* **2000,** *16* (19), 7355-7358.
162. Nakano, M.; Sugita, A.; Matsuoka, H.; Handa, T. Small-angle X-ray scattering and 13C NMR investigation on the internal structure of "Cubosomes". *Langmuir* **2001,** *17* (13), 3917-3922.
163. Svensson, O.; Thuresson, K.; Arnebrant, T. Interactions between chitosan-modified particles and mucin-coated surfaces. *J. Colloid Interf. Sci.* **2008,** *325* (2), 346-350.
164. Svensson, O.; Thuresson, K.; Arnebrant, T. Interactions between drug delivery particles and mucin in solution and at interfaces. *Langmuir* **2008,** *24* (6), 2573-2579.
165. Vandoolaeghe, P.; Rennie, A. R.; Campbell, R. A.; Thomas, R. K.; Hook, F.; Fragneto, G.; Tiberg, F.; Nylander, T. Adsorption of cubic liquid crystalline nanoparticles on model membranes. *Soft Matter* **2008,** *4* (11), 2267-2277.
166. Vandoolaeghe, P.; Rennie, A. R.; Campbell, R. A.; Nylander, T. Neutron reflectivity studies of the interaction of cubic-phase nanoparticles with phospholipid bilayers of different coverage. *Langmuir* **2009,** *25* (7), 4009-4020.
167. Vandoolaeghe, P.; Campbell, R. A.; Rennie, A. R.; Nylander, T. Adsorption of intact cubic liquid crystalline nanoparticles on hydrophilic surfaces: Lateral organization, interfacial stability, layer structure, and interaction mechanism. *J. Phys. Chem. C* **2009,** *113* (11), 4483-4494.
168. Landh, T. Phase-behavior in the system pine oil monoglycerides-poloxamer-407-water at 20-degrees-C *J. Phys. Chem.* **1994,** *98* (34), 8453-8467.
169. Siekmann, B.; Bunjes, H.; Koch, M. M. H.; Westesen, K. Preparation and structural investigations of colloidal dispersions prepared from cubic monoglyceride-water phases. *Int. J. Pharm.* **2002,** *244* (1-2), 33-43.
170. Nakano, M.; Teshigawara, T.; Sugita, A.; Leesajakul, W.; Taniguchi, A.; Kamo, T.; Matsuoka, H.; Handa, T. Dispersions of liquid crystalline phases of the monoolein/oleic acid/Pluronic F127 system. *Langmuir* **2002,** *18* (24), 9283-9288.
171. Popescu, G.; Barauskas, J.; Nylander, T.; Tiberg, F. Liquid crystalline phases and their dispersions in aqueous mixtures of glycerol monooleate and glyceryl monooleyl ether. *Langmuir* **2006,** *23* (2), 496-503.
172. Salonen, A.; Muller, F.; Glatter, O. Dispersions of internally liquid crystalline systems stabilized by charged disklike particles as pickering emulsions: Basic properties and time-resolved behavior. *Langmuir* **2008,** *24* (10), 5306-5314.
173. Muller, F.; Salonen, A.; Glatter, O. Monoglyceride-based cubosomes stabilized by Laponite: Separating the effects of stabilizer, pH and temperature. *Colloid Surface A* **2010,** *358* (1-3), 50-56.
174. Salonen, A.; Moitzi, C.; Salentinig, S.; Glatter, O. Material transfer in cubosome-emulsion mixtures: Effect of alkane chain length. *Langmuir* **2010,** *26* (13), 10670-10676.
175. Koynova, R.; Tenchov, B.; Rapp, G. Effect of PEG-lipid conjugates on the phase behavior of phosphatidylethanolamine dispersions. *Colloid Surface A* **1999,** *149* (1–3), 571-575.
176. Koynova, R.; Tenchov, B.; Rapp, G. Low amounts of PEG-lipid induce cubic phase in phosphatidylethanolamine dispersions. *BBA-Biomembranes* **1997,** *1326* (2), 167-170.
177. Johnsson, M.; Barauskas, J.; Tiberg, F. Cubic phases and cubic phase dispersions in a phospholipid-based system. *J. Am. Chem. Soc.* **2005,** *127* (4), 1076-1077.
178. Johnsson, M.; Edwards, K. Phase behavior and aggregate structure in mixtures of dioleoylphosphatidylethanolamine and poly(ethylene glycol)-lipids. *Biophys. J.* **2001,** *80* (1), 313-323.
179. Rangelov, S.; Almgren, M. Particulate and bulk bicontinuous cubic phases obtained from mixtures of glyceryl monooleate and copolymers bearing blocks of lipid-mimetic anchors in water. *J. Phys. Chem. B* **2005,** *109* (9), 3921-3929.

180. Angelov, B.; Angelova, A.; Garamus, V. M.; Drechsler, M.; Willumeit, R.; Mutafchieva, R.; Stepanek, P.; Lesieur, S. Earliest stage of the tetrahedral nanochannel formation in cubosome particles from unilamellar nanovesicles. *Langmuir* **2012,** *28* (48), 16647-16655.
181. Zeng, N.; Hu, Q.; Liu, Z.; Gao, X.; Hu, R.; Song, Q.; Gu, G.; Xia, H.; Yao, L.; Pang, Z.; Jiang, X.; Chen, J.; Fang, L. Preparation and characterization of paclitaxel-loaded DSPE-PEG-liquid crystalline nanoparticles (LCNPs) for improved bioavailability. *Int. J. Pharm.* **2012,** *424* (1–2), 58-66.
182. Almgren, M.; Rangelov, S. Polymorph dispersed particles from the bicontinuous cubic phase of glycerol monooleate stabilized by PEG-copolymers with lipid-mimetic hydrophobic anchors. *J. Disper. Sci. Technol.* **2006,** *27* (5), 599-609.
183. Gustafsson, J.; Nylander, T.; Almgren, M.; Ljusberg-Wahren, H. Phase behavior and aggregate structure in aqueous mixtures of sodium cholate and glycerol monooleate. *J. Colloid Interf. Sci.* **1999,** *211* (2), 326-335.
184. Spicer, P. T.; Small, W. B.; Lynch, M. L.; Burns, J. L. Dry powder precursors of cubic liquid crystalline nanoparticles (Cubosomes). *J. Nanopart. Res.* **2002,** *4* (4), 297-311.
185. Salonen, A.; Muller, F. o.; Glatter, O. Internally self-assembled submicrometer emulsions stabilized by spherical nanocolloids: Finding the free nanoparticles in the aqueous continuous phase. *Langmuir* **2010,** *26* (11), 7981-7987.
186. Alexandridis, P. Amphiphilic copolymers and their applications. *Curr. Opin. Colloid In.* **1996,** *1* (4), 490-501.
187. Mori, A.; Klibanov, A. L.; Torchilin, V. P.; Huang, L. Influence of the steric barrier activity of amphipathic poly(ethyleneglycol) and ganglioside GM1 on the circulation time of liposomes and on the target binding of immunoliposomes in vivo. **1991,** *284* (2), 263-266.
188. Martina, M.-S.; Nicolas, V.; Wilhelm, C.; Ménager, C.; Barratt, G.; Lesieur, S. The in vitro kinetics of the interactions between PEG-ylated magnetic-fluid-loaded liposomes and macrophages. **2007,** *28* (28), 4143-4153.
189. Martina, M.-S.; Wilhelm, C.; Lesieur, S. The effect of magnetic targeting on the uptake of magnetic-fluid-loaded liposomes by human prostatic adenocarcinoma cells. **2008,** *29* (30), 4137-4145.
190. Patton, J.; Carey, M. Watching fat digestion. *Science* **1979,** *204* (4389), 145-148.
191. Lindström, M.; Ljusberg-Wahren, H.; Larsson, K.; Borgström, B. Aqueous lipid phases of relevance to intestinal fat digestion and absorption. *Lipids* **1981,** *16* (10), 749-754.
192. Buchheim, W.; Larsson, K. Cubic lipid-protein-water phases. *J. Colloid Interf. Sci.* **1987,** *117* (2), 582-583.
193. Almgren, M.; Borne, J.; Feitosa, E.; Khan, A.; Lindman, B. Dispersed lipid liquid crystalline phases stabilized by a hydrophobically modified cellulose. *Langmuir* **2007,** *23* (5), 2768-2777.
194. Luo, Y.; Zhu, J.; Ma, Y.; Zhang, H. Dry coating, a novel coating technology for solid pharmaceutical dosage forms. *Int. J. Pharm.* **2008,** *358* (1–2), 16-22.
195. Kablitz, C. D.; Kappl, M.; Urbanetz, N. A. Parameters influencing polymer particle layering of the dry coating process. *Eur. J. Pharm. Biopharm.* **2008,** *69* (2), 760-768.
196. Konno, H.; Handa, T.; Alonzo, D. E.; Taylor, L. S. Effect of polymer type on the dissolution profile of amorphous solid dispersions containing felodipine. *Eur. J. Pharm. Biopharm.* **2008,** *70* (2), 493-499.
197. Guo, C.; Wang, J.; Cao, F.; Lee, R. J.; Zhai, G. Lyotropic liquid crystal systems in drug delivery. *Drug Discov. Today* **2010,** *15* (23–24), 1032-1040.
198. LjusbergWahern, H.; Nyberg, L.; Larsson, K. Dispersion of the cubic liquid crystalline phase - Structure preparation and functionality aspects. *Chim. Oggi.* **1996,** *14* (6), 40-43.
199. Shah, M. H.; Biradar, S. V.; Paradkar, A. R. Spray dried glyceryl monooleate–magnesium trisilicate dry powder as cubic phase precursor. *Int. J. Pharm.* **2006,** *323* (1–2), 18-26.
200. Libster, D.; Aserin, A.; Yariv, D.; Shoham, G.; Garti, N. Soft matter dispersions with ordered inner structures, stabilized by ethoxylated phytosterols. *Colloid Surface B* **2009,** *74* (1), 202-215.
201. Amar-Yuli, I.; Wachtel, E.; Shoshan, E. B.; Danino, D.; Aserin, A.; Garti, N. Hexosome and hexagonal phases mediated by hydration and polymeric stabilizer. *Langmuir* **2007,** *23* (7), 3637-3645.
202. Pecora, R. Dynamic light scattering measurement of nanometer particles in liquids. *J. Nanopart. Res.* **2000,** *2* (2), 123-131.
203. Wiese, H.; Horn, D. Single mode fibers in fiber optic quasielastic light scattering: A study of the dynamics of concentrated latex dispersions. *J. Chem. Phys.* **1991,** *94* (10), 6429-6443.

204. Wallace, S. J.; Li, J.; Nation, R. L.; Prankerd, R. J.; Velkov, T.; Boyd, B. J. Self-assembly behavior of colistin and its prodrug Colistin methanesulfonate: Implications for solution stability and solubilization. *J. Phys. Chem. B* **2010,** *114* (14), 4836-4840.
205. Laughlin, R. G.; Munyon, R. L. Diffusive interfacial transport: a new approach to phase studies. *J. Phys. Chem.* **1987,** *91* (12), 3299-3305.
206. Rosevear, F. B. The microscopy of the liquid crystalline neat and middle phases of soap and synthetic detergents *J. Am. Oil Chem. Soc.* **1954,** *31* (12), 628-639.
207. Rosevear, F. B. Liquid crystals - Mesomorphic phases of surfactant compositions. *J. Soc. Cosmet. Chem.* **1968,** *19* (9), 581-&.
208. Hyde, S. T. Identification of lyotropic liquid crystalline mesophases. In *Handbook of Applied Science and Colloid Chemistry* Holmberg, K., Ed.; John Wiley & Sons Ltd.: New York, 2001, pp 299-332.
209. Angelov, B.; Angelova, A.; Garamus, V. M.; Lebas, G.; Lesieur, S.; Ollivon, M.; Funari, S. S.; Willumeit, R.; Couvreur, P. Small-angle neutron and x-ray scattering from amphiphilic stimuli-responsive diamond-type bicontinuous cubic phase. *J. Am. Chem. Soc.* **2007,** *129* (44), 13474-13479.
210. Fong, C.; Krodkiewska, I.; Wells, D.; Boyd, B. J.; Booth, J.; Bhargava, S.; McDowall, A.; Hartley, P. G. Submicron dispersions of hexosomes based on novel glycerate surfactants. *Aust. J. Chem.* **2005,** *58* (9), 683-687.
211. Boyd, B. J.; Whittaker, D. V.; Khoo, S.-M.; Davey, G. Hexosomes formed from glycerate surfactants - Formulation as a colloidal carrier for irinotecan. *Int. J. Pharm.* **2006,** *318* (1-2), 154-162.
212. Sagalowicz, L.; Michel, M.; Adrian, M.; Frossard, P.; Rouvet, M.; Watzke, H. J.; Yaghmur, A.; De Campo, L.; Glatter, O.; Leser, M. E. Crystallography of dispersed liquid crystalline phases studded by cryo-transmission on electron microscopy. *J. Microsc-Oxford* **2006,** *221*, 110-121.
213. Amar-Yuli, D.; Garti, N. Transitions induced by solubilized fat into reverse hexagonal mesophases. *Colloid Surface B* **2005,** *43* (2), 72-82.
214. Almgren, M.; Edwards, K.; Karlsson, G. Cryo transmission electron microscopy of liposomes and related structures. *Colloid Surface A* **2000,** *174* (1-2), 3-21.
215. Borné, J.; Nylander, T.; Khan, A. Vesicle formation and other structures in aqueous dispersions of monoolein and sodium oleate. *J. Colloid Interf. Sci.* **2003,** *257* (2), 310-320.
216. Spicer, P. T. Progress in liquid crystalline dispersions: Cubosomes. *Curr. Opin. Colloid In.* **2005,** *10* (5-6), 274-279.
217. Ishida, O.; Maruyama, K.; Tanahashi, H.; Iwatsuru, M.; Sasaki, K.; Eriguchi, M.; Yanagie, H. Liposomes Bearing Polyethyleneglycol-Coupled Transferrin with Intracellular Targeting Property to the Solid Tumors In Vivo. *Pharm. Res.* **2001,** *18* (7), 1042-1048.
218. Maruyama, K.; Ishida, O.; Takizawa, T.; Moribe, K. Possibility of active targeting to tumor tissues with liposomes. **1999,** *40* (1–2), 89-102.
219. Mastrobattista, E.; Koning, G. A.; Storm, G. Immunoliposomes for the targeted delivery of antitumor drugs. *Adv. Drug Deliver. Rev.* **1999,** *40* (1–2), 103-127.
220. Park, J. W.; Kirpotin, D. B.; Hong, K.; Shalaby, R.; Shao, Y.; Nielsen, U. B.; Marks, J. D.; Papahadjopoulos, D.; Benz, C. C. Tumor targeting using anti-her2 immunoliposomes. *J. Control. Release* **2001,** *74* (1–3), 95-113.
221. Byrne, J. D.; Betancourt, T.; Brannon-Peppas, L. Active targeting schemes for nanoparticle systems in cancer therapeutics. *Adv. Drug Deliver. Rev.* **2008,** *60* (15), 1615-1626.
222. Moad, G.; Rizzardo, E.; Thang, S. H. Radical addition–fragmentation chemistry in polymer synthesis. *Polymer* **2008,** *49* (5), 1079-1131.
223. Keddie, D. J. A guide to the synthesis of block copolymers using reversible-addition fragmentation chain transfer (RAFT) polymerization. *Chem. Soc. Rev.* **2014,** *43* (2), 496-505.

Chapter 2

Steric Stabilisation of Self-Assembled Cubic Lyotropic Liquid Crystalline Nanoparticles: High Throughput Evaluation of Triblock Polyethylene oxide-Polypropylene oxide-Polyethylene oxide Copolymers

Josephine Y.T. Chong, Xavier Mulet, Lynne Waddington, Ben J. Boyd and Calum J. Drummond

Published: *Soft Matter* **2011**, 7, 4768-4777

Declaration for Chapter 2

Declaration by candidate

In the case of Chapter 2, the nature and extent of my contribution to the work was the following:

Nature of contribution	Extent of contribution (%)
Research design, performance of data collection and analysis, manuscript preparation	80

The following co-authors contributed to the work:

Name	Nature of contribution
Xavier Mulet	Supervision; intellectual input; input into manuscript preparation
Lynne Waddington	Intellectual input on cryo-TEM operation and analysis
Ben Boyd	Supervision; intellectual input; input into manuscript preparation
Calum Drummond	Supervision; intellectual input; input into manuscript preparation

Candidate's signature: [redacted] **Date:** **10.7.2014**

Declaration by co-authors

The undersigned hereby certify that:

(1) the above declaration correctly reflects the nature and extent of the candidate's contribution to this work, and the nature of the contribution of each of the co-authors.
(2) they meet the criteria for authorship in that they have participated in the conception, execution, or interpretation, of at least that part of the publication in their field of expertise;
(3) they take public responsibility for their part of the publication, except for the responsible author who accepts overall responsibility for the publication;
(4) there are no other authors of the publication according to these criteria;
(5) potential conflicts of interest have been disclosed to (a) granting bodies, (b) the editor or publisher of journals or other publications, and (c) the head of the responsible academic unit; and
(6) the original data are stored at the following location(s) and will be held for at least five years from the date indicated below:

Location of data storage: CSIRO Materials Science and Engineering, Ian Wark Laboratory, Bayview Avenue, Clayton 3168, Australia.

Co-authors' signature for Chapter 2:

Signed:  **Date:** **10.1.2014**

Xavier Mulet

Signed:  **Date:** **8.1.2014**

Lynne J. Waddington

Signed:  **Date:** **28.2.2014**

Ben J. Boyd

Signed:  **Date:** **12.4.2014**

Calum J. Drummond

Soft Matter

Cite this: *Soft Matter*, 2011, **7**, 4768

www.rsc.org/softmatter

PAPER

Steric stabilisation of self-assembled cubic lyotropic liquid crystalline nanoparticles: high throughput evaluation of triblock polyethylene oxide-polypropylene oxide-polyethylene oxide copolymers†

Josephine Y. T. Chong,[ab] Xavier Mulet,[ab] Lynne J. Waddington,[c] Ben J. Boyd*[b] and Calum J. Drummond*[a]

Received 2nd February 2011, Accepted 24th March 2011
DOI: 10.1039/c1sm05181d

Nanostructured cubic lyotropic liquid crystalline colloidal particles (Cubosomes™) are of interest for applications such as drug and biomedical imaging agent encapsulation systems. Maintaining the stability and integrity of these nanoparticles over time is essential for their storage and application. It is well known that the triblock polyethylene oxide-polypropylene oxide-polyethylene oxide (PEO-PPO-PEO) copolymer, Pluronic F127, imparts a steric barrier to aggregation of non-lamellar lyotropic liquid crystalline particles. However, few other stabilisers have been reported for these systems. Using high throughput methodologies to prepare and characterise dispersions of monoolein and phytantriol, the performance of a wide range of triblock PEO-PPO-PEO copolymers (Pluronics) was evaluated for optimal stabilisation of cubosomes. It is shown that Pluronic F108 is superior to Pluronic F127 as a stabiliser of monoolein based nanostructured particles, as it preserves the integrity of the double diamond inverse bicontinuous cubic phase internal structure of the particles, whilst maintaining colloidal stability.

Introduction

Cubosomes,‡ inverse bicontinuous cubic phase lyotropic liquid crystalline dispersions, have been garnering increasing attention due to their potential applications in nanomedicine.[1–3] Cubosomes have an internal ordered structure consisting of lipid bilayers and water channels, and are typically 100–200 nm in diameter, offering a large internal and external surface area. They differ from liposomes in that the internal region of the particle contains a high proportion of lipid, and a complex structure that provides for controlled release through diffusion. Their ability to be dispersed and stabilised as sub-micron nanostructured particles, and consequent suitability for intravenous administration, is key to their potential utility in drug delivery and as carriers for medical imaging agents.[4–10]

Cubosomes are commonly prepared using amphiphilic lipids that form bulk cubic phases.[11] The most commonly employed lipids are glyceride-based monoolein (GMO) (Fig. 1a), and phytantriol (3,7,11,15-tetramethylhexadecane-1,2,3-triol) (Fig. 1b), with recent efforts to identify new lipids capable of forming non-lamellar mesophases yielding entirely new classes of lipids.[10,12–17] These lipids are typically uncharged and their headgroup structure does not impart steric stabilisation to the cubosomes once formed in solution. Hence they will rapidly flocculate and phase separate as the bulk cubic phase in excess

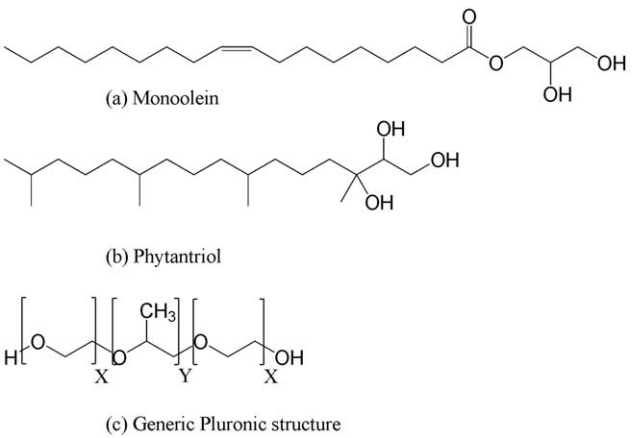

(a) Monoolein

(b) Phytantriol

(c) Generic Pluronic structure

Fig. 1 Chemical structures of (a) Monoolein, (b) Phytantriol and (c) the Pluronic stabiliser series.

[a]*CSIRO Materials Science and Engineering, Private Bag 10, Clayton, VIC 3169, Australia.* [redacted]

[b]*Drug Delivery, Disposition and Dynamics, Monash Institute of Pharmaceutical Sciences, Monash University, 381 Royal Parade, Parkville, VIC 3052, Australia.* [redacted]

[c]*CSIRO Materials Science and Engineering, 343 Royal Parade, Parkville, VIC 3052, Australia*

† Electronic supplementary information (ESI) available: Supplementary data set 1. See DOI: 10.1039/c1sm05181d

‡ Cubosome is a USPTO registered trademark of GS Development AB Corporation Sweden; Pluronic is a USPTO registered trademark with BASF corporation.

water shortly after dispersion. Consequently, to form stable cubosome dispersions the lipids must be dispersed in excess water in the presence of a stabiliser. Non-ionic block copolymers have been generally employed for this purpose.[2,7,18–20]

The most important criteria in selecting a stabiliser for cubosomes are (i) an ability to contribute to the formation of particles in the submicron size range with low size polydispersity; (ii) an effectiveness at low concentration of stabiliser; (iii) a long shelf-life over which the cubosomes are stabilised; and (iv) a limited effect on the internal structural integrity of the lyotropic liquid crystalline phase.

To date, only a few stabilisers have been used without altering the mesophase of the nanoparticles.[7,19,21–26] This is in part due to a lack of understanding of the fundamental nature of the interaction of the stabiliser with cubosome particles, and hence limited rational basis upon which to select the optimal structure of a stabiliser that provides both stabilisation and preservation of internal structure.

Pluronics (Fig. 1c) are a commercial group of triblock polyethylene oxide - polypropylene oxide - polyethylene oxide copolymers (PEO-PPO-PEO).[27] Despite the fact that the best known liquid crystal stabiliser is Pluronic F127,[7] in general the Pluronics have not been well explored for stabilisation properties for lyotropic liquid crystal particles. The fundamental drawback of Pluronic F127 is that the stabiliser concentration needs to be high, sometimes up to 1 wt. % of the total sample mass, to properly disperse non-lamellar crystalline particles. In addition, dispersion of bulk monoolein using Pluronic F127 can change the cubic phase symmetry of the self-assembled nanoparticle from Pn3m (double diamond) to Im3m (primitive) (Fig. 2), which is indicative of disruption and destabilisation of the internal liquid crystalline structure.[7]

Pluronics or poloxamers tend to be the most popular class of steric stabilisers available in the market for lyotropic liquid crystalline particles. Pluronic F127 is just one of the many Pluronics available. The difference between these Pluronic types is the varying number and ratios of ethylene oxide (EO) and propylene oxide (PO) units (Fig. 3 and Table 1). F127 specifically has an average molecular weight of 12600, with an average of 100 units of ethylene oxide and 67 units of propylene oxide. Preliminary studies have found limitations using Pluronic F127 as a lyotropic liquid crystal stabiliser, such as reduced polymer-particle association/affinity, resulting in more free F127 in solution than on the cubosome.[28] There are at least 30 other Pluronics marketed by the BASF corporation, with molecular weights ranging from 1100 (*i.e.* Pluronic L31) to 14600 (*i.e.* Pluronic F108) and sequentially varying EO and PO units.

Here we investigate twenty Pluronic tri-block copolymers as steric stabilisers for cubosomes. For brevity, the Pluronics are indicated in text using their BASF-assigned identifying code, for example F127 refers to Pluronic F127. We relate how the hydrophobic and hydrophilic components of the non-ionic molecules stabilise and preserve the integrity of lyotropic liquid crystalline particles, such as cubosomes, with a view to establishing the structure-property relationships in these classes of stabilisers.

The preparation of cubosomes was performed using recently developed techniques allowing for the screening and evaluation of the performance of various potential stabilisers.[29] Cubosomes were prepared from both phytantriol and monoolein to evaluate trends across different lipids. The specific Pluronic tri-block copolymers studied are indicated in Table 1 and Fig. 3. Characterisation of the internal structure of the dispersed

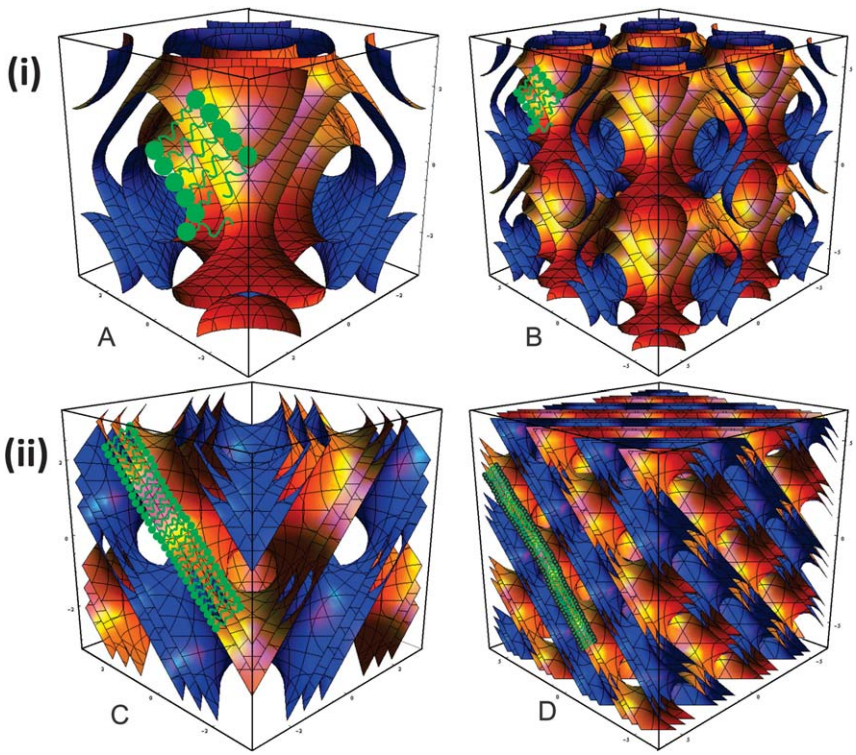

Fig. 2 Unit cell structure of (i) Im3m (A,B) and (ii) Pn3m (C,D) cubic phases. Figures were generated with Mathematica V7.

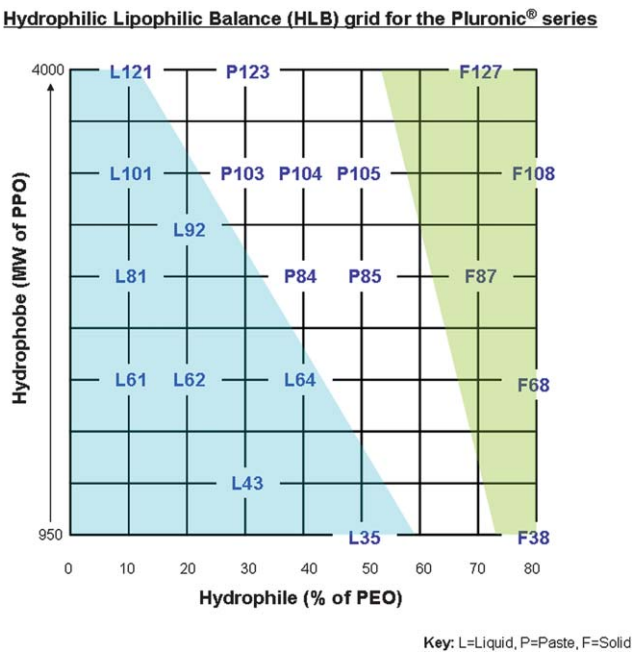

Fig. 3 HLB Grid of Pluronic series stabilisers used in study (adapted from BASF's Pluronic Grid[43]).

nanoparticles was undertaken using synchrotron small angle X-ray scattering (SAXS), necessary in light of their inherently low concentration and subsequently weak scattering. Further confirmation of the lyotropic liquid crystalline cubic structure was performed using cryo-TEM.

Materials

The amphiphiles used for cubosome formation were phytantriol (DSM Nutritional Products, NSW) and monoolein (1-oleoyl-rac-glycerol, Sigma Aldrich, NSW) (Fig. 1). These were dispersed by using poloxamers (Pluronic BASF Corp series: F127, P123, L121, P105, P104, P103, L101, L92, F87 NF, P85, L81, F68, L64, L62, L61, L53, F38 Pastille, L35 and F108 (kindly provided by Prof. Joe McGuire, Oregon State University, US)).

Methods

Preparation of nanostructured particles

Cubosomes were prepared in a 96-deep square well collection plate (Supelco®,USA) using an automated synthesis platform, Chemspeed Accelerator TM SLT2 (Chemspeed, Switzerland) as described by Mulet *et al.*[29] Briefly, 50 mg of lipid (to provide 100 mg mL^{-1} of dispersion) was dispensed per sample well, and 500 μl of a specific concentration (0.1, 0.5, 1.0 and 2.0 wt. %) of stabiliser in Milli Q water added. As the amount of high purity monoolein available was limited for this study samples containing Pluronic at 2.0 wt. % were only studied for phytantriol. Each sample was probe sonicated at an amplitude of five for five min total time at 1 Hz on/off cycle to prevent overheating.

Visual assessment of phase separation

The initial stability of dispersions was assessed visually through observation of the samples in the sample wells after sonication. A well dispersed sample contained no visible aggregates, and possessed a milky white consistency. In contrast, poorly dispersed samples were largely transparent systems with visible aggregates of lipid typically around the rim of the sample well. The visual assessment was used as an initial screen to rapidly exclude very poor dispersions from further study; the dispersions were graded using a scale where +++ indicates a homogeneous milky dispersion, ++ indicates cloudy dispersion with some aggregation apparent, + indicates a translucent dispersion where

Table 1 Structural and physicochemical data for Pluronic series stabilisers,[43] *F127 was used as positive control in these studies

Pluronic® Series Details								
Pluronic®	MW	Units of PO (Y)	Units of EO (X)	EO (%)	HLB	Cloud Point 1% Aqueous	Cloud Point 10% Aqueous	Schematic representation of PO/EO ratio
F108	14600	50	132	80	>24	>100	>100	
F68	8400	29	76	80	>24	>100	>100	
F38 Pastille	4700	16	43	80	>24	>100	>100	
F127*	12600	65	100	70	18–23	>100	>100	
F87NF	7700	40	61	70	>24	>100	>100	
P105	6500	56	37	50	12–18	91	92–96	
P85	4600	40	26	50	12–18	85	83–89	
L35	1900	16	11	50	18–23	73	78–82	
P104	5900	61	27	40	12–18	81	75–80	
P84	4200	43	19	40	12–18	74	70–76	
L64	2900	30	13	40	12–18	58	58–62	
P123	5750	69	19	30	7–12	90	85–91	
P103	4950	60	17	30	7–12	86	50–55	
L43	1850	22	6	30	7–12	42	30–34	
L92	3650	50	8	20	1–7	26	14–18	
L62	2500	34	6	20	1–7	32	22–26	
L121	4400	68	5	10	1–7	14	8–12	
L101	3800	59	4	10	1–7	15	9–12	
L81	2750	43	3	10	1–7	20	14–18	
L61	2000	31	2	10	1–7	24	15–19	

some lipid was dispersed but majority had aggregated and – indicates a clear and transparent aqueous phase coexisting with aggregated lipid phase with visually no lipid dispersed in the aqueous phase.

Both a positive and negative control were incorporated to ensure the expected outcomes were obtained from the sonication protocols used during HTP production of individual samples (500 μl) in 96 deep well plates. The negative control consisted of 50 mg (10 wt. %) of lipid with 500 μl of Milli Q water, whilst the positive control included the addition of steric stabiliser Pluronic F127 at 0.1, 0.5, 1.0 and 2.0 wt. % of the total sample mass.

Particle size

Particle size and polydispersity were determined using photon correlation spectroscopy (PCS) on a Malvern Zetasizer NanoZS (Malvern Instruments, Malvern, UK) at 25 °C, assuming a viscosity of pure water and presented as an average of three separate determinations. Measurements were conducted using 1 μl of sample diluted in 275 μl of Milli Q water, measured using automated settings in low-volume cuvettes.

Liquid crystal phase determination

The internal liquid crystalline structure of the dispersed particles was determined using small angle X-ray scattering (SAXS). Data was collected using the SAXS/WAXS beam line at the Australian Synchrotron using a beam wavelength $\lambda = 1.0322$ Å (15.0 keV) with a typical flux of 10^{13} photons/s. 2D diffraction patterns were recorded on a Dectris-Pilatus 1 M detector of 10 modules. The detector was offset to access a greater q-range. A silver behenate standard ($\lambda = 58.38$ Å) was used to calibrate the reciprocal space vector. The samples were loaded in special glass 1.5 mm capillaries (Hampton Research, USA) and positioned in a custom designed high throughput capillary holder capable of holding 34 capillaries with temperature controlled to ±0.1 °C between 20 and 75 °C. Temperature control was *via* a re-circulating water bath (Julabo, Germany). Exposure time for each sample was 1 s. SAXS data was analysed using an IDL-based AXcess software package, developed by Dr Heron at Imperial College, London.[30]

Cryo-transmission electron microscopy (Cryo-TEM)

A laboratory-built humidity-controlled vitrification system was used to prepare the samples for Cryo-TEM. Humidity was kept close to 80% for all experiments, and ambient temperature was 22 °C. 200-mesh copper grids coated with perforated carbon film (Lacey carbon film: ProSciTech, Qld, Australia) were glow discharged in nitrogen to render them hydrophilic. 4 μl aliquots of the sample were pipetted onto each grid, and after 30 s the grid was blotted manually using Whatman 541 filter paper, for 2 s. Blotting time was optimised for each sample. The grid was then plunged into liquid ethane cooled by liquid nitrogen. Vitrified grids were stored in liquid nitrogen until required.

The samples were examined using a Gatan 626 cryoholder (Gatan, Pleasanton, CA, USA) and Tecnai 12 Transmission Electron Microscope (FEI, Eindhoven, The Netherlands) at an operating voltage of 120 kV. At all times low dose procedures were followed, using an electron dose of 8–10 electrons/Å^2 for all imaging. Images were recorded using a Megaview III CCD camera and AnalySIS camera control software (Olympus) using magnifications in the range 30 000× to 97 000×.

Results

(i) Visual assessment of phase separation

The phytantriol and monoolein amphiphiles were dispersed in the presence of a range of Pluronics using the high-throughput (HTP) protocol described above. Colloidal stability was evaluated visually for 20 Pluronic block co-polymers as steric stabilisers of monoolein and phytantriol, and the results are summarised in Table 2. The effectiveness of the different Pluronics tested was established against negative and positive controls. The negative controls for monoolein and phytantriol, that is, samples without polymer stabilisation, showed no formation of dispersions, rather lipid aggregates were observed with an excess water component, these are labelled as (−). The positive control samples stabilised with increasing concentrations of Pluronic F127, showed dispersions as expected.

Phytantriol stabilised with Pluronic F127 at concentrations from 0.5 to 2.0 wt. % yielded well dispersed stable dispersions; the samples were milky white and without any visible aggregates in the dispersion or on the rim of the well (and hence were labelled with +++ in Table 2). Pluronic F127 provided better stability for phytantriol particles than for monoolein particles, in agreement with previous findings.[31] Specifically, monoolein was well dispersed by F127 at 1.0 wt. %, but cloudy dispersions with visible aggregates formed near the meniscus of the liquid contacted the well at 0.1 wt. % and 0.5 wt. %. When phytantriol was dispersed with F127 at the lowest Pluronic content (0.1 wt. %)

Table 2 Visual assessment of stability of dispersions using stabilisers in the Pluronic series; *F127 is used as the positive control; **Lipid in water is used as the negative control; Key: +++ Milky, ++Cloudy, +Translucent, −Clear, ● Not assessed

	Phytantriol (wt % of Pluronic added)				Monoolein (wt % of Pluronic added)		
Pluronic	0.1	0.5	1.0	2.0	0.1	0.5	1.0
F127*	+	+++	+++	+++	+	++	+++
F108	+	+++	+++	+++	+	+++	+++
P104	+	++	++	+++	+	++	+
P105	+	++	++	+++	—	++	+
P84	+	++	++	+++	●	●	+
P123	+	+	++	++	+	++	+
F68	+	+	++	+++	+	+	+
P85	+	+	++	++	●	●	+
F87	—	—	—	—	+	++	+
F38	—	—	—	—	●	●	—
L35	—	—	—	—	●	●	—
L43	—	—	—	—	●	●	—
L61	—	—	—	—	●	●	—
L62	—	—	—	—	●	●	—
L64	—	—	—	—	●	●	—
L81	—	—	—	—	●	●	—
L92	—	—	—	—	●	●	—
L101	—	—	—	—	●	●	—
P103	—	—	—	—	●	●	—
L121	—	—	—	—	●	●	—
Water**	—	—	—	—	—	—	—

a cloudy dispersion was formed with visible aggregates near the rim of the well.

Pluronics F108, F68, P105, P85, P104, P84 and P123 all formed dispersions of phytantriol and monoolein in water. In addition, F87 also provided dispersed monoolein particles even though it was not an effective stabiliser for phytantriol. Interestingly F108 out-performed all the other Pluronics on an equivalent wt. % basis including F127.

With respect to the Pluronic concentration, as anticipated there was a gradual improvement in dispersion stability with increasing concentration of stabiliser, ranging from 0.1 to 2.0 wt. %. Milky dispersions with less aggregation were obtained when using the higher stabiliser concentrations (*i.e.* 1.0 wt. % and 2.0 wt. %). However, with F127 and F108, milky dispersions were also apparent at the lower stabiliser concentration of 0.5 wt. %. There were a few translucent cloudy samples found with monoolein with Pluronics F87, P105, P104 and P123 at the stabiliser concentration of 0.5 wt. %. However these samples also had visible aggregates, indicating they were still not properly dispersed.

As a consequence of the visual assessment, stabilisers providing colloidal stability equivalent to or greater than that provided by F87 for phytantriol and monoolein (stabilisers above the cut-off line in Table 2) were progressed to SAXS studies to determine internal liquid crystalline nanostructure.

(ii) Particle size

A wide range of average particle sizes between 182 nm to 656 nm were obtained using the HTP preparation protocol. However the majority of the mean particle sizes recorded were within the 250–350 nm range. The polydispersity index (P.D.I.) of samples ranged from 0.01 to 0.4, with some multi-modal distributions being apparent. For the full record of particle sizes and polydispersity index obtained refer to Supplementary Data Set 1. For the most interesting Pluronic stabiliser, F108, when used to disperse monoolein at 1.0 wt. %, the average particle size was 187 nm and polydispersity index was 0.0, compared to Pluronic F127 at 243 nm with a P.D.I of 0.0. These extremely low polydispersity values, with magnitudes below an appropriate number of significant figures, are indicative of high quality uniform dispersions. The HTP production methodology, while suitable for initial rapid screening, is not an optimized preparation approach, and hence dispersions were not excluded from further SAXS studies solely on the basis of the particle sizing data but were mainly selected on the visual assessment of phase separation.

(iii) Phase determination by SAXS

Fig. 4 summarises the effect of the different Pluronic stabilisers on the phase behaviour of the amphiphiles used. The non-dispersed bulk phase formed by monoolein in excess water typically adopts the Q_{II}^{D} double diamond phase.[32] For the dispersed monoolein particles in this study, all stabilisers except for F108 had a significant effect on the internal phase structure. For example, monoolein F127 stabilised dispersions displayed a Q_{II}^{P} primitive inverse bicontinuous cubic phase (Im3m space group) (Fig. 5a & b). Typical Bragg reflections observed for a body-centred cubic phase with Im3m space group (Q_{229}) revealed 3 distinct Bragg peaks with relative positions in ratios $\sqrt{2}$, $\sqrt{4}$, $\sqrt{6}$ which can be indexed as hkl = 110, 200 and 211.

Only those dispersions stabilised with F108 retained the Q_{II}^{D} double diamond phase (Pn3m space group, Fig. 6a and b). Bragg peaks were observed with relative positions in ratios $\sqrt{2}$, $\sqrt{3}$, $\sqrt{4}$ which can be indexed as hkl = 110, 111 and 200 reflections characteristic of a double diamond cubic lattice of the Pn3m crystallographic space group (Q_{224}). For example, monoolein dispersed using F108 at 0.5 wt. % at 20 °C formed the diamond phase with a lattice parameter of 104.3 Å, compared to the equivalent dispersion with F127 which formed the primitive cubic phase, with a lattice parameter of 146.0 Å (Fig. 5 and 6).

The use of F108 to disperse monoolein also provided for improved stability of phase structure with increasing temperature compared to F127. F108-stabilised monoolein dispersions retained the Pn3m cubic phase symmetry at a concentration of 0.5 wt. % at all temperatures investigated (20, 30, 37 and 47 °C). In contrast, at 37 °C, monoolein dispersions containing 1.0 wt. % F108 presented co-existing phases; two Pn3m phases with lattice parameters of 90.6 Å and 100.4 Å (Fig. 7). Cubic symmetry was lost at 47 °C with 1 wt. % F108, and 1 unassignable Bragg reflection was observed.

Phytantriol mesophases were more stable than those of monoolein in the presence of Pluronics. Both F127 and F108, as well as several other stabilisers, retained a Pn3m cubic phase (Q_{224}) after forming dispersions with phytantriol (Fig. 4) with minimal differences in lattice dimensions. For example, phytantriol with 1.0 wt. % F108 at 20 °C had a lattice parameter of 68.0 Å, whilst the lattice parameter when using F127 at the same concentration was 69.3 Å. Similarly at 37 °C phytantriol dispersed with 1.0 wt. % F108 gave a lattice parameter of 64.1 Å, and F127 at the same concentration yielded 63.3 Å. The Pluronic concentration also had minimal effect on structure, for example phytantriol dispersed with F127 at 0.1, 0.5, and 2.0 wt. % formed diamond inverse bicontinuous cubic phase (Pn3m) with lattice parameters of 69.9 Å, 69.4 Å, 69.3 Å and 69.6 Å respectively at 20 °C. This observed phase stability was valid at all temperatures and across the different Pluronics tested. Overall there was no significant difference between the Pn3m cubic phases produced between the different types of Pluronic surfactants used with phytantriol (Fig. 5). The lattice parameters of the Pn3m cubic phases obtained from Pluronics F68, F87, F108 and F127 are comparable to that of the phytantriol in excess water bulk phase systems, with typical lattice parameters ranging from 68.2 Å to 63.2 Å, between temperatures of 20 °C and 45 °C.[33,34] The full data set for the small angle X-ray diffraction data (lattice parameter and phase behaviour) is available in the ESI.†

Fig. 8 shows the lattice parameters obtained from SAXS studies of self-assembled phytantriol colloidal dispersions stabilised with the Pluronics deemed to stabilise nanoparticles (as described above): F68, F87, F108, F127, P84, P104, P105 and P123 at 20, 30, 37 and 47 °C. The body-centred cubic phase with the Im3m space group (Q_{229}) was obtained using P84, P104 and P123 with phytantriol dispersions at 0.5, 1.0 and 2.0 wt. %. A decrease in lattice parameter with increasing temperature was observed in all cases. This commonly observed phenomenon

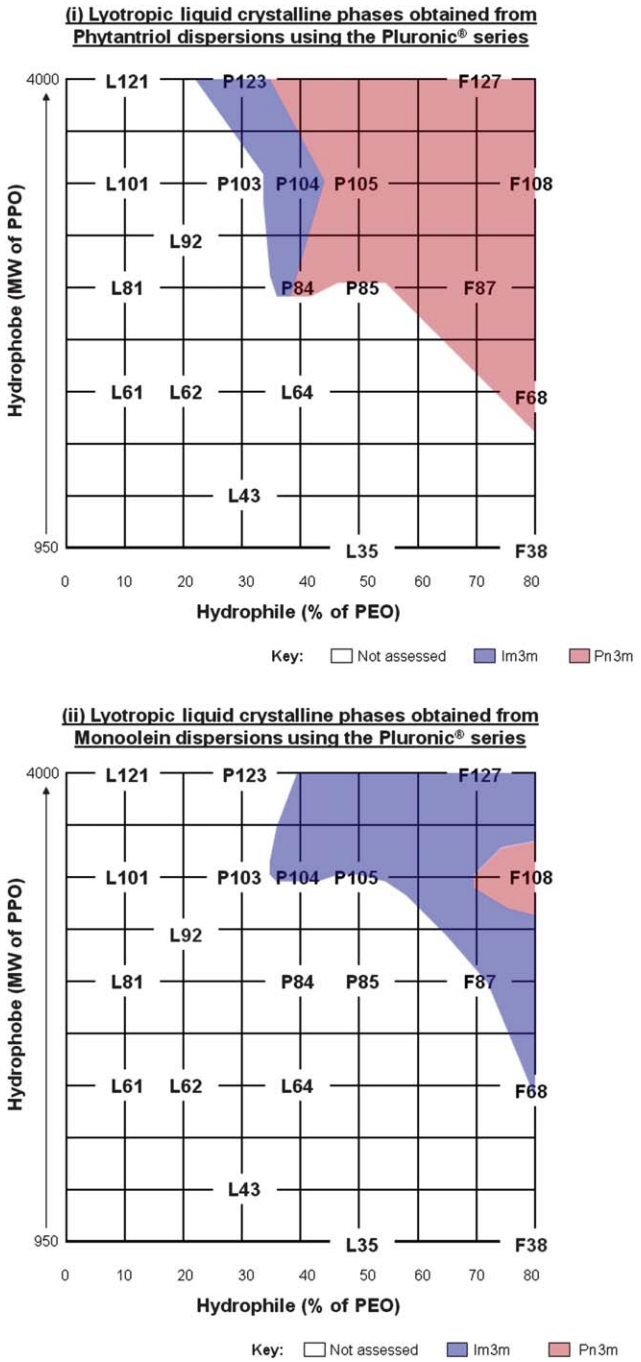

Fig. 4 Lyotropic liquid crystalline phases from SAXS data, resulting for dispersions of (i) phytantriol, and (ii) monoolein when stabilised using the Pluronic series. The Pn3m phase is represented in red and the Im3m phase in blue. Undispersed samples are shown in white.

reflects increasing chain splay of the small molecule self-assembling amphiphile with increasing temperature.

(iv) Cryo-transmission electron microscopy

Cryo-TEM images of individual particles were acquired for monoolein dispersions using Pluronic F108 as the stabiliser as it formed well dispersed Pn3m cubosomes at a low steric stabiliser concentration of 0.5 wt. % (Fig. 9). In Fig. 9(i), the cubic phase is

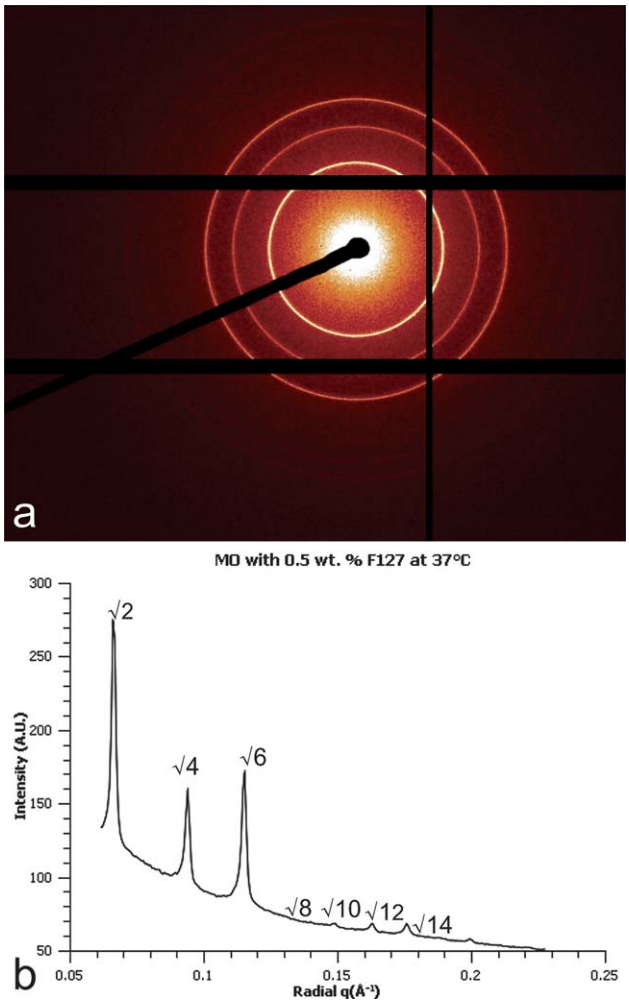

Fig. 5 (a) 2-Dimensional small angle X-ray scattering pattern for monoolein nanostructured particles stabilised with 0.5 wt. % F127 at 37 °C (b) Integrated data with Bragg peaks and peak assignment showing primitive inverse bicontinuous cubic phase (Im3m symmetry) with a lattice parameter of 134.1 ± 0.6 Å.

viewed along the [110 or 112] direction whilst in Fig. 9(ii)–9(iv) are aligned along the [111] plane. The cubosomes of monoolein and phytantriol made with 0.1, 0.5 and 1.0 wt. % of Pluronic F108 all displayed an internal cubic structure similar to that of the control standard of 1.0 wt. % Pluronic F127 with phytantriol.

Discussion

The ultimate utility of liquid crystalline particles such as cubosomes requires effective colloidal stabilisation with retention of internal nanostructure. The structure-property relationships governing stabilisation of these unique nanomaterials have yet to be properly established. The ubiquitous use of Pluronic F127 for the stabilisation of cubosomes highlights the Pluronic series as a suitable starting point for establishing these relationships, hence this manuscript has described high throughput approaches to assess this class of stabilisers for cubosome stabilisation.

The assessment of steric stabilisation of nanoparticles using the Pluronics presented in this manuscript demonstrates clearly

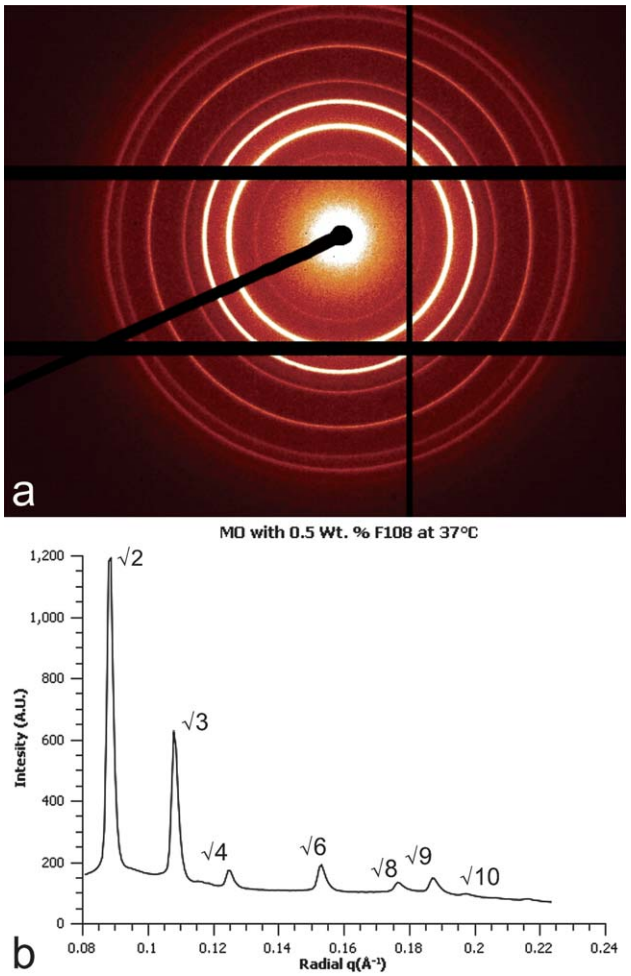

Fig. 6 (a) 2-Dimensional small angle X-ray scattering profile for monoolein nanostructured particles stabilised with 0.5 wt. % F108 at 37 °C (b) Integrated data with Bragg peaks and peak assignment showing double diamond inverse bicontinuous cubic phase (Pn3m symmetry) with a lattice parameter of 100.4 ± 0.01 Å.

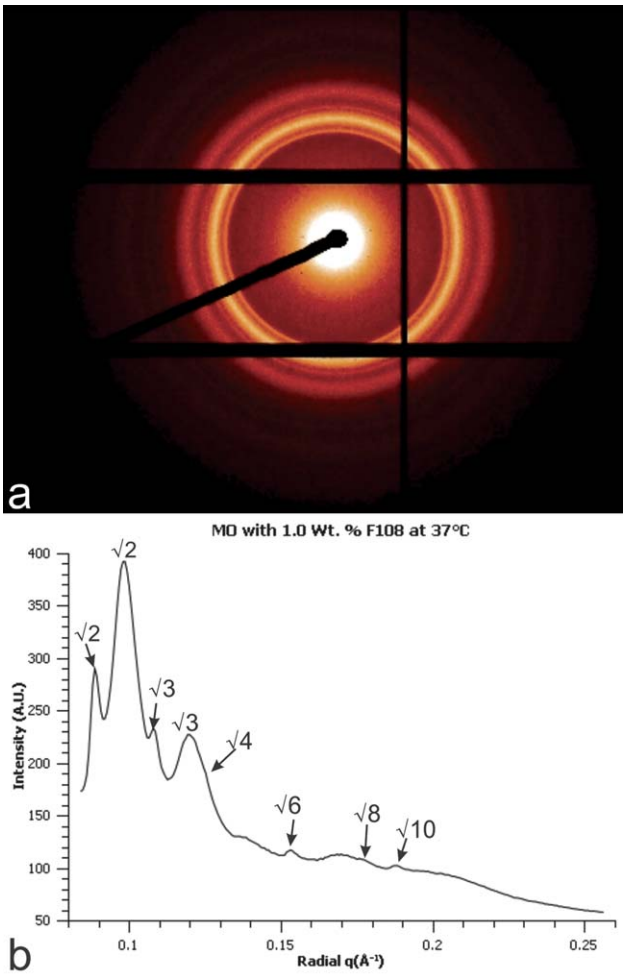

Fig. 7 (a) 2-Dimensional small angle X-ray scattering data for monoolein nanostructured particles stabilised with 1.0 wt. % F108 at 37 °C (b) Integrated data with Bragg peaks and peak assignment showing the presence of two double diamond inverse bicontinuous cubic phase (Pn3m symmetry) with lattice parameters of 90.6 and 100.4 ± 0.3 Å (the latter is identified with arrows).

the parameters that yield a good stabilising moiety. One of the most important parameters when considering the use of poly (ethylene oxide) as the hydrophilic domain of the stabiliser, is the length of the unit.

The stabilising effect of PEO is attributed to two characteristics, of which the first, a mixing effect, is driven by the balance of the PEO–solvent interaction relative to that of the inter PEO-PEO attractive forces. The systems presented in this manuscript are solvated in water for which PEO has a strong affinity. The other characteristic is the entropic effect of chain motion restriction or compression when two stabilised particles are in close proximity—the importance of this increases when the particle–particle separation is less than the adsorbed layer thickness. The impact of the combination of these mixing and entropic effects will increase as the number of adsorbed chains increases with respect to surface area unit and provide high levels of steric stabilisation.[35] Poly(ethylene oxide) surfactants are considered excellent dispersing agents due to their high water affinity, and the fact that these hydrated chains extend into the aqueous medium as coils that act as steric barriers to aggregation. It is considered that in order to be a good stabiliser, the poly

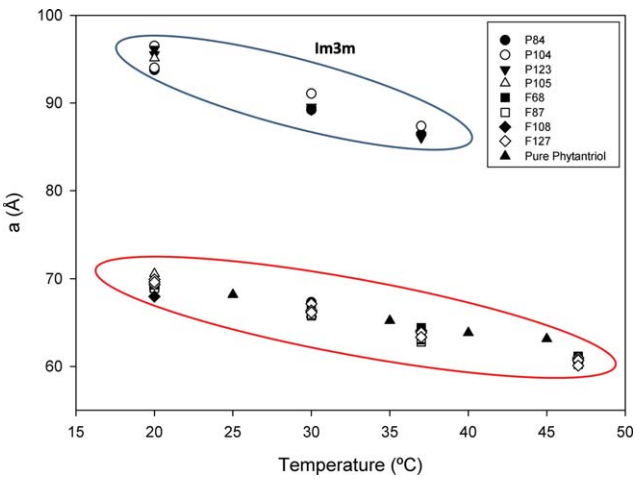

Fig. 8 Lattice parameter *vs.* temperature data for phytantriol dispersions stabilised by the Pluronic series.

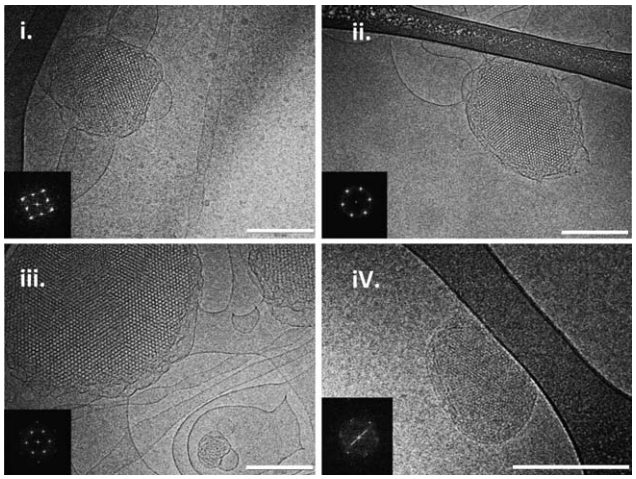

Fig. 9 Cryo-TEM images of dispersions formed using Pluronic F108 as stabiliser for monoolein (i)–(iii) and phytantriol (iv). F108 concentrations were (i) 0.1 wt. %, (ii) 0.5 wt. %, (iii) 1.0 wt. % and (iv) 1.0 wt. %. Scale bar is 200 nm.

(ethylene oxide) layer needs to be 20 repeat units long (about 25 Å)[33] This is in good agreement with the observations made for the Pluronics presented here: it appears that a number of repeat units of at least 19 with phytantriol and monoolein (*e.g.* P84 and P123 respectively) are necessary to form dispersions and 100 repeat units to form very stable dispersions for both lipids tested.

The reduced propensity for flocculation induced by greater poly(ethylene oxide) chain length is demonstrated through the observation that the Pluronic series L101 (4 PEO units), P103 (17 PEO units), P105 (37 PEO units) and F108 (132 PEO units) with a comparable molecular weight (3000) of hydrophobic poly (propylene oxide) (PPO), dispersed monoolein with differing efficiency. No dispersion was observed at short PEO lengths, a primitive cubic phase dispersion was produced at longer PEO length and a diamond inverse bicontinuous cubic phase with F108 at the longest PEO length formed.

Our studies confirm the fact that stabilising agents are required to be at a sufficiently high concentration to prevent flocculation. This flocculation results from the poor coverage of the particles at the lower concentrations—specifically 0.1 and 0.5 wt. % for this study. F108 proved to be a good stabiliser even at 0.5 wt. % for monoolein and phytantriol, which was better than our positive control possibly due to its long hydrophilic PEO chain.

The hydrophobic portion of the steric stabiliser, that is the PPO portion of the Pluronic stabilisers, is important to 'anchor' the stabiliser to the cubosome and enhance adsorption. The extent of the adsorption of the polymer on the surface of the nanoparticle is directly related to the length of the poly(propylene oxide) unit. A longer chain leads to increased adsorption and therefore increased stabilisation potential. The minimum hydrophobic domain length of the block co-polymer to successfully stabilise particles (++ in Table 2) is 40 PPO units (P85). A commonly proposed mechanism of particle flocculation is inter-particle bridging where flocculation is induced through a polymer spanning two particles or a polymer interacting with two particles' stabilisation spheres. A decrease in hydrophobic domain length and therefore reduced anchoring to the nanoparticles may promote such a flocculation effect. Whilst the propensity towards this behaviour may be assessed when comparing critical micelle concentration (CMCs) of the stabilisers, it is inconclusive for the Pluronic series presented here. Supplementary data 2 lists the Pluronics' CMCs, ordered using results from Batrakova *et al.*, which were determined at 37 °C, pH 7.4 using a florescence probe (pyrene) technique.[36,37] As polypropylene oxide length decreases, the CMC of the stabilising molecule increases; this can lead to reduced stabiliser absorbance onto the nanoparticle surface. Decreased stabiliser levels at the nanoparticle–water interface may cause a decrease in coverage on the particle surface thus increasing flocculation. Decreased stabiliser coverage may also increase the propensity for particle aggregation. The critical micelle concentrations of F127 (2.8×10^{-6} M) and F108 (2.2×10^{-5} M) are relatively low. Due to the high concentrations of stabiliser used in these experiments the adsorption on the surface of the nanoparticles is likely to be high. It should be noted however that phytantriol particles were stabilised using P105, P104, P84, F87, and F68, which have CMCs above and below that of F108 and F127. It follows that the CMC of the stabiliser alone does not permit the assessment of the ability of a polymer to form a good steric stabiliser.

The phase behaviour of the Pluronics studied is also of limited significance in the assessment of their performance as stabilisers of nanostructure particles. The polymer concentrations used are low (a maximum of 2.0 wt. %), thus limiting any polymeric self-assembly behaviour to the formation of "isotropic" micellar phases.[27]

The cloud point is another property that indicates the molecular self and solvent interactions of an alkylene oxide-based stabiliser at a given temperature. This is the temperature where the ethylene oxide moieties dehydrate, and the stabiliser will start to phase separate, resulting in the appearance of two phases, one polymer rich phase and one polymer poor phase, resulting in turbidity. Cloud points are typically measured using 1% aqueous amphiphile solution or 10% aqueous amphiphile solution. The results presented in this manuscript demonstrate that successful stabilisers *e.g.* F127 and F108 have a cloud point over 100 °C. Therefore in this study the experimental conditions are a long way from the temperature where ethylene oxide–ethylene oxide interactions are preferred over water–ethylene oxide interactions for the successful stabilisers.

The balance or ratio between the hydrophilic and hydrophobic molecular portion, otherwise known as the HLB of the stabilisers is a relative measure of the degree to which an amphiphile is hydrophilic or hydrophobic.[38–42] This property is also a key factor when determining the suitability of a steric stabiliser for forming dispersed lyotropic liquid crystalline structures, especially when forming them in excess water. The larger the HLB value the greater the hydrophilic nature of the polymer (the HLB values for the Pluronics are given in Table 1). The better polymers in terms of promoting stabilisation of nanoparticles, have relatively high HLB values. This is directly related to the large number of PEO units required to successfully stabilise the particles against flocculation. The majority of dispersions of phytantriol and monoolein that possessed the Pn3m cubic phase structure were formed when using a stabiliser with a HLB equal to or greater than 23. Those with a HLB less than 7 did not form any stable dispersions with both phytantriol and monoolein,

indicating that the more hydrophilic the stabiliser the more probable that it will form a dispersion and effectively stabilise a lyotropic liquid crystalline system. Another possible explanation for the success of F108 over F127 in forming double diamond symmetry cubosomes for monoolein dispersions may be due to its higher HLB: F108 has a greater hydrophilicity with a HLB value greater than 24, whereas F127 has a HLB value between 18–23.

Another important factor to note is that the hydrophobic domain may drive changes in lyotropic liquid crystalline phase behaviour of the nanoparticles. Such an effect is dependent upon the nature of the short-chained amphiphile itself and the polymer. For example F127 with 65 PPO units successfully stabilises phytantriol with little change to the phase behaviour when compared to bulk; however it does change the nature of the monoolein inverse bicontinuous unit cell. F108 which has a shorter hydrophobic domain with 50 PPO units does stabilise monoolein with little change to phase behaviour when compared to the bulk phase.[32]

A contributing factor to the stabilisation efficacy of the block copolymers is their molecular weight (MW). Stabilisers with the same HLB, such as F38, F68 and F108 but different MWs, display variations in stabilisation ability. For example F38 with a MW of 4700 was unable to form stable dispersions, while F68 with a higher MW of 8400 provided moderate stability (++) and F108 having the highest MW of 14600 formed the most stable dispersions (+++) of the group. The importance of the molecular weight of the polymers may be related to their capacity to be internalised within the lipidic lattice of the inverse bicontinuous cubic phase structure which has limited internal water channel size. Decreased internalisation of the polymer is anticipated to increase the fraction of stabiliser molecules available for adsorption at the surface of the nanoparticles, therefore enhancing their stabilising ability. All of the polymers presented in this study are commercially manufactured with molecular weight distributions that are relatively broad—such a distribution may have an effect on particle stabilisation, and future studies could incorporate polymers with narrower molecular weight distributions to elucidate this effect.

Therefore, the main factors indicating the potential success of a steric stabiliser are the MW and EO length, however further assessment in this area is required to distinguish which is of greater importance on the stabiliser's performance. We plan to apply the same methodologies across other classes of non-ionic stabilisers to further elucidate the most important structural parameters leading to effective cubosome stabilisation.

Conclusion

In this study high throughput screening approaches have confirmed that the HLB, MW and cloud point of Pluronic steric stabilisers indicate their ability to perform as effective stabilisers for liquid crystalline cubic phase particles. Pluronics that facilitate retention of Pn3m cubic phases while providing good colloidal stabilisation for dispersed liquid crystal particles have a hydrophilic-lipophilic balance (HLB) greater than 23, a cloud point greater than 100 °C, with an EO% over 50 and a molecular weight greater or equal to 6500. In the process it was discovered that Pluronic F108 is a more effective steric stabiliser of dispersed systems formed using phytantriol and monoolein than the more commonly used Pluronic F127. Hence Pluronic F127 is not the optimal triblock copolymer for the effective stabilisation of all lyotropic liquid crystalline particles.

Acknowledgements

Calum J. Drummond is the recipient of an ARC Federation Fellowship. Josephine YT Chong is the recipient of a CSIRO PhD studentship. Xavier Mulet is the recipient of a CSIRO-Monash University Collaborative Research Post-Doctoral Fellowship. We are grateful to the Australian Synchrotron for the opportunity to use the SAXS/WAXS beamline for this project.

References

1 C. Cervin, P. Vandoolaeghe, C. Nistor, F. Tiberg and M. Johnsson, *Eur. J. Pharm. Sci.*, 2009, **36**, 377–385.
2 B. J. Boyd, D. V. Whittaker, S. M. Khoo and G. Davey, *Int. J. Pharm.*, 2006, **309**, 218–226.
3 M. Malmsten, *J. Dispersion Sci. Technol.*, 2007, **28**, 63–72.
4 C. J. Drummond and C. Fong, *Curr. Opin. Colloid Interface Sci.*, 1999, **4**, 449–456.
5 P. T. Spicer, *Curr. Opin. Colloid Interface Sci.*, 2005, **10**, 274–279.
6 K. W. Lee, T. H. Nguyen, T. Hanley and B. J. Boyd, *Int. J. Pharm.*, 2009, **365**, 190–199.
7 A. Yaghmur and O. Glatter, *Adv. Colloid Interface Sci.*, 2009, **147–148**, 333–342.
8 M. Johnsson, J. Barauskas, A. Norlin and F. Tiberg, *J. Nanosci. Nanotechnol.*, 2006, **6**, 3017–3024.
9 G. Liu, C. E. Conn, L. J. Waddington, S. T. Mudie and C. J. Drummond, *Langmuir*, 2010, **26**, 2383–2391.
10 M. J. Moghaddam, L. de Campo, L. J. Waddington and C. J. Drummond, *Soft Matter*, 2010, **6**, 5915–5929.
11 T. Kaasgaard and C. J. Drummond, *Phys. Chem. Chem. Phys.*, 2006, **8**, 4957–4975.
12 S. M. Sagnella, C. E. Conn, I. Krodkiewska and C. J. Drummond, *Soft Matter*, 2009, **5**, 4823–4834.
13 C. E. Conn, C. Darmanin, S. M. Sagnella, X. Mulet, T. L. Greaves, J. N. Varghese and C. J. Drummond, *Soft Matter*, 2010, **6**, 4838–4846.
14 C. Fong, A. Weerawardena, S. M. Sagnella, X. Mulet, L. Waddington, I. Krodkiewska and C. J. Drummond, *Soft Matter*, 2010, **6**, 4727–4741.
15 X. Mulet, X. Gong, L. J. Waddington and C. J. Drummond, *ACS Nano*, 2009, **3**, 2789–2797.
16 C. Fong, D. Wells, I. Krodkiewska, A. Weerawardeena, J. Booth, P. G. Hartley and C. J. Drummond, *J. Phys. Chem. B*, 2007, **111**, 10713–10722.
17 S. M. Sagnella, X. Gong, M. J. Moghaddam, C. E. Conn, K. Kimpton, L. J. Waddington, I. Krodkiewska and C. J. Drummond, *Nanoscale*, 2011, **3**, 919–924.
18 P. T. Spicer, K. L. Hayden, M. L. Lynch, A. Ofori-Boateng and J. L. Burns, *Langmuir*, 2001, **17**, 5748–5756.
19 J. Barauskas, M. Johnsson, F. Johnson and F. Tiberg, *Langmuir*, 2005, **21**, 2569–2577.
20 O. Svensson, K. Thuresson and T. Arnebrant, *Langmuir*, 2008, **24**, 2573–2579.
21 B. J. Boyd, Y. D. Dong and T. Rades, *J. Liposome Res.*, 2009, **19**, 12–28.
22 P. T. Spicer, W. B. Small, M. L. Lynch and J. L. Burns, *J. Nanopart. Res.*, 2002, **4**, 297–311.
23 K. Larsson, *J. Phys. Chem.*, 1989, **93**, 7304–7314.
24 M. Almgren, J. Borne, E. Feitosa, A. Khan and B. Lindman, *Langmuir*, 2007, **23**, 2768–2777.
25 M. Uyama, M. Nakano, J. Yamashita and T. Handa, *Langmuir*, 2009, **25**, 4336–4338.
26 D. Libster, A. Aserin, D. Yariv, G. Shoham and N. Garti, *Colloids Surf., B*, 2009, **74**, 202–215.
27 G. Wanka, H. Hoffmann and W. Ulbricht, *Macromolecules*, 1994, **27**, 4145–4159.

28 A. Tilley and B. J. Boyd, Monash University Melbourne, VIC, 2010 (unpublished).
29 X. Mulet, D. F. Kennedy, C. E. Conn, A. Hawley and C. J. Drummond, *Int. J. Pharm.*, 2010, **395**, 290–297.
30 J. M. Seddon, A. M. Squires, C. E. Conn, O. Ces, A. J. Heron, X. Mulet, G. C. Shearman and R. H. Templer, *Philos. Trans. R. Soc. London, Ser. A*, 2006, **364**, 2635–2655.
31 C. E. Conn, X. Mulet, M. J. Moghaddam, C. Darmanin, L. J. Waddington, S. M. Sagnella, N. Kirby, J. N. Varghese and C. J. Drummond, *Soft Matter*, 2011, **7**, 567–578.
32 H. Qiu and M. Caffrey, *Biomaterials*, 2000, **21**, 223–234.
33 Y. D. Dong, A. W. Dong, I. Larson, M. Rappolt, H. Amenitsch, T. Hanley and B. J. Boyd, *Langmuir*, 2008, **24**, 6998–7003.
34 Y. D. Dong, I. Larson, T. Hanley and B. J. Boyd, *Langmuir*, 2006, **22**, 9512–9518.
35 D. H. Napper and A. Netschey, *J. Colloid Interface Sci.*, 1971, **37**, 528–535.
36 E. V. Batrakova, S. Li, D. W. Miller and A. V. Kabanov, *Pharm. Res.*, 1999, **16**, 1366–1372.
37 A. V. Kabanov, I. R. Nazarova, I. V. Astafieva, E. V. Batrakova, V. Y. Alakhov, A. A. Yaroslavov and V. A. Kabanov, *Macromolecules*, 1995, **28**, 2303–2314.
38 H. Schott, *J. Pharm. Sci.*, 1971, **60**, 648–649.
39 H. Schott, *J. Pharm. Sci.*, 1995, **84**, 1215–1222.
40 W. Griffin, *J. Soc. Cosmet. Chem.*, 1954, **5**, 259.
41 J. Davies, *Proceedings of the International Congress of Surface Activity*, 1957.
42 W. Griffin, *J. Soc. Cosmet. Chem.*, 1949, **1**, 311.
43 BASF-Corporation 2007 website. http://worldaccount.basf.com/wa/NAFTA~en_US/Catalog/ChemicalsNAFTA/pi/BASF/Brand/pluronic (accessed 18 October 2010).

Electronic Supplementary Material (ESI) for Soft Matter

Steric Stabilisation of Self-Assembled Cubic Lyotropic Liquid Crystalline Nanoparticles: High Throughput Evaluation of Triblock Polyethylene oxide-Polypropylene oxide-Polyethylene oxide Copolymers

Josephine Y.T. Chong [a,b], Xavier Mulet [a,b], Lynne J. Waddington[c], Ben J. Boyd*[b], Calum J. Drummond* [a]

Supplementary Data 1 - Pluronic stabilised nanoparticles characterisation including particle sizing, polydipersity (from dynamic light scattering data) with nanoparticle mesophase and lattice parameter (from small angle X-ray scattering).

			Phytantriol				**Monoolein**			
Stabiliser	*Temp (°C)*	Stabiliser *Conc. (Wt%)*	*Phase*	*Lattice parameter (Å)*	*Z-Ave (nm)*	*PDI*	*Phase*	*Lattice parameter (Å)*	*Z-Ave (nm)*	*PDI*
F108	20	0.1	·	·	·	·	Pn3m	104.3	314	0.0192
		0.5	·	·	·	·	Pn3m	104.3	348	0.0674
		1.0	Pn3m	68.0	263	7.41E-02	Pn3m	106.0	187	4.14E-15
	30	0.1	·	·	·	·	One ring		314	0.0192
		0.5	·	·	·	·	Pn3m	102.6	348	0.0674
		1.0	·	·	·	·	Pn3m	102.4	187	4.14E-15
	37	0.1	·	·	·	·	N/A	N/A	314	0.0192
		0.5	·	·	·	·	Pn3m	100.4	348	0.0674
		1.0	Pn3m	64.1	263	7.41E-02	Pn3m mix	90.6	187	4.14E-15
	47	0.1	·	·	·	·	Pn3m	91.0	314	0.0192
		0.5	·	·	·	·	Pn3m	91.1	348	0.0674
		1.0	·	·	·	·	One ring		187	4.14E-15
F68	20	0.5	Pn3m	69.3	351	0.28	One ring	N/A	·	·
		1.0	Pn3m	68.9	233	0.45	Im3m	139.9	132	0.0121
		2.0	Pn3m	69.4	262	0.42	·	·	·	·
	30	0.5	Pn3m	66.6	351	0.28	N/A	N/A	·	·
		1.0	Pn3m	66.2	233	0.45	N/A	N/A	132	0.0121
		2.0	Pn3m	66.8	262	0.42	·	·	·	·
	37	0.5	Pn3m	63.8	351	0.28	N/A	N/A	·	·
		1.0	Pn3m	63.5	233	0.45	N/A	N/A	132	0.0121
		2.0	Pn3m mix	64.4	262	0.42	·	·	·	·
	47	0.5	Pn3m	61.1	351	0.28	N/A	N/A	·	·
		1.0	Pn3m	60.5	233	0.45	N/A	N/A	132	0.0121
		2.0	Pn3m	61.0	262	0.42	·	·	·	·
F127	20	0.1	Pn3m	69.9	193	0.16	Im3m	141.2	·	·
		0.5	Pn3m	69.4	300	0.22	Im3m	146.0	194	Multi
		1.0	Pn3m	69.3	319	0.33	·	·	243	7.31E-16

		2.0	Pn3m	69.6	230	0.23	·	·	·	·
	30	0.1	Pn3m	67.1	193	0.16	Im3m	139.4	·	·
		0.5	Pn3m	66.3	300	0.22	Im3m	144.9	194	Multi
		1.0	Pn3m	66.4	319	0.33	·	·	243	7.31E-16
		2.0	Pn3m	66.1	230	0.23	·	·	·	·
	37	0.1	Pn3m	63.9	193	0.16	Im3m	130.7	·	·
		0.5	Pn3m	63.3	300	0.22	Im3m	134.1	194	Multi
		1.0	Pn3m	63.3	319	0.33	·	·	243	7.31E-16
		2.0	Pn3m	63.3	230	0.23	·	·	·	·
	47	0.1	Pn3m	61.0	193	0.16	Im3m	123.8	·	·
		0.5	Pn3m	60.8	300	0.22	Im3m	127.6	194	Multi
		1.0	Pn3m	60.7	319	0.33	·	·	243	7.31E-16
		2.0	Pn3m	60.1	230	0.23	·	·	·	·
F87 NF	20	0.5	Pn3m	68.9	440	0.61	N/A	N/A	671	4.21E-02
		1.0	Pn3m	69.3	429	0.47	Im3m	141.3	398	1.18E-01
		2.0	Pn3m	69.4	299	0.45	·	·	·	·
	30	0.5	Pn3m	65.8	440	0.61	Im3m	141.6	671	4.21E-02
		1.0	Pn3m	66.1	429	0.47	N/A	N/A	398	1.18E-01
		2.0	Pn3m	65.9	299	0.45	·	·	·	·
	37	0.5	Pn3m	62.8	440	0.61	N/A	N/A	671	4.21E-02
		1.0	Pn3m	63.0	429	0.47	N/A	N/A	398	1.18E-01
		2.0	Pn3m	63.2	299	0.45	·	·	·	·
	47	0.5	Pn3m	60.2	440	0.61	N/A	N/A	671	4.21E-02
		1.0	Pn3m	60.7	429	0.47	N/A	N/A	398	1.18E-01
		2.0	Pn3m	60.9	299	0.45	·	·	·	·
P105	20	0.1	N/A	N/A	355	0.15	N/A	N/A	·	·
		0.5	Pn3m	69.4	256	0.31	Im3m	150.2	656	1.58E-01
		1.0	Pn3m	69.6	295	0.32	N/A	N/A	105	1.94E-16
		2.0	Im3m/Pn3m	95.1/70.6	269	0.14	·	·	·	·
	30	0.1	N/A	N/A	355	0.15	N/A	N/A	·	·
		0.5	Pn3m	65.9	256	0.31	N/A	N/A	656	1.58E-01
		1.0	Pn3m	65.9	295	0.32	N/A	N/A	105	1.94E-16
		2.0	Pn3m	66.0	269	0.14	·	·	·	·
	37	0.1	N/A	N/A	355	0.15	N/A	N/A	·	·
		0.5	Pn3m	63.6	256	0.31	N/A	N/A	656	1.58E-01
		1.0	Pn3m	63.7	295	0.32	N/A	N/A	105	1.94E-16
		2.0	Pn3m	63.7	269	0.14	·	·	·	·
	47	0.1	N/A	N/A	355	0.15	N/A	N/A	·	·
		0.5	Pn3m	60.7	256	0.31	N/A	N/A	656	1.58E-01
		1.0	Pn3m	60.7	295	0.32	N/A	N/A	105	1.94E-16
		2.0	Pn3m	60.8	269	0.14	·	·	·	·

P104	20	0.5	N/A	N/A	334	0.17	N/A	N/A	349	1.17E-01
		1.0	Im3m	94.0	286	0.42	N/A	N/A	352	0.00639
		2.0	Im3m	96.5	296	0.43	·	·	·	·
	30	0.5	N/A	N/A	334	0.17	Im3m	143.8	349	1.17E-01
		1.0	One ring	N/A	286	0.42	Im3m	161.5	352	0.00639
		2.0	Im3m	91.1	296	0.43	·	·	·	·
	37	0.5	N/A	N/A	334	0.17	Im3m	135.0	349	1.17E-01
		1.0	One ring	N/A	286	0.42	Im3m	159.5	352	0.00639
		2.0	Im3m	87.4	296	0.43	·	·	·	·
	47	0.5	N/A	N/A	334	0.17	Im3m	124.3	349	1.17E-01
		1.0	N/A	N/A	286	0.42	Im3m	145.7	352	0.00639
		2.0	N/A	N/A	296	0.43	·	·	·	·
P123	20	0.5	N/A	N/A	224	0.34	·	·	·	·
		1.0	Im3m	95.5	197	0.12	N/A	N/A	538	1.81E-15
		2.0	Im3m	96.1	242	0.33	·	·	·	·
	30	0.5	N/A	N/A	224	0.34	·	·	·	·
		1.0	Im3m	89.2	197	0.12	N/A	N/A	538	1.81E-15
		2.0	Im3m	89.5	242	0.33	·	·	·	·
	37	0.5	N/A	N/A	224	0.34	·	·	·	·
		1.0	Im3m	86.1	197	0.12	N/A	N/A	538	1.81E-15
		2.0	Im3m	86.3	242	0.33	·	·	·	·
	47	0.5	N/A	N/A	224	0.34	·	·	·	·
		1.0	N/A	N/A	197	0.12	N/A	N/A	538	1.81E-15
		2.0	N/A	N/A	242	0.33	·	·	·	·
P84	20	0.1	Pn3m	69.4	336	multi	·	·	·	·
		0.5	Pn3m	68.9	379	multi	·	·	·	·
		1.0	Pn3m	69.2	471	2.11E-14	N/A	N/A	182	0.0475
		2.0	Im3m/Pn3m	93.8/69.5	594	0.0568	·	·	·	·
	30	0.1	Pn3m	67.3	336	multi	·	·	·	·
		0.5	N/A	N/A	379	multi	·	·	·	·
		1.0	Im3m	89.2	471	2.11E-14	N/A	N/A	182	0.0475
		2.0	N/A	N/A	594	0.0568	·	·	·	·
	37	0.1	N/A	N/A	336	multi	·	·	·	·
		0.5	N/A	N/A	379	multi	·	·	·	·
		1.0	Im3m	86.5	471	2.11E-14	N/A	N/A	182	0.0475
		2.0	N/A	N/A	594	0.0568	·	·	·	·
	47	0.1	N/A	N/A	336	multi	·	·	·	·
		0.5	N/A	N/A	379	multi	·	·	·	·
		1.0	N/A	N/A	471	2.11E-14	N/A	N/A	182	0.0475
		2.0	One ring	N/A	594	0.0568	·	·	·	·

Supplementary Data 2 – Pluronic's critical micelle concentration (CMC)

Pluronic	CMC ($1x10^{-6}$M)
L121	1
L101	2.1
P105	800*
F127	2.8, 800*
P104	3.4
P123	4.4
P103	6.1, 740*
F108	22, 510*
L81	23
P85	65
P84	71
L92	88
F87	91, 2200*
L61	110
L62	400, 7400*
L64	480, 8800*
F68	480, 1400*
L43	2200
F38	21000*

Critical micelle concentration for Pluronic stabilisers used in this study, all CMC values obtained from ref [1] [Pyrene Probe, 37°C] apart from values denoted by * which were obtained from ref [2].

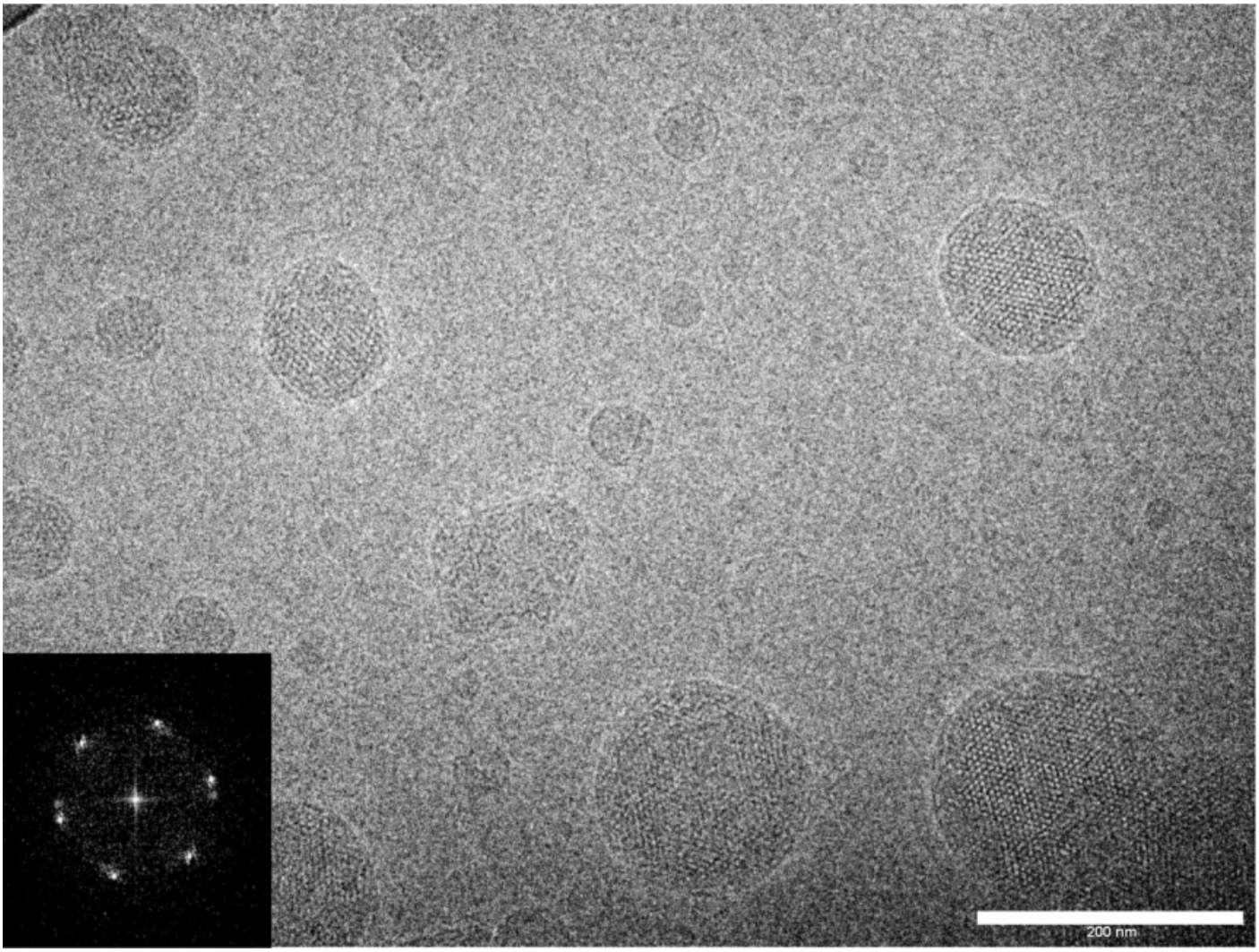

Figure S1 is representative of particle internal structure and order for 1.0 wt% F108 stabilised phytantriol dispersions.

References

1. E. V. Batrakova, S. Li, D. W. Miller and A. V. Kabanov, *Pharm. Res.*, 1999, **16**, 1366-1372.
2. J. R. Lopes and W. Loh, *Langmuir*, 1998, **14**, 750-756.

Chapter 3

High-Throughput Discovery of Novel Steric Stabilisers for Cubic Lyotropic Liquid Crystal Nanoparticle Dispersions

Josephine Y.T. Chong, Xavier Mulet, Lynne Waddington, Ben J. Boyd and Calum J. Drummond

Published: *Langmuir* **2012**, 28, 9223-9232

Declaration for Chapter 3

Declaration by candidate

In the case of Chapter 3, the nature and extent of my contribution to the work was the following:

Nature of contribution	Extent of contribution (%)
Research design, performance of data collection and analysis, manuscript preparation	80

The following co-authors contributed to the work:

Name	Nature of contribution
Xavier Mulet	Supervision; intellectual input; input into manuscript preparation
Lynne Waddington	Intellectual input on cryo-TEM operation and analysis
Ben Boyd	Supervision; intellectual input; input into manuscript preparation
Calum Drummond	Supervision; intellectual input; input into manuscript preparation

Candidate's signature: [redacted] **Date:** **10.7.2014**

Declaration by co-authors

The undersigned hereby certify that:

(7) the above declaration correctly reflects the nature and extent of the candidate's contribution to this work, and the nature of the contribution of each of the co-authors.

(8) they meet the criteria for authorship in that they have participated in the conception, execution, or interpretation, of at least that part of the publication in their field of expertise;

(9) they take public responsibility for their part of the publication, except for the responsible author who accepts overall responsibility for the publication;

(10) there are no other authors of the publication according to these criteria;

(11) potential conflicts of interest have been disclosed to (a) granting bodies, (b) the editor or publisher of journals or other publications, and (c) the head of the responsible academic unit; and

(12) the original data are stored at the following location(s) and will be held for at least five years from the date indicated below:

Location of data storage: CSIRO Materials Science and Engineering, Ian Wark Laboratory, Bayview Avenue, Clayton 3168, Australia.

Co-authors' signature for Chapter 3:

Signed:  **Date:** **10.1.2014**

Xavier Mulet

Signed:  **Date:** **8.1.2014**

Lynne J. Waddington

Signed:  **Date:** **28.2.2014**

Ben J. Boyd

Signed:  **Date:** **12.4.2014**

Calum J. Drummond

Langmuir

Article

pubs.acs.org/Langmuir

High-Throughput Discovery of Novel Steric Stabilizers for Cubic Lyotropic Liquid Crystal Nanoparticle Dispersions

Josephine Y. T. Chong,[†,‡] Xavier Mulet,[†,‡] Lynne J. Waddington,[§] Ben J. Boyd,*[,‡] and Calum J. Drummond*[,†]

[†]Commonwealth Scientific and Industrial Research Organisation (CSIRO) Materials Science and Engineering, Private Bag 10, Clayton, Victoria 3169, Australia

[‡]Drug Delivery, Disposition and Dynamics, Monash Institute of Pharmaceutical Sciences, Monash University (Parkville Campus), 381 Royal Parade, Parkville, Victoria 3052, Australia

[§]CSIRO Materials Science and Engineering, 343 Royal Parade, Parkville, Victoria 3052, Australia

Supporting Information

ABSTRACT: High-throughput methodologies have been employed to establish structure−property relationships and assess the effectiveness of nonionic steric stabilizers for inverse bicontinuous cubic lyotropic liquid crystalline nanoparticulate dispersions of monoolein and phytantriol. The ability of the stabilizers to disperse the lipids was compared with that of the commonly employed triblock poly(ethylene oxide)−poly(propylene oxide)−poly(ethylene oxide) copolymer Pluronic F127, which was used as a positive control. The poly(ethylene oxide) stearate class of stabilizers (commercially known as Myrj) were discovered to be effective as steric stabilizers for cubosomes, while retaining the internal nanostructure of the "parent" bulk phase. In particular, Myrj 59, with an average of 100 poly(ethylene oxide) units, was more effective than F127 at dispersing phytantriol, forming stable phytantriol cubosome dispersions at a concentration of 0.1 wt %, 5-fold lower than that achievable with Pluronic F127. The discovery of this new effective class of stabilizers for cubosomes, specifically enabled by high-throughput approaches, broadens the versatility of components from which to construct these interesting potential drug delivery and medical imaging nanoparticles.

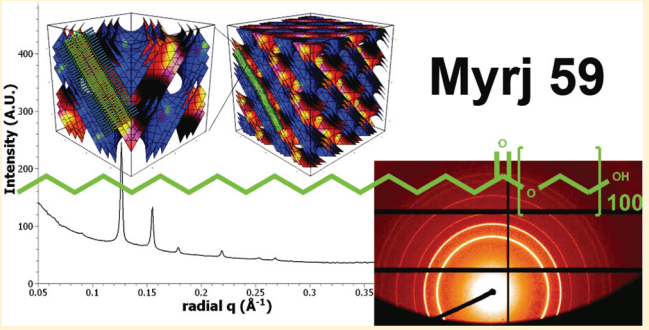

1. INTRODUCTION

Lyotropic liquid crystal engineering is an approach to achieve ordered nanostructured amphiphile self-assembly materials.[1] These liquid crystalline bulk materials are highly viscous and therefore not appropriate as drug delivery or medical imaging vehicles. For some applications of these materials, colloidal (nanoparticulate) dispersions are preferred.[2−5] Colloidal dispersions of these bulk materials have the potential to be used for intravenous administration because they are substantially less viscous and still retain the internal nanostructure of the bulk systems. Inverse phases of lyotropic liquid crystals have shown potential as controlled release agents, and their dispersed counterparts are being increasingly investigated as drug delivery vehicles.[4,6] Of particular interest are the inverse bicontinuous cubic phases and their dispersions that are capable of carrying water-soluble, hydrophobic and amphiphilic bioactive molecules, including peptides and proteins.[3,7,8] Often, the nanoparticles need to be kinetically stabilized by steric means to prevent flocculation of the dispersion and thus improve the shelf life. Since their inception, nanostructured inverse bicontinuous cubic lyotropic liquid crystalline particles have garnered increasing interest in biomedical applications, with potential applications in MRI imaging, biosensing, therapeutic delivery, and protein crystallization.[9−16] Recently, several studies exploiting the advantages of high-throughput approaches in the preparation of these cubosome dispersions have been reported. With this approach it has been possible to experimentally probe multidimensional compositional space (including variables such as temperature, buffer, or additive) successfully.[16−19] Typically steric stabilization of these colloidal particles is achieved by using a poly(ethylene oxide)−poly(propylene oxide)−poly(ethylene oxide) block copolymer, frequently Pluronic F127.[17,20,21]

To our knowledge, very few studies have investigated the potential of other classes of steric stabilizers for lyotropic liquid crystalline dispersions. A range of compounds and particles have been tested as stabilizers for lyotropic liquid crystal nanoparticles. In addition to Pluronics, examples of other stabilizer classes examined include clay particles, silica particles,

Received: November 24, 2011
Revised: May 22, 2012
Published: May 25, 2012

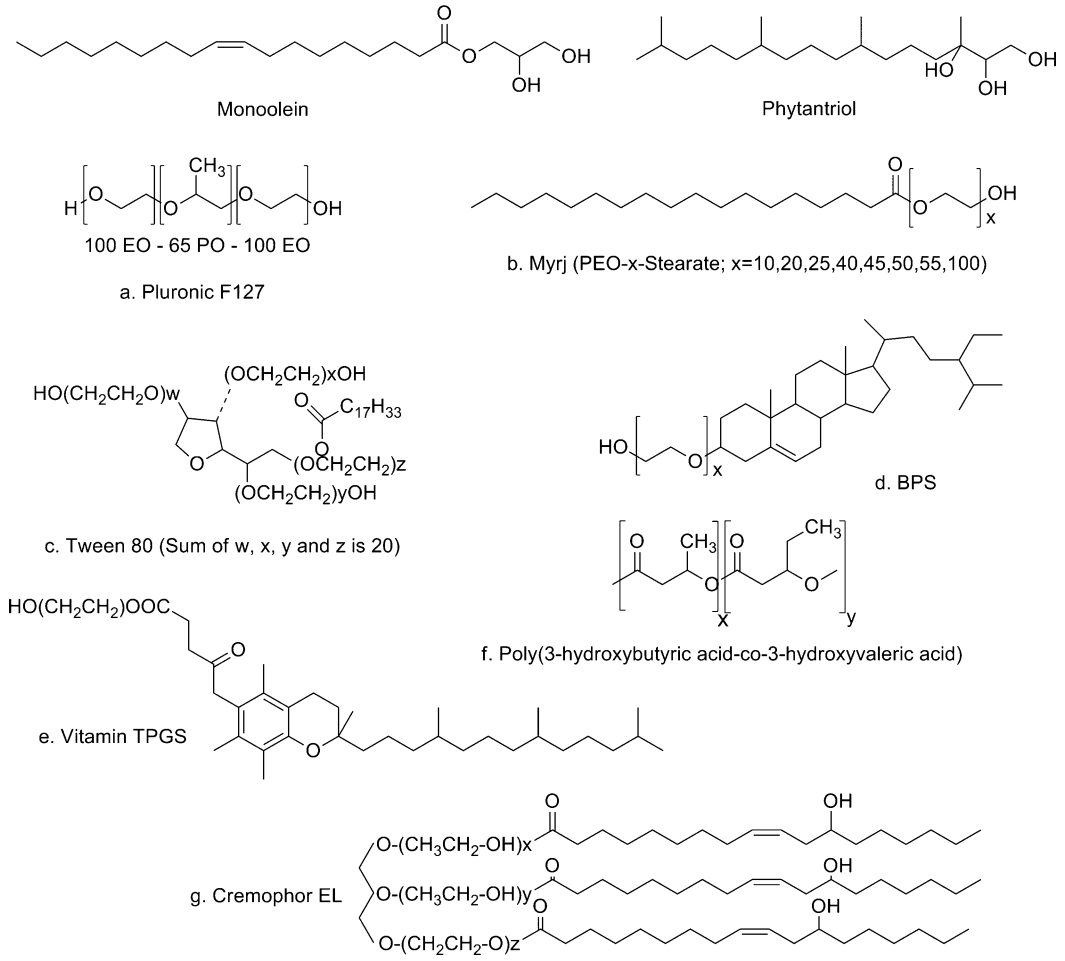

Figure 1. Chemical structure of monoolein and phytantriol and nonionic polymers as steric stabilizers: (a) Pluronic F127, (b) Myrj (x = PEO units), (c) Tween 80, (d) BPS, where x = 30 for BPS-30, (e) vitamin TPGS, (f) poly(3-hydroxybutyric acid-*co*-3-hydroxyvaleric acid), where x represents the 3-hydroxybutyrate (HB) unit and y the 3-hydroxyvalerate (HV) unit, and (g) Cremophor EL (where $x + y + z = 35$).

β-casein, polysorbates, modified cellulose, and ethoxylated phytosterol.[22−27]

A high-throughput assessment of the structure−property relationships for polymers from the Pluronic class in stabilizing lyotropic liquid crystalline dispersions has previously been performed.[17] It is important to conserve the internal structural integrity of cubosomes to enable the preservation of particle size and integrity, allowing for controlled usage in biomedical applications. The study revealed that a longer poly(ethylene oxide) (PEO) chain Pluronic, Pluronic F108 with 132 PEO units, was able to stabilize monoolein cubosomes without affecting the internal structure of the particles. However, the commonly used F127, with 100 PEO units, changes the monoolein cubic phase symmetry from its native double diamond inverse bicontinuous cubic phase (V_2^D) to a primitive cubic phase (V_2^P), indicative of disruption and destabilization of its internal liquid crystalline structure. This study by Chong et al. showed that both the hydrophilic and the hydrophobic domains determine the effectiveness of a steric stabilizer.[17] Furthermore, it was clear from the study that the balance between the hydrophobic anchoring domain size and the length of the hydrophilic steric repulsion chain plays an important role in overall stability.

In the current work we expand upon this research to investigate the structure−property relationships of a range of alternative steric stabilizer classes. Polymers that have been reported to confer repellency to surfaces share a number of properties such as hydrophilicity, presence of hydrogen bond acceptors but absence of hydrogen bond donors, and electrical neutrality.[28,29] PEO fits this profile, being an uncharged, hydrophilic polymer that is soluble in water. Due to its low toxicity and immunogenicity, PEO is considered to be the chemical moiety that yields the most effective steric repulsion barrier while improving the pharmacokinetics and pharmacodynamics of nanoscale drug delivery systems (e.g., stealth liposomes).[30−32] While PEO is regarded as an ideal headgroup, little is known about the ideal PEO chain length and the lipid anchoring chemical space has not been well explored.

In the study herein, we report the assessment of alternative, commercially available, nonionic steric stabilizers for monoolein and phytantriol cubosome systems. Using the same high-throughput methodologies employed in assessing the Pluronic series,[17] a number of potential alternative nonionic stabilizers were investigated. Polyethoxylated castor oil (Cremophor EL), polysorbates (Tween 80 and Tween 85), polyethoxylated phytosterols (BPS-05 and BPS-30 with 5 and 30 PEO units, respectively), D-α-tocopheryl poly(ethylene oxide) 1000 succinate (i.e., vitamin E TPGS), polyethoxylated stearates (Myrj series; the PEO lengths investigated were 10, 20, 25, 40, 45, 50, 55, and 100 PEO units), and a non-PEO-based polymer, poly(3-hydroxybutyric acid-*co*-3-hydroxyvaleric acid) (poly(hydroxyvaleric acid) (PHV) content 8 wt %) were assessed

dx.doi.org/10.1021/la301874v | *Langmuir* 2012, 28, 9223−9232

for their ability to stabilize cubosomes. The structures of the investigated steric stabilizers are shown in Figure 1. Selection of these PEO derivatives and poly(3-hydroxybutyric acid-*co*-3-hydroxyvaleric acid) was based on previous studies that had demonstrated their use as emulsifiers in food products, drug delivery systems, and application with lyotropic liquid crystals.[25,33−39]

The colloidal stability and retention of the nanostructure of cubosomes with these alternative steric stabilizing molecules were evaluated with the outlook of determining the structure−activity relationships for any successful family of stabilizers. The systems investigated were visually assessed for stabilization efficacy, followed by size measurement using dynamic light scattering (DLS) and characterization of the nanostructure of the dispersed nanoparticles using synchrotron small-angle X-ray scattering (SAXS). The temperature dependence of thermally induced inverse bicontinuous cubic (V_2) to inverse hexagonal (H_2) phase transitions can also provide information about the extent of lipid−stabilizer interactions. Hence, SAXS was also used to study the phase structure with increasing temperature. Further confirmation of the lyotropic liquid crystalline cubic structure was made by visualization of the particle morphology using cryogenic transmission electron microscopy (cryo-TEM).

2. MATERIALS AND METHODS

2.1. Materials. 3,7,11,15-Tetramethylhexadecane-1,2,3-triol (phytantriol) was obtained from DSM Nutritional Products, NSW, Australia, and monoolein (1-oleoyl-*rac*-glycerol) was obtained from Sigma-Aldrich, Castle Hill, NSW, Australia. Phytosterol ethoxylates (Nikkol BPS-05 and BPS-30, with PEO chain lengths of 5 and 30, respectively) were provided by Nikko Chemicals, Japan. Polyethoxylated castor oil (PEO-35-castor oil, Cremophor EL) was obtained from BASF, Mount Olive, NJ. Poly(oxyethylene) stearates (Nikkol MYS-10 V, MYS-25 V, MYS-45 V, and MYS-55 V, with 10, 25, 45, and 55 PEO units, respectively) were provided by Nikko Chemicals. Myrj S20 and Myrj S50, with 20 and 50 PEO units, respectively, were provided by Croda, Barcelona, Spain. Myrj 52 and Myrj 59, with 40 and 100 PEO units, respectively, were purchased from Sigma-Aldrich. Polysorbates Tween 80 and Tween 85 were from Sigma-Aldrich. D-*α*-Tocopheryl poly(ethylene oxide) 1000 succinate (vitamin E TPGS) was from Eastman, TN. Poly(3-hydroxybutyric acid-*co*-3-hydroxyvaleric acid) (biodegradable polymer, PHV content 8 wt %) was from Sigma-Aldrich.

Cubosome is a United States Patent and Trademark Office registered trademark of GS Development AB Corp., Sweden. Pluronic and Cremophor EL are USPTO registered trademarks of BASF Corp., Myrj is a USPTO registered trademark of Uniqema Americas LLC, Tween is a USPTO registered trademark of ICI Americas, Inc., and Nikkol is a USPTO registered trademark of Nikko Chemicals Co.

2.2. Preparation of Nanostructured Particles. Cubosomes were prepared in a 96-deep square well collection plate (Supelco) using an automated synthesis platform, Chemspeed Accelerator SLT2 (Chemspeed, Switzerland), as described by Mulet et al.[19] Briefly, 50 mg of lipid (to provide 100 mg/mL in the final dispersion, 10 wt % of the total sample mass) was dispensed in chloroform solution per sample well. Following overnight evaporation, any remaining solvent was removed using GeneVac Atlas evaporator model HT-4 (GeneVac, Ipswich, U.K.) at reduced pressure (3 mbar) and at 40 °C for at least 2 h. Subsequently, 500 μL of stabilizer solution in Milli-Q water was added (0.1, 0.5, 1.0, and 2.0 wt %). Each sample was probe sonicated (Chemspeed sonicator model SLT2, serial no. 1300/08) at an amplitude of 5 for a total of 5 min in a 1 Hz on/off cycle to minimize heating.

A sonication time of 5 min proved sufficient to form dispersions using Pluronic F127. As the principal goal of these experiments was to find novel stabilizers that would out-perform Pluronic F127, this length of sonication time was therefore considered a suitable energy input.

It is important to note that the sonication protocol has not been optimized for each concentration of each stabilizer. The aim of this study is to assess the performance of stabilizers against one another, and this can only be done if identical protocols are followed for each dispersion.

2.3. Dispersion Quality and Particle Size. The stability of dispersions immediately after preparation was assessed visually through observation of the samples in the sample wells after sonication. Due to the high-throughput nature of the research described herein and the very large numbers of samples involved, centrifugal accelerated stability assays as described by Libster et al. were not performed on the colloidal dispersions.[25] Therefore, the visual assessment was used as an initial screen to rapidly exclude poor dispersions from further study.

The appearance of a well-dispersed sample was characterized as having a milky white consistency with no visible large aggregates. In contrast, poorly dispersed samples were transparent in appearance with visible aggregates of lipid typically around the rim of the sample well. The dispersions were graded using a scale where "+++" indicates a homogeneous milky dispersion, "++" indicates a cloudy dispersion with some aggregation apparent, "+" indicates a translucent dispersion where some lipid was dispersed but the majority had aggregated, and "−" indicates a clear and transparent aqueous phase coexisting with an aggregated lipid phase with minimal lipid dispersed in the aqueous phase.

Both a positive control and a negative control were included to ensure the expected outcomes were obtained from the sonication protocols used for production of the dispersions. The negative control consisted of 50 mg of lipid without stabilizer in the aqueous phase, while for the positive controls Pluronic F127 was added at 0.1, 0.5, 1.0, and 2.0 wt % of the total sample mass.

Particle size and polydispersity were determined using DLS on a Malvern Zetasizer NanoZS (Malvern Instruments, Malvern, U.K.) at 25 °C, assuming a viscosity of pure water. Measurements were conducted using 1 μL of sample diluted in 275 μL of Milli-Q water, measured using automated settings in low-volume cuvettes. Dynamic light scattering using a DynaPro plate reader (Wyatt Technology, Santa Barbara, CA) was also used to determine the critical aggregation concentration (CAC) for the amphiphiles, and this is described in more detail in Supplementary Data 2 in the Supporting Information. Data statistics shown for particle size, polydispersity, and the CAC readings from the DLS instrument are averaged from three repeat measurements.

To rate the stabilizers, the stabilization abilities of the different moieties were compared against that of Pluronic F127. This approach means that polydispersity indices are not an ideal tool for the assessment of stabilization ability, but instead a range of parameters, including those from visual assessment, the effect on the mesophase, and phase transition temperatures, are all considered as relevant.

2.4. Characterization of Internal Structure and Particle Morphology. The internal liquid crystalline structure of the dispersed particles was determined by using SAXS. Data were collected using the SAXS/wide-angle X-ray scattering (WAXS) beamline at the Australian Synchrotron using a beam with wavelength λ = 1.033 Å (12.0 keV) with a typical flux of approximately 10^{13} photons/s. 2D diffraction patterns were recorded on a Decris-Pilatus 1 M detector of 10 modules. The detector was offset to access a greater q range. A silver behenate standard (λ = 58.38 Å) was used for calibration. The samples were loaded in special glass 1.5 mm capillaries (Hampton Research, Aliso Viejo, CA) and positioned in a custom-designed semi-high-throughput capillary holder capable of holding 34 capillaries with the temperature controlled to ±0.1 °C between 20 and 75 °C. Temperature control was via a recirculating water bath (Julabo, Germany). The exposure time for each sample was 1 s. SAXS data were analyzed using an IDL-based AXcess software package.[40]

A laboratory-built humidity-controlled vitrification system was used to prepare the samples for cryo-TEM. The humidity was kept close to 80% for all experiments, and the ambient temperature was 22 °C.

dx.doi.org/10.1021/la301874v | *Langmuir* 2012, 28, 9223−9232

Copper grids (200-mesh) coated with a perforated carbon film (lacey carbon film, ProSciTech, QLD, Australia) were glow discharged in nitrogen to render them hydrophilic. Aliquots of the sample (4 μL) were pipetted onto each grid, and after 30 s the grid was blotted manually using Whatman 541 filter paper for 2 s. The blotting time was optimized for each sample. The grid was then plunged into liquid ethane cooled by liquid nitrogen. Vitrified grids were stored in liquid nitrogen until required.

The samples were examined using a Gatan 626 cryoholder (Gatan, Pleasanton, CA) and Tecnai 12 transmission electron microscope (FEI, Eindhoven, The Netherlands) at an operating voltage of 120 kV. At all times low-dose procedures were followed using an electron dose of 8−10 electrons/Å^2 for all imaging. Images were recorded using a Megaview III charge-coupled device (CCD) camera and AnalySIS camera control software (Olympus) using magnifications in the range from 30000× to 97000×.

Molecular models of phytantriol, stearic acid, and monoolein were analyzed using the MM2 energy minimization force field in Chem3D Pro version 12.0 (CambridgeSoft, Cambridge, MA).

3. RESULTS

The most important criteria to consider in assessing the various stabilizers used in the preparation of inverse bicontinuous cubic phase liquid crystal nanoparticles are (i) their ability to enable the formation of dispersions, preferably with monodisperse particle size distribution, (ii) the relative effective concentration of the stabilizer, and (iii) retention of the internal lyotropic liquid crystalline phase.

3.1. Colloidal Stability. Colloidal stability was initially assessed visually to exclude very poor stabilizers from further study by SAXS and cryo-TEM. Table 1 shows the visual assessment of colloidal particle stability, immediately after particle preparation, using the sixteen stabilizers assessed at four different concentrations (0.1, 0.5, 1.0, and 2.0 wt % of the total sample mass). As expected from literature reports, the positive control, Pluronic F127, formed stable milky dispersions more readily with phytantriol than with monoolein at all four concentrations (0.1, 0.5, 1.0, and 2.0 wt %). The negative control system, using lipid only (i.e., phytantriol or monoolein) in water, did not provide stable particle dispersions.[17,21]

Table 1. Visual Assessment of the Stability of Dispersions Using Commercial Stabilizers[a]

	phytantriol				monoolein		
stabilizer	0.1 wt %	0.5 wt %	1.0 wt %	2.0 wt %	0.1 wt %	0.5 wt %	1.0 wt %
Pluronic F127[b]	+	+++	+++	+++	+	++	+++
PEO-100-stearate (Myrj 59)	+++	+++	+++	+++	−	+	++
PEO-55-stearate	+	+	++	++	−	+	+
PEO-50-stearate	+	+	++	++	−	+	+
PEO-45-stearate	+	+	++	++	−	+	+
PEO-40-stearate (Myrj 52)	−	+	+	++	●	+	+
PEO-25-stearate	−	+	+	+	−	+	+
PEO-20-stearate	−	−	+	+	−	−	+
PEO-10-stearate	−	−	−	+	−	−	−
vitamin TPGS	−	+	+	+	●	●	●
poly(3-hydroxybutyric acid-*co*-3-hydroxyvaleric acid)	−	−	+	+	●	●	●
Nikkol BPS-30	−	−	−	−	●	●	●
Nikkol BPS-05	−	−	−	−	●	●	●
Tween 85	−	−	−	−	●	●	●
Tween 80	−	−	−	−	●	●	●
Cremophor EL	−	−	−	−	●	●	●
no stabilizer[c]	−	−	−	−	−	−	−

[a]Key: +++, milky; ++, cloudy; +, translucent; −, clear; ●, not assessed. [b]F127 is used as the positive control. [c]Lipid in water is used as the negative control.

When the stabilizers were assessed for their effectiveness to disperse phytantriol, only Myrj 59 and Pluronic F127 formed uniform milky dispersions, while the remainder formed poorly stable, phase-separated mixtures. Myrj 59 actually outperformed the positive control Pluronic F127 in the formation of stable phytantriol dispersions at low concentrations. Milky dispersions were observed in the presence of only 0.1 wt % Myrj 59 compared to the translucent, poorly dispersed sample obtained when using 0.1 wt % Pluronic F127. Although the average particle size and polydispersity index (PDI) were higher for Myrj 59 (380.7 nm, PDI = 0.46) compared to Pluronic F127 (193.0 nm, PDI = 0.16), there were significant amounts of large nondispersed lipid aggregates present for the F127 system, which were not apparent for the Myrj 59 system. This finding highlights the caution that must be taken in comparing DLS data for these systems in isolation.

In contrast, Myrj 59 was a poor stabilizer for monoolein particles, as no stable dispersions were observed when using 0.1 wt % Myrj 59, and only a small quantity of monoolein was dispersed using 0.5 and 1.0 wt % stabilizer.

In the case of phytantriol dispersions, only two classes of stabilizers showed some stabilization ability, PEO-stearate surfactants and vitamin E TPGS at 0.5, 1.0, and 2.0 wt %, which were cloudy but displayed large visible aggregates indicative of poor stabilization. Dispersions were not formed with Myrj 52 or vitamin E TPGS at the lower stabilizer concentration (0.1 wt %) for phytantriol. Again, as observed for Myrj 59, dispersions with higher stability were formed when using phytantriol.

3.2. Internal Phase Structure for Dispersions. In the presence of excess water, but without stabilizer, at 20 °C phytantriol forms the double diamond cubic phase with a lattice parameter of 68.0 Å.[41] Under the same conditions the monoolein−water cubic phase also adopts a V_2^D mesophase, but with a lattice parameter of 112.8 Å.[17,42] Any deviation in phase structure observed after dispersion of the bulk material indicates an influence of the stabilizer on the internal nanostructure of the particles. Therefore, phase identification and unit cell measurement were performed on each of the successfully dispersed systems using synchrotron SAXS.[43]

It is common for monoolein dispersions in excess water with stabilizer to self-assemble into a V_2^P phase compared to the V_2^D lattice commonly observed in the bulk phase.[17,20] Undispersed RYLO, a distilled monoglyceride containing 92% C18:1, 6% C18:2, and 2% saturated acids, was found to form the V_2^P phase in the presence of 2 and 4 wt % F127 stabilizer in excess water. In contrast, dispersions of RYLO in the presence of 4 wt % F127 stabilizer in excess water formed V_2^D phases.[44]

For the F127-stabilized monoolein systems presented in this paper, our results agree with those of Nakano et al.[20] The differences in phase behavior compared to that reported by Gustafsson et al. at low stabilizer concentrations most likely arises from the different compositions of the lipids; in these studies we employed highly pure (99.0+%) monoolein, which does not contain other glyceride impurities, resulting in dispersions with the V_2^P internal nanostructure.[17] The absence

dx.doi.org/10.1021/la301874v | Langmuir 2012, 28, 9223−9232

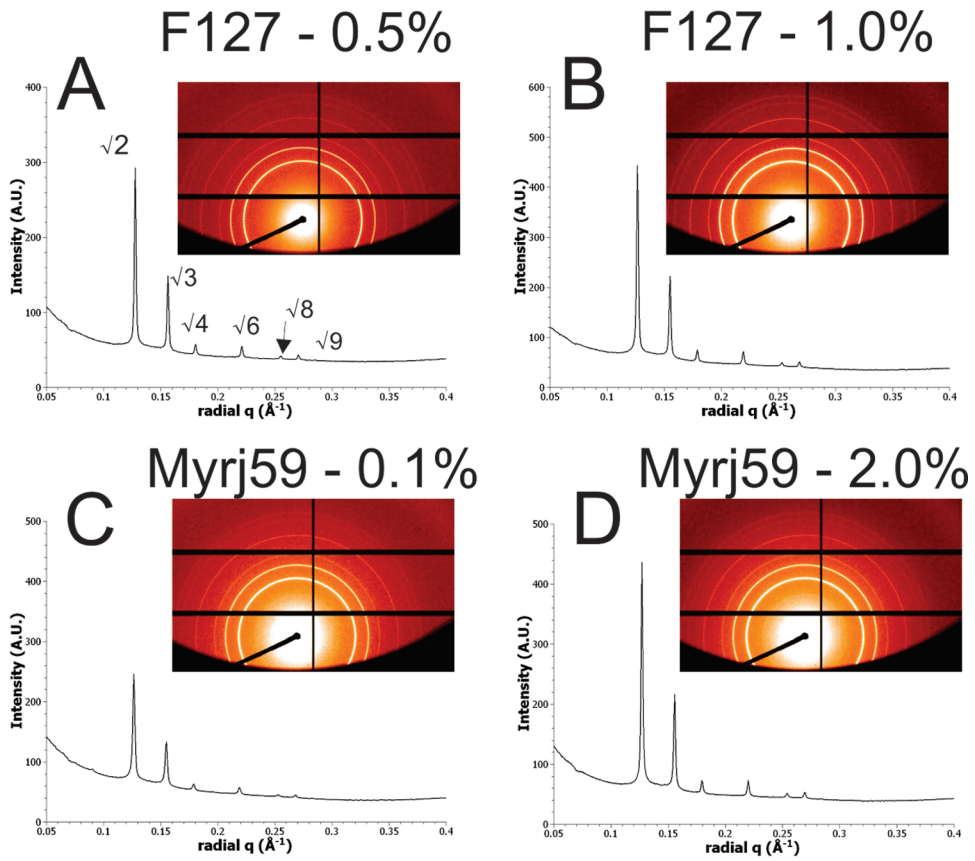

Figure 2. SAXS data and the assigned Bragg reflections for the double diamond (V_2^D) phase obtained at 37 °C for the F127 (A, lattice parameter *a* 63.3 Å; B, *a* = 63.3 Å) and Myrj 59 (C, *a* = 63.8 Å; D, *a* = 64.7 Å) stabilized phytantriol nanoparticles with the stabilizer and concentration (wt %) of the final dispersion using 100 mg/mL surfactant. Representative square root nomenclature is assigned in (A); this corresponds to a double diamond inverse bicontinuous cubic phase.

of glycerides with higher chain unsaturation may explain why the V_2^D phase was not observed.

Gustafsson et al. reported that RYLO was more easily dispersed to form cubosomes at higher stabilizer concentrations and that they then possessed the primitive cubic phase structure, as observed for monoolein in this study.[44,45] The lattice parameters measured for V_2^P monoolein cubosomes, with high F127 stabilizer concentrations, are 130−146 Å (see Supplementary Data 1 in the Supporting Information), which were similar to those quoted by Gustafsson et al. (130−140 Å).[44] Landh also reported the pine oil−water−-F127 phase diagram; although pine oil is rich in monoolein, it also contains a significant amount of lipidic impurities, again complicating direct comparison with the phase behavior of the systems containing neat monoolein in the current study.[46]

From the 16 stabilizers screened during visual assessment, only the dispersions of phytantriol stabilized using Myrj 59 provided comparable or improved stability compared to the positive control, Pluronic F127. Hence, only the results for Myrj 59 will be described in further detail. The structural information obtained using SAXS and DLS for the remaining stabilizers is reported in Supplementary Data 1 in the Supporting Information.

3.3. Myrj 59-Stabilized Cubosomes. The SAXS profiles and the assigned Bragg reflections obtained for the Myrj 59-stabilized phytantriol dispersions (0.1 and 2.0 wt % stabilizer) are shown in Figure 2 together with F127 systems (F127 at 0.5 and 1.0 wt %). With this figure we aim to demonstrate that there are few changes with respect to both phase and lattice parameter in comparing F127 to Myrj 59 as stabilizers for phytantriol. The Bragg reflections at positions $\sqrt{2}$, $\sqrt{3}$, $\sqrt{4}$, $\sqrt{6}$, $\sqrt{8}$, and $\sqrt{9}$ are clearly observed in the diffraction data obtained from all the samples, indicating that the double diamond phase was retained for the cubic phase. Myrj 59 therefore successfully dispersed phytantriol into V_2^D cubosomes. The lattice parameters derived from the peak positions did not change with increasing concentration of Myrj 59 (see Supplementary Data 1 in the Supporting Information) and were similar to that of the phytantriol in excess water−Pluronic F127 stabilizer. For example, phytantriol cubosomes stabilized with 2 wt % Pluronic F127 or Myrj 59 at 20 °C both exhibited a V_2^D phase, with lattice parameters of 69.9 and 69.6 Å, respectively (see Supplementary Data 1).

The V_2^P monoolein cubosomes displayed a clear difference in lattice parameter between those stabilized using Myrj 59 and Pluronic F127, in contrast to the phytantriol system. At 0.5 wt % Myrj 59, the cubosomes had a lattice parameter of 153 Å, which is 7 Å greater than for the equivalent F127 system (see Supplementary Data 1 in the Supporting Information).

Myrj 52 in contrast to Myrj 59 did not effectively stabilize the phytantriol cubosomes and induced a phase transition from the V_2^D phase to the V_2^P phase, with a consequent change in lattice parameter from 96 to 131 Å at 0.1 and 1.0 wt %, respectively.

Increasing temperature for both Myrj 59- and F127-stabilized phytantriol systems resulted in a steady decrease in the lattice parameter, consistent with the previously reported temperature

dx.doi.org/10.1021/la301874v | *Langmuir* 2012, 28, 9223−9232

dependence in these systems (see Supplementary Data 1 in the Supporting Information).[41] Figure 3 shows the phytantriol

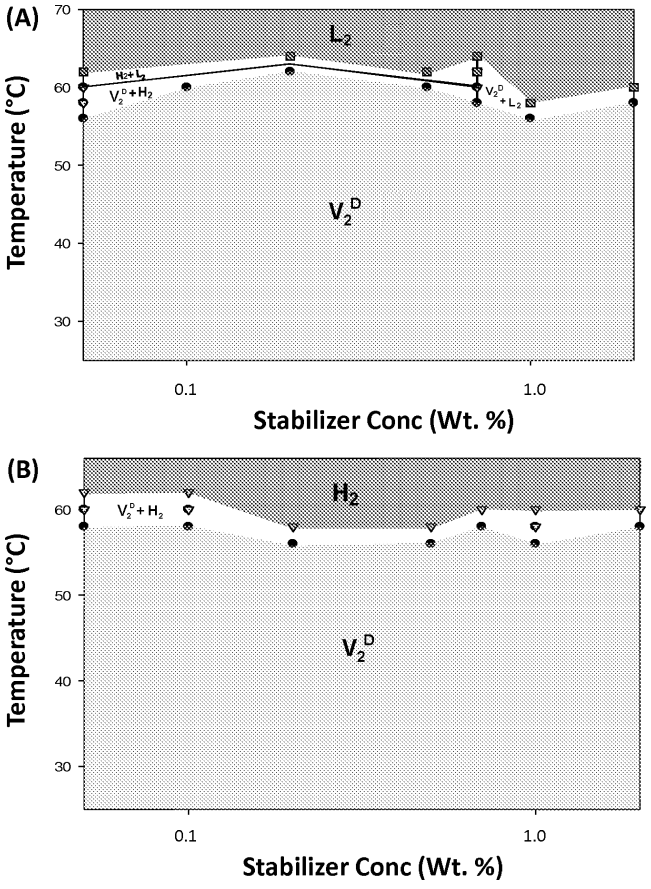

Figure 3. Phase diagrams for (A) Pluronic F127 and (B) PEO-100-stearate (Myrj 59) with 100 mg/mL phytantriol in Milli-Q water. Data points of the known phase structures are represented by the following shapes: solid circle, V_2^D; gray triangle, H_2; shaded square, L_2. Data points falling within the known phase boundary are omitted for clarity.

temperature-dependent phase behavior for the phytantriol dispersions stabilized using Myrj 59 and Pluronic F127. The Myrj 59 phytantriol cubosomes underwent a phase transition from a V_2^D phase to an H_2 structure between 56 and 59 °C (panel B). In contrast, the phytantriol dispersion stabilized using 1 wt % Pluronic F127 only exhibited a phase transition of V_2^D to a fluid isotropic phase (L_2) at 56 °C (Figures 3A and Figure 4). The temperature-dependent phase behavior for phytantriol dispersions stabilized using F127 (Figure 3A) showed that the H_2 structure was transiently observed over a narrow temperature range across several compositions, but not in others. It is likely that the coexisting H_2 phase was present but not observed during the 2 °C increments of the temperature scans. Furthermore, it was observed that F127 dispersions adopted the L_2 phase above 60 °C, which contrasts with Myrj 59 dispersions that formed an H_2 structure (Figure 3).

Although they were poorly dispersed, when Myrj 59 was used to disperse monoolein, the V_2^P cubosomes had a lattice parameter of 156.2 Å at 1.0 wt % Myrj 59 at 20 °C, higher than that observed when F127 was the stabilizer (see Supplementary Data 1 in the Supporting Information).

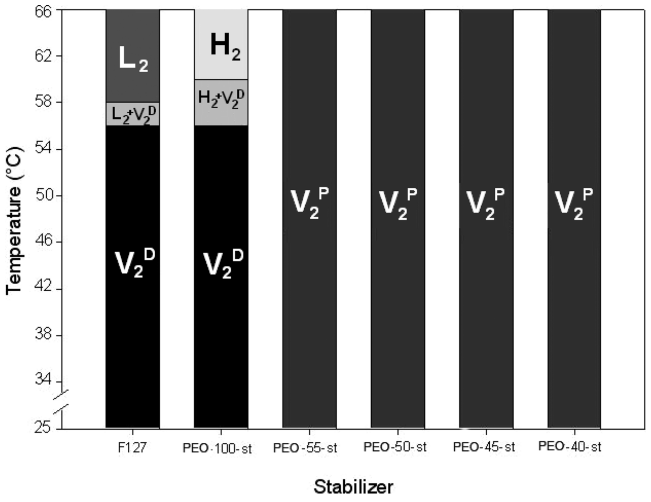

Figure 4. Comparison of phases obtained from SAXS temperature scans of phytantriol dispersions containing 1.0 wt % Pluronic F127, PEO-100-stearate (Myrj 59), PEO-55-stearate, PEO-50-stearate, PEO-45-stearate, and PEO-40-stearate in water.

Cryo-TEM was used to characterize the morphology of the Myrj 59-stabilized phytantriol dispersions with stabilizer concentrations of 0.1, 1.0, and 2.0 wt % in water (Figure 5).

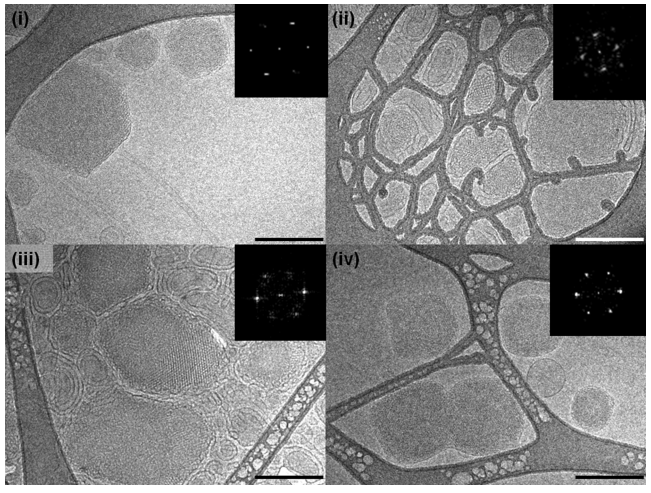

Figure 5. Cryo-TEM images of phytantriol cubosomes and vesicles using (i) Myrj 59, 0.1 wt %, (ii) Myrj 59, 1.0 wt %, (iii) Myrj 59, 2.0 wt %, and (iv) Pluronic F127 (control), 2.0 wt % (scale bar 200 nm). The insets show Fourier transformed images of the internal nanostructure of the particles. (i), (iii), and (iv) show V_2^D colloidal dispersions visualized through the [111] plane. In (ii) observation is through the [112] axis.

Well-dispersed cubosomes were observed at all concentrations. The particles imaged in Figure 5 all display internal long-range order. In Figure 5, panels i, iii, and iv, the observation plane is through the [111] plane with hexagonal packing clearly in the fast Fourier transform (FFT) insets. In Figure 5, panel ii, observation is through the [112] axis. This 2D hexagonal symmetry is indicative of an internal bicontinuous cubic structure.[47−49] The phytantriol cubosomes made with 0.1, 1.0, and 2.0 wt % Myrj 59 are similar in internal structure to those of the control (phytantriol with 2.0 wt % Pluronic F127). As commonly observed during the visualization of cubosomes by cryo-TEM, other vesicular structures were observed but it is

dx.doi.org/10.1021/la301874v | Langmuir 2012, 28, 9223−9232

difficult to quantify the proportion of vesicles in the relatively small sample size tested.[48] While perfect cubelike structures are sometimes seen and thought to be a result of ideal preparation conditions, a range of external particle morphologies are often captured.[45,50] In this study, the overall shapes of the nanoparticles themselves are varied, but as reported and confirmed by SAXS measurements, this does not affect the internal inverse bicontinuous cubic nature of the long-range ordering.[48,49,51,52]

4. DISCUSSION

To date the most frequently used material for the stabilization of inverse bicontinuous cubic phase colloidal dispersions has been the triblock copolymer Pluronic F127. Any potential new candidate for steric stabilization applications would be expected to demonstrate a comparable or improved performance in visual colloidal stability and particle size when compared to Pluronic F127.[17] The studies described herein have enabled the discovery of a new stabilizer (Myrj 59) that fulfills these criteria and has allowed us to assess the relevant structure−property relationships required for good steric stabilization.

Myrj 59 and PEO-55-stearate, despite having similar stearoylpoly(ethylene oxide) structures, have markedly different stabilizing abilities. The difference in efficiency of steric stabilization may be influenced by two factors.

First, the increased stability of phytantriol nanoparticles with Myrj 59 compared to PEO-55-stearate demonstrates the influence of the length of poly(ethylene oxide) chains on effective stabilization. Both Myrj 59 and PEO-55-stearate have the same 18-carbon-long, saturated aliphatic chain, but Myrj 59 has an average of 100 PEO units in the headgroup compared to 55 for PEO-55-stearate. The increased entropic effect of the 100 units compared to 55 units appears to be sufficient to stabilize phytantriol nanoparticles even at low concentrations of stabilizer.

The second factor to take into account is the localization of the polymer within the particle. PEO-stearate stabilizers with 55 or fewer PEO units changed the mesophase of the dispersed particles, with the V_2^P cubic phase being preferred, indicating increased internalization of the stabilizer within the particle nanostructure due to the shortened length of the poly(ethylene oxide) chain (Figure 4). These smaller amphiphiles may be able to penetrate into the particles more readily via the aqueous channels or by virtue of their greater hydrophobicity and hence partition tendency, driving the change in the mesophase. It is likely that this internalization results in less free amphiphile being available to provide surface coverage of the particles and therefore is consistent with the comparatively poorer colloidal stability.[53] The poor performance of the remainder of the shorter Myrj surfactants as stabilizers may also be due to the decreasing PEO chain length, which would be expected to have a reduced capacity to create sufficient steric hindrance to inhibit flocculation.

There was a clear trend between the CAC and stabilization across the Myrj series. Lower CAC values were obtained for the PEO-stearates with fewer PEO units; for PEO-20-stearate the CAC was 9.4×10^{-8} M (Supplementary Data 2 in the Supporting Information). The decrease in monomer concentration required to form aggregates demonstrates the reduced monomer water solubility as the PEO chain length is reduced.

The shorter chained PEO-stearates also showed significant influence over the nanostructure of the dispersed particles, changing the phase from V_2^D to V_2^P, consistent with the behavior of PEO-55-stearate. Again the phase disruption is attributed to increased internalization of amphiphiles into the inverse bicontinuous cubic phase structure, in particular the bilayer. This result highlights that the chemical nature of the PPO block of the Pluronic series is not a necessary factor to induce the phase transition, but that the size of the PEO unit and access to the internal domains appear to be the critical determinants.

Our studies confirm that the concentration of Pluronic F127 required to prevent flocculation is high (at least 0.5 wt %). Flocculation is likely to be the consequence of poor stabilizer coverage on the particle surface and was especially evident at the low F127 concentration (0.1 wt %). However, it was found that Myrj 59 was able to stabilize particles at 0.1 wt %, which is one-fifth of the lowest Pluronic F127 concentration able to make a stable dispersion (by weight). This shows that while Pluronic F127 provided stable dispersions with molar concentration greater than 3.96 mM (0.5 wt %), Myrj 59 provided stable dispersions with less stabilizer, even on a molar basis at 2.0 mM (0.1 wt %). At this low stabilizer concentration, Myrj 59 had a stabilization performance comparable to that of Pluronic F127 at a concentration of 1.0 wt % (7.9 mM). Their nominal average poly(ethylene oxide) chain lengths are both approximately 100 units (F127 possesses two PEO chains). Two possible reasons for the differences in their behavior are that, first, the polydispersity of the commercially manufactured surfactants plays a role in particle PEO coverage density and, second, the stabilizer is anchored differently into the nanoparticle structure. Myrj 59 has a stearoyl chain of 18 carbons and only 1 PEO 100 unit domain, compared to Pluronic F127, which possesses a central poly(propylene oxide) block 65 units in length to anchor to the nanoparticle, coupled at each end to two 100-unit-long PEO domains.

To attempt to further understand the role of the hydrophobicity of the surfactant in anchoring the stabilizer to the surface bilayer, we first examined their respective CACs. The CACs obtained for each stabilizer using DLS are shown in Supplementary Data 2.2 in the Supporting Information. Pluronic F127 had a CAC of 2.2×10^{-6} M, which was slightly larger than that for the CAC obtained using Myrj 59 (1.8×10^{-6} M), indicating similarities in their water solubility; hence, comparing the CACs of F127 and Myrj 59 does not discriminate between the two stabilizers. However, further clarification is provided by comparing the hydrophilic−lipophilic balance (HLB) of each polymer (Supplementary Data 2.2).[54] The greater lipophilicity of Myrj 59 compared to Pluronic F127 (HLBs of 18.8 and 24, respectively) would be expected to indicate the likelihood of increased association of the hydrophobic section of the amphiphile with the hydrophobic domain of the nanostructure particle. However, the structure of Pluronic F127 has twice the amount of PEO as that of Myrj 59, and this is taken into account when the hydrophobe/hydrophile ratios are calculated, so HLB is also not the ideal parameter with which to make such a comparison.

The likely affinity of the hydrophobe toward insertion into the bilayer may be better assessed by examining its octanol/water partition coefficient in isolation from the hydrophilic moieties. This parameter is often used as a strong indicator of the tendency of drug molecules to partition toward the bilayer rather than aqueous solution. The calculated octanol−water partition coefficient, herein expressed as log K_{ow}, of stearyl alcohol (representing the hydrophobic portion of Myrj 59) is 8.38 compared to that of propanol (representing the hydro-

dx.doi.org/10.1021/la301874v | Langmuir 2012, 28, 9223−9232

phobe for Pluronic F127) at 0.25.[55] If the partition coefficient is normalized to 100 poly(ethylene oxide) units, then the normalized log K_{ow} for Myrj 59 is 8.38 and that for Pluronic F127 is 1.76 ($\log(10^{0.25} \times 32.5)$). The hydrophobic section of Myrj 59 is more lipophilic than that of Pluronic F127, perhaps suggesting that Myrj 59 therefore has higher membrane affinity than Pluronic F127.

The stearate moiety of Myrj 59 seems to have greater affinity for binding with the phytantriol monolayer or bilayer compared to the monoolein-based aggregate. Hence, Myrj 59 appears to have preferential stabilization ability with phytantriol when compared to monoolein. This can most likely be attributed to the nature of the aliphatic chains of monoolein and phytantriol. The stearoyl group for Myrj, which does not possess the "kink" present in the oleyl chain of monoolein, may be more comparable in effective length or volume to phytantriol than the unsaturated monoolein chain. Both phytanyl and stearoyl are saturated chains which may pack preferentially when compared to the unsaturated oleoyl chain with stearoyl chains. While measurement of the energy-minimized chain length yielded chains extending to approximately 15 Å for both phytantriol and monoolein from the first carbon atom of the fatty tails to the terminal methyl group, it is clear that their relative volumes will vary significantly. For monoolein, Myrj 59 causes an apparent decrease in the negative curvature of the V_2^P mesophase (characterized by an increase in the lattice parameter; see Supplementary Data 1 in the Supporting Information) when compared to Pluronic F127 at a similar concentration (wt %). This suggests that Myrj 59 significantly affects the equilibrium mesophase structure and thus does not perform as well as F127 for this system.

Although other lyotropic liquid crystal phases (i.e., gyroid, lamellar) can be formed by monoolein, Landh highlighted the fact that the cubic phase of monoolein can exist in the presence of a significant amount of Pluronic F127 and attributed this to the clear amphiphilic nature of the stabilizer.[46] Furthermore, Landh hypothesized that the hydrophobic polypropylene part of the polymer Pluronic F127 resided closer to the polar−apolar interface rather than in the middle of the bilayer environment. The PEO domains were considered to be able to reside in the water channels. This theory has since been extended to the "capping" layer that surrounds liquid crystalline dispersions.[47,51] Anderson et al. proposed that, for the formation of dispersed cubic phases, one of the water channels needs to be open to the external aqueous environment.[56] The monoolein bilayer is thus considered to be a good solvent for the triblock copolymer. Our recent findings that F108 is able to successfully stabilize monoolein cubosomes supports this hypothesis.[17] The results in the current study indicate that the binding of Myrj 59 to phytantriol is higher than that of Pluronic F127.

Several other classes of stabilizers were investigated in addition to the Myrj series in the current study. However, they were all ruled out as they performed poorly compared to the positive control Pluronic F127. The phytosterol ethoxylates BPS-05 and BPS-30 have a bulky and stiff hydrophobic tail (Figure 1). This class of materials will have significantly different critical packing parameters and physiochemical behavior compared to nonionic surfactants that have a fatty acid residue as the hydrophobic anchor. Although Libster et al. were able to form inverse hexagonal phase dispersions of monoolein stabilized with BPS-30,[25] this was performed in the presence of tricaprylin. In the present study it was found that, in the absence of tricaprylin, we were unable to use BPS-30 to disperse particles consisting of monoolein or phytantriol. The use of phytosterol ethoxylates as stabilizers appears to require the presence of additional components for the formation of stable dispersions. In addition to poor binding to the particle due to a likely incompatibility between the hydrophobic tail structure and the monoolein or phytantriol bilayer, on the basis of findings with the Pluronic and Myrj series, the short EO lengths (5 and 30) for the stabilizers were also not sufficient to impart steric stabilization of phytantriol or monoolein dispersions. From the results obtained for both the Myrj stearates and Pluronics, the ideal EO length appears to be at least 100 PEO units.

In the present study, phytantriol was not well dispersed when using vitamin E TPGS as a steric stabilizer, as only a translucent sample with significant aggregated lipid could be produced. However, this contrasts with a study performed by Barauskas et al. in which V_2^P lyotropic liquid crystalline phytantriol dispersions were formed using vitamin E TPGS in water.[39] The difference in outcomes from the two studies may be accounted for by differences in sample preparation, with Barauskas et al. primarily using a vortex and a mechanical mixing protocol, which contrasts with the automated probe sonication method used in the present study. This highlights the importance of sample preparation upon successfully forming dispersions using different stabilizers.

5. CONCLUSION

This research clearly demonstrates differences in stabilization effectiveness between surfactant classes when employed as steric stabilizers for lyotropic liquid crystal dispersions. The length of the PEO chain was shown to be the primary determinant of whether the internal phase structure is retained in the presence of the stabilizer by modulating its internalization into the structure. In the case of a sufficiently long PEO group being present in the structure of the stabilizer, the hydrophobicity of the tail then dictates the relative efficiency of the surfactants to impart colloidal stability at low concentrations by virtue of the avidity for the bilayer. Finally, Myrj 59 was discovered to be an entirely new alternative, commercially available stabilizer for cubosomes. Even at the lowest stabilizer concentration tested (0.1 wt %), Myrj 59 formed well-dispersed phytantriol cubosomes. Surfactants with a reduced number of PEO units compared to Myrj 59 (i.e., <100 units) in the poly(oxyethylene) stearate series were less effective for stabilizing phytantriol cubosomes and induced a transition to primitive cubic phase cubosomes. Myrj 59 was less compatible with monoolein, where V_2^P cubosomes were observed, and provided poorer stability. The identification of Myrj 59 for this application opens new avenues for formulation and functionalization of these interesting delivery systems.

■ ASSOCIATED CONTENT

Supporting Information

Stabilizers DLS and SAXS data set and stabilizers CAC data set. This material is available free of charge via the Internet at http://pubs.acs.org.

■ AUTHOR INFORMATION

Corresponding Author

*[redacted]

[redacted]

Notes

The authors declare no competing financial interest.

■ ACKNOWLEDGMENTS

C.J.D. is the recipient of an Australian Research Council (ARC) Federation Fellowship. J.Y.T.C. is the recipient of a CSIRO Ph.D. studentship. X.M. is the recipient of a CSIRO-Monash University Collaborative Research Post-Doctoral Fellowship. This research was undertaken in part on the SAXS/WAXS beamline at the Australian Synchrotron, Victoria, Australia.

■ REFERENCES

(1) Fong, C.; Le, T.; Drummond, C. J. Lyotropic Liquid Crystal Engineering—Ordered Nanostructured Small Molecule Amphiphile Self-Assembly Materials by Design. *Chem. Soc. Rev.* **2012**, *41*, 1297−1322.

(2) Malmsten, M. Soft Drug Delivery Systems. *Soft Matter* **2006**, *2*, 760−769.

(3) Sagalowicz, L.; Leser, M. E.; Watzke, H. J.; Michel, M. Monoglyceride Self-Assembly Structures as Delivery Vehicles. *Trends Food Sci. Technol.* **2006**, *17*, 204−214.

(4) Yaghmur, A.; Glatter, O. Characterization and Potential Applications of Nanostructured Aqueous Dispersions. *Adv. Colloid Interface Sci.* **2009**, *147−48*, 333−342.

(5) Boyd, B. J.; Whittaker, D. V.; Khoo, S.-M.; Davey, G. Lyotropic Liquid Crystalline Phases Formed from Glycerate Surfactants as Sustained Release Drug Delivery Systems. *Int. J. Pharm.* **2006**, *309*, 218−226.

(6) Phan, S.; Fong, W.-K.; Kirby, N.; Hanley, T.; Boyd, B. J. Evaluating the Link between Self-Assembled Mesophase Structure and Drug Release. *Int. J. Pharm.* **2011**, *421*, 176−182.

(7) Guo, C.; Wang, J.; Cao, F.; Lee, R. J.; Zhai, G. Lyotropic Liquid Crystal Systems in Drug Delivery. *Drug Discovery Today* **2010**, *15*, 1032−1040.

(8) Angelova, A.; Angelov, B.; Mutafchieva, R.; Lesieur, S.; Couvreur, P. Self-Assembled Multicompartment Liquid Crystalline Lipid Carriers for Protein, Peptide, and Nucleic Acid Drug Delivery. *Acc. Chem. Res.* **2011**, *44*, 147−156.

(9) Larsson, K. Cubic Lipid-Water Phases—Structures and Biomembrane Aspects. *J. Phys. Chem.* **1989**, *93*, 7304−7314.

(10) Fraser, S. J.; Dawson, R. M.; Waddington, L. J.; Muir, B. W.; Mulet, X.; Hartley, P. G.; Separovic, F.; Polyzos, A. Development of Cubosomes as a Cell-Free Biosensing Platform. *Aust. J. Chem.* **2011**, *64*, 46−53.

(11) Nguyen, T. H.; Hanley, T.; Porter, C. J. H.; Larson, I.; Boyd, B. J. Phytantriol and Glyceryl Monooleate Cubic Liquid Crystalline Phases as Sustained-Release Oral Drug Delivery Systems for Poorly Water-Soluble Drugs II. In-Vivo Evaluation. *J. Pharm. Pharmacol.* **2010**, *62*, 856−865.

(12) Moghaddam, M. J.; de Campo, L.; Waddington, L. J.; Drummond, C. J. Chelating Phytanyl-EDTA Amphiphiles: Self-Assembly and Promise as Contrast Agents for Medical Imaging. *Soft Matter* **2010**, *6*, 5915−5929.

(13) Liu, G. Z.; Conn, C. E.; Waddington, L. J.; Mudie, S. T.; Drummond, C. J. Colloidal Amphiphile Self-Assembly Particles Composed of Gadolinium Oleate and Myverol: Evaluation as Contrast Agents for Magnetic Resonance Imaging. *Langmuir* **2010**, *26*, 2383−2391.

(14) Norling, T.; Lading, P.; Engstrom, S.; Larsson, K.; Krog, N.; Nissen, S. S. Formation of a Drug Delivery System Based on a Mixture of Monoglyceride and Trigycerides for Use in the Treatment of Periodontal-Disease. *J. Clin. Periodontol.* **1992**, *19*, 687−692.

(15) Spicer, P. T. Progress in Liquid Crystalline Dispersions: Cubosomes. *Curr. Opin. Colloid Interface Sci.* **2005**, *10*, 274−279.

(16) Conn, C. E.; Mulet, X.; Moghaddam, M. J.; Darmanin, C.; Waddington, L. J.; Sagnella, S. M.; Kirby, N.; Varghese, J. N.; Drummond, C. J. Enhanced Uptake of an Integral Membrane Protein, the Dopamine D2L Receptor, by Cubic Nanostructured Lipid Nanoparticles Doped with Ni(II) Chelated EDTA Amphiphiles. *Soft Matter* **2011**, *7*, 567−578.

(17) Chong, J. Y. T.; Mulet, X.; Waddington, L. J.; Boyd, B. J.; Drummond, C. J. Steric Stabilisation of Self-Assembled Cubic Lyotropic Liquid Crystalline Nanoparticles: High Throughput Evaluation of Triblock Polyethylene Oxide-Polypropylene Oxide-Polyethylene Oxide Copolymers. *Soft Matter* **2011**, *7*, 4768−4777.

(18) Muir, B. W.; Acharya, D. P.; Kennedy, D. F.; Mulet, X.; Evans, R. A.; Pereira, S. M.; Wark, K. L.; Boyd, B. J.; Nguyen, T.-H.; Hinton, T. M.; Waddington, L. J.; Kirby, N.; Wright, D. K.; Wang, H. X.; Egan, G. F.; Moffat, B. A. Metal-Free and MRI Visible Theranostic Lyotropic Liquid Crystal Nitroxide-Based Nanoparticles. *Biomaterials* **2012**, *33*, 2723−2733.

(19) Mulet, X.; Kennedy, D. F.; Conn, C. E.; Hawley, A.; Drummond, C. J. High Throughput Preparation and Characterisation of Amphiphilic Nanostructured Nanoparticulate Drug Delivery Vehicles. *Int. J. Pharm.* **2010**, *395*, 290−297.

(20) Nakano, M.; Teshigawara, T.; Sugita, A.; Leesajakul, W.; Taniguchi, A.; Kamo, T.; Matsuoka, H.; Handa, T. Dispersions of Liquid Crystalline Phases of the Monoolein/Oleic Acid/Pluronic F127 System. *Langmuir* **2002**, *18*, 9283−9288.

(21) Dong, Y.-D.; Larson, I.; Hanley, T.; Boyd, B. J. Bulk and Dispersed Aqueous Phase Behavior of Phytantriol: Effect of Vitamin E Acetate and F127 Polymer on Liquid Crystal Nanostructure. *Langmuir* **2006**, *22*, 9512−9518.

(22) Almgren, M.; Borne, J.; Feitosa, E.; Khan, A.; Lindman, B. Dispersed Lipid Liquid Crystalline Phases Stabilized by a Hydrophobically Modified Cellulose. *Langmuir* **2007**, *23*, 2768−2777.

(23) Barauskas, J.; Misiunas, A.; Gunnarsson, T.; Tiberg, F.; Johnsson, M. "Sponge" Nanoparticle Dispersions in Aqueous Mixtures of Diglycerol Monooleate, Glycerol Dioleate, and Polysorbate 80. *Langmuir* **2006**, *22*, 6328−6334.

(24) Dulle, M.; Glatter, O. Internally Self-Assembled Submicrometer Emulsions Stabilized with a Charged Polymer or with Silica Particles. *Langmuir* **2012**, *28*, 1136−41.

(25) Libster, D.; Aserin, A.; Yariv, D.; Shoham, G.; Garti, N. Soft Matter Dispersions with Ordered Inner Structures, Stabilized by Ethoxylated Phytosterols. *Colloids Surf., B* **2009**, *74*, 202−215.

(26) Uyama, M.; Nakano, M.; Yamashita, J.; Handa, T. Useful Modified Cellulose Polymers as New Emulsifiers of Cubosomes. *Langmuir* **2009**, *25*, 4336−4338.

(27) Zhai, J.; Waddington, L.; Wooster, T. J.; Aguilar, M.-I.; Boyd, B. J. Revisiting β-Casein as a Stabilizer for Lipid Liquid Crystalline Nanostructured Particles. *Langmuir* **2011**, *27*, 14757−14766.

(28) Wattendorf, U.; Merkle, H. P. PEGylation as a Tool for the Biomedical Engineering of Surface Modified Microparticles. *J. Pharm. Sci.* **2008**, *97*, 4655−4669.

(29) Ostuni, E.; Chapman, R. G.; Holmlin, R. E.; Takayama, S.; Whitesides, G. M. A Survey of Structure−Property Relationships of Surfaces That Resist the Adsorption of Protein. *Langmuir* **2001**, *17*, 5605−5620.

(30) Harris, J. M.; Martin, N. E.; Modi, M. Pegylation—A Novel Process for Modifying Pharmacokinetics. *Clin. Pharmacokinet.* **2001**, *40*, 539−551.

(31) Harris, J. M.; Chess, R. B. Effect of Pegylation on Pharmaceuticals. *Nat. Rev. Drug Discovery* **2003**, *2*, 214−221.

(32) Torchilin, V. P. Immunoliposomes and PEGylated Immunoliposomes: Possible Use for Targeted Delivery of Imaging Agents. *ImmunoMethods* **1994**, *4*, 244−258.

(33) Lionzo, M. I. Z.; Re, M. I.; Guterres, S. S.; Pohlmann, A. R. Microparticles Prepared with Poly(hydroxybutyrate-co-hydroxyvalerate) and Poly(epsilon-caprolactone) Blends to Control the Release of a Drug Model. *J. Microencapsulation* **2007**, *24*, 175−186.

(34) Goddeeris, C.; Goderis, B.; Van den Mooter, G. Lyotropic, Liquid Crystalline Nanostructures of Aqueous Dilutions of SMEDDS

Revealed by Small-Angle X-ray Scattering: Impact on Solubility and Drug Release. *Eur. J. Pharm. Sci.* **2010**, *40*, 110−117.
(35) Fehér, A.; Csányi, E.; Csóka, I.; Kovács, A.; Erős, I. Thermoanalytical Investigation of Lyotropic Liquid Crystals and Microemulsions for Pharmaceutical Use. *J. Therm. Anal. Calorim.* **2005**, *82*, 507−512.
(36) Jiao, J. Polyoxyethylated Nonionic Surfactants and Their Applications in Topical Ocular Drug Delivery. *Adv. Drug Delivery Rev.* **2008**, *60*, 1663−1673.
(37) Kayali, I.; Suhery, T.; Friberg, S. E.; Simion, F. A.; Rhein, L. D. Lyotropic Liquid-Crystals and the Structural Lipids of the Stratum-Corneum. *J. Pharm. Sci.* **1991**, *80*, 428−431.
(38) Leser, M. E.; Sagalowicz, L.; Michel, M.; Watzke, H. J. Self-Assembly of Polar Food Lipids. *Adv. Colloid Interface Sci.* **2006**, *123*, 125−136.
(39) Barauskas, J.; Johnsson, M.; Tiberg, F. Self-Assembled Lipid Superstructures: Beyond Vesicles and Liposomes. *Nano Lett.* **2005**, *5*, 1615−1619.
(40) Seddon, J. M.; Squires, A. M.; Conn, C. E.; Ces, O.; Heron, A. J.; Mulet, X.; Shearman, G. C.; Templer, R. H. Pressure-Jump X-Ray Studies of Liquid Crystal Transitions in Lipids. *Philos. Trans. R. Soc., A* **2006**, *364*, 2635−2655.
(41) Dong, Y.-D.; Dong, A. W.; Larson, I.; Rappolt, M.; Amenitsch, H.; Hanley, T.; Boyd, B. J. Impurities In Commercial Phytantriol Significantly Alter Its Lyotropic Liquid-Crystalline Phase Behavior. *Langmuir* **2008**, *24*, 6998−7003.
(42) Briggs, J.; Chung, H.; Caffrey, M. The Temperature-Composition Phase Diagram and Mesophase Structure Characterization of the Monoolein/Water System. *J. Phys. II* **1996**, *6*, 723−751.
(43) Tilley, A.; Dong, Y.-D.; Amenitsch, H.; Rappolt, M.; Boyd, B. J. Transfer of Lipid and Phase Reorganisation in Self-Assembled Liquid Crystal Nanostructured Particles Based on Phytantriol. *Phys. Chem. Chem. Phys.* **2011**, *13*, 3026−3032.
(44) Gustafsson, J.; Ljusberg-Wahren, H.; Almgren, M.; Larsson, K. Submicron Particles of Reversed Lipid Phases in Water Stabilized by a Nonionic Amphiphilic Polymer. *Langmuir* **1997**, *13*, 6964−6971.
(45) Gustafsson, J.; LjusbergWahren, H.; Almgren, M.; Larsson, K. Cubic Lipid-Water Phase Dispersed into Submicron Particles. *Langmuir* **1996**, *12*, 4611−4613.
(46) Landh, T. Phase-Behavior in the System Pine Oil Monoglycerides−Poloxamer-407−Water at 20 °C. *J. Phys. Chem.* **1994**, *98*, 8453−8467.
(47) Sagalowicz, L.; Mezzenga, R.; Leser, M. E. Investigating Reversed Liquid Crystalline Mesophases. *Curr. Opin. Colloid Interface Sci.* **2006**, *11*, 224−229.
(48) Sagalowicz, L.; Michel, M.; Adrian, M.; Frossard, P.; Rouvet, M.; Watzke, H. J.; Yaghmur, A.; De Campo, L.; Glatter, O.; Leser, M. E. Crystallography of Dispersed Liquid Crystalline Phases Studded by Cryo-Transmission on Electron Microscopy. *J. Microsc. (Oxford, U.K.)* **2006**, *221*, 110−121.
(49) Kuntsche, J.; Horst, J. C.; Bunjes, H. Cryogenic Transmission Electron Microscopy (Cryo-TEM) for Studying the Morphology of Colloidal Drug Delivery Systems. *Int. J. Pharm.* **2011**, *417*, 120−137.
(50) Barauskas, J.; Johnsson, M.; Johnson, F.; Tiberg, F. Cubic Phase Nanoparticles (Cubosome): Principles for Controlling Size, Structure, and Stability. *Langmuir* **2005**, *21*, 2569−2577.
(51) Johnsson, M.; Lam, Y.; Barauskas, J.; Tiberg, F. Aqueous Phase Behavior and Dispersed Nanoparticles of Diglycerol Monooleate/Glycerol Dioleate Mixtures. *Langmuir* **2005**, *21*, 5159−5165.
(52) Worle, G.; Siekmann, B.; Koch, M. H. J.; Bunjes, H. Transformation of Vesicular into Cubic Nanoparticles by Autoclaving of Aqueous Monoolein/Poloxamer Dispersions. *Eur. J. Pharm. Sci.* **2006**, *27*, 44−53.
(53) Delmas, T.; Piraux, H.; Couffin, A. C.; Texier, I.; Vinet, F.; Poulin, P.; Cates, M. E.; Bibette, J. How To Prepare and Stabilize Very Small Nanoemulsions. *Langmuir* **2011**, *27*, 1683−1692.
(54) Schott, H. Hydrophilic−Lipophilic Balance, Solubility Parameter, and Oil−Water Partition Coefficient as Universal Parameters of Nonionic Surfactants. *J. Pharm. Sci.* **1995**, *84*, 1215−1222.
(55) Tetko, I. V. G., J.; Todeschini, R.; Mauri, A.; Livingstone, D.; Ertl, P.; Palyulin, V. A.; Radchenko, E. V.; Zefirov, N. S.; Makarenko, A. S.; Tanchuk, V. Y.; Prokopenko, V. V. Virtual Computational Chemistry Laboratory—Design and Description. *J. Comput.-Aided Mol. Des* **2005**, *19*, 453−63.
(56) Andersson, S.; Jacob, M.; Lidin, S.; Larsson, K. Structure of the Cubosome—A Closed Lipid Bilayer Aggregate. *Z. Kristallogr.* **1995**, *210*, 315−318.

Supplementary Information Section

High-throughput Discovery of Novel Steric Stabilizers for Cubic Lyotropic Liquid Crystal Nanoparticle Dispersions

Josephine Y.T. Chong [a,b], Xavier Mulet [a,b], Lynne J. Waddington[c], Ben J. Boyd*[b], Calum J. Drummond* [a]

[a] CSIRO Materials Science and Engineering, Private Bag 10, Clayton VIC 3169, Australia.
[b] Monash Institute of Pharmaceutical Sciences, Monash University (Parkville campus), 381 Royal Parade, Parkville VIC 3052, Australia.
[c] CSIRO Materials Science and Engineering, 343 Royal Parade, Parkville VIC 3052, Australia.

Supplementary data 1 – Stabilizers DLS & SAXS data set (*P-*X* = PEO-*X*-stearate). Size and poly-dispersity measurements should not be used exclusively as precise indicators of particle stability, as these values can be misleading without considering sample appearance.

Stabilizer			Phytantriol				Monoolein			
	SAXS	Stabilizer	SAXS		DLS		SAXS		DLS	
	Temp (ºC)	Conc. (Wt%)	Phase	Lattice parameter (Å)	Z-Ave (nm)	PDI	Phase	Lattice parameter (Å)	Z-Ave (nm)	PDI
P-40* (Myrj 52)	20	0.1	V_2^P / V_2^D	96.0/71.4	454	0.21	·	·	·	·
		0.5	V_2^P	105.8	320	0.11	N/A	N/A	229	0.0181
		1	V_2^P	131	332	0.29	N/A	N/A	105	0.016
		2	One ring - not conclusive		333	0.09	·	·	·	·
	37	0.1	V_2^D	64.9	454	0.21	·	·	·	·
		0.5	V_2^P	96	320	0.11	N/A	N/A	229	0.0181
		1	V_2^P	107.1	332	0.29	N/A	N/A	105	0.016
		2	N/A	N/A	333	0.09	·	·	·	·
P-45*	20	1	V_2^P	120.4	315	0.05	·	·	·	·
	37	1	V_2^P	106.7	315	0.05	·	·	·	·
P-50*	20	1	V_2^P	107.5	257	0.03	·	·	·	·
	37	1	V_2^P	99.7	257	0.03	·	·	·	·
P-55*	20	1	V_2^P	103.3	346	0.05	·	·	·	·
	37	1	V_2^P	96.7	346	0.05	·	·	·	·
P-100* (Myrj 59)	20	0.1	V_2^D	69.4	381	0.46	V_2^P	151.6	287	0.0562
		0.5	V_2^D	70	263	0.27	V_2^P	153	304	multi
		1	V_2^D	70.1	250	0.15	V_2^P	156.2	671	0.055
		2	V_2^D	69.9	327	0.31	·	·	·	·
	37	0.1	V_2^D	63.8	381	0.46	N/A	N/A	287	0.0562
		0.5	V_2^D	64.2	263	0.27	V_2^P -mix	128	304	multi
		1	V_2^D	64.7	250	0.15	N/A	N/A	671	0.055
		2	V_2^D	64.7	327	0.31	·	·	·	·

Stabilizer	SAXS Temp (ºC)	Stabilizer Conc. (Wt%)	Phytantriol				Monoolein			
			SAXS		DLS		SAXS		DLS	
			Phase	Lattice parameter (Å)	Z-Ave (nm)	PDI	Phase	Lattice parameter (Å)	Z-Ave (nm)	PDI
Tween 80	20	0.1	N/A	N/A	478	0.44	·	·	·	·
		0.5	V_2^P / V_2^D	101.3/78.9	611	0.58	·	·	·	·
		1	V_2^P	114.25	1179	0.86	·	·	·	·
		2	N/A	N/A	242	0.38	·	·	·	·
	37	0.1	V_2^D	66.2	478	0.44	·	·	·	·
		0.5	V_2^P / V_2^D	92.4/70.8	611	0.58	·	·	·	·
		1	V_2^P	101.3	1179	0.86	·	·	·	·
		2	N/A	N/A	242	0.38	·	·	·	·
BPS30	20	0.1	V_2^P	96.1	338	0.53	·	·	·	·
		0.5	V_2^P	114.3	364	0.18	·	·	·	·
		1	N/A	N/A	309	0.13	·	·	·	·
		2	N/A	N/A	492	0.16	·	·	·	·
	37	0.1	V_2^P	93.1	338	0.53	·	·	·	·
		0.5	V_2^P	101.8	364	0.18	·	·	·	·
		1	N/A	N/A	309	0.13	·	·	·	·
		2	N/A	N/A	492	0.16	·	·	·	·
Vit TPGS	20	0.1	N/A	N/A	365	0.45	·	·	·	·
		0.5	N/A	N/A	373	0.41	·	·	·	·
		1	N/A	N/A	576	0.78	·	·	·	·
		2	N/A	N/A	917	0.81	·	·	·	·
	37	0.1	One ring - not conclusive		365	0.45	·	·	·	·
		0.5	N/A	N/A	373	0.41	·	·	·	·
		1	N/A	N/A	576	0.78	·	·	·	·
		2	N/A	N/A	917	0.81	·	·	·	·

Stabilizer			Phytantriol				Monoolein			
	SAXS	Stabilizer	SAXS		DLS		SAXS		DLS	
	Temp (ºC)	Conc. (Wt%)	Phase	Lattice parameter (Å)	Z-Ave (nm)	PDI	Phase	Lattice parameter (Å)	Z-Ave (nm)	PDI
Pluronic F127	20	0.1	V_2^D	69.9	193	0.16	V_2^P	141.2	·	·
		0.5	V_2^D	69.4	300	0.22	V_2^P	146	194	Multi
		1	V_2^D	69.3	319	0.33	·	·	243	7.31E-16
		2	V_2^D	69.6	230	0.23	·	·	·	·
	37	0.1	V_2^D	63.9	193	0.16	V_2^P	130.7	·	·
		0.5	V_2^D	63.3	300	0.22	V_2^P	134.1	194	Multi
		1	V_2^D	63.3	319	0.33	·	·	243	7.31E-16
		2	V_2^D	63.3	230	0.23	·	·	·	·

Supplementary data 2 – Stabilizers CAC data set

2.1 Critical Aggregation Concentration determination

The critical aggregation concentration (CAC) of each steric stabilizer was determined by using changes in scattered light intensity from dynamic light scattering (DLS) (Wyatt DynaPro Plate Reader, Wyatt Technology Corporation, US). This DLS instrument uses a 50 mW programmable laser (λ = 831.5 nm) with a detection at 158° and a thermostated sample chamber set to 25 °C. The viscosity and refractive index of water at 25°C, 0.8937 cP and 1.333, respectively were used for all measurements. In the absence of aggregates, the intensity of backscattered light is comparable to that of the solvent. In the presence of aggregates, the intensity of backscattered light increases with increasing concentration of aggregates.[1] Solutions were prepared in Milli-Q water by dilution from 20 mg/mL steric stabilizer stock solutions and analyzed using a polystyrene clear bottom low volume 384 well plate (Corning, USA). Ten acquisitions were collected for each sample to ensure reproducibility. Pluronic F127 served as a positive control and pure water wells were used as a blank. Intensity and size information was obtained from on the Wyatt DynaPro plate reader using the software package DYNAMICS v.7.

2.2 Table of Amphiphile HLB and CAC

Amphiphile	HLB	CAC (x 10^{-6} M)
Pluronic F127	22[2]	2.2
Vitamin TPGS	13[3]	1.7
Cremophor EL	13.5[4]	8.5
Tween 80	15[4]	1.9
Nikkol BPS-30	18[5]	1.4
PEO-20-Stearate	15[6]	9.4
PEO-25-Stearate	15[7]	6.7
PEO-40-Stearate	16.9[2]	4.1
PEO-45-Stearate	18[7]	3.8
PEO-50-Stearate	17.9[8]	3.4
PEO-55-Stearate	18[7]	3.2
PEO-100-Stearate	18.8[2]	1.8

HLB and CAC of the commercially available alternative amphiphiles. HLBs were obtained from literature and product websites. CACs were determined from dynamic light scattering experiments.

References (Supplementary data 2.1 and 2.2)

1. Wallace, S. J.; Li, J.; Nation, R. L.; Prankerd, R. J.; Velkov, T.; Boyd, B. J., *J. Phys. Chem. B* **2010,** 114, 4836-4840.
2. Schmidts, T.; Dobler, D.; Nissing, C.; Runkel, F., **2009,** 338, 184-192.
3. Mu, L.; Feng, S. S., **2002,** 80, 129-144.
4. Constantinides, P. P.; Yiv, S. H., **1995,** 115, 225-234.
5. Nikko Chemicals Shanghai Co., L. Polyoxyethylene phytosterol. http://www.nikkol.cn/Index.asp?page=details&id=373&categoryid=68 (19.11.2011).
6. CRODA Product summary; Myrj S20. http://www.croda.com/home.aspx?view=dtl&d=content&s=151&r=317&p=2138&prodID=793 (19.11.2011).
7. Nikko Chemicals Shanghai Co., L. Product Overview; Polyoxyethylene fatty acid ester. http://www.nikkol.cn/index.asp?page=category&categoryid=65 (19.11.2011).
8. CRODA Product summary; Myrj S50. http://www.croda.com/home.aspx?view=dtl&d=content&s=151&r=317&p=2138&prodID=796 (19.11.2011).

2.3 CAC data sets

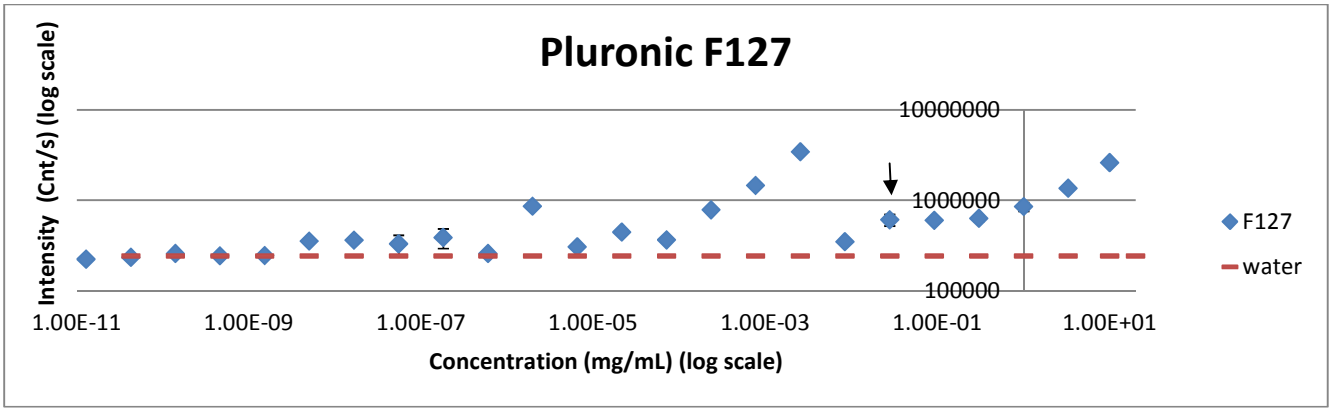

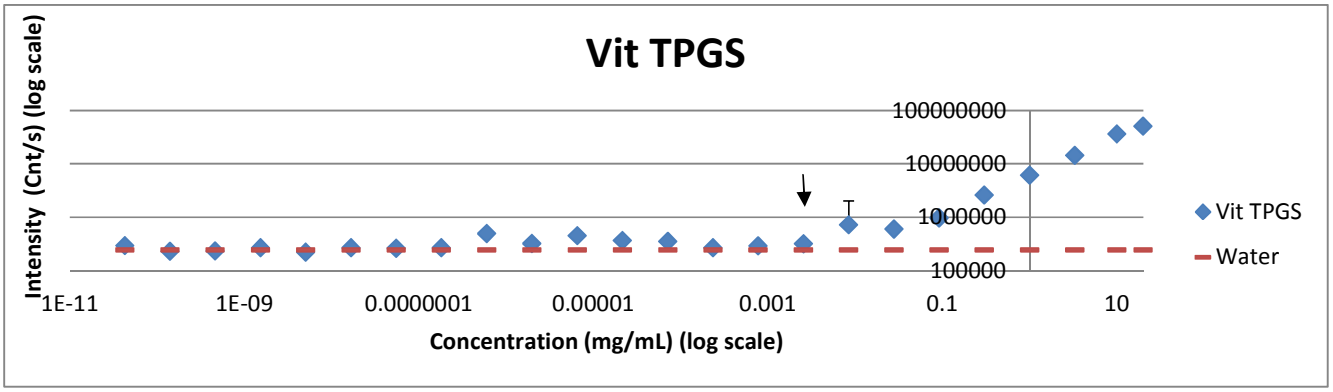

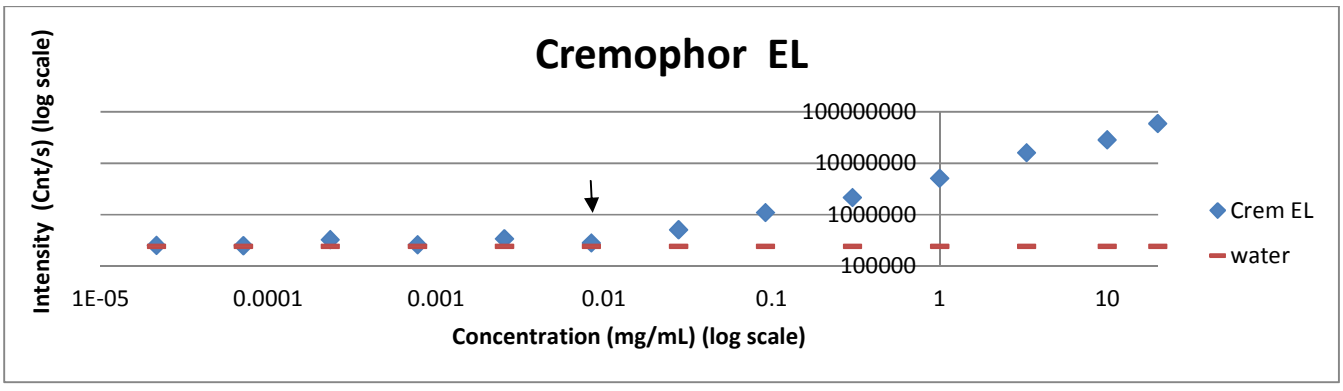

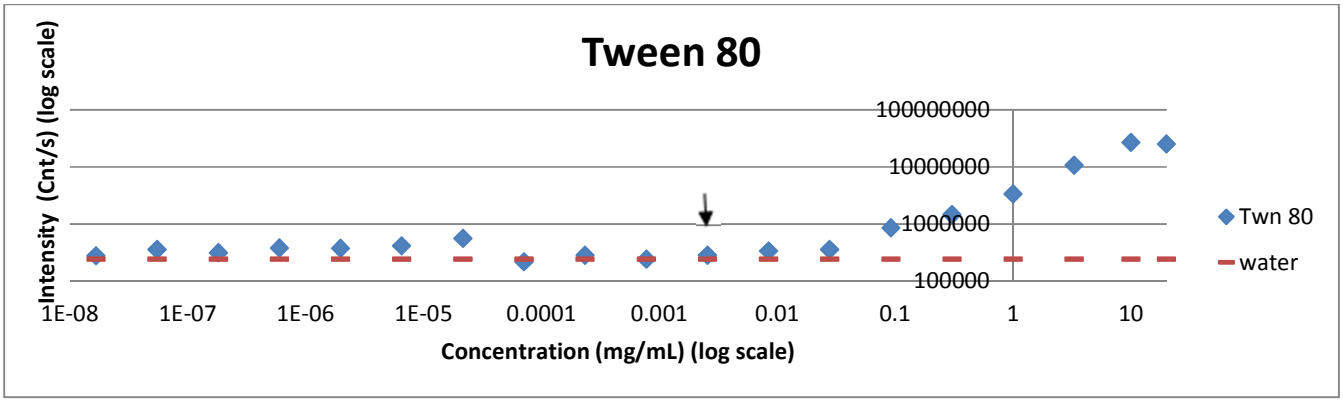
Tween 80
Intensity (Cnt/s) (log scale)
100000000
10000000
1000000
100000
1E-08
1E-07
1E-06
1E-05
0.0001
0.001
0.01
0.1
1
10
Concentration (mg/mL) (log scale)
Twn 80
water

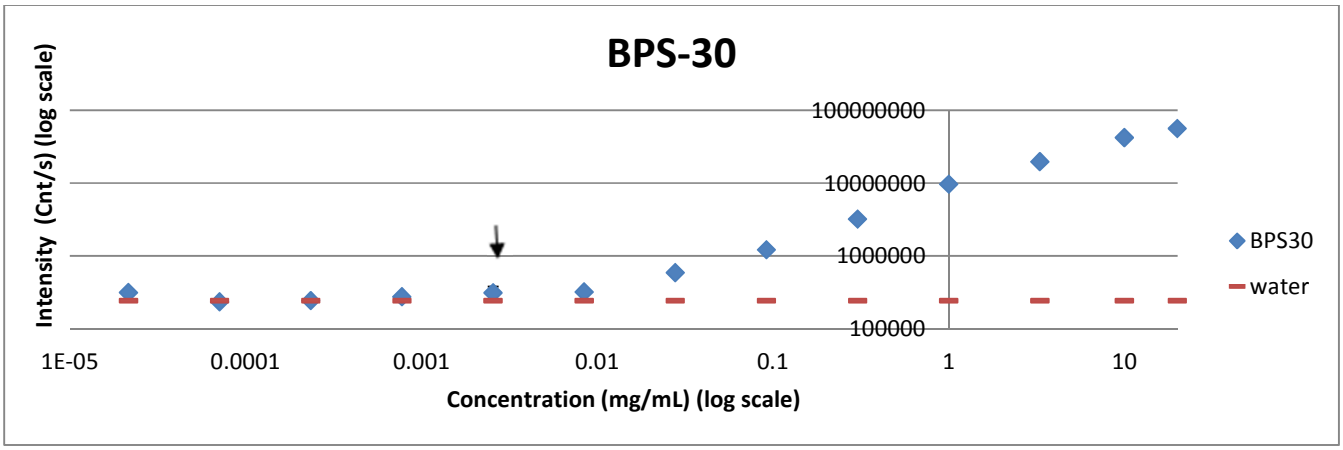
BPS-30
Intensity (Cnt/s) (log scale)
100000000
10000000
1000000
100000
1E-05
0.0001
0.001
0.01
0.1
1
10
Concentration (mg/mL) (log scale)
BPS30
water

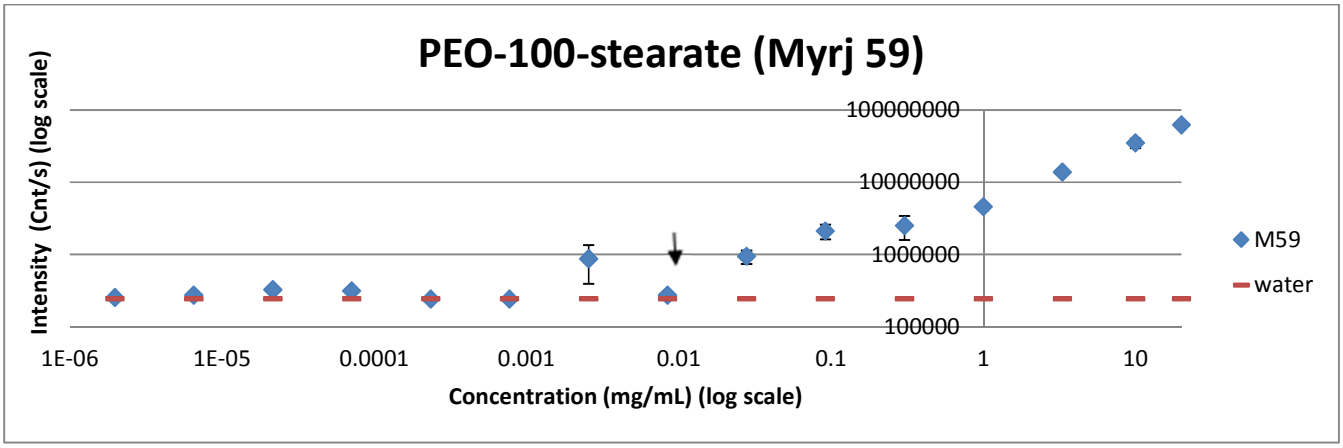
PEO-100-stearate (Myrj 59)
Intensity (Cnt/s) (log scale)
100000000
10000000
1000000
100000
1E-06
1E-05
0.0001
0.001
0.01
0.1
1
10
Concentration (mg/mL) (log scale)
M59
water

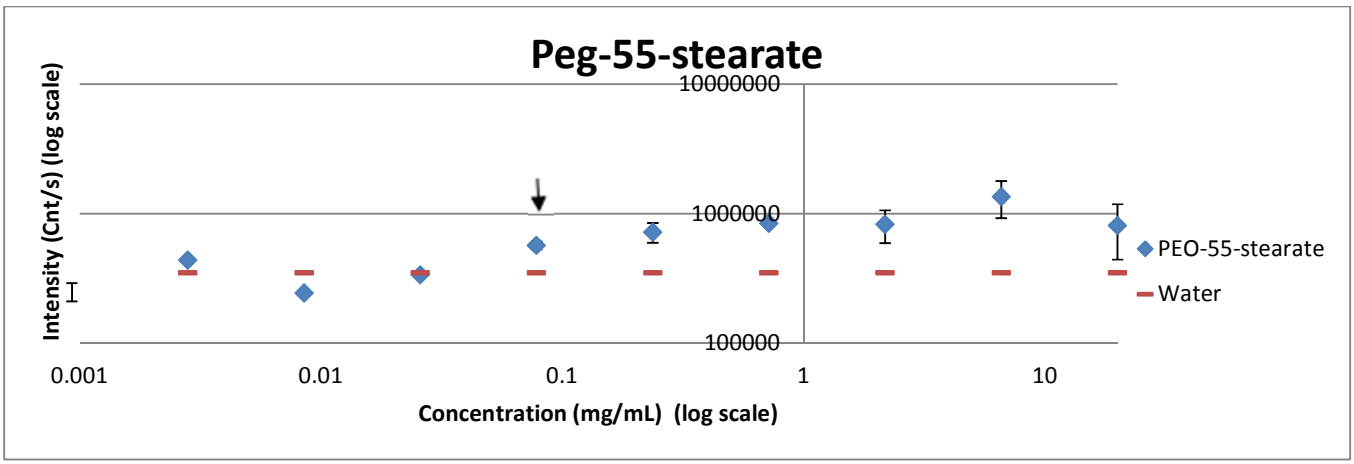
Peg-55-stearate
Intensity (Cnt/s) (log scale)
10000000
1000000
100000
0.001
0.01
0.1
1
10
Concentration (mg/mL) (log scale)
PEO-55-stearate
Water

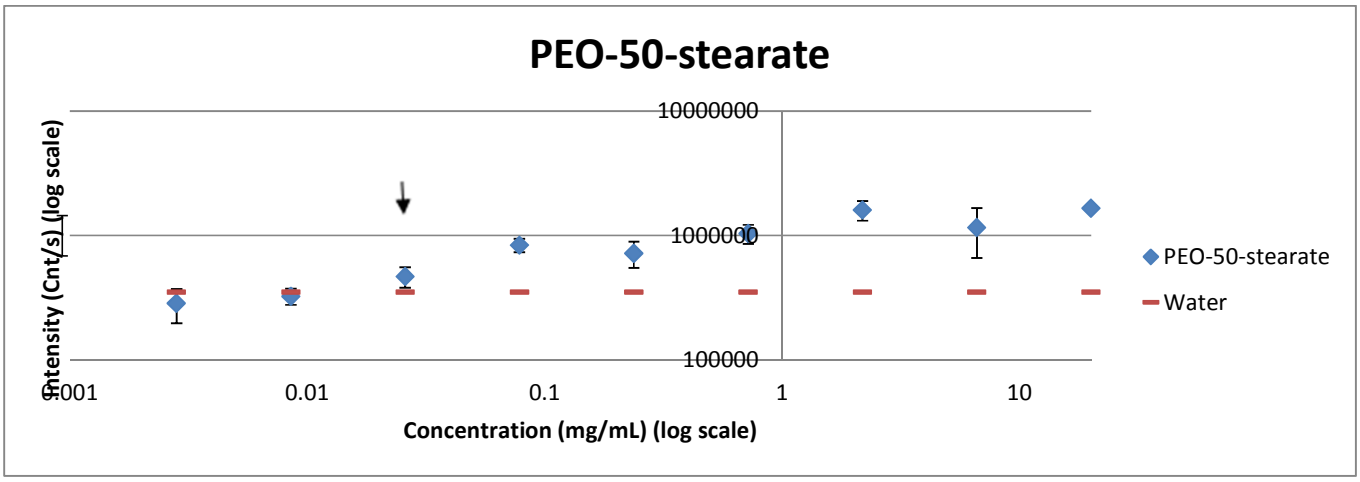
PEO-50-stearate
Intensity (Cnt/s) (log scale)
10000000
1000000
100000
0.001
0.01
0.1
1
10
Concentration (mg/mL) (log scale)
PEO-50-stearate
Water

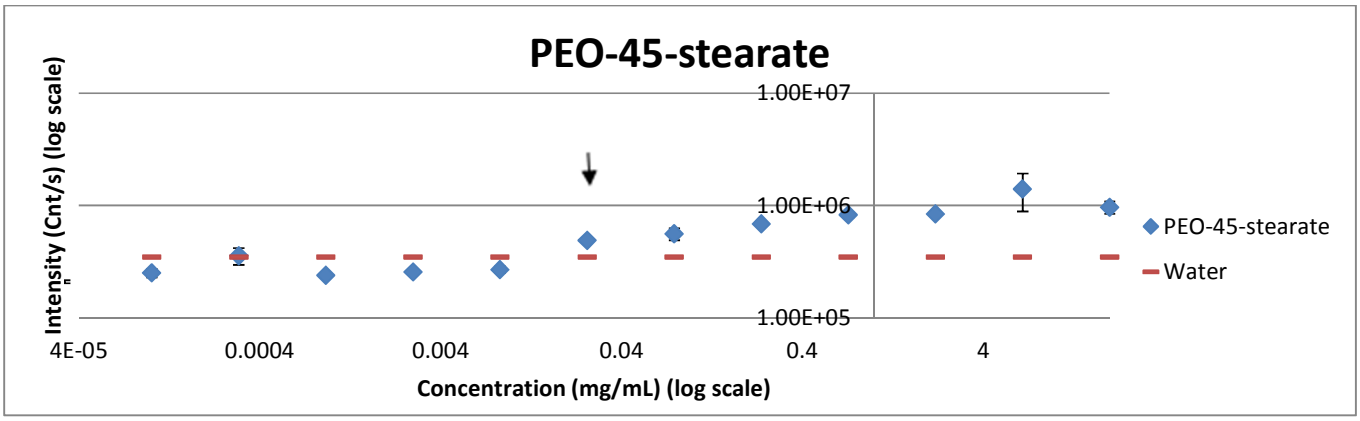
PEO-45-stearate
Intensity (Cnt/s) (log scale)
1.00E+07
1.00E+06
1.00E+05
4E-05
0.0004
0.004
0.04
0.4
4
Concentration (mg/mL) (log scale)
PEO-45-stearate
Water

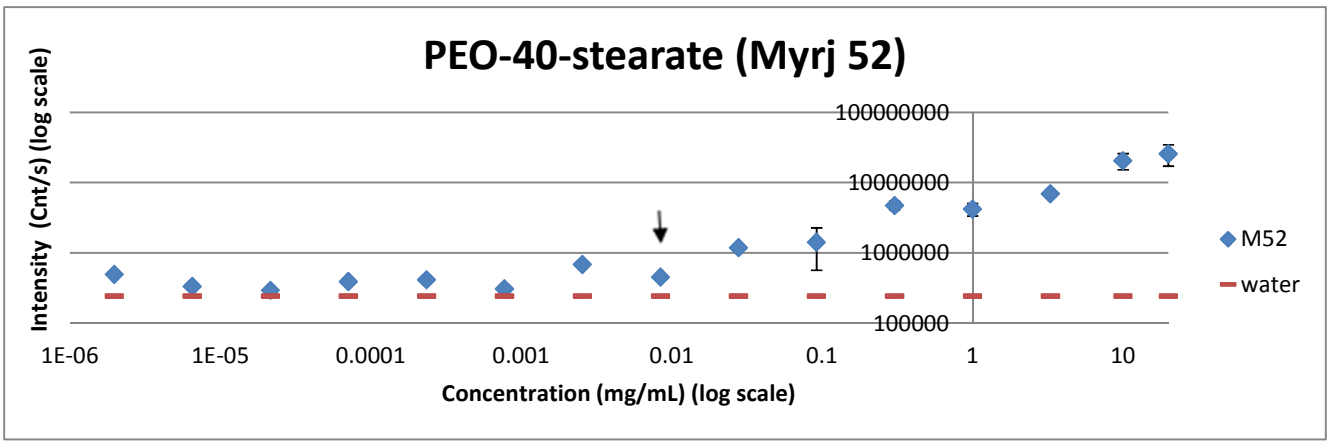
PEO-40-stearate (Myrj 52)
Intensity (Cnt/s) (log scale)
100000000
10000000
1000000
100000
1E-06
1E-05
0.0001
0.001
0.01
0.1
1
10
Concentration (mg/mL) (log scale)
M52
water

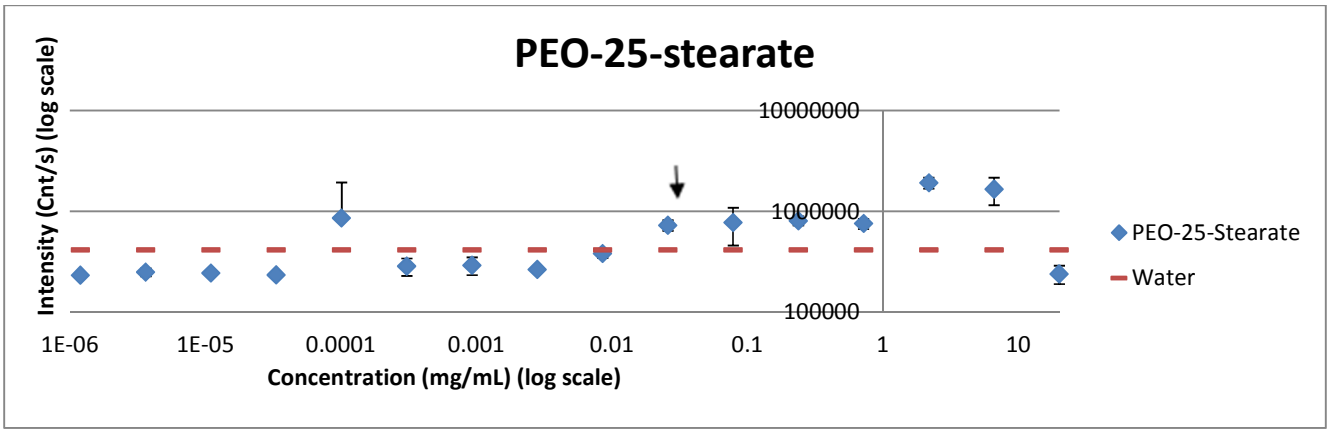
PEO-25-stearate
Intensity (Cnt/s) (log scale)
10000000
1000000
100000
1E-06
1E-05
0.0001
0.001
0.01
0.1
1
10
Concentration (mg/mL) (log scale)
PEO-25-Stearate
Water

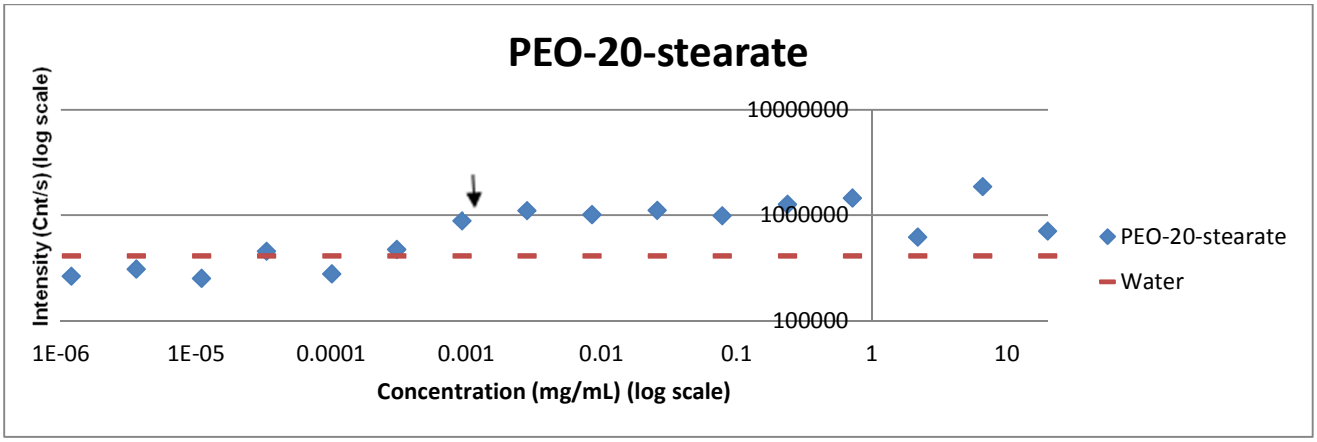
PEO-20-stearate
Intensity (Cnt/s) (log scale)
10000000
1000000
100000
1E-06
1E-05
0.0001
0.001
0.01
0.1
1
10
Concentration (mg/mL) (log scale)
PEO-20-stearate
Water

Chapter 4

Accelerated Stability Assay (ASA) for Colloidal Systems

Josephine Y.T. Chong, Xavier Mulet, Ben J. Boyd and Calum J. Drummond

Published: *ACS Combinatorial Science* (*Technology Note*) **2014**, 16, 205-210

Declaration for Chapter 4

Declaration by candidate

In the case of Chapter 4, the nature and extent of my contribution to the work was the following:

Nature of contribution	Extent of contribution (%)
Research design, development of methods, performance of data collection and analysis, manuscript preparation	85

The following co-authors contributed to the work:

Name	Nature of contribution
Xavier Mulet	Supervision; input into method development; intellectual input; input into manuscript preparation
Ben Boyd	Supervision; intellectual input; input into manuscript preparation
Calum Drummond	Supervision; intellectual input; input into manuscript preparation

Candidate's signature: [redacted] **Date:** **10.7.2014**

Declaration by co-authors

The undersigned hereby certify that:

(13) the above declaration correctly reflects the nature and extent of the candidate's contribution to this work, and the nature of the contribution of each of the co-authors.

(14) they meet the criteria for authorship in that they have participated in the conception, execution, or interpretation, of at least that part of the publication in their field of expertise;

(15) they take public responsibility for their part of the publication, except for the responsible author who accepts overall responsibility for the publication;

(16) there are no other authors of the publication according to these criteria;

(17) potential conflicts of interest have been disclosed to (a) granting bodies, (b) the editor or publisher of journals or other publications, and (c) the head of the responsible academic unit; and

(18) the original data are stored at the following location(s) and will be held for at least five years from the date indicated below:

Location of data storage: CSIRO Materials Science and Engineering, Ian Wark Laboratory, Bayview Avenue, Clayton 3168, Australia.

Co-authors' signature for Chapter 4:

Signed:  **Date:** **10.1.2014**

Xavier Mulet

Signed: 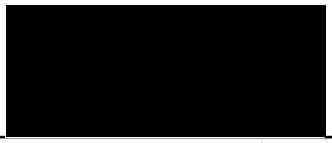 **Date:** **28.2.2014**

Ben J. Boyd

Signed:  **Date:** **12.4.2014**

Calum J. Drummond

ACS Combinatorial Science

Technology Note

pubs.acs.org/acscombsci

Accelerated Stability Assay (ASA) for Colloidal Systems

Josephine Y. T. Chong,[†,‡] Xavier Mulet,*[,†,‡] Ben J. Boyd,*[,‡] and Calum J. Drummond*[,†,§]

[†]CSIRO Materials Science and Engineering, Private Bag 10, Clayton, Victoria 3169, Australia

[‡]Drug Delivery, Disposition and Dynamics, Monash Institute of Pharmaceutical Science, Monash University (Parkville Campus), 381 Royal Parade, Parkville, Victoria 3052, Australia

[§]School of Applied Sciences, College of Science, Engineering and Health, RMIT University, GPO Box 2476, Melbourne, Victoria 3001, Australia

Supporting Information

ABSTRACT: Assessment of the stability of colloidal systems, in particular lyotropic liquid crystalline dispersions, such as cubosomes and hexosomes, is typically performed qualitatively or with limited throughput on specialized instruments. Here, an accelerated stability assay for colloidal particles has been developed in 384-well plates with standard laboratory equipment. These protocols enable quantitative assessments of colloidal stability. To demonstrate the applicability of the assay, several steric stabilizers for cubic phase nanostructured particles (cubosomes) have been compared to the current "gold standard" Pluronic F127.

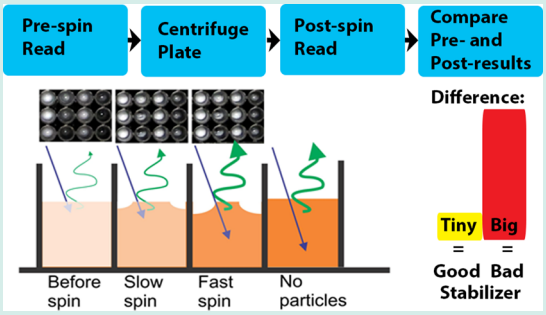

KEYWORDS: *cubosome, lyotropic liquid crystalline nanoparticle, colloidal stability, steric stabilization, accelerated stability assay*

Lyotropic liquid crystalline nanostructured particles have been explored for their potential in drug delivery systems. Liposomes, based on a 1D lamellar lyotropic liquid crystalline structure, have been extensively used as drug delivery vehicles with 12 clinically approved liposomal drug formulations on the market and twenty-two liposomal drugs undergoing clinical trials.[1,2] Particles based on other lyotropic liquid crystalline structures, such as cubosomes (dispersed inverse bicontinuous cubic phase) and hexosomes (dispersed inverse hexagonal phases) are being developed as potential drug delivery systems. The key advantages to these nanostructured particles with complex internal structure include their potential for controllable release and their increased lipid volume fraction per particle, which provides a lipophilic area for containing poorly water-soluble therapeutics.[3,4] These dispersed drug delivery systems typically consist of the lipid matrix, and a steric stabilizer, which provides the dispersion with varying degrees of stability, depending on the lipid and stabilizer combination and concentrations.[5,6]

The steric stabilizer is a key component of nanostructured particle preparation, particularly in the case of cubosomes and hexosomes where the internal interfacial area is high and may sequester stabilizer otherwise available for colloidal stability.[7] These cubosomes and hexosomes often consist of phytantriol as the core lipid matrix (Figure 1). A quantitative measure is required to assess the effectiveness of the steric stabilization conferred to lyotropic liquid crystalline nanostructured particles. Typically, the stabilizers used are amphiphilic polymers with the hydrophilic region consisting of one or more poly(ethylene glycol) (PEG) domains (e.g., Tween and Cremophor stabilizers). PEG has been shown to be able to form a stealth corona around liposomes, significantly reducing the rapid uptake of intravenously injected particulate drug carriers by cells of the mononuclear phagocyte system (MPS).[8,9] The most frequently used steric stabilizer for cubosomes and hexosomes is the nonionic triblock copolymer Pluronic F127. It consists of two blocks of PEG (100 monomer units on average) on either side of a poly(propylene oxide) domain (65 monomer units on average) (Figure 1). Pluronic F108 and Myrj 59 (PEG100-stearate), also represented in Figure 1, stabilize inverse bicontinuous cubic phases of phytantriol dispersions as, or more efficiently than Pluronic F127.[5,6]

Despite the advent of high-throughput preparation and characterization techniques to identify the effect of the steric stabilizer on lyotropic liquid crystal phase behavior,[3] there has so far been no assay available to screen new steric stabilizers over a large range of concentrations to quantifiably assess their effectiveness. The current norm is to use a visual assessment to determine if particle aggregation has occurred. This technique, however, is only suitable for differentiating poor stabilizers from stabilizers which are capable of producing milky dispersions void of aggregates. Dynamic light scattering may also be used to detect changes in particle size, however large aggregates (>1 μm) are typically difficult to detect as they fall outside of the detection range of typical laboratory instruments. Dynamic light scattering is therefore not a reliable measure of particle

Received: December 5, 2013
Revised: February 26, 2014
Published: March 27, 2014

   dx.doi.org/10.1021/co400155y | *ACS Comb. Sci.* 2014, 16, 205−210

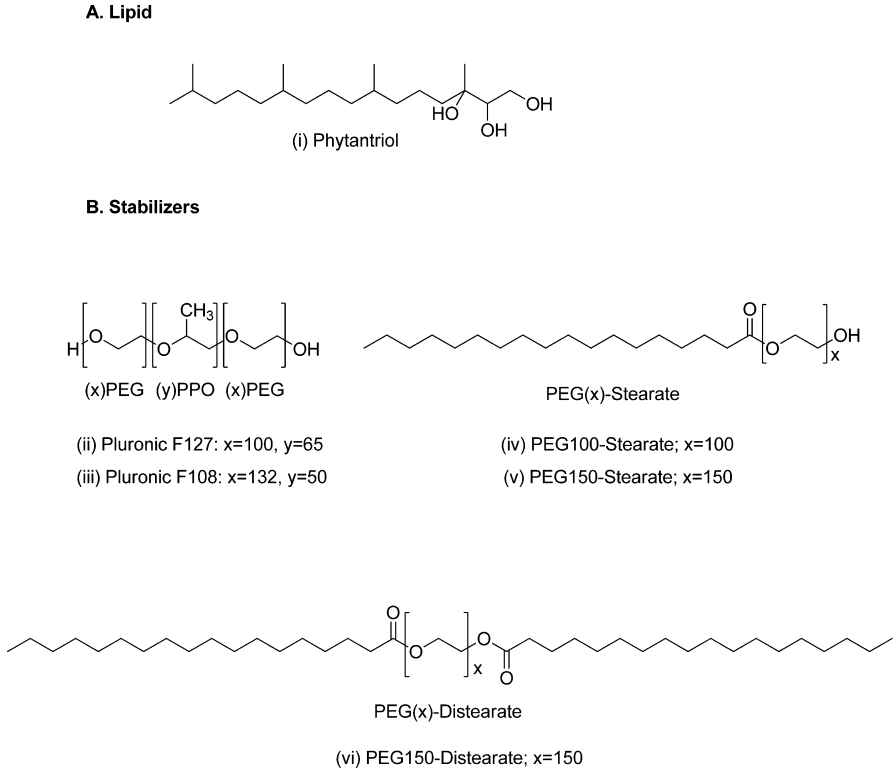

Figure 1. Chemical structures of (i) Phytantriol, (ii) Pluronic F127 (control steric stabilizer), (iii) Pluronic F108, (iv) PEG100-stearate, (v) PEG150-stearate, and (vi) PEG150-distearate.

stability as it may measure a net reduction in average size despite the presence of aggregates. At present, dispersion stability can be quantified by using a microprocessor-controlled analytical centrifuge that detects demixing phenomena (e.g., particle aggregation and clarification) of the dispersed systems during centrifugation over the whole sample length.[10,11] However, this is a low-throughput technique. Using a similar principle, detection of particle aggregation or clarification on centrifugation, herein we demonstrate the use of a fluorescence-based reproducible, alternative accelerated stability assessment technique which uses standard laboratory instruments (i.e., 96- or 384-well plate reader and plate centrifuge) to assess colloidal stability (Figure 2). A fluorescence approach was taken because of its high sensitivity to changes of sample stability, high signal to-noise and high reproducibility.

The principle of this assay is that the intensity of fluorescence measured is proportional to the quantity of particles dispersed in the solution. Centrifugation of the samples drives particle aggregation and these concentrate at the air water interface of the sample well. This is due to the low density of the lipid rich domain. Aggregation preferentially occurs on the edges of the multititer plate wells. The decrease in particle concentration in solution leads to reduced excitation and emission light scattering which results in an increase in emission signal in poorly stabilized samples. The magnitude of the change in fluorescence intensity following sample centrifugation correlates to particle aggregation and permits the quantification of the relative effectiveness of particle stabilization. Stable systems in which little aggregation occurs can be identified due to minimal change in fluorescence signal intensity before and after centrifugation (Figure 2).

The ability of this assay to quantifiably assess stabilizer performance is demonstrated by testing several steric stabilizers

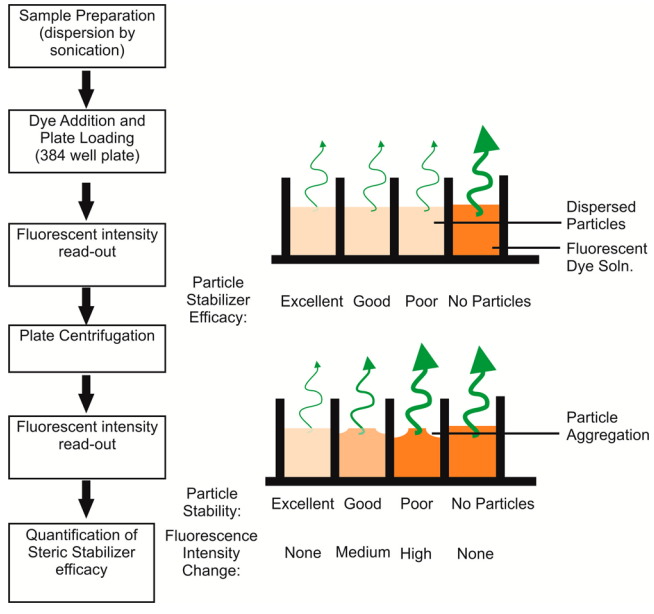

Figure 2. Schematic of the accelerated stability assay.

including Pluronic F108, Myrj 59 (PEG100-stearate), PEG150-stearate and PEG150-distearate, against Pluronic F127 as control (Figure 1). PEG150-stearate has a PEG domain of 150 monomer units on average compared to the 100 monomer units of Myrj 59 on average. In contrast to PEG150-stearate, PEG150-distearate is a molecule with two hydrophobic domains, one at each end of a PEG domain which is 150 monomer units long on average. Amphiphilic block configuration (i.e., terminal block ends using hydrophobic or hydrophilic blocks) of triblock copolymers used for steric

dx.doi.org/10.1021/co400155y | ACS Comb. Sci. 2014, 16, 205−210

stabilization may play an important part in stabilizer effectiveness.

The aim of this assay was to rapidly verify the effectiveness of a steric stabilizer for colloidal lyotropic liquid crystalline dispersions. Stabilizer effectiveness is dependent on a wide range of parameters, which includes stabilizer concentration, stabilizer structure (i.e., length of the amphiphilic domains, such as PEG length), temperature and buffer pH. This assay permits investigators to screen the effectiveness of steric stabilizers using centrifugation to accelerate the aggregation process within colloidal systems. Because of the relative densities of the aggregated lipid domain and the aqueous domain, this typically results in particle aggregation at the sample surface. As illustrated by Figure 2, particle aggregation occurred around the edge of the well, on the surface of the sample after centrifugation. Typically the longer centrifugation time and greater the spin speeds, the larger the dispersion destabilization observed.

Accelerated Stability Assay (ASA) with Different Concentrations of Pluronic F127. Demonstration of the discriminatory power of this assay was demonstrated using Pluronic F127, for inverse bicontinuous cubic phase dispersions (cubosomes) made up of phytantriol, because the dependence of stability on stabilizer concentration is well characterized. The ASA should differentiate quantifiably between known "poorly" stabilized (3 wt % Pluronic F127) and adequately stabilized (10 wt % Pluronic F127) dispersions. Consequently the colloidal stability of phytantriol cubosomes stabilized with Pluronic F127 at 3, 5, 7, 10, and 12 wt % stabilizer concentrations was tested using the ASA assay.

A change in fluorescence signal intensity from post and prespin cycles at 1800 rpm for 5 min was most evident for those with lower stabilizer concentrations (Figure 3). The magnitude of the fluorescence signal intensity change decreased with increased stabilizer concentration and therefore enhanced stability. For example, the change in fluorescence signal intensity for dispersions stabilized with 3 wt % Pluronic F127 was 1000 A.U. For the more stable dispersions (10 and 12 wt % Pluronic F127/phytantriol dispersions), this change was reduced by at least an order of magnitude. The magnitude of the change in fluorescence signal intensity is inversely proportional to particle stability. These reproducible and discernible changes make this assay suitable for the assessment of particle stability.

The fact that otherwise stable dispersions can be destabilized through further centrifugation means that this assay should be applicable to a range of systems. A second centrifugation spin at 2000 rpm for 5 min gives rise to further colloidal instability. The change in signal intensity doubled for all dispersions, while retaining the same inversely proportional trend with regard to stabilizer concentration seen after the first spin at 1800 rpm (Figure 3). This assay, with experiments performed in triplicates, is therefore adaptable to the differential effectiveness of stabilizers simply by increasing centrifugal speed or time.

It is imperative that to assess the stability of other steric stabilizers, a standard control calibration (in this case Pluronic F127) be present as part of the ASA performed. This was particularly important as the fluorescence detection system is sensitive to parameters such as concentration, bleaching and environmental variables. The ASA developed here demonstrates a practical accelerated method using standard laboratory instruments that has the ability to compare large data sets of samples (i.e., multiwell plate) in order to determine the steric stabilization effectiveness of various steric stabilizers compared to Pluronic F127.

Real Time Intrinsic Colloidal Stability. Aggregation is inevitable in colloidal systems that are not thermodynamically stable. Phytantriol dispersions stabilized with Pluronic F127 has poor stability at very low stabilizer concentrations (i.e., 1 wt %) shortly after sonication. To ensure that the ASA reflects the likely stability that would be expected to occur over time without centrifugation, but at accelerated time scales, a comparable experiment was performed using identical conditions and reagents with only the centrifugation aspect excluded. For this set of dispersions (phytantriol cubosomes stabilized with Pluronic F127 at 3, 5, 7, 10, and 12 wt %), fluorescence was measured daily over a two week time period. At 24 h following preparation, the dispersions with the lower stabilizer concentration were showing higher changes in signal intensity compared to the higher 10 wt % stabilizer concentration typically used in cubosome preparation (Figure 4). Over time, all samples produced higher fluorescence signal intensities, representative of gradual increase in particle aggregation occurring within all the samples. The changes in signal intensity were comparable to those obtained with the

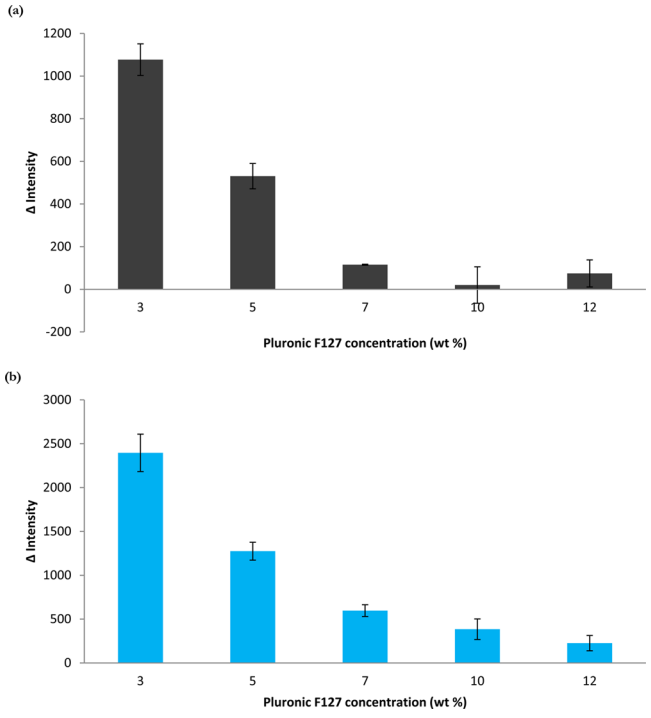

Figure 3. Pluronic F127 concentration vs Δ intensity after (a) 1800 rpm, (b) 2000 rpm for 5 min.

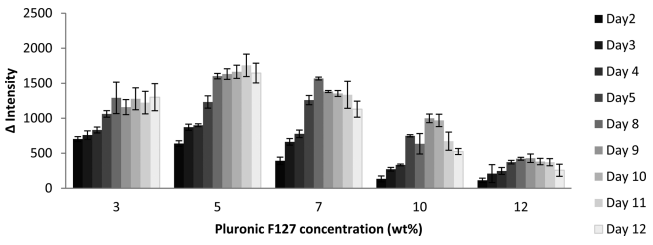

Figure 4. Pluronic F127 fluorescence signal intensity change progression with time (2 weeks).

dx.doi.org/10.1021/co400155y | ACS Comb. Sci. 2014, 16, 205−210

accelerated stability assay demonstrating its validity. In addition to increasing fluorescence signal intensities, visual cues of particle aggregation occurring in phytantriol cubosome systems over time also occurred for all five stabilizer concentrations, 3, 5, 7, 10, and 12 wt %, contained in 1.5 mL microcentrifuge tubes (see Supporting Information).

Using ASA to Compare Alternative Steric Stabilizers with Pluronic F127. To demonstrate the potential of this assay, we also quantified the performance of a range of previously reported and new steric stabilizers[5,6] Phytantriol dispersions stabilized using Pluronic F108, Myrj 59 (PEG100-stearate), PEG150-stearate, and PEG150-distearate, were made with the stabilizer concentrations that contained the same amount of PEG moles used in Pluronic F127 at 3, 5, 7, 10, and 12 wt % stabilizer concentrations. These concentrations were doubled for PEG-stearate dispersions to account for the two PEG blocks in Pluronic copolymers. It was determined that at the same molar concentration of PEG to Pluronic F127, Pluronic F108 had reduced change in fluorescence signal intensity, thus indicating that it has better stabilizer effectiveness than Pluronic F127 (Figures 5 and 6).

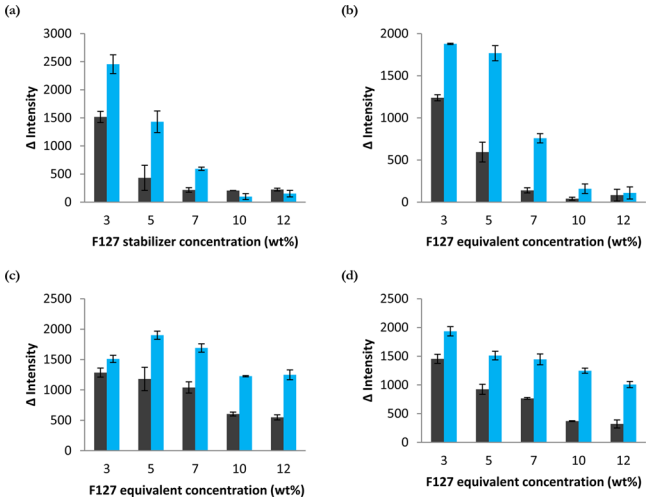

Figure 5. ASA graphs of (a) Pluronic F127—control steric stabilizer, (b) Pluronic F108, (c) PEG100-stearate (Myrj 59) and (d) PEG150-stearate. *X*-axis shows stabilizer concentration equivalent to PEG molar mass of control stabilizer, Pluronic F127 wt % concentrations. Results after the first spin 1800 rpm represented by left column (gray color). Results after second spin 2000 rpm represented by right column (blue color).

By contrast, dispersions stabilized with PEG-stearates (i.e., Myrj) displayed greater changes in fluorescence signal intensity compared to Pluronic F127, suggesting Pluronic F127 has better steric stabilizer effectiveness than both PEG100-stearate and PEG150-stearate for phytantriol dispersions. However, when comparing steric stabilizer performance within the PEG-stearate series, it was found that increasing the hydrophilic domain, or PEG length, from 100 monomer units on average (i.e., PEG100-stearate) to 150 monomer units on average (i.e., PEG150-stearate) improved the performance of the steric stabilizer. This is shown in Figures 5 and 6, where the results of dispersions stabilized with PEG150-stearate displayed smaller changes in its fluorescence signal intensity than dispersions stabilized with PEG100-stearate. Similarly to the Pluronic series, increasing the PEG length (i.e., > 100 PEG units) within the PEG-stearate steric stabilizer series improved the steric

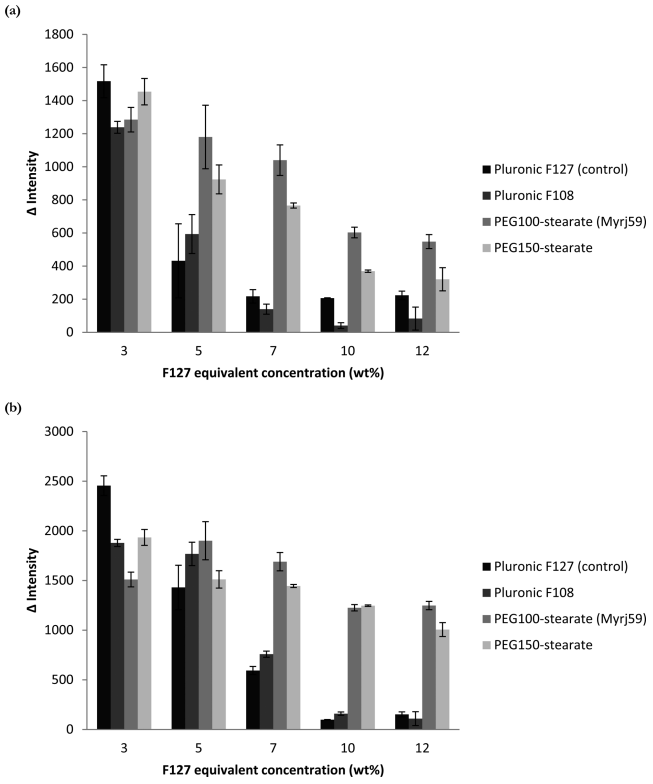

Figure 6. ASA graph of alternative steric stabilizers compared with Pluronic F127 after (a) first spin of 1800 rpm and (b) second spin of 2000 rpm. *X*-axis shows stabilizer concentration equivalent to PEG molar mass of control stabilizer, Pluronic F127 wt % concentrations.

stabilizer's effectiveness for stabilizing phytantriol dispersions. Furthermore, SAXS and cryo-TEM results confirmed that PEG150-stearate stabilized inverse bicontinuous (Q_2^D) phytantriol cubosomes in excess water (see Supporting Information).

Steric stabilizer concentration was also found to influence the effectiveness of the alternative steric stabilizers. As expected increasing stabilizer concentration improves the steric stabilizer's performance (Figure 5 and Figure 6).

A practical, reproducible accelerated stability assay for assessing stability of colloidal systems was reported, using a fluorescence plate reader and plate centrifugation equipment. The use of multiwell plates (i.e., 384-well plates) allows for accelerated methodologies to be pursued. This particular methodology has been optimized for quantification of the steric stabilizer effectiveness in cubic lyotropic liquid crystalline nanostructured particles, the protocols may, however, be adapted for quantifying stability in other colloidal and nanostructured particulate systems.

EXPERIMENTAL PROCEDURES

Materials. Pluronic F127, fluorescein sodium salt, Myrj 59 and 0.01 M phosphate buffered saline (PBS) solution (pH 7.4) were purchased from Sigma-Aldrich, Sydney, NSW, Australia. Phytantriol (3,7,11,15-tetramethylhexadecane-1,2,3-triol) was a gift from DSM Nutritional Products, Sydney, NSW, Australia. PEG-150-stearate and PEG-150-distearate were generously provided by HallStar Co., Bedford Park, Illinois, U.S.A. Pluronic F108 was a kind donation from Prof. Joe McGuire, Oregon State University, U.S.A. All chemicals were used without further purification.

dx.doi.org/10.1021/co400155y | *ACS Comb. Sci.* 2014, 16, 205−210

Preparation of Nanostructured Particles. Lyotropic liquid crystalline phase dispersions were prepared at a concentration of 100 mg/mL of phytantriol in 500 μL of 0.01 M PBS buffer solution, with 3, 5, 7, 10, and 12 wt % of steric stabilizer Pluronic F127. The range of Pluronic F127 stabilizer concentrations were selected to provide a variety of known poorly to excellently stabilized systems. Briefly, 50 mg of phytantriol was placed into each of five 1.5 mL centrifuge tubes. To each sample a Pluronic F127 steric stabilizer solution was added. The concentrations of Pluronic F127 tested were 3, 5, 7, 10, and 12 wt % (with respect to lipid) dissolved in 0.01 M PBS buffer solution. Samples were sonicated using a Misonix Ultrasonic Liquid Processor Microtip Probe Sonicator (Misonix Inc., NY, U.S.A.), with a 418 Misonix probe. The sequence programmed for the sonication of samples consisted of three programs, run in succession: program 1 settings 50 amplitude, 30 s process time, 3 s pulse-time on, 2 s pulse-time off; program 2 settings 45 amplitude, 1 min process time, 2 s pulse-time on, 4 s pulse-time off; and program 3 settings 40 amplitude, 1 min process time, 2 s pulse-time on, 4 s pulse-time off. The sequence resulted in a total sonication time of 2.5 min per sample. The sample temperature during sonication was monitored to prevent overheating of samples. The sample sonication temperature was observed to be consistent between 65 and 70 °C, during pulse sonication of samples.

Lyotropic liquid crystalline dispersions stabilized using the new stabilizers PEG150-stearate and PEG150-distearate were characterized using small-angle X-ray scattering (SAXS) and cryo-transmission electron microscopy (cryo-TEM). Briefly, the SAXS samples were loaded in special 1.5 mm capillaries (Hampton Research, U.S.A.) and positioned in a custom-designed capillary holder capable of holding 34 capillaries with the temperature controlled to ±1.0 °C between 20 and 75 °C. Temperature control was via a recirculating water bath (Julabo, Germany). SAXS was performed on dispersions at 25 and 37 °C. The exposure time for each sample was 1 s. SAXS data was analyzed using an IDL-based AXcess software package.[12]

A laboratory-built humidity-controlled vitrification system was used to prepare the samples for cryo-TEM. Humidity was kept close to 80% for all experiments, and ambient temperature was 22 °C. 200-Mesh copper grids coated with perforated carbon film (Lacey carbon film, ProSciTech, Queensland, Australia) were glow discharged in nitrogen to render them hydrophilic. Four microliter aliquots of the sample were pipetted onto each grid prior to plunging. After 30 s adsorption time, the grid was blotted manually using Whatman 541 filter paper, for 2 s. Blotting time was optimized for each sample. The grid was then plunged into liquid ethane cooled by liquid nitrogen. Frozen grids were stored in liquid nitrogen until required. The samples were examined using a Gatan 626 cryoholder (Gatan, Pleasanton, CA, U.S.A.) and Tecnai 12 transmission electron microscope (FEI, Eindhoven, the Netherlands) at an operating voltage of 120 kV. At all times, low dose procedures were followed, using an electron dose of 8−10 electrons/Å^2 for all imaging. Images were recorded using a Megaview III CCD camera and AnalySIS camera control software (Olympus) using magnifications in the range from 30 000× to 97 000×.

Accelerated Stability Assay (ASA) Optimization. A batch of poorly stabilized phytantriol dispersions (3 wt % stabilizer concentration) and standard phytantriol dispersions (10 wt % stabilizer concentration) were made to establish significant differences between the two extremes of colloidal stability. It should be noted that 1 wt % stabilizer was not used for the "poor stabilizing concentration" as the sample was required to be sufficiently dispersed and free of large aggregates. A 1:1 serial dilution of 10 mg/mL fluorescein dye in 0.01 M PBS solution was made with twenty-three sequential dilutions, resulting in the following dye concentrations: 10, 5, 2.5, 1.25, 6.3×10^{-1}, 3.1×10^{-1}, 1.6×10^{-1}, 7.8×10^{-2}, 3.9×10^{-2}, 2.0×10^{-2}, 9.8×10^{-3},4.9×10^{-3}, 2.4×10^{-3}, 1.2×10^{-3}, 6.1×10^{-4}, 3.1×10^{-4}, 1.5×10^{-4}, 7.6×10^{-5}, 3.8×10^{-5}, 1.9×10^{-5}, 9.5×10^{-6}, 4.8×10^{-6}, 2.4×10^{-6}, and 1.2×10^{-6} mg/mL. Fluorescein was used as a fluorescent dye due to its water solubility in PBS which results in minimal interaction with the lipid nanoparticles. Each dye solution was mixed at equal volumes with either a "poorly" stabilized (3 wt % stabilizer concentration) or the standard (10 wt % stabilizer concentration) phytantriol dispersion and pipetted into a Corning low volume, 384 round-well, black, with clear flat bottom, polystyrene microplate (product no. 3540). Adhesion of colloidal samples to the multititer plate walls will be sample dependent and should be taken into account during the application of this methodology. The optimization of this stability assay included testing plates with different well geometry (i.e., round or square). It is important to note that the round well geometry was found to be an important factor in the assay, as data obtained from plates with circular wells yielded highly reproducible data compared to square well geometries. Three repeats were made for each dye and cubosome mixture. Control samples consisted of three repeats of PBS and cubosome mixtures, as well as PBS and dye wells. Measurements of fluorescence intensity at emission wavelength of 530 nm, were taken pre- and postcentrifugation using a top-reading FlexStation 3 Multimode microplate reader (Molecular Devices Company, CA, U.S.A.), and processed on SoftMax Pro software. It is important to note that the top-read setting on this instrument is vital to obtaining usable ASA data sets, as the effect of particle aggregation after centrifugation occurs at the surface of the sample (top-end) of the well (Figure 2), and is only detected when using the "top-read" and not the "bottom-read" mode. The plate was spun at 645*g* (1800 rpm) for 5 min using Heraeus Multifuge ×3 Centrifuge (Thermo Scientific, Germany). The optimized dye concentration for the ASA was 3.1×10^{-4} mg/mL of fluorescein sodium salt in 0.01 M PBS buffer solution.

Final Accelerated Stability Assay (ASA) Protocol. Lyotropic liquid crystal phytantriol dispersions stabilized with 3, 5, 7, 10, and 12 wt % of Pluronic F127 were mixed at equal volumes with dye solution (i.e., 15 μL cubosome sample mixed with 15 μL dye solution) and pipetted into a 384 black round-well Corning plate. The same was done using PBS buffer solution instead of dye solution (3.1×10^{-4} mg/mL) for control samples. Negative control samples consisted of PBS buffer and dye solution. A minimum of three repeats were performed for each cubosome mixture with dye solution or PBS buffer solution. Fluorescence signal intensities were taken pre- and postcentrifugation (Figure 2). The centrifugation of plates was performed with a Heraeus Multifuge ×3 Centrifuge (Thermo Scientific, Germany). Fluorescence signal measurements were taken as described above. The plate was initially spun at 645*g* (1800 rpm) for 5 min, measured for fluorescence signal and then respun at 796*g* (2000 rpm) for 5 min. It was found that centrifugation speeds greater than 2000 rpm resulted in particle aggregation of all dispersions, resulting in less differentiation between "poor" and "well" dispersed

dx.doi.org/10.1021/co400155y | ACS Comb. Sci. 2014, 16, 205−210

samples, and results from lower speeds (i.e., <1000 rpm) were inconsistent and did not always result in particle aggregation of poor samples, which also led to less differentiation between the poor and well dispersed samples.

Intrinsic Colloidal Stability Study (i.e., Real-Time Nonaccelerated Stability Study). The aim of this stability assay was to accelerate the destabilization of dispersed liquid crystalline dispersions that would naturally occur with time. To ensure that the results obtained herein correlate with the effects of particle destabilization over time, dispersions were left to age without centrifugation and sample fluorescence measured. Samples of phytantriol dispersions in 0.01 M PBS buffer solution, stabilized with 3, 5, 7, 10, and 12 wt % of steric stabilizer Pluronic F127 were assessed over a two week time duration for any changes (i.e., particle aggregation). Samples were mixed with an equal volume of dye solution and pipetted into a 384 black round-well Corning plate. Control samples were mixed with equal volumes of PBS buffer solution. Additional controls such as PBS buffer solution and pure dye solution were tested, to monitor the natural decrease of the fluorescence signal from the dye over time using the same fluorescence method described above.

■ ASSOCIATED CONTENT

Ⓢ Supporting Information

Data sets obtained for the ASA fluorescence measurements, visual record of the time deterioration of stability study, and SAXS and cryo-TEM results for PEG150-stearate phytantriol dispersions. This material is available free of charge via the Internet at http://pubs.acs.org.

■ AUTHOR INFORMATION

Corresponding Authors

*[redacted]

Notes

The authors declare no competing financial interest.

■ ACKNOWLEDGMENTS

C.J.D. was the recipient of an Australian Research Council (ARC) Federation Fellowship. J.Y.T.C. was the recipient of a CSIRO Ph.D. studentship. X.M. was the recipient of a CSIRO-Monash University Collaborative research postdoctoral fellowship. B.J.B. is the recipient of an Australian Research Council (ARC) Future Fellowship (FT120100697). Some of the work presented here was obtained at the SAXS/WAXS beamline of the Australian Synchrotron.

■ REFERENCES

(1) Chang, H.-I.; Yeh, M.-K. Clinical Development of Liposome-Based Drugs: Formulation, Characterization, and Therapeutic Efficacy. *Int. J. Nanomed.* **2012**, *7*, 49−60.

(2) Zhang, J.-X.; Wang, K.; Mao, Z.-F.; Fan, X.; Jiang, D.-L.; Chen, M.; Cui, L.; Sun, K.; Dang, S.-C. Application of Liposomes in Drug Development—Focus on Gastroenterological Targets. *Int. J. Nanomed.* **2013**, *8*, 1325−1334.

(3) Mulet, X.; Kennedy, D. F.; Conn, C. E.; Hawley, A.; Drummond, C. J. High Throughput Preparation and Characterisation of Amphiphilic Nanostructured Nanoparticulate Drug Delivery Vehicles. *Int. J. Pharm.* **2010**, *395*, 290−297.

(4) Mulet, X.; Boyd, B. J.; Drummond, C. J. Advances in Drug Delivery and Medical Imaging Using Colloidal Lyotropic Liquid Crystalline Dispersions. *J. Colloid Interface Sci.* **2013**, *393*, 1−20.

(5) Chong, J. Y. T.; Mulet, X.; Waddington, L. J.; Boyd, B. J.; Drummond, C. J. Steric Stabilisation of Self-Assembled Cubic Lyotropic Liquid Crystalline Nanoparticles: High Throughput Evaluation of Triblock Polyethylene Oxide−Polypropylene Oxide−Polyethylene Oxide Copolymers. *Soft Matter* **2011**, *7*, 4768−4777.

(6) Chong, J. Y. T.; Mulet, X.; Waddington, L. J.; Boyd, B. J.; Drummond, C. J. High-Throughput Discovery of Novel Steric Stabilizers for Cubic Lyotropic Liquid Crystal Nanoparticle Dispersions. *Langmuir* **2012**, *28*, 9223−9232.

(7) Tilley, A. J.; Drummond, C. J.; Boyd, B. J. Disposition and Association of the Steric Stabilizer Pluronic (R) F127 in Lyotropic Liquid Crystalline Nanostructured Particle Dispersions. *J. Colloid Interface Sci.* **2013**, *392*, 288−296.

(8) Klibanov, A. L.; Maruyama, K.; Torchilin, V. P.; Huang, L. Amphipathic Polyethyleneglycols Effectively Prolong the Circulation Time of Liposomes. *FEBS Lett.* **1990**, *268*, 235−237.

(9) Gref, R.; Luck, M.; Quellec, P.; Marchand, M.; Dellacherie, E.; Harnisch, S.; Blunk, T.; Muller, R. H. 'Stealth' Corona-Core Nanoparticles Surface Modified by Polyethylene glycol (PEG): Influences of the Corona (PEG Chain Length and Surface Density) and of the Core Composition on Phagocytic Uptake and Plasma Protein Adsorption. *Colloids Surf., B* **2000**, *18*, 301−313.

(10) Libster, D.; Aserin, A.; Yariv, D.; Shoham, G.; Garti, N. Soft Matter Dispersions with Ordered Inner Structures, Stabilized by Ethoxylated Phytosterols. *Colloids Surf., B* **2009**, *74*, 202−215.

(11) Amar-Yuli, I.; Wachtel, E.; Shoshan, E. B.; Danino, D.; Aserin, A.; Garti, N. Hexosome and Hexagonal Phases Mediated by Hydration and Polymeric Stabilizer. *Langmuir* **2007**, *23*, 3637−3645.

(12) Seddon, J. M.; Squires, A. M.; Conn, C. E.; Ces, O.; Heron, A. J.; Mulet, X.; Shearman, G. C.; Templer, R. H. Pressure-Jump X-Ray Studies of Liquid Crystal Transitions in Lipids. *Philos. Trans. R. Soc. A* **2006**, *364*, 2635−2655.

Supplementary Information

An Accelerated Stability Assay (ASA) for Colloidal Systems

Josephine Y. T. Chong, Xavier Mulet, Ben J. Boyd, Calum J. Drummond

i. ASA Fluorescence measurements

Table 1. Data collected for Pluronic F127 stabilized phytantriol dispersions to establish ASA graphs

		3 wt%	5 wt%	7 wt%	10 wt%	12 wt%
Pre-spin	**Repeat 1**	4120	4239	4512	4062	4642
	Repeat 2	4146	4464	4719	4669	4852
	Repeat 3	4365	4841	4789	4845	4750
	Average	**4210**	**4515**	**4673**	**4525**	**4748**
Post-spin 1	**Repeat 1**	5118	4729	4627	4077	4559
1800 rpm (5min)	**Repeat 2**	5234	4967	4832	4559	4719
	Repeat 3	5510	5440	4907	5000	4743
	Average	**5287**	**5045**	**4789**	**4545**	**4674**
Post-spin 2	**Repeat 1**	6428	5480	5067	4430	4871
2000 rpm (5min)	**Repeat 2**	6386	5657	5280	4945	4989
	Repeat 3	7004	6230	5463	5354	5061
	Average	**6606**	**5789**	**5270**	**4910**	**4974**

ii. Visual record of the time deterioration of stability study

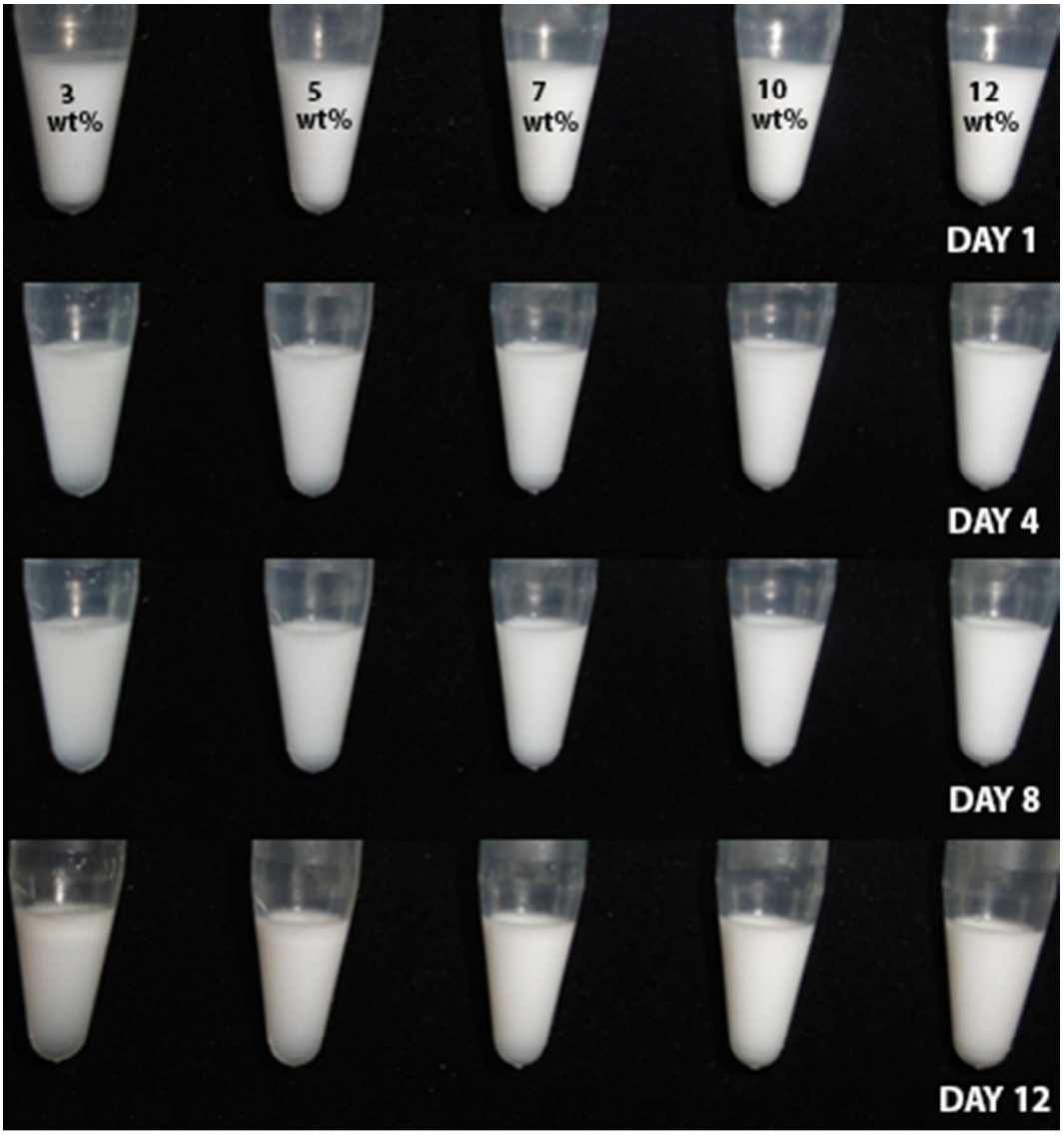

Figure 1a. Images of phytantriol dispersions sterically stabilized using control stabilizer Pluronic F127 at 3, 5, 7, 10 and 12 wt% at Day 1 (day dispersions were sonicated), Day 4, Day 8 and Day 12, showing natural creaming over time

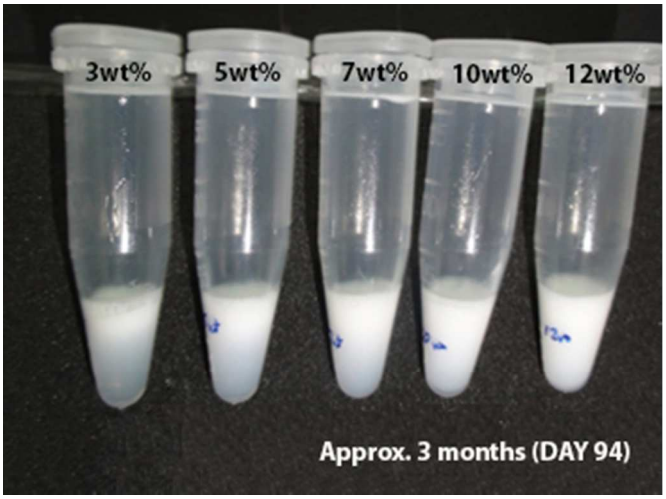

Figure 1b. Images of phytantriol dispersions sterically stabilized using control stabilizer Pluronic F127 at 3, 5, 7, 10 and 12 wt% after approximately 3 months (Day 94) showing natural creaming over time

iii. SAXS results for PEG150-stearate phytantriol dispersions

Table 2. SAXS results for PEG150-stearate phytantriol dispersions at 25 and 37 °C

Stabilizer Concentration (wt %)	Temperature (°C)	Phase	Lattice Parameter (Å)	Average particle size (nm)	PDI
3	25	Q_2^D	69.1	284	0.23
	37	Q_2^D	65.7		
5	25	Q_2^D	69.1	337	0.24
	37	Q_2^D	65.9		
7	25	Q_2^D	69.3	240	0.23
	37	Q_2^D	66.1		
10	25	Q_2^D	69.3	188	0.21
	37	Q_2^D	66.0		
12	25	Q_2^D	69.4	299	0.19
	37	Q_2^D	66.1		

iv. Cryo-TEM images for PEG150-stearate phytantriol dispersions

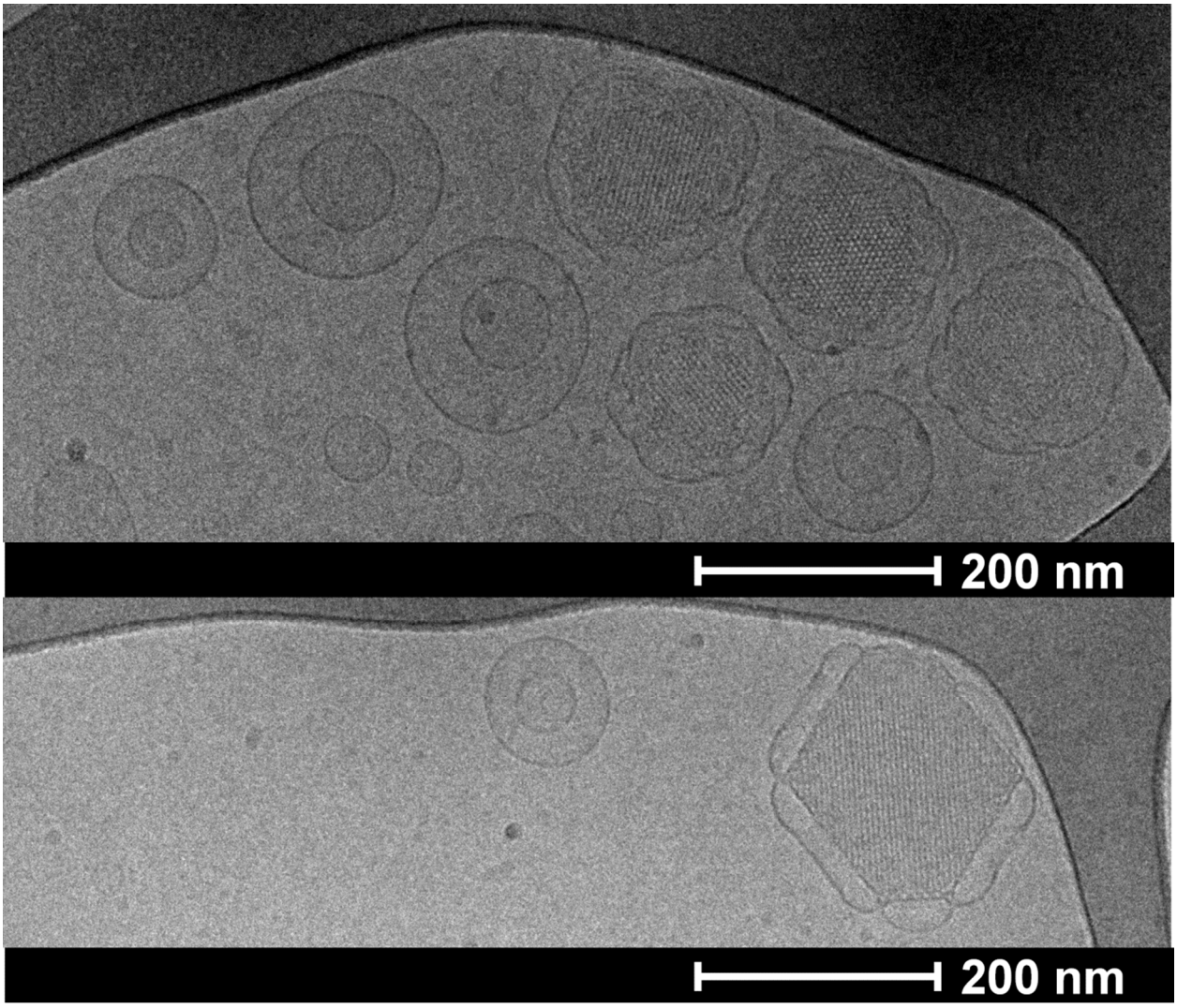

Figure 2. Cryo-TEM images of PEG150-stearate phytantriol dispersions in water using 10 wt% stabilizer concentration

Chapter 5

Novel steric stabilisers for lyotropic liquid crystalline nanoparticles: PEGylated-phytanyl copolymers

Josephine Y.T. Chong, Xavier Mulet, Daniel J. Keddie, Lynne Waddington, Stephen T. Mudie, Ben J. Boyd and Calum J. Drummond

SUBMITTED: *Langmuir* (submitted on 17.4.2014)

Declaration for Chapter 5

Declaration by candidate

In the case of Chapter 5, the nature and extent of my contribution to the work was the following:

Nature of contribution	Extent of contribution (%)
Research design, polymer synthesis and analysis, performance of data collection and analysis, manuscript preparation	80

The following co-authors contributed to the work:

Name	Nature of contribution
Xavier Mulet	Supervision; intellectual input; input into manuscript preparation
Daniel J. Keddie	Intellectual input on chloroform GPC operation and analysis
Lynne Waddington	Intellectual input on cryo-TEM operation and analysis
Stephen T. Mudie	Intellectual input on SAXS operation and analysis
Ben Boyd	Supervision; intellectual input; input into manuscript preparation
Calum Drummond	Supervision; intellectual input; input into manuscript preparation

Candidate's signature: [redacted] **Date:** **10.7.2014**

Declaration by co-authors

The undersigned hereby certify that:

(19) the above declaration correctly reflects the nature and extent of the candidate's contribution to this work, and the nature of the contribution of each of the co-authors.

(20) they meet the criteria for authorship in that they have participated in the conception, execution, or interpretation, of at least that part of the publication in their field of expertise;

(21) they take public responsibility for their part of the publication, except for the responsible author who accepts overall responsibility for the publication;

(22) there are no other authors of the publication according to these criteria;

(23) potential conflicts of interest have been disclosed to (a) granting bodies, (b) the editor or publisher of journals or other publications, and (c) the head of the responsible academic unit; and

(24) the original data are stored at the following location(s) and will be held for at least five years from the date indicated below:

Location of data storage: CSIRO Materials Science and Engineering, Ian Wark Laboratory, Bayview Avenue, Clayton 3168, Australia.

Co-authors' signature for Chapter 5:

Signed: [redacted] **Date:** **10.1.2014**

Xavier Mulet

Signed: [redacted] **Date:** **29.1.2014**

Daniel J. Keddie

Signed: [redacted] **Date:** **8.1.2014**

Lynne J. Waddington

Signed: [redacted] **Date:** **15.1.2014**

Stephen T. Mudie

Signed: [redacted] **Date:** **28.2.2014**

Ben J. Boyd

Signed: [redacted] **Date:** **12.4.2014**

Calum J. Drummond

Novel steric stabilizers for lyotropic liquid crystalline nanoparticles: PEGylated-phytanyl copolymers

Journal:	*Langmuir*
Manuscript ID:	la-2014-01471z.R1
Manuscript Type:	Article
Date Submitted by the Author:	n/a

Complete List of Authors:	Chong, Josephine; CSIRO, Materials Science and Engineering Mulet, Xavier; CSIRO, Materials Science and Engineering Keddie, Daniel; University of New England, School of Science and Technology Waddington, Lynne; CSIRO Materials Science and Engineering, Mudie, Stephen; CSIRO - Materials Science and Engineering, Boyd, Ben; Monash University, Drummond, Calum; CSIRO, Materials Science and Engineering

Novel steric stabilizers for lyotropic liquid crystalline nanoparticles: PEGylated-phytanyl copolymers

Josephine Y.T. Chong[a,b], Xavier Mulet[a,b], Daniel J. Keddie[a,c], Lynne Waddington[d], Stephen T. Mudie[e], Ben J. Boyd[b], Calum J. Drummond[a,f*]*

[a]CSIRO Materials Science and Engineering, Private Bag 10, Clayton, VIC 3169, Australia; [b]Drug Delivery, Disposition and Dynamics, Monash Institute of Pharmaceutical Science, Monash University (Parkville Campus), 381 Royal Parade, Parkville, VIC 3052, Australia; [c]Chemistry, School of Science and Technology, University of New England, NSW 2351, Australia; [d]CSIRO Materials Science and Engineering, 343 Royal Parade, Parkville, VIC 3052, Australia; [e]SAXS/WAXS beam line, Australian Synchrotron, 800 Blackburn Road, Clayton, VIC 3169, Australia; [f]School of Applied Sciences, College of Science, Engineering and Health, RMIT University, GPO Box 2476, Melbourne, VIC 3001, Australia

KEYWORDS: PEG-lipid, amphiphilic copolymer, lyotropic liquid crystalline nanostructured particle, steric stabilizer, cubosome

ABSTRACT

Lyotropic liquid crystalline nanostructured particles (e.g., cubosomes and hexosomes) are being investigated as delivery systems for therapeutics in biomedical and pharmaceutical applications. Long term stability of these particulate dispersions is generally provided by steric stabilizers, typically commercially available amphiphilic copolymers such as Pluronic® F127. Few examples exist of tailored molecular materials designed for lyotropic liquid crystalline nanostructured particle stabilization. A library of PEGylated-phytanyl copolymers (PEG-PHYT) with varying PEG molecular weights (200 to 14K Da) were synthesized to assess their performance as steric stabilizers for cubosomes and to establish structure-property relationships. The PEGylated-lipid copolymers were first found to self-

*[redacted]

assemble in excess water in the absence of cubosomes and also displayed thermotropic liquid crystal phase behaviour under cross polarized light microscopy. An accelerated stability assay was used to assess the performance of the copolymers, compared to Pluronic® F127, for stabilizing phytantriol-based cubosomes. Several of the PEGylated-lipid copolymers showed steric stabilizer effectiveness comparable to Pluronic® F127. Using synchrotron small angle X-ray scattering and cryo-transmission electron microscopy, the copolymers were shown to retain the native internal lyotropic liquid crystalline structure, double diamond cubic phase (Q_2^D), of phytantriol dispersions; an important attribute for controlling downstream performance.

1. Introduction

Inverse bicontinuous cubic and hexagonal lyotropic liquid crystalline dispersions of amphiphiles (i.e. cubosomes and hexosomes, respectively) are of interest in drug delivery applications due to their compartmentalized ordered internal structure, high lipid content and large surface area. Lipids, such as monoolein (GMO) and phytantriol, are common examples of amphiphile building-blocks for lyotropic liquid crystalline particles.[1-3] Their amphiphilic self-assembly features enables them to be compatible with both lipophilic and hydrophilic therapeutics or biomedical imaging agents.[4-7] Cubosome and hexosome dispersions are typically only colloidally stable for extended periods when in the presence of a steric stabilizer which prevents particle aggregation. The range of steric stabilizers that can successfully disperse lyotropic liquid crystalline particles remains limited.[8-10]

The current gold-standard in lyotropic liquid crystalline particle stabilization is Pluronic® F127 ("F127"). F127 is a poly(ethylene glycol)-poly(propylene oxide)-poly(ethylene glycol) non-ionic triblock copolymer (PEG-PPO-PEG), with an average molecular weight of 12 600, and approximately 100 PEG units on average on both sides of 65 PPO units on average.[11-16] Although popular, F127 has been shown to have restricted stabilizer effectiveness for the long term stability of cubosomes.[17] Alternative steric stabilizers that have been investigated for cubosomes include Pluronic® F108[16], β-casein[18], Myrj® 59[8], Laponite[19], modified cellulose[20], ethoxylated phytosterol[21], Polysorbate 80[8] and silica particles[22]. For amphiphilic stabilizers (e.g. F127), the lipophilic domain (e.g. PPO) anchors to the lipid bilayer of the lyotropic liquid crystalline system. The stabilizer thus has a strong affinity to the cubosome and this affinity can be tuned by altering lipid-to-stabilizer compatibility. The hydrophilic domain remains in the water or polar region of the self-assembled structures. Stabilizers have been found to associate with both the internal and external surfaces of the cubosomes.[17] The

hydrophilic domain often consists of PEG. This chemical moiety has been found to provide stealth *in vivo*[23] thus prolonging the circulation time of nanoparticles *in vivo*.[24-28]

Stabilizers can have an effect on the internal nanostructure of the dispersed lyotropic liquid crystalline particles. Studies using GMO-based cubosomes stabilized by F127, have shown that a transition between two cubic phases can be induced by the lipophilic domain (e.g. PPO) of the stabilizer being embedded in the cubosome bilayer. This drives a phase transition from the native double diamond phase to a primitive phase ($Q_2^{D}{}_{(Pn3m)}$ to $Q_2^{P}{}_{(Im3m)}$). In contrast, F127 adsorbs at the interface of phytantriol-based cubosome, with PPO occupying a finite interfacial area, limiting the available surface area for further stabilizer adsorption.[17] The association of the lipophile to the cubosome was found to be strong and irreversible as the stabilizer did not desorb from the cubosome after dilution of the system.[17] An effective steric stabilizer will therefore require a lipophile with a strong lipophilic affinity, whilst preserving the cubic internal nanostructure of the lyotropic liquid crystalline phase to ensure stability of the dispersion.

The limited chemical space explored, with respect to the nature of the steric stabilizers, can be attributed to the time-consuming nature of single sample preparation and material characterization techniques, impeding the progress of steric stabilizer screening. The development of high-throughput methodologies has recently enabled the implementation of rapid preparation and screening protocols[8, 16, 29-30] In previous work, a number of commercially-available polymers were examined as potential steric stabilizers for cubosomes. The Pluronic® polymer series[16] and later the Myrj® polymer series[8] were screened as stabilizers for phytantriol and monoolein cubosomes. Studies using the Pluronic® polymer series found that changes to the internal structure of the dispersions were directly linked to the internalization of the stabilizer within the lipidic structure. Eliminating or reducing the internalization of the stabilizer into the dispersed particles reduced the propensity for changes to the internal nanostructure. This was illustrated by the conservation of the double diamond cubic phase (Q_2^{D}) for monoolein dispersions when using Pluronic® F108, which has the longest PEG chain of the Pluronic®s commercially available. It was suggested that stabilizers with longer PEG chains (i.e. >100 PEG units on average) had increased presence on the surface of the particle, which alludes to the desire to investigate molecular structures with larger, controllable PEG content, such as custom synthesized copolymers. Pluronic®s are also difficult to functionalize where further functionality such as targeting by ligands to specific cell types is required. Custom copolymers for cubosomes are therefore attractive from both a colloidal stability and functionalization perspective.

PEGylated-lipid copolymers, have been reported for use in self-assembled drug delivery systems (e.g. micelle drug delivery systems).[31-33] Rouxhet *et al.* synthesized AB type PEGylated-lipid copolymers, with the lipid component consisting of monoglyceride.[33] These amphiphilic PEGylated-lipid copolymers were observed to self-assemble into micellar systems, as well as solubilise poorly water-soluble drugs. Such amphiphilic polymers with lipid-based hydrophobic domains could provide a suitable surface 'anchor' in lipid membranes and could therefore constitute a new class of steric stabilizers for cubosomes. Consequently, in the current study a series of PEGylated-lipid copolymer steric stabilizers incorporating a common lyotropic liquid crystal lipid, phytantriol, as the lipophilic component of the copolymers, was synthesized and characterized for their self-assembly behaviour and stabilization of cubosomes. The polycondensation synthesis employed (Scheme 1) was adapted from Rouxhet *et al.*[33] because it was an expedient way to develop some structure-performance relationships. Although there may be more controlled polymerization approaches reported[34-37], the Rouxhet *et al.*[33] approach was ultimately selected for synthetic simplicity and for amenity to a combinatorial chemistry approach. The novel PEGylated-lipid copolymer steric stabilizers were developed to contain a series of various PEG lengths (i.e. from 200 to 14K), and similarly to Rouxhet *et al*., various PEG to lipid ratios. The incremental variation of the steric stabilizer series allowed a comprehensive assessment of the structure-property relationship for the effectiveness of steric stabilization of lyotropic liquid crystalline nanostructured particles.

2. Materials and Methodology

2.1. Materials

Phytantriol (3,7,11,15-tetramethylhexadecane-1,2,3-triol) was a gift from DSM Nutritional Products, Wagga Wagga, NSW, Australia. Polyethylene glycol 200 and 400 were purchased from BDH Laboratory Reagents, Poole, UK. Polyethylene glycol 4000 was purchased from BDH Chemicals Australia, Port Fairy, VIC, Australia. Polyethylene glycol 600, 2000, 8000, 14000, succinic anhydride 99+%, 0.01 M phosphate buffered saline solution (pH 7.4), fluorescein sodium salt and Pluronic® F127 were purchased from Sigma-Aldrich, Sydney, NSW, Australia. Polyethylene glycol 800, 1000 and 6000 were purchased from ICI Australia Operations Pty Ltd, Melbourne, VIC, Australia. Polyethylene glycol 3000 and 10000 were purchased from Merck-Schuchardt, Hohenbrunn, Germany.

2.2. Methodology

2.2.1 Polymer Synthesis and Characterization

The copolymers were synthesized by polycondensation according to the synthesis pathway reported in Scheme 1.[33] Briefly phytantriol, succinic anhydride and polyethylene glycol were placed under nitrogen and the temperature raised to 180 °C. The reaction was maintained at 180 °C for 24 h. Different mol % ratios for developing five different copolymer series were made using a range of polyethylene glycol with molecular weights (MW) of 200, 400, 600, 800, 1000 (1K), 2000 (2K), 3000 (3K), 4000 (4K), 6000 (6K), 8000 (8K), 10000 (10K) and 14000 (14K). A total of 60 copolymers were synthesized in this study.

The nomenclature adopted for the copolymers assumed a 50 mol% SA content (based on the mol ratio of reactants), and indicates the PEG length and the PEG to phytantriol ratio. These polymers are indicated as $PEG(x)_yPHYT_z$, where x denoted the PEG length, y denotes the mol fraction of PEG in the polymer, z denotes the mol fraction of phytantriol. Thus, because the SA content is always 50 mol%, y+z = 50 mol% for all polymers.

The polymer composition and residual monomer content were analysed by NMR. The copolymers were dissolved in deuterated chloroform and spectra for structural assignments were obtained with a Bruker Avance 400 MHz spectrometer (^{1}H 400 MHz, ^{13}C 100 MHz).

Molecular weights of the polymers were determined by gel permeation chromatography (GPC) performed in chloroform (1.0 mL/min) at 30 °C using a Waters 2695 Separations Module, with a Waters 2414 Refractive Index Detector and a Waters 2996 Photodiode Array Detector, a series of four Polymer Laboratories PLGel columns (3 × 5 μm Miked-C and 1 × 3 μm Mixed-E), and Empower Pro Software. The GPC was calibrated with narrow polydispersity polystyrene standards (Polymer Laboratories EasiCal, M_w from 264 to 256,000), and molecular weights are reported as polystyrene equivalents based on the refractive index detector.

2.2.2 Polymer Self-Assembling Properties

The critical aggregation concentration (CAC) of the copolymers was determined by using changes in the scattered light intensity from dynamic light scattering (DLS). DLS was performed using a DynaPro plate reader (Wyatt Technology, Santa Barbara, CA). The DLS instrument uses a 50 mW programmable laser (λ = 831.5 nm) with a detection at 158° and a thermostated sample chamber set to 25 °C. The viscosity and refractive index of water at 25 °C, 0.8937 cP and 1.333 respectively, were used for all measurements. In the absence of aggregates the intensity of backscattered light is comparable to that of the solvent. In the presence of aggregates, the intensity of backscattered light increases with

increasing concentration of aggregates.[38] Solutions were prepared in double distilled water by dilution from 20 mg/mL stock solutions of the steric stabilizers and analysed using a polystyrene clear bottom low volume 384 well plate (Product #3540, Corning®, USA). Three repeats were made per sample. Ten acquisitions were collected for each sample to ensure reproducibility. Water wells were used as a blank. Intensity and size information was obtained from the Wyatt DynaPro plate reader using the software package DYNAMICS v.7. CAC measurements are averaged from the three repeat measurements.

Assessment of lyotropic phase behaviour of bulk copolymer in excess water was determined by using cross-polarized light microscopy (CPLM). Briefly, copolymer was melted onto a glass slide, covered with a cover slip and flooded with water for observation under a Nikon Eclipse 80i microscope (Nikon Corporation, Japan), with ×10 magnification, to obtain water penetration scans at temperatures 20 to 65 °C. Anisotropic phase behaviour was determined using cross-polarizers, to detect birefringent appearance of the sample.[39] Further assessment of lyotropic liquid crystalline phases occurring in the self-assembly of the copolymers in water was determined by using high throughput small angle X-ray scattering (SAXS), for two different systems; (i) with excess polymer (>60 % polymer content) and (ii) with excess water (>60 % hydration).

2.2.3 Preparation of Nanostructured Particles

Lyotropic liquid crystalline dispersions were formed at a concentration of 100 mg/mL of phytantriol in 500 μL of 0.01M phosphate buffered saline at pH 7.4 (PBS), with 1 wt% (i.e. 10 mg/mL) of each PEG-PHYT copolymer as the steric stabilizer. The copolymers with PEG MW≤1000 were dissolved in chloroform, containing 50 mg of phytantriol. These samples were then left in a vacuum desiccator over 14 days to ensure solvent removal. PBS (500 μl) was then added to each sample. Copolymers with PEG MW>1000 were dispersed in 500 μl of PBS. Once completely dispersed, phytantriol (50 mg) was added to each sample. Following combination of lipid, stabilizer and water, each sample was sonicated using a Misonix Ultrasonic Liquid Processor Microtip Probe Sonicator (Misonix Inc., NY, USA), with a 418 Misonix probe. The sequence programmed for the sonication of samples consisted of three programs, which were implemented in succession without any delay time: Program 1 settings: 50 Amplitude, 30s Process time, 3s Pulse-time On, 2s Pulse-time Off; Program 2 settings: 45 Amplitude, 1 min Process time, 2s Pulse-time On, 4s Pulse-time Off and Program 3 settings: 40 Amplitude, 1 min Process time, 2s Pulse-time On, 4s Pulse-time Off. The sequence resulted in a total sonication time

of 2.5 min per sample. The sample temperature during sonication was monitored and observed to be between 65 to 70 °C.

2.2.4 Characterization of Colloidal Stability, Internal Structure and Particle Morphology

The copolymers were assessed for performance as stabilizers for lyotropic liquid crystal dispersions using a visual assessment and an accelerated stability assay. An accelerated stability assay was developed to quantify the steric stabilizer effectiveness between fair to excellent lyotropic liquid crystal stabilizers that passed the initial visual assessment of particle stability.[40] Briefly, lyotropic liquid crystal phytantriol dispersions were mixed at equal volumes with hydrophilic dye solution, fluorescein sodium salt solution (3.1×10^{-4} mg/mL) (i.e. 15 μl cubosome sample mixed with 15 μl dye solution) and pipetted into a 384 black round well Corning® microplate. Control samples were prepared using 15 μl PBS and 15 μl dye solution. The same was done using PBS buffer solution instead of dye solution for control samples. Three repeats were made for each sample. Fluorescence signal intensities were taken pre- and post-centrifugation. The centrifugation of plates was performed with a Heraeus Multifuge ×3 Centrifuge (Thermo Scientific, Germany). Fluorescence signal measurements, with emission: 530 nm and excitation wavelength: 480 nm, were taken using a FlexStation3 Multi-mode Microplate Reader (Molecular Devices Company, CA, USA), and processed on SoftMax Pro software. The plate was initially spun at 645 × *g* (RCF) or 1800 RPM for 5 min, measured for fluorescence signal and then re-spun at 796 × *g* (RCF) or 2000 RPM for 5 min. Dispersions stabilized with F127 at 0.3, 0.5, 0.7, 1 and 1.2 wt% were used as a comparison for the ASA, where wt% is relative to total dispersion.

The principle of this assay is that aggregation (that typically results in increased creaming) correlates with increased fluorescence signal intensities. Therefore, the magnitude of the change in fluorescence signal intensity following centrifugation is proportional to creaming levels. In order to differentiate steric stabilizer efficacies, comparing changes in fluorescence signal intensities is required. Good steric stabilizers are able to maintain a stable colloidal dispersion over time and therefore after centrifugation. Thus, the less creaming that occurs within a sample during the accelerated stability assay (i.e. minimal change in fluorescence signal intensity), the more stable the colloidal dispersion. This is indicative of the effectiveness of the steric stabilizer and can be quantifiably compared to a control system, such as F127.

Particle size and polydispersity of dispersed samples were determined by dynamic light scattering using a DynaPro plate reader (Wyatt Technology, Santa Barbara, CA). Particle size and polydispersity from the DLS instrument were averaged from three repeat measurements. The viscosity of water was assumed and the samples were run at 25 °C.

Dispersed samples visually assessed to be milky white with little to no aggregation, were further assessed for lyotropic liquid crystalline nanostructured particle phase behaviour, using SAXS and cryo-TEM imaging. SAXS can be used to establish the phase structure (i.e. internal long range order of the liquid crystal lattice) of the dispersed particle samples at selected temperatures. SAXS data was collected at the Australian Synchrotron using a beam with wavelength λ = 1.033 Å and a typical flux of approximately 10^{13} photons/s. 2D diffraction patterns were recorded on a Dectris-Pilatus2 1-M detector. A silver behenate standard (d-spacing = 58.38 Å) was used for q-scale calibration. The samples were loaded into Quartz Glass 1.5 mm capillaries (Hampton Research, USA) and positioned in a custom-designed sample holder capable of holding 34 capillaries and the temperature controlled to ±1.0 °C between 20 and 75 °C.[30] Temperature control was via a recirculating water bath (Huber, Germany). SAXS was performed on dispersions from 25 to 65 °C at 5 °C increments. The exposure time for each sample was 1 s. SAXS data was analysed using an IDL-based software package: AXcess.[41]

A laboratory-built humidity-controlled vitrification system was used to prepare the samples for cryo-TEM. Humidity was kept close to 80% for all experiments, and ambient temperature was 22 °C. These were the optimal conditions for sample preparation of lyotropic liquid crystalline nanostructured particle samples. Copper grids (200-mesh) coated with perforated carbon film (Lacey carbon film: ProSciTech, Kirwan, Qld, Australia) were glow discharged in nitrogen to render them hydrophilic. Aliquots of the sample (4 μl) were pipetted onto each grid prior to plunging. After 30 sec adsorption time, the grid was blotted manually using Whatman 541 filter paper, for 2 sec. Blotting time was optimized for each sample. The grid was then plunged into liquid ethane cooled by liquid nitrogen. Frozen grids were stored in liquid nitrogen until required. The samples were examined using a Gatan 626 cryoholder (Gatan, Pleasanton, CA, USA) and Tecnai 12 Transmission Electron Microscope (FEI, Eindhoven, The Netherlands) at an operating voltage of 120 kV. At all times low dose procedures were followed, using an electron dose of 8-10 electrons/Å^2 for all imaging. Images were recorded using a FEI Eagle 4k × 4k CCD camera at magnifications in the range 15 000x to 40 000x.

3. Results

A library of sixty PEGylated-lipid copolymers (PEG-PHYT) was synthesized using the polycondensation scheme (Scheme 1) adapted from Rouxhet *et al.*.[33]

Part I – Copolymers

3.1 Polymer characterization

Polymers composed of 10 to 40 mol% PEG with molecular weights between 200 and 14K Da, 10 to 40 mol% phytantriol (PHYT) and all containing 50 mol% succinic anhydride (SA) were synthesized. The polycondensation of the different monomers, represented in Scheme 1 will lead to random copolymers. Weight-averaged molecular weight (M_w), number-average molecular weight (M_n) and dispersity ($M_w/M_n = Đ$) of the synthesized polymers were determined by GPC using chloroform as the eluent and shown in Table 1. The dispersities were determined to be between 1.1 and 2.7, with most copolymers having $Đ<1.5$.

3.2 Polymer self-assembling properties

The self-assembly behaviour of the polymers in excess water was characterized using dynamic light scattering to determine their critical aggregation concentration. Subsequently, the cross-polarized light microscopy technique was used to establish whether the polymers formed thermotropic liquid crystalline phases and whether lyotropic liquid crystals were formed in the presence of water.

3.2.1 Critical aggregation concentration (CAC) and Gibbs free energy of aggregation (ΔG_{agg})

The critical aggregation concentration of each polymer, with a PEG moiety greater than 45 units on average (i.e. PEG2K), was established using dynamic light scattering as shown in Table 1. The scattered light intensity was measured over a serial dilution of the copolymers in water. Copolymers with PEG MW ≤1K were excluded from the study due to their very low water solubility.

As expected, increasing the molar percentage (PEG mol%) of PEG units within the polymers typically resulted in a corresponding increase in CAC (Table 1). This trend was most pronounced across the 10, 20, 25, 30 and 40 PEG mol% copolymers with higher PEG molecular weights (i.e. ≥PEG6K). For example, the CACs for the PEG8K copolymers increased gradually with PEG molar ratio (Figure 1).

Increasing the PEG MW of the copolymer series while maintaining the same molar percentage of PEG to lipid generally resulted in an increase in the CAC. For example, the CAC generally increased for PEG2K (CAC value of 0.2 μM) to PEG14K (CAC value of 8.2 μM) in the 40 PEG mol% series (Table 1).

The Gibbs free energy of aggregation (ΔG_{agg}) in all cases is negative confirming the spontaneity of aggregate formation and the spontaneity is generally observed to be much higher for soluble copolymers with a lower PEG mol% (i.e. 10 PEG mol%) (Table 1 and Figure 1).

3.2.2 Self-Assembly of copolymers using cross-polarized light microscopy (CPLM)

Polymer self-assembly was examined using cross-polarized light microscopy to assess the thermotropic and lyotropic phase behaviour properties. Temperature and penetration scans of PEG-PHYT copolymers with 10, 20, 25, 30 and 40 PEG mol%, where the PEG MW is 1K to 14K, were performed over a temperature range of 20 to 60 °C. The polymer series showed some anisotropic and isotropic phases, indicative of liquid crystalline properties (see Supplementary Material for data).[39]

Lyotropic liquid crystalline phase behaviour in excess water

Upon hydration in water, at either 25 °C or 30 °C, twenty-three of the sixty copolymers that were synthesized displayed an isotropic band near the water interface. The high viscosity upon shearing of this band suggested that it may be a cubic phase. The majority of copolymers that displayed cubic isotropic bands had a PEG molecular weight range between 1K and 14K and their PEG molar ratio typically between 10 and 30%.

One particular example, $PEG10K_{10}PHYT_{40}$, displayed an isotropic region, believed to be a cubic phase, above 35 °C, which slowly formed and expanded until the entire copolymer material dissolved, leaving only an aqueous solution visible on the microscope slide at 55 °C. A representative water penetration scan at 40 °C for this copolymer is shown in Figure 2.

The self-assembly behaviour of the copolymers was also assessed using SAXS, for two different systems; (i) with high polymer (>60 % polymer content) and (ii) with high water (>60 % hydration) to attempt to determine whether long range order existed in the samples as an indication of formation of lyotropic liquid crystalline structure formation. No long-range order, typical of lyotropic crystalline phases, was detected during SAXS analysis of these systems. This indicated

that the anisotropic and isotropic phases observed during CPLM were not able to persist at high hydration levels, and therefore are most likely type I (normal phases) phases. This is comparable to the behaviour of F127, which has been reported to also form type I lyotropic liquid crystalline structures (isotropic phase and micellar cubic phase, Q_1).[42]

Part II – Performance as Steric Stabilizers for Cubosomes

3.3 Colloidal Stability

3.3.1 Visual Assessment & DLS

A well-dispersed cubosome sample has a milky white, aggregate-free appearance. This provides a good indication of stabilizer effectiveness. Dispersions which are translucent with visible aggregates are poorly stabilised. To perform a rapid initial screen of the stabilization capability of the copolymers, the phytantriol dispersions were assessed visually and complemented with particle sizing measurements using dynamic light scattering. Visual assessment was performed on all dispersions, which were formed using 100 mg/mL of phytantriol in PBS buffer solution, using 1 wt% of the new copolymers (Table 2).

It was found that copolymers which had a PEG MW <1K were unable to form stable dispersions, with large aggregates visible in the aqueous medium. Despite a slight cloudiness in the dispersions formed using $PEG800_{30}PHYT_{20}$ and $PEG800_{40}PHYT_{10}$, they were still poor quality dispersions with large visible aggregates (stability score -/+). It is apparent that the hydrophilic PEG chain ≥PEG1K is required to create a steric barrier on the surface of the lyotropic liquid crystalline nanostructured particles for steric repulsion of neighbouring colloids. In agreement with Kim *et al.* it was found that longer hydrophilic chain lengths (i.e. >PEG1K) provided better stabilization.[43] Copolymers that were not able to stabilize particles were therefore excluded from further investigations. The remaining dispersions were found to have a similar 'milky' appearance to those dispersions stabilized using F127 (the positive control known to effectively stabilize cubosomes).

The stability of the dispersions prepared using PEG6K copolymers was found to be dependent on the PEG molar ratio, with 10, 20 and 25 mol% scoring ++ and 30 and 40 mol% scoring +++. This indicates that a higher PEG to lipid ratio reduced the degree of aggregation. In contrast, copolymers with higher PEG molecular weights, such as PEG8K and PEG10K, displayed the reverse trend. Both PEG3K and PEG4K copolymers with 20, 25 and 40 mol% produced the

most stable (+++) dispersions. Overall the most stable dispersions were seen for the 20, 25 and 40 PEG mol% copolymer series, typically with PEG MW values between PEG1K and PEG6K.

Particle size and polydispersity index of the dispersions were measured using dynamic light scattering (see Supplementary Materials for data). Although there are variations in the PEG content (i.e. varying PEG mol% or PEG MW) of the PEG-PHYT copolymer series employed to stabilize phytantriol dispersions, there was no discernible trend revealed by the particle size measurements obtained that may highlight this. The average particle size of the dispersions measured using DLS was between 174 and 386 nm. It should be noted that DLS determination of particle size is not a clear indication of colloidal stability when measured in isolation because large phase-separating aggregates may not be detected by the technique, leading to a misleading average particle size distribution.

3.3.2 Accelerated stability assay (ASA) for steric stabilizer effectiveness

The effectiveness of PEG-PHYT copolymer as a steric stabilizer for stabilizing phytantriol dispersions was quantified with an accelerated stability assay, developed for the quantification of lyotropic liquid crystalline nanoparticle steric stabilizers compared to control stabilizer F127.[40] Steric stabilization of phytantriol cubosomes by F127 was assessed at 0.3, 0.5, 0.7, 1 and 1.2 wt% to provide comparison of systems to 'poorly' (i.e. 0.3 wt%) and 'well' (i.e. 1 wt%) stabilized systems based on previous experience with F127. Only stabilizers with a visual assessment score of either a ++ or +++ were assessed.

ASA results for F127 were in agreement with previous ASA results for this system[40], with greater aggregation (i.e. increased creaming) correlating with increased fluorescence signal intensities. As expected, at 0.3 wt% F127, the greatest aggregation was observed during the ASA, correlating with the greatest increase in fluorescence signal. By increasing the F127 concentration, better steric stabilizer effectiveness was observed, with the optimal stabilizer concentration established to be 1 wt% (Figure 3).

With all the phytantriol dispersions stabilized at the same copolymer concentration of 1 wt%, a clear trend of decreasing change in fluorescence signal intensity was seen within the $PEG_{20}PHYT_{30}$ series with increasing PEG MW from 2K to 14K (Figure 3), with smaller changes in fluorescence signal intensity indicating better steric stabilizer effectiveness. Longer hydrophilic moieties (i.e. longer PEG chains) for the copolymer steric stabilizer provided better steric stabilization. This is illustrated in the $PEG_{20}PHYT_{30}$ copolymer series (Figure 3).

The accelerated stability assay results indicate that amphiphilic copolymers PEG-PHYT with larger PEG molar ratios, such as the copolymer series with 30 PEG mol%, are more effective steric stabilizers as a smaller change in fluorescence signal intensity was obtained. This is illustrated in Figure 3, where both $PEG4K_{30}PHYT_{20}$ and $PEG6K_{30}PHYT_{20}$ copolymers have the least change in fluorescence signal intensities.

ASA results also revealed that some of the copolymers provided comparable stability to that of F127 at 1 wt% (Figure 3). Specifically $PEG6K_{30}PHYT_{20}$ and copolymers from the $PEG_{20}PHYT_{30}$ stabilizers series, with PEG MW 8K to 14K.

3.3.3 Lyotropic phase behaviour of dispersions stabilized with PEG-PHYT copolymers

The PEG-PHYT copolymers were successful at sterically stabilizing inverse bicontinuous cubic phase nanostructured particles, at 1 wt% stabilizer concentration. All phytantriol dispersions stabilized at this concentration using PEG-PHYT copolymers, with PEG MW ≥1K at 25 °C yielded a SAXS diffraction pattern indicative of a cubic (Q_2^D or Q_2^P) lyotropic liquid crystal phase (Figure 4). This corresponded to a Pn3m or Im3m space group symmetry respectively. Cubosomes with a Pn3m space group symmetry, double diamond phase (Q_2^D), which is characteristic of the bulk phase formed by phytantriol in excess water, were stabilized by PEG-PHYT copolymers with PEG MW ≥3K (i.e. ≥68 PEG units on average) (Figure 4). These Q_2^D cubosomes had an average lattice parameter of 66.8 Å at 25 °C that decreased in size with increasing temperature. This is comparable to the lattice parameter recorded for phytantriol Q_2^D cubosomes stabilized by F127 (66.4 Å) at 25 °C. All the copolymers in the 25, 30 and 40 PEG mol% series, with PEG MW ≥3K (i.e. ≥68 PEG units on average) were able to stabilize cubosomes with a Q_2^D cubic phase at physiological temperature of 37 °C (Figure 4). Cubosomes with a primitive phase internal structure, Im3m space group symmetry (Q_2^P), were observed in phytantriol dispersions stabilized using PEG-PHYT copolymers with PEG MW≤2K (i.e. ≤45 PEG units on average). These Q_2^P cubosomes had an average lattice parameter of 98.1 Å at 25 °C, which decreased with increasing temperature.

Phase transitions, such as from the cubic (Q_2^D) to the hexagonal (H_2) phase, can be induced by increasing the temperature of the lyotropic liquid crystal dispersion. The higher the phase transition temperature the more resilient the structure is to thermal changes. Higher phase transition temperatures were observed for phytantriol dispersions stabilized using PEG-PHYT copolymers, where the PEG block was of equal or greater molar ratio to the hydrophobic block (i.e. 25, 30 or 40 PEG mol% copolymer series). For example, phytantriol dispersions stabilized with the $PEG_{25}PHYT_{25}$ copolymer series, where PEG MW 3K-8K (i.e. 68-181 PEG units on average), displayed cubic to hexagonal phase transition temperatures greater or equal to 50 °C. The hexagonal (H_2) phase obtained in SAXS for the dispersions stabilized with the copolymers

had an average lattice parameter of 40.0 Å, which decreased with increasing temperatures. Copolymers in the 25 PEG mol% copolymer series exceeding PEG MW 8K (i.e. >181 PEG units on average) had relatively lower cubic to hexagonal transition temperatures, which were as low as 40 °C. This indicates for the 25 PEG mol% copolymer series, very high PEG lengths are not beneficial to maintain the particle cubic phase at moderate temperatures (i.e. ≥40 °C).

The overall trend observed for the novel PEG-PHYT copolymer steric stabilizers, with PEG MW >2K (i.e. >45 PEG units on average), was that as the hydrophilic portion of the steric stabilizer structure was increased (i.e. >10 PEG mol% series) the higher the observed cubic to hexagonal phase transition temperature for phytantriol stabilized dispersions (Figure 5). The highest cubic to hexagonal phase transition temperatures (i.e. 55 °C) were observed for phytantriol dispersions stabilized with copolymers with PEG MW≥8K (i.e. >181 PEG units on average) from the $PEG_{30}PHYT_{20}$ and $PEG_{40}PHYT_{10}$ series. Thus, it was generally observed that the copolymer series with PEG molar ratios of 30 and 40 mol%, were able to maintain a stable Q_2^D cubic phase over a greater temperature range than the rest of the copolymers. In particular, the $PEG_{30}PHYT_{20}$ series, where PEG MW ≥6K (i.e. ≥136 PEG units on average), display both high cubic to hexagonal phase transition temperatures and ASA results that indicate it is an effective steric stabilizer, which is better than or comparable to the stabilizer effectiveness of standard control steric stabilizer F127.

Cryo-TEM was performed to further confirm the type of lyotropic liquid crystalline phase present in the aqueous dispersion of phytantriol. Cryo-TEM images taken of phytantriol nanoparticles stabilized with 1 wt% of $PEG6K_{25}PHYT_{25}$ in PBS at room temperature (25 °C) are shown in Figure 6. Cubosomes as well as vesicular structures were observed under cryo-TEM. Although cubosomes of different sizes were present, the majority of the nanostructured particles were approximately 200 nm in diameter. The Fourier transform of the internal structure of the particle (Figure 6 inset) shows a hexagonal arrangement. The internal structure is observed along the [111] axis, and the crystallographic planes observed are of the (110) type. This is compatible with the space group symmetries of Pn3m, Im3m, Ia3d or H_{II}. However, considering the SAXS results of this sample, it is most likely the cubic structure with Pn3m space group symmetry. It should be noted that results from cryo-TEM analysis are not a complete/comprehensive representation of the entire sample size, as only a small fraction of the actual sample is examined under the microscope, and therefore results obtained are used to compliment the SAXS results/data, to determine lyotropic liquid crystalline behaviour.

4. Discussion

4.1. PEG-PHYT Copolymer Self Assembly Properties

Amphiphilic copolymers typically self-assemble in the presence of water in order to minimize interfacial free energy.[44-46] The PEGylated-lipid (PEG-PHYT) copolymers self-assembled, with aggregation detected at 25 °C. These critical aggregation concentrations for the PEG-PHYT copolymers displayed a general trend, where the greater the proportion of lipophilic moiety (i.e. PHYT mol%) in the copolymer structure for a given PEG content, generally the lower the CAC value.

These findings were in reasonable agreement with the literature for micelle formation using AB diblock copolymers, where the increase in the length of a hydrophobic block at a given length of a hydrophilic block causes a noticeable decrease in CMC value and increase in micelle stability.[47-50] Although the copolymers in this study cannot be considered to be a diblock structure, their behaviour is at least somewhat consistent with that of diblocks. The same trend applied to the copolymers with lower PEG molecular weights (i.e. <6K) within the same PEG molar ratio copolymer series. This trend is evident from the CAC values for the copolymer series with a PEG molar ratio >10 mol%. These findings again were in general agreement with literature on micelle formation using AB diblock copolymers, where the increase in the length of a hydrophilic block at a given length of a hydrophobic block results in a small rise of the CMC value.[47, 49, 51]

The general trend obtained in this study of higher CAC values for PEGylated-phytanyl copolymers with longer PEG lengths, is also in accordance to Rosen *et al.* where a series of 2-dodecyloxypoly(ethenoxyethanol) surfactants were synthesized with different amounts of PEG (i.e. 2, 3, 4, 5, 7 and 8 PEG units) and higher CMC values were reported for surfactants with longer PEG chains.[52] Rouxhet *et al*. also reported a similar trend in which higher CAC values were determined for the PEGylated-monoglyceride copolymers with longer PEG lengths (i.e. 9 to 48 PEG units on average). CMCs have been found to decrease strongly with increasing alkyl chain length of the surfactant.[53] Thus, in agreement with Kwon *et al.* for AB diblock copolymers, both the hydrophilic and hydrophobic blocks influence the micelle CMC value, with the hydrophobic block playing a more crucial role.[48, 54]

The Gibbs free energy of aggregation for the PEGylated-phytanyl copolymer series in this study were found to display a similar trend to the Gibbs free energy of micellation of the 2-dodecyloxypoly(ethenoxyethanol) surfactant series reported by Rosen *et al.*[52], whereby greater negative ΔG_{agg} values were generally observed for surfactants with a lower PEG content and/or shorter PEG length (Figure 1). This general trend was most obvious in the $PEG(x)_{40}PHYT_{10}$ series, illustrated by Figure 1. Figure 1 displays an asymptotic relationship occurring between the copolymer's PEG

length (i.e. number of PEG units) and its Gibbs free energy of aggregation, whereby increasing the copolymer's PEG length increases the value of Gibbs free energy of aggregation. However, increasing the copolymer's PEG length past 90 PEG units was found to incur little to no change to the value of the Gibbs free energy of aggregation, with a maximum ΔG_{agg} value of -28.1 kJ mol^{-1} reported.

The CAC values of known commercially-available cubosome steric stabilizers, Myrj® 59 and F127, were also found to be similar to several of the novel PEGylated-lipid (PEG-PHYT) copolymers. In particular, the CAC for $PEG6K_{30}PHYT_{20}$ copolymer was 1.9 μM, which is highly comparable to the CAC values of the commercial stabilizers, F127 (2.1 μM) and Myrj® 59 (1.8 μM).[8]

The lyotropic liquid crystalline phase behavior displayed under CPLM by the PEGylated-lipid copolymers are consistent with the lyotropic liquid crystalline phase behavior reported by Fong *et al.* for monodispersed non-ionic phytanyl ethylene oxide surfactants ($Phytanyl(EO)_n$, where n = 1 to 8) and non-ionic isoprenoid-type hexahydrofarnesyl ethylene oxide surfactants ($HFarnesyl(EO)_n$, where n = 1 to 8), where hexagonal, lamellar (L_α) phase, inverse cubic (Q_{II}) and isotropic phases (L_2) were reported.[55-56]

4.2. Steric Stabilization of Lyotropic Liquid Crystalline Nanostructured Particles

Phytantriol-based cubosomes were successfully sterically-stabilized by the PEG-PHYT copolymers. SAXS results where PEG MW >2K, at 1 wt% copolymer, the Q_2^D internal cubic phase was maintained at both 25 °C and physiological temperature, 37 °C, in agreement with the behavior of F127. The average particle size for the phytantriol Q_2^D cubosomes stabilized using the PEG-PHYT copolymers, was between 200 and 300 nm in diameter, which is also comparable to phytantriol cubosomes stabilized with F127. Furthermore, the stability assessment by ASA showed that some of the copolymers (e.g. $PEG_{30}PHYT_{20}$ series, where PEG MW >6K) provided steric stabilization for phytantriol cubosomes comparable to F127 at 1 wt% stabilizer concentration. This confirms that an essentially random copolymer structure can be as effective as an ABA triblock copolymer to provide steric stabilization for lyotropic liquid crystalline nanostructured particles. It is felt that the PEG-PHYT copolymers behave as block systems rather than random copolymers due to their amphiphilic nature. This type of behavior, displayed by random copolymers, has also been reported before for random polymers with varying hydrophilic and lipophilic characteristics.[57]

One of the important macromolecular features for a copolymer structure to be an effective steric stabilizer for cubosomes is having an asymmetrical amphiphilic structure containing a larger hydrophilic domain than the hydrophobic moiety (i.e. $PEG_{30}PHYT_{20}$ series, PEG MW ≥6K). It was shown that copolymers that had a PEG MW <1K were unable to successfully form dispersions, indicating the importance of PEG length when designing a steric stabilizer for cubosomes. For these PEGylated-lipid copolymers, a minimum of 22 ethylene glycol monomer units on average (i.e. PEG1K) was required for cubosomes to be stabilized (i.e. either Q_2^P or Q_2^D cubic phase). More specifically for obtaining phytantriol cubosomes with Q_2^D cubic phase, the copolymers were required to have at least 68 units on average of PEG (i.e. ≥PEG3K). These findings are comparable to results obtained using vitamin E TPGS, a known PEG-lipid stabilizer for phytantriol cubosomes.[58] Vitamin E TPGS, which has a PEG length of 22 PEG units on average (i.e. PEG1K), forms phytantriol dispersions with Q_2^P cubic internal structure, which is in accordance with the results herein where phytantriol dispersions stabilized using PHYT-PEG copolymers, with 22 PEG units on average, also formed Q_2^P cubosomes.

Pluronic® stabilizers required a minimum of 26 PEG units on average to stabilize phytantriol dispersions with a cubic phase (i.e. either Q_2^P or Q_2^D cubic phase).[16] To obtain the Q_2^D cubic phases, Pluronic® stabilizers require at least 61 units on average of PEG in each hydrophilic arm, with HLB value >24.[16] Thus, regardless of whether the stabilizer is a PEGylated-lipid copolymer (i.e. PEG-PHYT) or triblock (i.e. PEG-PPO-PEG, Pluronic®) copolymer, the minimum PEG length required to sterically stabilize phytantriol Q_2^D cubosome dispersions is ≥61 PEG units on average, with a HLB value >17. Similarly, when using Myrj® (PEG-stearate) series to stabilize phytantriol cubosomes, the stabilizers with PEG length <68 PEG units on average gave particles with Q_2^P internal structure, while ≥68 PEG units on average gave phytantriol cubosomes with Q_2^D structure.[40] The increased entropic effect of the 68 units on average (i.e. PEG3K) compared to 45 units on average (i.e. PEG2K) appears to be sufficient to stabilize phytantriol nanostructured particles, even when using copolymers with a low PEG molar content.

A key factor to take into account for shorter PEG chain length PEG-PHYT copolymers causing a change in structure for phytantriol cubosomes, from the parent Q_2^D phase to the Q_2^P structure, is the localization of the polymer within the lipid matrix. PEG-PHYT stabilizers with 45 or fewer PEG units on average changes the mesophase of the dispersed nanostructured particles, indicating increased internalization of the stabilizer within the lipid matrix due to the shortened length of the PEG chain. These smaller amphiphiles may be able to penetrate into the particles more readily via the aqueous channels or by virtue of their greater hydrophobicity and hence partition tendency, driving the change

in the mesophase. It is likely that this internalization results in less free amphiphile being available to provide surface coverage of the particles and therefore is consistent with the poorer colloidal stability. The poorer performance of the remainder of the shorter PEG-PHYT surfactants (i.e. ≤22 PEG units on average) may also be due to the decreasing PEG chain length, which would be expected to have a reduced capacity to create sufficient steric hindrance to inhibit flocculation.

Phytantriol dispersions stabilized with copolymers consisting of a longer hydrophilic moiety, $PEG_{30}PHYT_{20}$ series, where PEG MW ≥6K, resulted in higher cubic to hexagonal phase transition temperatures (i.e. >50 °C). Furthermore, these copolymers were effective steric stabilizers for phytantriol dispersions, illustrated and quantified using the ASA screening experiments (Figure 3), without compromising structure formation.

As well as establishing that the novel steric stabilizer copolymer (PEG-PHYT) requires a minimum PEG length to establish steric stability of lyotropic liquid crystalline nanostructured particles, it should also be noted that it can be disadvantageous to make a steric stabilizer "too" hydrophilic (i.e. 40 PEG mol% copolymer series). For example, the dispersions which were stabilized with copolymers in the $PEG_{40}PHYT_{10}$ series, where PEG MW is 4K and 6K, displayed ASA results with lower steric stabilizer effectiveness than those stabilized with a lower PEG molar ratio (i.e. $PEG_{30}PHYT_{20}$ series) at the same PEG length (Figure 3). In addition to having a lower steric stabilizer effectiveness, phytantriol dispersions stabilized with copolymers from the $PEG_{40}PHYT_{10}$ series were also shown to have lower cubic to hexagonal phase transition temperatures than those stabilized using stabilizers from the $PEG_{30}PHYT_{20}$ series (Figure 5). This indicates that the copolymer stabilizer series does appear to have a maximum 'hydrophilic threshold' (i.e. >30 PEG mol%) at which the effectiveness of the steric stabilizer is compromised when exceeded. The diminished steric stabilizer effectiveness by copolymers with an extremely large hydrophilic domain (i.e. $PEG_{40}PHYT_{10}$ series) could be due to: (i) the water solubility being too high and the stabilizer not adsorbing sufficiently to the particle surface or (ii) flocculation of the particles caused by 'bridging' mechanisms by the extended PEG chains of neighbouring particles interacting with each other.[59] Thus, it is recommended that when designing a steric stabilizer copolymer structure, the hydrophilic moiety should not exceed 60% of the total amphiphilic structure. The optimal PEG-PHYT copolymer stabilizer parameters (i.e. PEG length and mol%) lie between 68 to 136 PEG units on average and between 20 to 40 PEG mol%, for producing good quality dispersions (i.e. devoid of aggregates), which maintain a Q_2^D cubic phase at 37 °C (see Supplementary Material).

Having established the design rules for copolymer-based stabilizers that provide good quality stable dispersions while retaining the parent internal phase structure, future efforts will be directed towards preparing copolymers with more defined structures using controlled polymerization approaches such as reversible addition-fragmentation chain transfer (RAFT)[37, 60] and the inclusion of functionalizable monomer units to facilitate attachment of targeting ligands to drive the progress in the cubosome field from 'static' delivery particles, to biologically interactive delivery systems better suited for theranostic applications.

5. Conclusion

The novel PEGylated-phytanyl copolymers displayed self-assembly properties in water. A select number successfully sterically stabilized cubic lyotropic liquid crystalline nanostructured particles. Application of these amphiphilic PEGylated-lipid copolymers in other lipid-based self-assembly systems seems prospective. As lyotropic liquid crystalline nanoparticles (i.e. cubosomes) are further developed for biomedical applications, developing steric stabilizers with optimal performance is a crucial part. The amphiphilic copolymer PEG-PHYT series synthesized in this study has illustrated the potential of using customized steric stabilizers. Equivalent steric stabilizer effectiveness comparable to "gold standard" Pluronic® F127 can be achieved using this novel copolymer series.

FIGURES

(i)

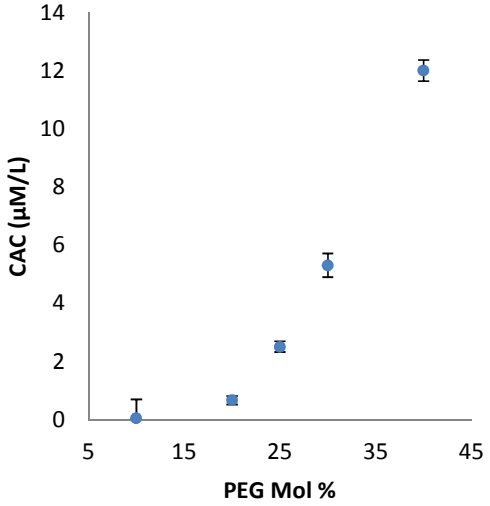

(ii)

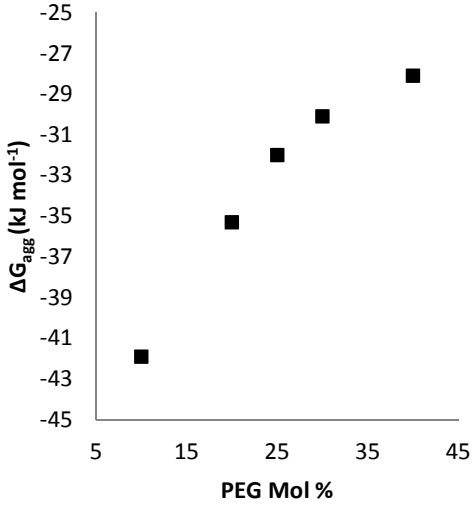

(iii)

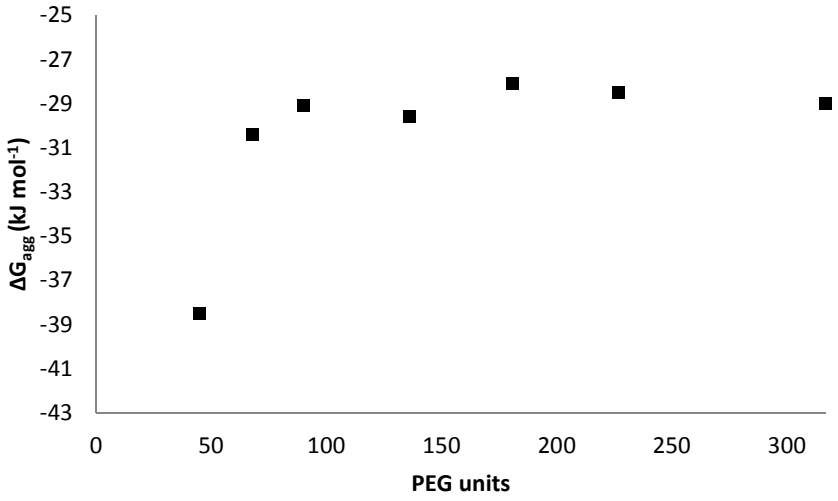

Figure 1. (i) CAC and (ii) ΔG_{agg} values for PEG8K$_y$PHYT$_z$, where *y*: 10 to 40 mol% and *z*: 10 to 40 mol%. (iii) ΔG_{agg} values vs. PEG units for PEG(x)$_{40}$PHYT$_{10}$ Error bars represent the standard deviation

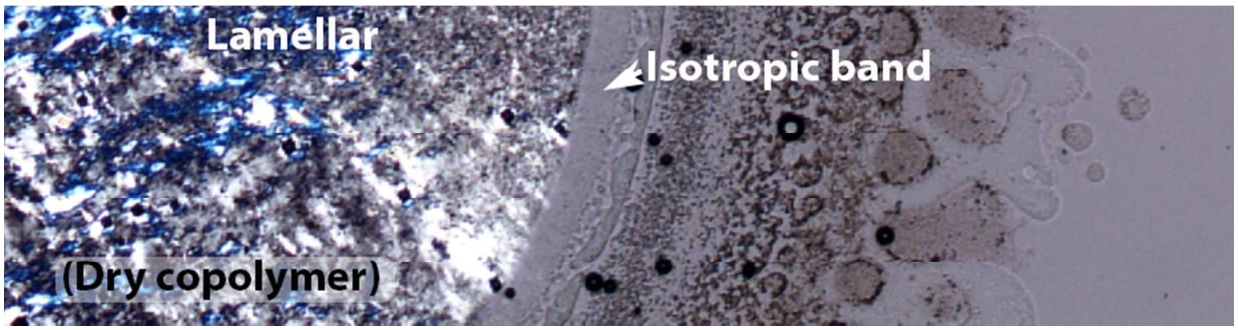

Figure 2. Water penetration scan of PEG10K$_{10}$PHYT$_{40}$ in excess water at 40 °C, displaying multiple bands (i.e. isotropic band). Dry copolymer is to the left of the figure, whist the excess water region is on the right of the image. 100x magnification

(a) **(b)**

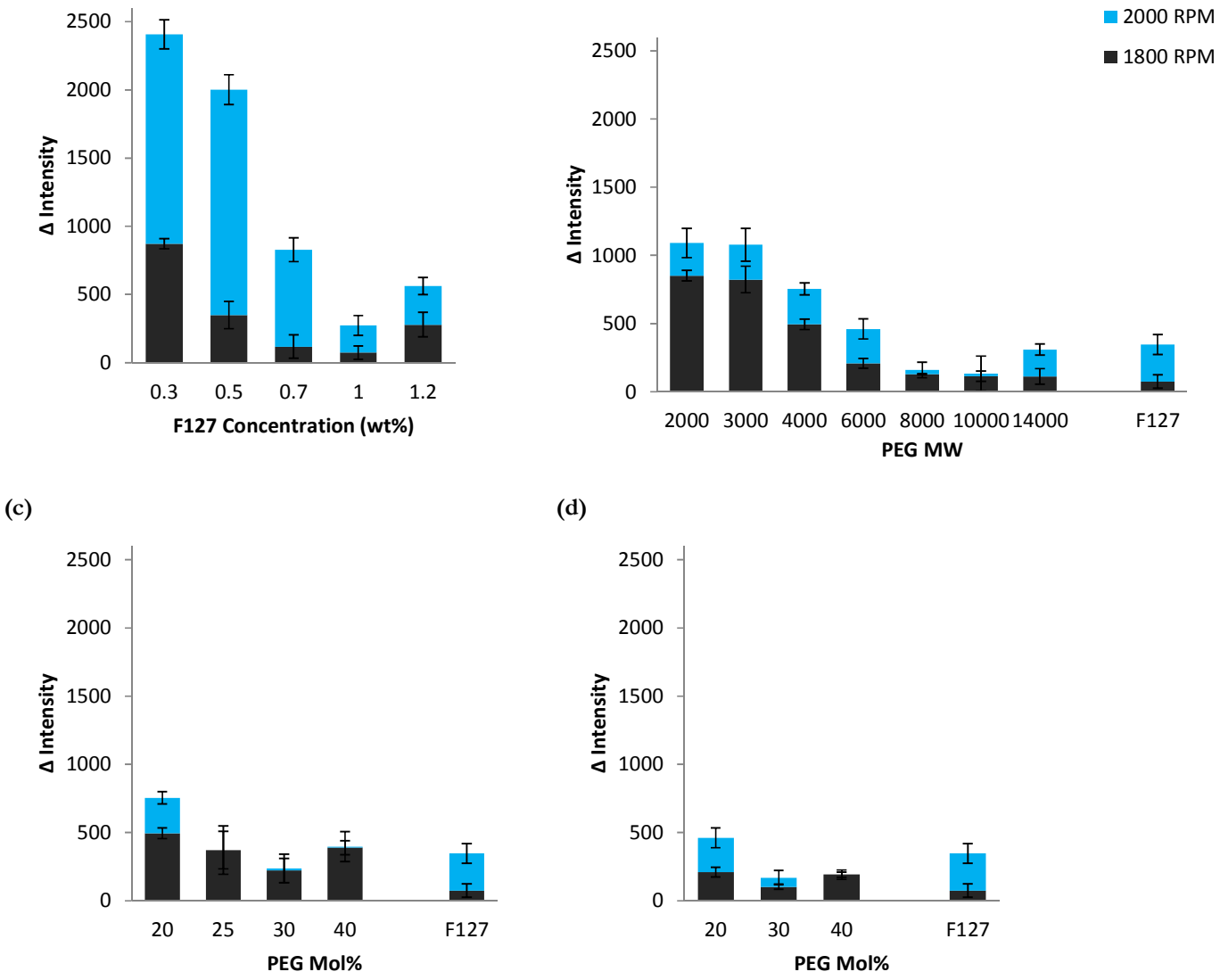

Figure 3. Accelerated stability assay results for (a) F127 (Control stabilizer) at 0.3 ,0.5, 0.7, 1 and 1.2 wt% stabilizer concentration, (b) $PEG_{20}PHYT_{30}$ copolymer series, where PEG MW: 2K to 14K, (c) PEG4K-PHYT copolymer (from 20, 25, 30 and 40 PEG mol% copolymer series) and (d) PEG6K-PHYT copolymer (from 20, 30 and 40 PEG mol% copolymer series). ASA results after first spin 1800 RPM are represented in grey columns, whilst ASA results after second spin 2000 RPM are represented in blue columns. Steric stabilizer concentration for ASA results presented in (b), (c) and (d) are 1 wt%, with control standard steric stabilizer F127 at 1 wt% presented to the right.

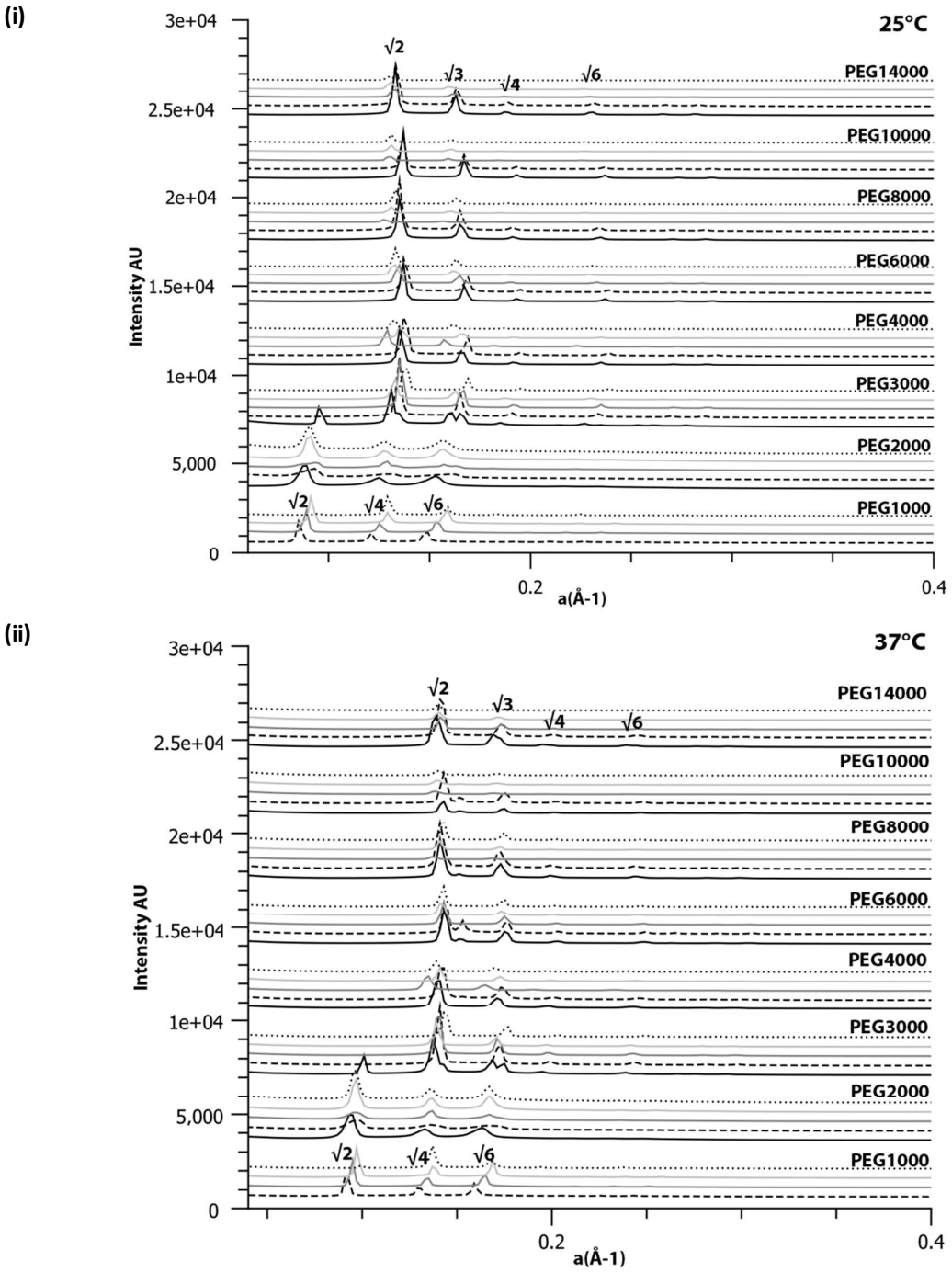

Figure 4. SAXS diffraction patterns at (i) room temperature (25 °C) and (ii) physiological temperature (37 °C) of phytantriol dispersions stabilized with PEG-PHYT copolymers where PEG mol %: 10% (1st, black line), 20% (2nd, black dash-line), 25% (3rd, dark grey line), 30% (4th, light grey line), 40% (5th, light grey dotted line), and PEG MW between 1K and 14K

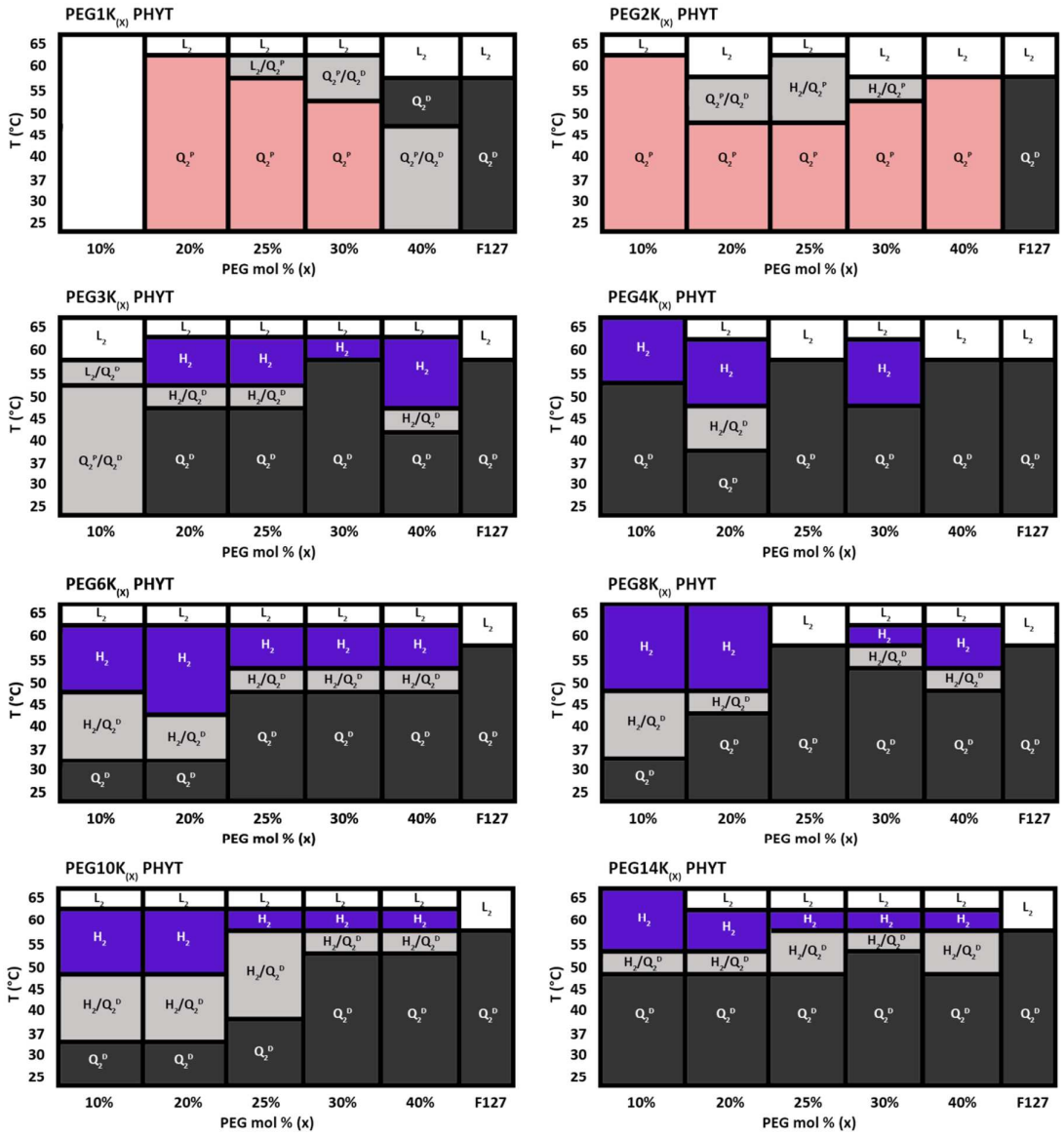

Figure 5. Lyotropic liquid crystalline (LLC) phases obtained during SAXS; temperature (°C) vs. PEG mol% over 8 different PEG MWs within the 5 different copolymer series. Order of tables placed from low PEG MW (PEG1K) to high PEG MW (PEG14K). These tables show the effect of increasing PEG density (or respectively the decreasing lipid ratio in copolymer) on LLC phase behaviour under increasing temperature (25-65°C).

(i)

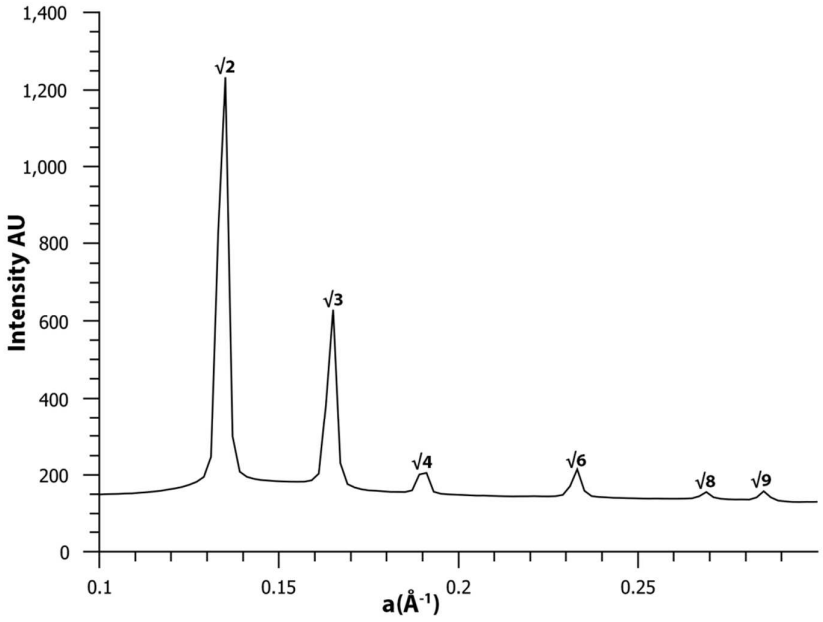

ii)

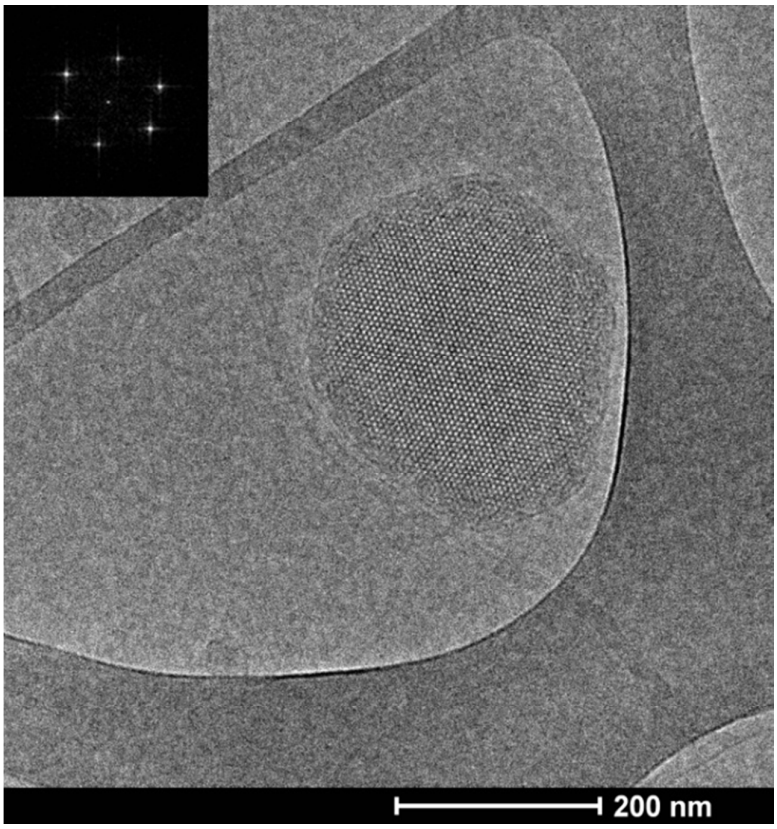

Figure 6. (i) SAXS diffraction pattern and (ii) cryo-TEM image observed in the [111] axis plane (inset shows FFT), of a phytantriol dispersion sterically stabilized using $PEG6K_{25}PHYT_{25}$ at 1 wt% stabilizer concentration

SCHEMES

Scheme 1. Synthesis scheme of the copolymers made of polyethylene glycol (PEG), phytantriol (PHYT) and succinic anhydride (SA) by polycondensation. PEG MW is denoted with (x), whilst the number of PEG units, SA units and PHYT units on average are denoted by *n*, *o* and *p* respectively. Polyethylene glycol units were calculated in accordance to $C_{2n}H_{4n+2}O_{n+1}$

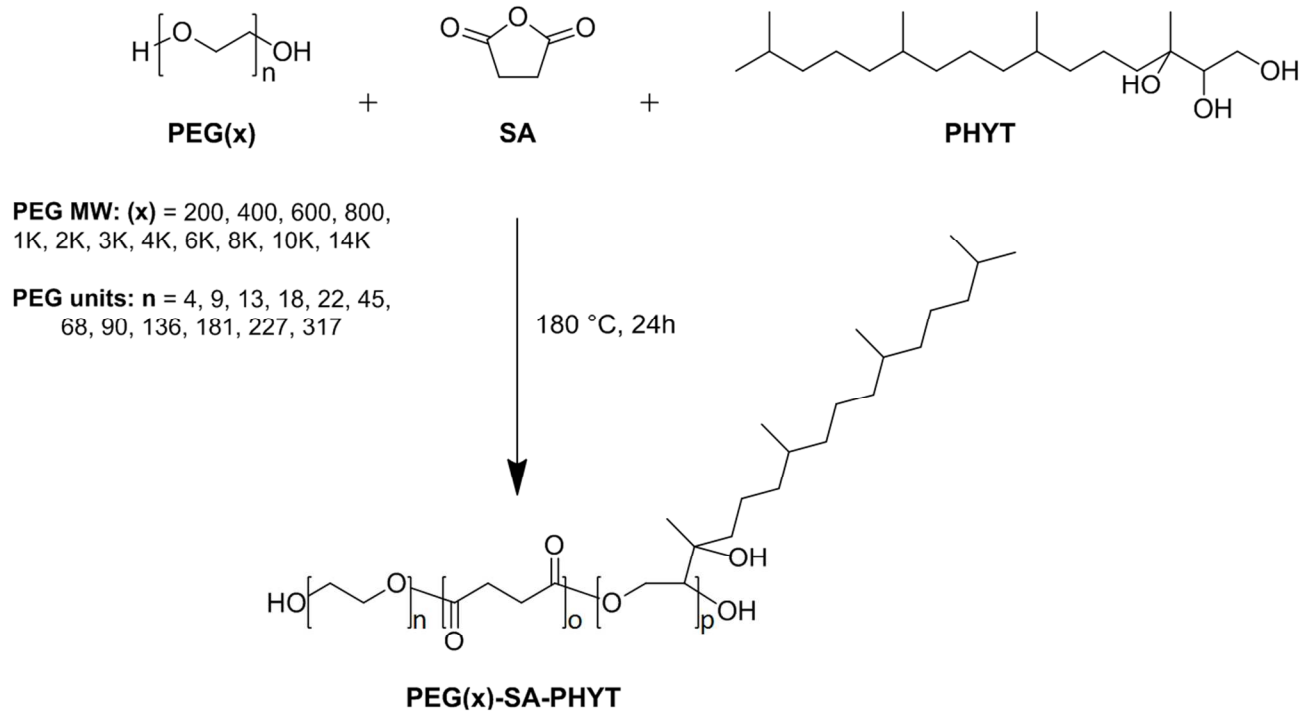

TABLES

Table 1. PEG-PHYT copolymers molecular weights (M_w, M_n), dispersity ($Đ$), physical state at room temperature 25 °C (S), hydrophilic-lipophilic balance (HLB) and critical aggregation concentration (CAC). [a]Apparent weight-averaged molecular weight (M_w), number-average molecular weight (M_n) and dispersity ($Đ$) of the phytanyl-based PEGylated copolymers determined by chloroform gel permeation chromatography, with the molecular weights in polystyrene equivalents. Dispersity is calculated using M_w/M_n. [b]The physical state of the copolymers at room temperature (25 °C) - L, Liquid; W/G, Waxy/Gel; W/S, Waxy/Solid; S, Solid. [c]HLB calculated using Griffin's method for non-ionic surfactants HLB=20*M_h/M, where M_h is the molecular mass of the hydrophilic portion of the molecule and M is the molecular mass of the whole molecule[61] [d]CAC – with micromole (μM) calculation using MW

determined by chloroform gel permeation chromatography (GPC) [e]Gibbs free energy of aggregation[62] (ΔG_{agg}) calculated using: $\Delta G_{agg} = RT \ln(CAC)$ where R is the universal gas constant and T is the absolute temperature

Polymer composition (mol%)		M_w[a]	M_n[a]	$Đ$[a]	S[b]	HLB[c]	CAC (μM)[d]	ΔG_{agg} (kJ mol^{-1})[e]
	PEG(x)							
PEG(x)$_{10}$PHYT$_{40}$	PEG200	1629	1358	1.3	L	6.9		
	PEG400	1259	914	1.4	L	8.1		
	PEG600	1259	901	1.4	L	9.1		
	PEG800	1278	869	1.5	L	9.9		
	PEG1K	1812	1014	1.8	W/G	10.6		
	PEG2K	5351	4965	1.1	W/S	13.1	1.6	-33.1
	PEG3K	5870	2150	2.7	W/G	14.5	0.02	-44.3
	PEG4K	8089	7353	1.1	W/G	15.5	1	-34.2
	PEG6K	13721	11442	1.2	S	16.6	0.2	-38.2
	PEG8K	20379	17886	1.1	S	17.3	0.05	-41.9
	PEG10K	16585	11414	1.5	S	17.8	0.06	-41.4
	PEG14K	28775	23985	1.2	S	18.3	0.1	-40.0
PEG(x)$_{20}$PHYT$_{30}$	PEG200	1700	1385	1.2	L	9.5		
	PEG400	2005	1466	1.4	L	11.3		
	PEG600	1644	1118	1.5	L	12.6		
	PEG800	2354	1406	1.7	L	13.6		
	PEG1K	3195	1696	1.9	W/G	14.3		
	PEG2K	5437	4425	1.2	W/S	16.4	1.6	-33.1
	PEG3K	8054	6283	1.3	W/G	17.4	1	-34.2
	PEG4K	9345	7193	1.3	W/G	17.9	2.7	-31.8
	PEG6K	12430	9219	1.3	S	18.5	2	-32.5
	PEG8K	38805	33867	1.1	S	18.9	0.7	-35.3
	PEG10K	13307	9171	1.5	S	19.1	1.9	-32.7
	PEG14K	27782	21954	1.3	S	19.3	0.9	-34.5
PEG(x)$_{25}$PHYT$_{25}$	PEG200	1660	1366	1.2	L	11.0		
	PEG400	1641	1086	1.5	L	12.9		
	PEG600	1580	993	1.6	L	14.2		
	PEG800	2184	1304	1.7	L	15.0		
	PEG1K	3124	1646	1.9	W/G	15.7		
	PEG2K	5356	4510	1.2	W/S	17.4	0.5	-35.9
	PEG3K	8687	7325	1.2	W/S	18.1	1	-34.3
	PEG4K	6312	2444	2.6	W/G	18.5	12	-28.1
	PEG6K	13395	10717	1.2	S	19.0	1.9	-32.7
	PEG8K	10422	3870	2.7	S	19.2	2.5	-32.0
	PEG10K	18852	13884	1.4	S	19.4	1.4	-33.4
	PEG14K	25429	13969	1.8	S	19.5	3	-31.5
PEG(x)$_{30}$PHYT$_{20}$	PEG200	2898	2301	1.3	L	12.5		
	PEG400	2074	1483	1.4	L	14.4		
	PEG600	1800	1171	1.5	L	15.5		
	PEG800	2362	1334	1.8	L	16.3		
	PEG1K	3970	2459	1.6	W/G	16.8		
	PEG2K	5182	4274	1.2	W/S	18.2	0.5	-35.8
	PEG3K	6761	5935	1.1	S	18.7	3.8	-30.9
	PEG4K	7907	7243	1.1	S	19.0	9.8	-28.6
	PEG6K	13602	11132	1.2	S	19.3	1.9	-32.7
	PEG8K	14594	7765	1.9	S	19.5	5.3	-30.1
	PEG10K	19276	14231	1.4	S	19.6	4	-30.8
	PEG14K	27161	20671	1.3	S	19.7	2.9	-31.6
PEG(x)$_{40}$PHYT$_{10}$	PEG200	1717	1324	1.3	L	15.9		
	PEG400	1895	1195	1.6	L	17.3		
	PEG600	2148	1310	1.6	L	18.0		
	PEG800	2885	1548	1.9	L	18.4		
	PEG1K	4820	2246	2.0	W/G	18.6		
	PEG2K	5109	4327	1.2	W/S	19.3	0.2	-38.5
	PEG3K	16254	12261	1.3	S	19.5	4.8	-30.4
	PEG4K	9600	7877	1.2	S	19.6	8	-29.1
	PEG6K	12198	8977	1.4	S	19.7	6.4	-29.6
	PEG8K	20426	18107	1.1	S	19.8	12	-28.1
	PEG10K	22290	17483	1.3	S	19.8	10	-28.5
	PEG14K	28529	23227	1.2	S	19.9	8.2	-29.0

Table 2. Visual assessment of the stability of phytantriol dispersions using 1 wt% PEG-PHYT copolymers as steric stabilizer. Key: +++ milky sample with no visible aggregates. ++ milky sample with few visible aggregates, + milky/cloudy sample with aggregates, - translucent sample with large aggregates [samples rated (-) were not progressed to ASA or SAXS assessment]

PEG(x)-PHYT [Mol%]		$PEG(x)_{10}PHYT_{40}$	$PEG(x)_{20}PHYT_{30}$	$PEG(x)_{25}PHYT_{25}$	$PEG(x)_{30}PHYT_{20}$	$PEG(x)_{40}PHYT_{10}$
PEG MW (x)	PEG200	-	-	-	-	-
	PEG400	-	-	-	-	-
	PEG600	-	-	-	-	-
	PEG800	-	-	-	-/+	-/+
	PEG1K	+	+++	+++	++	+++
	PEG2K	++	+++	++	++	+++
	PEG3K	+++	+++	+++	+	+++
	PEG4K	++	+++	+++	+++	+++
	PEG6K	++	++	++	+++	+++
	PEG8K	+++	++	++	+	+
	PEG10K	+++	++	++	+	+
	PEG14K	++	++	+++	+	+

Supporting Information

Datasets obtained of the NMR, CAC, CPLM, CAC, DLS and SAXS results for PEG-PHYT copolymers and their phytantriol dispersions. This material is available free of charge via the Internet at http://pubs.acs.org.

ACKNOWLEDGMENT

Calum J. Drummond was the recipient of an Australian Research Council (ARC) Federation Fellowship. Josephine Y.T. Chong was the recipient of an Australian Postgraduate Award and a CSIRO Ph.D. studentship. Xavier Mulet was the recipient of a CSIRO-Monash University Collaborative research postdoctoral fellowship. Ben J. Boyd is the recipient of an Australian Research Council (ARC) Future Fellowship (FT120100697). This research was undertaken in part at the SAXS/WAXS beamline at the Australian Synchrotron, Victoria, Australia.

REFERENCES

1. Koynova, R.; Caffrey, M. An index of lipid phase diagrams. *Chem. Phys. Lipids* **2002,** *115* (1–2), 107-219.
2. Seddon, J. M.; Bartle, E. A.; Mingins, J. Inverse cubic liquid-crystalline phases of phospholipids and related lyotropic systems. *J. Phys.-Condes. Matter* **1990,** *2*, SA285-SA290.
3. Seddon, J. M.; Hogan, J. L.; Warrender, N. A.; Pebaypeyroula, E. *Structural studies of phospholipid cubic phases* 1990; Vol. 81. p 189-197.
4. Yaghmur, A.; Glatter, O. Characterization and potential applications of nanostructured aqueous dispersions. *Adv. Colloid Interfac.* **2009,** *147-48*, 333-342.
5. Fraser, S. J.; Dawson, R. M.; Waddington, L. J.; Muir, B. W.; Mulet, X.; Hartley, P. G.; Separovic, F.; Polyzos, A. Development of Cubosomes as a Cell-Free Biosensing Platform. *Aust. J. Chem.* **2011,** *64* (1), 46-53.
6. Mulet, X.; Boyd, B. J.; Drummond, C. J. Advances in drug delivery and medical imaging using colloidal lyotropic liquid crystalline dispersions. *J. Colloid Interf. Sci.* **2013,** *393* (0), 1-20.
7. Spicer, P. T. Progress in liquid crystalline dispersions: Cubosomes. *Curr. Opin. Colloid In.* **2005,** *10* (5-6), 274-279.
8. Chong, J. Y. T.; Mulet, X.; Waddington, L. J.; Boyd, B. J.; Drummond, C. J. High-Throughput Discovery of Novel Steric Stabilizers for Cubic Lyotropic Liquid Crystal Nanoparticle Dispersions. *Langmuir* **2012,** *28* (25), 9223-9232.
9. Sagalowicz, L.; Guillot, S.; Acquistapace, S.; Schmitt, B.; Maurer, M.; Yaghmur, A.; de Campo, L.; Rouvet, M.; Leser, M.; Glatter, O. Influence of Vitamin E Acetate and Other Lipids on the Phase Behavior of Mesophases Based on Unsaturated Monoglycerides. *Langmuir* **2013,** *29* (26), 8222-8232.
10. Guillot, S.; Salentinig, S.; Chemelli, A.; Sagalowicz, L.; Leser, M. E.; Glatter, O. Influence of the Stabilizer Concentration on the Internal Liquid Crystalline Order and the Size of Oil-Loaded Monolinolein-Based Dispersions. *Langmuir* **2010,** *26* (9), 6222-6229.
11. Gustafsson, J.; Ljusberg-Wahren, H.; Almgren, M.; Larsson, K. Submicron particles of reversed lipid phases in water stabilized by a nonionic amphiphilic polymer. *Langmuir* **1997,** *13* (26), 6964-6971.
12. Spicer, P. T.; Hayden, K. L.; Lynch, M. L.; Ofori-Boateng, A.; Burns, J. L. Novel process for producing cubic liquid crystalline nanoparticles (cubosomes). *Langmuir* **2001,** *17* (19), 5748-5756.
13. Dong, Y. D.; Larson, I.; Hanley, T.; Boyd, B. J. Bulk and dispersed aqueous phase behavior of phytantriol: Effect of vitamin E acetate and F127 polymer on liquid crystal nanostructure. *Langmuir* **2006,** *22* (23), 9512-9518.
14. Nakano, M.; Teshigawara, T.; Sugita, A.; Leesajakul, W.; Taniguchi, A.; Kamo, T.; Matsuoka, H.; Handa, T. Dispersions of liquid crystalline phases of the monoolein/oleic acid/Pluronic F127 system. *Langmuir* **2002,** *18* (24), 9283-9288.
15. Kojarunchitt, T.; Hook, S.; Rizwan, S.; Rades, T.; Baldursdottir, S. Development and characterisation of modified poloxamer 407 thermoresponsive depot systems containing cubosomes. *Int. J. Pharm.* **2011,** *408* (1-2), 20-26.
16. Chong, J. Y. T.; Mulet, X.; Waddington, L. J.; Boyd, B. J.; Drummond, C. J. Steric stabilisation of self-assembled cubic lyotropic liquid crystalline nanoparticles: high throughput evaluation of triblock polyethylene oxide-polypropylene oxide-polyethylene oxide copolymers. *Soft Matter* **2011,** *7* (10), 4768-4777.

17. Tilley, A. J.; Drummond, C. J.; Boyd, B. J. Disposition and association of the steric stabilizer Pluronic® F127 in lyotropic liquid crystalline nanostructured particle dispersions. *J. Colloid Interf. Sci.* **2013,** *392* (0), 288-296.
18. Zhai, J. L.; Waddington, L.; Wooster, T. J.; Aguilar, M. I.; Boyd, B. J. Revisiting beta-Casein as a Stabilizer for Lipid Liquid Crystalline Nanostructured Particles. *Langmuir* **2011,** *27* (24), 14757-14766.
19. Muller, F.; Salonen, A.; Glatter, O. Phase behavior of Phytantriol/water bicontinuous cubic Pn3m cubosomes stabilized by Laponite disc-like particles. *J. Colloid Interf. Sci.* **2010,** *342* (2), 392-398.
20. Uyama, M.; Nakano, M.; Yamashita, J.; Handa, T. Useful Modified Cellulose Polymers as New Emulsifiers of Cubosomes. *Langmuir* **2009,** *25* (8), 4336-4338.
21. Libster, D.; Aserin, A.; Yariv, D.; Shoham, G.; Garti, N. Soft matter dispersions with ordered inner structures, stabilized by ethoxylated phytosterols. *Colloid Surf., B* **2009,** *74* (1), 202-215.
22. Dulle, M.; Glatter, O. Internally Self-Assembled Submicrometer Emulsions Stabilized with a Charged Polymer or with Silica Particles. *Langmuir* **2012,** *28* (2), 1136-1141.
23. Li, S. D.; Huang, L. Stealth nanoparticles: High density but sheddable PEG is a key for tumor targeting. *J. Control. Release* **2010,** *145* (3), 178-181.
24. Gref, R.; Luck, M.; Quellec, P.; Marchand, M.; Dellacherie, E.; Harnisch, S.; Blunk, T.; Muller, R. H. 'Stealth' corona-core nanoparticles surface modified by polyethylene glycol (PEG): influences of the corona (PEG chain length and surface density) and of the core composition on phagocytic uptake and plasma protein adsorption. *Colloid Surf., B* **2000,** *18* (3-4), 301-313.
25. Allen, T. M.; Hansen, C. Pharmacokinetics of stealth versus conventional liposomes - Effect of dose. *Biochim. Biophys. Acta* **1991,** *1068* (2), 133-141.
26. Immordino, M. L.; Dosio, F.; Cattel, L. Stealth liposomes: review of the basic science, rationale, and clinical applications, existing and potential. *Int. J. Nanomed.* **2006,** *1* (3), 297-315.
27. Knop, K.; Hoogenboom, R.; Fischer, D.; Schubert, U. S. Poly(ethylene glycol) in Drug Delivery: Pros and Cons as Well as Potential Alternatives. *Angew. Chem.-Int. Edit.* **2010,** *49* (36), 6288-6308.
28. Photos, P. J.; Bacakova, L.; Discher, B.; Bates, F. S.; Discher, D. E. Polymer vesicles in vivo: correlations with PEG molecular weight. *J. Control. Release* **2003,** *90* (3), 323-334.
29. Mulet, X.; Kennedy, D. F.; Conn, C. E.; Hawley, A.; Drummond, C. J. High throughput preparation and characterisation of amphiphilic nanostructured nanoparticulate drug delivery vehicles. *Int. J. Pharm.* **2010,** *395* (1-2), 290-297.
30. Mulet, X.; Conn, C. E.; Fong, C.; Kennedy, D. F.; Moghaddam, M. J.; Drummond, C. J. High-Throughput Development of Amphiphile Self-Assembly Materials: Fast-Tracking Synthesis, Characterization, Formulation, Application and Understanding. *Acc. Chem. Res.* **2013,** *46* (7), 1497-1505.
31. Takeoka, S.; Mori, K.; Ohkawa, H.; Sou, K.; Tsuchida, E. Synthesis and assembly of poly(ethylene glycol)-lipids with mono-, di-, and tetraacyl chains and a poly(ethylene glycol) chain of various molecular weights. *J. Am. Chem. Soc.* **2000,** *122* (33), 7927-7935.
32. Lee, J. H.; Jung, S. W.; Kim, I. S.; Jeong, Y. I.; Kim, Y. H.; Kim, S. H. Polymeric nanoparticle composed of fatty acids and poly(ethylene glycol) as a drug carrier. *Int. J. Pharm.* **2003,** *251* (1-2), 23-32.

33. Rouxhet, L.; Dinguizli, M.; Dwan'Isa, J. P. L.; Ould-Ouali, L.; Twaddle, P.; Nathan, A.; Brewster, M. E.; Rosenblatt, J.; Arien, A.; Preat, V. Monoglyceride-based self-assembling copolymers as carriers for poorly water-soluble drugs. *Int. J. Pharm.* **2009,** *382* (1-2), 244-253.
34. Lutz, J.-F. Polymerization of oligo(ethylene glycol) (meth)acrylates: Toward new generations of smart biocompatible materials. *J. Polym. Sci. A Polym. Chem.* **2008,** *46* (11), 3459-3470.
35. Heroguez, V.; Gnanou, Y.; Fontanille, M. Novel Amphiphilic Architectures by Ring-Opening Metathesis Polymerization of Macromonomers. *Macromolecules* **1997,** *30* (17), 4791-4798.
36. Murphy, J. J.; Kawasaki, T.; Fujiki, M.; Nomura, K. Precise Synthesis of Amphiphilic Polymeric Architectures by Grafting Poly(ethylene glycol) to End-Functionalized Block ROMP Copolymers. *Macromolecules* **2005,** *38* (4), 1075-1083.
37. Moad, G.; Rizzardo, E.; Thang, S. H. Radical addition–fragmentation chemistry in polymer synthesis. *Polymer* **2008,** *49* (5), 1079-1131.
38. Wallace, S. J.; Li, J.; Nation, R. L.; Prankerd, R. J.; Velkov, T.; Boyd, B. J. Self-assembly behavior of colistin and its prodrug Colistin methanesulfonate: Implications for solution stability and solubilization. *J. Phys. Chem. B* **2010,** *114* (14), 4836-4840.
39. Rosevear, F. B. The microscopy of the liquid crystalline neat and middle phases of soap and synthetic detergents *J. Am. Oil Chem. Soc.* **1954,** *31* (12), 628-639.
40. Chong, J. Y. T.; Mulet, X.; Boyd, B. J.; Drummond, C. J. Accelerated Stability Assay (ASA) for Colloidal Systems. *ACS Comb. Sci.* **2014,** *16* (5), 205-210.
41. Seddon, J. M.; Squires, A. M.; Conn, C. E.; Ces, O.; Heron, A. J.; Mulet, X.; Shearman, G. C.; Templer, R. H. Pressure-Jump X-Ray Studies of Liquid Crystal Transitions in Lipids. *Philos. T. R. Soc. A.* **2006,** *364* (1847), 2635-2655.
42. Sarkar, B.; Lakshmichand, J.; Alexandridis, P. Self-Assembly of Amphiphilic Block Copolymers in Ternary Solvent Mixtures: Lyotropic Liquid Crystalline Phase Behavior and Structure. *Macromol. Chem. Physic.* **2012,** *213* (23), 2514-2528.
43. Kim, S.-C.; Suh, S.-H.; Seong, B.-S. Effect of polymer size and chain length on depletion interactions between two colloids. *J. Chem. Phys.* **2007,** *127* (11), 114903.
44. Murray, R. C.; Hartley, G. S. Equilibrium between micelles and simple ions, with particular reference to the solubility of long-chain salts. *T. Faraday Soc.* **1935,** *31* (0), 183-189.
45. Shinoda, K.; Hutchinson, E. Pseudo-phase seperation model for thermodynamic calculations on micellar solutions. *J. Phys. Chem.* **1962,** *66* (4), 577-582.
46. Tiddy, G. J. T. Surfactant-water liquid crystal phases. *Phys. Rep.* **1980,** *57* (1), 1-46.
47. Nagarajan, R.; Ganesh, K. Block copolymer self-assembly in selective solvents: theory of solubilization in spherical micelles. *Macromolecules* **1989,** *22* (11), 4312-4325.
48. Kwon, G.; Naito, M.; Yokoyama, M.; Okano, T.; Sakurai, Y.; Kataoka, K. Micelles based on AB block copolymers of poly(ethylene oxide) and poly(.beta.-benzyl L-aspartate). *Langmuir* **1993,** *9* (4), 945-949.
49. Astafieva, I.; Zhong, X. F.; Eisenberg, A. Critical micellization phenomena in block polyelectrolyte solutions. *Macromolecules* **1993,** *26* (26), 7339-7352.
50. Tong, L.; Shen, Z.; Zhang, S.; Li, Y.; Lu, G.; Huang, X. Synthesis and characterization of perfluorocyclobutyl aryl ether-based amphiphilic diblock copolymer. *Polymer* **2008,** *49* (21), 4534-4540.
51. Torchilin, V. P. Structure and design of polymeric surfactant-based drug delivery systems. *J. Control. Release* **2001,** *73* (2-3), 137-172.

52. Rosen, M. J.; Cohen, A. W.; Dahanayake, M.; Hua, X. Y. Relationship of structure to properties in surfactants. 10. Surface and thermodynamic properties of 2-dodecyloxypoly(ethenoxyethanol)s, C12H25(OC2H4)XOH, in aqueous solution. *J. Phys. Chem.* **1982,** *86* (4), 541-545.
53. Holmberg, K.; Jönsson, B.; Kronberg, B.; Lindman, B. *Surfactants and Polymers in Aqueous Solution*; John Wiley & Sons, Ltd: Chichester, 1998.
54. Kwon, G.; Yokoyama, M.; Okano, T.; Sakurai, Y.; Kataoka, K. Biodistribution of Micelle-Forming Polymer–Drug Conjugates. *Pharm. Res.* **1993,** *10* (7), 970-974.
55. Fong, C.; Weerawardena, A.; Sagnella, S. M.; Mulet, X.; Waddington, L.; Krodkiewska, I.; Drummond, C. J. Monodisperse nonionic phytanyl ethylene oxide surfactants: high throughput lyotropic liquid crystalline phase determination and the formation of liposomes, hexosomes and cubosomes. *Soft Matter* **2010,** *6* (19), 4727-4741.
56. Fong, C.; Weerawardena, A.; Sagnella, S. M.; Mulet, X.; Krodkiewska, I.; Chong, J.; Drummond, C. J. Monodisperse Nonionic Isoprenoid-Type Hexahydrofarnesyl Ethylene Oxide Surfactants: High Throughput Lyotropic Liquid Crystalline Phase Determination. *Langmuir* **2011,** *27* (6), 2317-2326.
57. Maiez-Tribut, S.; Pascault, J. P.; Soulé, E. R.; Borrajo, J.; Williams, R. J. J. Nanostructured Epoxies Based on the Self-Assembly of Block Copolymers: A New Miscible Block That Can Be Tailored to Different Epoxy Formulations. *Macromolecules* **2007,** *40* (4), 1268-1273.
58. Barauskas, J.; Johnsson, M.; Tiberg, F. Self-Assembled Lipid Superstructures: Beyond Vesicles and Liposomes. *Nano Lett.* **2005,** *5* (8), 1615-1619.
59. Rosen, M. J.; Kunjappu, J. T. Dispersion and Aggregation of Solids in Liquid Media by Surfactants. In *Surfactants and Interfacial Phenomena*; John Wiley & Sons, Inc., 2012, pp 368-391.
60. Keddie, D. J. A guide to the synthesis of block copolymers using reversible-addition fragmentation chain transfer (RAFT) polymerization. *Chem. Soc. Rev.* **2014,** *43* (2), 496-505.
61. Griffin, W. C. Calculation of HLB Values of Non-Ionic Surfactants. *J. Soc. Cosmet. Chem.* **1954,** *5*, 249.
62. Rosen, M. J. Micelle Formation by Surfactants. In *Surfactants and Interfacial Phenomena*; John Wiley & Sons, Inc., 2004, pp 105-177.

TOC graphic

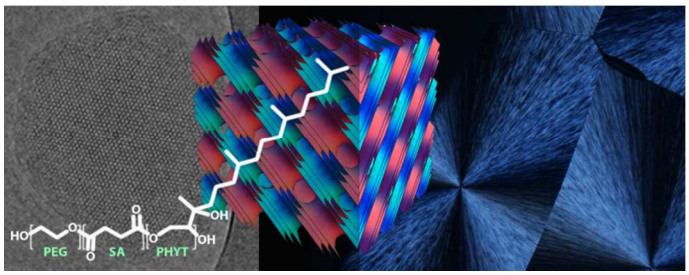

Graphic for Langmuir Journal Cover

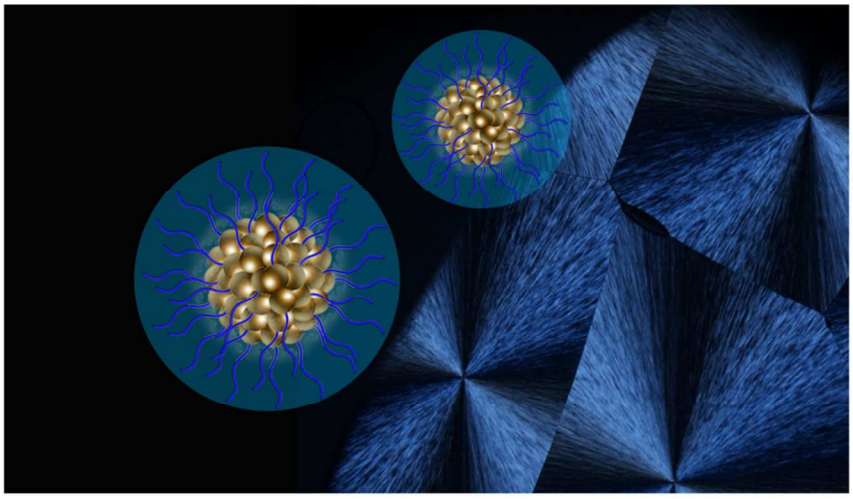

Supplementary Materials

Novel steric stabilizers for lyotropic liquid crystalline nanoparticles: PEGylated-phytanyl copolymers

Josephine Y.T. Chong, Xavier Mulet, Daniel J. Keddie, Lynne Waddington, Stephen T. Mudie, Ben J. Boyd, Calum J. Drummond

Representative ^{1}H NMR spectrum of $PEG(x)_{25}PHYT_{25}$ copolymer series (x=200-14K)

$PEG200_{25}PHYT_{25}$

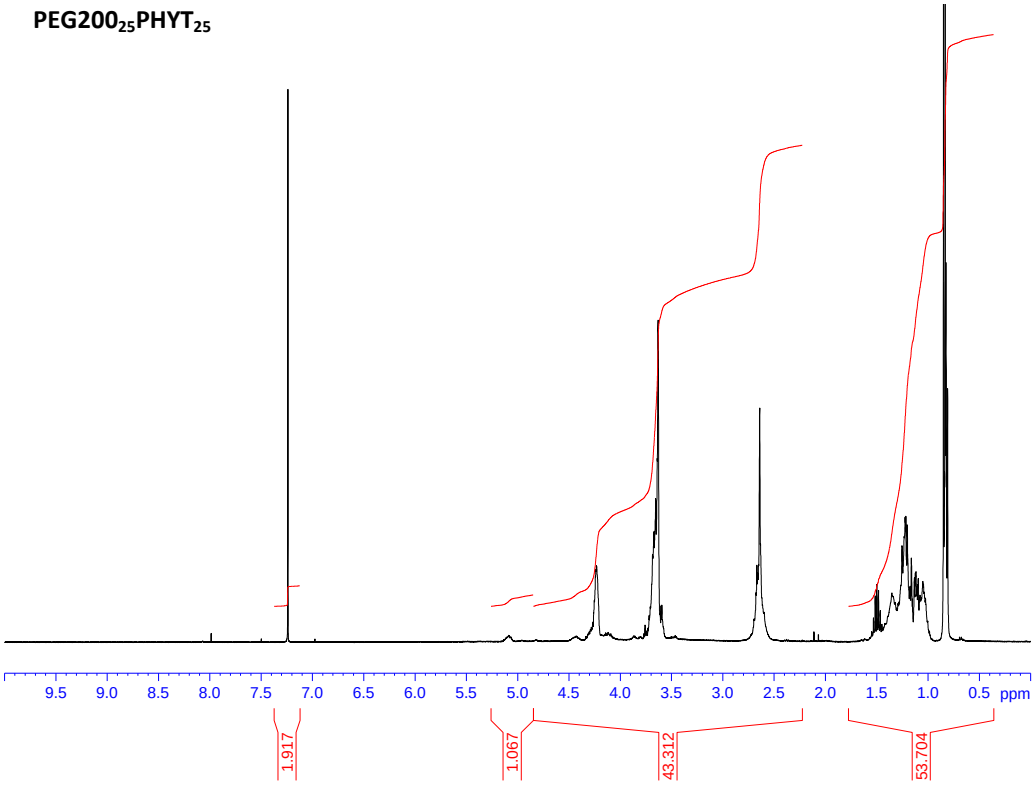

$PEG400_{25}PHYT_{25}$

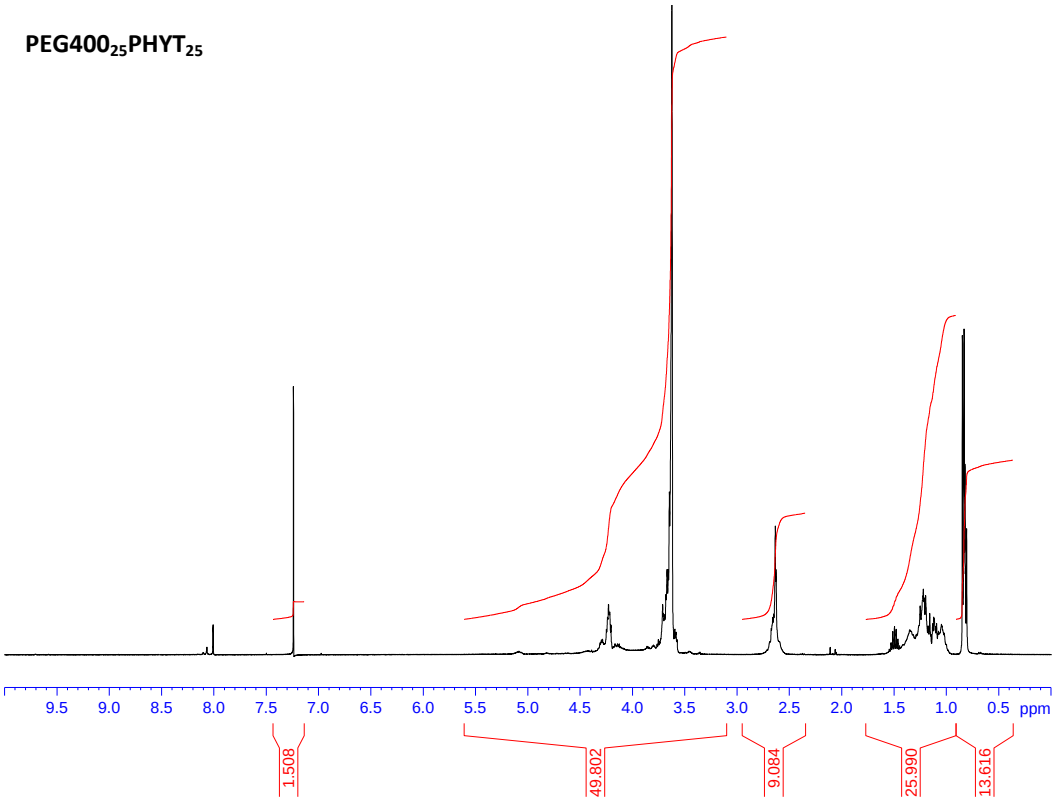

PEG600$_{25}$PHYT$_{25}$

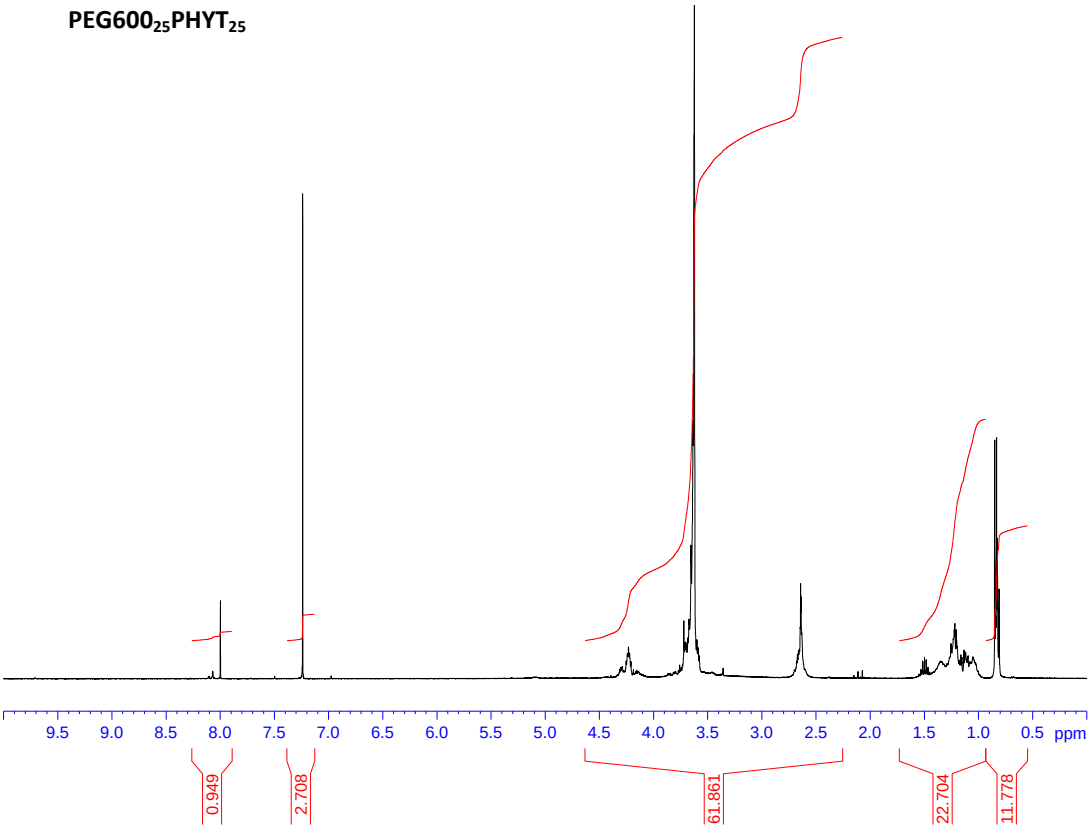

PEG800$_{25}$PHYT$_{25}$

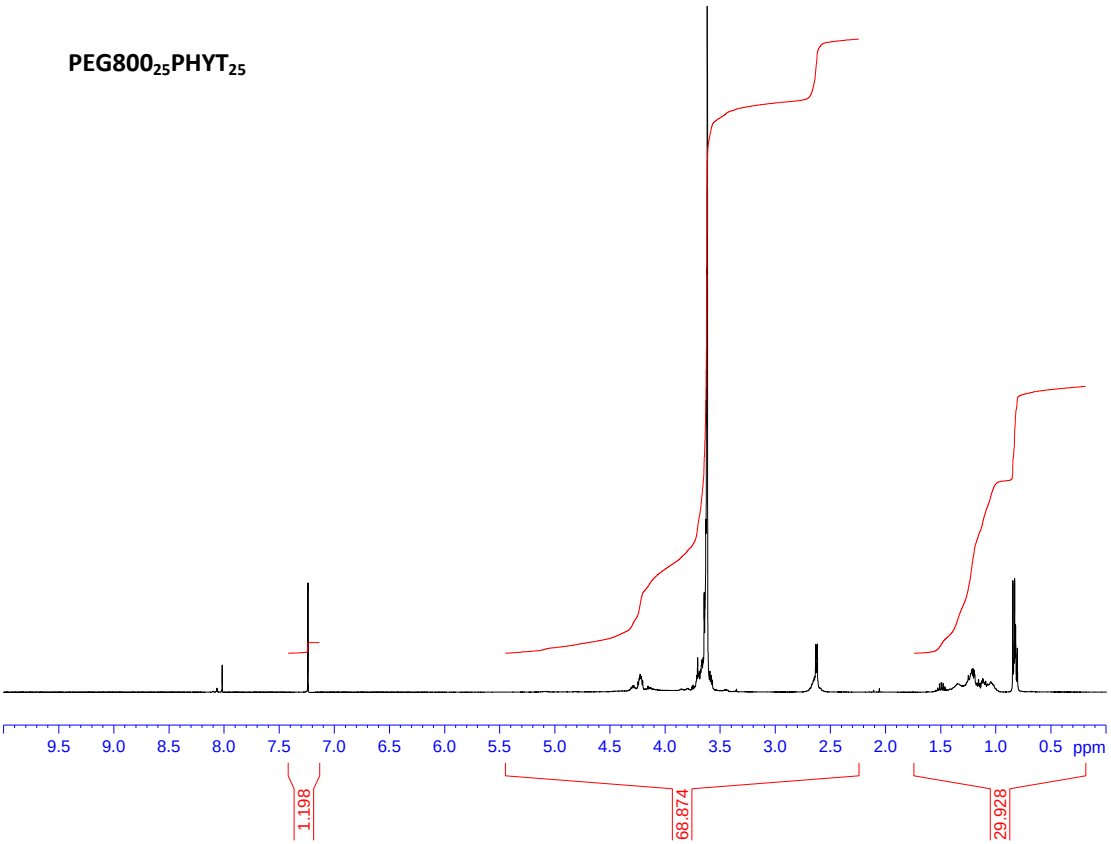

PEG1K$_{25}$PHYT$_{25}$

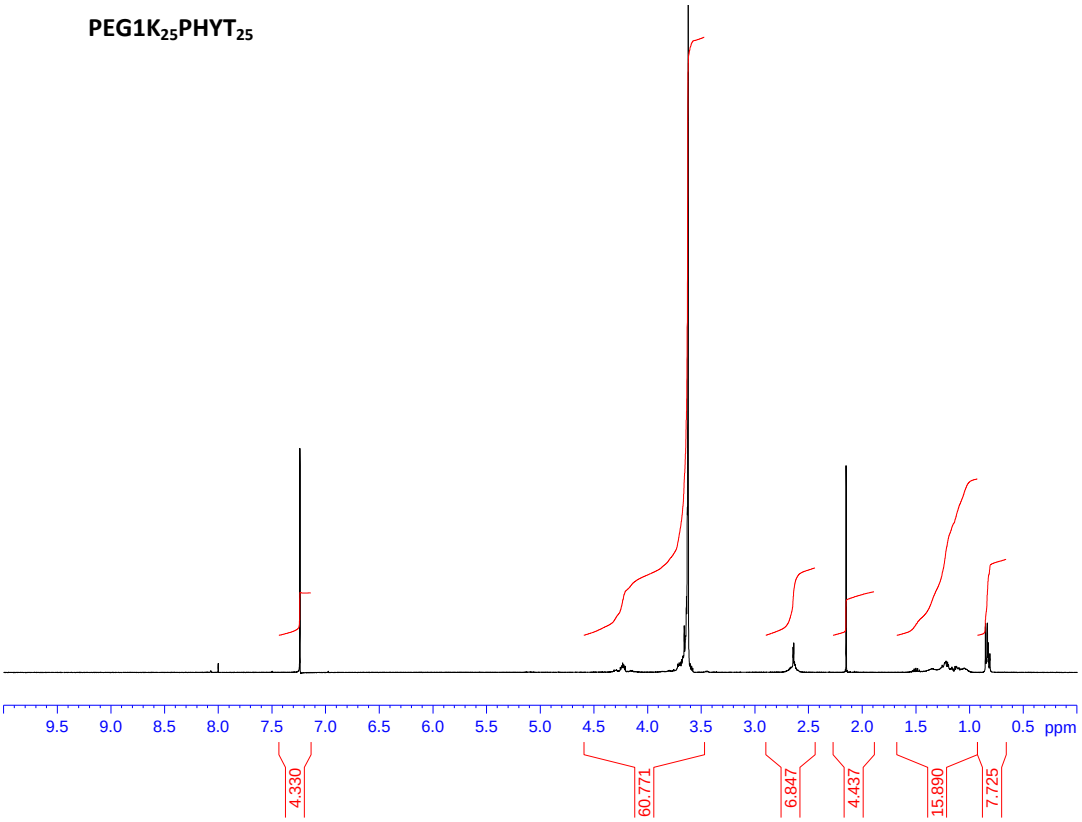

PEG2K$_{25}$PHYT$_{25}$

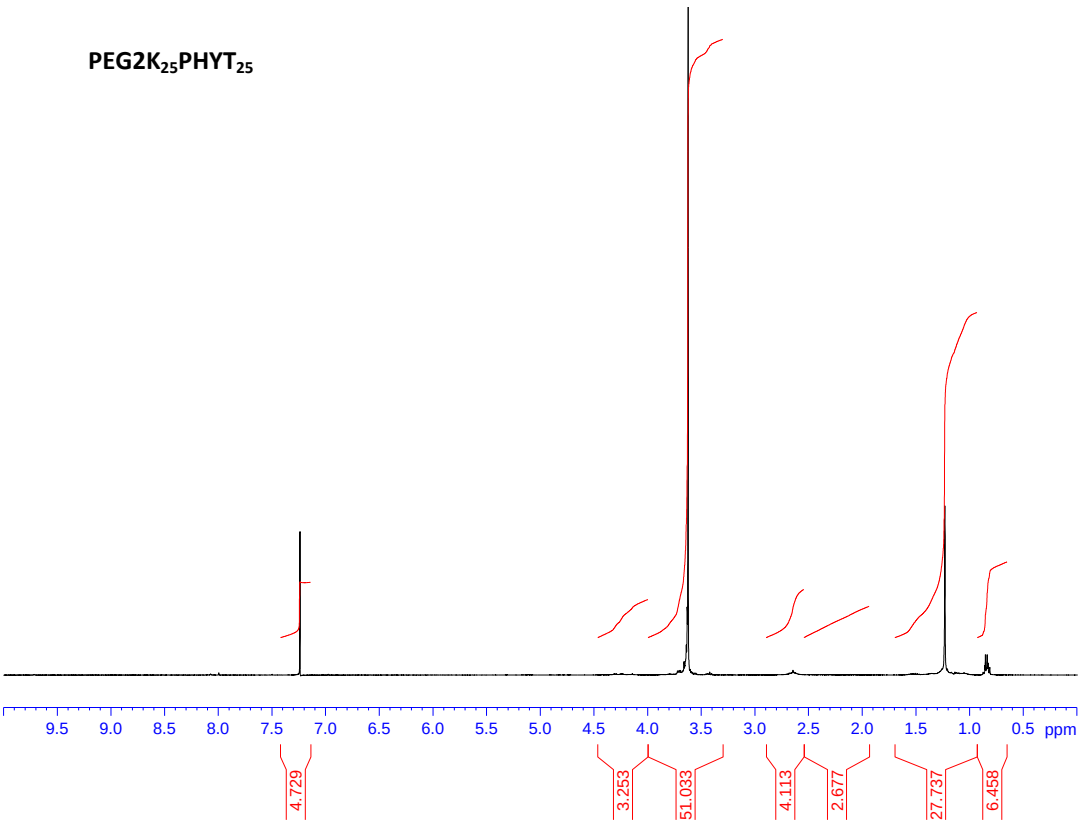

PEG3K$_{25}$PHYT$_{25}$

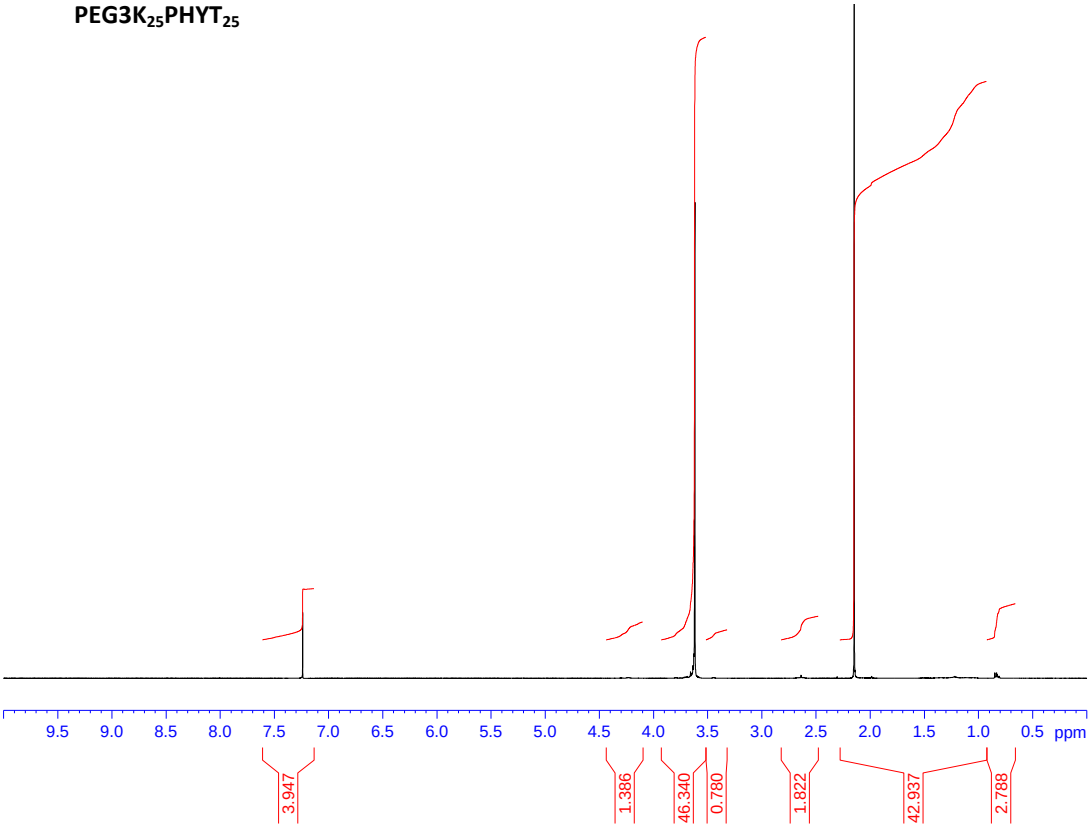

PEG4K$_{25}$PHYT$_{25}$

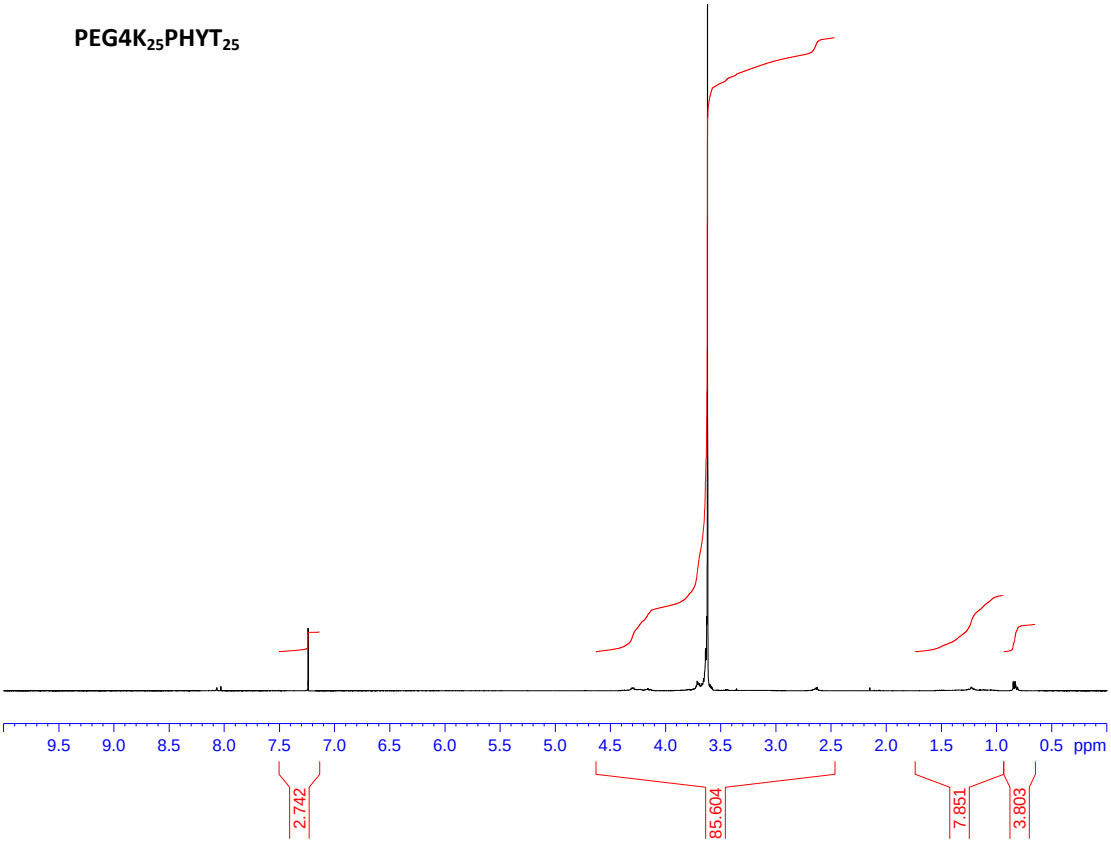

PEG6K$_{25}$PHYT$_{25}$

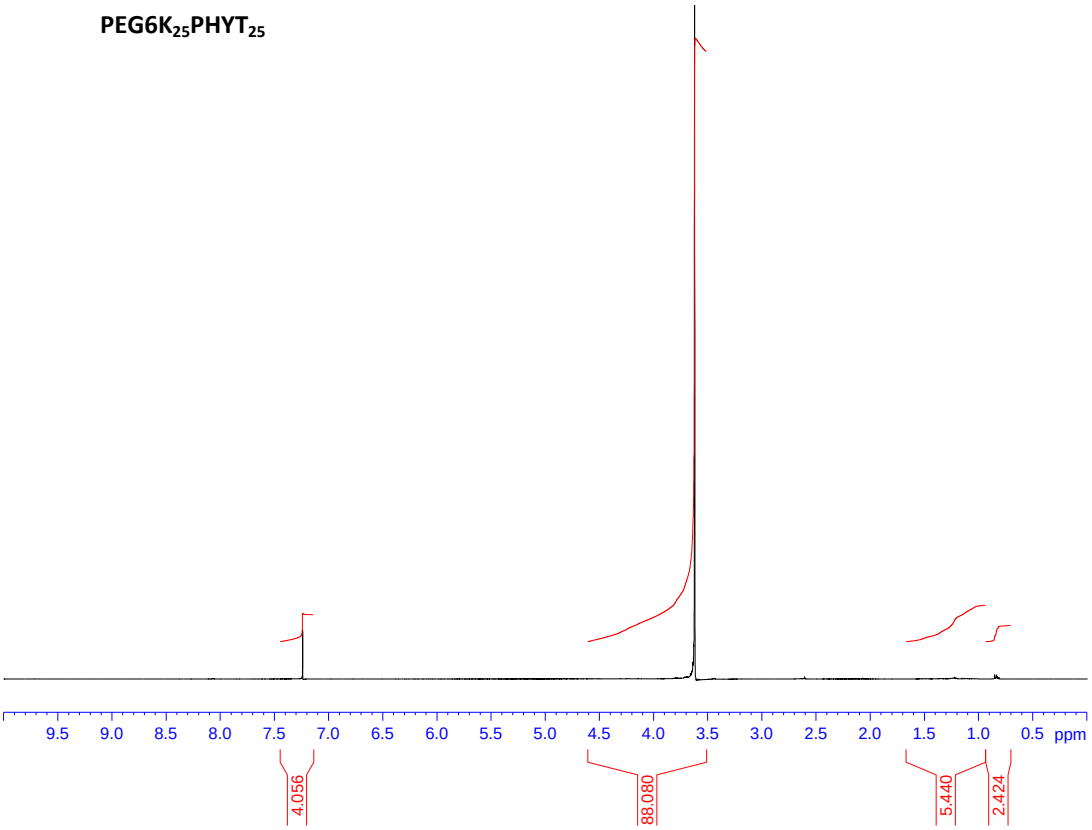

PEG8K$_{25}$PHYT$_{25}$

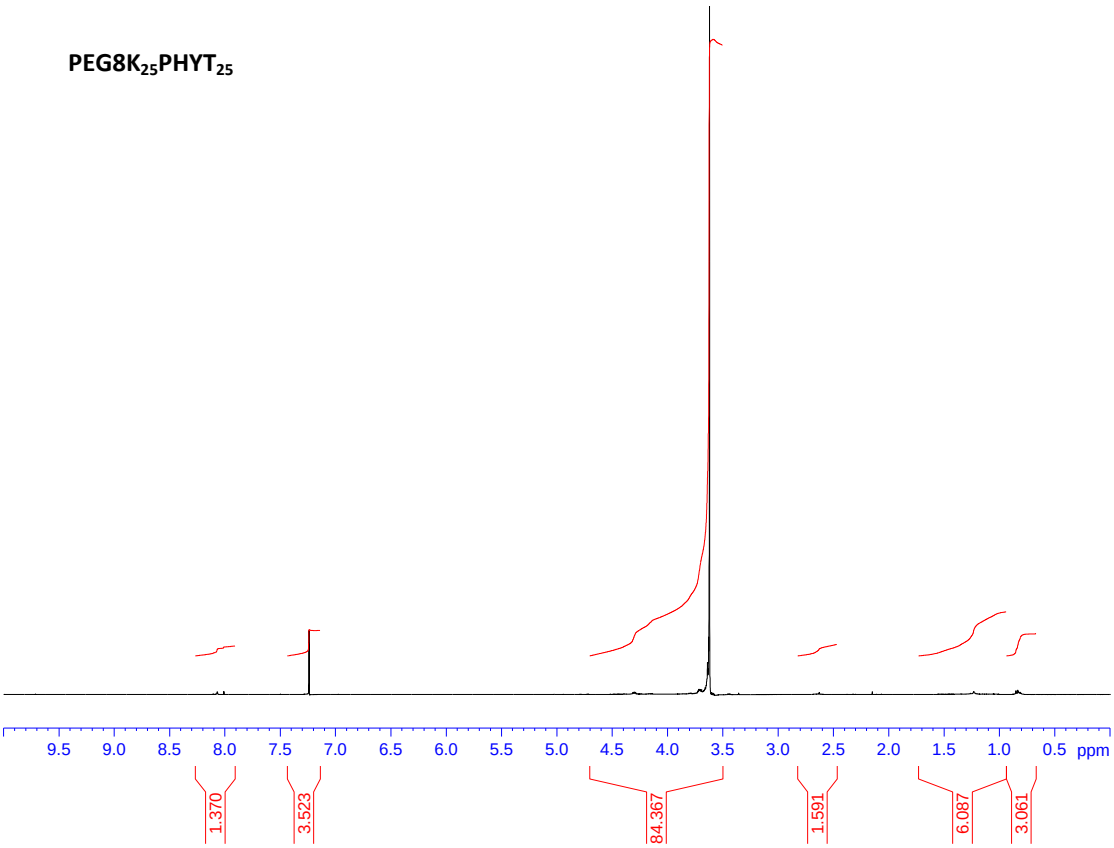

PEG10K$_{25}$PHYT$_{25}$

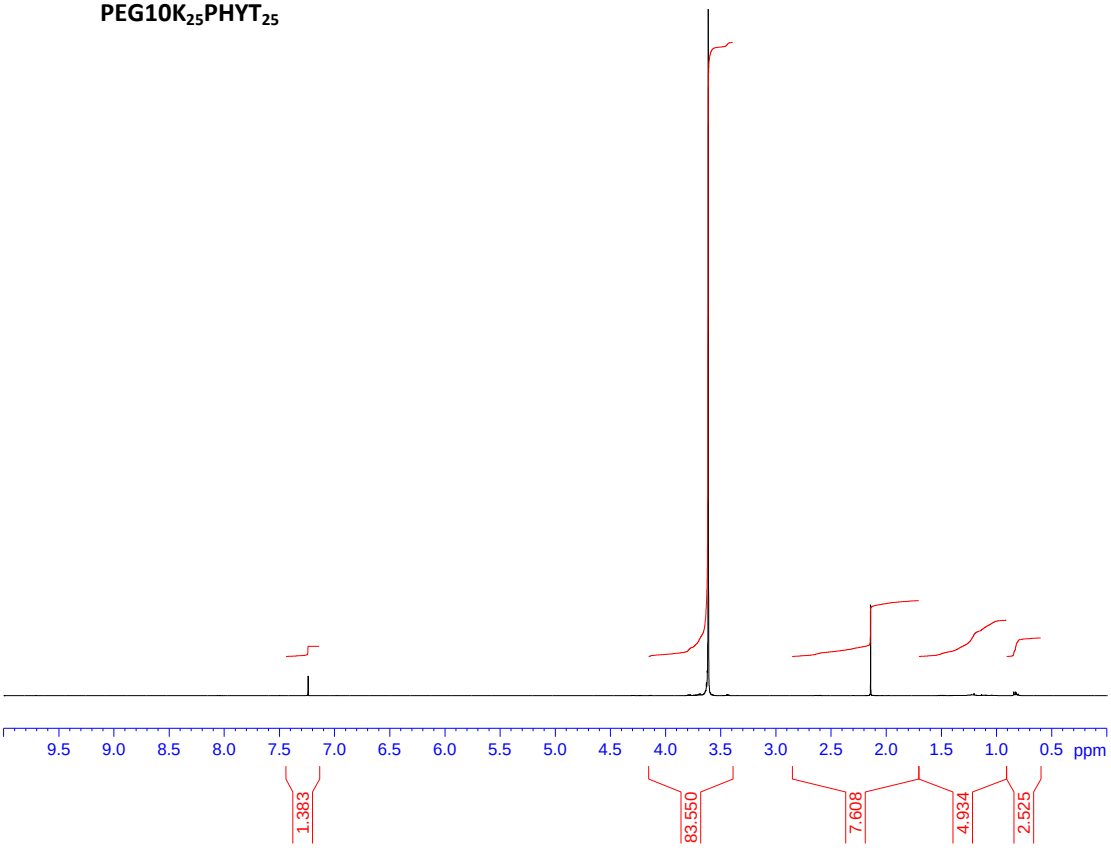

PEG14K$_{25}$PHYT$_{25}$

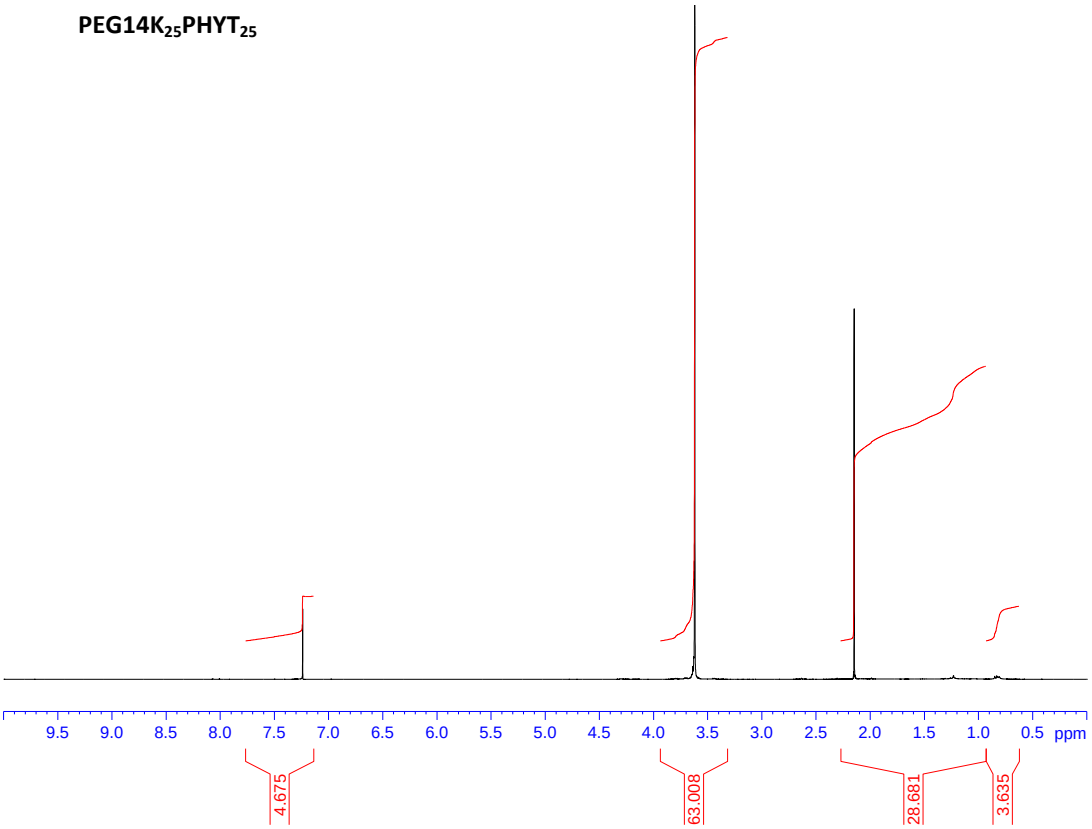

Critical aggregation concentration (CAC) data

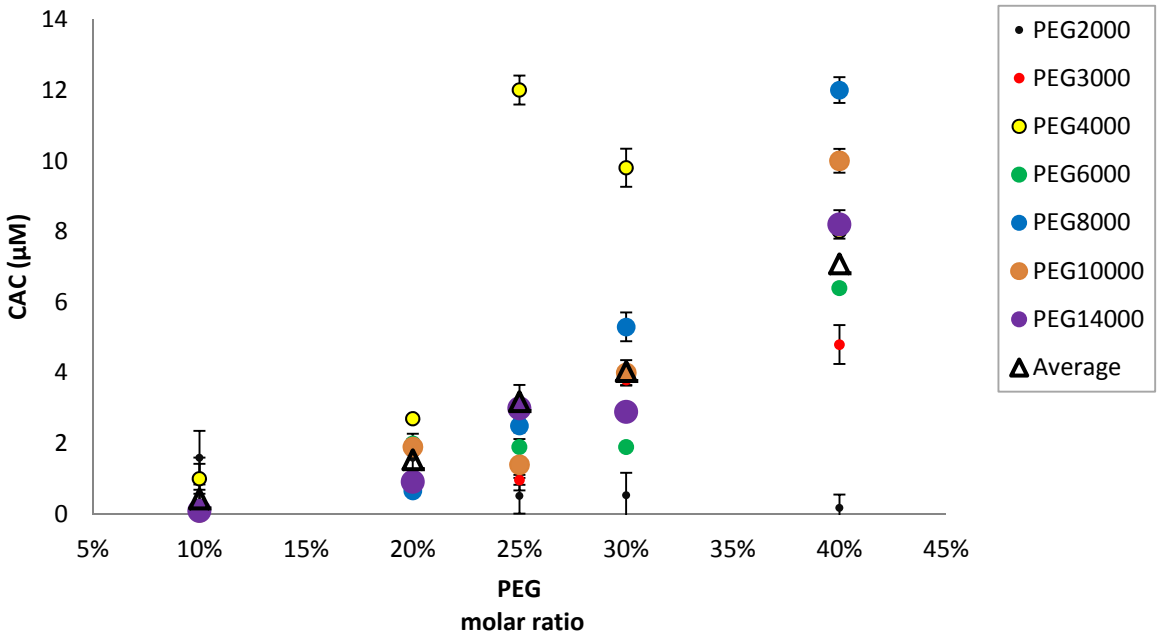

Figure 1. CAC vs. Copolymer's PEG molar ratio (10 to 40%) of the PEG-PHYT copolymers

CAC graphs

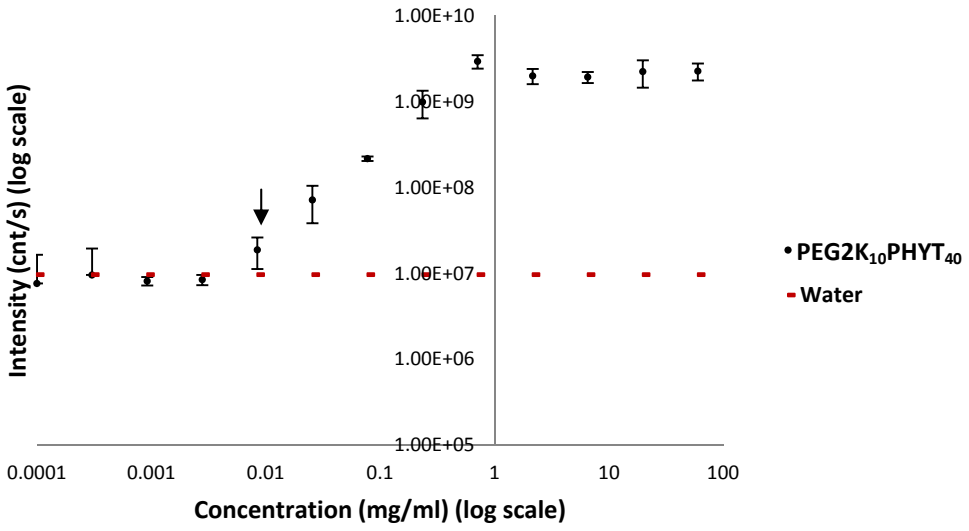

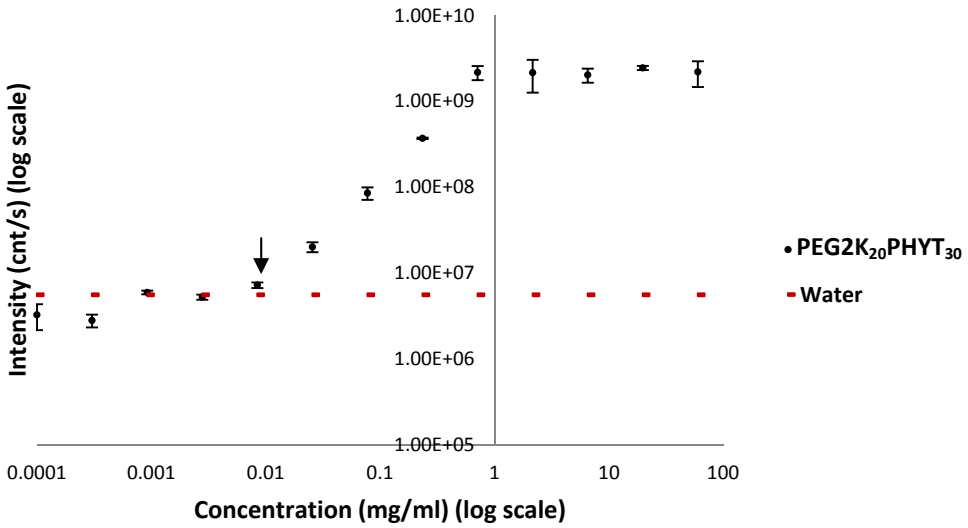
1.00E+10
1.00E+09
1.00E+08
1.00E+07
1.00E+06
1.00E+05
Intensity (cnt/s) (log scale)
0.0001
0.001
0.01
0.1
1
10
100
Concentration (mg/ml) (log scale)
PEG2K20PHYT30
Water

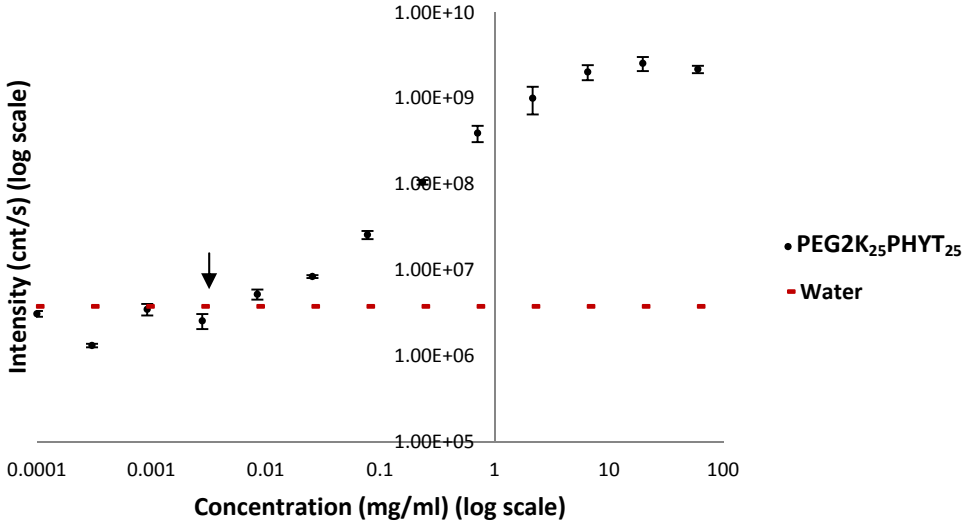
1.00E+10
1.00E+09
1.00E+08
1.00E+07
1.00E+06
1.00E+05
Intensity (cnt/s) (log scale)
0.0001
0.001
0.01
0.1
1
10
100
Concentration (mg/ml) (log scale)
PEG2K25PHYT25
Water

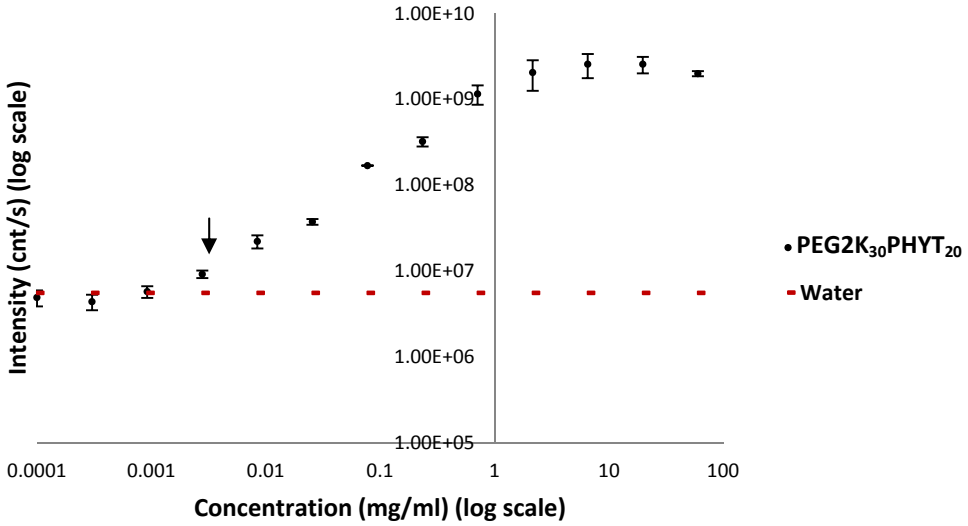
1.00E+10
1.00E+09
1.00E+08
1.00E+07
1.00E+06
1.00E+05
Intensity (cnt/s) (log scale)
0.0001
0.001
0.01
0.1
1
10
100
Concentration (mg/ml) (log scale)
PEG2K30PHYT20
Water

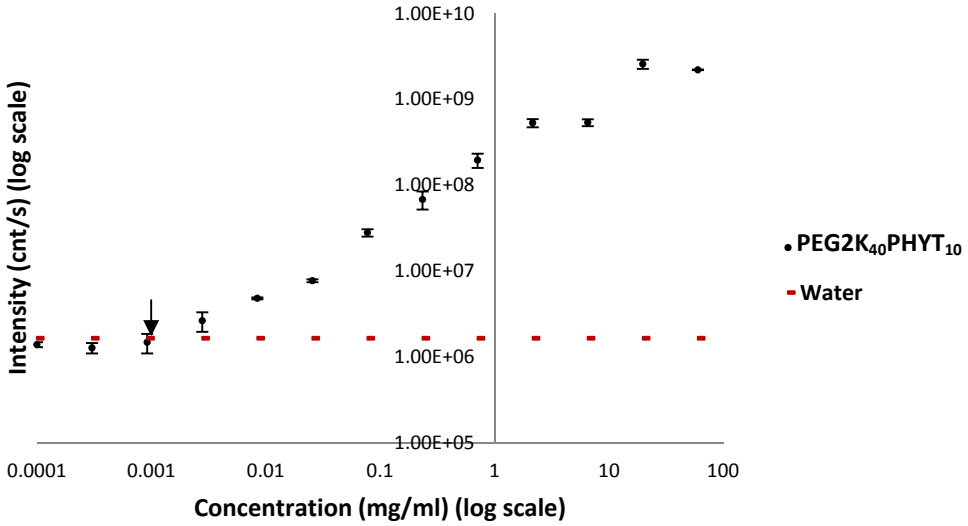
1.00E+10
1.00E+09
1.00E+08
1.00E+07
1.00E+06
1.00E+05
Intensity (cnt/s) (log scale)
0.0001
0.001
0.01
0.1
1
10
100
Concentration (mg/ml) (log scale)
PEG2K40PHYT10
Water

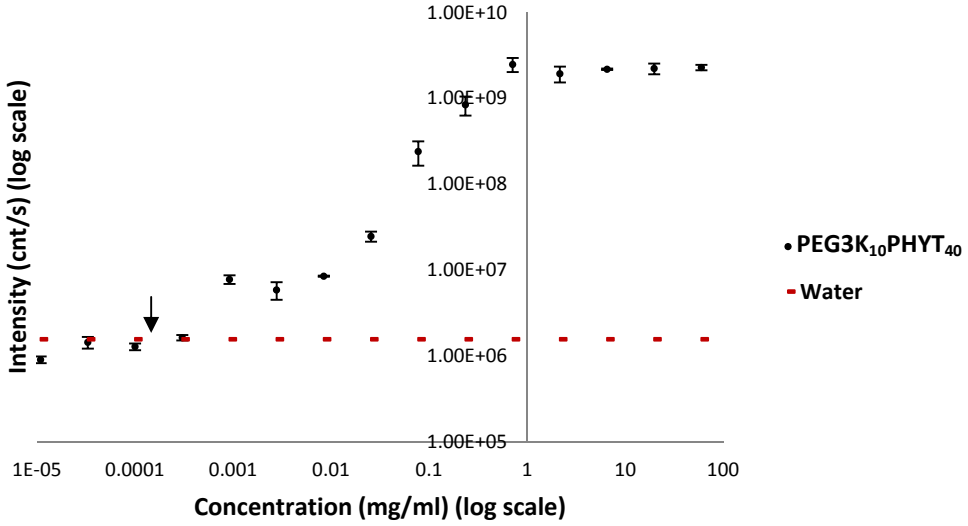
1.00E+10
1.00E+09
1.00E+08
1.00E+07
1.00E+06
1.00E+05
Intensity (cnt/s) (log scale)
1E-05
0.0001
0.001
0.01
0.1
1
10
100
Concentration (mg/ml) (log scale)
PEG3K10PHYT40
Water

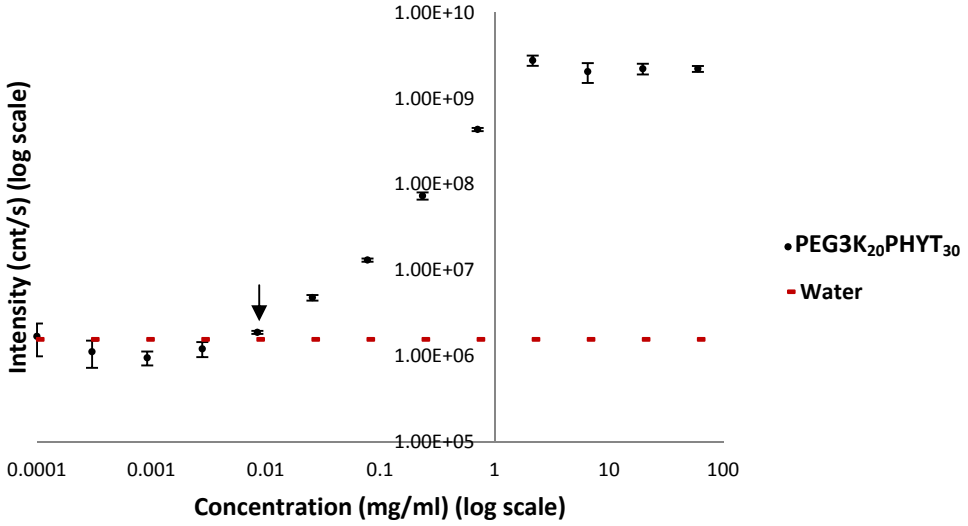
1.00E+10
1.00E+09
1.00E+08
1.00E+07
1.00E+06
1.00E+05
Intensity (cnt/s) (log scale)
0.0001
0.001
0.01
0.1
1
10
100
Concentration (mg/ml) (log scale)
PEG3K20PHYT30
Water

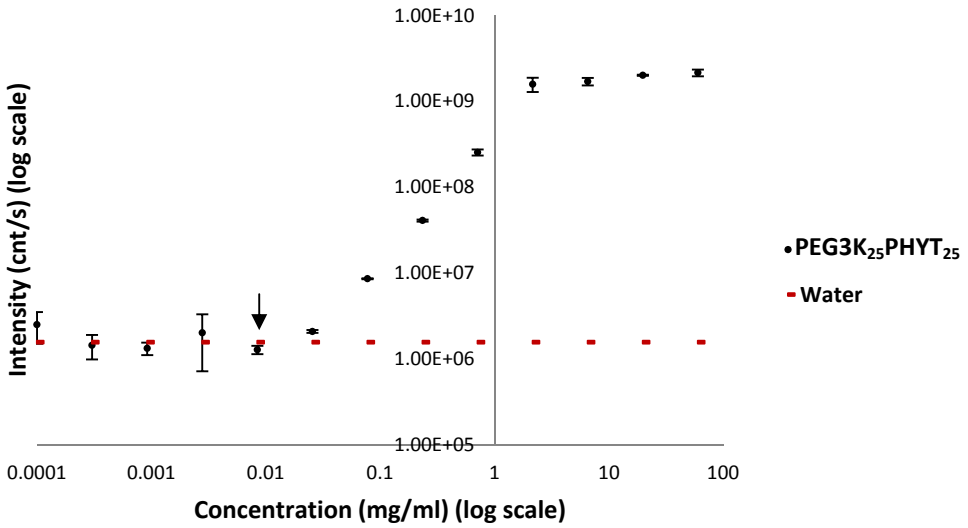
1.00E+10
1.00E+09
1.00E+08
1.00E+07
1.00E+06
1.00E+05
Intensity (cnt/s) (log scale)
0.0001
0.001
0.01
0.1
1
10
100
Concentration (mg/ml) (log scale)
PEG3K25PHYT25
Water

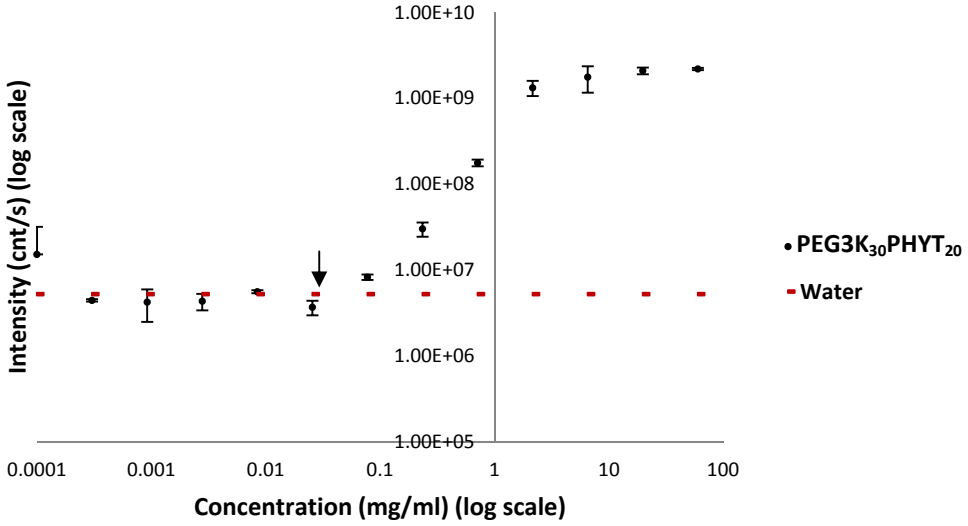
1.00E+10
1.00E+09
1.00E+08
1.00E+07
1.00E+06
1.00E+05
Intensity (cnt/s) (log scale)
0.0001
0.001
0.01
0.1
1
10
100
Concentration (mg/ml) (log scale)
PEG3K30PHYT20
Water

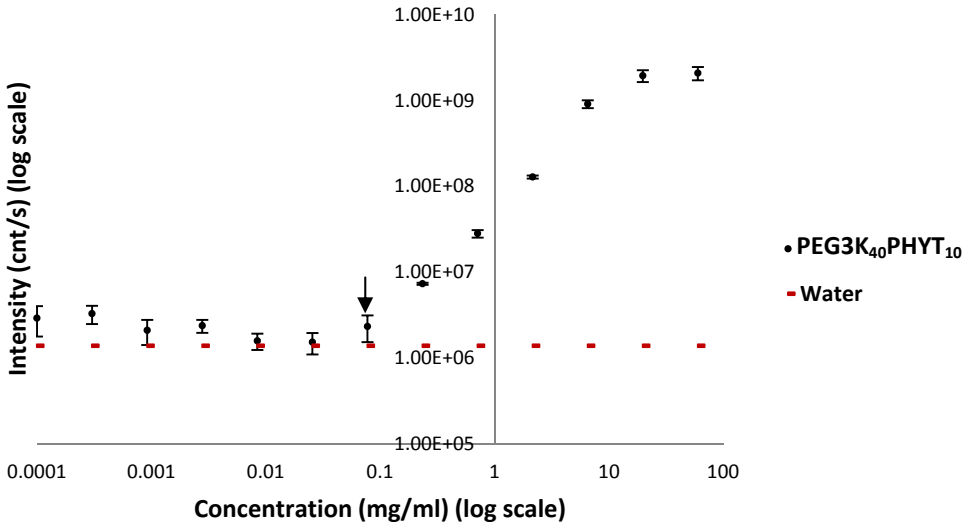
1.00E+10
1.00E+09
1.00E+08
1.00E+07
1.00E+06
1.00E+05
Intensity (cnt/s) (log scale)
0.0001
0.001
0.01
0.1
1
10
100
Concentration (mg/ml) (log scale)
PEG3K40PHYT10
Water

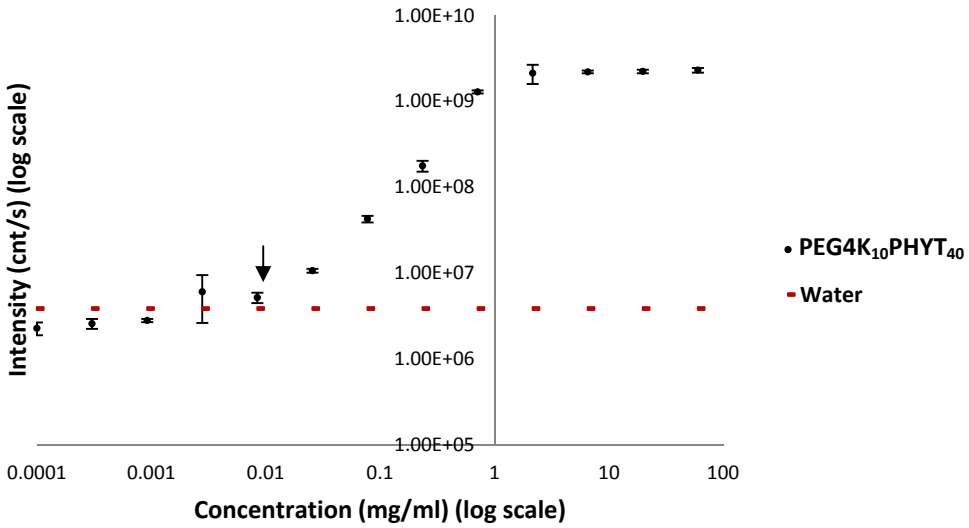
1.00E+10
1.00E+09
1.00E+08
1.00E+07
1.00E+06
1.00E+05
Intensity (cnt/s) (log scale)
0.0001
0.001
0.01
0.1
1
10
100
Concentration (mg/ml) (log scale)
PEG4K10PHYT40
Water

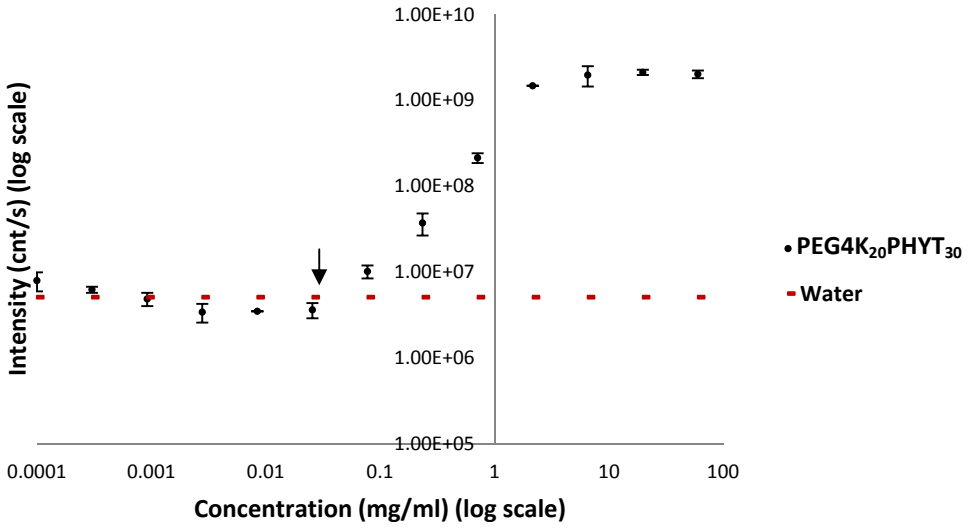
1.00E+10
1.00E+09
1.00E+08
1.00E+07
1.00E+06
1.00E+05
Intensity (cnt/s) (log scale)
0.0001
0.001
0.01
0.1
1
10
100
Concentration (mg/ml) (log scale)
PEG4K20PHYT30
Water

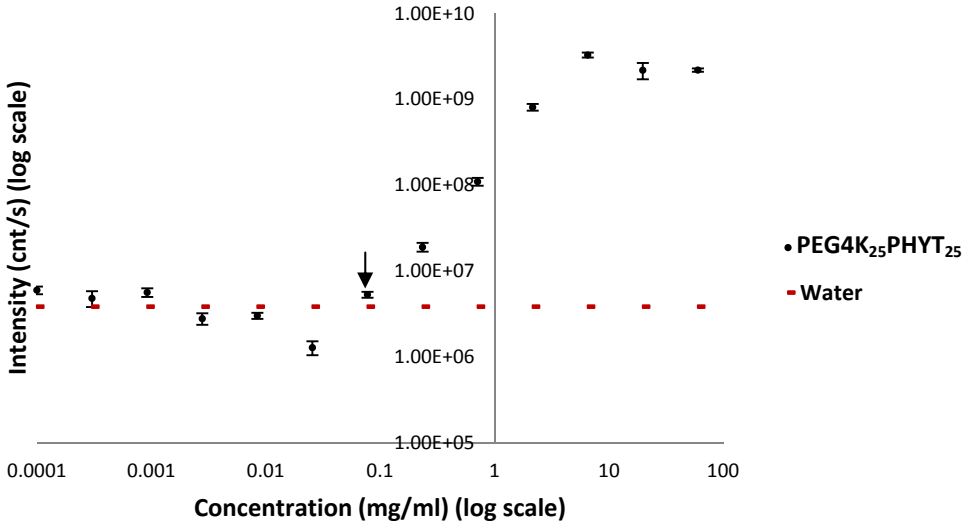
1.00E+10
1.00E+09
1.00E+08
1.00E+07
1.00E+06
1.00E+05
Intensity (cnt/s) (log scale)
0.0001
0.001
0.01
0.1
1
10
100
Concentration (mg/ml) (log scale)
PEG4K25PHYT25
Water

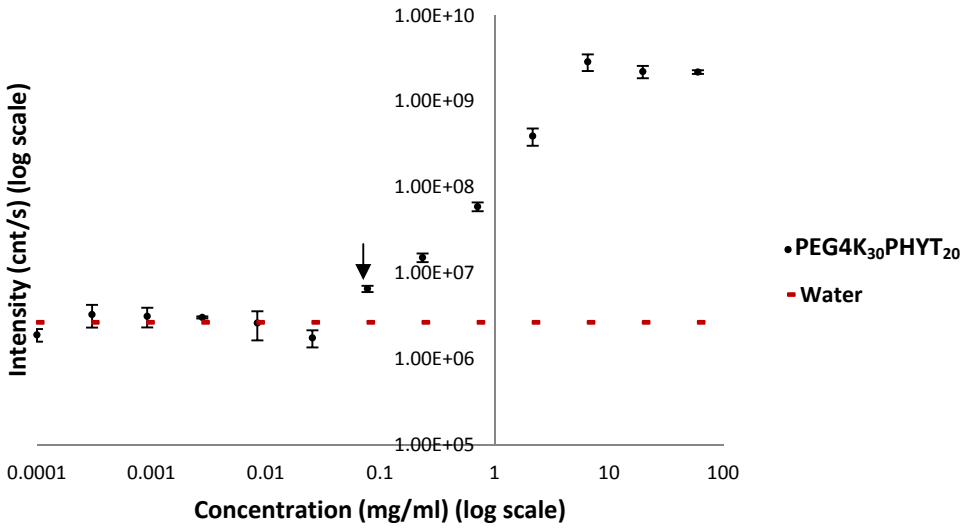
1.00E+10
1.00E+09
1.00E+08
1.00E+07
1.00E+06
1.00E+05
Intensity (cnt/s) (log scale)
0.0001
0.001
0.01
0.1
1
10
100
Concentration (mg/ml) (log scale)
PEG4K30PHYT20
Water

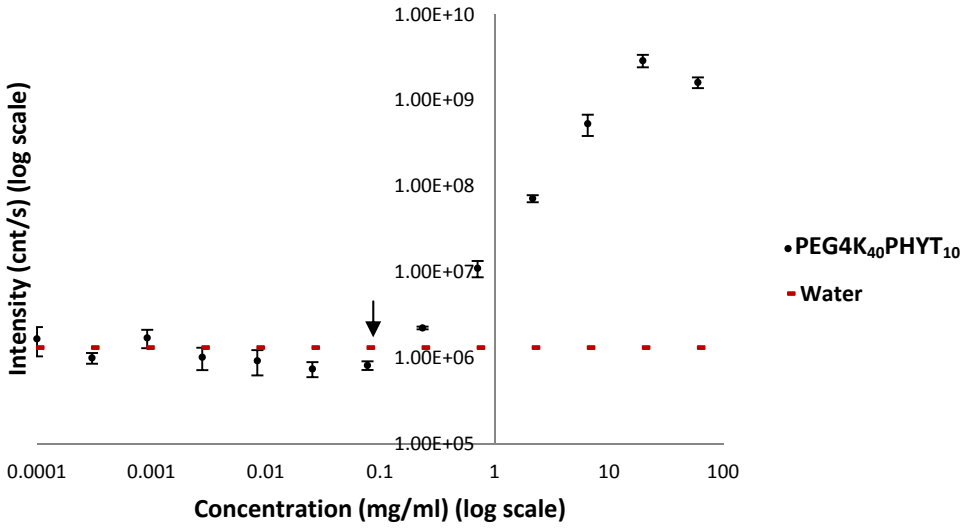
1.00E+10
1.00E+09
1.00E+08
1.00E+07
1.00E+06
1.00E+05
Intensity (cnt/s) (log scale)
0.0001
0.001
0.01
0.1
1
10
100
Concentration (mg/ml) (log scale)
PEG4K40PHYT10
Water

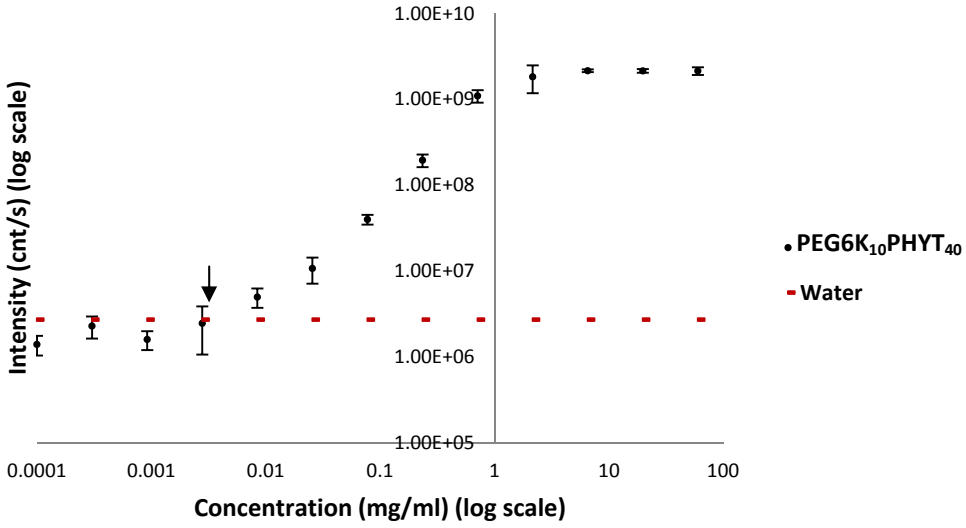
1.00E+10
1.00E+09
1.00E+08
1.00E+07
1.00E+06
1.00E+05
Intensity (cnt/s) (log scale)
0.0001
0.001
0.01
0.1
1
10
100
Concentration (mg/ml) (log scale)
PEG6K10PHYT40
Water

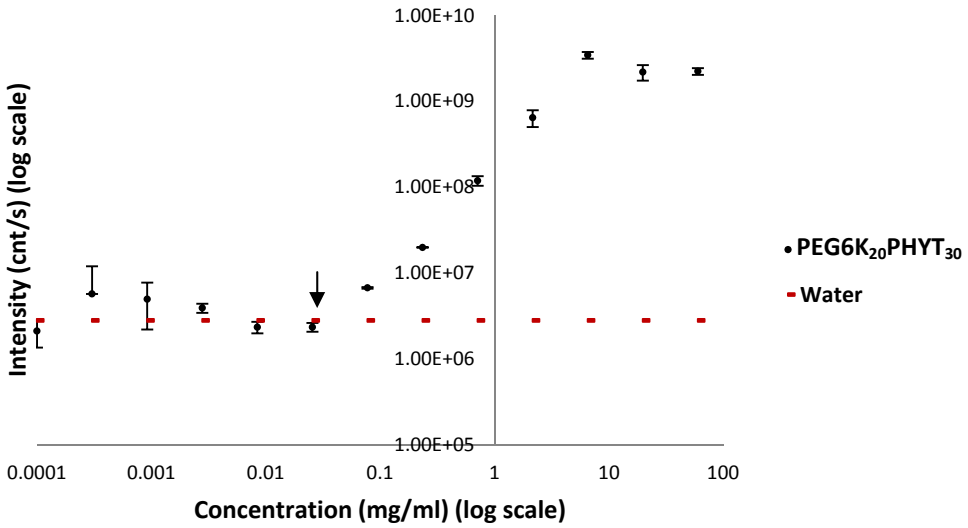
1.00E+10
1.00E+09
1.00E+08
1.00E+07
1.00E+06
1.00E+05
Intensity (cnt/s) (log scale)
0.0001
0.001
0.01
0.1
1
10
100
Concentration (mg/ml) (log scale)
PEG6K20PHYT30
Water

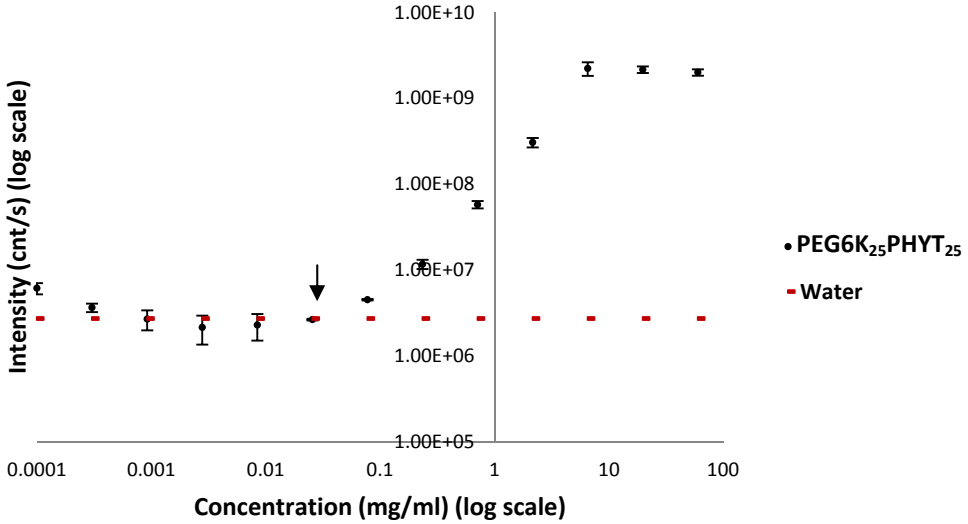
1.00E+10
1.00E+09
1.00E+08
1.00E+07
1.00E+06
1.00E+05
Intensity (cnt/s) (log scale)
0.0001
0.001
0.01
0.1
1
10
100
Concentration (mg/ml) (log scale)
PEG6K25PHYT25
Water

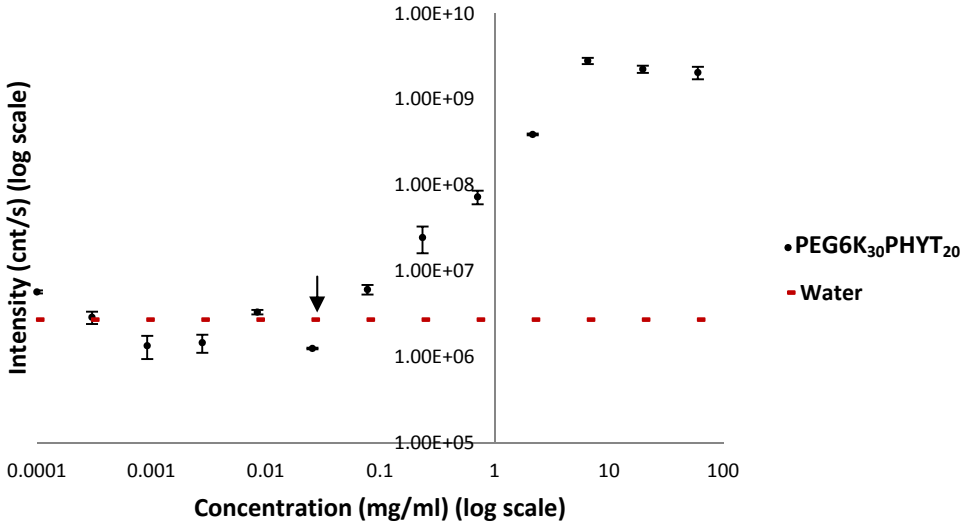
1.00E+10
1.00E+09
1.00E+08
1.00E+07
1.00E+06
1.00E+05
Intensity (cnt/s) (log scale)
0.0001
0.001
0.01
0.1
1
10
100
Concentration (mg/ml) (log scale)
PEG6K30PHYT20
Water

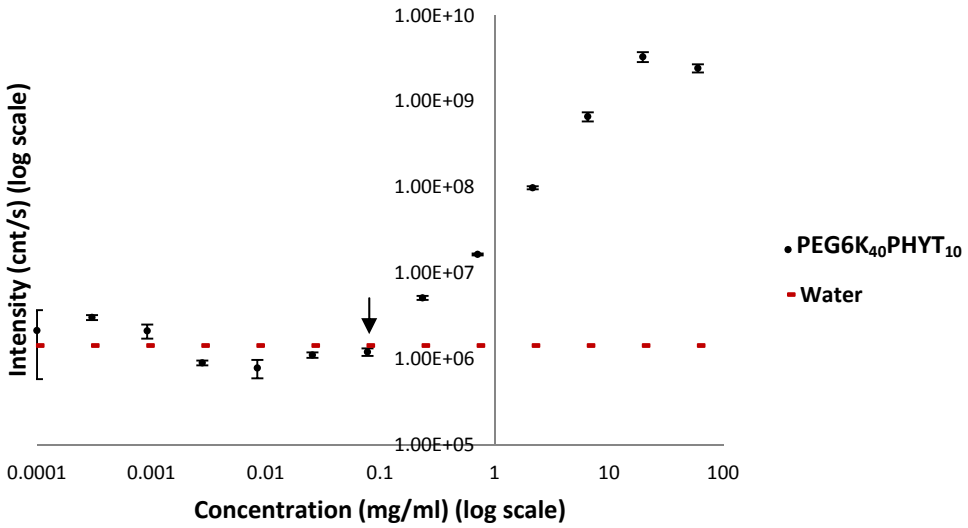
1.00E+10
1.00E+09
1.00E+08
1.00E+07
1.00E+06
1.00E+05
Intensity (cnt/s) (log scale)
0.0001
0.001
0.01
0.1
1
10
100
Concentration (mg/ml) (log scale)
PEG6K40PHYT10
Water

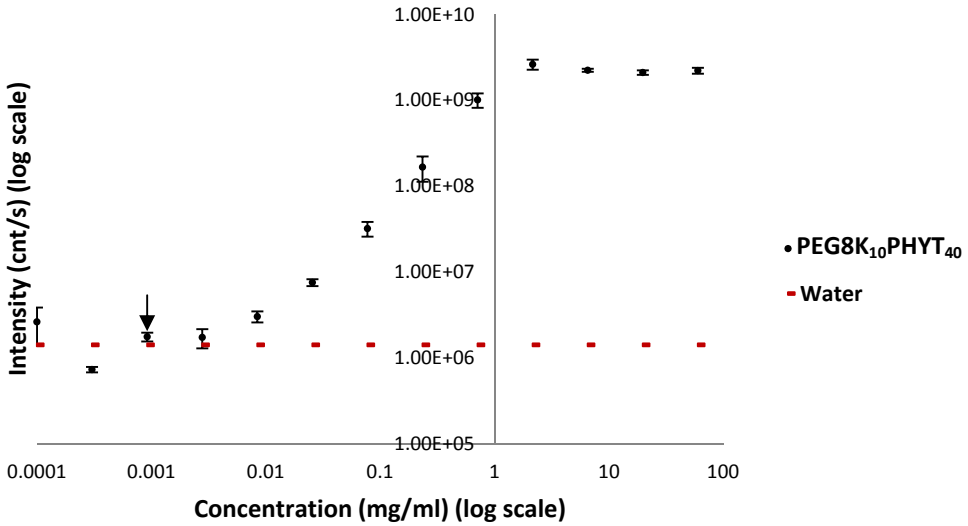
1.00E+10
1.00E+09
1.00E+08
1.00E+07
1.00E+06
1.00E+05
Intensity (cnt/s) (log scale)
0.0001
0.001
0.01
0.1
1
10
100
Concentration (mg/ml) (log scale)
PEG8K10PHYT40
Water

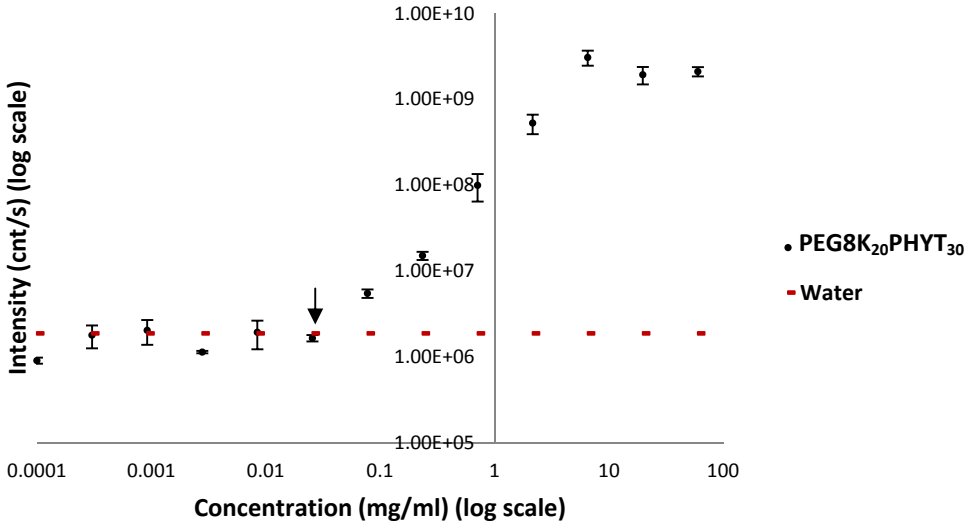
1.00E+10
1.00E+09
1.00E+08
1.00E+07
1.00E+06
1.00E+05
Intensity (cnt/s) (log scale)
0.0001
0.001
0.01
0.1
1
10
100
Concentration (mg/ml) (log scale)
PEG8K20PHYT30
Water

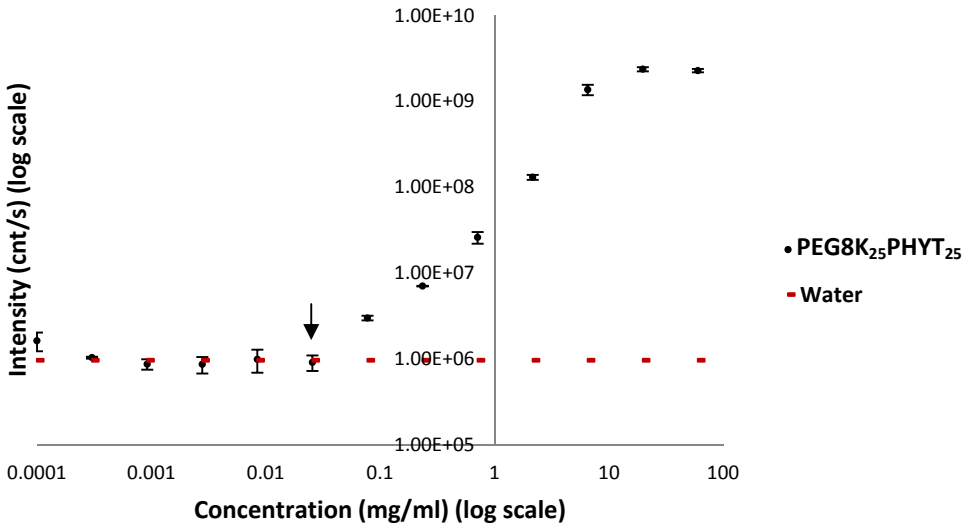
1.00E+10
1.00E+09
1.00E+08
1.00E+07
1.00E+06
1.00E+05
Intensity (cnt/s) (log scale)
0.0001
0.001
0.01
0.1
1
10
100
Concentration (mg/ml) (log scale)
PEG8K25PHYT25
Water

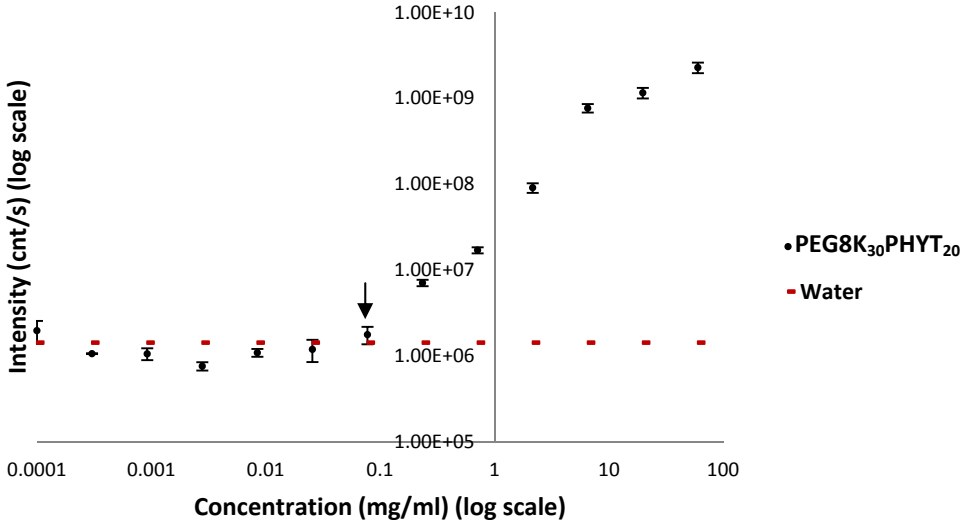
1.00E+10
1.00E+09
1.00E+08
1.00E+07
1.00E+06
1.00E+05
Intensity (cnt/s) (log scale)
0.0001
0.001
0.01
0.1
1
10
100
Concentration (mg/ml) (log scale)
PEG8K30PHYT20
Water

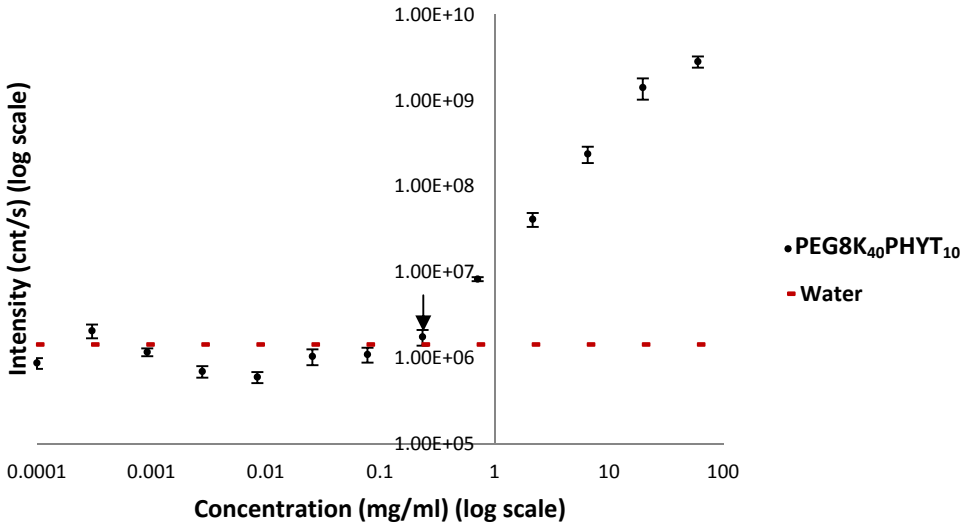
1.00E+10
1.00E+09
1.00E+08
1.00E+07
1.00E+06
1.00E+05
Intensity (cnt/s) (log scale)
0.0001
0.001
0.01
0.1
1
10
100
Concentration (mg/ml) (log scale)
PEG8K40PHYT10
Water

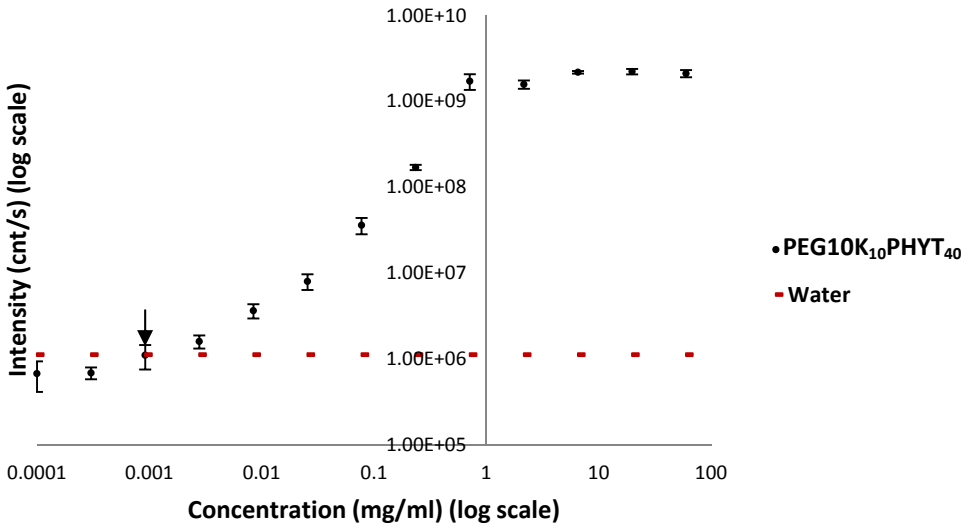
1.00E+10
1.00E+09
1.00E+08
1.00E+07
1.00E+06
1.00E+05
Intensity (cnt/s) (log scale)
0.0001
0.001
0.01
0.1
1
10
100
Concentration (mg/ml) (log scale)
PEG10K10PHYT40
Water

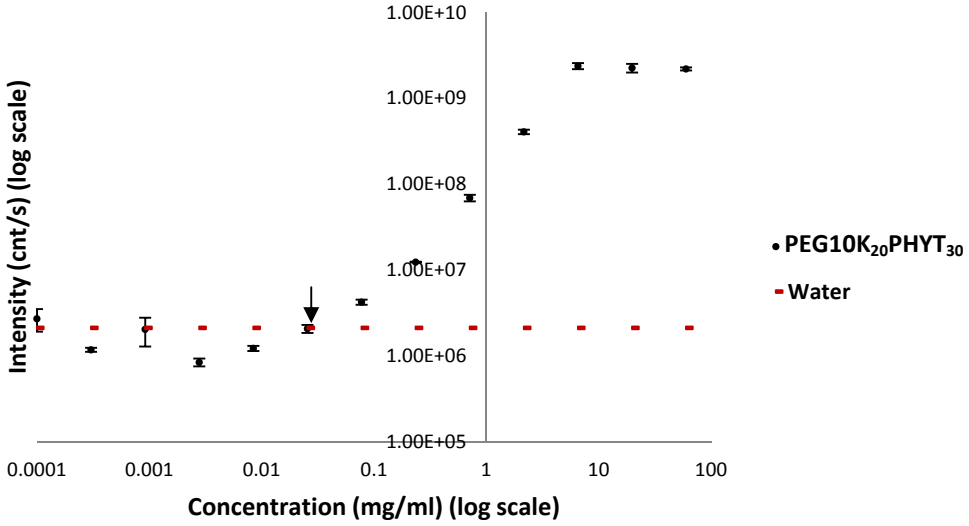
1.00E+10
1.00E+09
1.00E+08
1.00E+07
1.00E+06
1.00E+05
Intensity (cnt/s) (log scale)
0.0001
0.001
0.01
0.1
1
10
100
Concentration (mg/ml) (log scale)
PEG10K20PHYT30
Water

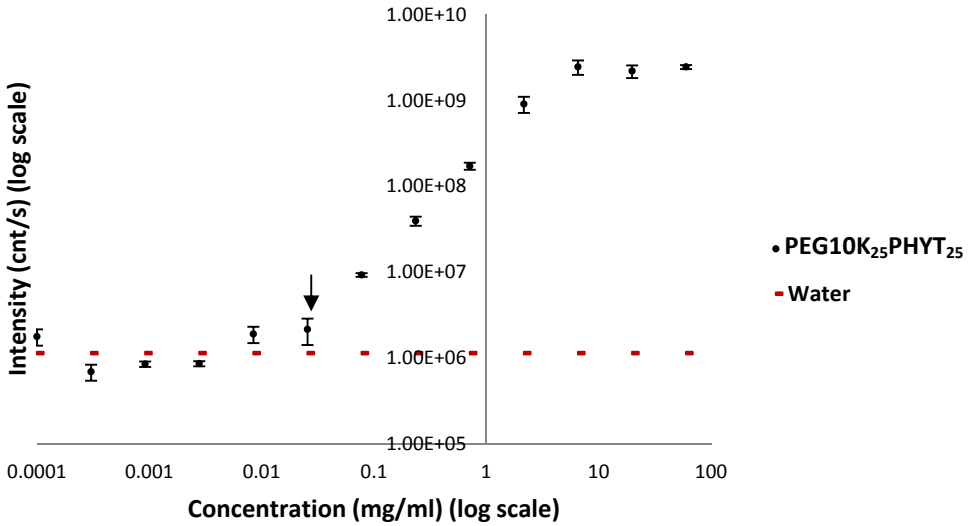
1.00E+10
1.00E+09
1.00E+08
1.00E+07
1.00E+06
1.00E+05
Intensity (cnt/s) (log scale)
0.0001
0.001
0.01
0.1
1
10
100
Concentration (mg/ml) (log scale)
PEG10K25PHYT25
Water

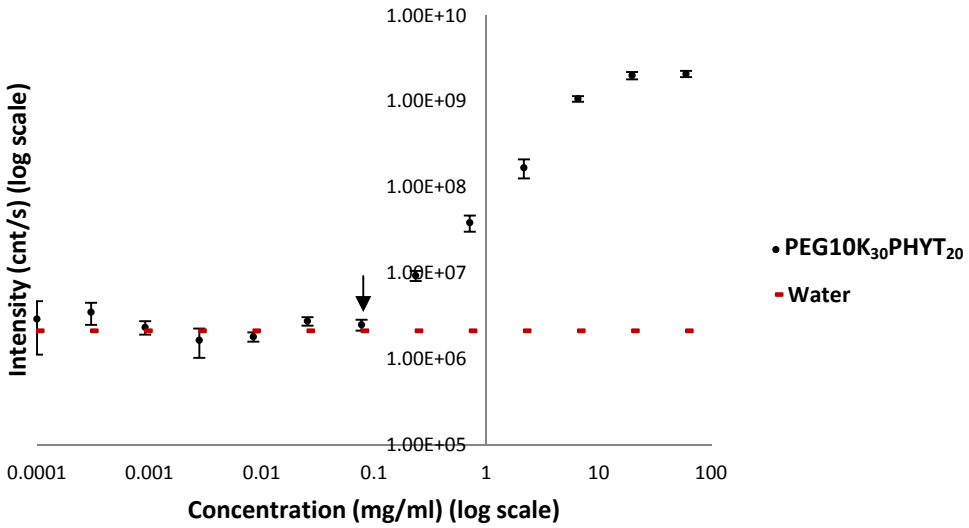
1.00E+10
1.00E+09
1.00E+08
1.00E+07
1.00E+06
1.00E+05
Intensity (cnt/s) (log scale)
0.0001
0.001
0.01
0.1
1
10
100
Concentration (mg/ml) (log scale)
PEG10K30PHYT20
Water

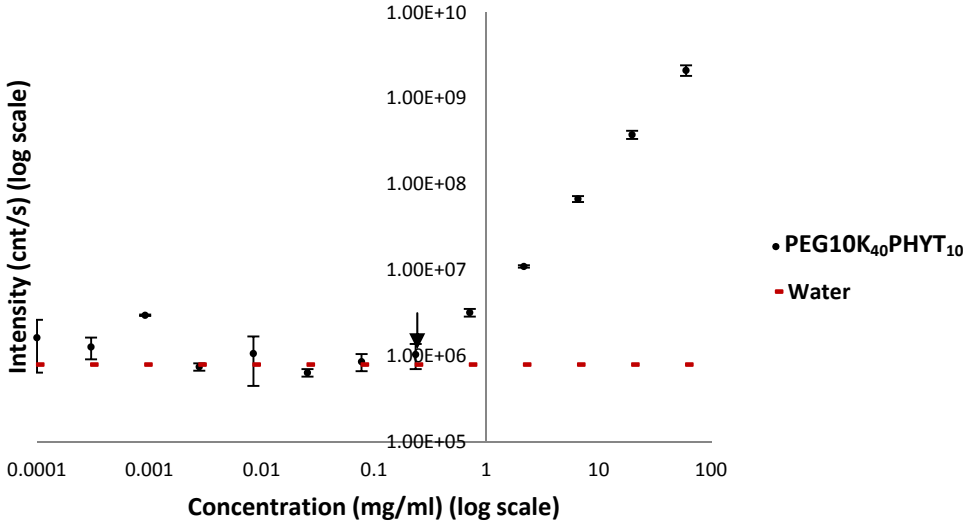
1.00E+10
1.00E+09
1.00E+08
1.00E+07
1.00E+06
1.00E+05
Intensity (cnt/s) (log scale)
0.0001
0.001
0.01
0.1
1
10
100
Concentration (mg/ml) (log scale)
PEG10K40PHYT10
Water

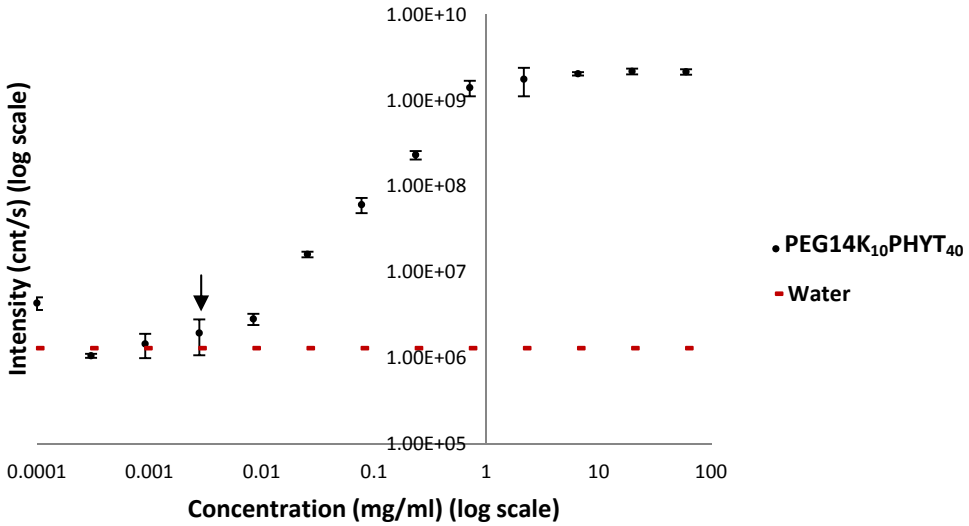
1.00E+10
1.00E+09
1.00E+08
1.00E+07
1.00E+06
1.00E+05
Intensity (cnt/s) (log scale)
0.0001
0.001
0.01
0.1
1
10
100
Concentration (mg/ml) (log scale)
PEG14K10PHYT40
Water

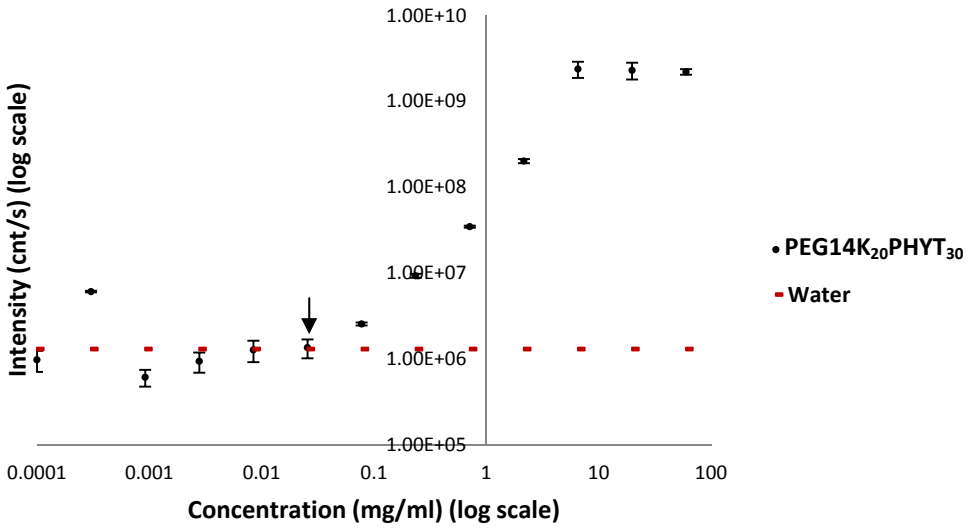
1.00E+10
1.00E+09
1.00E+08
1.00E+07
1.00E+06
1.00E+05
Intensity (cnt/s) (log scale)
0.0001
0.001
0.01
0.1
1
10
100
Concentration (mg/ml) (log scale)
PEG14K20PHYT30
Water

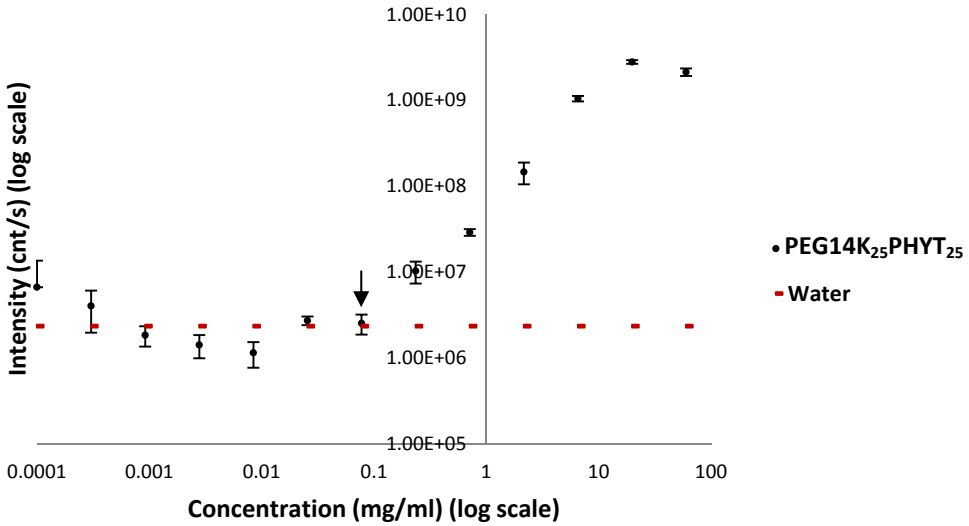
1.00E+10
1.00E+09
1.00E+08
1.00E+07
1.00E+06
1.00E+05
Intensity (cnt/s) (log scale)
0.0001
0.001
0.01
0.1
1
10
100
Concentration (mg/ml) (log scale)
PEG14K25PHYT25
Water

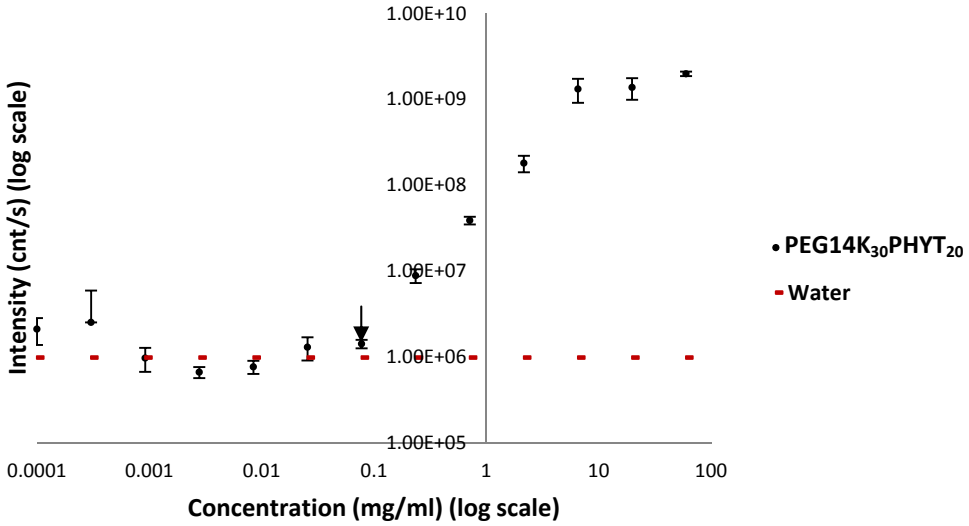
1.00E+10
1.00E+09
1.00E+08
1.00E+07
1.00E+06
1.00E+05
Intensity (cnt/s) (log scale)
0.0001
0.001
0.01
0.1
1
10
100
Concentration (mg/ml) (log scale)
PEG14K30PHYT20
Water

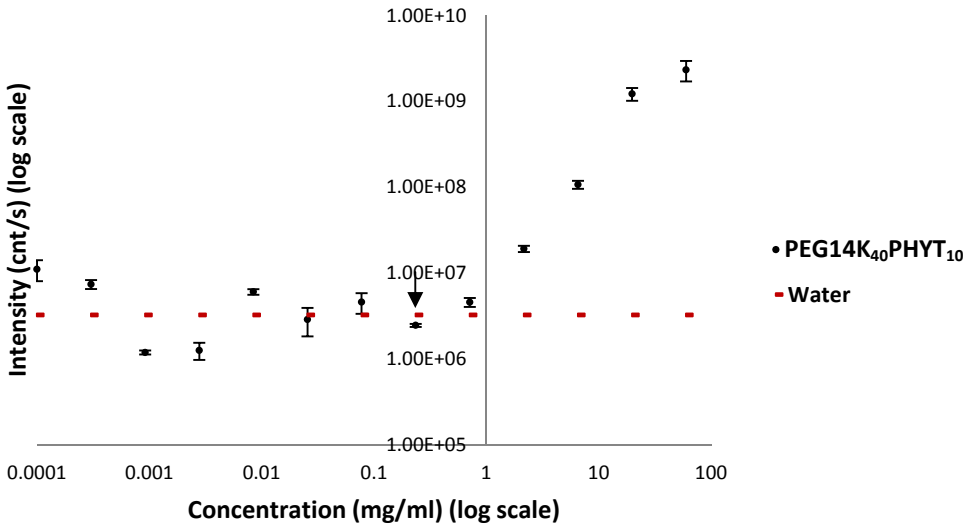
1.00E+10
1.00E+09
1.00E+08
1.00E+07
1.00E+06
1.00E+05
Intensity (cnt/s) (log scale)
0.0001
0.001
0.01
0.1
1
10
100
Concentration (mg/ml) (log scale)
PEG14K40PHYT10
Water

Thermotropic phase behaviour using cross-polarized light microscopy (CPLM)

Table 1. Thermotropic phase behaviour (I, isotropic, B, Birefringent, H, hexagonal, Sm, smectic) of the polymers at 20 °C. H* are hexagonal displays of both fan-type and mosaic optical patterns. CPLM images showing optical structures can be found in Appendix 1.

PEG mol%	10%	20%	25%	30%	40%
PEG1K	I	I/B	I/B	Sm	Sm
PEG2K	Sm	Sm	Sm	Sm	Sm
PEG3K	Sm	Sm	Sm	Sm	Sm
PEG4K	Sm	Sm	Sm	H	Sm
PEG6K	H*	H	Sm	H	Sm
PEG8K	H	H	Sm	H	Sm
PEG10K	Sm	H	H	H	H*
PEG14K	Sm	H	H	H	Sm

The dry copolymer thermotropic phase behaviour was initially observed at 20 °C under cross-polarisers (Table 1). Hexagonal phases were observed for some of the polymers with PEG chain lengths greater than 90 PEG units (i.e. >PEG4000) (Figure 1a).The majority of the PEG(x)/SA/PHYT copolymers displayed smectic optical textures (Figure 1b & 6c).

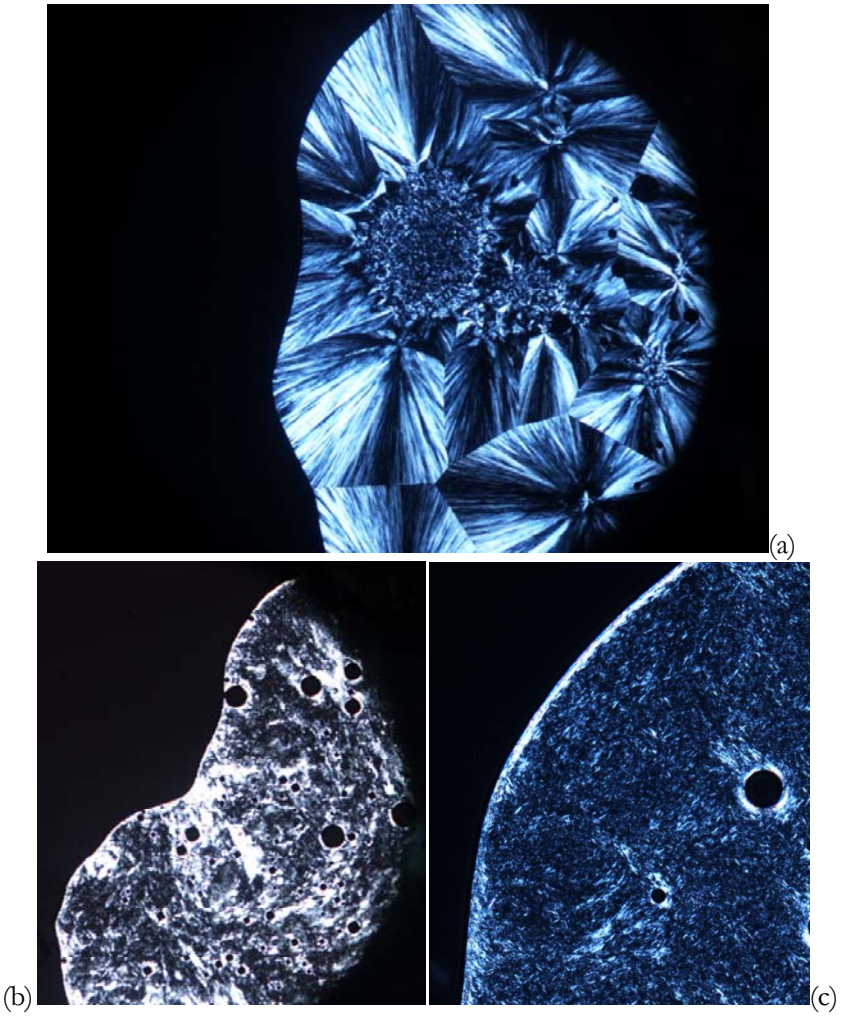

Figure 2. Example of (a) hexagonal phase observed with copolymer $PEG10K_{20}PHYT_{30}$, (b) smectic phase observed with copolymer $PEG10K_{10}PHYT_{40}$ and (c) smectic phase observed with copolymer $PEG14K_{10}PHYT_{40}$, under cross-polarized light microscopy at 20 °C.

Cross-polarized light microscopy (CPLM) data

The phase behaviour of each copolymer was assessed by observation of the characteristic optical textures of anisotropic and isotropic phases when observed through polarised light. The textures of the birefringent materials were typically indicative lamellar phases, hexagonal phases whilst the non-viscous isotropic phases were identified as micellar phases.

	Dry(20°C)	20 °C	25 °C	30 °C	37 °C	40 °C	45 °C	50 °C	55 °C	60 °C	65 °C
F127 (Control)		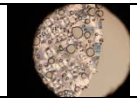	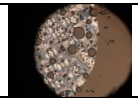	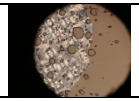	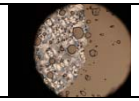	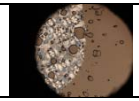	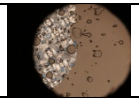	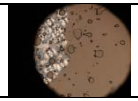	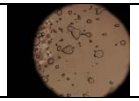	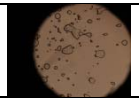	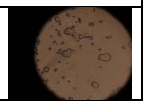

	Dry(20°C)	20 °C	25 °C	30 °C	35 °C	37 °C	40 °C	45 °C	50 °C	55 °C	60 °C	65 °C
$PEG1K_{10}PHYT_{40}$			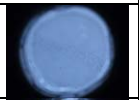	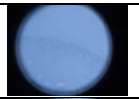	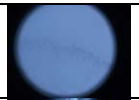	N.A	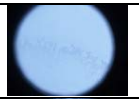		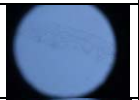	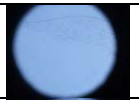		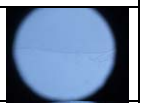
$PEG1K_{20}PHYT_{30}$		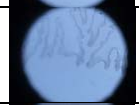	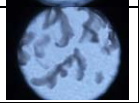	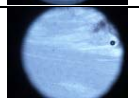	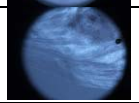	N.A	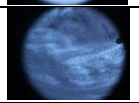		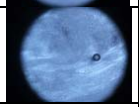	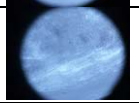	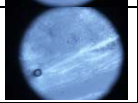	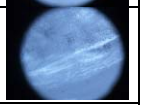
$PEG1K_{25}PHYT_{25}$	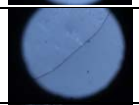	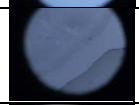	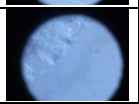	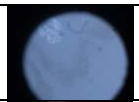	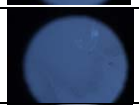	N.A	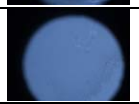	N.A	N.A	N.A	N.A	N.A
$PEG1K_{30}PHYT_{20}$	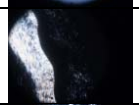					N.A		N.A	N.A	N.A	N.A	N.A
$PEG1K_{40}PHYT_{10}$							N.A	N.A	N.A	N.A	N.A	N.A

	Dry(20°C)	20 °C	25 °C	30 °C	35 °C	37 °C	40 °C	45 °C	50 °C	55 °C	60 °C	65 °C
$PEG2K_{10}PHYT_{40}$		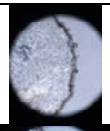										
$PEG2K_{20}PHYT_{30}$	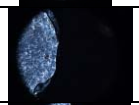	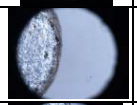	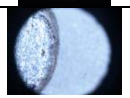	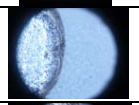	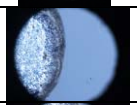	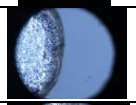	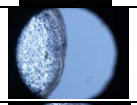	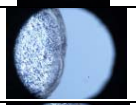	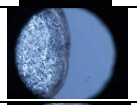	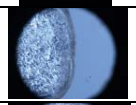	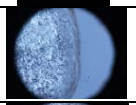	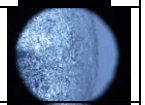
$PEG2K_{25}PHYT_{25}$	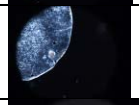	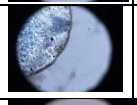				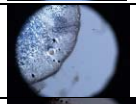	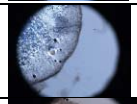			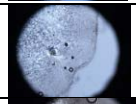	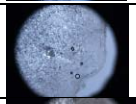	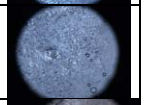
$PEG2K_{30}PHYT_{20}$				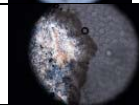								
$PEG2K_{40}PHYT_{10}$												

	Dry(20°C)	20 °C	25 °C	30 °C	35 °C	37 °C	40 °C	45 °C	50 °C	55 °C	60 °C	65 °C
$PEG3K_{10}PHYT_{40}$												
$PEG3K_{20}PHYT_{30}$												N.A
$PEG3K_{25}PHYT_{25}$										N.A	N.A	N.A
$PEG3K_{30}PHYT_{20}$												
$PEG3K_{40}PHYT_{10}$												N.A

	Dry(20°C)	20 °C	25 °C	30 °C	35 °C	37 °C	40 °C	45 °C	50 °C	55 °C	60 °C	65 °C
$PEG4K_{10}PHYT_{40}$	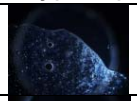	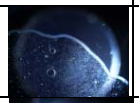			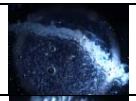					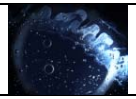		
$PEG4K_{20}PHYT_{30}$	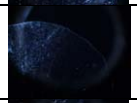				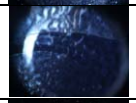	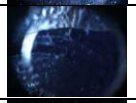		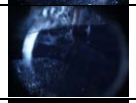	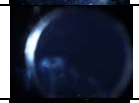	N.A	N.A	N.A
$PEG4K_{25}PHYT_{25}$		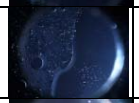	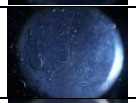									N.A
$PEG4K_{30}PHYT_{20}$	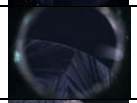	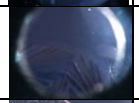		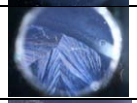	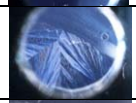		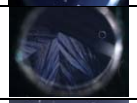	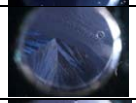				N.A
$PEG4K_{40}PHYT_{10}$									N.A	N.A	N.A	N.A

	Dry(20°C)	20 °C	25 °C	30 °C	35 °C	37 °C	40 °C	45 °C	50 °C	55 °C	60 °C
$PEG6K_{10}PHYT_{40}$											N.A
$PEG6K_{20}PHYT_{30}$											N.A
$PEG6K_{25}PHYT_{25}$											
$PEG6K_{30}PHYT_{20}$											
$PEG6K_{40}PHYT_{10}$											

	Dry(20°C)	20 °C	25 °C	30 °C	35 °C	37 °C	40 °C	45 °C	50 °C	55 °C	60 °C	65 °C
$PEG8K_{10}PHYT_{40}$	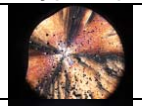	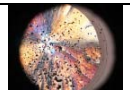					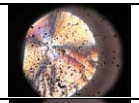			N.A	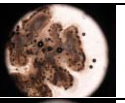	N.A
$PEG8K_{20}PHYT_{30}$	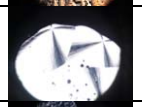	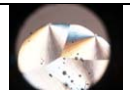			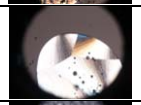			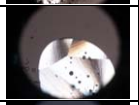		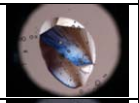		N.A
$PEG8K_{25}PHYT_{25}$	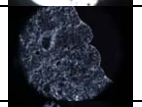	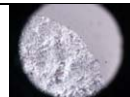	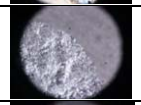	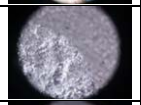	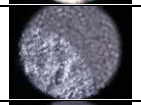	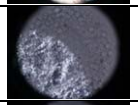	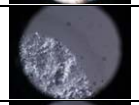	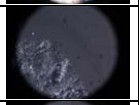		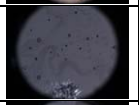		N.A
$PEG8K_{30}PHYT_{20}$	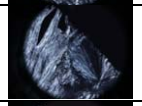	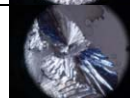	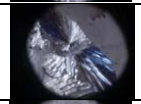	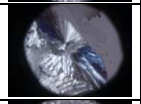	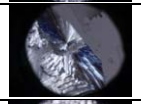	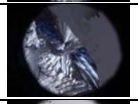	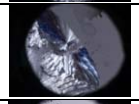	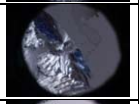				N.A
$PEG8K_{40}PHYT_{10}$												

	Dry(20°C)	20 °C	25 °C	30 °C	35 °C	37 °C	40 °C	45 °C	50 °C	55 °C	60 °C
$PEG10K_{10}PHYT_{40}$											N.A
$PEG10K_{20}PHYT_{30}$											
$PEG10K_{25}PHYT_{25}$											
$PEG10K_{30}PHYT_{20}$											
$PEG10K_{40}PHYT_{10}$											

	Dry(20°C)	20 °C	25 °C	30 °C	35 °C	37 °C	40 °C	45 °C	50 °C	55 °C	60 °C	65 °C
$PEG14K_{10}PHYT_{40}$	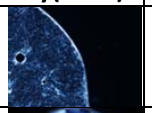	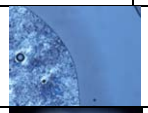	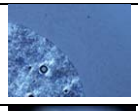	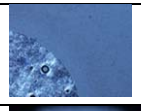	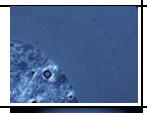	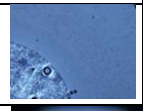	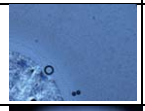	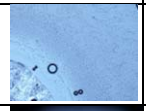			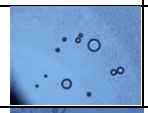	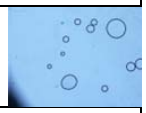
$PEG14K_{20}PHYT_{30}$			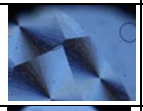	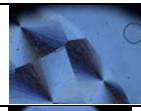				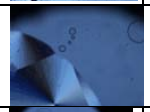				N.A
$PEG14K_{25}PHYT_{25}$	N.A				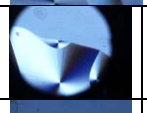					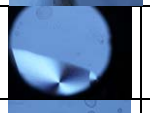	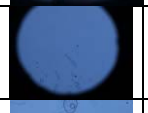	N.A
$PEG14K_{30}PHYT_{20}$	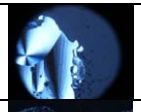											N.A
$PEG14K_{40}PHYT_{10}$												N.A

Anisotropic and isotropic phase behaviour using CPLM

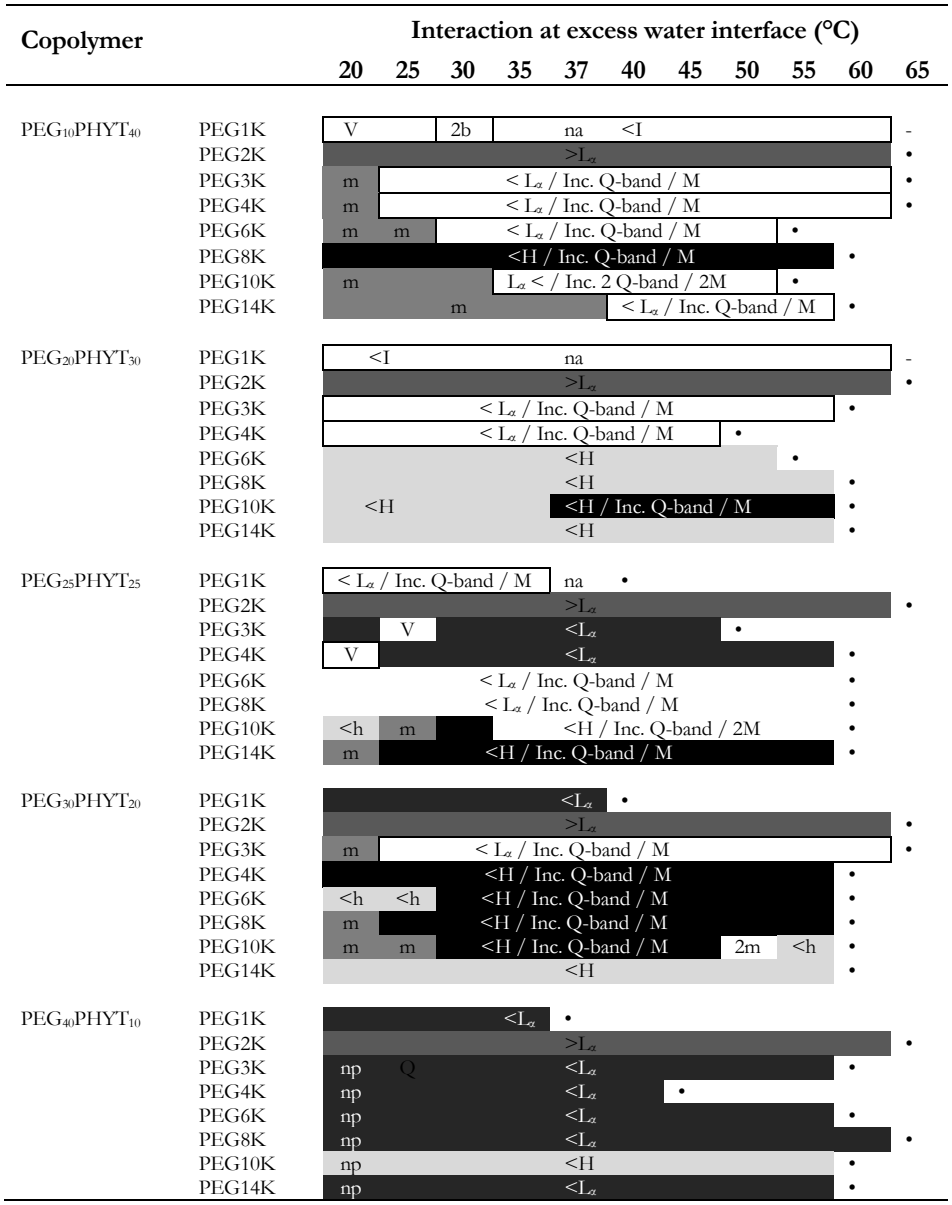

Legend:

•	No longer present (all dissolved)
N/A	Result not available
<H	Sequential reduction of H phase at higher temp
M	Micelle
Np	nanoparticles
<H / Inc. Q-band / M	Reduction in Hex which is next to an increasing cubic band appearing in access water which is next to micelles furthest from the polymer surface
2m	Reduction in Hex which is next to an increasing cubic band appearing in access water which is next to small micelle band which is next to bigger micelles (2m = 2 micelle groups) furthest from the polymer surface
<Lα	reduction of lamellar phase with increasing temperature, sometimes with "np" nanoparticles formation seen at the interface where the water meets the polymer
>Lα	expansion, with edges of polymer in contact with water swollen and less biorefringent as temperature increase
V	cubic band

Figure 3. Anisotropic and isotropic phases observed during water penetration scans of the copolymer in excess water under cross polarized light microscopy (CPLM) from 20 °C to 65 °C.

Small Angle X-ray Scattering (SAXS) & Dynamic Light Scattering (DLS) data

$PEG(x)_{10}PHYT_{40}$		Sol		SAXS		DLS	
PEG MW (x)	**Conc wt %**	**500µl**	**Temp (°C)**	**Phase**	**Lattice Parameter (Å)**	**Z-Ave (nm)**	**PDI**
	1	PBS	25	Q_2^P	101.34	299.4	0.40
PEG2K	1	PBS	30	Q_2^P	99.01		
	1	PBS	37	Q_2^P	95.09		
	1	PBS	40	Q_2^P	93.55		
	1	PBS	45	Q_2^P	90.26		
	1	PBS	50	Q_2^P	88.49		
	1	PBS	55	Q_2^P	87.27		
	1	PBS	60	Q_2^P	88.59		
	1	PBS	65	L_2			
	1	PBS	25	Q_2^P/Q_2^D	93.12/68.08	385.6	0.44
PEG3K	1	PBS	30	Q_2^P/Q_2^D	92.11/66.43		
	1	PBS	37	Q_2^P/Q_2^D	88.59/64.61		
	1	PBS	40	Q_2^P/Q_2^D	87.63/64.24		
	1	PBS	45	Q_2^P/Q_2^D	86.03/63.19		
	1	PBS	50	mix/Q_2^D	-/61.68		
	1	PBS	55	Q_2^D	60.67		
	1	PBS	60	L_2			
	1	PBS	65	L_2			
	1	PBS	25	Q_2^D	65.65	234.7	0.24
PEG4K	1	PBS	30	Q_2^D	64.64		
	1	PBS	37	Q_2^D	63.64		
	1	PBS	40	Q_2^D	63.45		
	1	PBS	45	Q_2^D	63.19		
	1	PBS	50	Q_2^D	60.99		
	1	PBS	55	H_2	40.08		
	1	PBS	60	H_2	39.49		
	1	PBS	65	H_2	39.03		
	1	PBS	25	Q_2^D	65.11	340.7	0.34
PEG6K	1	PBS	30	Q_2^D	63.57		
	1	PBS	37	Q_2^D/H_2	62.07/41.39		
	1	PBS	40	Q_2^D/H_2	62.10/41.26		
	1	PBS	45	Q_2^D/H_2	60.63/40.58		
	1	PBS	50	H_2	40.01		
	1	PBS	55	H_2	39.45		
	1	PBS	60	H_2	38.80		
	1	PBS	65	L_2			
	1	PBS	25	Q_2^D	65.71	222.4	0.24
PEG8K	1	PBS	30	Q_2^D	64.44		
	1	PBS	37	Q_2^D/H_2	63.07/41.86		
	1	PBS	40	Q_2^D	62.94		
	1	PBS	45	Q_2^D/H_2	61.11/40.74		
	1	PBS	50	H_2	40.22		
	1	PBS	55	H_2	39.65		
	1	PBS	60	H_2	39.05		
	1	PBS	65	H_2	38.64		
	1	PBS	25	Q_2^D	65.11	334.0	0.27
PEG10K	1	PBS	30	Q_2^D	63.63		
	1	PBS	37	Q_2^D/H_2	62.50/41.52		
	1	PBS	40	Q_2^D/H_2	62.35/41.37		
	1	PBS	45	Q_2^D/H_2	60.81/40.77		
	1	PBS	50	H_2	40.14		
	1	PBS	55	H_2	39.59		
	1	PBS	60	H_2	39.01		
	1	PBS	65	L_2			
	1	PBS	25	Q_2^D	67.00	302.7	0.40
PEG14K	1	PBS	30	Q_2^D	65.52		Multi-modal
	1	PBS	37	Q_2^D	64.16		
	1	PBS	40	Q_2^D	64.07		
	1	PBS	45	Q_2^D	62.75		
	1	PBS	50	Q_2^D/H_2	60.57/40.45		
	1	PBS	55	H_2	39.98		
	1	PBS	60	H_2	39.32		
	1	PBS	65	H_2	38.81		

$PEG(x)_{20}PHYT_{30}$		Sol		SAXS		DLS	
PEG MW (x)	**Conc wt %**	**500µl**	**Temp (°C)**	**Phase**	**Lattice Parameter(Å)**	**Z-Ave (nm)**	**PDI**
	1	PBS	25	Q_2^P	104.18	242.6	Multi-modal
PEG1K	1	PBS	30	Q_2^P	101.67		
	1	PBS	37	Q_2^P	96.94		
	1	PBS	40	Q_2^P	95.01		
	1	PBS	45	Q_2^P	92.24		
	1	PBS	50	Q_2^P	89.71		
	1	PBS	55	Q_2^P	88.42		
	1	PBS	60	Q_2^P	88.59		
	1	PBS	65	L_2			
	1	PBS	25	Q_2^P	97.52	257.1	Multi-modal
PEG2K	1	PBS	30	Q_2^P	95.46		
	1	PBS	37	Q_2^P	92.34		
	1	PBS	40	Q_2^P	90.45		
	1	PBS	45	Q_2^P	88.99		
	1	PBS	50	Q_2^P/Q_2^D	87.91/62.21		
	1	PBS	55	Q_2^P/Q_2^D	88.18/62.24		
	1	PBS	60	L_2			
	1	PBS	65	L_2			
	1	PBS	25	Q_2^D	66.04	580.8	Multi-modal
PEG3K	1	PBS	30	Q_2^D	64.85		
	1	PBS	37	Q_2^D	63.28		
	1	PBS	40	Q_2^D	62.81		
	1	PBS	45	Q_2^D	61.79		
	1	PBS	50	Q_2^D/H_2	60.77/40.29		
	1	PBS	55	H_2	39.88		
	1	PBS	60	H_2	39.43		
	1	PBS	65	L_2			
	1	PBS	25	Q_2^D	64.58	284	0.26
PEG4K	1	PBS	30	Q_2^D	63.27		
	1	PBS	37	Q_2^D	62.67		
	1	PBS	40	Q_2^D/H_2	62.20/41.17		
	1	PBS	45	Q_2^D/H_2	60.85/40.43		
	1	PBS	50	H_2	39.97		
	1	PBS	55	H_2	39.37		
	1	PBS	60	H_2	38.85		
	1	PBS	65	L_2			
	1	PBS	25	Q_2^D	64.60	251.5	0.24
PEG6K	1	PBS	30	Q_2^D	63.26		
	1	PBS	37	Q_2^D/H_2	61.86/41.14		
	1	PBS	40	Q_2^D/H_2	61.90/41.04		
	1	PBS	45	H_2	40.36		
	1	PBS	50	H_2	39.66		
	1	PBS	55	H_2	39.04		
	1	PBS	60	H_2	38.53		
	1	PBS	65	L_2			
	1	PBS	25	Q_2^D	65.22	266.9	0.31
PEG8K	1	PBS	30	Q_2^D	64.54		
	1	PBS	37	Q_2^D	63.13		
	1	PBS	40	Q_2^D	63.08		
	1	PBS	45	Q_2^D/H_2	61.29/40.75		
	1	PBS	50	H_2	40.21		
	1	PBS	55	H_2	39.61		
	1	PBS	60	H_2	39.01		
	1	PBS	65	H_2	38.56		
	1	PBS	25	Q_2^D	65.15	338.2	0.237
PEG10K	1	PBS	30	Q_2^D	63.69		Multi-modal
	1	PBS	37	Q_2^D/H_2	62.21/41.43		
	1	PBS	40	Q_2^D/H_2	62.23/41.13		
	1	PBS	45	Q_2^D/H_2	60.86/40.62		
	1	PBS	50	H_2	40.01		
	1	PBS	55	H_2	39.39		
	1	PBS	60	H_2	38.79		
	1	PBS	65	L_2			
	1	PBS	25	Q_2^D	66.62	369.3	0.24
PEG14K	1	PBS	30	Q_2^D	64.99		
	1	PBS	37	Q_2^D	62.83		
	1	PBS	40	Q_2^D	62.86		
	1	PBS	45	Q_2^D	62.03		
	1	PBS	50	Q_2^D/H_2	60.34/40.34		
	1	PBS	55	H_2	39.80		
	1	PBS	60	H_2	39.16		
	1	PBS	65	L_2			

$PEG(x)_{25}PHYT_{25}$		Sol		SAXS		DLS	
PEG MW (x)	**Conc wt %**	**500µl**	**Temp (°C)**	**Phase**	**Lattice Parameter(Å)**	**Z-Ave (nm)**	**PDI**
	1	PBS	25	Q_2^P	100.38	310	Multi-
PEG1K	1	PBS	30	Q_2^P	97.95		modal
	1	PBS	37	Q_2^P	93.90		
	1	PBS	40	Q_2^P	92.13		
	1	PBS	45	Q_2^P	89.90		
	1	PBS	50	Q_2^P	87.61		
	1	PBS	55	Q_2^P	87.12		
	1	PBS	60	Q_2^P	88.13		
	1	PBS	65	L_2			
	1	PBS	25	Q_2^P/Q_2^D	94.96/69.28	174.4	Multi-
PEG2K	1	PBS	30	Q_2^P	95.70		modal
	1	PBS	37	Q_2^P	92.52		
	1	PBS	40	Q_2^P	91.15		
	1	PBS	45	Q_2^P	89.62		
	1	PBS	50	Q_2^P/Q_2^D	88.15/62.03		
	1	PBS	55	Q_2^P/H_2	88.24/40.99		
	1	PBS	60	L_2			
	1	PBS	65	L_2			
	1	PBS	25	Q_2^D	65.60	574.5	0.24
PEG3K	1	PBS	30	Q_2^D	64.69		Multi-
	1	PBS	37	Q_2^D	63.53		Modal
	1	PBS	40	Q_2^D	63.19		
	1	PBS	45	Q_2^D	62.04		
	1	PBS	50	Q_2^D/H^2	60.64/40.25		
	1	PBS	55	H^2	39.88		
	1	PBS	60	H^2	39.30		
	1	PBS	65	L_2			
	1	PBS	25	Q_2^D	69.20	259.9	0.26
PEG4K	1	PBS	30	Q_2^D	67.59		
	1	PBS	37	Q_2^D	66.20		
	1	PBS	40	Q_2^D	65.92		
	1	PBS	45	Q_2^D	65.42		
	1	PBS	50	Q_2^D	63.28		
	1	PBS	55	Q_2^D	60.69		
	1	PBS	60	L_2			
	1	PBS	65	L_2			
	1	PBS	25	Q_2^D	66.23	337.2	Multi-
PEG6K	1	PBS	30	Q_2^D	64.62		modal
	1	PBS	37	Q_2^D	62.19		
	1	PBS	40	Q_2^D	62.21		
	1	PBS	45	Q_2^D	61.67		
	1	PBS	50	Q_2^D/H^2	60.11/40.25		
	1	PBS	55	H^2	39.72		
	1	PBS	60	H^2	39.09		
	1	PBS	65	L_2			
	1	PBS	25	Q_2^D	69.75	229.5	Multi-
PEG8K	1	PBS	30	Q_2^D	67.78		modal
	1	PBS	37	Q_2^D	64.66		
	1	PBS	40	Q_2^D	64.72		
	1	PBS	45	Q_2^D	64.60		
	1	PBS	50	Q_2^D	62.23		
	1	PBS	55	Q_2^D	59.90		
	1	PBS	60	n/a			
	1	PBS	65	n/a			
	1	PBS	25	Q_2^D	68.43	310.9	Multi-
PEG10K	1	PBS	30	Q_2^D	66.35		modal
	1	PBS	37	Q_2^D	64.29		
	1	PBS	40	Q_2^D	64.33		
	1	PBS	45	Q_2^D/H^2	64.11/40.59		
	1	PBS	50	Q_2^D	61.41		
	1	PBS	55	Q_2^D/H^2	59.58/40.13		
	1	PBS	60	H^2	39.52		
	1	PBS	65	n/a			
	1	PBS	25	Q_2^D	67.24	386.7	Multi-
PEG14K	1	PBS	30	Q_2^D	65.56		modal
	1	PBS	37	Q_2^D	62.77		
	1	PBS	40	Q_2^D	62.63		
	1	PBS	45	Q_2^D	61.09		
	1	PBS	50	Q_2^D/H^2	60.03/40.60		
	1	PBS	55	Q_2^D/H^2	59.25/39.98		
	1	PBS	60	H^2	39.31		
	1	PBS	65	L_2			

$PEG(x)_{30}PHYT_{20}$		Sol	SAXS			DLS	
PEG MW (x)	**Conc wt %**	**500µl**	**Temp (°C)**	**Phase**	**Lattice Parameter(Å)**	**Z-Ave (nm)**	**PDI**
	1	PBS	25	Q_2^P	97.43	332.1	Multi-
PEG1K	1	PBS	30	Q_2^P	95.03		modal
	1	PBS	37	Q_2^P	91.42		
	1	PBS	40	Q_2^P	89.78		
	1	PBS	45	Q_2^P	87.68		
	1	PBS	50	Q_2^P/Q_2^D	85.78/63.05		
	1	PBS	55	Q_2^P/Q_2^D	86.27/61.09		
	1	PBS	60	L_2			
	1	PBS	65	L_2			
	1	PBS	25	Q_2^P	98.61	253.3	0.23
PEG2K	1	PBS	30	Q_2^P	95.90		
	1	PBS	37	Q_2^P	92.34		
	1	PBS	40	Q_2^P	91.06		
	1	PBS	45	Q_2^P	89.01		
	1	PBS	50	Q_2^P	87.49		
	1	PBS	55	Q_2^P/H^2	87.10/40.95		
	1	PBS	60	L_2			
	1	PBS	65	L_2			
	1	PBS	25	Q_2^D	67.10	506.8	Multi-
PEG3K	1	PBS	30	Q_2^D	65.91		modal
	1	PBS	37	Q_2^D	63.89		
	1	PBS	40	Q_2^D	63.27		
	1	PBS	45	Q_2^D	63.09		
	1	PBS	50	Q_2^D	62.09		
	1	PBS	55	Q_2^D	60.03		
	1	PBS	60	H^2	39.65		
	1	PBS	65	L_2			
	1	PBS	25	Q_2^D	65.64	275.4	
PEG4K	1	PBS	30	Q_2^D	63.97		
	1	PBS	37	Q_2^D	63.18		
	1	PBS	40	Q_2^D	63.21		
	1	PBS	45	Q_2^D	61.29		
	1	PBS	50	H^2	40.15		
	1	PBS	55	H^2	39.53		
	1	PBS	60	H^2	38.88		
	1	PBS	65	L_2			
	1	PBS	25	Q_2^D	67.29	330.7	0.40
PEG6K	1	PBS	30	Q_2^D	65.49		
	1	PBS	37	Q_2^D	62.80		
	1	PBS	40	Q_2^D	62.79		
	1	PBS	45	Q_2^D	61.57		
	1	PBS	50	Q_2^D/H^2	60.05/40.26		
	1	PBS	55	H^2	39.90		
	1	PBS	60	H^2	39.22		
	1	PBS	65	L_2			
	1	PBS	25	Q_2^D	68.06	495.5	Multi-
PEG8K	1	PBS	30	Q_2^D	66.10		modal
	1	PBS	37	Q_2^D	63.19		
	1	PBS	40	Q_2^D	63.14		
	1	PBS	45	Q_2^D	61.51		
	1	PBS	50	Q_2^D	60.82		
	1	PBS	55	Q_2^D/H^2	59.48/40.09		
	1	PBS	60	H^2	39.47		
	1	PBS	65	L_2			
	1	PBS	25	Q_2^D	67.97	290	Multi-
PEG10K	1	PBS	30	Q_2^D	66.04		modal
	1	PBS	37	Q_2^D	63.75		
	1	PBS	40	Q_2^D	63.79		
	1	PBS	45	Q_2^D	63.29		
	1	PBS	50	Q_2^D	60.90		
	1	PBS	55	Q_2^D/H^2	59.38/40.06		
	1	PBS	60	H^2	39.41		
	1	PBS	65	n/a			
	1	PBS	25	Q_2^D	68.20	354.2	0.21
PEG14K	1	PBS	30	Q_2^D	66.38		
	1	PBS	37	Q_2^D	63.44		
	1	PBS	40	Q_2^D	63.30		
	1	PBS	45	Q_2^D	62.80		
	1	PBS	50	Q_2^D	60.77		
	1	PBS	55	Q_2^D/H^2	59.56/40.14		
	1	PBS	60	H	39.53		
	1	PBS	65	L_2			

$PEG(x)_{40}PHYT_{10}$		Sol		SAXS		DLS	
PEG MW (x)	**Conc wt %**	**500µl**	**Temp (°C)**	**Phase**	**Lattice Parameter(Å)**	**Z-Ave (nm)**	**PDI**
	1	PBS	25	Q_2^P/Q_2^D	96.92/68.69	350.9	0.24
PEG1K	1	PBS	30	Q_2^P/Q_2^D	94.40/66.93		Multi-
	1	PBS	37	Q_2^P/Q_2^D	91.40/64.85		modal
	1	PBS	40	Q_2^P/Q_2^D	87.78/64.62		
	1	PBS	45	Q_2^P/Q_2^D	87.50/64.58		
	1	PBS	50	$2(Q_2^D)$	63.78/60.75		
	1	PBS	55	$2(Q_2^D)$	61.59/59.89		
	1	PBS	60	L_2			
	1	PBS	65	L_2			
	1	PBS	25	Q_2^P	98.70	231.5	0.30
PEG2K	1	PBS	30	Q_2^P	96.31		
	1	PBS	37	Q_2^P	92.59		
	1	PBS	40	Q_2^P	91.21		
	1	PBS	45	Q_2^P	89.34		
	1	PBS	50	Q_2^P	87.80		
	1	PBS	55	Q_2^P	86.64		
	1	PBS	60	L_2			
	1	PBS	65	L_2			
	1	PBS	25	Q_2^D	64.40	459.1	Multi-
PEG3K	1	PBS	30	Q_2^D	63.48		modal
	1	PBS	37	Q_2^D	61.86		
	1	PBS	40	Q_2^D	61.45		
	1	PBS	45	Q_2^D/H^2	60.89/40.58		
	1	PBS	50	H^2	40.04		
	1	PBS	55	H^2	39.42		
	1	PBS	60	H^2	38.80		
	1	PBS	65	L_2			
	1	PBS	25	Q_2^D	67.35	319.4	Multi-
PEG4K	1	PBS	30	Q_2^D	65.43		modal
	1	PBS	37	Q_2^D	64.14		
	1	PBS	40	Q_2^D	64.18		
	1	PBS	45	Q_2^D	63.58		
	1	PBS	50	Q_2^D	61.58		
	1	PBS	55	Q_2^D	59.47		
	1	PBS	60	L_2			
	1	PBS	65	n/a			
	1	PBS	25	Q_2^D	66.82	311.8	0.24
PEG6K	1	PBS	30	Q_2^D	65.06		Multi-
	1	PBS	37	Q_2^D	62.41		modal
	1	PBS	40	Q_2^D	62.36		
	1	PBS	45	Q_2^D	61.55		
	1	PBS	50	Q_2^D/H^2	59.93/40.21		
	1	PBS	55	H^2	39.75		
	1	PBS	60	H^2	39.11		
	1	PBS	65	L_2			
	1	PBS	25	Q_2^D	66.74	285.5	0.27
PEG8K	1	PBS	30	Q_2^D	65.09		Multi-
	1	PBS	37	Q_2^D	62.35		modal
	1	PBS	40	Q_2^D	62.02		
	1	PBS	45	Q_2^D	60.95		
	1	PBS	50	Q_2^D/H^2	59.91/40.45		
	1	PBS	55	H^2	39.82		
	1	PBS	60	H^2	39.14		
	1	PBS	65	L_2			
	1	PBS	25	Q_2^D	67.97	263.1	0.236
PEG10K	1	PBS	30	Q_2^D	65.96		Multi-
	1	PBS	37	Q_2^D	63.56		modal
	1	PBS	40	Q_2^D	63.58		
	1	PBS	45	Q_2^D	63.23		
	1	PBS	50	Q_2^D	60.96		
	1	PBS	55	Q_2^D/H^2	59.42/39.89		
	1	PBS	60	H^2	39.40		
	1	PBS	65	n/a			
	1	PBS	25	Q_2^D	68.36	372.9	Multi-
PEG14K	1	PBS	30	Q_2^D	66.71		modal
	1	PBS	37	Q_2^D	63.59		
	1	PBS	40	Q_2^D	63.50		
	1	PBS	45	Q_2^D	61.70		
	1	PBS	50	Q_2^D/H^2	60.50/40.48		
	1	PBS	55	Q_2^D	59.45		
	1	PBS	60	H^2	39.56		
	1	PBS	65	n/a			

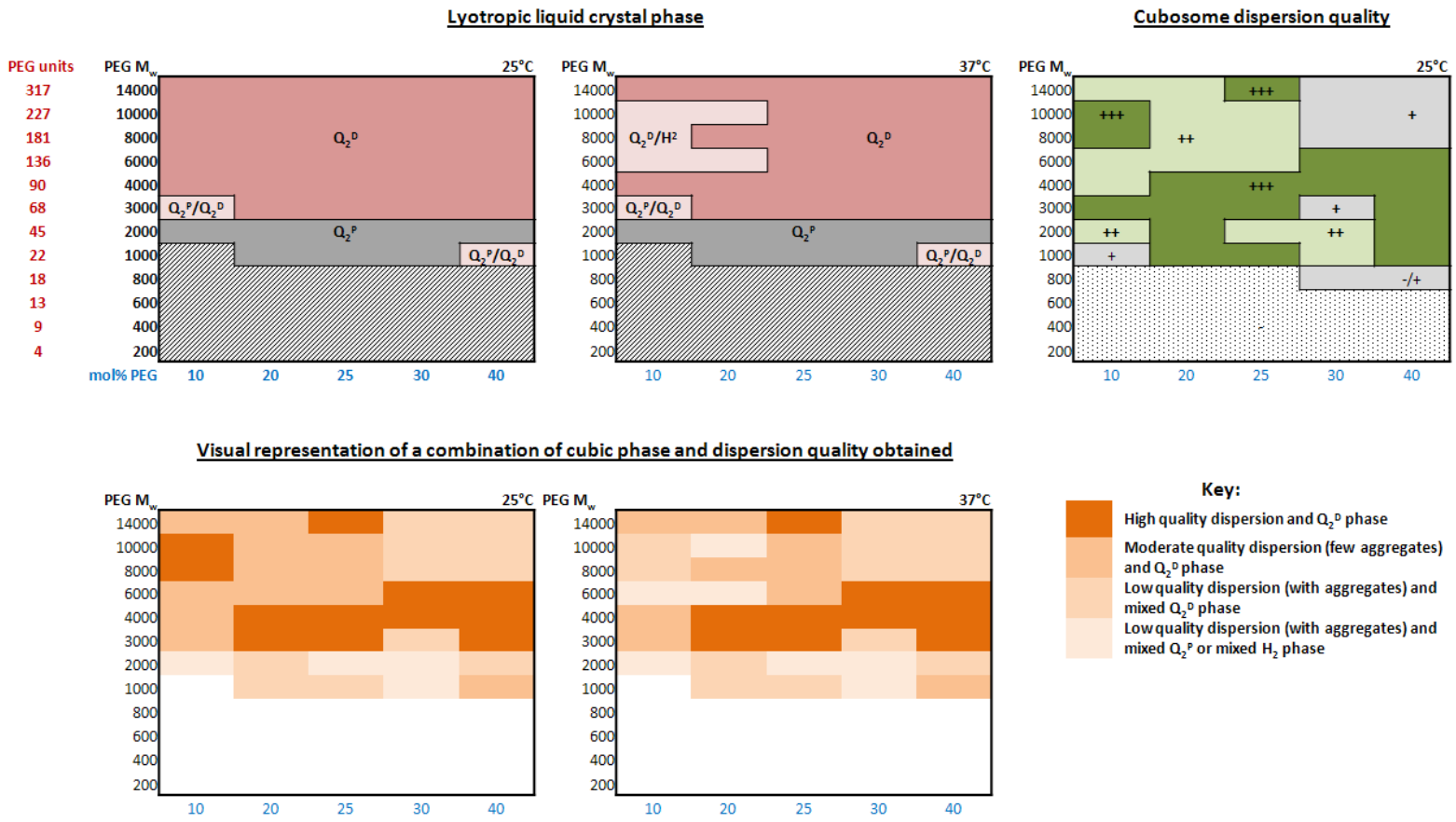

Figure 4. Visual representation of the lyotropic liquid crystal phases obtained from SAXS at 25 °C and 37 °C (Top left) and their corresponding dispersion quality at 25 °C (Top right). Visual representations of a combination of the cubic phase and its dispersion quality are presented for temperature 25 °C and 37 °C (Below), with the key for the shading on the bottom right

Chapter 6

The synthesis, self-assembly and application of amphiphilic brush copolymers as custom designed novel lyotropic liquid crystalline nanostructured particle steric stabilisers

Josephine Y.T. Chong, Xavier Mulet, Almar Postma, Daniel J. Keddie, Lynne Waddington, Ben J. Boyd and Calum J. Drummond

Part 1 (Chapter 6.1)

Polymer synthesis and self-assembly

Part 2 (Chapter 6.2)

Novel steric stabiliser for cubosomes

Chapter 6.1

RAFT preparation and aqueous self-assembly of amphiphilic poly(octadecyl acrylate)-*block*-poly(polyethylene glycol methyl ether acrylate) copolymers

Josephine Y.T. Chong, Daniel J. Keddie, Almar Postma, Xavier Mulet, Ben J. Boyd and Calum J. Drummond

SUBMITTED: *Colloid and Polymer Science* (submitted on 23.5.2014)

Declaration for Chapter 6.1

Declaration by candidate

In the case of Chapter 6.1, the nature and extent of my contribution to the work was the following:

Nature of contribution	Extent of contribution (%)
Research design, polymer synthesis and analysis, performance of data collection and analysis, manuscript preparation	75

The following co-authors contributed to the work:

Name	Nature of contribution
Daniel J. Keddie	Intellectual input on RAFT polymerisation and preparation; input into manuscript preparation
Almar Postma	Intellectual input on RAFT polymerisation and preparation; input into manuscript preparation
Xavier Mulet	Supervision; intellectual input; input into manuscript preparation
Ben Boyd	Supervision; intellectual input; input into manuscript preparation
Calum Drummond	Supervision; intellectual input; input into manuscript preparation

Candidate's signature: [redacted] **Date:** **10.7.2014**

Declaration by co-authors

The undersigned hereby certify that:

(25) the above declaration correctly reflects the nature and extent of the candidate's contribution to this work, and the nature of the contribution of each of the co-authors.

(26) they meet the criteria for authorship in that they have participated in the conception, execution, or interpretation, of at least that part of the publication in their field of expertise;

(27) they take public responsibility for their part of the publication, except for the responsible author who accepts overall responsibility for the publication;

(28) there are no other authors of the publication according to these criteria;

(29) potential conflicts of interest have been disclosed to (a) granting bodies, (b) the editor or publisher of journals or other publications, and (c) the head of the responsible academic unit; and

(30) the original data are stored at the following location(s) and will be held for at least five years from the date indicated below:

Location of data storage: CSIRO Materials Science and Engineering, Ian Wark Laboratory, Bayview Avenue, Clayton 3168, Australia.

Co-authors' signature for Chapter 6.1:

Signed:  **Date:** **29.1.2014**

Daniel J. Keddie

Signed:  **Date:** **8.1.2014**

Almar Postma

Signed:  **Date:** **10.1.2014**

Xavier Mulet

Signed:  **Date:** **28.2.2014**

Ben J. Boyd

Signed:  **Date:** **12.4.2014**

Calum J. Drummond

RAFT preparation and the aqueous self-assembly of amphiphilic poly(octadecyl acrylate)-block-poly(polyethylene glycol methyl ether acrylate) copolymers

Journal:	*Colloid and Polymer Science*
Manuscript ID:	Draft
Manuscript Type:	Original Contribution
Date Submitted by the Author:	n/a
Complete List of Authors:	Chong, Josephine; CSIRO, CMSE; Monash University, Drug Delivery, Disposition and Dynamics Keddie, Daniel; University of New England, Chemistry, School of Science and Technology; CSIRO, CMSE Postma, Almar; CSIRO, CMSE Mulet, Xavier; CSIRO, CMSE Boyd, Ben; Monash University, Drug Delivery, Disposition and Dynamics Drummond, Calum; RMIT University, School of Applied Sciences, College of Science, Engineering and Health; CSIRO, CMSE
Keywords:	amphiphilic brush copolymer, PEGylated copolymer, self-assembly, RAFT end-group, diblock copolymer

RAFT preparation and the aqueous self-assembly of amphiphilic poly(octadecyl acrylate)-*block*-poly(polyethylene glycol methyl ether acrylate) copolymers

Josephine Y.T. Chong[a,b], *Daniel J. Keddie*[a,c], *Almar Postma*[a], *Xavier Mulet*[a,b], *Ben J. Boyd*[b*], *Calum J. Drummond*[a,d*]

[a] CSIRO Materials Science and Engineering, Private Bag 10, Clayton, VIC 3169, Australia; [b] Drug Delivery, Disposition and Dynamics, Monash Institute of Pharmaceutical Science, Monash University, 381 Royal Parade, Parkville, VIC 3052, Australia; [c] Chemistry, School of Science and Technology, University of New England, NSW 2351, Australia; [d] School of Applied Sciences, College of Science, Engineering and Health, RMIT University, GPO Box 2476, Melbourne, VIC 3001, Australia

ABSTRACT

Reversible addition-fragmentation chain transfer (RAFT) polymerisation was used to prepare novel amphiphilic poly(octadecyl acrylate)-*block*-poly(polyethylene glycol methyl ether acrylate) (P(ODA)-*b*-P(PEGA-OMe)) copolymers. These polymers were reduced to remove the dodecyl RAFT end-group, via radical-induced reduction using a hypophosphite salt, *N*-ethylpiperidine hypophosphite (EPHP). The resulting brush-like diblock copolymers were characterised by proton nuclear magnetic resonance (^{1}H NMR) and gel permeation chromatography (GPC). Investigation of the self-assembly behaviour of both the reduced and RAFT-group functional polymers in excess water determined by dynamic light scattering (DLS), cryo-transmission electron microscopy (cryo-TEM) and cross-polarised light microscopy (CPLM), indicated that all the copolymers form micellar aggregates in excess water. The hydrophobic dodecyltrithiocarbonate RAFT end-group, which is located on the terminal end of the hydrophilic domain, significantly influences the self-assembly behaviour of the copolymers in water.

KEYWORDS amphiphilic brush copolymer, PEGylated copolymer, self-assembly, RAFT end-group, diblock copolymer

INTRODUCTION

Amphiphilic block copolymers attract considerable research attention because of their ability to self-assemble into micelles, vesicles and other morphologies when immersed in selective solvents. Due to their interesting morphologies and properties, block copolymer micelle systems are studied from the perspective of colloidal science, synthesis of advanced materials, drug and gene delivery and biomedical application.[1-7] Micelle-based drug delivery systems have been considered to have select advantages over some other particulate-based carriers, which make them well studied systems. These include retaining a long circulation time *in vivo* (the so-called 'stealth' effect), enhancement of solubility for incorporating hydrophobic drugs, and enhanced permeability and retention effect (EPR effect) in tumour tissue (i.e., passive targeting).[8-12]

In order to promote the stealth effect in micelle systems to foster the EPR effect, prevention of protein adsorption and cell adhesion are required through the use of polymers with low surface energy, such as polyethylene glycol (PEG).[13, 14] PEG is a hydrophilic, non-toxic, water-soluble, synthetic polymer. PEG has been found to provide surfaces with stealth and anti-fouling properties as a result of its hydrophilicity, high surface water mobility and low interfacial free energy with water.[14] Although traditionally linear amphiphilic copolymers containing PEG have

* [redacted]

been used for micelle systems, it has been found that the molecular architecture of PEG is important, with non-linear chains (i.e., star-shaped and brush-shaped) being more effective than the linear counterparts at preventing non-specific protein adsorption.[15-18] The increased effectiveness is due to a larger surface area occupied per chain and a higher surface mobility of PEG in a brush-type copolymer configuration.[19] Brush copolymers were also reported to enhance the stability of micelles more than their plain/linear analogues.[20]

In addition to forming micelles some amphiphilic copolymers also have the ability to stabilise lyotropic liquid crystalline nanostructured bicontinuous cubic particles (e.g., triblock copolymer, Pluronic® F127). Although various steric stabilisers for lyotropic liquid crystalline nanostructured particles exhibiting different polymer architectures have been reported[21-23], an amphiphilic brush copolymer has to our knowledge never been used for this purpose. It would be interesting to develop amphiphilic brush copolymer structures for sterically stabilising lyotropic liquid crystalline nanostructured particles (e.g., cubosomes) as non-linear structures (e.g., hyperbranched polyglycerols)[24-28] are often reported to be advantageous over linear structures for stabilisation.

There are three main approaches for the synthesis of amphiphilic brush copolymers[29], which includes grafting-through (i.e., homo- and copolymerisation of macromonomers)[30-33], grafting-from (i.e., grafting side chains from the backbone)[34-37] and grafting-onto (i.e., attachment of side chains to the backbone)[38-43]. Presently, a variety of well-defined amphiphilic polymers with various architectures have been synthesised by controlled/"living" polymerisation methods, such as atom transfer radical polymerisation (ATRP)[44-46], ring-opening polymerisation (ROP)[45, 47, 48], nitroxide-mediated free radical polymerisation (NMP)[49-51], ring-opening metathesis polymerisation (ROMP)[45, 52, 53] and reversible addition-fragmentation chain transfer (RAFT) polymerisation[54-59]. RAFT has been used to prepare brush-type copolymers based on PEG, which self-assemble in water into interesting micelle morphologies.[55, 56, 60]

However, the presence of the thiocarbonylthio end-groups in the polymer post-RAFT polymerisation means that the polymers may be coloured and eventually release an odour over time, due to the decomposition of the thiocarbonylthio groups and the evolution of volatile sulphur-containing compounds.[61, 62] In addition to the unwanted colour and odour, it has also been observed that the thiocarbonylthio group can be toxic and fatal to an assay of fibroblast cells.[63-67] These drawbacks can be disadvantageous in some applications (i.e., biomedical or cosmetic), and can be easily circumvented by the removal of the thiocarbonylthio end-groups, through one of several post-polymerisation modifications.[62, 68-70] Radical-induced reduction is one popular method, which uses a hypophosphite salt, *N*-ethylpiperidine hypophosphite (EPHP).[71] EPHP is a very effective hydrogen donor and work-up is simplified to a water wash.

In the present work, we report on the preparation of six brush-type amphiphilic diblock copolymers with poly(polyethylene glycol methyl ether acrylate) (P(PEGA-OMe)) as the hydrophilic brush block and poly(octadecyl acrylate) (P(ODA)) as the hydrophobic brush block, via consecutive RAFT polymerisations. P(ODA) has recently been used to make a homopolymer used in pH responsive micelles for photosensitive therapeutics.[72] The amphiphilic diblock copolymers were synthesised to have a short hydrophobic block and a long hydrophilic block with synthesis beginning with the hydrophobic block and resulted in the RAFT end-group residing on the terminal end of the hydrophilic block. This sequence in which the blocks were polymerised was primarily chosen because of the potential to create an active targeting system by adding an active targeting moiety to the terminal end of the PEG block by RAFT end-group functionalisation. In addition, the sequence performance made it easier to characterise the block extension by GPC, as the peaks were resolved from one another and also the ODA monomer is not very soluble in many solvents that P(PEGA-OMe) is soluble in except for chloroform, which is a less than ideal solvent in which to perform radical polymerisation.

To assess the effects of the RAFT end-group on the self-assembly behaviour of the copolymers, radical-induced reduction was performed on all six copolymers to remove the RAFT end-group shortly after their polymerisation. The self-assembly properties of the copolymers pre- and post-reduction were studied, as it has been reported that the presence of the hydrophobic RAFT end-group has a significant impact on the ability of a polymer to self-assemble.[73-75] It was discovered by Du *et al.* that a small amount of hydrophobic RAFT end-groups (e.g., dodecyl end-group) on hydrophilic homopolymers were the main driving force for the formation of homopolymer micelles and complex micelles.[74] Therefore it was of interest to investigate the effects of the removal of the hydrophobic, dodecyl RAFT end-groups from the hydrophilic domain of the amphiphilic diblock copolymer. The self-assembly properties of these brush copolymers were studied using dynamic light scattering (DLS) and cross-

polarised light microscopy (CPLM). The morphologies of micelles formed during self-assembly in water were also characterised using cryo-transmission electron microscopy (cryo-TEM).

In addition to studying the self-assembly behaviour of these brush copolymers and the effect of the RAFT end-group, these copolymers were also synthesised to assess their potential to serve as steric stabilisers with potential for active targeting capabilities for lyotropic liquid crystalline nanostructured bicontinuous cubic particles. The liquid crystalline phase behaviour of the polymers themselves was explored in this study by using cross-polarised light microscopy, and the steric stabilisation potential of the polymer is explored later in a separate complementary paper.[76] However, to reiterate, the focus of this paper was to investigate the self-assembly properties of these amphiphilic brush copolymers as they are interesting in their own right as possible micellar drug delivery systems.

MATERIALS AND METHODS

Materials

Octadecyl acrylate (97%) (ODA) was purchased from Sigma-Aldrich (Milwaukee, USA). Poly(ethylene glycol) methyl ether acrylate (M_n 480), *N*-ethylpiperidine hypophosphite (EPHP) and RAFT agent, cyanomethyl dodecyl trithiocarbonate were purchased from Sigma-Aldrich (St Louis, USA). 2,2´-azobis(isobutyronitrile) (AIBN) was purchased from Acros Organics (Geel, Belgium) and purified by recrystallisation twice from methanol prior to use. Toluene, acetone and chloroform solvents were purchased from Merck Chemicals (Darmstadt, Germany). 1,1´-azobis(cyclohexanecarbonitrile) (Vazo™ 88) was purchased from DuPont (Wilmington, USA).

Methodology

Synthesis of macro-RAFT agent poly(octadecyl acrylate) (P(ODA))

Two poly(octadecyl acrylate) macro-RAFT agents were synthesised. The first P(ODA) block (RAFT 1 P(ODA)) was prepared by dissolving 2 g cyanomethyl dodecylcarbonotrithioate (RAFT agent), 15 g ODA and 7.6 mg AIBN in 18 mL of toluene. Aliquots of this stock solution were then transferred into glass ampoules which were degassed and flame sealed. The ampoules were then placed in an oil bath and heated at 60 °C for 16 h. The second P(ODA) block (RAFT 2 P(ODA)) was then prepared repeating this process using 1 g cyanomethyl dodecylcarbonotrithioate, 15 g ODA and 15.2 mg AIBN in 18 mL of toluene. Toluene was removed and then polymer was precipitated from acetone. Three precipitations were performed for the first P(ODA) block and two precipitations were performed for the second P(ODA) block. The molar mass (M_n) for RAFT 1 P(ODA) was 2710, with M_w/M_n=1.04 and for RAFT 2 P(ODA) M_n=3850, with M_w/M_n=1.07.

Synthesis of poly(octadecyl acrylate)-*block*-poly(polyethylene glycol methyl ether acrylate) (P(ODA)-b-P(PEGA-OMe))

To synthesise poly(octadecyl acrylate)-*block*-poly(polyethylene glycol methyl ether acrylate) polymers, 12 g poly(ethylene glycol) methyl ether acrylate (PEGA-OMe), 1.15 g RAFT 1 P(ODA) and 16.5 mg AIBN, were dissolved in 50 mL of toluene. Aliquots of this stock solution were then transferred into three glass ampoules which were degassed and flame sealed. The ampoules were then placed in an oil bath and heated at 60 °C. The first ampoule was heated for 2 h. The second ampoule was heated for 4 h. The third ampoule was heated for 6 h. This produced three different poly(polyethylene glycol methyl ether acrylate) block length polymers. This process was repeated using the second P(ODA) block, using 12 g poly(ethylene glycol) methyl ether acrylate (PEGA-OMe), 1.85 g RAFT 2 P(ODA) and 16.5 mg AIBN, in 50 mL of toluene. In total six amphiphilic P(ODA)-*b*-P(PEGA-OMe)) polymers were synthesised. Toluene was removed and all polymers were purified by dialysis. Dialysis involved placing the polymer into dialysis tubing (MWCO 3500) and then submerging the polymer and tubing in deionised water (DI). Dialysis of the polymers was completed over three days. The molar mass and dispersity values for the copolymers were: $P(ODA)_6$-*b*-$P(PEGA\text{-}OMe)_{27}$ M_n=15400, with M_w/M_n=1.33; $P(ODA)_6$-*b*-$P(PEGA\text{-}OMe)_{35}$ M_n=17500, with M_w/M_n=1.33; $P(ODA)_6$-*b*-$P(PEGA\text{-}OMe)_{39}$ M_n=17900, with M_w/M_n=1.32; $P(ODA)_{10}$-*b*-$P(PEGA\text{-}OMe)_{23}$ M_n=14100, with M_w/M_n=1.46; $P(ODA)_{10}$-*b*-$P(PEGA\text{-}OMe)_{31}$ M_n=15700, with M_w/M_n=1.42; and $P(ODA)_{10}$-*b*-$P(PEGA\text{-}OMe)_{34}$ M_n=16700, with M_w/M_n=1.41.

Reduction of P(ODA)-*b*-P(PEGA-OMe)

Reduction of poly(octadecyl acrylate)-*block*-poly(polyethylene glycol methyl ether acrylate) to remove the RAFT end-group was performed through radical-induced reduction using a hypophosphite salt, *N*-ethylpiperidine hypophosphite (EPHP). Briefly, polymers were prepared in glass ampoules with EPHP and initiator Vazo™ 88, mixed with a small amount of toluene. These ampoules were then degassed and flame-sealed before being placed in an oil bath and heated at 100 °C for 16 h (Scheme 3). The quantity of EPHP and initiator Vazo™ 88 used was calculated according to the amount of polymer used; 1 M of polymer required 0.4 M of initiator Vazo™ 88 and 10 M of EPHP. As one example 0.5 g of $P(ODA)_6$-*b*-$P(PEGA\text{-}OMe)_{27}$ was reduced using 0.06 g EPHP and 0.003 g of initiator Vazo™ 88. Polymers were then transferred into round bottom flasks and solvent removed by rotary evaporation (Rotavapor® R-210, BUCHI, Switzerland). All polymers were purified over three days by dialysis using membrane cut off 3500 Da.

Characterisation of P(ODA)-*b*-P(PEGA-OMe)

Polymers were characterised using proton nuclear magnetic resonance (^{1}H NMR), chloroform and tetrahydrofuran gel permeation chromatography (GPC). Tetrahydrofuran GPC was used post-reduction for the photodiode array detector to analyse the polymers between 305-310 nm wavelengths for the detection of the RAFT end-group. The polymer composition and residual monomer content were analysed by proton nuclear magnetic resonance (NMR). The copolymers were dissolved in deuterated chloroform and spectra for structural assignments were obtained with a Bruker Avance 400 MHz spectrometer (^{1}H 400 MHz, ^{13}C 100 MHz).

Molar masses of the polymers were determined by GPC performed in chloroform (1.0 mL/min) at 30 °C using a Waters 2695 Separations Module, with a Waters 2414 Refractive Index Detector and a Waters 2996 Photodiode Array Detector, a series of four Polymer Laboratories PLGel columns (3 × 5 µm Miked-C and 1 × 3 µm Mixed-E), and Empower Pro Software. The GPC was calibrated with narrow dispersity polystyrene standards (Polymer Laboratories EasiCal, M_w from 264 to 256,000), and molecular weights are reported as polystyrene equivalents based on the refractive index detector.

Self-assembling behaviour of P(ODA)-*b*-P(PEGA-OMe)

Self-assembling behaviour of the P(ODA)-*b*-P(PEGA-OMe) polymers was determined by dynamic light scattering (DLS), cryo-transmission electron microscopy (cryo-TEM) and cross-polarised light microscopy (CPLM). Critical aggregation concentration (CAC) and particle size was determined by DLS[22], performed using a DynaPro plate reader (Wyatt Technology, Santa Barbara, CA). Data shown for CAC measurements from the DLS instrument are averaged from three repeat measurements. Aggregation and self-assembly of P(ODA)-*b*-P(PEGA-OMe) polymers in excess water was confirmed with cryo-TEM. Cryo-TEM images were obtained for a reduced P(ODA)-*b*-PEGA-OMe brush copolymer in excess water, using a Gatan 626 cryoholder (Gatan, Pleasanton, CA, USA) and Tecnai 12 Transmission Electron Microscope (FEI, Eindhoven, The Netherlands) at an operating voltage of 120 KV. Images were recorded using a FEI Eagle 4k × 4k CCD camera at magnifications between 15000x and 42000x, using an electron dose of 8-10 electrons/Å^2.

Lyotropic phase behaviour of bulk copolymer in excess water was determined using cross-polarised light microscopy. CPLM was performed using a Nikon Eclipse 80i microscope (Nikon Corporation, Tokyo, Japan), using ×10 magnification, for obtaining water penetration scans with temperature ranging from 20 to 65 °C.

RESULTS AND DISCUSSION

Polymer synthesis and characterisation

Six brush-type amphiphilic diblock copolymers, P(ODA)-*b*-P(PEGA-OMe), were prepared via two consecutive RAFT polymerisations (Scheme 1 and 2): (i) synthesis of well-defined P(ODA) *via* RAFT polymerisation of P(ODA), using cyanomethyl dodecylcarbonotrithioate as the RAFT agent, and (ii) synthesis of the well-defined diblock copolymer, *via* RAFT polymerisation of P(PEGA-OMe), using the P(ODA) obtained above as the macro-RAFT agent. Three copolymers with varying PEGA units were composed with 6 P(ODA) units on average and

another three copolymers with 10 P(ODA) units on average. The size, structure, and composition of the polymers and copolymers were studied by GPC (Figure 1) and ^{1}H NMR spectroscopy (Figure 2).

An example of one of the GPC chromatograms for the P(ODA)-*b*-P(PEGA-OMe) copolymers, P(ODA)$_{10}$-*b*-P(PEGA-OMe)$_{34}$ is shown in Figure 1(i) to have a shorter retention time post-RAFT polymerisation and broader peak than its precursor P(ODA) block (i.e., 10 P(ODA) units on average). The shorter retention time indicates an increase in molar mass and shows successful diblock copolymer formation, whilst the broader molar mass distribution reflects the pendant PEG chain molar mass distribution of PEGA-OMe monomer. The removal of the RAFT end-group, which has a UV signal between 305–310 nm, was observed by the absence of its distinctive/characteristic signal detected at 306 nm in UV traces using GPC with a UV detector (Figure 1(ii) and Supplementary Materials), and was further confirmed by the elimination of its distinctive peak around 4.8 ppm in the ^{1}H NMR spectra of the polymers post-reduction (see Supplementary Materials). The reduced polymers also lacked the yellow pigmentation and odour, which are characteristic traits of the RAFT end-group that were present in the pre-reduced polymers. The combination of these results indicates the successful removal of the RAFT end-group from the amphiphilic diblock copolymers. These results are consistent in all copolymers and the GPC chromatograms for all the polymers can be found in the Supplementary Materials. Dialysis was also shown to be effective in removing residual PEGA-OMe monomers after RAFT polymerisation of P(ODA)-*b*-P(PEGA-OMe) copolymers, as the second peak (i.e., at approximately 34 min) indicative of the presence of PEGA-OMe monomers, was completely removed post-dialysis (see Supplementary Materials).

Figure 2 shows a stack plot of the ^{1}H NMR spectra of P(ODA)$_{10}$-*b*-P(PEGA-OMe)$_{23}$ pre- and post-reduction and the P(ODA)$_{10}$ block. The stack plot shows the successful synthesis of the amphiphilic diblock copolymer and the successful removal of the RAFT end-group (absence of a distinctive peak around 4.8 ppm is indicative of the RAFT end-group) in the reduced polymer spectrum. All ^{1}H NMR stacked spectra of the P(ODA)-*b*-P(PEGA-OMe) copolymers were found to be consistent and are available in the Supplementary Materials.

The number-average molar mass (M_n) and the molar mass dispersity (M_w/M_n) of the corresponding P(ODA)-*b*-P(PEGA-OMe) copolymers, obtained from both GPC and ^{1}H NMR spectroscopy results, are listed in Table 1. Table 1 shows that the M_n for the P(ODA)-*b*-P(PEGA-OMe) copolymers obtained from GPC and ^{1}H NMR spectroscopy results, are in fairly good agreement with their theoretical value. For three of the copolymers in Table 1, the M_n of 20 700 for P(ODA)$_6$-*b*-P(PEGA-OMe)$_{39}$, 18 200 for P(ODA)$_{10}$-*b*-P(PEGA-OMe)$_{31}$ and 19 600 for P(ODA)$_{10}$-*b*-P(PEGA-OMe)$_{34}$, deduced from ^{1}H NMR spectroscopy results, are also in fairly good agreement with the corresponding theoretical values of 20 900, 22 100 and 23 700 respectively. However, they are much larger than corresponding M_n of 17 900, 15 700 and 16 700, from GPC. The deviations in molar mass are expected from the fact that the hydrodynamic volumes of the brush-type copolymers differ from those of the linear polystyrene standards. The dispersity value for P(ODA)-*b*-P(PEGA-OMe) copolymers with 6 P(ODA) units on average is 1.3 and broadens slightly to 1.4 with 10 P(ODA) units on average.

Self-assembly behaviour of P(ODA)-*b*-P(PEG-OMe)

P(ODA)-*b*-P(PEGA-OMe) amphiphilic brush copolymers self-assembled in water, at room temperature (25 °C). All P(ODA)-*b*-P(PEGA-OMe) amphiphilic brush copolymers had calculated hydrophilic lipophilic balance (HLB) values greater than 15 (Table 2), indicating that they are moderately hydrophilic, although slightly less hydrophilic than Pluronic® F127[21]. The critical aggregation concentration determined by DLS, is defined as the concentration of surfactant above which aggregates form and all additional surfactants added to the system contributed to aggregate formation. The CAC values for the P(ODA)-*b*-P(PEGA-OMe) copolymers were lower for copolymers with a longer P(ODA) block (i.e., 10 units on average) than shorter a P(ODA) block (i.e. 6 units on average), with similar P(PEGA-OMe) block lengths (Table 2). This trend was found in both pre- and post-reduced copolymers. For example, P(ODA)-*b*-P(PEGA-OMe) copolymers with 23 or 27 P(PEGA-OMe) units on average, obtained a lower CAC value of 0.14 μM (pre-reduction) and 0.43 μM (post-reduction), when possessing 10 P(ODA) units on average than 6 P(ODA) units on average, which resulted in a higher CAC value of 3.7 μM (pre- and post-reduction). It has been reported that increasing the size of the insoluble domain (i.e. increasing the hydrophobic length) will significantly decrease/lower the CAC value.[77-80]

In addition to the copolymers with a shorter P(ODA) block having a lower CAC value, it was observed that the pre-reduced copolymers had a lower CAC value than the post-reduced copolymers. This is in agreement with the notion

that the presence of the hydrophobic RAFT end-groups have a contributing hydrophobic effect on the self-assembly behaviour of the polymers, resulting in lower CAC values. The presence of the RAFT end-group had a more significant effect on the CAC value for the amphiphilic brush diblock copolymers with a larger hydrophobic domain (i.e., 10 P(ODA) units on average), where the hydrophobic domain contributed approximately 20% of the polymer mass, compared with those with a smaller hydrophobic domain (i.e., 6 P(ODA) units on average) where the hydrophobic domain contributed approximately 10% (i.e., a tenth) of the polymer mass, as the CACs post-reduction varied only with the copolymer series with 10 P(ODA) units on average. In this case, $P(ODA)_{10}$-*b*-$P(PEGA\text{-}OMe)_{23}$ had a CAC of 0.14 µM, with a Gibbs free energy of aggregation ($\Delta G°_{agg}$) value of -39.1 kJ/mol, prior to reduction of the RAFT end-group from the copolymer. Post-reduction $P(ODA)_{10}$-*b*-$P(PEGA\text{-}OMe)_{23}$ had a larger CAC of 0.43 µM and $\Delta G°_{agg}$ value of -36.3 kJ/mol. This illustrates that the presence of the dodecyl RAFT end-group on the terminal end of the P(PEGA-OMe) block in the P(ODA)-*b*-P(PEGA-OMe) copolymers increases the hydrophobic effect on the overall self-assembly of P(ODA)-*b*-P(PEGA-OMe) copolymers in water, in agreement with Du *et al.*[74] This change in CAC and $\Delta G°_{agg}$ value is also more apparent in the copolymers with the shorter hydrophilic block (i.e., 23 P(PEGA-OMe) units on average) than for copolymers with a longer hydrophilic block (i.e., 34 P(PEGA-OMe) units on average). We propose this is due to the latter having a more hydrophilic structure (HLB of 16.9) which overcomes the impact of the hydrophobic effect of the dodecyl RAFT end-group on the copolymer. This may explain the similarities in the pre- and post-reduction CAC and $\Delta G°_{agg}$ values for the $P(ODA)_6$-*b*-P(PEGA-OMe) copolymer series, which have greater hydrophilic HLB values of 16.8, 17.6 and 17.8, than those in the $P(ODA)_{10}$-*b*-P(PEGA-OMe) copolymer series and a hydrophobic domain which is only approximately a tenth of the copolymer mass.

The presence of RAFT end-groups has also been reported to affect the self-assembly behaviour of poly(*N*-isopropylacrylamide) (PNIPAM).[74, 81-84] PNIPAM is a thermo-sensitive polymer commonly used to form hydrogels, which exhibits a phase transition at the lower critical solution temperature (LCST) around 32 °C. The LCST was reported to be influenced by the presence of additives, secondary copolymerisation monomer and modification of the end-group of the polymer chain.[68-71] The presence of a RAFT dodecyl chain terminal group was reported to lower the LCST of PNIPAM due to its hydrophobicity, which upon modification by radical-induced reduction resulted in an increased LCST.[83, 85, 86]

For brush-type amphiphilic copolymers, several studies on the morphology of micelles formed on self-assembly in water have been reported.[55, 80, 87-89] Figure 3 shows the cryo-TEM image of self-assembled micelles of $P(ODA)_{10}$-*b*-$P(PEGA\text{-}OMe)_{34}$ copolymer in water, which appear to be spherical in shape and similar to the self-assembly structures of an amphiphilic diblock molecular brushes observed by Li *et al.*[90] Spherical self-assembly structures were also reported by Tong *et al.* for amphiphilic diblock copolymers with a 'brush' hydrophobic domain, even though their triblock copolymer analogues were found to have additional self-assembled morphologies (i.e., cylindrical rods) at increased hydrophobic content.[79, 80] The architecture of the block copolymer (i.e., diblock or triblock) has also been reported to influence micelle size and formation due to block or segment stretching/coiling.[91] Micelle sizes measured using DLS were between 27-49 nm for the $P(ODA)_6$-*b*-P(PEGA-OMe) series copolymers and 90-157 nm for the $P(ODA)_{10}$-*b*-P(PEGA-OMe) series copolymers (Table 2). The increase of the micelle size in the latter copolymer series, is a direct reflection of the increase in length of the hydrophobic block (P(ODA)) of the copolymer, from 6 units to 10 units on average. Although the micelle size represented in the cryo-TEM images in figure 3 appears to be smaller than detected by DLS, it has been reported that particle size (i.e., hydrodynamic diameter) determined by using DLS has typically been found to be significantly larger than those determined by cryo-TEM.[92-94]

Liquid crystalline phase behaviour

Cross-polarised light microscopy was used to identify liquid crystal behaviour of both neat polymer and polymer exposed to excess water. All neat P(ODA)-*b*-P(PEGA-OMe) copolymers displayed some birefringence under cross polarizers at 20 °C indicating their crystalline nature. However, the birefringence was most prominent in copolymers that were more hydrophobic (i.e., HLB <16.9), such as $P(ODA)_6$-*b*-$P(PEGA\text{-}OMe)_{27}$, $P(ODA)_{10}$-*b*-$P(PEGA\text{-}OMe)_{23}$ and $P(ODA)_{10}$-*b*-$P(PEGA\text{-}OMe)_{31}$ (Figure 4 and Supplementary Materials). Birefringence observed under CPLM is characteristic of crystalline material (e.g., liquid crystals) due to their anisotropic nature.

When subjected to hydration with water the interface between the polymer and the water expanded for all the P(ODA)-*b*-P(PEGA-OMe) copolymers. This is seen for both (i) non reduced and (ii) reduced polymers, as seen in

Figure 5. In Figure 5(i), a more defined interface, of the hydrated polymer region, between the water and dry polymer can be seen for a non-reduced P(ODA)-*b*-P(PEGA-OMe) copolymer. In contrast a less defined interface region, between the water and dry polymer is seen, for a reduced P(ODA)-*b*-P(PEGA-OMe) copolymer in Figure 5(ii). Here, there appears to be a greater expansion of the polymer area during hydration and dissolution into the water solution. This is proposed to be due to the removal of the hydrophobic RAFT end-group, following reduction of the P(ODA)-*b*-P(PEGA-OMe) copolymer, leading to a higher water solubility of the reduced polymer. Polymers with a shorter hydrophobic chain (i.e., $P(ODA)_6$) also dispersed into the excess water, at lower temperatures in comparison to the copolymers with a longer hydrophobic chain (i.e., $P(ODA)_{10}$). This is likely to be due to less hydrophobic interaction between the chains (i.e., lower dispersion forces due to shorter chains). The phases formed for all of the copolymers in excess water had isotropic textures, which is characteristic of the micellar phase, further confirming the self-assembly ability of these copolymers in water, enabling the determination of their CAC values.

CONCLUSION

Poly(octadecyl acrylate)-*block*-poly(polyethylene glycol methyl ether acrylate) amphiphilic polymers were successfully polymerised using RAFT polymerisation[57]. However, the presence of the dodecylthiocarbonate RAFT end-group after polymerisation was found to affect the self-assembly behaviour of the polymer in water. Reports on the influence of RAFT end-group on polymer behaviour have been few and limited[68-71,74], with none exploring its impact on an amphiphilic brush copolymer. This study is relevant to validating the effect of the RAFT end-group on polymer self-assembly. The presence of the dodecyl RAFT end-group was found to increase the hydrophobicity of the copolymer and because of its location on the terminal end of the hydrophilic domain of the amphiphilic polymer, its self-assembly behaviour was similar to that of an ABA triblock copolymer with hydrophobic terminal ends, instead of its proposed AB diblock copolymer structure. It is therefore important to remove the RAFT end-group to allow full exposure/extension of the hydrophilic PEG block in water, for optimal stealth and/or steric barrier for self-assembly applications of the copolymer.

This study is also novel in investigating the liquid crystalline behaviour of amphiphilic brush copolymers, which were also synthesized as novel/custom steric stabilizers for lyotropic liquid crystalline nanostructured bicontinuous cubic particles. This series of custom amphiphilic brush copolymers, varying in PEGA-OMe length and ODA length, were found to possess liquid crystalline phase behaviour and self-assembled into micellar structures in excess water. In addition, to synthesising amphiphilic brush copolymers that have the capability to be used as micelle drug delivery carriers, the RAFT end-groups can also be functionalised to provide active targeting functionality to the colloidal system (e.g., functionalised micelles[95, 96]). These are options that make this copolymer an exciting candidate as steric stabilisers for amphiphile self-assembling colloidal particles (e.g., cubosomes). This potential is explored in a separate complementary paper.[76]

FIGURES

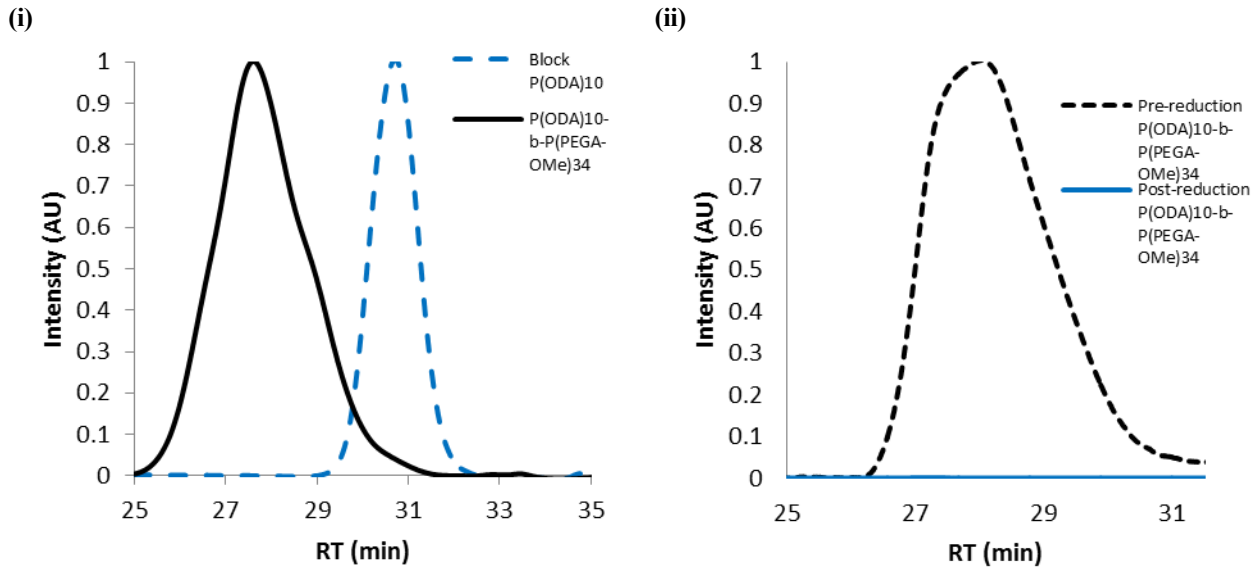

Figure 1. GPC chromatography of $P(ODA)_{10}$ macroRAFT agent and $P(ODA)_{10}$-*b*-$P(PEGA\text{-}OMe)_{34}$: (i) After RAFT polymerisation and (ii) UV detection at 306 nm pre- and post-reduction

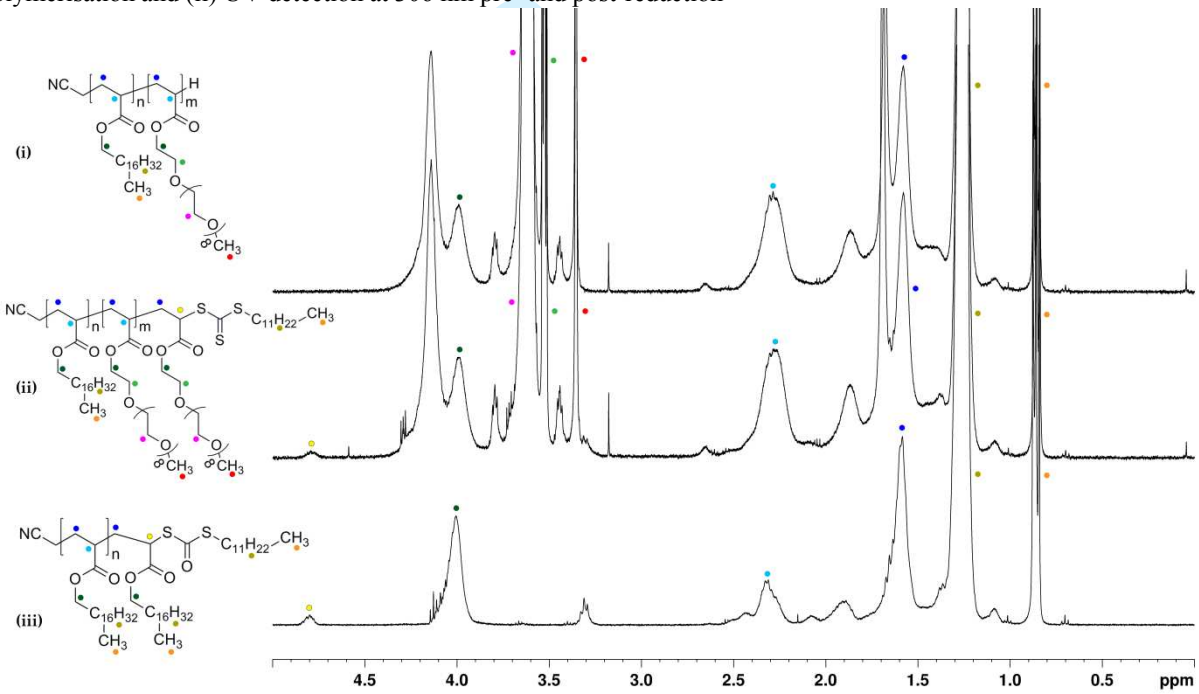

Figure 2. ^{1}H NMR spectra of (i) reduced $P(ODA)_{10}$-*b*-$P(PEGA\text{-}OMe)_{23}$ [n:10 and m:23], (ii) non-reduced $P(ODA)_{10}$-*b*-$P(PEGA\text{-}OMe)_{23}$ [n:10 and m:22] and (iii) P(ODA) with the RAFT end-group [n:9] (see Supplementary Materials for ^{1}H NMR spectra of other copolymers)

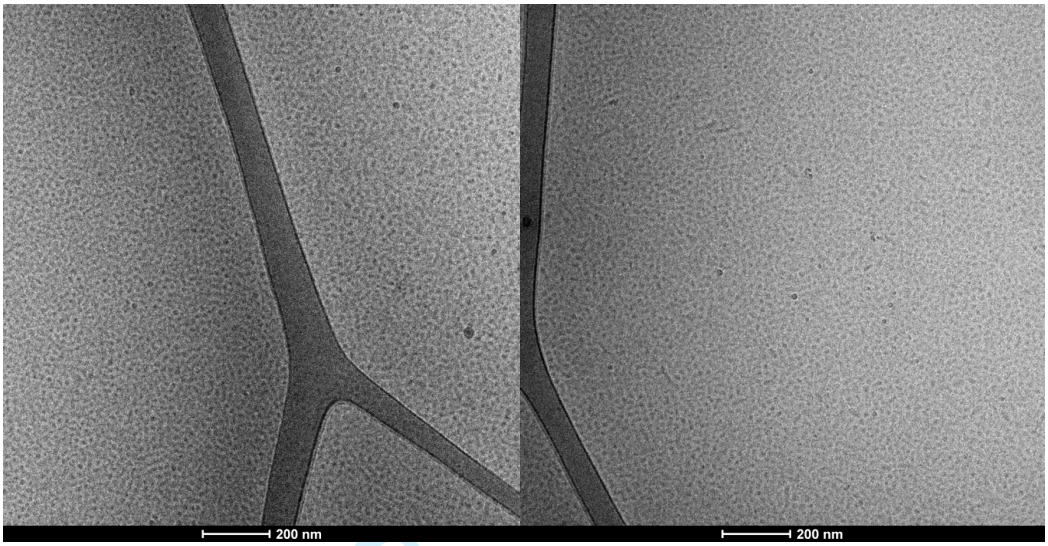

Figure 3. Cryo-TEM image of $P(ODA)_{10}$-*b*-$P(PEGA\text{-}OMe)_{34}$ in water

(i) **(ii)**

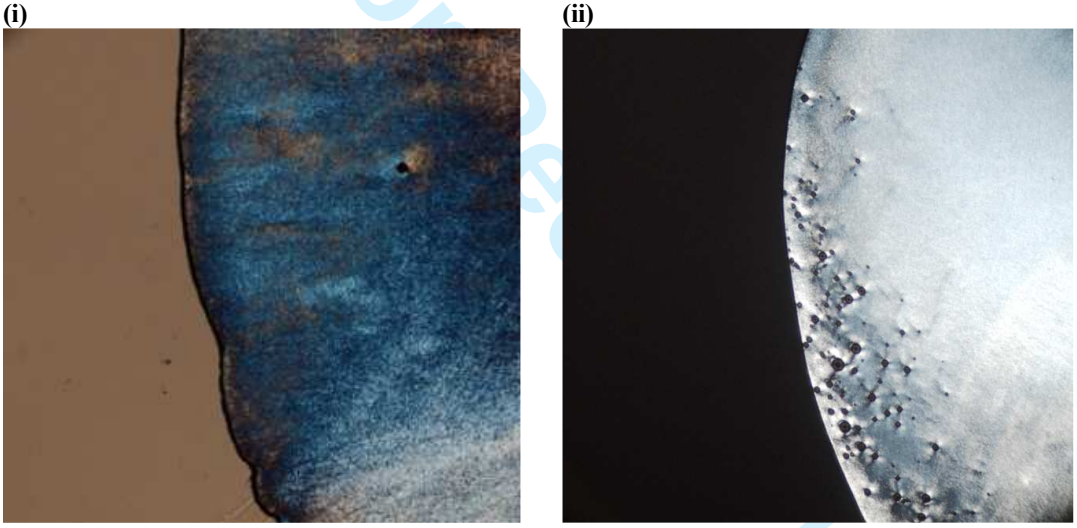

Figure 4. Image of neat $P(ODA)_{10}$-*b*-$P(PEGA\text{-}OMe)_{23}$ copolymer under CPLM (×10 magnification) at 20 °C (i) pre-reduction, (ii) post-reduction

(i) **(ii)**

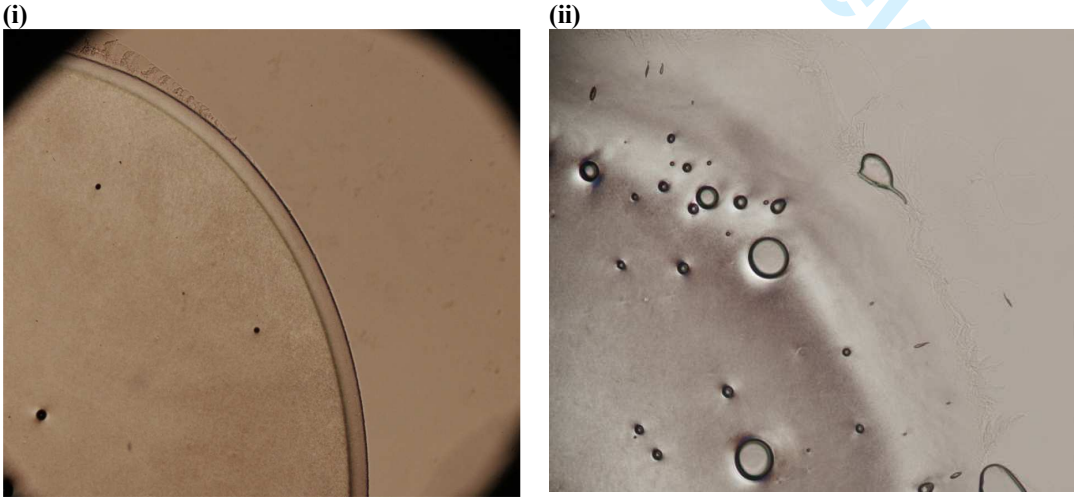

Figure 5. Image of $P(ODA)_{10}$-*b*-$P(PEGA\text{-}OMe)_{34}$ in excess water under CPLM (×10 magnification) at 20 °C (i) pre-reduction, (ii) post-reduction. Polymer is on the left of the images, with the water region on the right.

SCHEMES

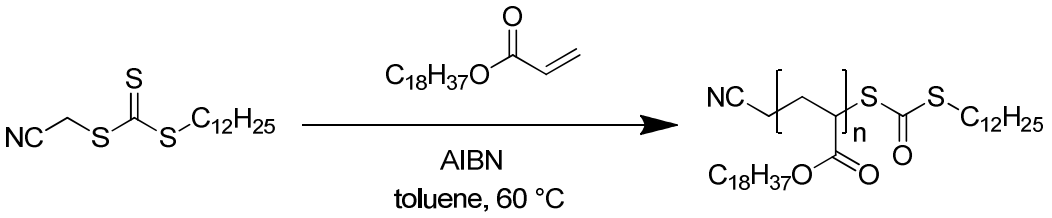

Scheme 1. Synthesis scheme of macro-RAFT agent, P(ODA)

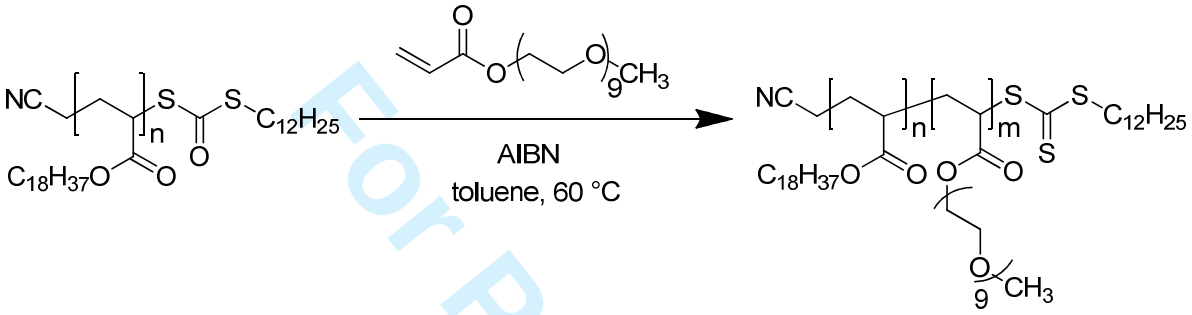

Scheme 2. Block extension of P(ODA) to obtain P(ODA)-*b*-P(PEGA-OMe)

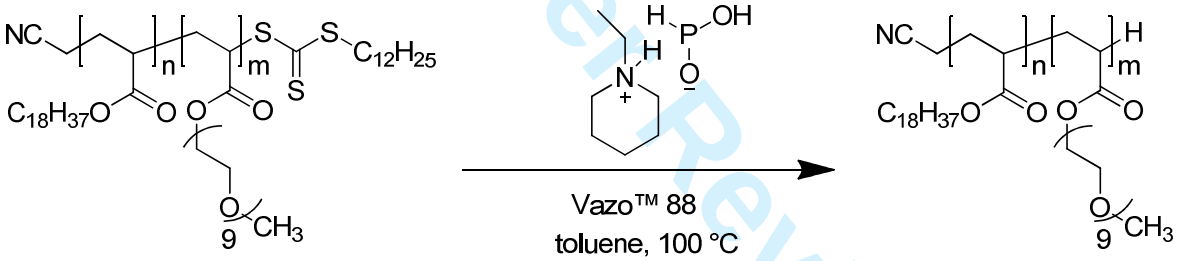

Scheme 3. Radical-induced reduction scheme of P(ODA)-*b*-P(PEGA-OMe)

TABLES

Table 1. P(ODA)-*b*-P(PEGA-OMe) number average molar mass (M_n), dispersity (M_w/M_n), [a] Number-average molar mass (M_n) determined by ^{1}H NMR [b] Number-average molar mass (M_n) and dispersity (M_w/M_n) determined by chloroform gel permeation chromatography, with the molar mass in polystyrene equivalents.

Polymer P(ODA)-*b*-P(PEGA-OMe)	Units ODA	Units PEGA	M_n Theory	M_n[a] NMR	M_n[b] GPC	M_w/M_n [b] GPC
$P(ODA)_{6}$-*b*-$P(PEGA\text{-}OMe)_{27}$	5.6	27.1	14500	15200	15400	1.33
$P(ODA)_{6}$-*b*-$P(PEGA\text{-}OMe)_{35}$	5.6	35.1	19400	19000	17500	1.33
$P(ODA)_{6}$-*b*-$P(PEGA\text{-}OMe)_{39}$	5.6	38.7	20900	20700	17900	1.32
$P(ODA)_{10}$-*b*-$P(PEGA\text{-}OMe)_{23}$	9.9	23.1	17500	14600	14100	1.46
$P(ODA)_{10}$-*b*-$P(PEGA\text{-}OMe)_{31}$	9.9	30.7	22100	18200	15700	1.42
$P(ODA)_{10}$-*b*-$P(PEGA\text{-}OMe)_{34}$	9.9	33.5	23700	19600	16700	1.41

Table 2. P(ODA)-*b*-P(PEGA-OMe) copolymers hydrophilic-lipophilic balance (HLB), critical aggregation concentration (CAC), aggregate size determined by DLS and Gibbs free energy of aggregation ($\Delta G°_{agg}$). [a] HLB calculated using Griffin's method for non-ionic surfactants HLB=20*Mh/M, where Mh is the molecular mass of the hydrophilic portion of the molecule and M is the molecular mass of the whole molecule[97] [b] CAC – with mol calculation using M_n determined by ^{1}H NMR [c] Gibbs free energy of aggregation ($\Delta G°_{agg}$) calculated using: $\Delta G°_{agg} = RT\ ln\ CAC$

		Pre-reduction				Post-reduction			
Polymer P(ODA)-*b*-P(PEGA-OMe)	HLB[a]	CAC (μM)[b]	Size (nm)	PDI	$\Delta G°_{agg}$ (kJ/mol)[c]	CAC (μM)[b]	PDI	Size (nm)	$\Delta G°_{agg}$ (kJ/mol)[c]
$P(ODA)_{6}$-*b*-$P(PEGA\text{-}OMe)_{27}$	16.8	3.7	49	Multimodal	-31.0	3.7	Multimodal	48	-31.0
$P(ODA)_{6}$-*b*-$P(PEGA\text{-}OMe)_{35}$	17.6	4.1	34	Multimodal	-30.8	4.1	Multimodal	27	-30.8
$P(ODA)_{6}$-*b*-$P(PEGA\text{-}OMe)_{39}$	17.8	5.1	39	Multimodal	-30.2	5.1	Multimodal	31	-30.2
$P(ODA)_{10}$-*b*-$P(PEGA\text{-}OMe)_{23}$	15.8	0.14	109	Multimodal	-39.1	0.43	Multimodal	90	-36.3
$P(ODA)_{10}$-*b*-$P(PEGA\text{-}OMe)_{31}$	16.7	0.15	108	Multimodal	-39.0	0.46	Multimodal	157	-36.2
$P(ODA)_{10}$-*b*-$P(PEGA\text{-}OMe)_{34}$	16.9	0.19	114	Multimodal	-38.4	1.8	Multimodal	118	-32.8

Supporting Information

This material is available.

ACKNOWLEDGMENT
Calum J. Drummond was the recipient of an Australian Research Council (ARC) Federation Fellowship. Josephine Y.T. Chong was the recipient of a CSIRO Ph.D. studentship. Xavier Mulet was the recipient of a CSIRO-Monash University Collaborative research postdoctoral fellowship. Ben J. Boyd is the recipient of an ARC Future Fellowship (FT120100697).

REFERENCES

1. Savić, R., et al. (2003) Micellar Nanocontainers Distribute to Defined Cytoplasmic Organelles. *Science 300*(5619): 615-618
2. Kataoka, K., A. Harada, and Y. Nagasaki (2001) Block copolymer micelles for drug delivery: design, characterization and biological significance. *Adv. Drug Deliv. Rev. 47*(1): 113-131
3. Rösler, A., G.W.M. Vandermeulen, and H.-A. Klok (2001) Advanced drug delivery devices via self-assembly of amphiphilic block copolymers. *Adv. Drug. Deliv. Rev. 53*(1): 95-108
4. Gaucher, G., et al. (2005) Block copolymer micelles: preparation, characterization and application in drug delivery. *J. Control. Release 109*(1–3): 169-188
5. Jenekhe, S.A. and X.L. Chen (1998) Self-Assembled Aggregates of Rod-Coil Block Copolymers and Their Solubilization and Encapsulation of Fullerenes. *Science 279*(5358): 1903-1907
6. Yasugi, K., et al. (1999) Preparation and characterization of polymer micelles from poly(ethylene glycol)-poly(d,l-lactide) block copolymers as potential drug carrier. *J. Control. Release 62*(1–2): 89-100
7. Massey, J., et al. (1998) Self-Assembly of a Novel Organometallic−Inorganic Block Copolymer in Solution and the Solid State: Nonintrusive Observation of Novel Wormlike Poly(ferrocenyldimethylsilane)-b-Poly(dimethylsiloxane) Micelles. *J. Am. Chem. Soc. 120*(37): 9533-9540
8. Lukyanov, A.N. and V.P. Torchilin (2004) Micelles from lipid derivatives of water-soluble polymers as delivery systems for poorly soluble drugs. *Adv. Drug Deliver. Rev. 56*(9): 1273-1289
9. Rapoport, N. (2007) Physical stimuli-responsive polymeric micelles for anti-cancer drug delivery. *Prog. Polym. Sci. 32*(8–9): 962-990
10. Kedar, U., et al. (2010) Advances in polymeric micelles for drug delivery and tumor targeting. *Nanomedicine: NBM 6*(6): 714-729
11. Maeda, H., et al. (2000) Tumor vascular permeability and the EPR effect in macromolecular therapeutics: a review. *J. Control. Release 65*(1–2): 271-284
12. Iyer, A.K., et al. (2006) Exploiting the enhanced permeability and retention effect for tumor targeting. *Drug Discov. Today 11*(17–18): 812-818
13. Gref, R., et al. (2000) 'Stealth' corona-core nanoparticles surface modified by polyethylene glycol (PEG): influences of the corona (PEG chain length and surface density) and of the core composition on phagocytic uptake and plasma protein adsorption. *Colloid. Surface. B 18*(3–4): 301-313
14. Lee, J.H. and S.H. Oh (2002) MMA/MPEOMA/VSA copolymer as a novel blood-compatible material: Effect of PEO and negatively charged side chains on protein adsorption and platelet adhesion. *J. Biomed. Mater. Res. 60*(1): 44-52
15. Irvine, D.J., et al. (1998) Comparison of tethered star and linear poly(ethylene oxide) for control of biomaterials surface properties. *J. Biomed. Mater. Res. 40*(3): 498-509
16. Irvine, D.J., A.M. Mayes, and L. Griffith-Cima (1996) Self-Consistent Field Analysis of Grafted Star Polymers. *Macromolecules 29*(18): 6037-6043
17. Groll, J., et al. (2005) Comparison of Coatings from Reactive Star Shaped PEG-stat-PPG Prepolymers and Grafted Linear PEG for Biological and Medical Applications. *Biomacromolecules 6*(2): 956-962
18. Gunkel, G., et al. (2011) Effect of Polymer Brush Architecture on Antibiofouling Properties. *Biomacromolecules 12*(11): 4169-4172
19. Bozukova, D., et al. (2008) Imparting Antifouling Properties of Poly(2-hydroxyethyl methacrylate) Hydrogels by Grafting Poly(oligoethylene glycol methyl ether acrylate). *Langmuir 24*(13): 6649-6658
20. Xu, P., et al. (2004) Enhanced Stability of Core−Surface Cross-Linked Micelles Fabricated from Amphiphilic Brush Copolymers. *Biomacromolecules 5*(5): 1736-1744

21. Chong, J.Y.T., et al. (2011) Steric stabilisation of self-assembled cubic lyotropic liquid crystalline nanoparticles: High throughput evaluation of triblock polyethylene oxide-polypropylene oxide-polyethylene oxide copolymers. *Soft Matter 7*(10): 4768-4777
22. Chong, J.Y.T., et al. (2012) High-throughput discovery of novel steric stabilizers for cubic lyotropic liquid crystal nanoparticle dispersions. *Langmuir 28*(25): 9223-9232
23. Chong, J.Y.T., et al. (2014) Novel steric stabilizers for lyotropic liquid crystalline nanoparticles: PEGylated-phytanyl copolymers. *Langmuir (Submitted)*
24. Kainthan, R.K. and D.E. Brooks (2007) In vivo biological evaluation of high molecular weight hyperbranched polyglycerols. *Biomaterials 28*(32): 4779-4787
25. Knop, K., et al. (2010) Poly(ethylene glycol) in Drug Delivery: Pros and Cons as Well as Potential Alternatives. *Angew. Chem.-Int. Edit. 49*(36): 6288-6308
26. Calderón, M., et al. (2010) Dendritic Polyglycerols for Biomedical Applications. *Adv. Mater. 22*(2): 190-218
27. Neoh, K.G. and E.T. Kang (2011) Functionalization of inorganic nanoparticles with polymers for stealth biomedical applications. *Polym. Chem. 2*(4): 747-759
28. Amoozgar, Z. and Y. Yeo (2012) Recent advances in stealth coating of nanoparticle drug delivery systems. *Wiley Interdiscip. Rev. Nanomed. Nanobiotechnol. 4*(2): 219-233
29. Zhang, M. and A.H.E. Müller (2005) Cylindrical polymer brushes. *J. Polym. Sci. A. 43*(16): 3461-3481
30. Wintermantel, M., et al. (1996) Molecular Bottlebrushes. *Macromolecules 29*(3): 978-983
31. Tsukahara, Y., et al. (1989) Study on the radical polymerization behavior of macromonomers. *Macromolecules 22*(4): 1546-1552
32. Tsukahara, Y., et al. (1990) Radical polymerization behavior of macromonomers. 2. Comparison of styrene macromonomers having a methacryloyl end group and a vinylbenzyl end group. *Macromolecules 23*(25): 5201-5208
33. Wintermantel, M., et al. (1994) Rodlike combs. *Macromol. Rapid Commun. 15*(3): 279-284
34. Beers, K.L., et al. (1998) The Synthesis of Densely Grafted Copolymers by Atom Transfer Radical Polymerization. *Macromolecules 31*(26): 9413-9415
35. Cheng, G., et al. (2001) Amphiphilic Cylindrical Core−Shell Brushes via a "Grafting From" Process Using ATRP. *Macromolecules 34*(20): 6883-6888
36. Börner, H.G., et al. (2001) Synthesis of Molecular Brushes with Block Copolymer Side Chains Using Atom Transfer Radical Polymerization. *Macromolecules 34*(13): 4375-4383
37. Zhang, M., et al. (2003) Amphiphilic cylindrical brushes with poly(acrylic acid) core and poly(n-butyl acrylate) shell and narrow length distribution. *Polymer 44*(5): 1449-1458
38. Schappacher, M., et al. (1999) Synthesis, dimensions and solution properties of linear and macrocyclic poly(chloroethyl vinyl ether)-g-polystyrene comblike polymers. *Macromol. Chem. Phys. 200*(10): 2377-2386
39. Schappacher, M., J. Bernard, and A. Deffieux (2003) Functional Polystyrene Combs and Dendrigrafts, 1. *Macromol. Chem. Phys. 204*(5-6): 762-769
40. Deffieux, A. and M. Schappacher (1999) Synthesis and Characterization of Star and Comb Polystyrenes Using Isometric Poly(chloroethyl vinyl ether) Oligomers as Reactive Backbone. *Macromolecules 32*(6): 1797-1802
41. Ryu, S.W. and A. Hirao (2000) Anionic Synthesis of Well-Defined Poly(m-halomethylstyrene)s and Branched Polymers via Graft-onto Methodology. *Macromolecules 33*(13): 4765-4771
42. Keddie, D.J., et al. (2011) Amphiphilic Silicone Architectures via Anaerobic Thiol–Ene Chemistry. *Org. Lett. 13*(22): 6006-6009
43. Farrugia, B.L., et al. (2012) An investigation into the effect of amphiphilic siloxane oligomers on dermal fibroblasts. *J. Biomed. Mater. Res. A 100A*(7): 1919-1927
44. Börner, H.G., et al. (2002) Synthesis of Molecular Brushes with Gradient in Grafting Density by Atom Transfer Polymerization. *Macromolecules 35*(9): 3387-3394
45. Xie, M., et al. (2008) Well-Defined Brush Copolymers with High Grafting Density of Amphiphilic Side Chains by Combination of ROP, ROMP, and ATRP. *Macromolecules 41*(23): 9004-9010
46. Pyun, J., T. Kowalewski, and K. Matyjaszewski (2003) Synthesis of Polymer Brushes Using Atom Transfer Radical Polymerization. *Macromol. Rapid Comm. 24*(18): 1043-1059
47. Villarroya, S., et al. (2006) Synthesis of Graft Copolymers by the Combination of ATRP and Enzymatic ROP in scCO2. *Macromolecules 39*(26): 9080-9086

48. Xu, X., et al. (2006) Synthesis of well-defined, brush-type, amphiphilic [poly(styrene-co-2-hydroxyethyl methacrylate)-graft-poly(ε-caprolactone)]-b-poly(ethylene oxide)-b-[poly(styrene-co-2-hydroxyethyl methacrylate)-graft-poly(ε-caprolactone)] and its aggregation behavior inaqueous media. *J. Polym. Sci. A. 44*(15): 4396-4408
49. Li, J., X. Chen, and Y.-C. Chang (2005) Preparation of End-Grafted Polymer Brushes by Nitroxide-Mediated Free Radical Polymerization of Vaporized Vinyl Monomers. *Langmuir 21*(21): 9562-9567
50. Hawker, C.J., et al. (1997) "Living" free radical polymerization of macromonomers: Preparation of well defined graft copolymers. *Macromol. Chem. Phys. 198*(1): 155-166
51. Schierholz, K., et al. (2003) Acrylamide-Based Amphiphilic Block Copolymers via Nitroxide-Mediated Radical Polymerization. *Macromolecules 36*(16): 5995-5999
52. Nomura, K., S. Takahashi, and Y. Imanishi (2001) Synthesis of Poly(macromonomer)s by Repeating Ring-Opening Metathesis Polymerization (ROMP) with Mo(CHCMe2Ph)(NAr)(OR)2 Initiators. *Macromolecules 34*(14): 4712-4723
53. Notestein, J.M., L.-B.W. Lee, and R.A. Register (2002) Well-Defined Diblock Copolymers via Termination of Living ROMP with Anionically Polymerized Macromolecular Aldehydes. *Macromolecules 35*(6): 1985-1987
54. Cheng, Z., et al. (2005) Dual-Brush-Type Amphiphilic Triblock Copolymer with Intact Epoxide Functional Groups from Consecutive RAFT Polymerizations and ATRP. *Macromolecules 38*(16): 7187-7192
55. Cheng, et al. (2005) Brush-Type Amphiphilic Diblock Copolymers from "Living"/Controlled Radical Polymerizations and Their Aggregation Behavior. *Langmuir 21*(16): 7180-7185
56. Lian, X., et al. (2010) Synthesis and Self-Assembly of Amphiphilic Asymmetric Macromolecular Brushes. *Macromolecules 43*(18): 7434-7445
57. Keddie, D.J. (2014) A guide to the synthesis of block copolymers using reversible-addition fragmentation chain transfer (RAFT) polymerization. *Chem. Soc. Rev. 43*(2): 496-505
58. Perrier, S. and P. Takolpuckdee (2005) Macromolecular design via reversible addition–fragmentation chain transfer (RAFT)/xanthates (MADIX) polymerization. *J. Polym. Sci. A. 43*(22): 5347-5393
59. Hosta-Rigau, L., et al. (2012) Surface-Adhered Composite Poly(Vinyl Alcohol) Physical Hydrogels: Polymersome-Aided Delivery of Therapeutic Small Molecules. *Adv. Healthcare Mater. 1*(6): 791-795
60. Zehm, D., et al. (2011) Synthesis and self-assembly of amphiphilic semi-brush and dual brush block copolymers in solution and on surfaces. *Polym. Chem. 2*(1): 137-147
61. Haeussler, M., et al., *Controlled Synthesis of Multifunctional Polymers by RAFT for Personal Care Applications*, in *Polymers for Personal Care and Cosmetics*. 2013, American Chemical Society. p. 157-172.
62. Chong, Y.K., et al. (2007) Thiocarbonylthio End Group Removal from RAFT-Synthesized Polymers by Radical-Induced Reduction. *Macromolecules 40*(13): 4446-4455
63. Stenzel, M.H., et al. (2004) Amphiphilic Block Copolymers Based on Poly(2-acryloyloxyethyl phosphorylcholine) Prepared via RAFT Polymerisation as Biocompatible Nanocontainers. *Macromol. Biosci. 4*(4): 445-453
64. Zhang, L., et al. (2007) Shell-Cross-Linked Micelles Containing Cationic Polymers Synthesized via the RAFT Process: Toward a More Biocompatible Gene Delivery System. *Biomacromolecules 8*(9): 2890-2901
65. Boyer, C., et al. (2009) Bioapplications of RAFT Polymerization. *Chem. Rev. 109*(11): 5402-5436
66. Pissuwan, D., et al. (2010) In Vitro Cytotoxicity of RAFT Polymers. *Biomacromolecules 11*(2): 412-420
67. Nguyen, T.L.U., et al. (2007) Core-shell microspheres with surface grafted poly(vinyl alcohol) as drug carriers for the treatment of hepatocellular carcinoma. *J. Polym. Sci. A. 45*(15): 3256-3272
68. Chen, M., G. Moad, and E. Rizzardo (2009) Thiocarbonylthio end group removal from RAFT-synthesized polymers by a radical-induced process. *J. Polym. Sci. A Polym. Chem. 47*(23): 6704-6714
69. Moad, G., E. Rizzardo, and S.H. Thang (2011) End-functional polymers, thiocarbonylthio group removal/transformation and reversible addition–fragmentation–chain transfer (RAFT) polymerization. *Polym. Int. 60*(1): 9-25
70. Willcock, H. and R.K. O'Reilly (2010) End group removal and modification of RAFT polymers. *Polym. Chem. 1*(2): 149-157
71. Jang, D.O. and D.H. Cho (2002) Radical deoxygenation of alcohols and vicinal diols with N-ethylpiperidine hypophosphite in water. *Tetrahedron Lett. 43*(34): 5921-5924
72. Taillefer, J., et al. (2000) Preparation and characterization of pH-responsive polymeric micelles for the delivery of photosensitizing anticancer drugs. *J. Pharm. Sci. 89*(1): 52-62

73. Lavine, M.S. (2011) The Ends of the Story. *Science 333*(6041): 386
74. Du, J., et al. (2011) Self-Assembly of Hydrophilic Homopolymers: A Matter of RAFT End Groups. *Small 7*(14): 2070-2080
75. Zhu, Y., L. Liu, and J. Du (2012) Probing into Homopolymer Self-Assembly: How Does Hydrogen Bonding Influence Morphology? *Macromolecules 46*(1): 194-203
76. Chong, J.Y.T., et al. (2014) Novel RAFT amphiphilic brush copolymer steric stabilizers for cubosomes: Poly(octadecyl acrylate)-block-poly(polyethylene glycol methyl ether acrylate). *(Submitted)*
77. Astafieva, I., X.F. Zhong, and A. Eisenberg (1993) Critical micellization phenomena in block polyelectrolyte solutions. *Macromolecules 26*(26): 7339-7352
78. Alexandridis, P., J.F. Holzwarth, and T.A. Hatton (1994) Micellization of Poly(ethylene oxide)-Poly(propylene oxide)-Poly(ethylene oxide) Triblock Copolymers in Aqueous Solutions: Thermodynamics of Copolymer Association. *Macromolecules 27*(9): 2414-2425
79. Tong, L., et al. (2008) Synthesis and characterization of perfluorocyclobutyl aryl ether-based amphiphilic diblock copolymer. *Polymer 49*(21): 4534-4540
80. Tong, L., et al. (2009) PTPFCBBMA-b-PEG-b-PTPFCBBMA amphiphilic triblock copolymer: Synthesis and self-assembly behavior. *Polymer 50*(11): 2341-2348
81. Chen, S., X. Jiang, and L. Sun (2013) Effects of end groups on the thermal response of poly(N-isopropylacrylamide) microgels. *J. Appl. Polym. Sci. 130*(2): 1164-1171
82. Chang, K., Z.T. Dicke, and L.J. Taite (2012) Engineering a sharp physiological transition state for poly(n-isopropylacrylamide) through structural control. *J. Polym. Sci. A Polym. Chem. 50*(5): 976-985
83. Vogt, A.P. and B.S. Sumerlin (2008) Tuning the Temperature Response of Branched Poly(N-isopropylacrylamide) Prepared by RAFT Polymerization. *Macromolecules 41*(20): 7368-7373
84. Skrabania, K., et al. (2006) Design, Synthesis, and Aqueous Aggregation Behavior of Nonionic Single and Multiple Thermoresponsive Polymers†. *Langmuir 23*(1): 84-93
85. Plummer, R., D.J.T. Hill, and A.K. Whittaker (2006) Solution Properties of Star and Linear Poly(N-isopropylacrylamide). *Macromolecules 39*(24): 8379-8388
86. Rimmer, S., et al. (2007) Highly branched poly-(N-isopropylacrylamide)s with arginine-glycine-aspartic acid (RGD)- or COOH-chain ends that form sub-micron stimulus-responsive particles above the critical solution temperature. *Soft Matter 3*(8): 971-973
87. Hussain, H., K.Y. Mya, and C. He (2008) Self-Assembly of Brush-Like Poly[poly(ethylene glycol) methyl ether methacrylate] Synthesized via Aqueous Atom Transfer Radical Polymerization. *Langmuir 24*(23): 13279-13286
88. Holder, S.J., et al. (2003) ABA triblock copolymers: from controlled synthesis to controlled function. *J. Mater. Chem. 13*(11): 2771-2778
89. Vriezema, D.M., et al. (2004) Electroformed Giant Vesicles from Thiophene-Containing Rod−Coil Diblock Copolymers. *Macromolecules 37*(12): 4736-4739
90. Li, Z., et al. (2010) Synthesis of Hetero-Grafted Amphiphilic Diblock Molecular Brushes and Their Self-Assembly in Aqueous Medium. *Macromolecules 43*(3): 1182-1184
91. Bonné, T.B., et al. (2007) Effect of Polymer Architecture of Amphiphilic Poly(2-oxazoline) Copolymers on the Aggregation and Aggregate Structure. *Macromol. Chem. Phys. 208*(13): 1402-1408
92. Hans, M., et al. (2005) Synthesis and Characterization of mPEG−PLA Prodrug Micelles. *Biomacromolecules 6*(5): 2708-2717
93. Coldren, B., et al. (2003) From Vesicle Size Distributions to Bilayer Elasticity via Cryo-Transmission and Freeze-Fracture Electron Microscopy. *Langmuir 19*(14): 5632-5639
94. Schuetz, P., et al. (2011) Controlling the micellar morphology of binary PEO-PCL block copolymers in water-THF through controlled blending. *Soft Matter 7*(2): 749-759
95. Wei, T., et al. (2013) Functionalized Nanoscale Micelles Improve Drug Delivery for Cancer Therapy in Vitro and in Vivo. *Nano Lett. 13*(6): 2528-2534
96. Sutton, D., et al. (2007) Functionalized Micellar Systems for Cancer Targeted Drug Delivery. *Pharm. Res. 24*(6): 1029-1046
97. Griffin, W.C. (1954) Calculation of HLB Values of Non-Ionic Surfactants. *J. Soc. Cosmet. Chem. 5*: 249

Supplementary Information

RAFT preparation and the aqueous self-assembly of amphiphilic poly(octadecyl acrylate)-*block*-poly(polyethylene glycol methyl ether acrylate) copolymers

Josephine Y.T. Chong[a,b], *Daniel J. Keddie*[a,c], *Almar Postma*[a], *Xavier Mulet*[a,b], *Ben J. Boyd*[b*], *Calum J. Drummond*[a,d*]

[a] CSIRO Materials Science and Engineering, Private Bag 10, Clayton, VIC 3169, Australia; [b] Drug Delivery, Disposition and Dynamics, Monash Institute of Pharmaceutical Science, Monash University, 381 Royal Parade, Parkville, VIC 3052, Australia; [c] Chemistry, School of Science and Technology, University of New England, NSW 2351, Australia; [d] School of Applied Sciences, College of Science, Engineering and Health, RMIT University, GPO Box 2476, Melbourne, VIC 3001, Australia

[redacted]

^{1}H NMR DATA

*(i) Reduced polymer, (ii) Non-reduced polymer, (iii) P(ODA) with end-group. *Highlighted peak indicates end-group presence*

1. ^{1}H NMR spectrum of

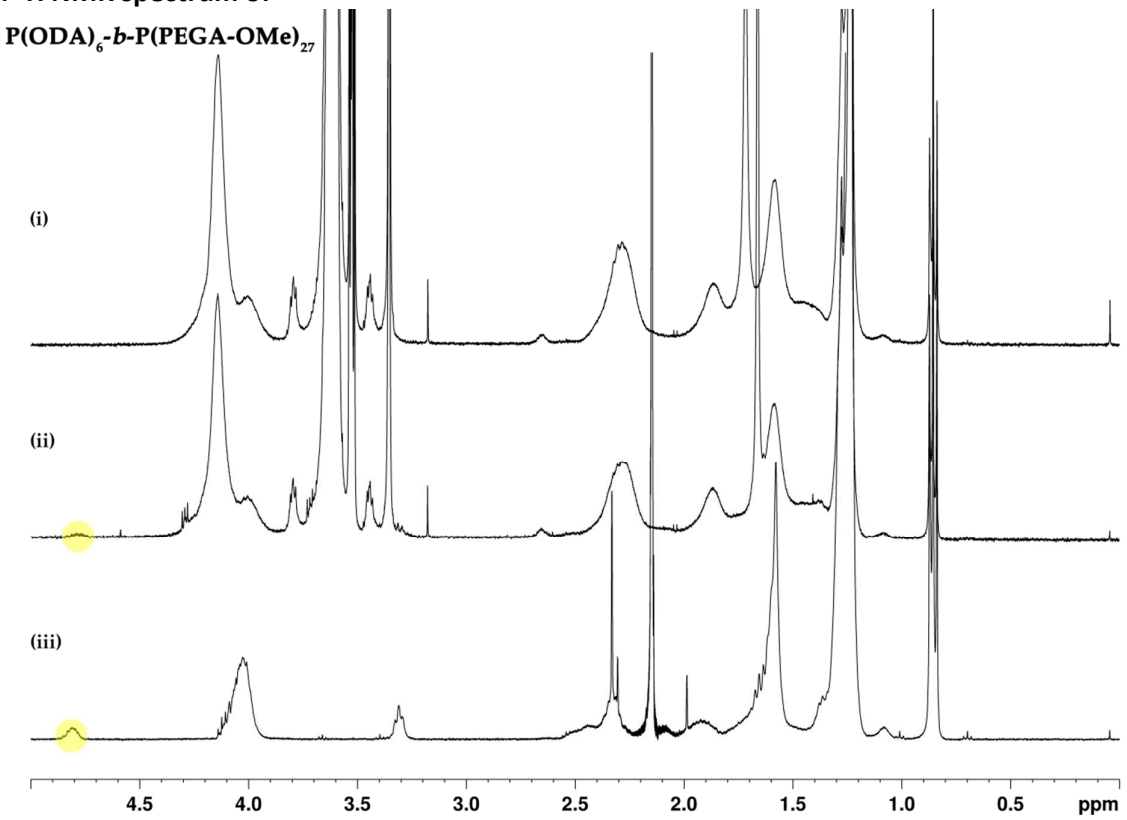

2. ^{1}H NMR spectrum of

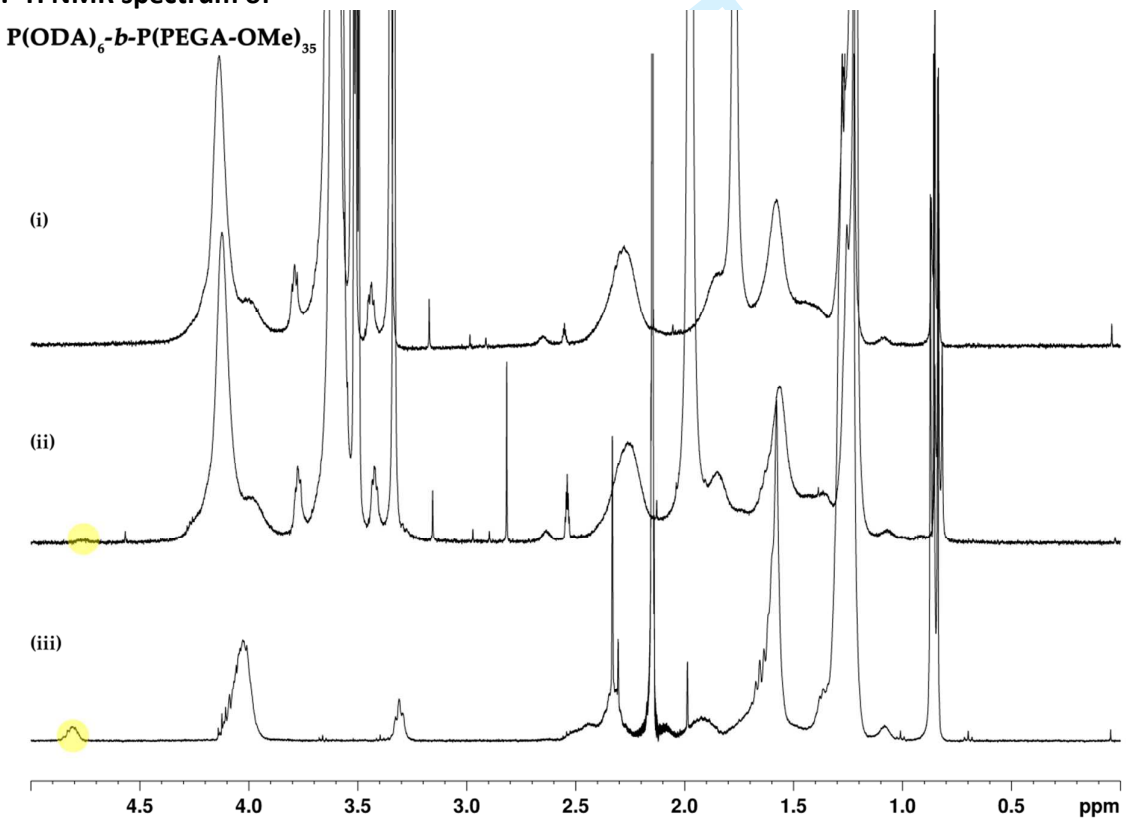

^{1}H NMR spectrum of

P(ODA)$_6$-*b*-P(PEGA-OMe)$_{39}$

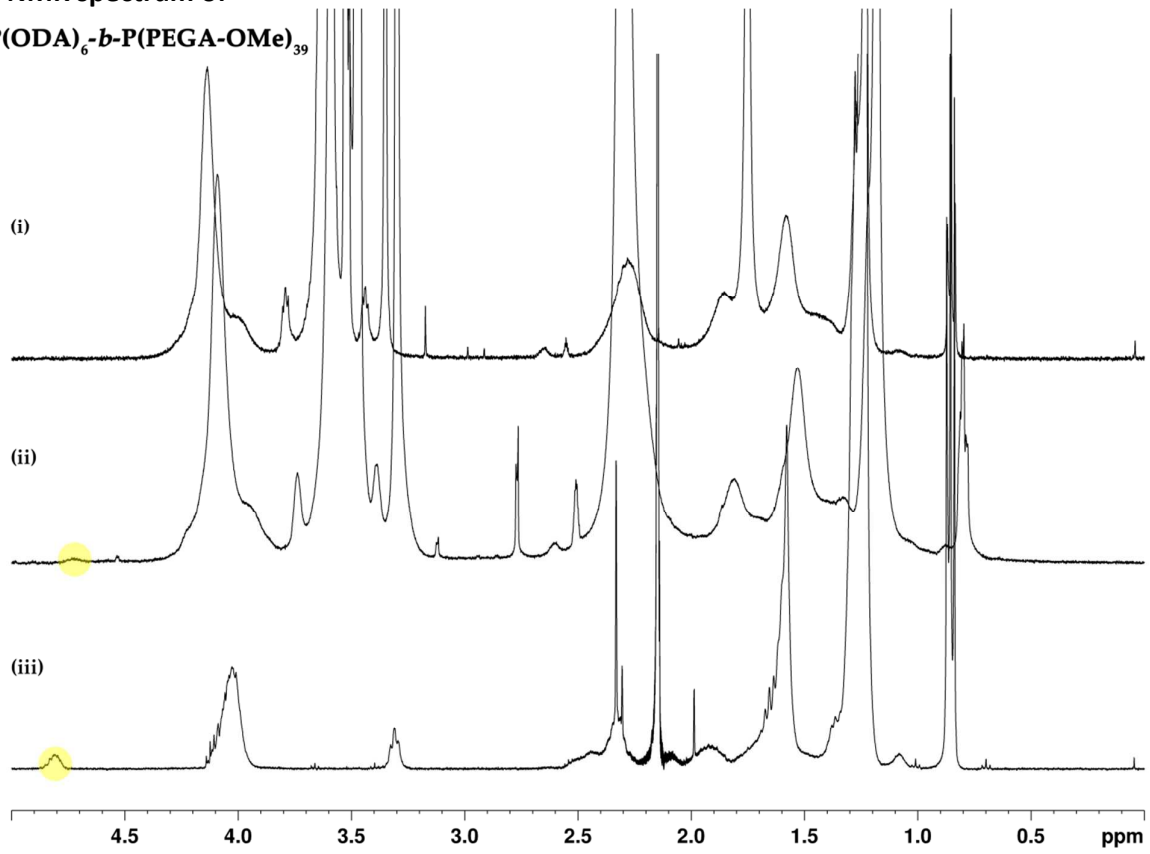

4. ^{1}H NMR spectrum of

P(ODA)$_{10}$-*b*-P(PEGA-OMe)$_{23}$

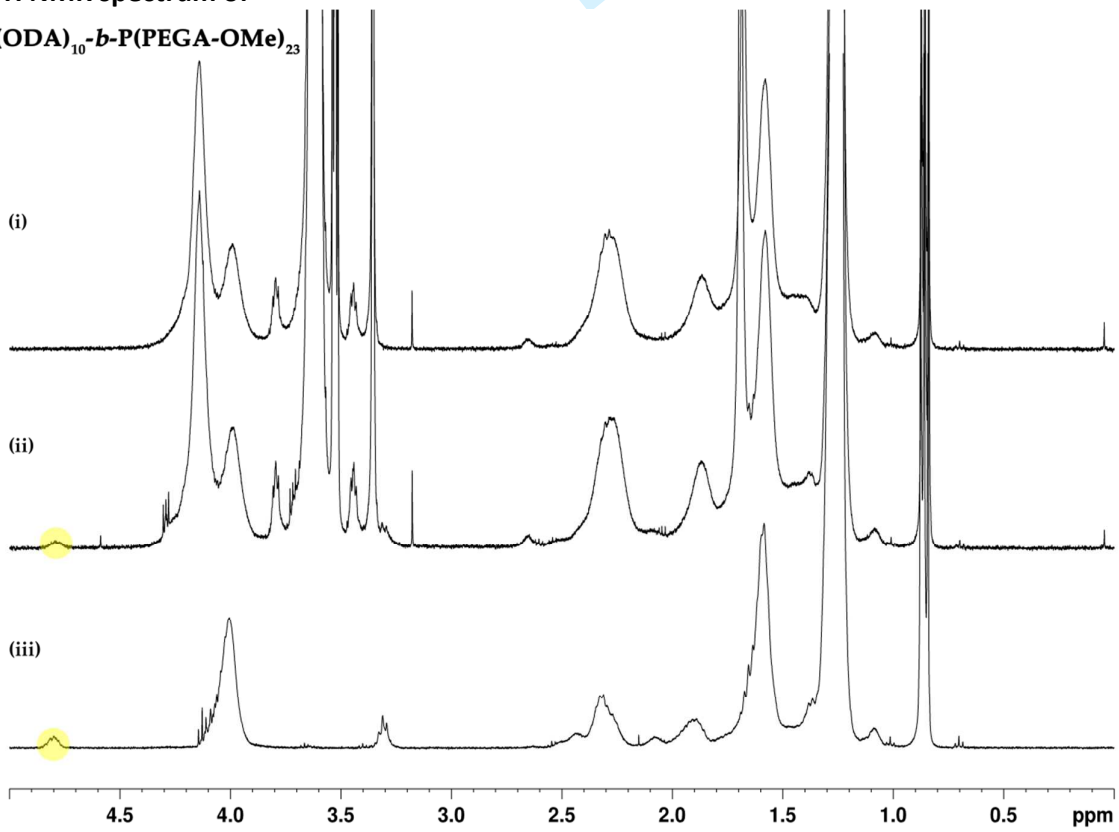

5. ^{1}H NMR spectrum of

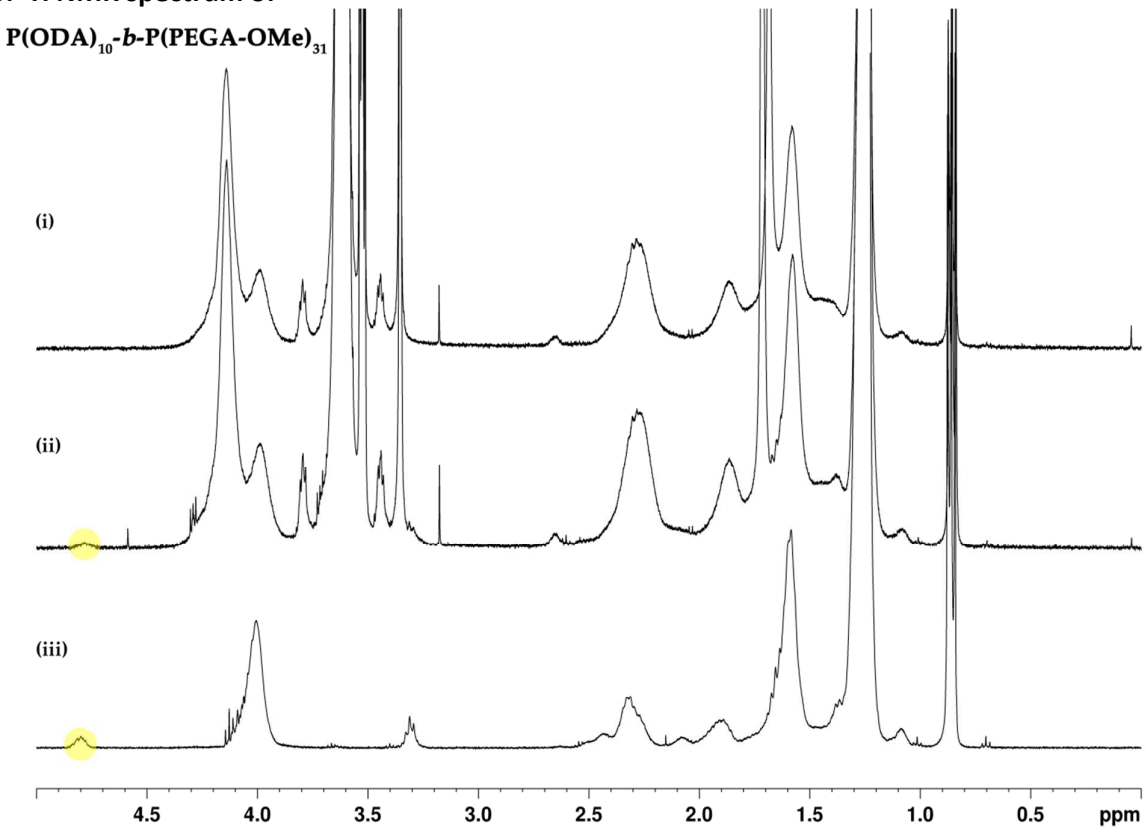

6. ^{1}H NMR spectrum of

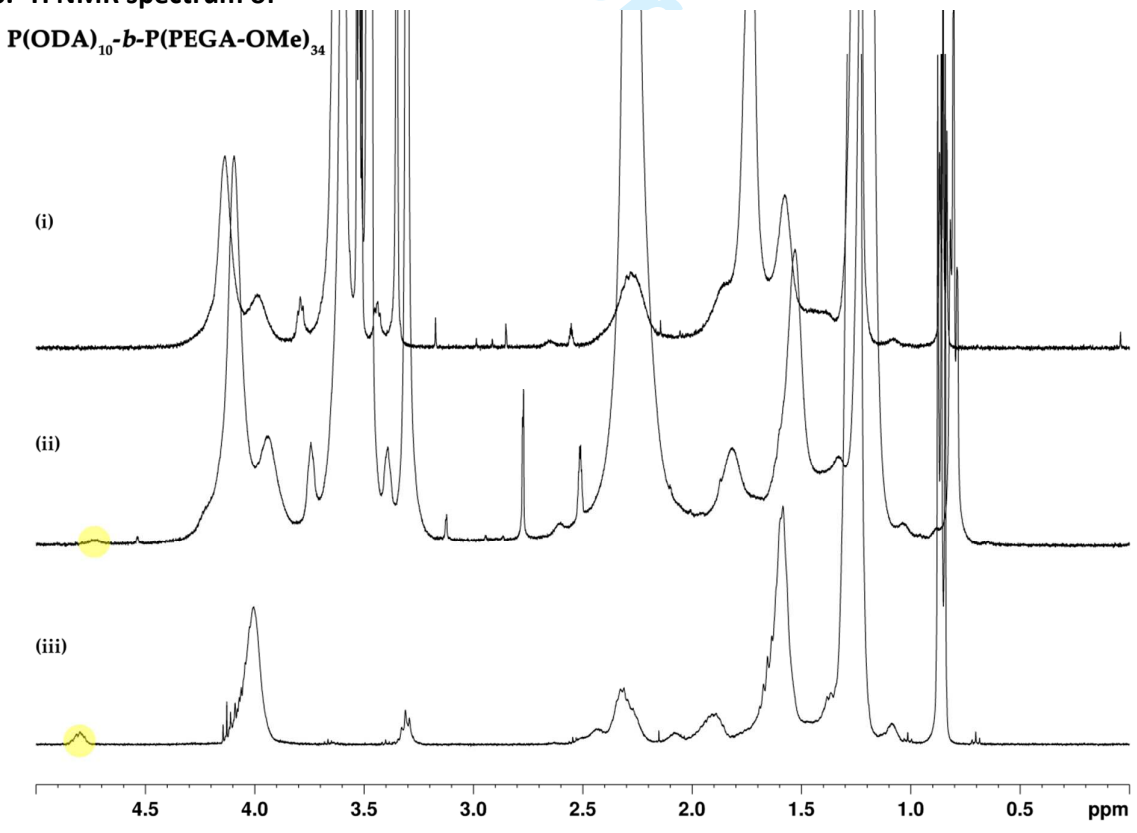

GEL PERMEATION CHROMATOGRAPHY (GPC) DATA (Chloroform solvent)

1a.

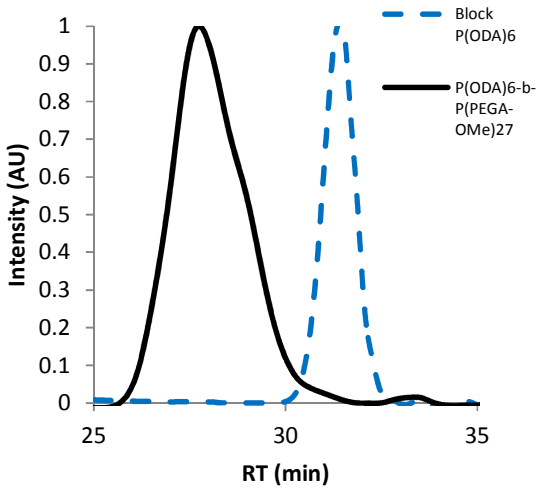

1b. After dialysis

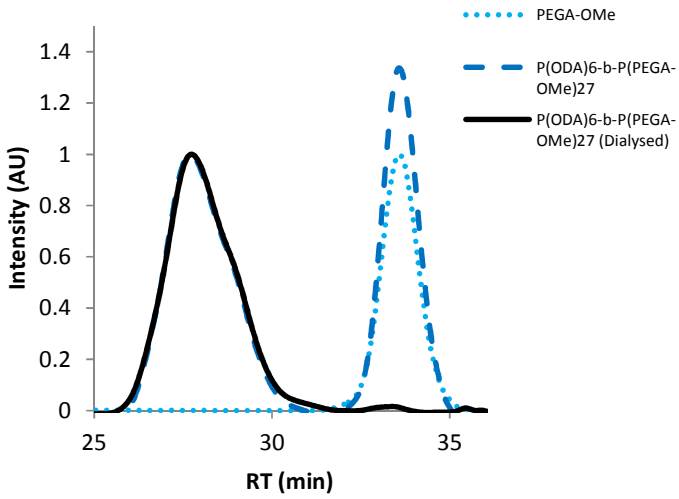

2a.

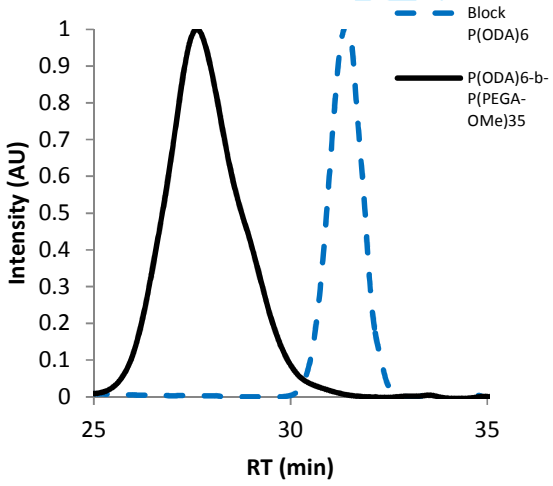

2b.

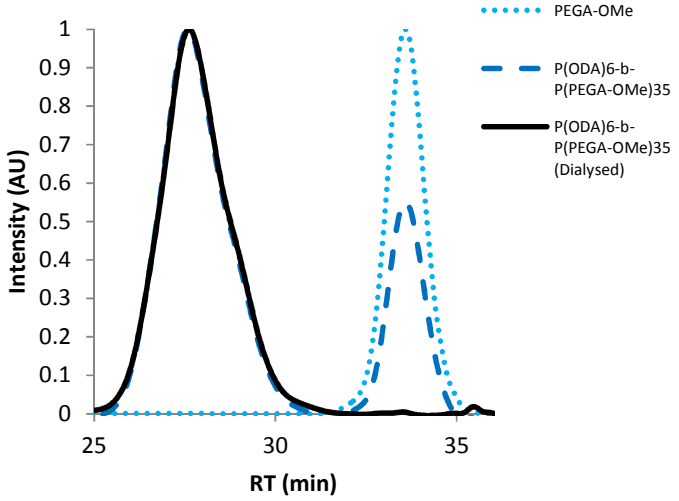

3a.

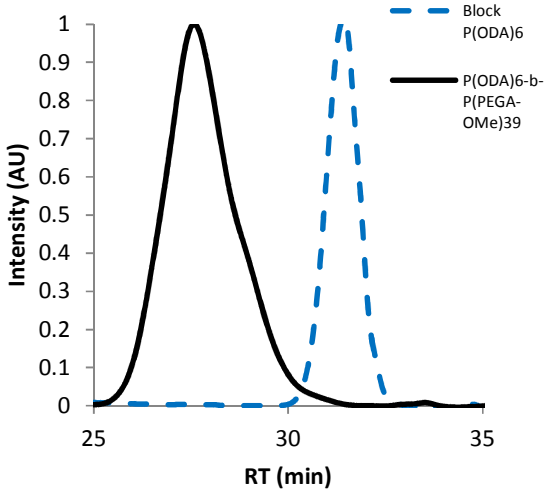

3b.

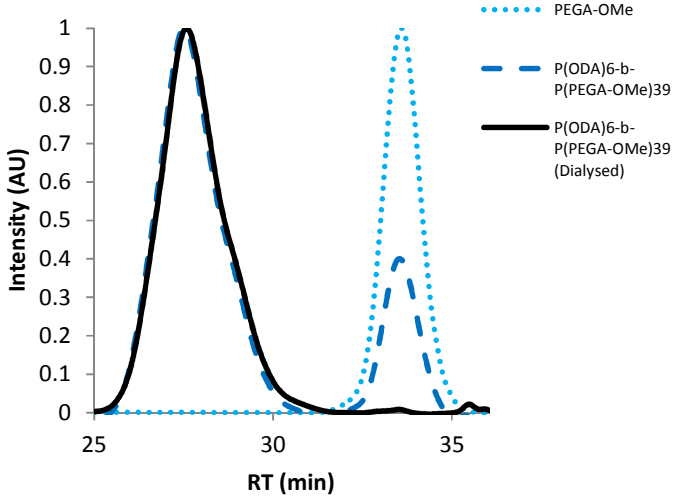

4a.

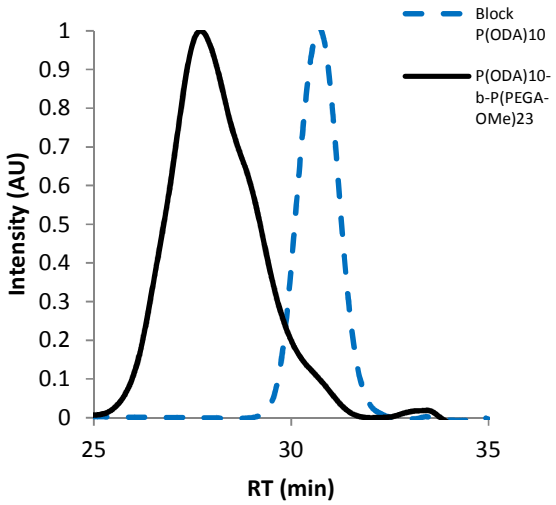

4b. After dialysis

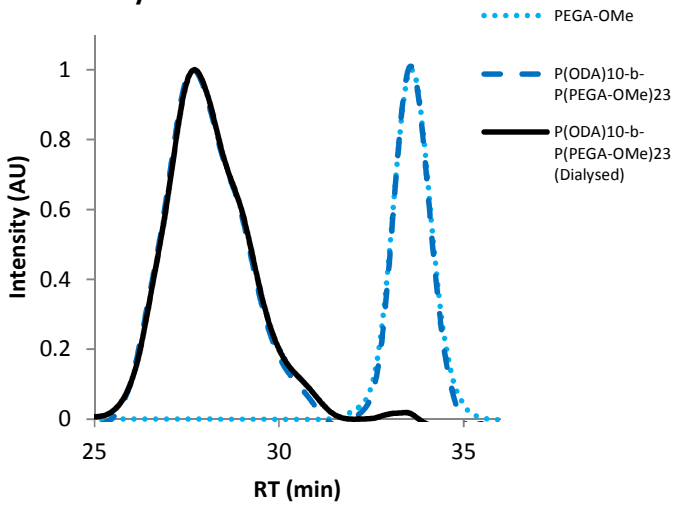

5a.

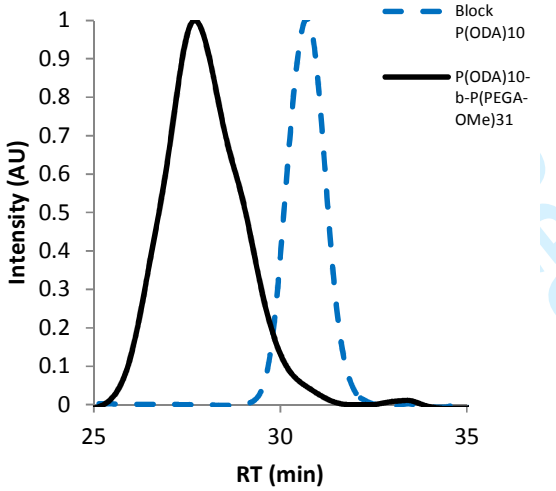

5b.

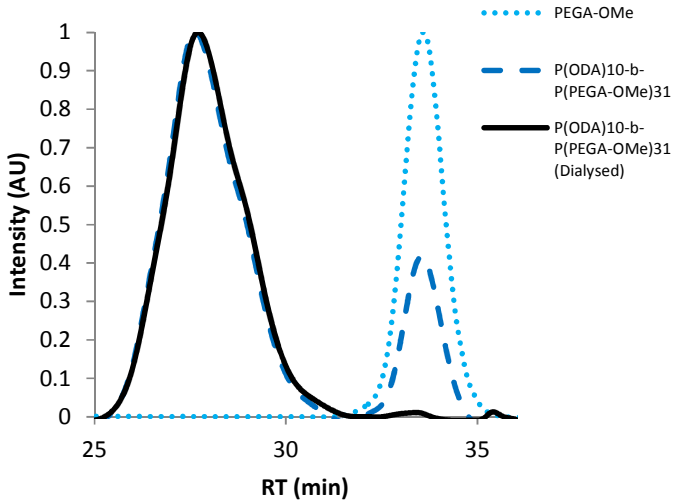

6a.

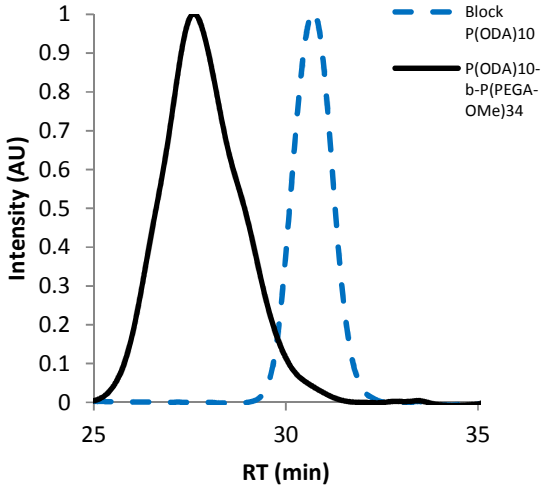

6b.

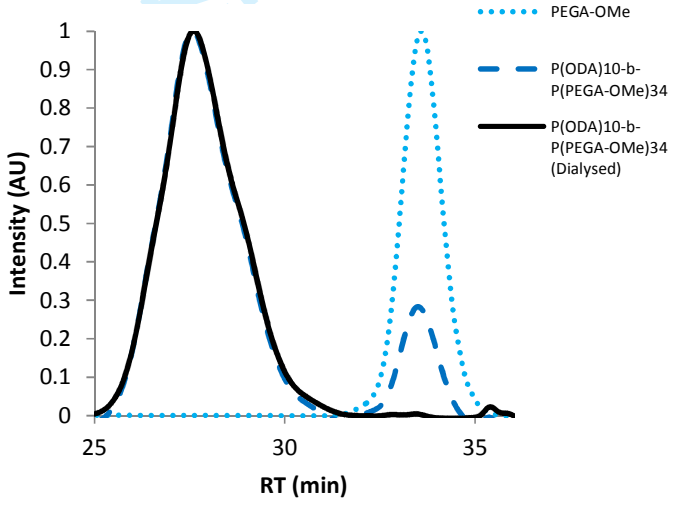

GPC DATA Pre and Post Reduction (THF solvent)

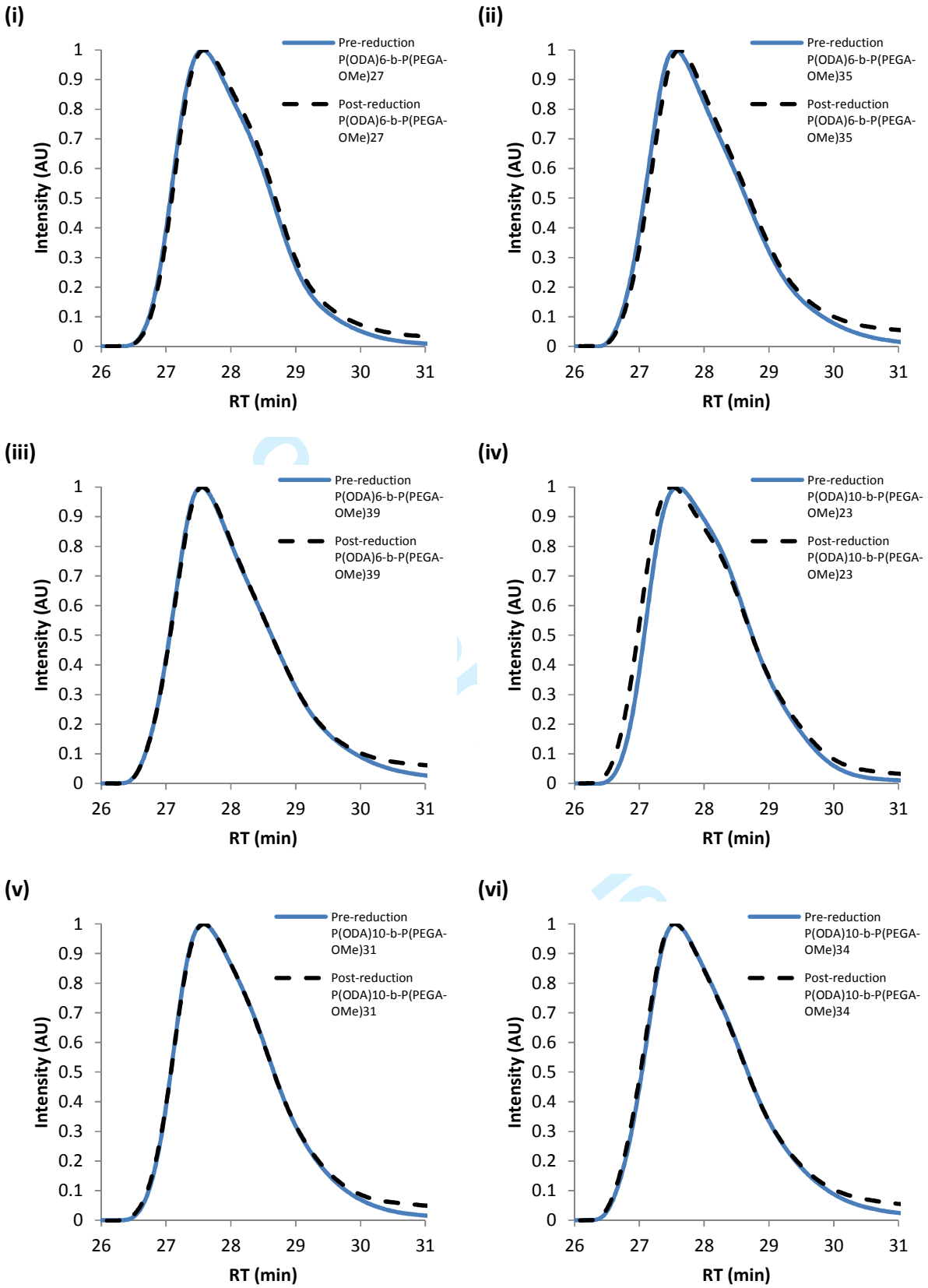

UV GPC data (RT 306 nm) – RAFT signal present between 305 – 310 nm

(i)

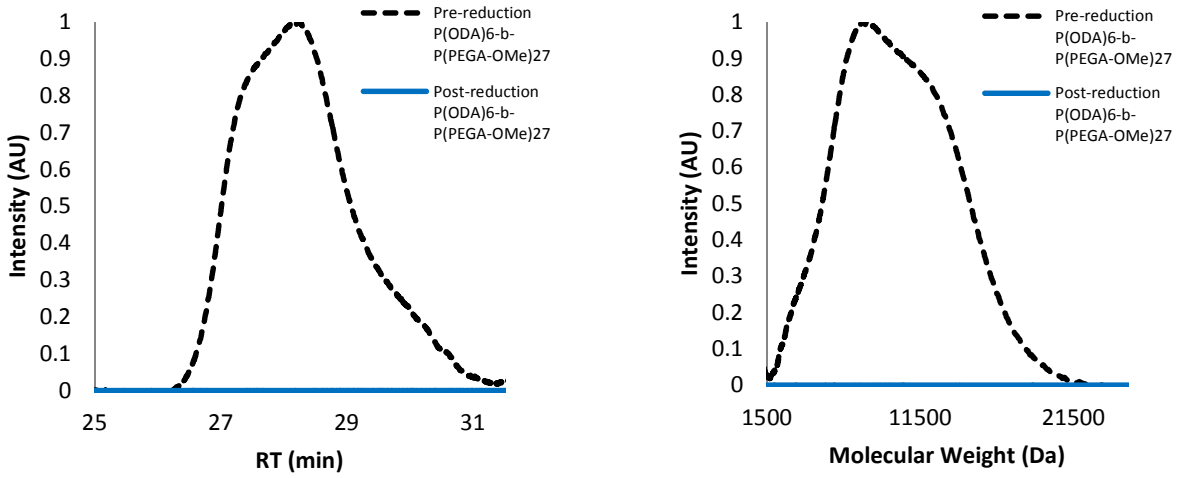

(ii)

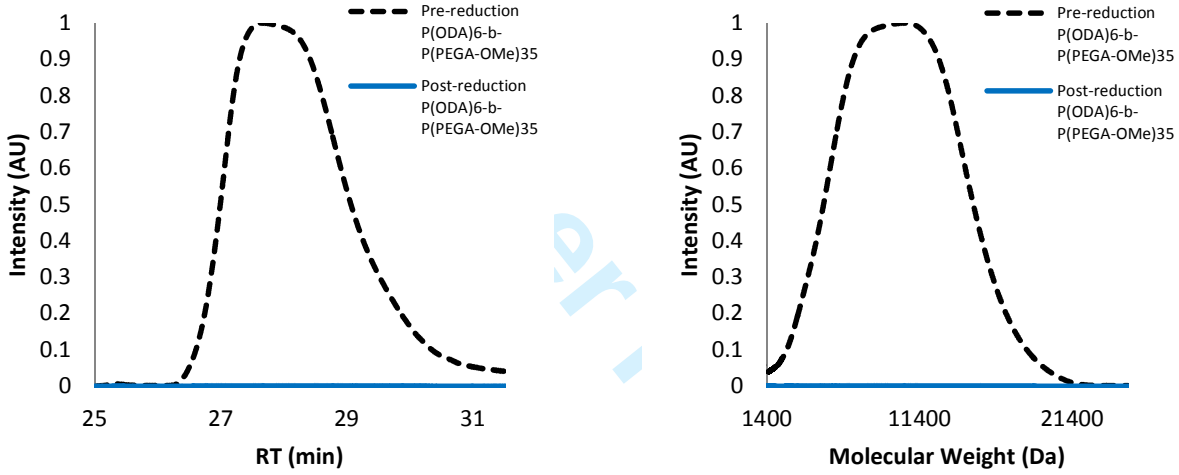

(iii)

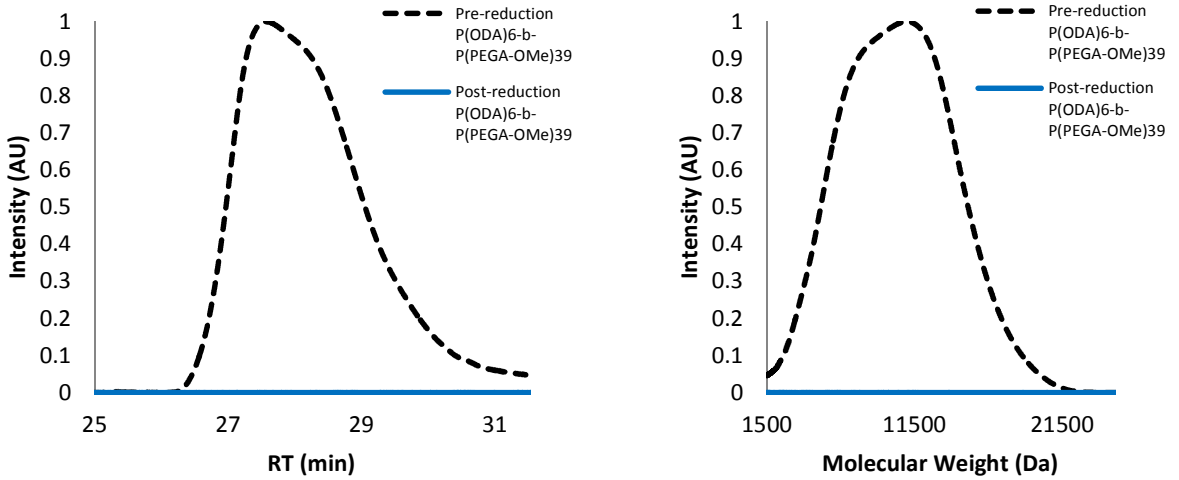

(iv)

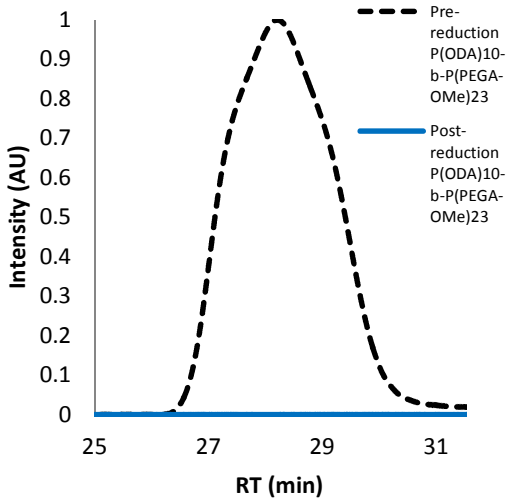
Intensity (AU)
RT (min)
Pre-reduction P(ODA)10-b-P(PEGA-OMe)23
Post-reduction P(ODA)10-b-P(PEGA-OMe)23

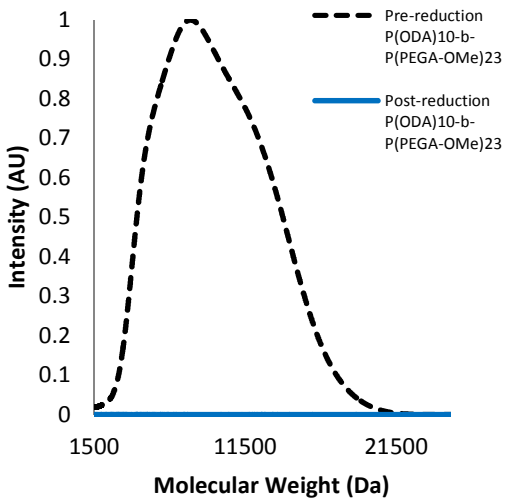
Intensity (AU)
Molecular Weight (Da)
Pre-reduction P(ODA)10-b-P(PEGA-OMe)23
Post-reduction P(ODA)10-b-P(PEGA-OMe)23

(v)

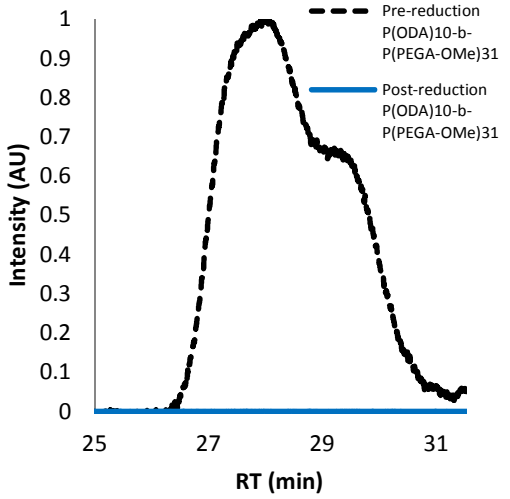
Intensity (AU)
RT (min)
Pre-reduction P(ODA)10-b-P(PEGA-OMe)31
Post-reduction P(ODA)10-b-P(PEGA-OMe)31

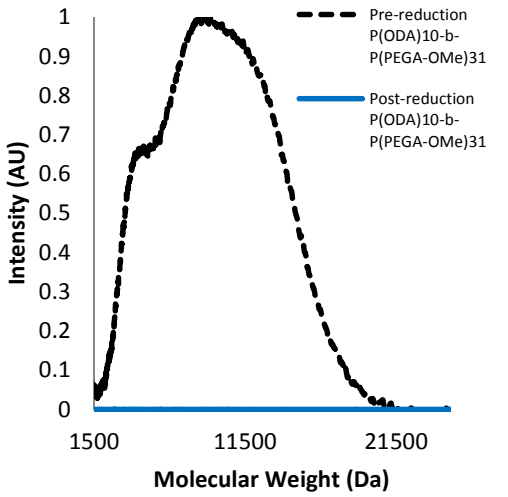
Intensity (AU)
Molecular Weight (Da)
Pre-reduction P(ODA)10-b-P(PEGA-OMe)31
Post-reduction P(ODA)10-b-P(PEGA-OMe)31

(vi)

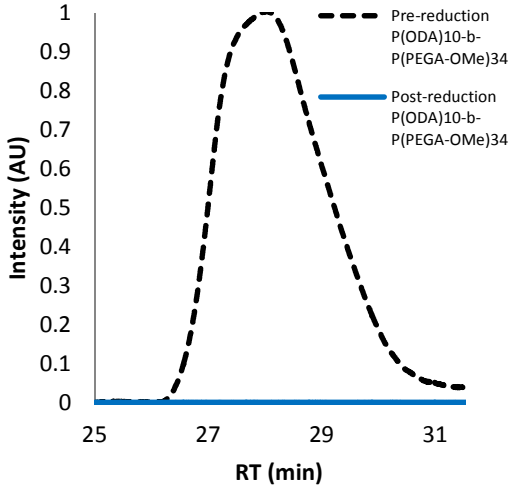
Intensity (AU)
RT (min)
Pre-reduction P(ODA)10-b-P(PEGA-OMe)34
Post-reduction P(ODA)10-b-P(PEGA-OMe)34

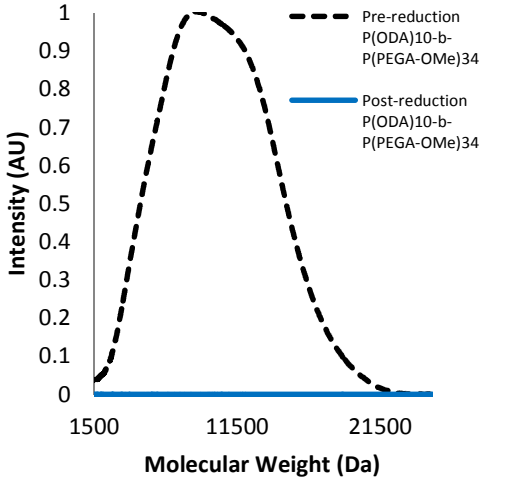
Intensity (AU)
Molecular Weight (Da)
Pre-reduction P(ODA)10-b-P(PEGA-OMe)34
Post-reduction P(ODA)10-b-P(PEGA-OMe)34

A. PRE-REDUCTION CAC GRAPHS

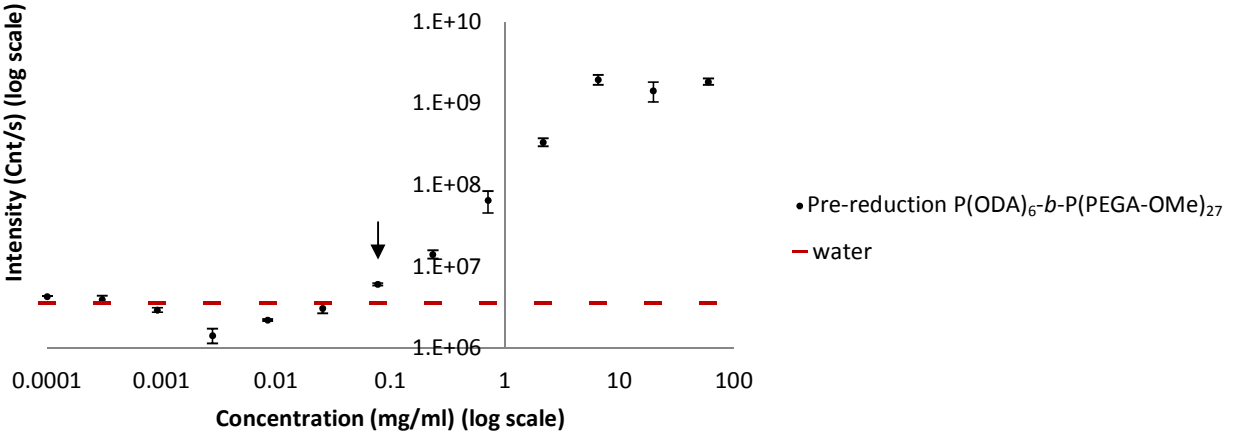

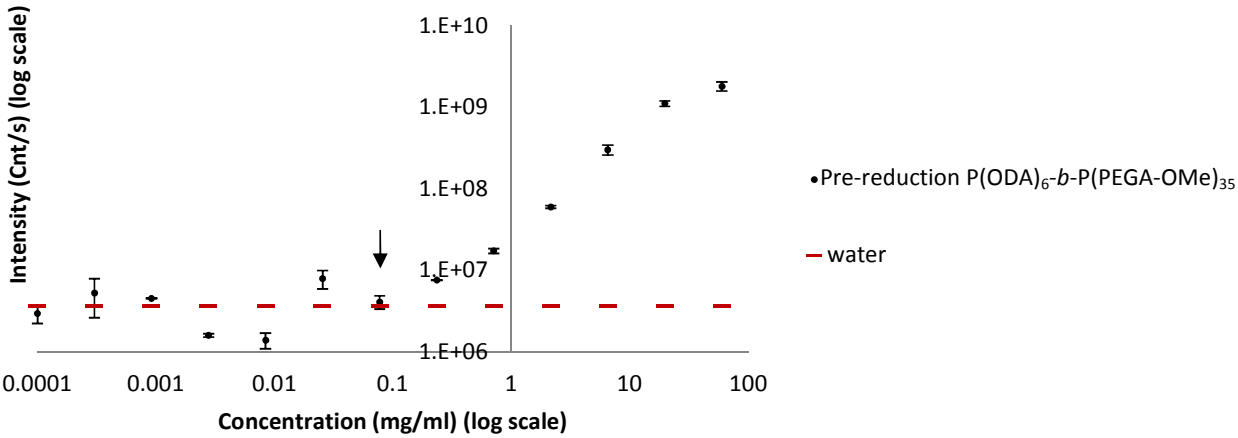

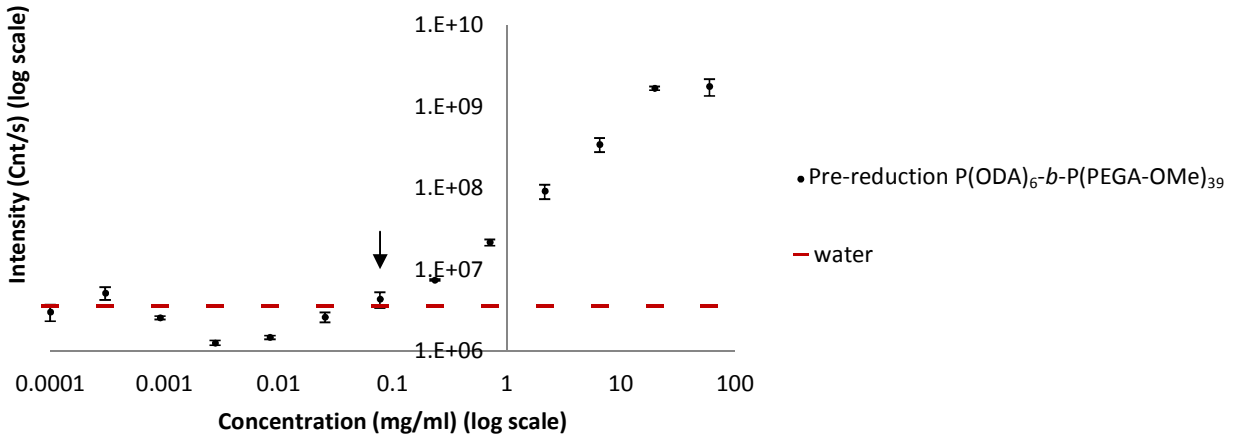

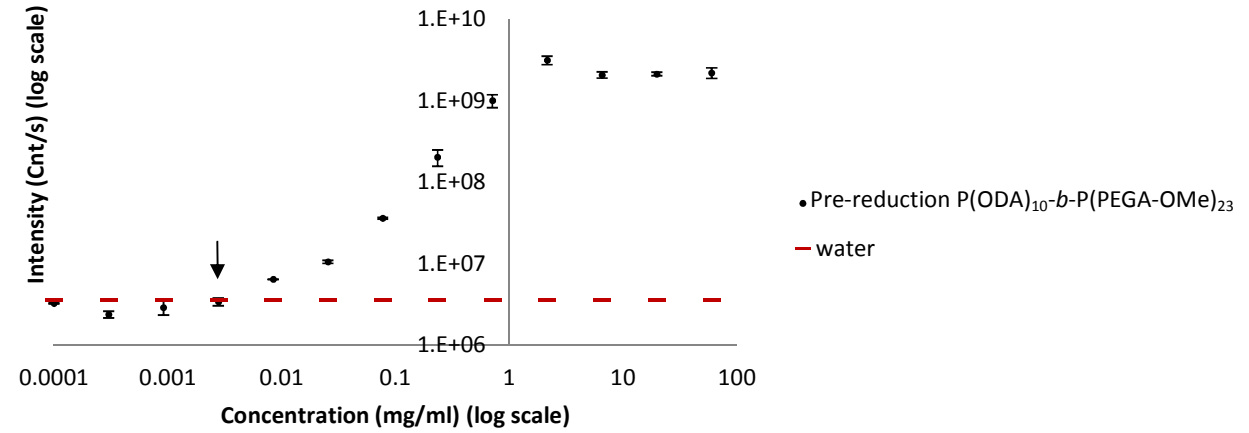
Intensity (Cnt/s) (log scale)
1.E+10
1.E+09
1.E+08
1.E+07
1.E+06
0.0001
0.001
0.01
0.1
1
10
100
Concentration (mg/ml) (log scale)
Pre-reduction P(ODA)10-b-P(PEGA-OMe)23
water

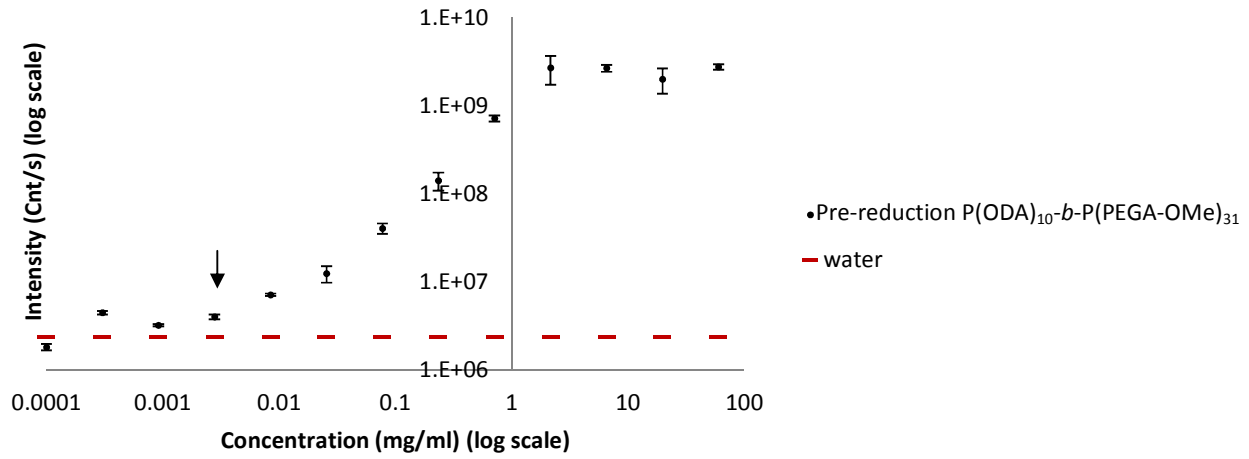
Intensity (Cnt/s) (log scale)
1.E+10
1.E+09
1.E+08
1.E+07
1.E+06
0.0001
0.001
0.01
0.1
1
10
100
Concentration (mg/ml) (log scale)
Pre-reduction P(ODA)10-b-P(PEGA-OMe)31
water

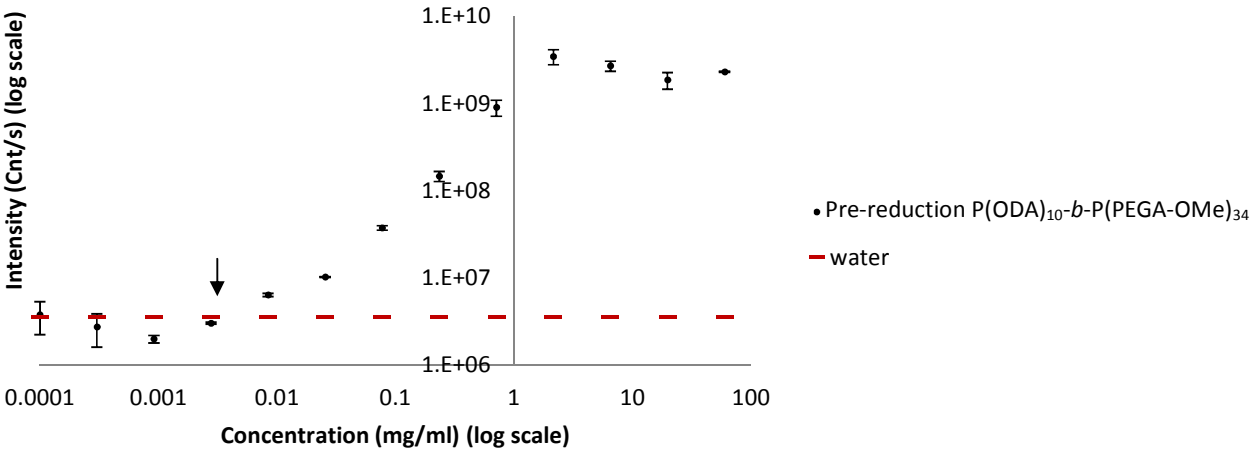
Intensity (Cnt/s) (log scale)
1.E+10
1.E+09
1.E+08
1.E+07
1.E+06
0.0001
0.001
0.01
0.1
1
10
100
Concentration (mg/ml) (log scale)
Pre-reduction P(ODA)10-b-P(PEGA-OMe)34
water

B. POST-REDUCTION CAC GRAPHS

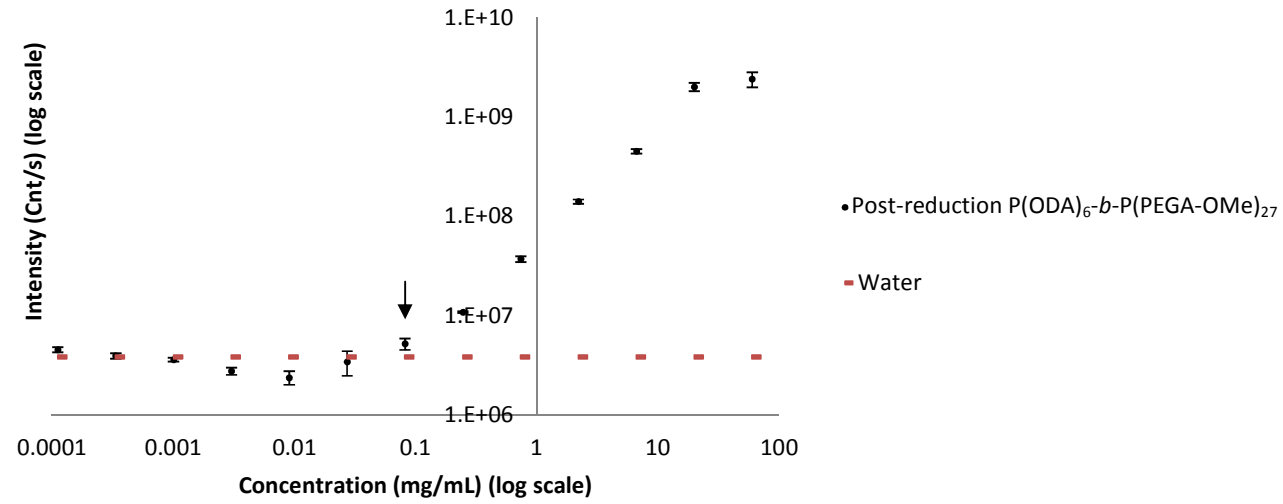

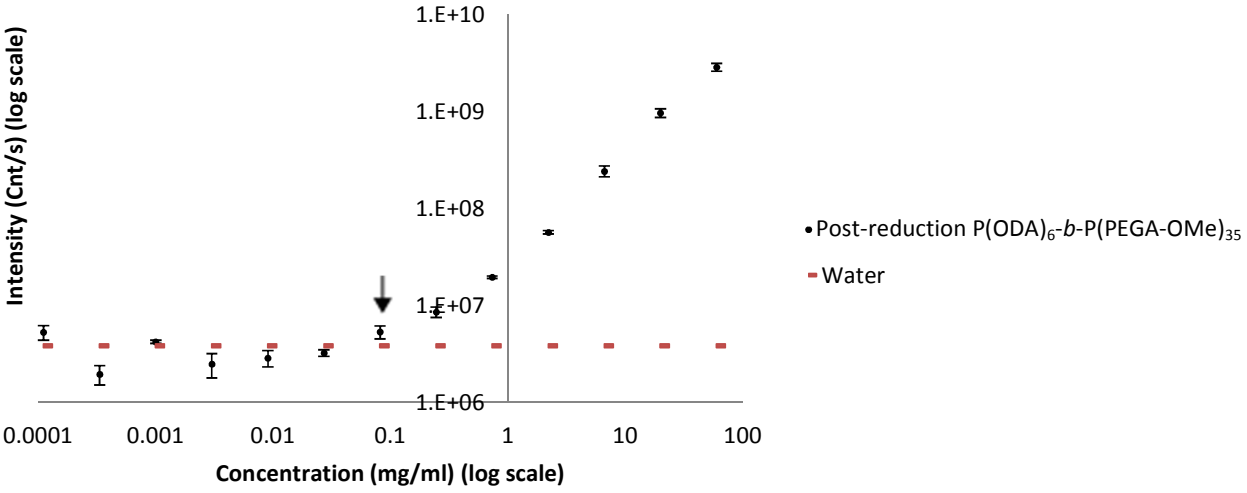

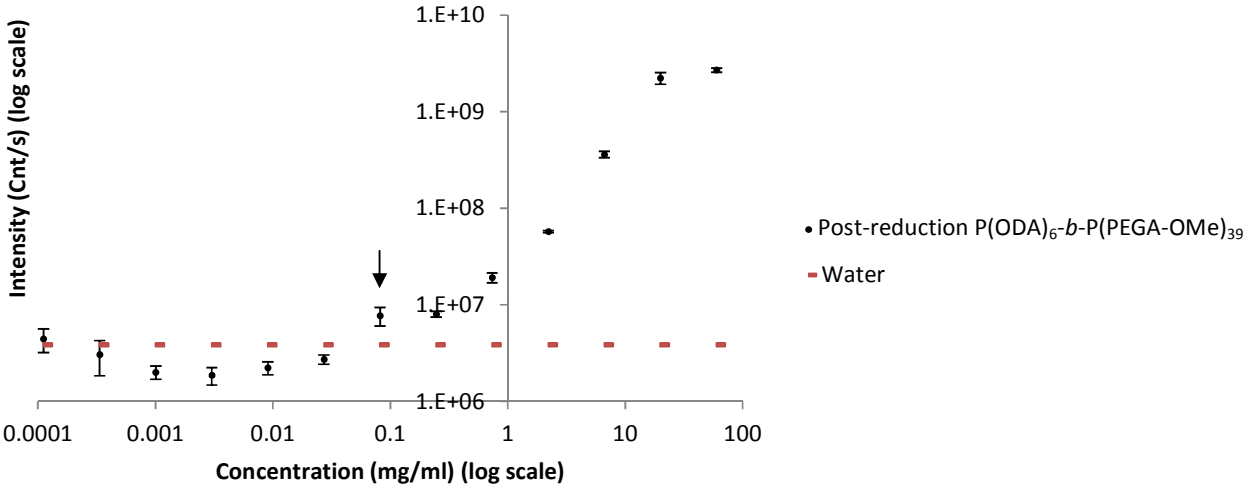

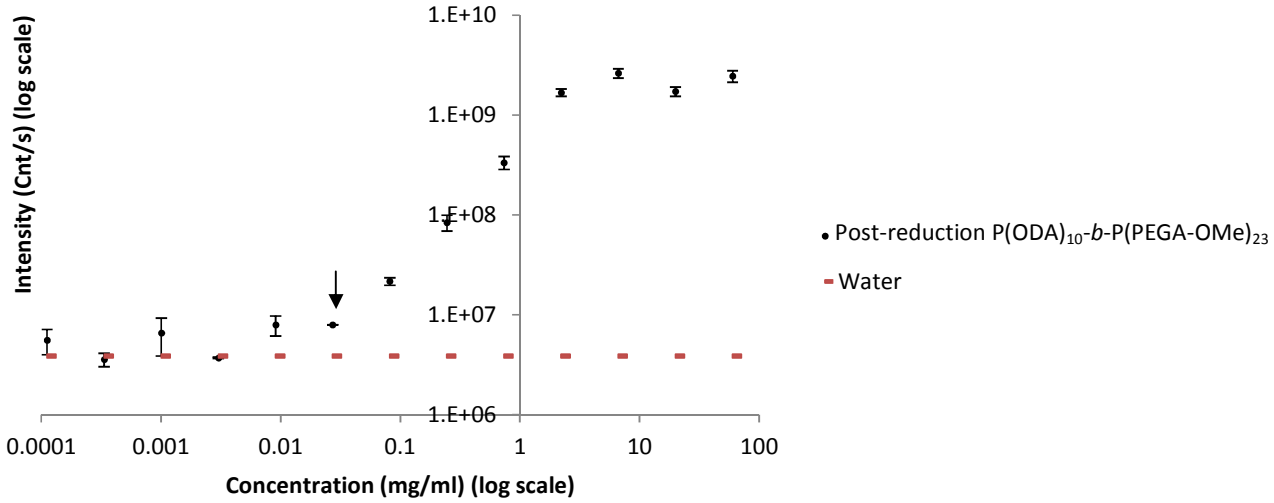
Intensity (Cnt/s) (log scale)
1.E+10
1.E+09
1.E+08
1.E+07
1.E+06
0.0001
0.001
0.01
0.1
1
10
100
Concentration (mg/ml) (log scale)
Post-reduction P(ODA)10-b-P(PEGA-OMe)23
Water

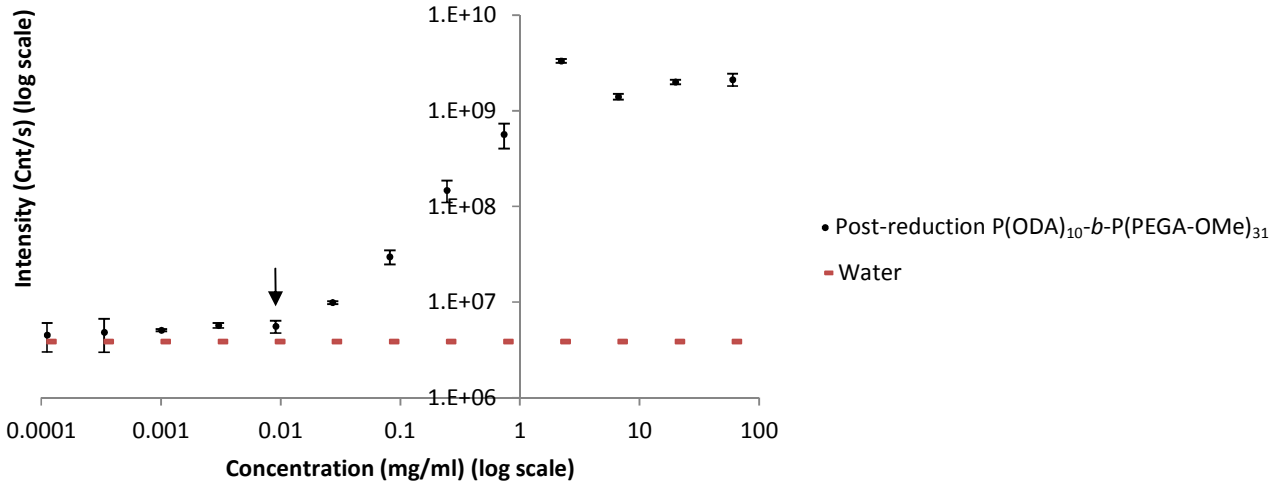
Intensity (Cnt/s) (log scale)
1.E+10
1.E+09
1.E+08
1.E+07
1.E+06
0.0001
0.001
0.01
0.1
1
10
100
Concentration (mg/ml) (log scale)
Post-reduction P(ODA)10-b-P(PEGA-OMe)31
Water

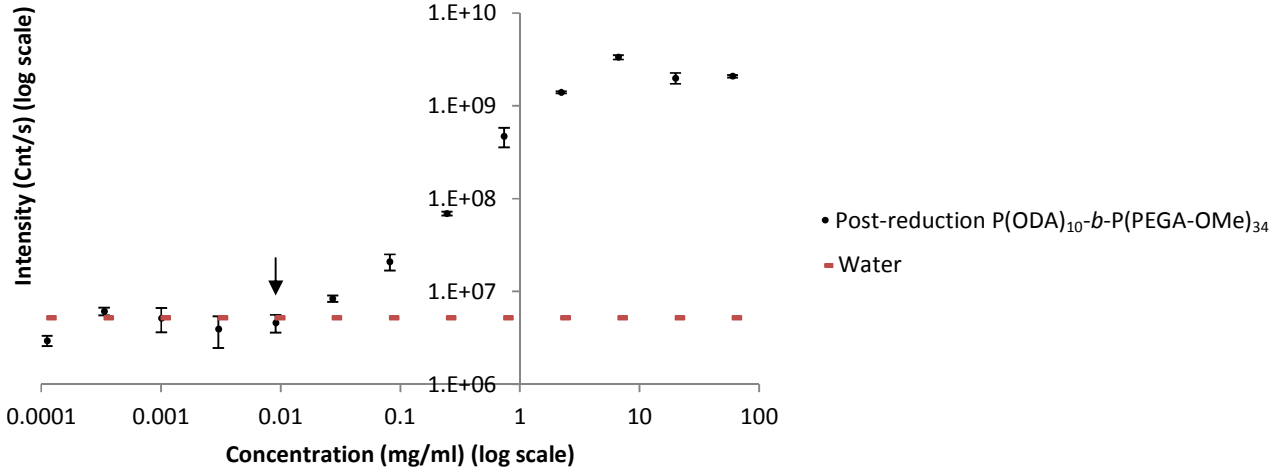
Intensity (Cnt/s) (log scale)
1.E+10
1.E+09
1.E+08
1.E+07
1.E+06
0.0001
0.001
0.01
0.1
1
10
100
Concentration (mg/ml) (log scale)
Post-reduction P(ODA)10-b-P(PEGA-OMe)34
Water

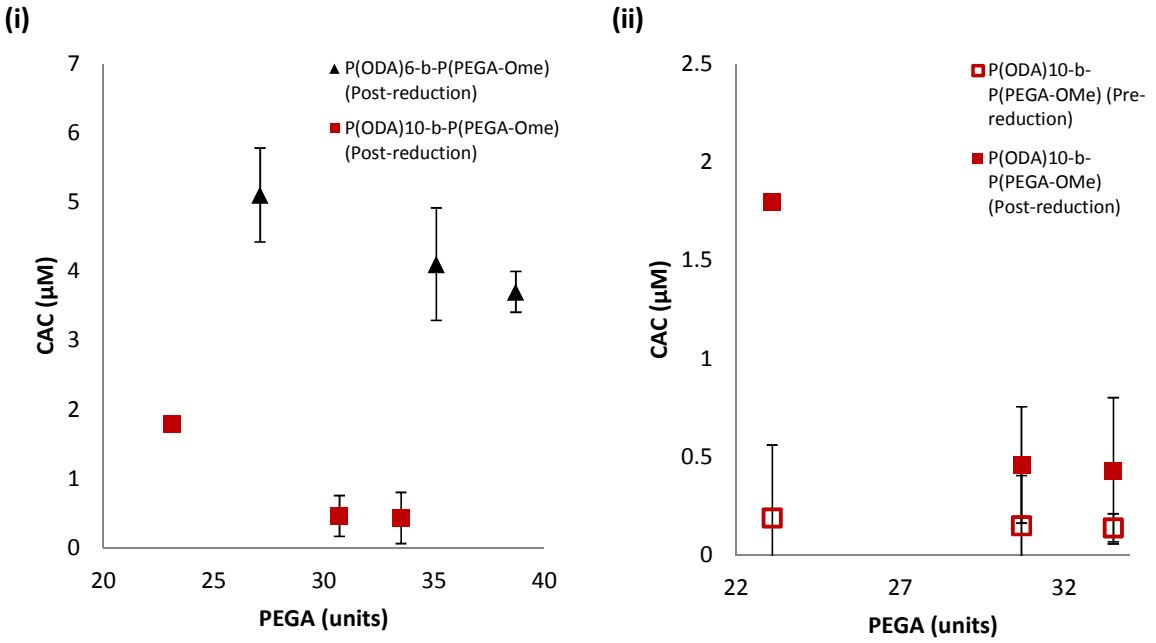

Figure 1. CAC (μM) vs. Copolymer's PEGA length post-reduction for (i) $P(ODA)_6$-*b*-P(PEGA-OMe) (▲) and $P(ODA)_{10}$-*b*-P(PEGA-OMe) (■); and (ii) $P(ODA)_{10}$-*b*-P(PEGA-OMe) (□ Pre-, ■ Post-reduction). Error bars represent the standard deviation

CROSS-POLARIZED LIGHT MICROSCOPY (CPLM) DATA

The phase behaviour of each copolymer was assessed by observation of the characteristic optical textures of anisotropic and isotropic phases when observed through polarised light. The textures of the birefringent materials were typically indicative lamellar phases, hexagonal phases whilst the non-viscous isotropic phases were identified as micellar phases.

Copolymer	DRY	Interaction at excess water interface (°C)									
	20	20	25	30	35	40	45	50	55	60	65
$P(ODA)_6$-*b*-$P(PEGA\text{-}OMe)_{27}$	B							•			
Post reduction	B							•			
$P(ODA)_6$-*b*-$P(PEGA\text{-}OMe)_{35}$	I				•						
Post reduction	B							•			
$P(ODA)_6$-*b*-$P(PEGA\text{-}OMe)_{39}$	B					•					
Post reduction	B					•					
$P(ODA)_{10}$-*b*-$P(PEGA\text{-}OMe)_{23}$	B								•		
Post reduction	B								•		
$P(ODA)_{10}$-*b*-$P(PEGA\text{-}OMe)_{31}$	B							•			
Post reduction	B									•	
$P(ODA)_{10}$-*b*-$P(PEGA\text{-}OMe)_{34}$	B								•		
Post reduction	B									•	

•-No longer present (all dissolved)
B - birefringence
I – Isotropic

Table 1. Anisotropic and isotropic phases observed during water penetration scans of the copolymer in excess water under cross polarised light microscopy (CPLM) from 20 °C to 65 °C.

CPLM IMAGES

	Dry(20°C)	20 °C	25 °C	30 °C	35 °C	40 °C	45 °C	50 °C	55 °C	60 °C
Pre-reduction $P(ODA)_6$-*b*-$P(PEGA\text{-}OMe)_{27}$	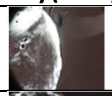	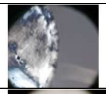	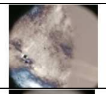	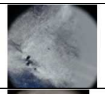	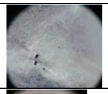	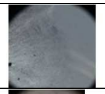		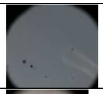		
Post-reduction $P(ODA)_6$-*b*-$P(PEGA\text{-}OMe)_{27}$		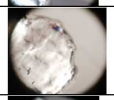	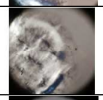		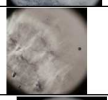			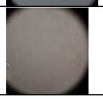		
Pre-reduction $P(ODA)_6$-*b*-$P(PEGA\text{-}OMe)_{35}$	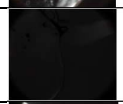	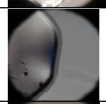	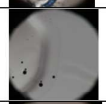	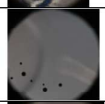	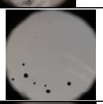					
Post-reduction $P(ODA)_6$-*b*-$P(PEGA\text{-}OMe)_{35}$	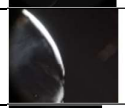			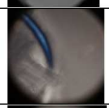	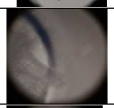					
Pre-reduction $P(ODA)_6$-*b*-$P(PEGA\text{-}OMe)_{39}$										
Post-reduction $P(ODA)_6$-*b*-$P(PEGA\text{-}OMe)_{39}$					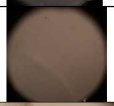					
Pre-reduction $P(ODA)_{10}$-*b*-$P(PEGA\text{-}OMe)_{23}$										
Post-reduction $P(ODA)_{10}$-*b*-$P(PEGA\text{-}OMe)_{23}$										
Pre-reduction $P(ODA)_{10}$-*b*-$P(PEGA\text{-}OMe)_{31}$										
Post-reduction $P(ODA)_{10}$-*b*-$P(PEGA\text{-}OMe)_{31}$										
Pre-reduction $P(ODA)_{10}$-*b*-$P(PEGA\text{-}OMe)_{34}$										
Post-reduction $P(ODA)_{10}$-*b*-$P(PEGA\text{-}OMe)_{34}$										

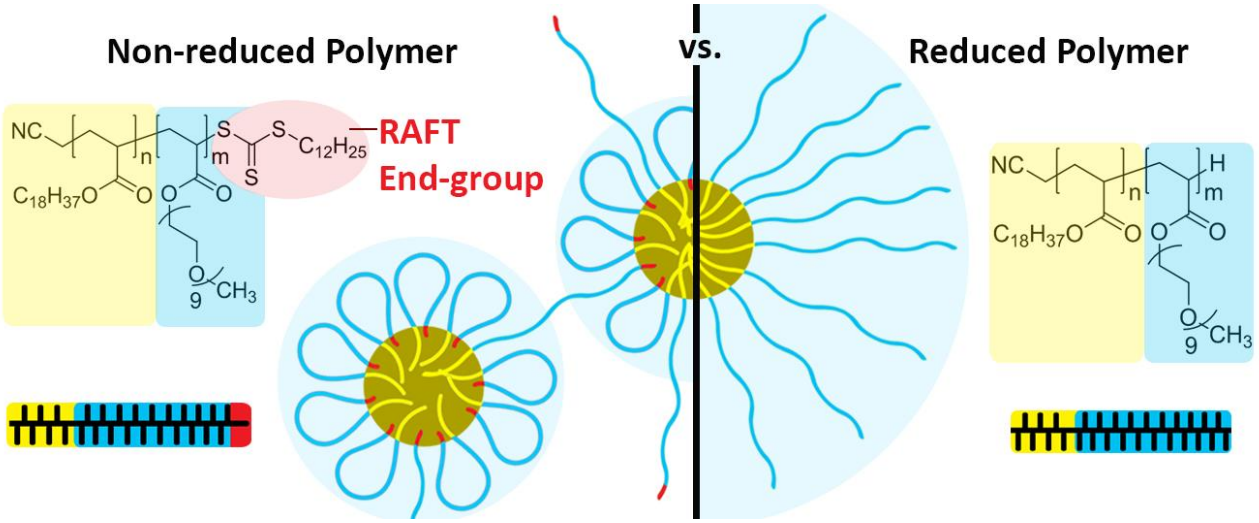

TOC graphic

Chapter 6.2

Novel RAFT amphiphilic brush copolymer steric stabilisers for cubosomes: Poly(octadecyl acrylate)-*block*-poly(polyethylene glycol methyl ether acrylate)

Josephine Y.T. Chong, Xavier Mulet, Almar Postma, Daniel J. Keddie, Lynne Waddington, Ben J. Boyd and Calum J. Drummond

SUBMITTED: *Soft Matter* (submitted on 15.5.2014)

Declaration for Chapter 6.2

Declaration by candidate

In the case of Chapter 6.2, the nature and extent of my contribution to the work was the following:

Nature of contribution	Extent of contribution (%)
Research design, performance of data collection and analysis, manuscript preparation	80

The following co-authors contributed to the work:

Name	Nature of contribution
Xavier Mulet	Supervision; intellectual input; input into manuscript preparation
Almar Postma	Intellectual input on RAFT polymerisation and preparation; input into manuscript preparation
Daniel J. Keddie	Intellectual input on RAFT polymerisation and preparation; input into manuscript preparation
Lynne Waddington	Intellectual input on cryo-TEM operation and analysis
Ben Boyd	Supervision; intellectual input; input into manuscript preparation
Calum Drummond	Supervision; intellectual input; input into manuscript preparation

Candidate's signature: [redacted] **Date:** **10.7.2014**

Declaration by co-authors

The undersigned hereby certify that:

(31) the above declaration correctly reflects the nature and extent of the candidate's contribution to this work, and the nature of the contribution of each of the co-authors.

(32) they meet the criteria for authorship in that they have participated in the conception, execution, or interpretation, of at least that part of the publication in their field of expertise;

(33) they take public responsibility for their part of the publication, except for the responsible author who accepts overall responsibility for the publication;

(34) there are no other authors of the publication according to these criteria;

(35) potential conflicts of interest have been disclosed to (a) granting bodies, (b) the editor or publisher of journals or other publications, and (c) the head of the responsible academic unit; and

(36) the original data are stored at the following location(s) and will be held for at least five years from the date indicated below:

Location of data storage: CSIRO Materials Science and Engineering, Ian Wark Laboratory, Bayview Avenue, Clayton 3168, Australia.

Co-authors' signature for Chapter 6.2:

Signed: [redacted] **Date:** **10.1.2014**

Xavier Mulet

Signed: [redacted] **Date:** **8.1.2014**

Almar Postma

Signed: [redacted] **Date:** **29.1.2014**

Daniel J. Keddie

Signed: [redacted] **Date:** **8.1.2014**

Lynne J. Waddington

Signed: [redacted] **Date:** **28.2.2014**

Ben J. Boyd

Signed: [redacted] **Date:** **12.4.2014**

Calum J. Drummond

Soft Matter

Novel RAFT amphiphilic brush copolymer steric stabilisers for cubosomes: Poly(octadecyl acrylate)-block-poly(polyethylene glycol methyl ether acrylate)

Journal:	*Soft Matter*
Manuscript ID:	Draft
Article Type:	Paper
Date Submitted by the Author:	n/a

Complete List of Authors:	Chong, Josephine; CSIRO, CSIRO Materials Science and Engineering; Monash University, Drug Delivery, Disposition and Dynamics Mulet, Xavier; CSIRO, Molecular & Health Technology Postma, Almar; CSIRO, CMHT Keddie, Daniel; University of New England, Chemistry, School of Science and Technology; CSIRO, Materials Science and Engineering Waddington, Lynne; CSIRO, Molecular & Health Technologies Boyd, Ben; Monash University, Monash Institute of Pharmaceutical Sciences Drummond, Calum; RMIT University, School of Applied Sciences

Soft Matter

PAPER

Novel RAFT amphiphilic brush copolymer steric stabilisers for cubosomes: poly(octadecyl acrylate)-*block*-poly(polyethylene glycol methyl ether acrylate)†

Cite this: DOI: 10.1039/c4sm01064g

Josephine Y. T. Chong,[ab] Xavier Mulet,[ab] Almar Postma,[a] Daniel J. Keddie,[ac] Lynne J. Waddington,[d] Ben J. Boyd*[b] and Calum J. Drummond*[ae]

Received 15th May 2014
Accepted 12th July 2014

DOI: 10.1039/c4sm01064g

www.rsc.org/softmatter

Copolymers, particularly Pluronic®s, are typically used to sterically stabilise colloidal nanostructured particles composed of a lyotropic liquid crystalline bicontinuous cubic phase (cubosomes). There is a need to design and assess new functionalisable stabilisers for these colloidal drug delivery systems. Six amphiphilic brush copolymers, poly(octadecyl acrylate)-*block*-poly(polyethylene glycol methyl ether acrylate) (P(ODA)-*b*-P(PEGA-OMe)), synthesised by reversible addition–fragmentation chain transfer (RAFT), were assessed as novel steric stabilisers for cubosomes. It was found that increasing the density of PEG on the nanostructured particle surface by incorporating a PEG brush design (*i.e.*, brush copolymer), provided comparable and/or increased stabilisation effectiveness compared to a linear PEG structure, Pluronic® F127, which is extensively used for steric stabilisation of cubosomes. Assessment was conducted both prior to and following the removal of the dodecyl trithiocarbonate end-group, by free radical-induced reduction. The reduced (P(ODA)-*b*-P(PEGA-OMe) copolymers were more effective steric stabilisers for phytantriol and monoolein colloidal particle dispersions than their non-reduced analogues. High throughput characterisation methodologies, including an accelerated stability assay (ASA) and synchrotron small angle X-ray scattering (SAXS), were implemented in this study for the rapid assessment of steric stabiliser effectiveness and lyotropic liquid crystalline phase identification. Phytantriol cubosomes stabilised with P(ODA)-*b*-P(PEGA-OMe) copolymers exhibited a double diamond cubic phase (Q_2^D), whilst monoolein cubosomes exhibited a primitive cubic phase (Q_2^P), analogous to those formed using Pluronic® F127.

Introduction

Lyotropic liquid crystalline nanostructured particles, such as cubosomes, are of significant interest due to their well-defined, ordered internal structure. These self-assembled structures possess a high volume fraction of lipid and large internal surface area for loading with both hydrophilic and lipophilic therapeutics and biomedical imaging agents.[1–7] Lipids, such as phytantriol and monoolein (GMO) (structures in Fig. 1) are common examples of building blocks for these lyotropic liquid crystalline phase systems.[8] As amphiphiles with both lipophilic and hydrophilic domains, these lipids readily self-assemble in aqueous environments.[9–11] However, lyotropic liquid crystalline nanostructured particles in aqueous solutions can only be colloidally stable for extended periods in the presence of a stabiliser. Currently the range of steric stabilisers for lyotropic liquid crystalline nanostructured particles remains limited, with the most commonly employed stabiliser being Pluronic® F127.[12–17]

Pluronic® F127 ("F127") is an amphiphilic triblock copolymer, with a number average molar mass of 12 600, consisting of 100 units on average of polyethylene glycol (PEG) on both sides of a 65-unit long polypropylene oxide (PPO) block (Fig. 1). F127 has been extensively used for sterically stabilising lyotropic liquid crystalline bicontinuous cubic nanostructured

[a]*CSIRO Materials Science and Engineering, Private Bag 10, Clayton, VIC 3169, Australia.* [redacted]

[b]*Drug Delivery, Disposition and Dynamics, Monash Institute of Pharmaceutical Science, Monash University, Parkville Campus, 381 Royal Parade, Parkville, VIC 3052, Australia.* [redacted]

[c]*Department of Chemistry, School of Science and Technology, University of New England, NSW 2351, Australia*

[d]*CSIRO Materials Science and Engineering, 343 Royal Parade, Parkville, VIC 3052, Australia*

[e]*School of Applied Sciences, College of Science, Engineering and Health, RMIT University, GPO Box 2476, Melbourne, VIC 3001, Australia*

† Electronic supplementary information (ESI) available: Datasets obtained of the visual assessment, ASA, DLS and SAXS results for P(ODA)-*b*-P(PEGA-OMe) copolymers and their phytantriol or monoolein dispersions. See DOI: 10.1039/c4sm01064g

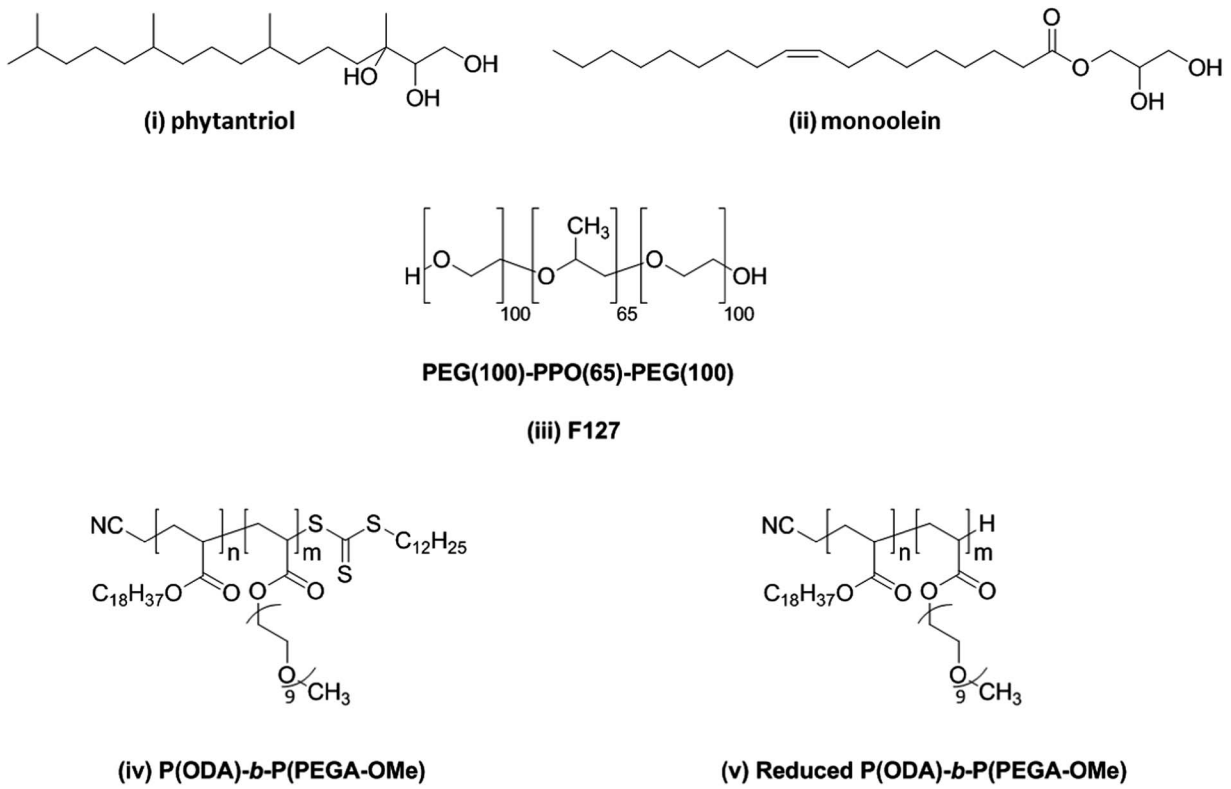

Fig. 1 Chemical structures of (i) phytantriol, (ii) monoolein, (iii) F127 (control steric stabiliser), (iv) P(ODA)-*b*-P(PEGA-OMe) (non-reduced) and (v) P(ODA)-*b*-P(PEGA-OMe) (reduced).

particles. Although F127 is an effective steric stabiliser for cubosomes, it may not always be the most effective steric stabiliser available for different lipids.[17,18] Alternative steric stabilisers known for stabilising lyotropic liquid crystalline colloidal particles include β-casein,[19] silica particles,[20] laponite,[21] modified cellulose,[22] ethoxylated phytosterol,[23] polysorbate 80,[24] Pluronic® F108 (ref. 17) and Myrj® 59.[25] Discovery of the alternative steric stabilisers: Pluronic® F108 and Myrj® 59, were enabled by the development of high-throughput methodologies, which has facilitated implementation of high-throughput preparation and screening protocols.[17,25–27]

Previous studies on steric stabilisers possessing different architectures have shown varying degrees of effectiveness of steric stabilisation.[17,18,25,28] In previous work, an amphiphilic brush copolymer, poly(octadecyl acrylate)-*block*-poly(polyethylene glycol methyl ether acrylate) (P(ODA)-*b*-P(PEGA-OMe)) was synthesised, using reversible addition–fragmentation chain transfer (RAFT) polymerisation (Fig. 1 and Table 1).[29,30] These P(ODA)-*b*-P(PEGA-OMe) copolymers showed self-assembly behaviour in excess water and were noted to be potential candidates for self-assembled drug delivery systems, such as micelles.[30] Although the amphiphilic 'brush' copolymer structure has to our knowledge never been reported for use in the steric stabilisation of lyotropic liquid crystalline nanostructured particles, a polymer brush structure with branching arms of PEG was thought to be an effective design for steric stabilisers because of reports that non-linear structures (*i.e.*, hyperbranched polyglycerols) were advantageous over linear structures. Some of these advantages include antifouling,[31,32] protein resistance,[33,34] less susceptibility to oxidation or thermal stresses than PEG,[34] longer plasma half-lives indicating stealth[35–39] properties and prolonging particle circulation.[40,41]

In this study, custom synthesised amphiphilic brush copolymers (P(ODA)-*b*-P(PEGA-OMe)) are assessed for their effectiveness at sterically stabilising cubosomes. The significance of this study is to establish new stabiliser designs/structures that are not commercially available to improve effectiveness of steric stabilisation, whilst validating the use of controlled RAFT synthesised materials for colloidal systems. Synthesising custom steric stabilisers is relatively new, as previous studies in this field/area have predominantly investigated the stability of cubosome dispersions using commercially available surfactants/copolymers (*e.g.* Pluronic®, Tween®, Myrj®).[17,25] The advantages of customising and synthesising steric stabilisers are twofold. Firstly having the ability to tune stabilisers will allow opportunities for optimising stabilisation for different lipids. Secondly functionalising stabilisers through the functional groups afforded by the RAFT agent at the end of the hydrophilic domain permits the attachment of targeting moieties (*e.g.* antibodies or antibody fragments). This will allow the development and use of active targeting systems. Active targeting cubosome systems have not been reported and are important in advancing the use of these colloidal systems for drug delivery applications. The P(ODA)-*b*-P(PEGA-OMe) copolymers

Table 1 Properties of amphiphilic copolymers P(ODA)-*b*-P(PEGA-OMe): number average molar mass (M_n), dispersity (M_w/M_n)

Polymer P(ODA)-*b*-P(PEGA-OMe)	M_n, theory	M_n[a], NMR	M_n[b], GPC	M_w/M_n[b], GPC
$P(ODA)_6$-*b*-$P(PEGA\text{-}OMe)_{27}$	14 500	15 200	15 400	1.33
$P(ODA)_6$-*b*-$P(PEGA\text{-}OMe)_{35}$	19 400	19 000	17 500	1.33
$P(ODA)_6$-*b*-$P(PEGA\text{-}OMe)_{39}$	20 900	20 700	17 900	1.32
$P(ODA)_{10}$-*b*-$P(PEGA\text{-}OMe)_{23}$	17 500	14 600	14 100	1.46
$P(ODA)_{10}$-*b*-$P(PEGA\text{-}OMe)_{31}$	22 100	18 200	15 700	1.42
$P(ODA)_{10}$-*b*-$P(PEGA\text{-}OMe)_{34}$	23 700	19 600	16 700	1.41

[a] Number-average molar mass (M_n) determined by ^{1}H NMR. [b] Number-average molar mass (M_n) and dispersity (M_w/M_n) determined by chloroform gel permeation chromatography, with the molar mass in polystyrene equivalents. Reproduced from ref. 30.

were synthesised with the intent to potentially functionalise the terminal RAFT end-group *via* thiol-conjugation to produce actively targeted drug delivery systems. Even though it is possible to functionalise the end of Pluronic® surfactants[42] these copolymers have a unique design (*i.e.*, brush structure), which may be more effective for the steric stabilisation of cubosomes.

Therefore herein we assess the use of these amphiphilic brush copolymers as novel steric stabilisers for cubosomes and compare their effectiveness as stabilisers to the standard control steric stabiliser, F127 (Fig. 1(iii)). Both reduced (RAFT end-group removed; (Fig. 1(v)) and non-reduced P(ODA)-*b*-P(PEGA-OMe (Fig. 1(iv)) were assessed. Colloidal particle dispersions prepared using both phytantriol and monoolein (Fig. 1(i) and (ii)) as the core lipids, stabilised with P(ODA)-*b*-P(PEGA-OMe) copolymers were characterised for their effectiveness at providing steric stabilisation using visual assessment and an accelerated stability assay (ASA).[18] Particle size was determined using dynamic light scattering (DLS) and characterisation of lyotropic liquid crystal internal structure and particle morphology were determined using synchrotron small-angle X-ray scattering (SAXS) and cryo-transmission electron microscopy (cryo-TEM).

Materials and methods

Materials

Phytantriol (3,7,11,15-tetramethylhexadecane-1,2,3-triol) was obtained from DSM Nutritional Products, NSW. Monoolein (1-oleoyl-*rac*-glycerol ≥99%), Pluronic® F127, fluorescein sodium salt and 0.01 M phosphate buffered saline (PBS) solution (pH 7.4) were purchased from Sigma-Aldrich, NSW. P(ODA)-*b*-P(PEGA-OMe) amphiphilic brush copolymers, in their non-reduced and reduced states, were synthesised by RAFT polymerisation.[30]

Methods

Preparation of lyotropic liquid crystalline bicontinuous cubic nanostructured colloidal particles. All dispersions contained lipid (phytantriol/monoolein) at 50 mg lipid per 500 μL of aqueous phase. Control lyotropic liquid crystal dispersions were formed using F127 (control steric stabiliser) at 0.3, 0.5, 0.7, 1, 1.2, 1.5 and 2 wt% of the total sample mass, in 0.01 M PBS buffer solution. The buffer solution was replaced with Milli Q water for cryo-TEM samples. Lyotropic liquid crystal dispersions stabilised with both reduced and non-reduced P(ODA)-*b*-P(PEGA-OMe) copolymers, were made using 0.1, 0.5, 0.7 and 1 wt% stabiliser concentrations for initial visual assessment and SAXS analysis. For the accelerated stability assay, the molar concentrations of copolymer equivalent to F127 at 0.7, 1, 1.2, 1.5 and 2 wt% were calculated for reduced P(ODA)-*b*-P(PEGA-OMe) copolymers and used to prepare phytantriol and monoolein dispersions. These dispersions were also analysed using SAXS.

Two methods were used to prepare cubosome dispersions in 1.5 mL Eppendorf tubes. The first method required steric stabiliser to be dissolved in water, before being added to the lipid. This method was used for steric stabilisers with high water solubility: Pluronic® F127 and the reduced P(ODA)-*b*-P(PEGA-OMe) copolymers.

The second method was applied to the less water soluble stabilisers, such as the non-reduced P(ODA)-*b*-P(PEGA-OMe) copolymers, which possessed a dodecyl thiocarbonate RAFT end-group. The second method required the steric stabiliser to be dissolved into the lipid, by dissolving both components together with chloroform. In the second methodology, it is important to remove the chloroform before adding the water or PBS buffer solution to the stabiliser/lipid mix, as the presence of chloroform can affect the quality of the dispersion. This was done by placing these samples in a vacuum desiccator over 14 days to remove the chloroform by evaporation. Full removal of chloroform was verified using ^{1}H NMR, using deuterated methanol as the NMR solvent.

The resulting contents of the tube were sonicated using a probe ultra-sonicator (Misonix Ultrasonic Liquid Processor Microtip Probe Sonicator with a 418 Misonix probe (Misonix Inc., NY, USA)). Two different processing sequences were used for the sonication of cubosome dispersions. For the sonication of phytantriol samples, three programs were processed in succession without any delay time: program 1 settings: 50 amplitude, 30 s process time, 3 s pulse-time on, 2 s pulse-time off; program 2 settings: 45 amplitude, 1 min process time, 2 s pulse-time on, 4 s pulse-time off; and program 3 settings: 40 amplitude, 1 min process time, 2 s pulse-time on, 4 s pulse-time off. The sequence resulted in a total sonication time of 2.5 min per sample.

For the sonication of monoolein samples the three programs were: program 1 settings: 50 amplitude, 1 min process time, 1 s pulse-time on, 10 s pulse-time off; program 2 settings: 45

amplitude, 1 min process time, 1 s pulse-time on, 10 s pulse-time off; and program 3 settings: 40 amplitude, 1 min process time, 1 s pulse-time on, 10 s pulse-time off. The sequence resulted in a total sonication time of 3 min per sample. The sample temperature during sonication was measured using a temperature probe and monitored to prevent overheating of samples. The sample sonication temperature was observed to be consistent between 65 °C to 70 °C, during pulse sonication of samples.

Characterisation of the effectiveness of the copolymer stabilisers. The P(ODA)-*b*-P(PEGA-OMe) copolymers were assessed for their ability to perform as steric stabilisers by visual assessment and an accelerated stability assay.[18] The protocol used for ASA was developed to distinguish between fair to excellent stabilisers that passed the initial visual assessment of particle stability. Only dispersions given a visual assessment score of +++ out of +++, which is the typical scoring for milky, aggregate-free dispersions, equivalent in appearance to the dispersions prepared using control stabiliser F127 at 1 wt% stabiliser concentration, were assessed with ASA.[18]

Briefly, phytantriol dispersions were mixed at equal volumes with dye solution (*i.e.*, 15 μL cubosome sample mixed with 15 μL dye) and pipetted into a 384 black round well Corning® plate. The same was prepared using PBS buffer solution instead of dye solution (3.1×10^{-4} mg mL^{-1}) for control samples. Negative control samples consisted of PBS and dye. Each cubosome mixture with dye or PBS buffer was prepared in triplicate. Fluorescence signal intensities were taken pre and post-centrifugation. The centrifugation of plates was performed with a Heraeus Multifuge ×3 Centrifuge (Thermo Scientific, Germany). Fluorescence signal measurements were taken using FlexStation3 Multi-mode Microplate Reader (Molecular Devices Company, CA, USA), and processed on SoftMax Pro software. The plate was initially centrifuged at 645 × *g* (1800 rpm) for 5 min, measured for fluorescence signal and then re-centrifuged at 796 × *g* (2000 rpm) for 5 min. Phytantriol dispersions stabilised with F127 at 0.3, 0.5, 0.7, 1 and 1.2 wt% were used as a control standard for the ASA.

The intensity of the fluorescence measured in the ASA is proportional to the quantity of particles dispersed in the solution.[18] Using centrifugation to accelerate the occurrence of particle aggregation within a dispersed sample, poorly and well stabilised systems can be distinguished from samples which appear to be well dispersed. Poorly stabilised systems have greater particle aggregation post-centrifugation and therefore greater changes in fluorescence signal intensities pre- and post-centrifugation. In contrast, good steric stabilisers are able to maintain colloidal stability after centrifugation and therefore have fewer changes in fluorescence signal intensities pre- and post-centrifugation. Thus, lesser changes in fluorescence signal intensities pre- and post-centrifugation indicate greater steric stabiliser effectiveness.[18]

Characterisation of the internal structure and morphology of lyotropic liquid crystal colloidal particles. Particle size and polydispersity of dispersed samples was determined by dynamic light scattering using a DynaPro plate reader (Wyatt Technology, Santa Barbara, CA). Data statistics shown for particle size and polydispersity from the DLS instrument are averaged from three repeat measurements. Samples which passed the visual assessment for determining 'good' steric stabilisers were then further analysed using small angle X-ray scattering and cryo-TEM imaging. SAXS is required for establishing the internal phase behaviour (*i.e.*, internal long range order of the crystal lattice) of the dispersed samples under various thermal conditions.

SAXS data was collected at the Australian Synchrotron using a beam with wavelength $\lambda = 1.033$ Å (12.0 keV) with a typical flux of approximately 10^{13} photons per s.[43] 2D diffraction patterns were recorded on a Dectris-Pilatus 1M detector of 10 modules. The detector was offset to access a greater q range. A silver behenate standard (lamellar repeat distance of 58.38 Å) was used for calibration. The samples were loaded in 96 well plates and positioned in a custom-designed plate holder capable of holding two plates at a time, within a temperature adjustable sample holder chamber, with the temperature controlled to ±1.0 °C between 20 and 75 °C. Temperature control was *via* a recirculating water bath (Julabo, Germany). SAXS was performed on dispersions using a temperature range from room temperature (25 °C) with 5 °C increments to 65 °C. The exposure time for each sample was 0.5 s. SAXS data was analysed using an IDL-based AXcess software package.[44]

Particle structure and morphology was further clarified using cryo-TEM imaging. Samples were prepared in a laboratory-built humidity-controlled vitrification system. Humidity was kept close to 80% for all experiments, and ambient temperature was 22 °C. 200-mesh copper grids coated with perforated carbon film (Lacey carbon film: ProSciTech, Qld, Australia) were glow discharged in nitrogen to render them hydrophilic. Preparation of samples involved 4 μL aliquots of the sample pipetted onto each grid prior to plunging. Samples were left for 30 seconds to be adsorbed onto the grid and excess sample was removed *via* manual blotting of the grid for approximately 2 seconds, using Whatman 541 filter paper. Blotting time was optimised for each sample. The grid was then plunged into liquid ethane cooled by liquid nitrogen and frozen grids were then stored in liquid nitrogen until required. The samples were examined using a Gatan 626 cryoholder (Gatan, Pleasanton, CA, USA) and Tecnai 12 Transmission Electron Microscope (FEI, Eindhoven, The Netherlands) at an operating voltage of 120 kV. At all times low dose procedures were followed, using an electron dose of 8–10 electrons per $Å^2$ for all imaging. Images were recorded using a FEI Eagle 4k × 4k CCD camera at magnifications between 15 000× and 42 000×.

Results

Reduced copolymers provide improved colloidal stability over non-reduced copolymers

The amphiphilic brush copolymers, P(ODA)-*b*-P(PEGA-OMe), were able to sterically stabilise phytantriol and monoolein dispersions in both PBS buffer solution and water. The reduced P(ODA)-*b*-P(PEGA-OMe) copolymers were superior to the non-reduced analogues in stabilising phytantriol and monoolein dispersions, creating milky white dispersions with no visible aggregates. These polymers were given the highest visual assessment score (*i.e.*, +++), which was comparable to

dispersions stabilised by the standard control stabiliser, F127 (Tables 2 and 3 and ESI†).

Both phytantriol and monoolein dispersions, stabilised with reduced P(ODA)-*b*-P(PEGA-OMe) copolymers, had an average particle size ranging between 180 and 400 nm in diameter. In contrast, non-reduced P(ODA)-*b*-P(PEGA-OMe) copolymers, which possess a dodecyl trithiocarbonate RAFT end-group, produced milky white phytantriol dispersions, with visible aggregates present after sonication. These dispersions were found to have an average particle size ranging between 110 and 340 nm. Furthermore, non-reduced P(ODA)-*b*-P(PEGA-OMe) copolymers were unable to form stable monoolein dispersions. The poor stability of dispersions produced using non-reduced P(ODA)-*b*-P(PEGA-OMe) copolymers is due to the presence of the hydrophobic end-group at the hydrophilic moiety of the P(ODA)-*b*-P(PEGA-OMe) copolymer likely facilitating particle bridging and flocculation.

Poorly stabilised cubosome systems with visible aggregates have also been previously been reported for using a stabiliser with hydrophobic terminal blocks (*i.e.* PEG150-distearate).[18] Limitations within the dynamic light scattering equipment may lead to large aggregates being undetected and therefore results from DLS should always be accompanied with the visual assessment of the particle dispersions. Consequently, only phytantriol and monoolein dispersions stabilised using the reduced P(ODA)-*b*-P(PEGA-OMe) copolymers were further assessed using the accelerated stability assay.

Reduced amphiphilic brush copolymers provide comparable steric stabiliser effectiveness to F127

It was generally found that stabilisers that had a longer hydrophobic block (*i.e.*, 10 ODA repeat units) provided greater colloidal stability than stabilisers with a shorter hydrophobic

Table 2 Visual assessment of the stability of phytantriol dispersions using 0.1, 0.5, 0.7 and 1 wt% P(ODA)-*b*-P(PEGA-OMe) copolymers as steric stabiliser. Key: +++ milky sample with no visible aggregates. ++ milky sample with few visible aggregates, + milky/cloudy sample with aggregates, – translucent sample with large aggregates [not progressed through to ASA or SAXS studies]

			Stabiliser concentration			
Stabiliser	ODA	PEGA	0.1 wt%	0.5 wt%	0.7 wt%	1 wt%
$P(ODA)_6$-*b*-$P(PEGA\text{-}OMe)_{27}$	5.6	27.1	–	+	++	++
Reduced			+	++	+++	+++
$P(ODA)_6$-*b*-$P(PEGA\text{-}OMe)_{35}$	5.6	35.1	–	+	++	++
Reduced			+	++	+++	+++
$P(ODA)_6$-*b*-$P(PEGA\text{-}OMe)_{39}$	5.6	38.7	+	+	++	++
Reduced			+	++	+++	+++
$P(ODA)_{10}$-*b*-$P(PEGA\text{-}OMe)_{23}$	9.9	23.1	–	++	++	++
Reduced			+	++	+++	+++
$P(ODA)_{10}$-*b*-$P(PEGA\text{-}OMe)_{31}$	9.9	30.7	–	++	++	++
Reduced			+	++	+++	+++
$P(ODA)_{10}$-*b*-$P(PEGA\text{-}OMe)_{34}$	9.9	33.5	+	++	++	++
Reduced			+	++	+++	+++
Control	PPO	PEG				
F127	65	100	+	+++	+++	+++

Table 3 Visual assessment of the stability of monoolein dispersions using 0.1, 0.5, 0.7 and 1 wt% P(ODA)-*b*-P(PEGA-OMe) copolymers as steric stabiliser

			Stabiliser concentration			
Stabiliser	ODA	PEGA	0.1 wt%	0.5 wt%	0.7 wt%	1 wt%
$P(ODA)_6$-*b*-$P(PEGA\text{-}OMe)_{27}$	5.6	27.1	–	–	–	–
Reduced			–	–	++	+++
$P(ODA)_6$-*b*-$P(PEGA\text{-}OMe)_{35}$	5.6	35.1	–	–	–	–
Reduced			–	–	+++	+++
$P(ODA)_6$-*b*-$P(PEGA\text{-}OMe)_{39}$	5.6	38.7	–	–	–	–
Reduced			–	–	+++	+++
$P(ODA)_{10}$-*b*-$P(PEGA\text{-}OMe)_{23}$	9.9	23.1	–	–	–	–
Reduced			–	–	++	+++
$P(ODA)_{10}$-*b*-$P(PEGA\text{-}OMe)_{31}$	9.9	30.7	–	–	–	–
Reduced			–	–	+++	+++
$P(ODA)_{10}$-*b*-$P(PEGA\text{-}OMe)_{34}$	9.9	33.5	–	–	–	–
Reduced			–	–	+++	+++
Control	PPO	PEG				
F127	65	100	–	–	++	+++

block (*i.e.*, 6 ODA repeat units), for both phytantriol and monoolein dispersions (Fig. 2 and ESI†). This may be due to increased stabiliser affinity to the nanostructured particle through increased hydrophobicity, provided by a longer hydrophobic block.

It is also shown that increasing hydrophilicity within both the 6 and 10 ODA unit copolymer series (*e.g.*, $P(ODA)_6$-*b*-$P(PEGA\text{-}OMe)_{39}$ and $P(ODA)_{10}$-*b*-$P(PEGA\text{-}OMe)_{34}$ copolymers respectively) also improved the effectiveness of a stabiliser at providing colloidal stability for both phytantriol and monoolein dispersions (Fig. 2 and ESI†). This increased steric stabilizer effectiveness may be due to increased steric hindrance as a result of increasing the number of units of PEG arms in the copolymer brush structure.

The reduced copolymer that provided the most effective colloidal stability for both lipid systems (*i.e.*, phytantriol and monoolein) was found to be $P(ODA)_{10}$-*b*-$P(PEGA\text{-}OMe)_{34}$, which showed better or comparable steric stabiliser effectiveness to standard control steric stabiliser, F127 (Fig. 2 and ESI†). This is the amphiphilic brush copolymer stabiliser with the longest hydrophobic (*i.e.*, 10 ODA units) and hydrophilic (*i.e.*, 34 PEGA-OMe units) block in the series.

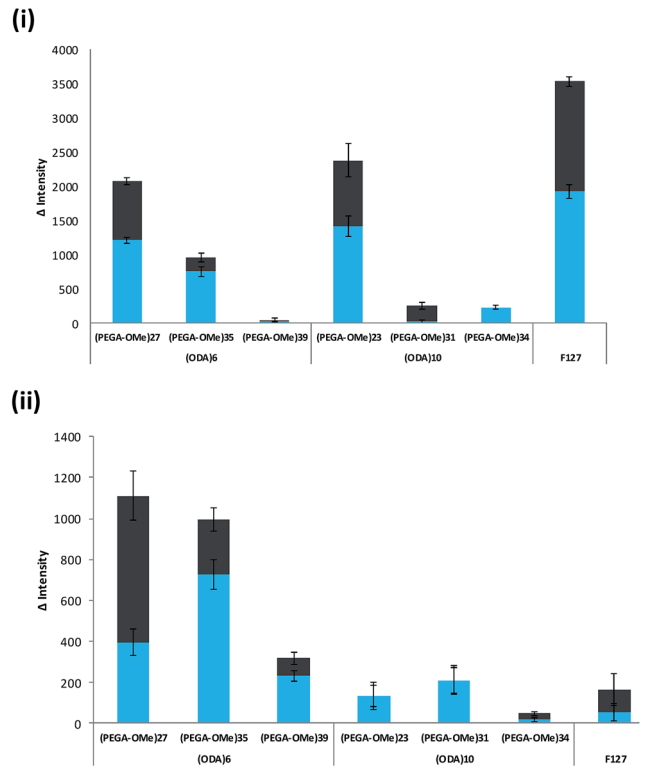

Fig. 2 Accelerated stability assay results for (i) phytantriol and (ii) monoolein dispersions stabilised with 1.5 wt% of reduced: $P(ODA)_6$-*b*-$P(PEGA\text{-}OMe)_{27}$, $P(ODA)_6$-*b*-$P(PEGA\text{-}OMe)_{35}$, $P(ODA)_6$-*b*-$P(PEGA\text{-}OMe)_{39}$, $P(ODA)_{10}$-*b*-$P(PEGA\text{-}OMe)_{23}$, $P(ODA)_{10}$-*b*-$P(PEGA\text{-}OMe)_{31}$, $P(ODA)_{10}$-*b*-$P(PEGA\text{-}OMe)_{34}$ and F127. Samples are initially spun at 645 × *g* for 5 min and then further spun at 796 × *g* for 5 min. ASA results after first spin 645 × *g* are represented by the bottom column (blue color), whilst ASA results after second spin 796 × *g* are represented by the top column (grey colour) see ESI† for other ASA results.

Reduced copolymers were less disruptive to the lyotropic liquid crystalline bicontinuous cubic phase compared to non-reduced copolymers

Phytantriol dispersions stabilised with 1 wt% of non-reduced P(ODA)-*b*-P(PEGA-OMe) brush copolymers, presented a mixed Q_2^D cubic and hexagonal (H_2) phase at room temperature (25 °C) (Fig. 3 and 4(i)).

In fact, all phytantriol dispersions, with each of the six non-reduced P(ODA)-*b*-P(PEGA-OMe) brush copolymers at 0.7 and 1 wt%, possessed the hexagonal (H_2) internal phase at physiological temperature of 37 °C (Fig. 4 and ESI†).

In contrast, phytantriol dispersions stabilised with reduced P(ODA)-*b*-P(PEGA-OMe) brush copolymers with various steric stabiliser concentrations (*i.e.*, 0.1, 0.5, 0.7 and 1 wt% and also with mol equivalent concentrations to F127: 0.7, 1, 1.2, 1.5 and

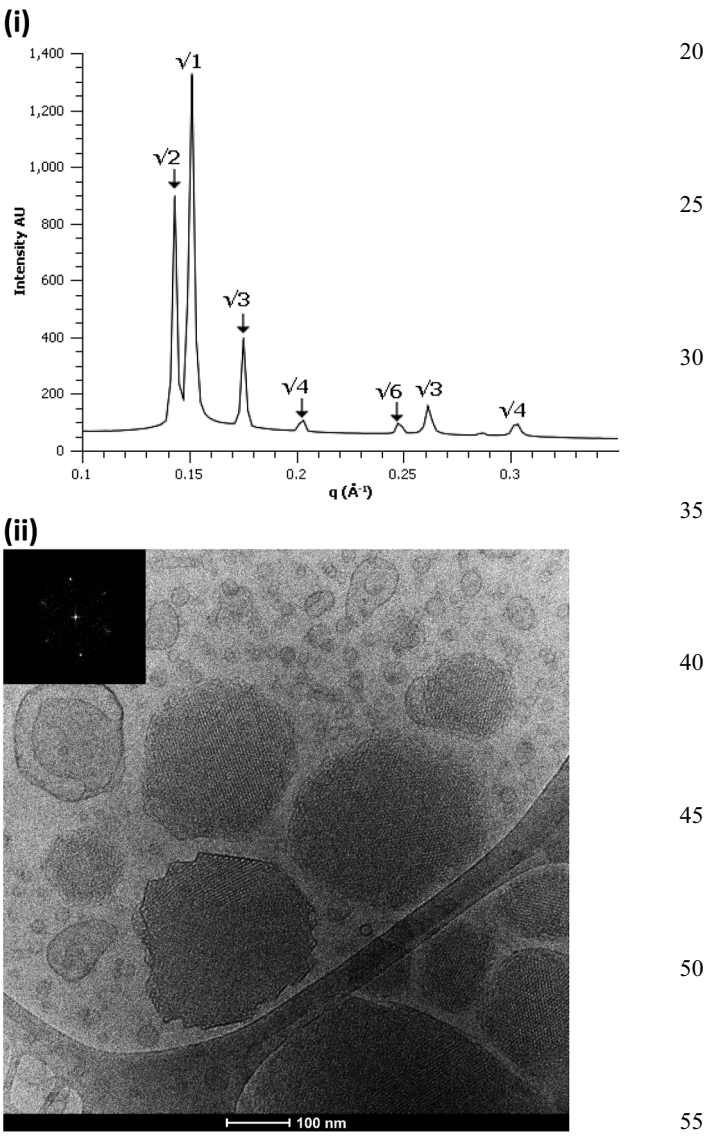

Fig. 3 (i) SAXS diffraction pattern (arrows indicate Q_2^D cubic phase and other peaks indicate H_2 hexagonal phase) and (ii) cryo-TEM image observed in the [111] axis plane for phytantriol dispersion stabilised with 1 wt% non-reduced $P(ODA)_6$-*b*-$P(PEGA\text{-}OMe)_{39}$ copolymer at 25 °C.

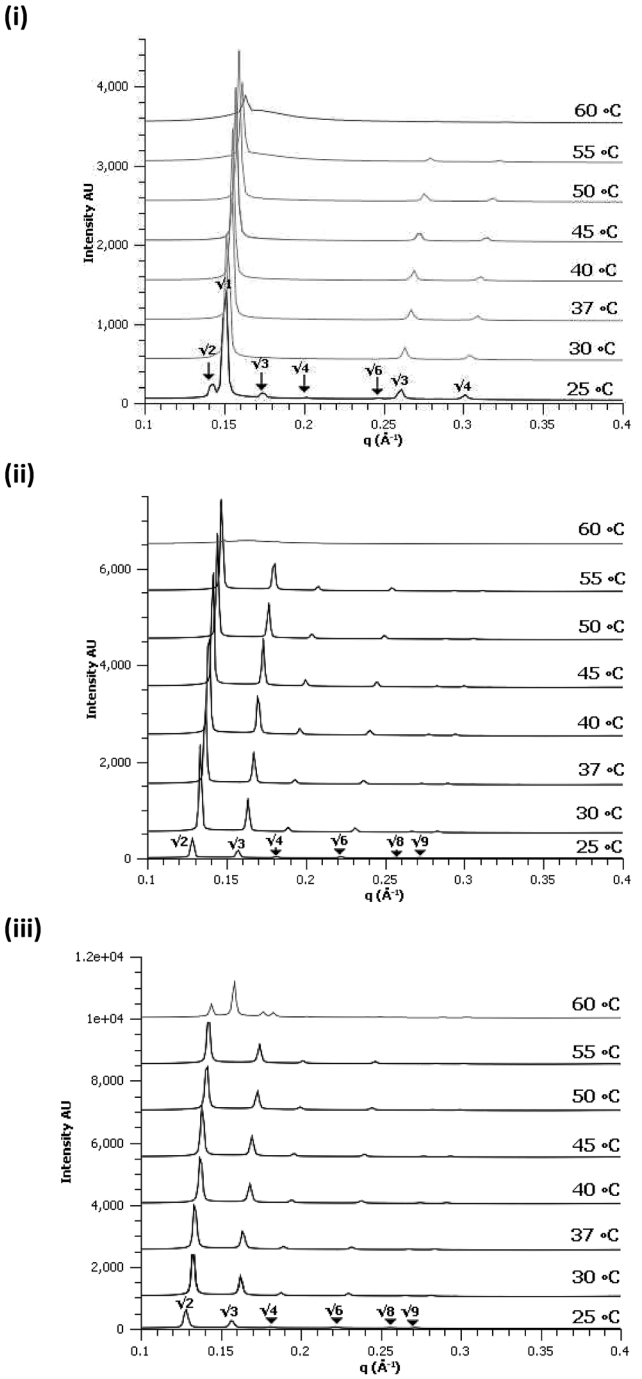

Fig. 4 Stacked SAXS diffraction pattern, at 25 to 60 °C, for phytantriol dispersions stabilised with 1 wt% of (i) non-reduced $P(ODA)_{10}$-*b*-$P(PEGA\text{-}OMe)_{34}$ copolymer, (ii) reduced $P(ODA)_{10}$-*b*-$P(PEGA\text{-}OMe)_{34}$ copolymer and (iii) F127 (control stabiliser). Arrows indicate Q_2^D cubic phase.

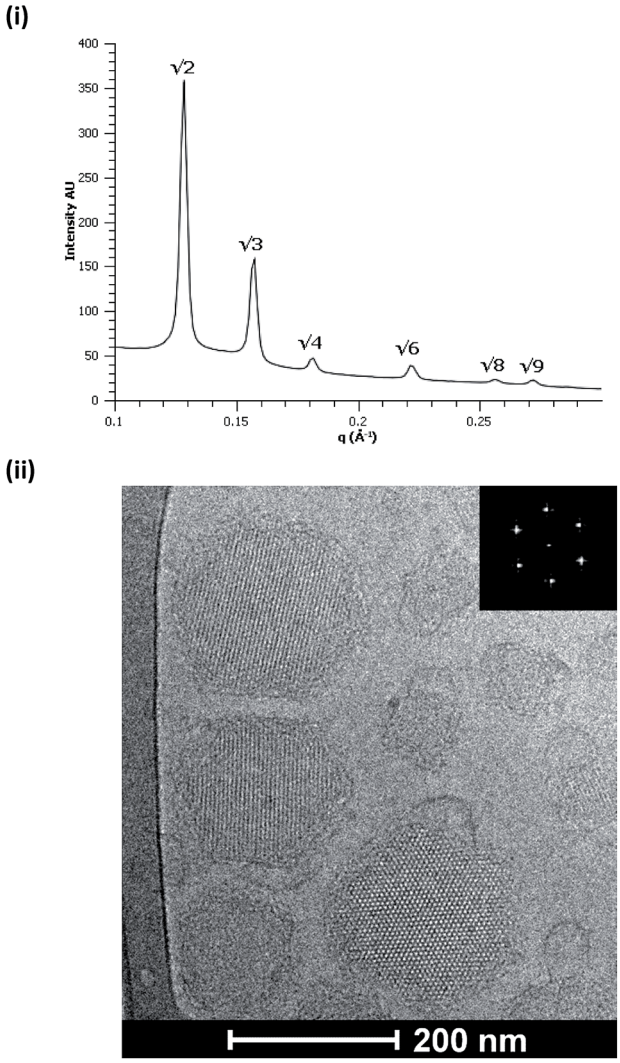

Fig. 5 (i) SAXS diffraction patterns and (ii) cryo-TEM images for phytantriol dispersion stabilised with reduced $P(ODA)_{10}$-*b*-$P(PEGA\text{-}OMe)_{34}$ copolymer at 25 °C using mol equivalent stabiliser concentration to F127 at 1.5 wt%.

2 wt%) were identified to retain the Q_2^D cubic phase at room temperature (25 °C) (Fig. 4 and 5). These phytantriol dispersions had a phase transition temperature from Q_2^D to H_2 at 60 °C, identical to that when stabilised using F127 (Fig. 4). The Q_2^D phytantriol cubosomes stabilised with 1 wt% of $P(ODA)_{10}$-*b*-$P(PEGA\text{-}OMe)_{34}$ had an average lattice parameter of 69.0 Å at 25 °C, which decreased in lattice parameter as the temperature was increased. This result is comparable with literature reports[14,17,19,25] of phytantriol systems stabilised by F127 at the same concentration (*e.g.*, lattice parameter of 68.6 Å at 25 °C).[14]

The reduced P(ODA)-*b*-P(PEGA-OMe) brush copolymers also stabilised monoolein dispersions at various stabiliser concentrations (*i.e.*, mol equivalent concentrations to F127: 0.7, 1, 1.2, 1.5 and 2 wt%) with the internal primitive Q_2^P cubic phase (Fig. 6 and 7). The Q_2^P cubic phase did not change phase as the temperature was increased up to 66 °C while taking SAXS profiles (Fig. 7). This is similar to F127 stabilised monoolein dispersions, which also resulted in a Q_2^P cubic phase, which did not change phase with increasing temperatures up to 66 °C (Fig. 7). The Q_2^P monoolein cubosomes stabilised with 1 wt% of $P(ODA)_{10}$-*b*-$P(PEGA\text{-}OMe)_{34}$ had an average lattice parameter of 149.8 Å at 25 °C, which decreased as the temperature was increased. This result is comparable with literature reports of GMO systems stabilised by F127 at the same concentration (*e.g.*, 130–140 Å at 25 °C).[12,14,17,19,25]

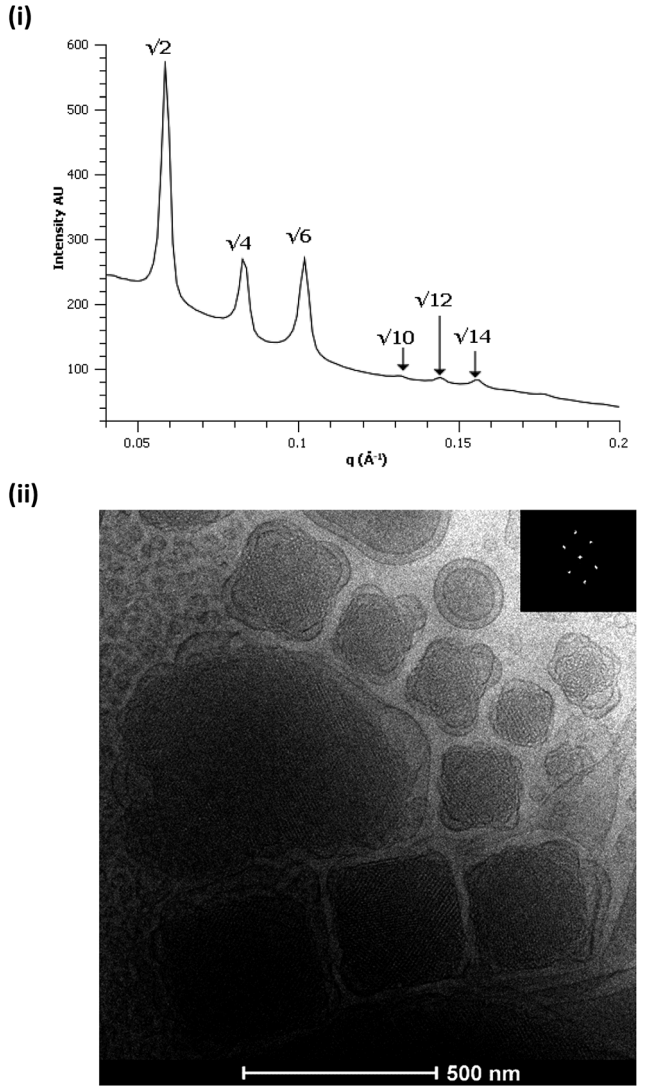

Fig. 6 (i) SAXS diffraction patterns and (ii) cryo-TEM images for monoolein dispersion stabilised with reduced $P(ODA)_{10}$-*b*-$P(PEGA\text{-}OMe)_{34}$ copolymer at 25 °C using mol equivalent stabiliser concentration to F127 at 1.5 wt%.

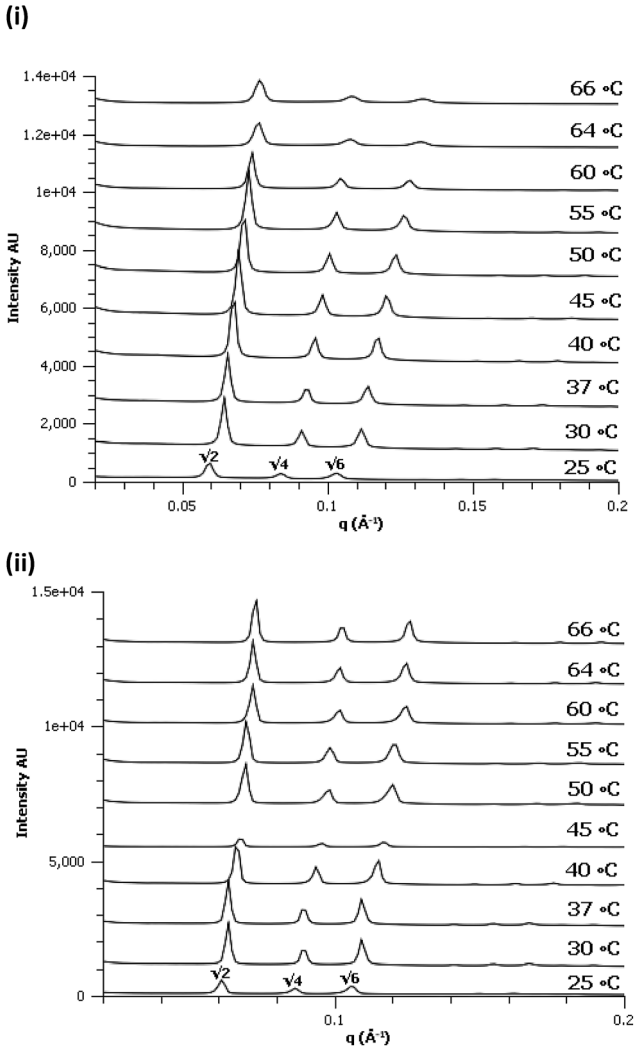

Fig. 7 Stacked SAXS diffraction patterns, at 25 to 66 °C, for monoolein dispersions stabilised with 10 wt% of (i) reduced $P(ODA)_{10}$-*b*-$P(PEGA\text{-}OMe)_{34}$ copolymer or (ii) F127 (control stabiliser).

Cubosomes as well as vesicular structures were observed under cryo-TEM. Although cubosomes of different sizes existed, the majority of the nanostructured particles were approximately 200 nm in diameter as seen in Fig. 5 and 6. The Fourier transform of the internal structure of the particle (Fig. 5ii insert) shows a hexagonal arrangement with interplanar distances of about 6 nm. The internal structure is observed along the [111] axis, and the crystallographic planes observed are of the (110) type. This is compatible with the cubic structure of *Pn*3*m* symmetry with a lattice size of 8.5 nm.

Discussion

The structure of the copolymer used for steric stabilisation of lyotropic liquid crystalline bicontinuous cubic nanostructured particles is important. Although linear block copolymers (*e.g.*, F127) have been commonly/traditionally used as steric stabilisers for cubosomes, this study has shown that more complex polymer designs, such as amphiphilic brush copolymers, can also be a viable alternative structural option for sterically stabilising cubosome dispersions. There are two trends that are prevalent from previous studies[17,18,25,28] for improving the effectiveness of a steric stabiliser, which are gained by altering the structure of the stabiliser and these are: (1) increasing the hydrophilic block length (*i.e.*, increasing the PEG length) and/or (2) increasing the number of hydrophilic blocks (*i.e.*, increasing the number of PEG blocks in the copolymer structure).

The first trend can be seen in the Myrj®, Pluronic® and PEGylated-phytanyl copolymer stabiliser series, whereby increasing the length of the PEG domain on the stabiliser created greater colloidal stability for cubosome dispersions.[18,28] For example, copolymers with 150 PEG units (*i.e.*, Myrj®: PEG-150-stearate) or 132 PEG unit (*i.e.*, Pluronic® F108) were found to be more effective stabilisers than their corresponding copolymers with only 100 PEG units on average (*i.e.*, Myrj® 59

and Pluronic® F127).[18] In agreement with this trend it was observed in this study that increasing the hydrophilic PEGA-OMe block length (*e.g.*, from 23 to 34 PEGA-OMe units) of the brush copolymer stabilisers, also resulted in more effective stabilisation of both phytantriol and monoolein cubosome dispersions. Although the PEG length within the PEGA-OMe 'brush-arms' remained the same (*i.e.*, 9 PEG units on average), increasing the units of PEGA-OMe in the hydrophilic block increases the overall hydrophilicity of the copolymer causing a similar effect to increasing the PEG length of a stabiliser as seen in previous studies.[17,18,25,28]

The latter trend of improving the effectiveness of the steric stabiliser by increasing the number of hydrophilic domains in its amphiphilic structure can also be seen when comparing stabilisers from the Myrj® and Pluronic® series (*i.e.*, Myrj® 59 and Pluronic® F127, which both have 100 PEG units on average). It was found that doubling the number of PEG domains in a steric stabiliser from a linear diblock copolymer (Myrj® 59) with one PEG block, to a triblock copolymer (Pluronic® F127) with two PEG blocks, resulted in improved effectiveness of the steric stabiliser at maintaining colloidal cubosome dispersions.[18] In a similar notion, increasing the PEG density in the structure of a stabiliser by using a brush configuration, such as the P(ODA)-*b*-P(PEGA-OMe) brush copolymers used in this study, has also shown to improve steric stabilisation effectiveness, especially over the triblock copolymer, F127. The improved steric stabiliser effectiveness produced by increasing the quantity/density of PEG arms in the hydrophilic PEGA-OMe brush structure is most likely due to it having a greater surface area-to-volume ratio than a linear copolymer structure, consequently allowing there to be increased steric hindrance coverage for the nanostructured particle.

The length of the hydrophobic domain of the P(ODA)-*b*-P(PEGA-OMe) brush copolymers was also found to influence its effectiveness as a steric stabiliser. When comparing the stabilisation of cubosome dispersions using brush copolymers with a similar hydrophilic domain size but different hydrophobic domain sizes (*e.g.*, $P(ODA)_6$-*b*-$P(PEGA\text{-}OMe)_{27}$ *vs.* $P(ODA)_{10}$-*b*-$P(PEGA\text{-}OMe)_{23}$), it was found that copolymers with a longer hydrophobic domain (*i.e.*, 10 ODA units) were more effective steric stabilisers. Similarly, it has previously been reported that increasing the length of the hydrophobic domain in PEGylated-phytanyl steric stabilisers also results in improved steric stabilisation of cubosome dispersions.[28] Improved stabilisation due to larger hydrophobic domains is likely caused by the stronger affinity created between the stabiliser and the nanostructured particle after increasing the hydrophobicity of the stabiliser.

Although these custom P(ODA)-*b*-P(PEGA-OMe) brush copolymers were synthesised with intent to optimally sterically stabilise monoolein and phytantriol cubosome dispersions, their brush copolymer structure has to our knowledge never been reported for stabilising lyotropic liquid crystalline nanostructured particles. However, this study validates the use and effectiveness of an amphiphilic brush copolymer structure for sterically stabilising cubosome dispersions of different lipid compositions (*i.e.*, both monoolein and phytantriol). Cubosome dispersions stabilised using P(ODA)-*b*-P(PEGA-OMe) brush copolymers were found to have similar phase behaviours to those stabilised with F127. Although the brush copolymer structure is different to that of triblock copolymer (*i.e.*, Pluronic® F127), its ability to sterically stabilise cubosome dispersions could be attributed to the ratio of the amphiphilic domains; with a longer hydrophilic block than hydrophobic block, and a hydrophilic lipophilic balance (HLB) value greater or equal to 17, being favourable characteristics.

This study has also affirmed the possibility of polymerising novel custom steric stabilisers for cubosomes using RAFT polymerisation. However, this polymerisation technique results in the presence of a hydrophobic RAFT end-group. Results have shown that it is important to use the reduced form of the RAFT polymerised stabilisers for achieving optimal stability of phytantriol and/or monoolein cubosome dispersions because the presence of a dodecyl trithiocarbonate RAFT end-group, located on the terminal end of the hydrophilic block, significantly decreases the effectiveness of the P(ODA)-*b*-P(PEGA-OMe) brush copolymers as steric stabilisers. It is likely that due to the hydrophobic nature of the end-group the non-reduced copolymer acted like a triblock copolymer with hydrophobic end blocks, instead of its intended amphiphilic diblock brush copolymer structure. As reported in a previous study the position of the hydrophilic and hydrophobic blocks in an amphiphilic triblock copolymer used as a steric stabiliser is important.[18] Only triblock copolymers with hydrophilic end blocks are effective stabilisers as structures with hydrophobic ends have the tendency to promote aggregation *via* particle bridging.

In addition to discovering a novel steric stabiliser structure, this study allows us to pursue/view custom steric stabilisers as viable options for stabilising lyotropic liquid crystalline nanostructured particles (*e.g.*, cubosomes) for drug delivery systems. Advantages of customising the design of steric stabilisers include the ability to optimise the structure and block lengths for stabilising dispersions for different lipids and also allow options for functionalisation. Functionalisation of the steric stabiliser, specifically attaching a functional/targeting moiety (*e.g.*, antibody fragment) to the terminal end of the hydrophilic domain, would consequently allow site specific targeting (*e.g.*, tumour sites) of the nanostructured particle and thus enable active drug delivery of these systems to be explored. This would also have broader implications and applications of these systems for MRI imaging and drug delivery applications, as these systems are versatile and multifaceted with the capacity to contain either hydrophilic or hydrophobic therapeutics, imaging/contrast agents[45] and other nano-structures (*e.g.*, gold nanorods)[46] that can act as switches for initiating controlled drug release. With the combination of specific site drug delivery and locating its position in the body and also controlling the drug release, the potential for more effective drug treatments with less adverse side-effects is possible.

Conclusion

Poly(octadecyl acrylate)-*block*-poly(polyethylene glycol methyl ether acrylate) amphiphilic brush copolymers are efficient novel

steric stabilisers for lyotropic liquid crystalline nanostructured colloidal particles. When comparing non-reduced and reduced P(ODA)-*b*-P(PEGA-OMe) brush copolymers for their steric stabiliser effectiveness, it was found that reduced brush copolymers, provided significantly better steric stabilisation without the dodecyl trithiocarbonate RAFT end-group. However, the stabilisation of cubosomes using the non-reduced P(ODA)-*b*-P(PEGA-OMe) brush copolymers, demonstrates potential for custom brush copolymer stabilisers to functionalise the RAFT copolymer end-group for active targeting of the cubosome, whilst maintaining steric stabilisation.

The most effective steric stabiliser of the P(ODA)-*b*-P(PEGA-OMe) brush copolymer series, for both phytantriol and monoolein cubosome dispersions, consisted of the longest hydrophilic and hydrophobic brush blocks, $P(ODA)_{10}$-*b*-$P(PEGA\text{-}OMe)_{34}$. However, all six reduced P(ODA)-*b*-P(PEGA-OMe) brush copolymers were able to sterically stabilise monoolein and phytantriol dispersions, with either equivalent or better steric stabiliser effectiveness to the standard control stabiliser, Pluronic® F127. This demonstrates the potential of exploring new custom polymers and/or different copolymer structures for improving the steric stabilisation of lyotropic liquid crystalline nanostructured particles. Furthermore, this study initiates the opportunity to develop novel custom functionalised steric stabilisers for exploring active targeting in these lyotropic liquid crystalline nanostructured particle systems, for drug delivery and MRI imaging applications.

Acknowledgements

Calum J. Drummond was the recipient of an Australian Research Council (ARC) Federation Fellowship. Josephine Y. T. Chong was the recipient of a CSIRO Ph.D. studentship. Xavier Mulet was the recipient of a CSIRO-Monash University Collaborative research postdoctoral fellowship. Ben J. Boyd is the recipient of an ARC Future Fellowship (FT120100697). This research was undertaken in part at the SAXS/WAXS beamline at the Australian Synchrotron, Victoria, Australia.

Notes and references

1 G. Garg and S. Saraf, *Biol. Pharm. Bull.*, 2007, **30**, 350–353.
2 S. Andersson, M. Jacob, S. Lidin and K. Larsson, *Z. Kristallogr.*, 1995, **210**, 315–318.
3 A. Yaghmur and O. Glatter, *Adv. Colloid Interface Sci.*, 2009, **147–148**, 333–342.
4 I. Amar-Yuli, E. Wachtel, E. Ben Shoshan, D. Danino, A. Aserin and N. Garti, *Langmuir*, 2007, **23**, 3637–3645.
5 S. J. Fraser, R. M. Dawson, L. J. Waddington, B. W. Muir, X. Mulet, P. G. Hartley, F. Separovic and A. Polyzos, *Aust. J. Chem.*, 2011, **64**, 46–53.
6 X. Mulet, B. J. Boyd and C. J. Drummond, *J. Colloid Interface Sci.*, 2013, **393**, 1–20.
7 P. T. Spicer, *Curr. Opin. Colloid Interface Sci.*, 2005, **10**, 274–279.
8 C. Fong, T. Le and C. J. Drummond, *Chem. Soc. Rev.*, 2012, **41**, 1297–1322.
9 R. Koynova and M. Caffrey, *Chem. Phys. Lipids*, 2002, **115**, 107–219.
10 J. M. Seddon, E. A. Bartle and J. Mingins, *J. Phys.: Condens. Matter*, 1990, **2**, SA285–SA290.
11 J. M. Seddon, J. L. Hogan, N. A. Warrender and E. Pebaypeyroula, Structural studies of phospholipid cubic phases, 1990. 4
12 J. Gustafsson, H. Ljusberg-Wahren, M. Almgren and K. Larsson, *Langmuir*, 1997, **13**, 6964–6971.
13 P. T. Spicer, K. L. Hayden, M. L. Lynch, A. Ofori-Boateng and J. L. Burns, *Langmuir*, 2001, **17**, 5748–5756.
14 Y. D. Dong, I. Larson, T. Hanley and B. J. Boyd, *Langmuir*, 2006, **22**, 9512–9518.
15 M. Nakano, T. Teshigawara, A. Sugita, W. Leesajakul, A. Taniguchi, T. Kamo, H. Matsuoka and T. Handa, *Langmuir*, 2002, **18**, 9283–9288.
16 T. Kojarunchitt, S. Hook, S. Rizwan, T. Rades and S. Baldursdottir, *Int. J. Pharm.*, 2011, **408**, 20–26.
17 J. Y. T. Chong, X. Mulet, L. J. Waddington, B. J. Boyd and C. J. Drummond, *Soft Matter*, 2011, **7**, 4768–4777.
18 J. Y. T. Chong, X. Mulet, B. J. Boyd and C. J. Drummond, *ACS Comb. Sci.*, 2014, **16**, 205–210.
19 J. L. Zhai, L. Waddington, T. J. Wooster, M. I. Aguilar and B. J. Boyd, *Langmuir*, 2011, **27**, 14757–14766.
20 M. Dulle and O. Glatter, *Langmuir*, 2012, **28**, 1136–1141.
21 F. Muller, A. Salonen and O. Glatter, *J. Colloid Interface Sci.*, 2010, **342**, 392–398.
22 M. Uyama, M. Nakano, J. Yamashita and T. Handa, *Langmuir*, 2009, **25**, 4336–4338.
23 D. Libster, A. Aserin, D. Yariv, G. Shoham and N. Garti, *Colloids Surf., B*, 2009, **74**, 202–215.
24 J. Barauskas, A. Misiunas, T. Gunnarsson, F. Tiberg and M. Johnsson, *Langmuir*, 2006, **22**, 6328–6334.
25 J. Y. T. Chong, X. Mulet, L. J. Waddington, B. J. Boyd and C. J. Drummond, *Langmuir*, 2012, **28**, 9223–9232.
26 X. Mulet, D. F. Kennedy, C. E. Conn, A. Hawley and C. J. Drummond, *Int. J. Pharm.*, 2010, **395**, 290–297.
27 X. Mulet, C. E. Conn, C. Fong, D. F. Kennedy, M. J. Moghaddam and C. J. Drummond, *Acc. Chem. Res.*, 2013, **46**, 1497–1505.
28 J. Y. T. Chong, X. Mulet, D. J. Keddie, L. J. Waddington, S. T. Mudie, B. J. Boyd and C. J. Drummond, *Langmuir*, 2014, submitted. 5
29 D. J. Keddie, *Chem. Soc. Rev.*, 2014, **43**, 496–505.
30 J. Y. T. Chong, D. J. Keddie, A. Postma, X. Mulet, B. J. Boyd and C. J. Drummond, *J. Colloid Interface Sci.*, 2014, submitted.
31 G. Gunkel, M. Weinhart, T. Becherer, R. Haag and W. T. S. Huck, *Biomacromolecules*, 2011, **12**, 4169–4172.
32 I. Banerjee, R. C. Pangule and R. S. Kane, *Adv. Mater.*, 2011, **23**, 690–718.
33 Y. Zhuang, Q. Zhu, C. Tu, D. Wang, J. Wu, Y. Xia, G. Tong, L. He, B. Zhu, D. Yan and X. Zhu, *J. Mater. Chem.*, 2012, **22**, 23852–23860.
34 C. Siegers, M. Biesalski and R. Haag, *Chem.–Eur. J.*, 2004, **10**, 2831–2838.

35 R. K. Kainthan and D. E. Brooks, *Biomaterials*, 2007, **28**, 4779–4787.
36 K. Knop, R. Hoogenboom, D. Fischer and U. S. Schubert, *Angew. Chem., Int. Ed.*, 2010, **49**, 6288–6308.
37 M. Calderón, M. A. Quadir, S. K. Sharma and R. Haag, *Adv. Mater.*, 2010, **22**, 190–218.
38 K. G. Neoh and E. T. Kang, *Polym. Chem.*, 2011, **2**, 747–759.
39 Z. Amoozgar and Y. Yeo, *Wiley Interdiscip. Rev.: Nanomed. Nanobiotechnol.*, 2012, **4**, 219–233.
40 K. Maruyama, S. Okuizumi, O. Ishida, H. Yamauchi, H. Kikuchi and M. Iwatsuru, *Int. J. Pharm.*, 1994, **111**, 103–107.
41 A. M. Hofmann, F. Wurm, E. Hühn, T. Nawroth, P. Langguth and H. Frey, *Biomacromolecules*, 2010, **11**, 568–574.
42 A. V. Kabanov, E. V. Batrakova, N. S. Meliknubarov, N. A. Fedoseev, T. Y. Dorodnich, V. Y. Alakhov, V. P. Chekhonin, I. R. Nazarova and V. A. Kabanov, *J. Controlled Release*, 1992, **22**, 141–157.
43 N. M. Kirby, S. T. Mudie, A. M. Hawley, D. J. Cookson, H. D. T. Mertens, N. Cowieson and V. Samardzic-Boban, *J. Appl. Crystallogr.*, 2013, **46**, 1670–1680.
44 J. M. Seddon, A. M. Squires, C. E. Conn, O. Ces, A. J. Heron, X. Mulet, G. C. Shearman and R. H. Templer, *Philos. Trans. R. Soc., A*, 2006, **364**, 2635–2655.
45 B. W. Muir, D. P. Acharya, D. F. Kennedy, X. Mulet, R. A. Evans, S. M. Pereira, K. L. Wark, B. J. Boyd, T. H. Nguyen, T. M. Hinton, L. J. Waddington, N. Kirby, D. K. Wright, H. X. Wang, G. E. Egan and B. A. Moffat, *Biomaterials*, 2012, **33**, 2723–2733.
46 W.-K. Fong, T. L. Hanley, B. Thierry, N. Kirby, L. J. Waddington and B. J. Boyd, *Langmuir*, 2012, **28**, 14450–14460.

Supplementary Information

Novel RAFT amphiphilic brush copolymer steric stabilizers for cubosomes: Poly(octadecyl acrylate)-*block*-poly(polyethylene glycol methyl ether acrylate)

Josephine Y.T. Chong, Xavier Mulet, Almar Postma, Daniel J. Keddie, Lynne J. Waddington, Ben J. Boyd, Calum J. Drummond

Visual assessment of reduced P(ODA)-*b*-P(PEGA-OMe) stabilized monoolein and phytantriol dispersions used for ASA

Stabilizer	Lipid	Stabilizer Concentration				
		0.7 Mol eq.	1 Mol eq.	1.2 Mol eq.	1.5 Mol eq.	2 Mol eq.
$P(ODA)_{6}$-*b*-$P(PEGA\text{-}OMe)_{27}$	PHYT	+++	+++	+++	+++	+++
	GMO	++	+++	+++	+++	+++
$P(ODA)_{6}$-*b*-$P(PEGA\text{-}OMe)_{35}$	PHYT	+++	+++	+++	+++	+++
	GMO	+++	+++	+++	+++	+++
$P(ODA)_{6}$-*b*-$P(PEGA\text{-}OMe)_{39}$	PHYT	+++	+++	+++	+++	+++
	GMO	+++	+++	+++	+++	+++
$P(ODA)_{10}$-*b*-$P(PEGA\text{-}OMe)_{23}$	PHYT	+++	+++	+++	+++	+++
	GMO	++	+++	+++	+++	+++
$P(ODA)_{10}$-*b*-$P(PEGA\text{-}OMe)_{31}$	PHYT	+++	+++	+++	+++	+++
	GMO	+++	+++	+++	+++	+++
$P(ODA)_{10}$-*b*-$P(PEGA\text{-}OMe)_{34}$	PHYT	+++	+++	+++	+++	+++
	GMO	+++	+++	+++	+++	+++
Control F127	PHYT	+++	+++	+++	+++	+++
	GMO	++	+++	+++	+++	+++

Table 2. Visual assessment of the stability of phytantriol and monoolein dispersions using 0.7, 1, 1.2, 1.5 and 2 mol% P(ODA)-*b*-P(PEGA-OMe) copolymers as steric stabilizer. Key: +++ milky sample with no visible aggregates. ++ milky sample with few visible aggregates, + milky/cloudy sample with aggregates, - translucent sample with large aggregates [not used in ASA or SAXS] Note: 0.7 Mol eq. is the Mol equivalent concentration to F127 at 0.7 wt% stabilizer concentration

Accelerated stability assay results for P(ODA)-*b*-P(PEGA-OMe) stabilized dispersions

i. Phytantriol dispersions

Results: Bottom (blue) column 645 xg, Top (grey) column 796 xg

Stabilizer concentration

0.7 wt %

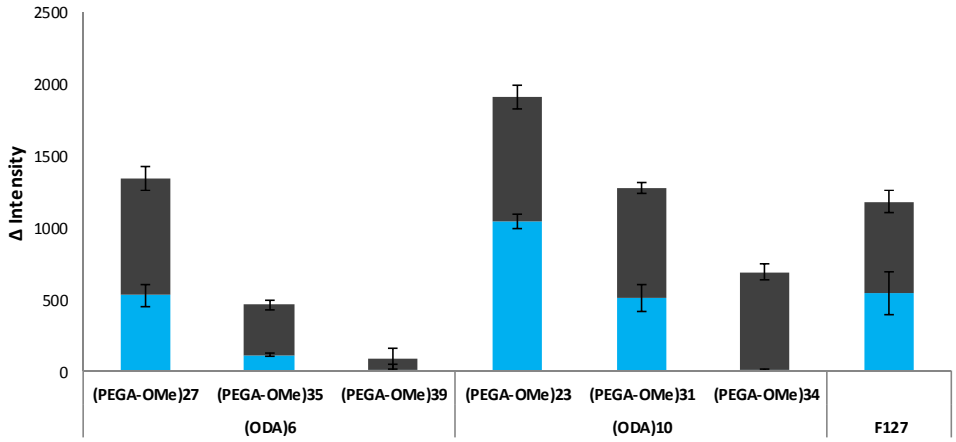

1 wt %

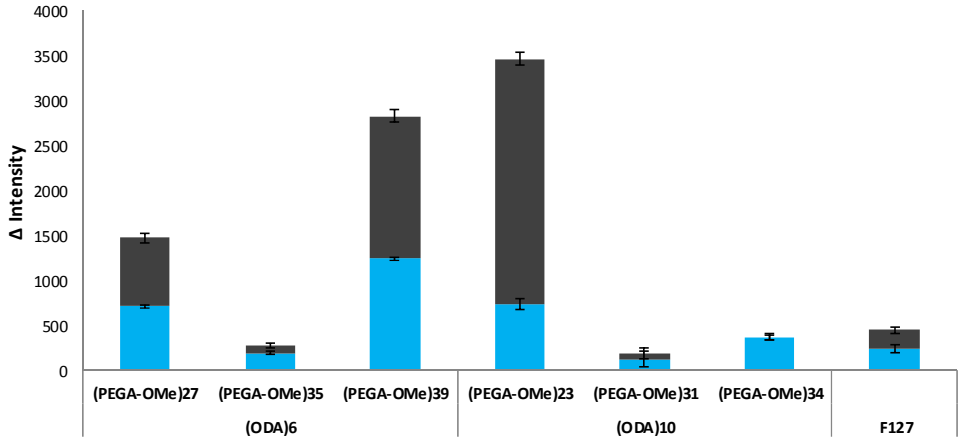

1.2 wt %

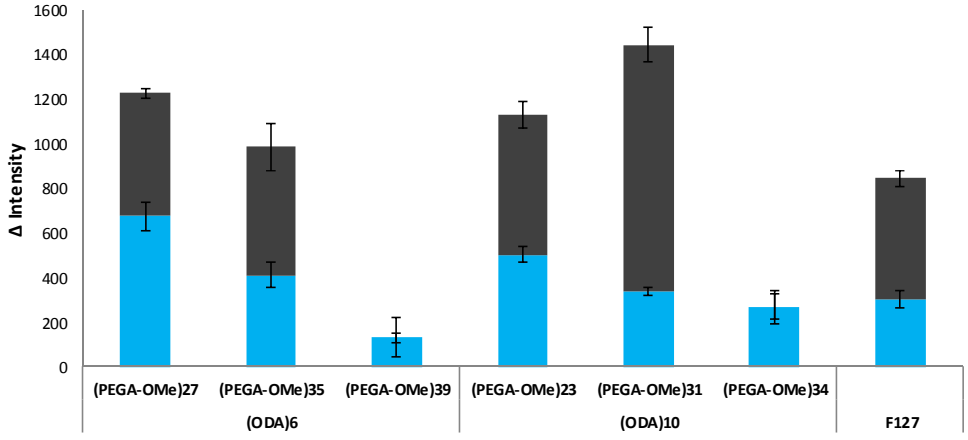

1.5 wt %

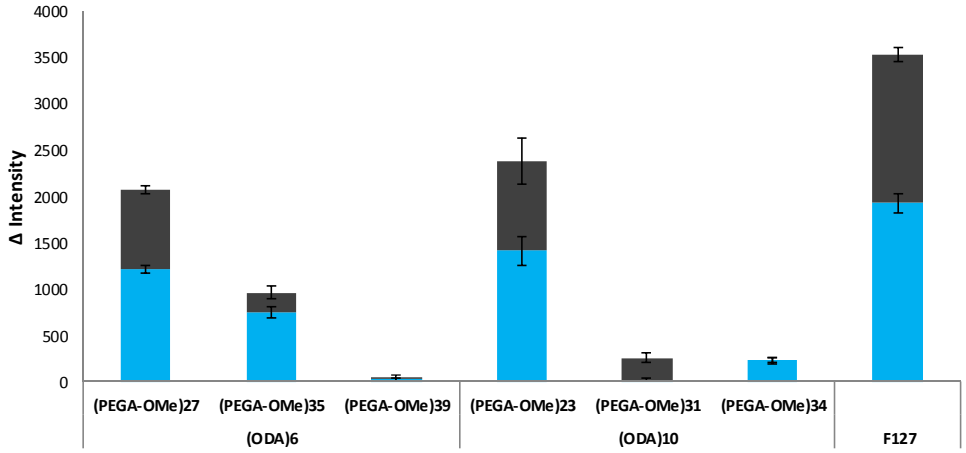
4000
3500
3000
2500
2000
1500
1000
500
0
Δ Intensity
(PEGA-OMe)27
(PEGA-OMe)35
(PEGA-OMe)39
(PEGA-OMe)23
(PEGA-OMe)31
(PEGA-OMe)34
(ODA)6
(ODA)10
F127

2 wt %

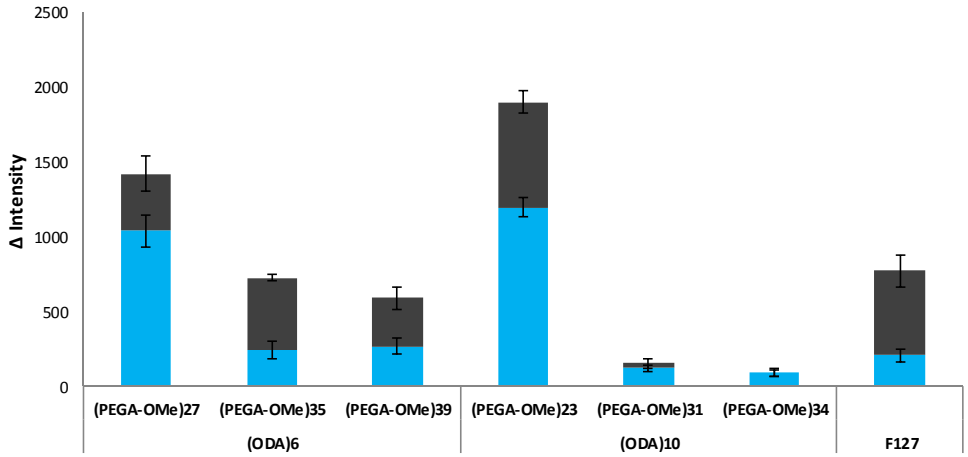
2500
2000
1500
1000
500
0
Δ Intensity
(PEGA-OMe)27
(PEGA-OMe)35
(PEGA-OMe)39
(PEGA-OMe)23
(PEGA-OMe)31
(PEGA-OMe)34
(ODA)6
(ODA)10
F127

ii. Monoolein dispersions

Stabilizer concentration

0.7 wt %

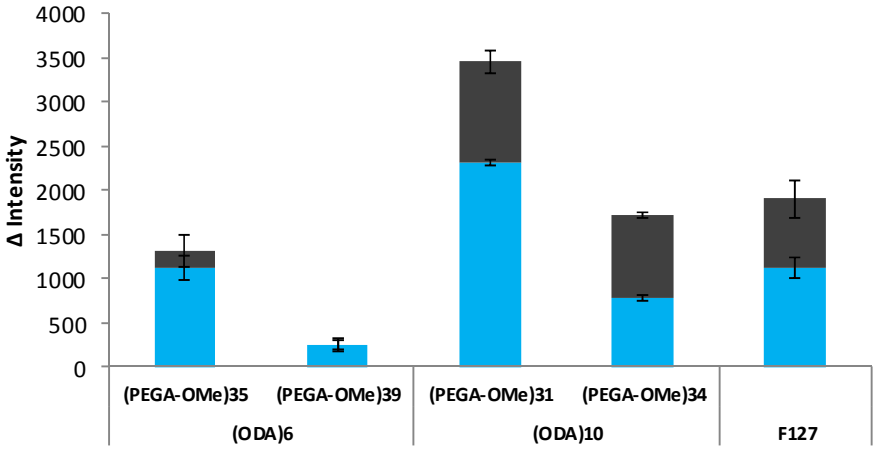

1 wt %

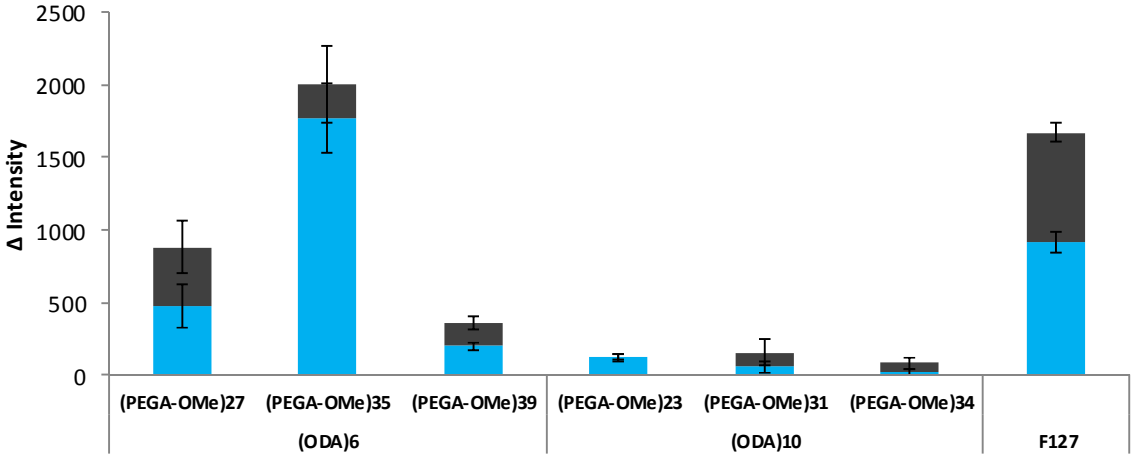

1.2 wt %

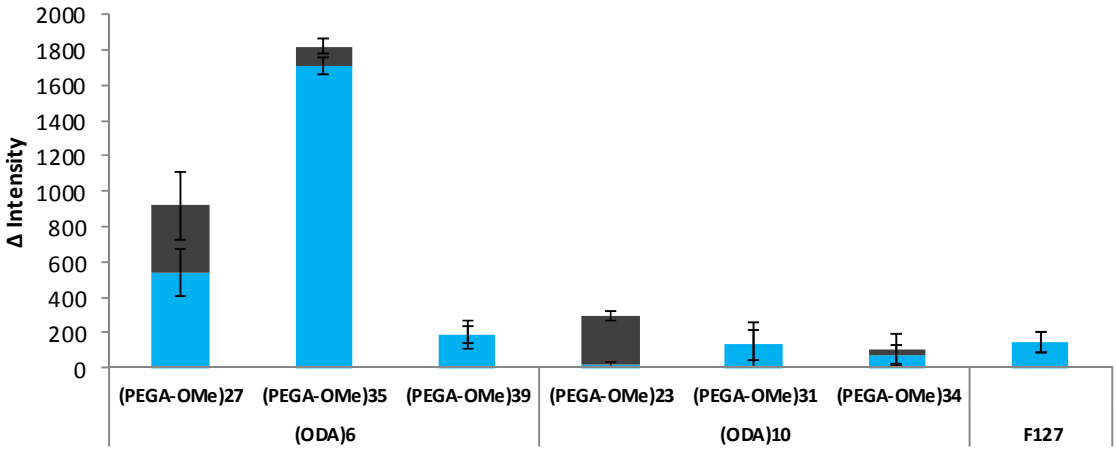

1.5 wt %

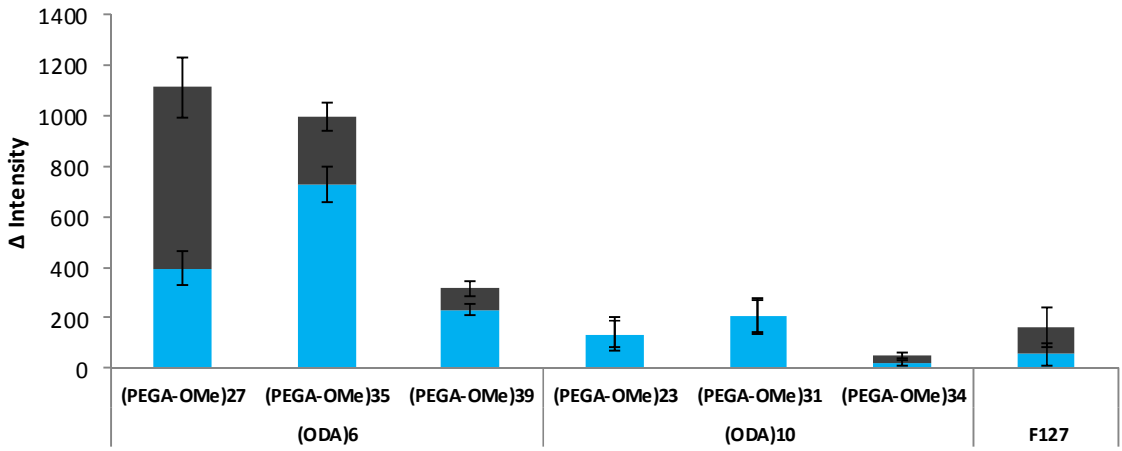
Δ Intensity
1400
1200
1000
800
600
400
200
0
(PEGA-OMe)27
(PEGA-OMe)35
(PEGA-OMe)39
(PEGA-OMe)23
(PEGA-OMe)31
(PEGA-OMe)34
(ODA)6
(ODA)10
F127

2 wt %

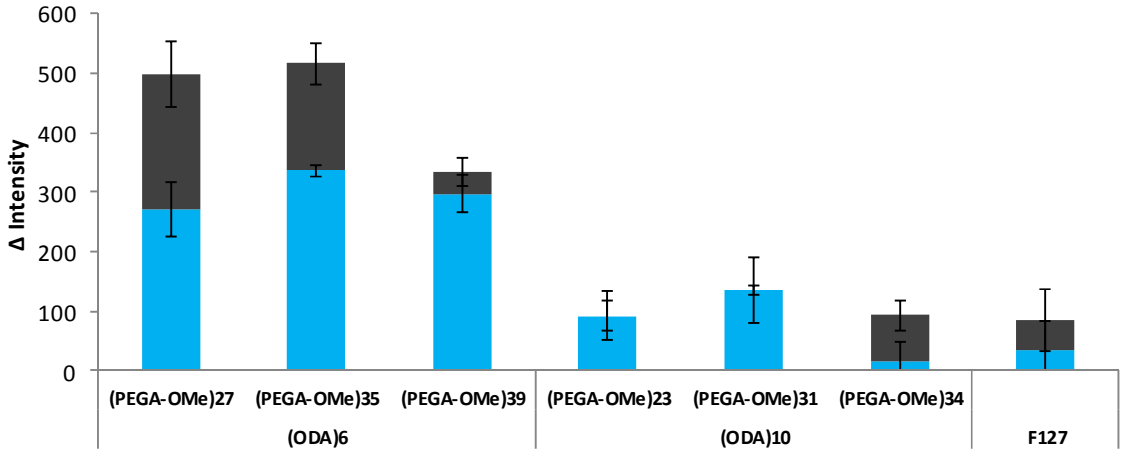
Δ Intensity
600
500
400
300
200
100
0
(PEGA-OMe)27
(PEGA-OMe)35
(PEGA-OMe)39
(PEGA-OMe)23
(PEGA-OMe)31
(PEGA-OMe)34
(ODA)6
(ODA)10
F127

Lyotropic liquid phases of non reduced and reduced P(ODA)-*b*-P(PEGA-OMe) stabilized phytantriol dispersions

i. $P(ODA)_6$-*b*-P(PEGA-OMe) copolymers

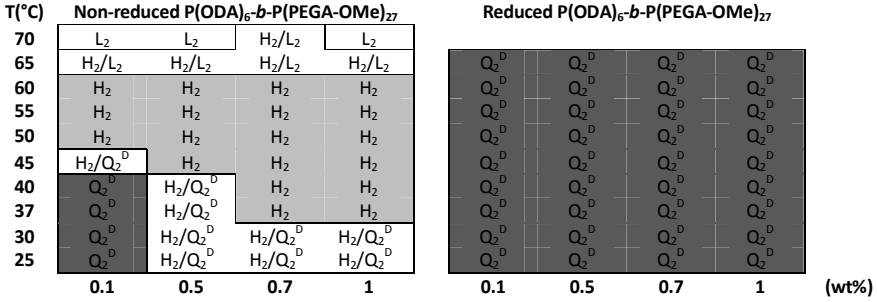

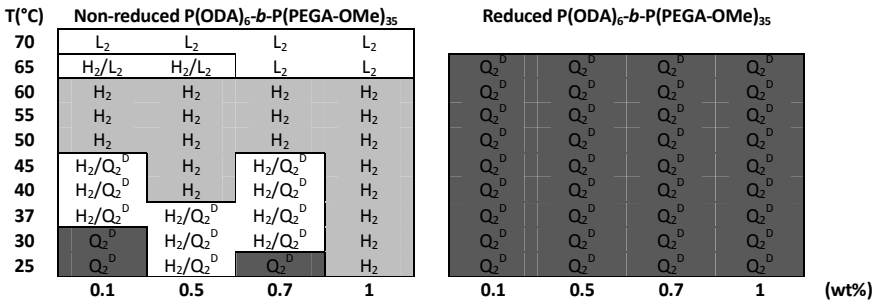

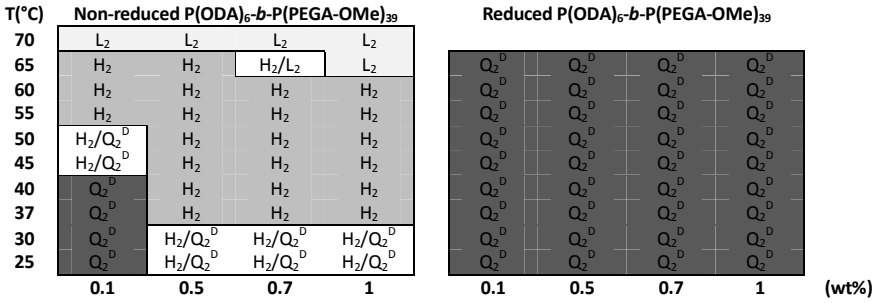

ii. $P(ODA)_{10}$-*b*-P(PEGA-OMe) copolymers

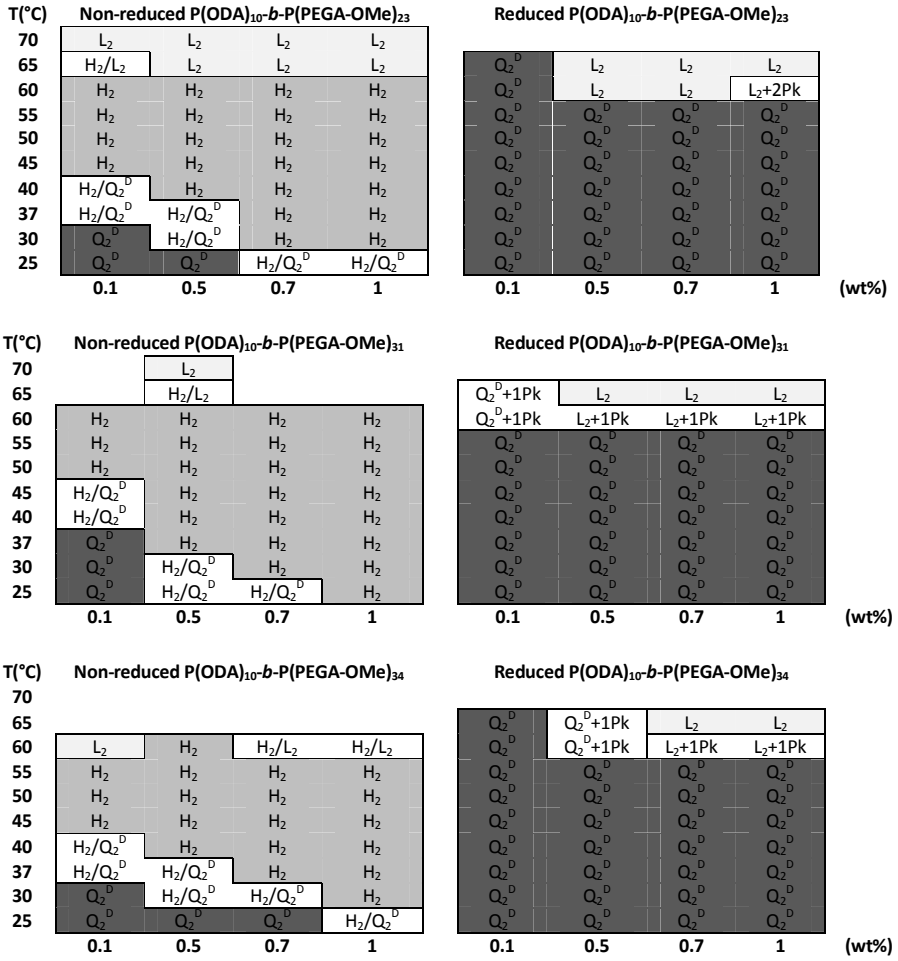

Lyotropic liquid phase diagrams of reduced P(ODA)-*b*-P(PEGA-OMe) stabilized dispersions

i. P(ODA)$_6$-*b*-P(PEGA-OMe) copolymers

Reduced P(ODA)$_6$-*b*-P(PEGA-OMe)$_{27}$

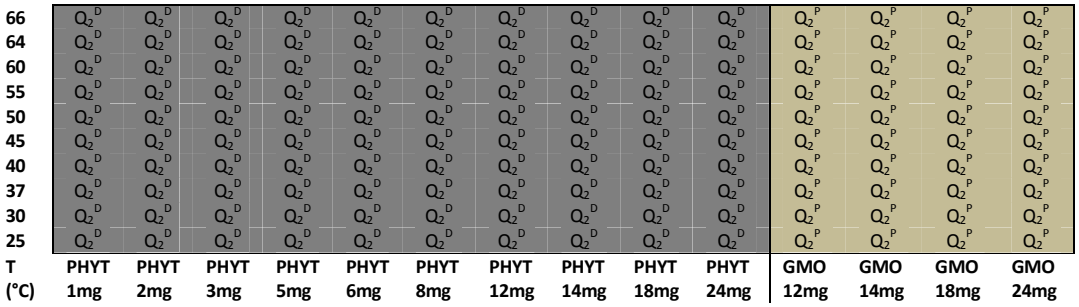

Reduced P(ODA)$_6$-*b*-P(PEGA-OMe)$_{35}$

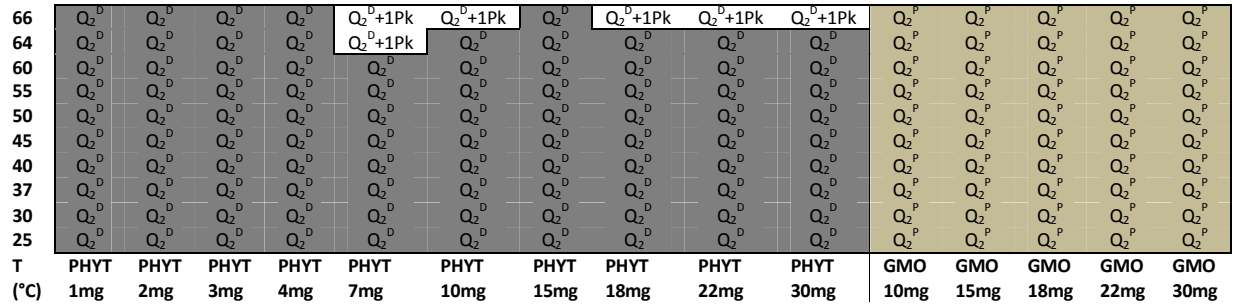

Reduced P(ODA)$_6$-*b*-P(PEGA-OMe)$_{39}$

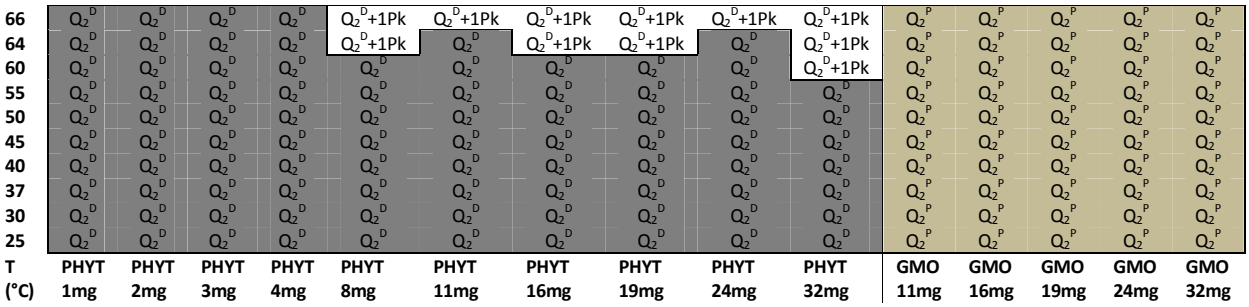

ii. P(ODA)$_{10}$-*b*-P(PEGA-OMe) copolymers

Reduced P(ODA)$_{10}$-*b*-P(PEGA-OMe)$_{23}$

66	Q_2^D	L_2	L_2	L_2	L_2	L_2	L_2	L_2	Q_2^D/L_2	Q_2^D/L_2	Q_2^P/Q_2^D	Q_2^P/Q_2^D	Q_2^P	Q_2^P
64	Q_2^D	L_2	L_2	Q_2^D/L_2	L_2	L_2	L_2	L_2	Q_2^D/L_2	Q_2^D/L_2	Q_2^P	Q_2^P+1Pk	Q_2^P	Q_2^P
60	Q_2^D	L_2	L_2	Q_2^D/L_2	L_2	L_2	L_2	L_2	Q_2^D/L_2	Q_2^D/L_2	Q_2^P	Q_2^P	Q_2^P	Q_2^P
55	Q_2^D	Q_2^D	Q_2^D	Q_2^D	Q_2^D	Q_2^D	Q_2^D	Q_2^D	Q_2^D	Q_2^D	Q_2^P	Q_2^P	Q_2^P	Q_2^P
50	Q_2^D	Q_2^D	Q_2^D	Q_2^D	Q_2^D	Q_2^D	Q_2^D	Q_2^D	Q_2^D	Q_2^D	Q_2^P	Q_2^P	Q_2^P	Q_2^P
45	Q_2^D	Q_2^D	Q_2^D	Q_2^D	Q_2^D	Q_2^D	Q_2^D	Q_2^D	Q_2^D	Q_2^D	Q_2^P	Q_2^P	Q_2^P	Q_2^P
40	Q_2^D	Q_2^D	Q_2^D	Q_2^D	Q_2^D	Q_2^D	Q_2^D	Q_2^D	Q_2^D	Q_2^D	Q_2^P	Q_2^P	Q_2^P	Q_2^P
37	Q_2^D	Q_2^D	Q_2^D	Q_2^D	Q_2^D	Q_2^D	Q_2^D	Q_2^D	Q_2^D	Q_2^D	Q_2^P	Q_2^P	Q_2^P	Q_2^P
30	Q_2^D	Q_2^D	Q_2^D	Q_2^D	Q_2^D	Q_2^D	Q_2^D	Q_2^D	Q_2^D	Q_2^D	Q_2^P	Q_2^P	Q_2^P	Q_2^P
25	Q_2^D	Q_2^D	Q_2^D	Q_2^D	Q_2^D	Q_2^D	Q_2^D	Q_2^D	Q_2^D	Q_2^D	Q_2^P	Q_2^P	Q_2^P	Q_2^P
T	PHYT	PHYT	PHYT	PHYT	PHYT	PHYT	PHYT	PHYT	PHYT	PHYT	GMO	GMO	GMO	GMO
(°C)	1mg	2mg	3mg	5mg	5.8mg	8mg	11mg	13mg	17mg	23mg	11mg	13mg	17mg	23mg

Reduced P(ODA)$_{10}$-*b*-P(PEGA-OMe)$_{31}$

66	Q_2^D	Q_2^D+1Pk	L_2	L_2	L_2	L_2	L_2	L_2	L_2	L_2	L_2	Q_2^P	Q_2^P	Q_2^P	Q_2^P	Q_2^P
64	Q_2^D	Q_2^D+1Pk	L_2	L_2	L_2	L_2	L_2	L_2	L_2	L_2	L_2	Q_2^P	Q_2^P	Q_2^P	Q_2^P	Q_2^P
60	Q_2^D	Q_2^D+1Pk	L_2+1Pk	L_2+1Pk	L_2+1Pk	L_2+1Pk	L_2	L_2	L_2	L_2	L_2	Q_2^P	Q_2^P	Q_2^P	Q_2^P	Q_2^P
55	Q_2^D	Q_2^D	Q_2^D	Q_2^D	Q_2^D	Q_2^D	Q_2^D	Q_2^D	Q_2^D	Q_2^D	Q_2^D	Q_2^P	Q_2^P	Q_2^P	Q_2^P	Q_2^P
50	Q_2^D	Q_2^D	Q_2^D	Q_2^D	Q_2^D	Q_2^D	Q_2^D	Q_2^D	Q_2^D	Q_2^D	Q_2^D	Q_2^P	Q_2^P	Q_2^P	Q_2^P	Q_2^P
45	Q_2^D	Q_2^D	Q_2^D	Q_2^D	Q_2^D	Q_2^D	Q_2^D	Q_2^D	Q_2^D	Q_2^D	Q_2^D	Q_2^P	Q_2^P	Q_2^P	Q_2^P	Q_2^P
40	Q_2^D	Q_2^D	Q_2^D	Q_2^D	Q_2^D	Q_2^D	Q_2^D	Q_2^D	Q_2^D	Q_2^D	Q_2^D	Q_2^P	Q_2^P	Q_2^P	Q_2^P	Q_2^P
37	Q_2^D	Q_2^D	Q_2^D	Q_2^D	Q_2^D	Q_2^D	Q_2^D	Q_2^D	Q_2^D	Q_2^D	Q_2^D	Q_2^P	Q_2^P	Q_2^P	Q_2^P	Q_2^P
30	Q_2^D	Q_2^D	Q_2^D	Q_2^D	Q_2^D	Q_2^D	Q_2^D	Q_2^D	Q_2^D	Q_2^D	Q_2^D	Q_2^P	Q_2^P	Q_2^P	Q_2^P	Q_2^P
25	Q_2^D	Q_2^D	Q_2^D	Q_2^D	Q_2^D	Q_2^D	Q_2^D	Q_2^D	Q_2^D	Q_2^D	Q_2^D	Q_2^P	Q_2^P	Q_2^P	Q_2^P	Q_2^P
T	PHYT	PHYT	PHYT	PHYT	PHYT	PHYT	PHYT	PHYT	PHYT	PHYT	PHYT	GMO	GMO	GMO	GMO	GMO
(°C)	1mg	2mg	3mg	4mg	5mg	7mg	10mg	14mg	17mg	21mg	29mg	10mg	17mg	18mg	21mg	29mg

Reduced P(ODA)$_{10}$-*b*-P(PEGA-OMe)$_{34}$

66	Q_2^D	Q_2^D+1Pk	L_2	L_2	L_2	L_2	L_2	L_2	L_2	L_2	Q_2^P+1Pk	Q_2^P	Q_2^P	Q_2^P	Q_2^P	Q_2^P
64	Q_2^D	Q_2^D+1Pk	L_2	L_2	L_2	L_2	L_2	L_2	L_2	L_2	Q_2^P	Q_2^P	Q_2^P	Q_2^P	Q_2^P	Q_2^P
60	Q_2^D	Q_2^D+1Pk	L_2+1Pk	L_2+1Pk	L_2+1Pk	L_2+1Pk	L_2+1Pk	L_2	L_2	L_2	Q_2^P	Q_2^P	Q_2^P	Q_2^P	Q_2^P	Q_2^P
55	Q_2^D	Q_2^D	Q_2^D	Q_2^D	Q_2^D	Q_2^D	Q_2^D	Q_2^D	Q_2^D	Q_2^D	Q_2^P	Q_2^P	Q_2^P	Q_2^P	Q_2^P	Q_2^P
50	Q_2^D	Q_2^D	Q_2^D	Q_2^D	Q_2^D	Q_2^D	Q_2^D	Q_2^D	Q_2^D	Q_2^D	Q_2^P	Q_2^P	Q_2^P	Q_2^P	Q_2^P	Q_2^P
45	Q_2^D	Q_2^D	Q_2^D	Q_2^D	Q_2^D	Q_2^D	Q_2^D	Q_2^D	Q_2^D	Q_2^D	Q_2^P	Q_2^P	Q_2^P	Q_2^P	Q_2^P	Q_2^P
40	Q_2^D	Q_2^D	Q_2^D	Q_2^D	Q_2^D	Q_2^D	Q_2^D	Q_2^D	Q_2^D	Q_2^D	Q_2^P	Q_2^P	Q_2^P	Q_2^P	Q_2^P	Q_2^P
37	Q_2^D	Q_2^D	Q_2^D	Q_2^D	Q_2^D	Q_2^D	Q_2^D	Q_2^D	Q_2^D	Q_2^D	Q_2^P	Q_2^P	Q_2^P	Q_2^P	Q_2^P	Q_2^P
30	Q_2^D	Q_2^D	Q_2^D	Q_2^D	Q_2^D	Q_2^D	Q_2^D	Q_2^D	Q_2^D	Q_2^D	Q_2^P	Q_2^P	Q_2^P	Q_2^P	Q_2^P	Q_2^P
25	Q_2^D	Q_2^D	Q_2^D	Q_2^D	Q_2^D	Q_2^D	Q_2^D	Q_2^D	Q_2^D	Q_2^D	Q_2^P	Q_2^P	Q_2^P	Q_2^P	Q_2^P	Q_2^P
T	PHYT	PHYT	PHYT	PHYT	PHYT	PHYT	PHYT	PHYT	PHYT	PHYT	GMO	GMO	GMO	GMO	GMO	
(°C)	1mg	2mg	3mg	4mg	7mg	10mg	15mg	18mg	23mg	31mg	10mg	15mg	18mg	23mg	31mg	

Small Angle X-ray Scattering (SAXS) & Dynamic Light Scattering (DLS) data

Stabilizer					Sol		SAXS		DLS	
P(ODA)-*b*-P(PEGA-OMe)	**ODA (units)**	**PEGA (units)**	**Conc (wt%)**	**Lipid**	**500µl**	**Temp (°C)**	**Phase**	**Lattice Parameter (Å)**	**Z-Ave (nm)**	**PDI**
			1	PHYT	PBS	25	Q_2^D/H_2	62.39/41.62		
$P(ODA)_{6}$-*b*-$P(PEGA\text{-}OMe)_{27}$ (Non-reduced)	**5.6**	27.1	1	PHYT	PBS	30	Q_2^D/H_2	61.65/41.32	109.9	3.94E-01
			1	PHYT	PBS	37	H_2	40.82		
			1	PHYT	PBS	40	H_2	40.55		
			1	PHYT	PBS	45	H_2	40.14		
			1	PHYT	PBS	50	H_2	39.78		
			1	PHYT	PBS	55	H_2	39.44		
			1	PHYT	PBS	60	H_2	39.04		
			1	PHYT	PBS	65	H_2/Broad (L_α)	38.26		
			1	PHYT	PBS	70	Broad (L_α)	-		
			1	PHYT	PBS	25	H_2	41.17		
$P(ODA)_{6}$-*b*-$P(PEGA\text{-}OMe)_{35}$ (Non-reduced)	**5.6**	35.1	1	PHYT	PBS	30	H_2	40.69	236.4	Multi-modal
			1	PHYT	PBS	37	H_2	40.13		
			1	PHYT	PBS	40	H_2	39.90		
			1	PHYT	PBS	45	H_2	39.50		
			1	PHYT	PBS	50	H_2	39.15		
			1	PHYT	PBS	55	H_2	38.77		
			1	PHYT	PBS	60	H_2	38.37		
			1	PHYT	PBS	65	Broad (L_α)	-		
			1	PHYT	PBS	70	Broad (L_α)	-		
			1	PHYT	PBS	25	Q_2^D/H_2	62.13/41.59		
$P(ODA)_{6}$-*b*-$P(PEGA\text{-}OMe)_{39}$ (Non-reduced)	**5.6**	38.7	1	PHYT	PBS	30	Q_2^D/H_2	61.23/41.14	269.1	Multi-modal
			1	PHYT	PBS	37	H_2	40.66		
			1	PHYT	PBS	40	H_2	40.43		
			1	PHYT	PBS	45	H_2	40.03		
			1	PHYT	PBS	50	H_2	39.62		
			1	PHYT	PBS	55	H_2	39.35		
			1	PHYT	PBS	60	H_2	38.89		
			1	PHYT	PBS	65	Broad (L_α)	-		
			1	PHYT	PBS	70	Broad (L_α)	-		
			1	PHYT	PBS	25	Q_2^D/H_2	62.20/41.64		
$P(ODA)_{10}$-*b*-$P(PEGA\text{-}OMe)_{23}$ (Non-reduced)	**9.9**	23.1	1	PHYT	PBS	30	H_2	41.25	338.1	Multi-modal
			1	PHYT	PBS	37	H_2	40.69		
			1	PHYT	PBS	40	H_2	40.47		
			1	PHYT	PBS	45	H_2	40.05		
			1	PHYT	PBS	50	H_2	39.59		
			1	PHYT	PBS	55	H_2	39.15		
			1	PHYT	PBS	60	H_2	38.74		
			1	PHYT	PBS	65	Broad (L_α)	-		
			1	PHYT	PBS	70	Broad (L_α)	-		
			1	PHYT	PBS	25	H_2	41.68		
$P(ODA)_{10}$-*b*-$P(PEGA\text{-}OMe)_{31}$ (Non-reduced)	**9.9**	30.7	1	PHYT	PBS	30	H_2	41.27	260.4	Multi-modal
			1	PHYT	PBS	37	H_2	40.66		
			1	PHYT	PBS	40	H_2	40.35		
			1	PHYT	PBS	45	H_2	39.72		
			1	PHYT	PBS	50	H_2	39.32		
			1	PHYT	PBS	55	H_2	38.75		
			1	PHYT	PBS	60	H_2	38.14		
			1	PHYT	PBS	25	Q_2^D/H_2	62.52/41.79		
$P(ODA)_{10}$-*b*-$P(PEGA\text{-}OMe)_{34}$ (Non-reduced)	**9.9**	33.5	1	PHYT	PBS	30	H_2	41.36	285.9	Multi-modal
			1	PHYT	PBS	37	H_2	40.73		
			1	PHYT	PBS	40	H_2	40.50		
			1	PHYT	PBS	45	H_2	40.00		
			1	PHYT	PBS	50	H_2	39.47		
			1	PHYT	PBS	55	H_2	38.98		
			1	PHYT	PBS	60	H_2/Broad (L_α)	38.49		

Stabilizer					Sol		SAXS		DLS	
P(ODA)-*b*-P(PEGA-OMe)	**ODA (units)**	**PEGA (units)**	**Conc (wt%)**	**Lipid**	**500µl**	**Temp (°C)**	**Phase**	**Lattice Parameter (Å)**	**Z-Ave (nm)**	**PDI**
$P(ODA)_6$-*b*-$P(PEGA\text{-}OMe)_{27}$ (Non-reduced)	**5.6**	27.1	0.7	PHYT	PBS	25	Q_2^D/H_2	62.08/41.55		
			0.7	PHYT	PBS	30	Q_2^D/H_2	61.29/41.13	221.1	Multi-modal
			0.7	PHYT	PBS	37	H_2	40.64		
			0.7	PHYT	PBS	40	H_2	40.42		
			0.7	PHYT	PBS	45	H_2	40.04		
			0.7	PHYT	PBS	50	H_2	39.70		
			0.7	PHYT	PBS	55	H_2	39.34		
			0.7	PHYT	PBS	60	H_2	38.84		
			0.7	PHYT	PBS	65	H_2/Broad (L_2)	38.35		
			0.7	PHYT	PBS	70	H_2/Broad (L_2)	38.07		
$P(ODA)_6$-*b*-$P(PEGA\text{-}OMe)_{35}$ (Non-reduced)	**5.6**	35.1	0.7	PHYT	PBS	25	Q_2^D	63.64		
			0.7	PHYT	PBS	30	Q_2^D/H_2	62.65/41.74	298.8	4.84E-01
			0.7	PHYT	PBS	37	Q_2^D/H_2	61.37/41.12		
			0.7	PHYT	PBS	40	Q_2^D/H_2	60.92/40.97		
			0.7	PHYT	PBS	45	Q_2^D/H_2	60.21/40.70		
			0.7	PHYT	PBS	50	H_2	40.26		
			0.7	PHYT	PBS	55	H_2	39.71		
			0.7	PHYT	PBS	60	H_2	39.31		
			0.7	PHYT	PBS	65	Broad (L_2)	-		
			0.7	PHYT	PBS	70	Broad (L_2)	-		
$P(ODA)_6$-*b*-$P(PEGA\text{-}OMe)_{39}$ (Non-reduced)	**5.6**	38.7	0.7	PHYT	PBS	25	Q_2^D/H_2	62.16/41.58		
			0.7	PHYT	PBS	30	Q_2^D/H_2	61.41/41.21	298.7	Multi-modal
			0.7	PHYT	PBS	37	H_2	40.71		
			0.7	PHYT	PBS	40	H_2	40.46		
			0.7	PHYT	PBS	45	H_2	40.05		
			0.7	PHYT	PBS	50	H_2	39.65		
			0.7	PHYT	PBS	55	H_2	39.35		
			0.7	PHYT	PBS	60	H_2	38.90		
			0.7	PHYT	PBS	65	H_2/Broad (L_2)	38.19		
			0.7	PHYT	PBS	70	Broad (L_2)	-		
$P(ODA)_{10}$-*b*-$P(PEGA\text{-}OMe)_{23}$ (Non-reduced)	**9.9**	23.1	0.7	PHYT	PBS	25	Q_2^D/H_2	62.17/41.65		
			0.7	PHYT	PBS	30	H_2	41.19	344.7	Multi-modal
			0.7	PHYT	PBS	37	H_2	40.59		
			0.7	PHYT	PBS	40	H_2	40.35		
			0.7	PHYT	PBS	45	H_2	39.93		
			0.7	PHYT	PBS	50	H_2	39.51		
			0.7	PHYT	PBS	55	H_2	38.08		
			0.7	PHYT	PBS	60	H_2	38.65		
			0.7	PHYT	PBS	65	Broad (L_2)	-		
			0.7	PHYT	PBS	70	Broad (L_2)	-		
$P(ODA)_{10}$-*b*-$P(PEGA\text{-}OMe)_{31}$ (Non-reduced)	**9.9**	30.7	0.7	PHYT	PBS	25	Q_2^D/H_2	62.12/41.68		
			0.7	PHYT	PBS	30	H_2	41.30	273.1	Multi-modal
			0.7	PHYT	PBS	37	H_2	40.71		
			0.7	PHYT	PBS	40	H_2	40.39		
			0.7	PHYT	PBS	45	H_2	39.86		
			0.7	PHYT	PBS	50	H_2	39.39		
			0.7	PHYT	PBS	55	H_2	38.91		
			0.7	PHYT	PBS	60	H_2	38.36		
$P(ODA)_{10}$-*b*-$P(PEGA\text{-}OMe)_{34}$ (Non-reduced)	**9.9**	33.5	0.7	PHYT	PBS	25	Q_2^D	63.20		
			0.7	PHYT	PBS	30	Q_2^D/H_2	62.25/41.53	252.5	Multi-modal
			0.7	PHYT	PBS	37	H_2/1 ring	41.18		
			0.7	PHYT	PBS	40	H_2	40.94		
			0.7	PHYT	PBS	45	H_2	40.39		
			0.7	PHYT	PBS	50	H_2	39.83		
			0.7	PHYT	PBS	55	H_2	39.32		
			0.7	PHYT	PBS	60	H_2/Broad (L_2)	38.83		

Stabilizer					Sol		SAXS		DLS	
P(ODA)-*b*-P(PEGA-OMe)	**ODA (units)**	**PEGA (units)**	**Conc (wt%)**	**Lipid**	**500µl**	**Temp (°C)**	**Phase**	**Lattice Parameter (Å)**	**Z-Ave (nm)**	**PDI**
			0.5	PHYT	PBS	25	Q_2^D/H_2	62.51/41.67		
$P(ODA)_6$-*b*-$P(PEGA\text{-}OMe)_{27}$ (Non-reduced)	**5.6**	27.1	0.5	PHYT	PBS	30	Q_2^D/H_2	61.64/41.18	297.9	3.94E-01
			0.5	PHYT	PBS	37	Q_2^D/H_2	60.54/40.79		
			0.5	PHYT	PBS	40	Q_2^D/H_2	60.13/40.66		
			0.5	PHYT	PBS	45	H_2	40.26		
			0.5	PHYT	PBS	50	H_2	39.96		
			0.5	PHYT	PBS	55	H_2	39.53		
			0.5	PHYT	PBS	60	H_2	39.13		
			0.5	PHYT	PBS	65	H_2/Broad(L_2)	38.59		
			0.5	PHYT	PBS	70	Broad(L_2)	-		
			0.5	PHYT	PBS	25	Q_2^D/H_2	62.90/41.84		
$P(ODA)_6$-*b*-$P(PEGA\text{-}OMe)_{35}$ (Non-reduced)	**5.6**	35.1	0.5	PHYT	PBS	30	Q_2^D/H_2	61.92/41.40	384.9	3.31E-01
			0.5	PHYT	PBS	37	Q_2^D/H_2	60.99/40.94		
			0.5	PHYT	PBS	40	H_2	40.71		
			0.5	PHYT	PBS	45	H_2	40.33		
			0.5	PHYT	PBS	50	H_2	39.93		
			0.5	PHYT	PBS	55	H_2	39.52		
			0.5	PHYT	PBS	60	H_2	39.07		
			0.5	PHYT	PBS	65	H_2/Broad(L_2)	38.43		
			0.5	PHYT	PBS	70	Broad(L_2)	-		
			0.5	PHYT	PBS	25	Q_2^D/H_2	62.38/41.62		
$P(ODA)_6$-*b*-$P(PEGA\text{-}OMe)_{39}$ (Non-reduced)	**5.6**	38.7	0.5	PHYT	PBS	30	Q_2^D/H_2	61.65/41.30	335.5	Multi-modal
			0.5	PHYT	PBS	37	H_2	40.82		
			0.5	PHYT	PBS	40	H_2	40.55		
			0.5	PHYT	PBS	45	H_2	40.14		
			0.5	PHYT	PBS	50	H_2	39.78		
			0.5	PHYT	PBS	55	H_2	39.44		
			0.5	PHYT	PBS	60	H_2	39.04		
			0.5	PHYT	PBS	65	H_2	38.26		
			0.5	PHYT	PBS	70	Broad(L_2)	-		
			0.5	PHYT	PBS	25	Q_2^D	63.31		
$P(ODA)_{10}$-*b*-$P(PEGA\text{-}OMe)_{23}$ (Non-reduced)	**9.9**	23.1	0.5	PHYT	PBS	30	Q_2^D/hint H_2	62.10/41.48	400.5	Multi-modal
			0.5	PHYT	PBS	37	Q_2^D/hint H_2	61.10/41.23		
			0.5	PHYT	PBS	40	H_2	41.01		
			0.5	PHYT	PBS	45	H_2	40.60		
			0.5	PHYT	PBS	50	H_2	40.20		
			0.5	PHYT	PBS	55	H_2	39.79		
			0.5	PHYT	PBS	60	H_2	39.41		
			0.5	PHYT	PBS	65	Broad(L_2)	-		
			0.5	PHYT	PBS	70	Broad(L_2)	-		
			0.5	PHYT	PBS	25	Q_2^D/H_2	62.78/41.81		
$P(ODA)_{10}$-*b*-$P(PEGA\text{-}OMe)_{31}$ (Non-reduced)	**9.9**	30.7	0.5	PHYT	PBS	30	Q_2^D/H_2	61.84/41.52	407.5	Multi-modal
			0.5	PHYT	PBS	37	H_2	40.94		
			0.5	PHYT	PBS	40	H_2	40.70		
			0.5	PHYT	PBS	45	H_2	40.25		
			0.5	PHYT	PBS	50	H_2	39.82		
			0.5	PHYT	PBS	55	H_2	39.36		
			0.5	PHYT	PBS	60	H_2	38.95		
			0.5	PHYT	PBS	65	H_2/Broad(L_2)	38.18		
			0.5	PHYT	PBS	70	Broad(L_2)	-		
			0.5	PHYT	PBS	25	Q_2^D	63.28		
$P(ODA)_{10}$-*b*-$P(PEGA\text{-}OMe)_{34}$ (Non-reduced)	**9.9**	33.5	0.5	PHYT	PBS	30	Q_2^D/H_2	62.33/41.58	249.2	Multi-modal
			0.5	PHYT	PBS	37	Q_2^D/H_2	61.17/41.23		
			0.5	PHYT	PBS	40	H_2	40.98		
			0.5	PHYT	PBS	45	H_2	40.38		
			0.5	PHYT	PBS	50	H_2	39.81		
			0.5	PHYT	PBS	55	H_2	39.38		
			0.5	PHYT	PBS	60	H_2	38.81		

Stabilizer					Sol		SAXS		DLS	
P(ODA)-*b*-P(PEGA-OMe)	**ODA (units)**	**PEGA (units)**	**Conc (wt%)**	**Lipid**	**500µl**	**Temp (°C)**	**Phase**	**Lattice Parameter (Å)**	**Z-Ave (nm)**	**PDI**
			0.1	PHYT	PBS	25	Q_2^D	64.59		
$P(ODA)_6$-*b*-$P(PEGA\text{-}OMe)_{27}$ (Non-reduced)	**5.6**	27.1	0.1	PHYT	PBS	30	Q_2^D	63.65	409.9	Multi-modal
			0.1	PHYT	PBS	37	Q_2^D	62.21		
			0.1	PHYT	PBS	40	Q_2^D	61.58/41.10		
			0.1	PHYT	PBS	45	Q_2^D/H_2	60.71/40.89		
			0.1	PHYT	PBS	50	H_2	40.61		
			0.1	PHYT	PBS	55	H_2	40.18		
			0.1	PHYT	PBS	60	H_2	39.72		
			0.1	PHYT	PBS	65	H_2/Broad (L_2)	39.08		
			0.1	PHYT	PBS	70	Broad (L_2)	-		
			0.1	PHYT	PBS	25	Q_2^D	64.47		
$P(ODA)_6$-*b*-$P(PEGA\text{-}OMe)_{35}$ (Non-reduced)	**5.6**	35.1	0.1	PHYT	PBS	30	Q_2^D	63.25	389.5	Multi-modal
			0.1	PHYT	PBS	37	Q_2^D/hint H_2	61.59/41.27		
			0.1	PHYT	PBS	40	Q_2^D/H_2	61.47/41.07		
			0.1	PHYT	PBS	45	Q_2^D/H_2	60.79/40.73		
			0.1	PHYT	PBS	50	H_2	40.30		
			0.1	PHYT	PBS	55	H_2	38.89		
			0.1	PHYT	PBS	60	H_2	39.38		
			0.1	PHYT	PBS	65	H_2/Broad (L_2)	38.65		
			0.1	PHYT	PBS	70	Broad (L_2)	-		
			0.1	PHYT	PBS	25	Q_2^D	65.23		
$P(ODA)_6$-*b*-$P(PEGA\text{-}OMe)_{39}$ (Non-reduced)	**5.6**	38.7	0.1	PHYT	PBS	30	Q_2^D	64.11	311.9	Multi-modal
			0.1	PHYT	PBS	37	Q_2^D	62.63		
			0.1	PHYT	PBS	40	Q_2^D	61.91		
			0.1	PHYT	PBS	45	Q_2^D/H_2	61.16/40.95		
			0.1	PHYT	PBS	50	Q_2^D/H_2	60.62/40.69		
			0.1	PHYT	PBS	55	H_2	40.31		
			0.1	PHYT	PBS	60	H_2	39.92		
			0.1	PHYT	PBS	65	H_2	39.19		
			0.1	PHYT	PBS	70	Broad (L_2)	-		
			0.1	PHYT	PBS	25	Q_2^D	63.88		
$P(ODA)_{10}$-*b*-$P(PEGA\text{-}OMe)_{23}$ (Non-reduced)	**9.9**	23.1	0.1	PHYT	PBS	30	Q_2^D	62.64	286.2	Multi-modal
			0.1	PHYT	PBS	37	Q_2^D/H_2	61.31/41.32		
			0.1	PHYT	PBS	40	Q_2^D/H_2	61.04/41.18		
			0.1	PHYT	PBS	45	H_2	40.78		
			0.1	PHYT	PBS	50	H_2	40.35		
			0.1	PHYT	PBS	55	H_2	39.97		
			0.1	PHYT	PBS	60	H_2	39.51		
			0.1	PHYT	PBS	65	H_2/Broad (L_2)	38.77		
			0.1	PHYT	PBS	70	Broad (L_2)	-		
			0.1	PHYT	PBS	25	Q_2^D	64.96		
$P(ODA)_{10}$-*b*-$P(PEGA\text{-}OMe)_{31}$ (Non-reduced)	**9.9**	30.7	0.1	PHYT	PBS	30	Q_2^D	63.48	301.0	Multi-modal
			0.1	PHYT	PBS	37	Q_2^D	61.97		
			0.1	PHYT	PBS	40	Q_2^D/H_2	61.36/41.10		
			0.1	PHYT	PBS	45	Q_2^D/H_2	60.78/40.99		
			0.1	PHYT	PBS	50	H_2	40.59		
			0.1	PHYT	PBS	55	H_2	40.10		
			0.1	PHYT	PBS	60	H_2	39.69		
			0.1	PHYT	PBS	65	Nothing	-		
			0.1	PHYT	PBS	70	Nothing	-		
			0.1	PHYT	PBS	25	Q_2^D	64.63		
$P(ODA)_{10}$-*b*-$P(PEGA\text{-}OMe)_{34}$ (Non-reduced)	**9.9**	33.5	0.1	PHYT	PBS	30	Q_2^D	63.53	206.6	Multi-modal
			0.1	PHYT	PBS	37	Q_2^D/hint H_2	61.77/41.33		
			0.1	PHYT	PBS	40	Q_2^D/H_2	61.26/41.25		
			0.1	PHYT	PBS	45	H_2	40.62		
			0.1	PHYT	PBS	50	H_2	40.12		
			0.1	PHYT	PBS	55	H_2	39.52		
			0.1	PHYT	PBS	60	Broad (L_2)	-		

Stabilizer					Sol		SAXS		DLS	
P(ODA)-*b*-P(PEGA-OMe)	**ODA (units)**	**PEGA (units)**	**Conc (wt%)**	**Lipid**	**500µl**	**Temp (°C)**	**Phase**	**Lattice Parameter (Å)**	**Z-Ave (nm)**	**PDI**
			1	PHYT	PBS	25	Q_2^D	69.38	284.7	1.56E-03
$P(ODA)_6$-*b*-$P(PEGA\text{-}OMe)_{27}$ (Reduced)	**5.6**	27.1	1	PHYT	PBS	30	Q_2^D	67.01		
			1	PHYT	PBS	37	Q_2^D	66.27		
			1	PHYT	PBS	40	Q_2^D	64.53		
			1	PHYT	PBS	45	Q_2^D	64.01		
			1	PHYT	PBS	50	Q_2^D	62.17		
			1	PHYT	PBS	55	Q_2^D	61.59		
			1	PHYT	PBS	60	Q_2^D	60.43		
			1	PHYT	PBS	65	Q_2^D	60.13		
			1	PHYT	PBS	70	Q_2^D	59.55		
			1	PHYT	PBS	25	Q_2^D	69.29	182.6	1.70E-03
$P(ODA)_6$-*b*-$P(PEGA\text{-}OMe)_{35}$ (Reduced)	**5.6**	35.1	1	PHYT	PBS	30	Q_2^D	66.89		
			1	PHYT	PBS	37	Q_2^D	66.63		
			1	PHYT	PBS	40	Q_2^D	64.33		
			1	PHYT	PBS	45	Q_2^D	63.98		
			1	PHYT	PBS	50	Q_2^D	61.95		
			1	PHYT	PBS	55	Q_2^D	61.42		
			1	PHYT	PBS	60	Q_2^D	60.14		
			1	PHYT	PBS	65	Q_2^D	59.82		
			1	PHYT	PBS	70	Q_2^D	59.15		
			1	PHYT	PBS	25	Q_2^D	69.28	300.7	1.69E-03
$P(ODA)_6$-*b*-$P(PEGA\text{-}OMe)_{39}$ (Reduced)	**5.6**	38.7	1	PHYT	PBS	30	Q_2^D	66.93		
			1	PHYT	PBS	37	Q_2^D	66.83		
			1	PHYT	PBS	40	Q_2^D	64.23		
			1	PHYT	PBS	45	Q_2^D	63.91		
			1	PHYT	PBS	50	Q_2^D	61.88		
			1	PHYT	PBS	55	Q_2^D	61.36		
			1	PHYT	PBS	60	Q_2^D	59.99		
			1	PHYT	PBS	65	Q_2^D	59.70		
			1	PHYT	PBS	70	Q_2^D	58.99		
			1	PHYT	PBS	25	Q_2^D	68.98	364.9	1.86E-03
$P(ODA)_{10}$-*b*-$P(PEGA\text{-}OMe)_{23}$ (Reduced)	**9.9**	23.1	1	PHYT	PBS	30	Q_2^D	66.57		
			1	PHYT	PBS	37	Q_2^D	64.96		
			1	PHYT	PBS	40	Q_2^D	64.03		
			1	PHYT	PBS	45	Q_2^D	62.83		
			1	PHYT	PBS	50	Q_2^D	61.82		
			1	PHYT	PBS	55	Q_2^D	60.62		
			1	PHYT	PBS	60	Q_2^D/L_2	59.68		
			1	PHYT	PBS	65	Q_2^D/L_2	58.96		
			1	PHYT	PBS	70	L^2	-		
			1	PHYT	PBS	25	Q_2^D	69.00	300.5	6.78E-04
$P(ODA)_{10}$-*b*-$P(PEGA\text{-}OMe)_{31}$ (Reduced)	**9.9**	30.7	1	PHYT	PBS	30	Q_2^D	66.38		
			1	PHYT	PBS	37	Q_2^D	64.91		
			1	PHYT	PBS	40	Q_2^D	63.85		
			1	PHYT	PBS	45	Q_2^D	62.70		
			1	PHYT	PBS	50	Q_2^D	61.53		
			1	PHYT	PBS	55	Q_2^D	60.41		
			1	PHYT	PBS	60	L_2 + 1Pk	-		
			1	PHYT	PBS	65	L_2	-		
			1	PHYT	PBS	70	L^2	-		
			1	PHYT	PBS	25	Q_2^D	69.04	268.5	1.52E-03
$P(ODA)_{10}$-*b*-$P(PEGA\text{-}OMe)_{34}$ (Reduced)	**9.9**	33.5	1	PHYT	PBS	30	Q_2^D	66.35		
			1	PHYT	PBS	37	Q_2^D	64.85		
			1	PHYT	PBS	40	Q_2^D	63.77		
			1	PHYT	PBS	45	Q_2^D	62.63		
			1	PHYT	PBS	50	Q_2^D	61.40		
			1	PHYT	PBS	55	Q_2^D	60.26		
			1	PHYT	PBS	60	L_2 + 1Pk	-		
			1	PHYT	PBS	64	L_2	-		
			1	PHYT	PBS	66	L^2	-		

Stabilizer					Sol		SAXS		DLS	
P(ODA)-*b*-P(PEGA-OMe)	**ODA (units)**	**PEGA (units)**	**Conc (wt%)**	**Lipid**	**500µl**	**Temp (°C)**	**Phase**	**Lattice Parameter (Å)**	**Z-Ave (nm)**	**PDI**
			0.7	PHYT	PBS	25	Q_2^D	69.25	441.4	1.47E-03
$P(ODA)_{6}$-*b*-$P(PEGA\text{-}OMe)_{27}$ (Reduced)	**5.6**	27.1	0.7	PHYT	PBS	30	Q_2^D	66.88		
			0.7	PHYT	PBS	37	Q_2^D	66.25		
			0.7	PHYT	PBS	40	Q_2^D	64.45		
			0.7	PHYT	PBS	45	Q_2^D	63.91		
			0.7	PHYT	PBS	50	Q_2^D	62.11		
			0.7	PHYT	PBS	55	Q_2^D	61.55		
			0.7	PHYT	PBS	60	Q_2^D	60.45		
			0.7	PHYT	PBS	64	Q_2^D	60.17		
			0.7	PHYT	PBS	66	Q_2^D	59.53		
			0.7	PHYT	PBS	25	Q_2^D	69.32	502.4	1.14E-03
$P(ODA)_{6}$-*b*-$P(PEGA\text{-}OMe)_{35}$ (Reduced)	**5.6**	35.1	0.7	PHYT	PBS	30	Q_2^D	67.06		
			0.7	PHYT	PBS	37	Q_2^D	66.99		
			0.7	PHYT	PBS	40	Q_2^D	64.34		
			0.7	PHYT	PBS	45	Q_2^D	64.09		
			0.7	PHYT	PBS	50	Q_2^D	61.96		
			0.7	PHYT	PBS	55	Q_2^D	61.52		
			0.7	PHYT	PBS	60	Q_2^D	60.25		
			0.7	PHYT	PBS	64	Q_2^D	59.95		
			0.7	PHYT	PBS	66	Q_2^D	59.28		
			0.7	PHYT	PBS	25	Q_2^D	69.23	508.9	1.79E-03
$P(ODA)_{6}$-*b*-$P(PEGA\text{-}OMe)_{39}$ (Reduced)	**5.6**	38.7	0.7	PHYT	PBS	30	Q_2^D	66.81		
			0.7	PHYT	PBS	37	Q_2^D	66.61		
			0.7	PHYT	PBS	40	Q_2^D	64.17		
			0.7	PHYT	PBS	45	Q_2^D	63.81		
			0.7	PHYT	PBS	50	Q_2^D	61.81		
			0.7	PHYT	PBS	55	Q_2^D	61.33		
			0.7	PHYT	PBS	60	Q_2^D	60.07		
			0.7	PHYT	PBS	64	Q_2^D	59.78		
			0.7	PHYT	PBS	66	Q_2^D	59.08		
			0.7	PHYT	PBS	25	Q_2^D	68.92	400.7	1.10E-03
$P(ODA)_{10}$-*b*-$P(PEGA\text{-}OMe)_{23}$ (Reduced)	**9.9**	23.1	0.7	PHYT	PBS	30	Q_2^D	66.52		
			0.7	PHYT	PBS	37	Q_2^D	64.85		
			0.7	PHYT	PBS	40	Q_2^D	63.94		
			0.7	PHYT	PBS	45	Q_2^D	62.81		
			0.7	PHYT	PBS	50	Q_2^D	61.55		
			0.7	PHYT	PBS	55	Q_2^D	60.47		
			0.7	PHYT	PBS	60	L_2	-		
			0.7	PHYT	PBS	64	L_2	-		
			0.7	PHYT	PBS	66	L_2	-		
			0.7	PHYT	PBS	25	Q_2^D	68.98	389.9	7.87E-04
$P(ODA)_{10}$-*b*-$P(PEGA\text{-}OMe)_{31}$ (Reduced)	**9.9**	30.7	0.7	PHYT	PBS	30	Q_2^D	66.44		
			0.7	PHYT	PBS	37	Q_2^D	64.77		
			0.7	PHYT	PBS	40	Q_2^D	63.83		
			0.7	PHYT	PBS	45	Q_2^D	62.72		
			0.7	PHYT	PBS	50	Q_2^D	61.29		
			0.7	PHYT	PBS	55	Q_2^D	60.27		
			0.7	PHYT	PBS	60	L_2 + 1Pk	-		
			0.7	PHYT	PBS	64	L_2	-		
			0.7	PHYT	PBS	66	L^2	-		
			0.7	PHYT	PBS	25	Q_2^D	69.00	540.7	8.97E-04
$P(ODA)_{10}$-*b*-$P(PEGA\text{-}OMe)_{34}$ (Reduced)	**9.9**	33.5	0.7	PHYT	PBS	30	Q_2^D	66.36		
			0.7	PHYT	PBS	37	Q_2^D	64.74		
			0.7	PHYT	PBS	40	Q_2^D	63.75		
			0.7	PHYT	PBS	45	Q_2^D	62.60		
			0.7	PHYT	PBS	50	Q_2^D	61.17		
			0.7	PHYT	PBS	55	Q_2^D	60.16		
			0.7	PHYT	PBS	60	L_2 + 1Pk	-		
			0.7	PHYT	PBS	64	L_2	-		
			0.7	PHYT	PBS	66	L^2	-		

Stabilizer					Sol		SAXS		DLS	
P(ODA)-*b*-P(PEGA-OMe)	**ODA (units)**	**PEGA (units)**	**Conc (wt%)**	**Lipid**	**500µl**	**Temp (°C)**	**Phase**	**Lattice Parameter (Å)**	**Z-Ave (nm)**	**PDI**
			0.5	PHYT	PBS	25	Q_2^D	69.15	432.5	1.26E-03
$P(ODA)_6$-*b*-$P(PEGA\text{-}OMe)_{27}$ (Reduced)	**5.6**	27.1	0.5	PHYT	PBS	30	Q_2^D	66.77		
			0.5	PHYT	PBS	37	Q_2^D	66.19		
			0.5	PHYT	PBS	40	Q_2^D	64.41		
			0.5	PHYT	PBS	45	Q_2^D	63.86		
			0.5	PHYT	PBS	50	Q_2^D	62.04		
			0.5	PHYT	PBS	55	Q_2^D	61.54		
			0.5	PHYT	PBS	60	Q_2^D	60.55		
			0.5	PHYT	PBS	64	Q_2^D	60.28		
			0.5	PHYT	PBS	66	Q_2^D	59.64		
			0.5	PHYT	PBS	25	Q_2^D	69.26	390.2	1.63E-03
$P(ODA)_6$-*b*-$P(PEGA\text{-}OMe)_{35}$ (Reduced)	**5.6**	35.1	0.5	PHYT	PBS	30	Q_2^D	66.83		
			0.5	PHYT	PBS	37	Q_2^D	66.62		
			0.5	PHYT	PBS	40	Q_2^D	64.39		
			0.5	PHYT	PBS	45	Q_2^D	63.95		
			0.5	PHYT	PBS	50	Q_2^D	62.02		
			0.5	PHYT	PBS	55	Q_2^D	61.54		
			0.5	PHYT	PBS	60	Q_2^D	60.48		
			0.5	PHYT	PBS	64	Q_2^D	60.27		
			0.5	PHYT	PBS	66	Q_2^D	59.55		
			0.5	PHYT	PBS	25	Q_2^D	69.30	525.9	1.15E-03
$P(ODA)_6$-*b*-$P(PEGA\text{-}OMe)_{39}$ (Reduced)	**5.6**	38.7	0.5	PHYT	PBS	30	Q_2^D	66.90		
			0.5	PHYT	PBS	37	Q_2^D	66.91		
			0.5	PHYT	PBS	40	Q_2^D	64.26		
			0.5	PHYT	PBS	45	Q_2^D	64.11		
			0.5	PHYT	PBS	50	Q_2^D	61.88		
			0.5	PHYT	PBS	55	Q_2^D	61.51		
			0.5	PHYT	PBS	60	Q_2^D	60.33		
			0.5	PHYT	PBS	64	Q_2^D	60.19		
			0.5	PHYT	PBS	66	Q_2^D	59.34		
			0.5	PHYT	PBS	25	Q_2^D	68.92	418.2	1.85E-03
$P(ODA)_{10}$-*b*-$P(PEGA\text{-}OMe)_{23}$ (Reduced)	**9.9**	23.1	0.5	PHYT	PBS	30	Q_2^D	66.51		
			0.5	PHYT	PBS	37	Q_2^D	64.93		
			0.5	PHYT	PBS	40	Q_2^D	63.97		
			0.5	PHYT	PBS	45	Q_2^D	62.96		
			0.5	PHYT	PBS	50	Q_2^D	61.47		
			0.5	PHYT	PBS	55	Q_2^D	60.53		
			0.5	PHYT	PBS	60	L_2	-		
			0.5	PHYT	PBS	64	L_2	-		
			0.5	PHYT	PBS	66	L_2	-		
			0.5	PHYT	PBS	25	Q_2^D	68.62	414.1	7.94E-04
$P(ODA)_{10}$-*b*-$P(PEGA\text{-}OMe)_{31}$ (Reduced)	**9.9**	30.7	0.5	PHYT	PBS	30	Q_2^D	66.05		
			0.5	PHYT	PBS	37	Q_2^D	65.65		
			0.5	PHYT	PBS	40	Q_2^D	64.31		
			0.5	PHYT	PBS	45	Q_2^D	63.59		
			0.5	PHYT	PBS	50	Q_2^D	62.36		
			0.5	PHYT	PBS	55	Q_2^D	61.73		
			0.5	PHYT	PBS	60	Q_2^D + 1Pk	60.77		
			0.5	PHYT	PBS	64	Q_2^D + 1Pk	60.40		
			0.5	PHYT	PBS	66	Q_2^D + 1Pk	60.25		
			0.5	PHYT	PBS	25	Q_2^D	68.70	386.8	1.50E-03
$P(ODA)_{10}$-*b*-$P(PEGA\text{-}OMe)_{34}$ (Reduced)	**9.9**	33.5	0.5	PHYT	PBS	30	Q_2^D	65.96		
			0.5	PHYT	PBS	37	Q_2^D	65.63		
			0.5	PHYT	PBS	40	Q_2^D	64.21		
			0.5	PHYT	PBS	45	Q_2^D	63.54		
			0.5	PHYT	PBS	50	Q_2^D	62.24		
			0.5	PHYT	PBS	55	Q_2^D	61.58		
			0.5	PHYT	PBS	60	Q_2^D + 1Pk	60.63		
			0.5	PHYT	PBS	64	Q_2^D + 1Pk	60.34		
			0.5	PHYT	PBS	66	Q_2^D + 1Pk	60.26		

Stabilizer					Sol		SAXS		DLS	
P(ODA)-*b*-P(PEGA-OMe)	**ODA (units)**	**PEGA (units)**	**Conc (wt%)**	**Lipid**	**500µl**	**Temp (°C)**	**Phase**	**Lattice Parameter (Å)**	**Z-Ave (nm)**	**PDI**
			0.1	PHYT	PBS	25	Q_2^D	69.06	440.1	7.52E-04
$P(ODA)_6$-*b*-$P(PEGA\text{-}OMe)_{27}$ (Reduced)	**5.6**	27.1	0.1	PHYT	PBS	30	Q_2^D	66.90		
			0.1	PHYT	PBS	37	Q_2^D	66.84		
			0.1	PHYT	PBS	40	Q_2^D	64.44		
			0.1	PHYT	PBS	45	Q_2^D	64.13		
			0.1	PHYT	PBS	50	Q_2^D	62.50		
			0.1	PHYT	PBS	55	Q_2^D	62.21		
			0.1	PHYT	PBS	60	Q_2^D	60.91		
			0.1	PHYT	PBS	64	Q_2^D	60.67		
			0.1	PHYT	PBS	66	Q_2^D	59.96		
			0.1	PHYT	PBS	25	Q_2^D	69.23	320.1	1.69E-03
$P(ODA)_6$-*b*-$P(PEGA\text{-}OMe)_{35}$ (Reduced)	**5.6**	35.1	0.1	PHYT	PBS	30	Q_2^D	67.06		
			0.1	PHYT	PBS	37	Q_2^D	67.10		
			0.1	PHYT	PBS	40	Q_2^D	64.35		
			0.1	PHYT	PBS	45	Q_2^D	64.11		
			0.1	PHYT	PBS	50	Q_2^D	62.48		
			0.1	PHYT	PBS	55	Q_2^D	62.09		
			0.1	PHYT	PBS	60	Q_2^D	60.73		
			0.1	PHYT	PBS	64	Q_2^D	60.51		
			0.1	PHYT	PBS	66	Q_2^D	59.71		
			0.1	PHYT	PBS	25	Q_2^D	68.88	537.9	1.81E-03
$P(ODA)_6$-*b*-$P(PEGA\text{-}OMe)_{39}$ (Reduced)	**5.6**	38.7	0.1	PHYT	PBS	30	Q_2^D	66.26		
			0.1	PHYT	PBS	37	Q_2^D	66.16		
			0.1	PHYT	PBS	40	Q_2^D	64.38		
			0.1	PHYT	PBS	45	Q_2^D	64.12		
			0.1	PHYT	PBS	50	Q_2^D	62.48		
			0.1	PHYT	PBS	55	Q_2^D	61.98		
			0.1	PHYT	PBS	60	Q_2^D	60.78		
			0.1	PHYT	PBS	64	Q_2^D	60.13		
			0.1	PHYT	PBS	66	Q_2^D	59.95		
			0.1	PHYT	PBS	25	Q_2^D	68.60	556.7	1.20E-03
$P(ODA)_{10}$-*b*-$P(PEGA\text{-}OMe)_{23}$ (Reduced)	**9.9**	23.1	0.1	PHYT	PBS	30	Q_2^D	66.12		
			0.1	PHYT	PBS	37	Q_2^D	65.69		
			0.1	PHYT	PBS	40	Q_2^D	64.33		
			0.1	PHYT	PBS	45	Q_2^D	63.61		
			0.1	PHYT	PBS	50	Q_2^D	62.43		
			0.1	PHYT	PBS	55	Q_2^D	61.75		
			0.1	PHYT	PBS	60	Q_2^D	60.82		
			0.1	PHYT	PBS	64	Q_2^D	60.28		
			0.1	PHYT	PBS	66	Q_2^D	60.12		
			0.1	PHYT	PBS	25	Q_2^D	68.68	406.8	8.64E-04
$P(ODA)_{10}$-*b*-$P(PEGA\text{-}OMe)_{31}$ (Reduced)	**9.9**	30.7	0.1	PHYT	PBS	30	Q_2^D	65.92		
			0.1	PHYT	PBS	37	Q_2^D	65.60		
			0.1	PHYT	PBS	40	Q_2^D	64.14		
			0.1	PHYT	PBS	45	Q_2^D	63.49		
			0.1	PHYT	PBS	50	Q_2^D	62.15		
			0.1	PHYT	PBS	55	Q_2^D	61.52		
			0.1	PHYT	PBS	60	Q_2^D	60.51		
			0.1	PHYT	PBS	64	Q_2^D	60.01		
			0.1	PHYT	PBS	66	Q_2^D	59.85		
			0.1	PHYT	PBS	25	Q_2^D	68.69	454.3	2.05E-03
$P(ODA)_{10}$-*b*-$P(PEGA\text{-}OMe)_{34}$ (Reduced)	**9.9**	33.5	0.1	PHYT	PBS	30	Q_2^D	65.79		
			0.1	PHYT	PBS	37	Q_2^D	65.57		
			0.1	PHYT	PBS	40	Q_2^D	64.00		
			0.1	PHYT	PBS	45	Q_2^D	63.46		
			0.1	PHYT	PBS	50	Q_2^D	62.03		
			0.1	PHYT	PBS	55	Q_2^D	61.40		
			0.1	PHYT	PBS	60	Q_2^D	60.38		
			0.1	PHYT	PBS	64	Q_2^D	60.03		
			0.1	PHYT	PBS	66	Q_2^D	59.91		

Stabilizer					Sol		SAXS			DLS
P(ODA)-*b*-P(PEGA-OMe)	**ODA (units)**	**PEGA (units)**	**Conc (Mol eq.)**	**Lipid**	**500µl**	**Temp (°C)**	**Phase**	**Lattice Parameter (Å)**	**Z-Ave (nm)**	**PDI**
			2	PHYT	PBS	25	Q_2^D	68.86	193.6	1.05E-03
$P(ODA)_6$-*b*-$P(PEGA\text{-}OMe)_{27}$ (Reduced)	**5.6**	27.1	2	PHYT	PBS	30	Q_2^D	66.89		
			2	PHYT	PBS	37	Q_2^D	65.81		
			2	PHYT	PBS	40	Q_2^D	64.60		
			2	PHYT	PBS	45	Q_2^D	63.79		
			2	PHYT	PBS	50	Q_2^D	62.70		
			2	PHYT	PBS	55	Q_2^D	62.02		
			2	PHYT	PBS	60	Q_2^D	61.13		
			2	PHYT	PBS	64	Q_2^D	60.64		
			2	PHYT	PBS	66	Q_2^D	60.13		
			2	PHYT	PBS	25	Q_2^D	69.07	224.7	1.16E-03
$P(ODA)_6$-*b*-$P(PEGA\text{-}OMe)_{35}$ (Reduced)	**5.6**	35.1	2	PHYT	PBS	30	Q_2^D	66.90		
			2	PHYT	PBS	37	Q_2^D	66.10		
			2	PHYT	PBS	40	Q_2^D	64.46		
			2	PHYT	PBS	45	Q_2^D	63.79		
			2	PHYT	PBS	50	Q_2^D	62.52		
			2	PHYT	PBS	55	Q_2^D	61.89		
			2	PHYT	PBS	60	Q_2^D	60.95		
			2	PHYT	PBS	64	Q_2^D	60.61		
			2	PHYT	PBS	66	Q_2^D + 1Pk	59.96		
			2	PHYT	PBS	25	Q_2^D	69.03	215.7	1.93E-03
$P(ODA)_6$-*b*-$P(PEGA\text{-}OMe)_{39}$ (Reduced)	**5.6**	38.7	2	PHYT	PBS	30	Q_2^D	66.70		
			2	PHYT	PBS	37	Q_2^D	66.04		
			2	PHYT	PBS	40	Q_2^D	64.33		
			2	PHYT	PBS	45	Q_2^D	63.73		
			2	PHYT	PBS	50	Q_2^D	62.25		
			2	PHYT	PBS	55	Q_2^D	61.63		
			2	PHYT	PBS	60	Q_2^D + 1Pk	60.72		
			2	PHYT	PBS	64	Q_2^D + 1Pk	60.31		
			2	PHYT	PBS	66	Q_2^D + 1Pk	59.66		
			2	PHYT	PBS	25	Q_2^D	68.60	330.8	1.12E-03
$P(ODA)_{10}$-*b*-$P(PEGA\text{-}OMe)_{23}$ (Reduced)	**9.9**	23.1	2	PHYT	PBS	30	Q_2^D	66.45		
			2	PHYT	PBS	37	Q_2^D	65.56		
			2	PHYT	PBS	40	Q_2^D	64.59		
			2	PHYT	PBS	45	Q_2^D	63.46		
			2	PHYT	PBS	50	Q_2^D	62.69		
			2	PHYT	PBS	55	Q_2^D	61.88		
			2	PHYT	PBS	60	Q_2^D/L_2	60.80		
			2	PHYT	PBS	64	Q_2^D/L_2	60.07		
			2	PHYT	PBS	66	Q_2^D/L_2	59.96		
			2	PHYT	PBS	25	Q_2^D	69.02	293.8	1.53E-03
$P(ODA)_{10}$-*b*-$P(PEGA\text{-}OMe)_{31}$ (Reduced)	**9.9**	30.7	2	PHYT	PBS	30	Q_2^D	66.46		
			2	PHYT	PBS	37	Q_2^D	65.88		
			2	PHYT	PBS	40	Q_2^D	64.64		
			2	PHYT	PBS	45	Q_2^D	63.70		
			2	PHYT	PBS	50	Q_2^D	62.84		
			2	PHYT	PBS	55	Q_2^D	62.07		
			2	PHYT	PBS	60	L_2	-		
			2	PHYT	PBS	64	L_2	-		
			2	PHYT	PBS	66	L_2	-		
			2	PHYT	PBS	25	Q_2^D	69.10	302.1	2.17E-03
$P(ODA)_{10}$-*b*-$P(PEGA\text{-}OMe)_{34}$ (Reduced)	**9.9**	33.5	2	PHYT	PBS	30	Q_2^D	66.34		
			2	PHYT	PBS	37	Q_2^D	65.79		
			2	PHYT	PBS	40	Q_2^D	64.42		
			2	PHYT	PBS	45	Q_2^D	63.51		
			2	PHYT	PBS	50	Q_2^D	62.62		
			2	PHYT	PBS	55	Q_2^D	61.80		
			2	PHYT	PBS	60	L_2	-		
			2	PHYT	PBS	64	L_2	-		
			2	PHYT	PBS	66	L_2	-		

Stabilizer					Sol		SAXS		DLS	
P(ODA)-*b*-P(PEGA-OMe)	**ODA (units)**	**PEGA (units)**	**Conc (Mol eq.)**	**Lipid**	**500µl**	**Temp (°C)**	**Phase**	**Lattice Parameter (Å)**	**Z-Ave (nm)**	**PDI**
			1.5	PHYT	PBS	25	Q_2^D	69.76	292.7	1.86E-03
$P(ODA)_6$-*b*-$P(PEGA\text{-}OMe)_{27}$ (Reduced)	**5.6**	27.1	1.5	PHYT	PBS	30	Q_2^D	67.26		
			1.5	PHYT	PBS	37	Q_2^D	66.62		
			1.5	PHYT	PBS	40	Q_2^D	64.71		
			1.5	PHYT	PBS	45	Q_2^D	64.16		
			1.5	PHYT	PBS	50	Q_2^D	62.55		
			1.5	PHYT	PBS	55	Q_2^D	61.99		
			1.5	PHYT	PBS	60	Q_2^D	61.04		
			1.5	PHYT	PBS	64	Q_2^D	60.78		
			1.5	PHYT	PBS	66	Q_2^D	60.21		
			1.5	PHYT	PBS	25	Q_2^D	69.21	235.6	1.60E-03
$P(ODA)_6$-*b*-$P(PEGA\text{-}OMe)_{35}$ (Reduced)	**5.6**	35.1	1.5	PHYT	PBS	30	Q_2^D	66.97		
			1.5	PHYT	PBS	37	Q_2^D	66.02		
			1.5	PHYT	PBS	40	Q_2^D	64.44		
			1.5	PHYT	PBS	45	Q_2^D	63.72		
			1.5	PHYT	PBS	50	Q_2^D	62.23		
			1.5	PHYT	PBS	55	Q_2^D	61.63		
			1.5	PHYT	PBS	60	Q_2^D	60.75		
			1.5	PHYT	PBS	64	Q_2^D	60.52		
			1.5	PHYT	PBS	66	Q_2^D + 1Pk	59.80		
			1.5	PHYT	PBS	25	Q_2^D	69.53	181.4	1.21E-03
$P(ODA)_6$-*b*-$P(PEGA\text{-}OMe)_{39}$ (Reduced)	**5.6**	38.7	1.5	PHYT	PBS	30	Q_2^D	67.12		
			1.5	PHYT	PBS	37	Q_2^D	66.80		
			1.5	PHYT	PBS	40	Q_2^D	64.41		
			1.5	PHYT	PBS	45	Q_2^D	63.77		
			1.5	PHYT	PBS	50	Q_2^D	62.06		
			1.5	PHYT	PBS	55	Q_2^D	61.34		
			1.5	PHYT	PBS	60	Q_2^D	60.73		
			1.5	PHYT	PBS	64	Q_2^D	60.42		
			1.5	PHYT	PBS	66	Q_2^D + 1Pk	59.52		
			1.5	PHYT	PBS	25	Q_2^D	68.63	335.4	1.26E-03
$P(ODA)_{10}$-*b*-$P(PEGA\text{-}OMe)_{23}$ (Reduced)	**9.9**	23.1	1.5	PHYT	PBS	30	Q_2^D	66.37		
			1.5	PHYT	PBS	37	Q_2^D	65.48		
			1.5	PHYT	PBS	40	Q_2^D	64.46		
			1.5	PHYT	PBS	45	Q_2^D	63.38		
			1.5	PHYT	PBS	50	Q_2^D	62.50		
			1.5	PHYT	PBS	55	Q_2^D	61.62		
			1.5	PHYT	PBS	60	Q_2^D/L_2	60.62		
			1.5	PHYT	PBS	64	Q_2^D/L_2	59.56		
			1.5	PHYT	PBS	66	Q_2^D/L_2	59.42		
			1.5	PHYT	PBS	25	Q_2^D	68.89	285.1	7.47E-03
$P(ODA)_{10}$-*b*-$P(PEGA\text{-}OMe)_{31}$ (Reduced)	**9.9**	30.7	1.5	PHYT	PBS	30	Q_2^D	66.36		
			1.5	PHYT	PBS	37	Q_2^D	65.64		
			1.5	PHYT	PBS	40	Q_2^D	64.40		
			1.5	PHYT	PBS	45	Q_2^D	63.47		
			1.5	PHYT	PBS	50	Q_2^D	62.52		
			1.5	PHYT	PBS	55	Q_2^D	61.73		
			1.5	PHYT	PBS	60	L_2	-		
			1.5	PHYT	PBS	64	L_2	-		
			1.5	PHYT	PBS	66	L_2	-		
			1.5	PHYT	PBS	25	Q_2^D	69.08	232.7	2.03E-03
$P(ODA)_{10}$-*b*-$P(PEGA\text{-}OMe)_{34}$ (Reduced)	**9.9**	33.5	1.5	PHYT	PBS	30	Q_2^D	66.41		
			1.5	PHYT	PBS	37	Q_2^D	65.65		
			1.5	PHYT	PBS	40	Q_2^D	64.33		
			1.5	PHYT	PBS	45	Q_2^D	63.25		
			1.5	PHYT	PBS	50	Q_2^D	62.44		
			1.5	PHYT	PBS	55	Q_2^D	61.48		
			1.5	PHYT	PBS	60	L_2	-		
			1.5	PHYT	PBS	64	L_2	-		
			1.5	PHYT	PBS	66	L_2	-		

Stabilizer					Sol		SAXS		DLS	
P(ODA)-*b*-P(PEGA-OMe)	**ODA (units)**	**PEGA (units)**	**Conc (Mol eq.)**	**Lipid**	**500µl**	**Temp (°C)**	**Phase**	**Lattice Parameter (Å)**	**Z-Ave (nm)**	**PDI**
			1.2	PHYT	PBS	25	Q_2^D	69.63	410.6	1.77E-03
$P(ODA)_6$-*b*-$P(PEGA\text{-}OMe)_{27}$ (Reduced)	**5.6**	27.1	1.2	PHYT	PBS	30	Q_2^D	67.27		
			1.2	PHYT	PBS	37	Q_2^D	66.44		
			1.2	PHYT	PBS	40	Q_2^D	64.69		
			1.2	PHYT	PBS	45	Q_2^D	64.06		
			1.2	PHYT	PBS	50	Q_2^D	62.39		
			1.2	PHYT	PBS	55	Q_2^D	61.77		
			1.2	PHYT	PBS	60	Q_2^D	60.89		
			1.2	PHYT	PBS	64	Q_2^D	60.64		
			1.2	PHYT	PBS	66	Q_2^D	60.01		
			1.2	PHYT	PBS	25	Q_2^D	69.34	314.7	1.64E-03
$P(ODA)_6$-*b*-$P(PEGA\text{-}OMe)_{35}$ (Reduced)	**5.6**	35.1	1.2	PHYT	PBS	30	Q_2^D	67.02		
			1.2	PHYT	PBS	37	Q_2^D	66.13		
			1.2	PHYT	PBS	40	Q_2^D	64.37		
			1.2	PHYT	PBS	45	Q_2^D	63.73		
			1.2	PHYT	PBS	50	Q_2^D	62.09		
			1.2	PHYT	PBS	55	Q_2^D	61.46		
			1.2	PHYT	PBS	60	Q_2^D	60.53		
			1.2	PHYT	PBS	64	Q_2^D	60.31		
			1.2	PHYT	PBS	66	Q_2^D + 1Pk	59.63		
			1.2	PHYT	PBS	25	Q_2^D	69.45	442.8	1.66E-03
$P(ODA)_6$-*b*-$P(PEGA\text{-}OMe)_{39}$ (Reduced)	**5.6**	38.7	1.2	PHYT	PBS	30	Q_2^D	67.16		
			1.2	PHYT	PBS	37	Q_2^D	66.86		
			1.2	PHYT	PBS	40	Q_2^D	64.35		
			1.2	PHYT	PBS	45	Q_2^D	63.78		
			1.2	PHYT	PBS	50	Q_2^D	61.93		
			1.2	PHYT	PBS	55	Q_2^D	61.27		
			1.2	PHYT	PBS	60	Q_2^D	60.55		
			1.2	PHYT	PBS	64	Q_2^D + 1Pk	60.19		
			1.2	PHYT	PBS	66	Q_2^D + 1Pk	59.42		
			1.2	PHYT	PBS	25	Q_2^D	68.98	478.0	1.72E-03
$P(ODA)_{10}$-*b*-$P(PEGA\text{-}OMe)_{23}$ (Reduced)	**9.9**	23.1	1.2	PHYT	PBS	30	Q_2^D	66.64		
			1.2	PHYT	PBS	37	Q_2^D	65.57		
			1.2	PHYT	PBS	40	Q_2^D	64.50		
			1.2	PHYT	PBS	45	Q_2^D	63.43		
			1.2	PHYT	PBS	50	Q_2^D	62.46		
			1.2	PHYT	PBS	55	Q_2^D	61.51		
			1.2	PHYT	PBS	60	L_2	-		
			1.2	PHYT	PBS	64	L_2	-		
			1.2	PHYT	PBS	66	L_2	-		
			1.2	PHYT	PBS	25	Q_2^D	68.81	409.9	1.34E-03
$P(ODA)_{10}$-*b*-$P(PEGA\text{-}OMe)_{31}$ (Reduced)	**9.9**	30.7	1.2	PHYT	PBS	30	Q_2^D	66.32		
			1.2	PHYT	PBS	37	Q_2^D	65.43		
			1.2	PHYT	PBS	40	Q_2^D	64.26		
			1.2	PHYT	PBS	45	Q_2^D	63.26		
			1.2	PHYT	PBS	50	Q_2^D	62.31		
			1.2	PHYT	PBS	55	Q_2^D	61.39		
			1.2	PHYT	PBS	60	L_2	-		
			1.2	PHYT	PBS	64	L_2	-		
			1.2	PHYT	PBS	66	L_2	-		
			1.2	PHYT	PBS	25	Q_2^D	69.10	513.7	1.74E-03
$P(ODA)_{10}$-*b*-$P(PEGA\text{-}OMe)_{34}$ (Reduced)	**9.9**	33.5	1.2	PHYT	PBS	30	Q_2^D	66.44		
			1.2	PHYT	PBS	37	Q_2^D	65.52		
			1.2	PHYT	PBS	40	Q_2^D	64.20		
			1.2	PHYT	PBS	45	Q_2^D	63.10		
			1.2	PHYT	PBS	50	Q_2^D	62.25		
			1.2	PHYT	PBS	55	Q_2^D	61.26		
			1.2	PHYT	PBS	60	L_2	-		
			1.2	PHYT	PBS	64	L_2	-		
			1.2	PHYT	PBS	66	L_2	-		

Stabilizer					Sol		SAXS		DLS	
P(ODA)-*b*-P(PEGA-OMe)	**ODA (units)**	**PEGA (units)**	**Conc (Mol eq.)**	**Lipid**	**500µl**	**Temp (°C)**	**Phase**	**Lattice Parameter (Å)**	**Z-Ave (nm)**	**PDI**
$P(ODA)_{6}$-*b*-$P(PEGA\text{-}OMe)_{27}$ (Reduced)	**5.6**	27.1	1	PHYT	PBS	25	Q_2^D	69.54	299.7	1.48E-03
			1	PHYT	PBS	30	Q_2^D	67.16		
			1	PHYT	PBS	37	Q_2^D	66.10		
			1	PHYT	PBS	40	Q_2^D	64.54		
			1	PHYT	PBS	45	Q_2^D	63.89		
			1	PHYT	PBS	50	Q_2^D	62.26		
			1	PHYT	PBS	55	Q_2^D	61.65		
			1	PHYT	PBS	60	Q_2^D	60.68		
			1	PHYT	PBS	64	Q_2^D	60.44		
			1	PHYT	PBS	66	Q_2^D	59.81		
$P(ODA)_{6}$-*b*-$P(PEGA\text{-}OMe)_{35}$ (Reduced)	**5.6**	35.1	1	PHYT	PBS	25	Q_2^D	69.56	412.0	1.29E-03
			1	PHYT	PBS	30	Q_2^D	67.28		
			1	PHYT	PBS	37	Q_2^D	66.92		
			1	PHYT	PBS	40	Q_2^D	64.52		
			1	PHYT	PBS	45	Q_2^D	64.10		
			1	PHYT	PBS	50	Q_2^D	62.09		
			1	PHYT	PBS	55	Q_2^D	61.51		
			1	PHYT	PBS	60	Q_2^D	60.55		
			1	PHYT	PBS	64	Q_2^D	60.27		
			1	PHYT	PBS	66	Q_2^D	59.53		
$P(ODA)_{6}$-*b*-$P(PEGA\text{-}OMe)_{39}$ (Reduced)	**5.6**	38.7	1	PHYT	PBS	25	Q_2^D	69.17	296.8	9.28E-04
			1	PHYT	PBS	30	Q_2^D	66.65		
			1	PHYT	PBS	37	Q_2^D	65.63		
			1	PHYT	PBS	40	Q_2^D	64.04		
			1	PHYT	PBS	45	Q_2^D	63.42		
			1	PHYT	PBS	50	Q_2^D	61.70		
			1	PHYT	PBS	55	Q_2^D	61.02		
			1	PHYT	PBS	60	Q_2^D	60.09		
			1	PHYT	PBS	64	Q_2^D + 1Pk	59.67		
			1	PHYT	PBS	66	Q_2^D + 1Pk	59.11		
$P(ODA)_{10}$-*b*-$P(PEGA\text{-}OMe)_{23}$ (Reduced)	**9.9**	23.1	1	PHYT	PBS	25	Q_2^D	69.01	364.0	1.16E-03
			1	PHYT	PBS	30	Q_2^D	66.65		
			1	PHYT	PBS	37	Q_2^D	65.44		
			1	PHYT	PBS	40	Q_2^D	64.36		
			1	PHYT	PBS	45	Q_2^D	63.27		
			1	PHYT	PBS	50	Q_2^D	62.26		
			1	PHYT	PBS	55	Q_2^D	61.22		
			1	PHYT	PBS	60	L_2	-		
			1	PHYT	PBS	64	L_2	-		
			1	PHYT	PBS	66	L_2	-		
$P(ODA)_{10}$-*b*-$P(PEGA\text{-}OMe)_{31}$ (Reduced)	**9.9**	30.7	1	PHYT	PBS	25	Q_2^D	68.99	252.9	1.47E-03
			1	PHYT	PBS	30	Q_2^D	66.48		
			1	PHYT	PBS	37	Q_2^D	65.42		
			1	PHYT	PBS	40	Q_2^D	64.22		
			1	PHYT	PBS	45	Q_2^D	63.15		
			1	PHYT	PBS	50	Q_2^D	62.19		
			1	PHYT	PBS	55	Q_2^D	61.20		
			1	PHYT	PBS	60	L_2	-		
			1	PHYT	PBS	64	L_2	-		
			1	PHYT	PBS	66	L_2	-		
$P(ODA)_{10}$-*b*-$P(PEGA\text{-}OMe)_{34}$ (Reduced)	**9.9**	33.5	1	PHYT	PBS	25	Q_2^D	69.03	243.1	1.92E-03
			1	PHYT	PBS	30	Q_2^D	66.40		
			1	PHYT	PBS	37	Q_2^D	65.28		
			1	PHYT	PBS	40	Q_2^D	64.12		
			1	PHYT	PBS	45	Q_2^D	62.96		
			1	PHYT	PBS	50	Q_2^D	62.03		
			1	PHYT	PBS	55	Q_2^D	60.93		
			1	PHYT	PBS	60	L_2 + 1Pk	-		
			1	PHYT	PBS	64	L_2	-		
			1	PHYT	PBS	66	L_2	-		

Stabilizer					Sol		SAXS		DLS	
P(ODA)-*b*-P(PEGA-OMe)	**ODA (units)**	**PEGA (units)**	**Conc (Mol eq.)**	**Lipid**	**500µl**	**Temp (°C)**	**Phase**	**Lattice Parameter (Å)**	**Z-Ave (nm)**	**PDI**
			0.7	PHYT	PBS	25	Q_2^D	69.50	476.7	2.91E-03
$P(ODA)_6$-*b*-$P(PEGA\text{-}OMe)_{27}$ (Reduced)	**5.6**	27.1	0.7	PHYT	PBS	30	Q_2^D	67.16		
			0.7	PHYT	PBS	37	Q_2^D	66.39		
			0.7	PHYT	PBS	40	Q_2^D	64.53		
			0.7	PHYT	PBS	45	Q_2^D	63.92		
			0.7	PHYT	PBS	50	Q_2^D	62.16		
			0.7	PHYT	PBS	55	Q_2^D	61.52		
			0.7	PHYT	PBS	60	Q_2^D	60.54		
			0.7	PHYT	PBS	64	Q_2^D	60.26		
			0.7	PHYT	PBS	66	Q_2^D	59.68		
			0.7	PHYT	PBS	25	Q_2^D	69.47	444.0	4.38E-03
$P(ODA)_6$-*b*-$P(PEGA\text{-}OMe)_{35}$ (Reduced)	**5.6**	35.1	0.7	PHYT	PBS	30	Q_2^D	67.12		
			0.7	PHYT	PBS	37	Q_2^D	66.68		
			0.7	PHYT	PBS	40	Q_2^D	64.42		
			0.7	PHYT	PBS	45	Q_2^D	63.96		
			0.7	PHYT	PBS	50	Q_2^D	62.02		
			0.7	PHYT	PBS	55	Q_2^D	61.42		
			0.7	PHYT	PBS	60	Q_2^D	60.33		
			0.7	PHYT	PBS	64	Q_2^D	60.08		
			0.7	PHYT	PBS	66	Q_2^D + 1Pk	59.39		
			0.7	PHYT	PBS	25	Q_2^D	69.37	436.1	9.36E-04
$P(ODA)_6$-*b*-$P(PEGA\text{-}OMe)_{39}$ (Reduced)	**5.6**	38.7	0.7	PHYT	PBS	30	Q_2^D	67.09		
			0.7	PHYT	PBS	37	Q_2^D	60.84		
			0.7	PHYT	PBS	40	Q_2^D	64.30		
			0.7	PHYT	PBS	45	Q_2^D	63.83		
			0.7	PHYT	PBS	50	Q_2^D	61.92		
			0.7	PHYT	PBS	55	Q_2^D	61.27		
			0.7	PHYT	PBS	60	Q_2^D	60.18		
			0.7	PHYT	PBS	64	Q_2^D	59.95		
			0.7	PHYT	PBS	66	Q_2^D + 1Pk	59.18		
			0.7	PHYT	PBS	25	Q_2^D	69.01	261.2	9.73E-04
$P(ODA)_{10}$-*b*-$P(PEGA\text{-}OMe)_{23}$ (Reduced)	**9.9**	23.1	0.7	PHYT	PBS	30	Q_2^D	66.65		
			0.7	PHYT	PBS	37	Q_2^D	65.28		
			0.7	PHYT	PBS	40	Q_2^D	64.22		
			0.7	PHYT	PBS	45	Q_2^D	63.09		
			0.7	PHYT	PBS	50	Q_2^D	61.99		
			0.7	PHYT	PBS	55	Q_2^D	60.93		
			0.7	PHYT	PBS	60	L_2	-		
			0.7	PHYT	PBS	64	L_2	-		
			0.7	PHYT	PBS	66	L_2	-		
			0.7	PHYT	PBS	25	Q_2^D	68.96	494.5	1.84E-03
$P(ODA)_{10}$-*b*-$P(PEGA\text{-}OMe)_{31}$ (Reduced)	**9.9**	30.7	0.7	PHYT	PBS	30	Q_2^D	66.40		
			0.7	PHYT	PBS	37	Q_2^D	65.20		
			0.7	PHYT	PBS	40	Q_2^D	64.09		
			0.7	PHYT	PBS	45	Q_2^D	62.96		
			0.7	PHYT	PBS	50	Q_2^D	61.93		
			0.7	PHYT	PBS	55	Q_2^D	60.84		
			0.7	PHYT	PBS	60	L_2	-		
			0.7	PHYT	PBS	64	L_2	-		
			0.7	PHYT	PBS	66	L_2	-		
			0.7	PHYT	PBS	25	Q_2^D	69.06	483.7	1.71E-03
$P(ODA)_{10}$-*b*-$P(PEGA\text{-}OMe)_{34}$ (Reduced)	**9.9**	33.5	0.7	PHYT	PBS	30	Q_2^D	66.42		
			0.7	PHYT	PBS	37	Q_2^D	65.16		
			0.7	PHYT	PBS	40	Q_2^D	64.01		
			0.7	PHYT	PBS	45	Q_2^D	62.84		
			0.7	PHYT	PBS	50	Q_2^D	61.84		
			0.7	PHYT	PBS	55	Q_2^D	60.67		
			0.7	PHYT	PBS	60	L_2 + 1Pk	-		
			0.7	PHYT	PBS	64	L_2	-		
			0.7	PHYT	PBS	66	L_2	-		

Stabilizer					Sol		SAXS		DLS	
P(ODA)-*b*-P(PEGA-OMe)	**ODA (units)**	**PEGA (units)**	**Conc (Mol eq.)**	**Lipid**	**500µl**	**Temp (°C)**	**Phase**	**Lattice Parameter (Å)**	**Z-Ave (nm)**	**PDI**
			0.5	PHYT	PBS	25	Q_2^D	69.40	454.1	1.82E-03
$P(ODA)_6$-*b*-$P(PEGA\text{-}OMe)_{27}$ (Reduced)	**5.6**	27.1	0.5	PHYT	PBS	30	Q_2^D	67.02		
			0.5	PHYT	PBS	37	Q_2^D	66.24		
			0.5	PHYT	PBS	40	Q_2^D	64.49		
			0.5	PHYT	PBS	45	Q_2^D	63.93		
			0.5	PHYT	PBS	50	Q_2^D	62.13		
			0.5	PHYT	PBS	55	Q_2^D	61.50		
			0.5	PHYT	PBS	60	Q_2^D	60.39		
			0.5	PHYT	PBS	64	Q_2^D	60.10		
			0.5	PHYT	PBS	66	Q_2^D	59.54		
			0.5	PHYT	PBS	25	Q_2^D	69.34	402.1	1.60E-03
$P(ODA)_6$-*b*-$P(PEGA\text{-}OMe)_{35}$ (Reduced)	**5.6**	35.1	0.5	PHYT	PBS	30	Q_2^D	66.96		
			0.5	PHYT	PBS	37	Q_2^D	66.51		
			0.5	PHYT	PBS	40	Q_2^D	64.34		
			0.5	PHYT	PBS	45	Q_2^D	63.87		
			0.5	PHYT	PBS	50	Q_2^D	61.97		
			0.5	PHYT	PBS	55	Q_2^D	61.36		
			0.5	PHYT	PBS	60	Q_2^D	60.16		
			0.5	PHYT	PBS	64	Q_2^D + 1Pk	59.89		
			0.5	PHYT	PBS	66	Q_2^D + 1Pk	59.26		
			0.5	PHYT	PBS	25	Q_2^D	69.32	405.4	2.42E-03
$P(ODA)_6$-*b*-$P(PEGA\text{-}OMe)_{39}$ (Reduced)	**5.6**	38.7	0.5	PHYT	PBS	30	Q_2^D	66.98		
			0.5	PHYT	PBS	37	Q_2^D	66.79		
			0.5	PHYT	PBS	40	Q_2^D	64.27		
			0.5	PHYT	PBS	45	Q_2^D	63.82		
			0.5	PHYT	PBS	50	Q_2^D	61.92		
			0.5	PHYT	PBS	55	Q_2^D	61.30		
			0.5	PHYT	PBS	60	Q_2^D	60.01		
			0.5	PHYT	PBS	64	Q_2^D + 1Pk	59.78		
			0.5	PHYT	PBS	66	Q_2^D + 1Pk	59.05		
			0.5	PHYT	PBS	25	Q_2^D	68.98	282.5	1.75E-03
$P(ODA)_{10}$-*b*-$P(PEGA\text{-}OMe)_{23}$ (Reduced)	**9.9**	23.1	0.5	PHYT	PBS	30	Q_2^D	66.60		
			0.5	PHYT	PBS	37	Q_2^D	65.10		
			0.5	PHYT	PBS	40	Q_2^D	64.08		
			0.5	PHYT	PBS	45	Q_2^D	62.91		
			0.5	PHYT	PBS	50	Q_2^D	61.77		
			0.5	PHYT	PBS	55	Q_2^D	60.66		
			0.5	PHYT	PBS	60	L_2	-		
			0.5	PHYT	PBS	64	L_2	-		
			0.5	PHYT	PBS	66	L_2	-		
			0.5	PHYT	PBS	25	Q_2^D	68.97	250.5	1.42E-03
$P(ODA)_{10}$-*b*-$P(PEGA\text{-}OMe)_{31}$ (Reduced)	**9.9**	30.7	0.5	PHYT	PBS	30	Q_2^D	66.37		
			0.5	PHYT	PBS	37	Q_2^D	65.04		
			0.5	PHYT	PBS	40	Q_2^D	63.95		
			0.5	PHYT	PBS	45	Q_2^D	62.81		
			0.5	PHYT	PBS	50	Q_2^D	61.69		
			0.5	PHYT	PBS	55	Q_2^D	60.56		
			0.5	PHYT	PBS	60	L_2 + 1Pk	-		
			0.5	PHYT	PBS	64	L_2	-		
			0.5	PHYT	PBS	66	L_2	-		
			0.5	PHYT	PBS	25	Q_2^D	69.01	262.3	1.96E-03
			0.5	PHYT	PBS	30	Q_2^D	66.41		
			0.5	PHYT	PBS	37	Q_2^D	64.83		
			0.5	PHYT	PBS	40	Q_2^D	63.82		
			0.5	PHYT	PBS	45	Q_2^D	62.68		
			0.5	PHYT	PBS	50	Q_2^D	61.42		
			0.5	PHYT	PBS	55	Q_2^D	60.33		
			0.5	PHYT	PBS	60	L_2 + 1Pk	-		
			0.5	PHYT	PBS	64	L_2	-		
			0.5	PHYT	PBS	66	L_2	-		
			0.5	PHYT	PBS	25	Q_2^D	69.09	380.4	2.01E-03
$P(ODA)_{10}$-*b*-$P(PEGA\text{-}OMe)_{34}$ (Reduced)	**9.9**	33.5	0.5	PHYT	PBS	30	Q_2^D	66.41		
			0.5	PHYT	PBS	37	Q_2^D	65.03		
			0.5	PHYT	PBS	40	Q_2^D	63.91		
			0.5	PHYT	PBS	45	Q_2^D	62.74		
			0.5	PHYT	PBS	50	Q_2^D	61.63		
			0.5	PHYT	PBS	55	Q_2^D	60.43		
			0.5	PHYT	PBS	60	L_2 + 1Pk	-		
			0.5	PHYT	PBS	64	L_2	-		
			0.5	PHYT	PBS	66	L_2	-		

Stabilizer					Sol		SAXS		DLS	
P(ODA)-*b*-P(PEGA-OMe)	**ODA (units)**	**PEGA (units)**	**Conc (Mol eq.)**	**Lipid**	**500µl**	**Temp (°C)**	**Phase**	**Lattice Parameter (Å)**	**Z-Ave (nm)**	**PDI**
			2	GMO	PBS	25	Q_2^P	155.19	237.7	7.08E-04
$P(ODA)_6$-*b*-$P(PEGA\text{-}OMe)_{27}$ (Reduced)	**5.6**	27.1	2	GMO	PBS	30	Q_2^P	152.05		
			2	GMO	PBS	37	Q_2^P	154.99		
			2	GMO	PBS	40	Q_2^P	139.55		
			2	GMO	PBS	45	Q_2^P	139.16		
			2	GMO	PBS	50	Q_2^P	134.07		
			2	GMO	PBS	55	Q_2^P	132.24		
			2	GMO	PBS	60	Q_2^P	129.07		
			2	GMO	PBS	64	Q_2^P	128.28		
			2	GMO	PBS	66	Q_2^P	128.34		
			2	GMO	PBS	25	Q_2^P	151.13	150.8	1.51E-03
$P(ODA)_6$-*b*-$P(PEGA\text{-}OMe)_{35}$ (Reduced)	**5.6**	35.1	2	GMO	PBS	30	Q_2^P	150.59		
			2	GMO	PBS	37	Q_2^P	150.11		
			2	GMO	PBS	40	Q_2^P	137.32		
			2	GMO	PBS	45	Q_2^P	134.76		
			2	GMO	PBS	50	Q_2^P	131.24		
			2	GMO	PBS	55	Q_2^P	128.64		
			2	GMO	PBS	60	Q_2^P	127.49		
			2	GMO	PBS	64	Q_2^P	127.28		
			2	GMO	PBS	66	Q_2^P	127.88		
			2	GMO	PBS	25	Q_2^P	148.82	141.1	1.10E-03
$P(ODA)_6$-*b*-$P(PEGA\text{-}OMe)_{39}$ (Reduced)	**5.6**	38.7	2	GMO	PBS	30	Q_2^P	143.04		
			2	GMO	PBS	37	Q_2^P	143.18		
			2	GMO	PBS	40	Q_2^P	132.93		
			2	GMO	PBS	45	Q_2^P	132.07		
			2	GMO	PBS	50	Q_2^P	127.74		
			2	GMO	PBS	55	Q_2^P	126.63		
			2	GMO	PBS	60	Q_2^P	124.69		
			2	GMO	PBS	64	Q_2^P	124.49		
			2	GMO	PBS	66	Q_2^P	124.66		
			2	GMO	PBS	25	Q_2^P	160.13	264.2	1.30E-03
$P(ODA)_{10}$-*b*-$P(PEGA\text{-}OMe)_{23}$ (Reduced)	**9.9**	23.1	2	GMO	PBS	30	Q_2^P	143.04		
			2	GMO	PBS	37	Q_2^P	140.38		
			2	GMO	PBS	40	Q_2^P	134.60		
			2	GMO	PBS	45	Q_2^P	130.32		
			2	GMO	PBS	50	Q_2^P	126.65		
			2	GMO	PBS	55	Q_2^P	123.25		
			2	GMO	PBS	60	Q_2^P	121.60		
			2	GMO	PBS	64	Q_2^P	119.62		
			2	GMO	PBS	66	Q_2^P	119.28		
			2	GMO	PBS	25	Q_2^P	154.52	211.8	1.53E-03
$P(ODA)_{10}$-*b*-$P(PEGA\text{-}OMe)_{31}$ (Reduced)	**9.9**	30.7	2	GMO	PBS	30	Q_2^P	142.59		
			2	GMO	PBS	37	Q_2^P	143.17		
			2	GMO	PBS	40	Q_2^P	136.38		
			2	GMO	PBS	45	Q_2^P	133.80		
			2	GMO	PBS	50	Q_2^P	129.81		
			2	GMO	PBS	55	Q_2^P	127.55		
			2	GMO	PBS	60	Q_2^P	125.52		
			2	GMO	PBS	64	Q_2^P	124.46		
			2	GMO	PBS	66	Q_2^P	124.32		
			2	GMO	PBS	25	Q_2^P	155.13	217.0	1.86E-03
$P(ODA)_{10}$-*b*-$P(PEGA\text{-}OMe)_{34}$ (Reduced)	**9.9**	33.5	2	GMO	PBS	30	Q_2^P	144.40		
			2	GMO	PBS	37	Q_2^P	143.57		
			2	GMO	PBS	40	Q_2^P	137.29		
			2	GMO	PBS	45	Q_2^P	133.64		
			2	GMO	PBS	50	Q_2^P	130.96		
			2	GMO	PBS	55	Q_2^P	127.63		
			2	GMO	PBS	60	Q_2^P	126.18		
			2	GMO	PBS	64	Q_2^P	124.54		
			2	GMO	PBS	66	Q_2^P	124.34		

Stabilizer					Sol		SAXS		DLS	
P(ODA)-*b*-P(PEGA-OMe)	**ODA (units)**	**PEGA (units)**	**Conc (Mol eq.)**	**Lipid**	**500µl**	**Temp (°C)**	**Phase**	**Lattice Parameter (Å)**	**Z-Ave (nm)**	**PDI**
			1.5	GMO	PBS	25	Q_2^P	149.11	216.1	1.60E-03
$P(ODA)_6$-*b*-$P(PEGA\text{-}OMe)_{27}$ (Reduced)	**5.6**	27.1	1.5	GMO	PBS	30	Q_2^P	149.16		
			1.5	GMO	PBS	37	Q_2^P	149.87		
			1.5	GMO	PBS	40	Q_2^P	135.83		
			1.5	GMO	PBS	45	Q_2^P	134.53		
			1.5	GMO	PBS	50	Q_2^P	130.87		
			1.5	GMO	PBS	55	Q_2^P	128.35		
			1.5	GMO	PBS	60	Q_2^P	126.08		
			1.5	GMO	PBS	64	Q_2^P	124.84		
			1.5	GMO	PBS	66	Q_2^P	124.67		
			1.5	GMO	PBS	25	Q_2^P	147.90	257.9	1.60E-03
$P(ODA)_6$-*b*-$P(PEGA\text{-}OMe)_{35}$ (Reduced)	**5.6**	35.1	1.5	GMO	PBS	30	Q_2^P	148.65		
			1.5	GMO	PBS	37	Q_2^P	147.99		
			1.5	GMO	PBS	40	Q_2^P	134.23		
			1.5	GMO	PBS	45	Q_2^P	131.89		
			1.5	GMO	PBS	50	Q_2^P	128.83		
			1.5	GMO	PBS	55	Q_2^P	126.46		
			1.5	GMO	PBS	60	Q_2^P	125.07		
			1.5	GMO	PBS	64	Q_2^P	125.33		
			1.5	GMO	PBS	66	Q_2^P	125.65		
			1.5	GMO	PBS	25	Q_2^P	148.32	132.1	1.40E-03
$P(ODA)_6$-*b*-$P(PEGA\text{-}OMe)_{39}$ (Reduced)	**5.6**	38.7	1.5	GMO	PBS	30	Q_2^P	139.89		
			1.5	GMO	PBS	37	Q_2^P	139.83		
			1.5	GMO	PBS	40	Q_2^P	129.04		
			1.5	GMO	PBS	45	Q_2^P	128.74		
			1.5	GMO	PBS	50	Q_2^P	124.93		
			1.5	GMO	PBS	55	Q_2^P	121.61		
			1.5	GMO	PBS	60	Q_2^P	122.07		
			1.5	GMO	PBS	64	Q_2^P	122.10		
			1.5	GMO	PBS	66	Q_2^P	121.60		
			1.5	GMO	PBS	25	Q_2^P	155.20	270.5	1.86E-03
$P(ODA)_{10}$-*b*-$P(PEGA\text{-}OMe)_{23}$ (Reduced)	**9.9**	23.1	1.5	GMO	PBS	30	Q_2^P	139.94		
			1.5	GMO	PBS	37	Q_2^P	137.11		
			1.5	GMO	PBS	40	Q_2^P	132.16		
			1.5	GMO	PBS	45	Q_2^P	128.11		
			1.5	GMO	PBS	50	Q_2^P	124.50		
			1.5	GMO	PBS	55	Q_2^P	120.96		
			1.5	GMO	PBS	60	Q_2^P	119.37		
			1.5	GMO	PBS	64	Q_2^P	116.36		
			1.5	GMO	PBS	66	Q_2^P	115.66		
			1.5	GMO	PBS	25	Q_2^P	151.91	256.6	1.88E-03
$P(ODA)_{10}$-*b*-$P(PEGA\text{-}OMe)_{31}$ (Reduced)	**9.9**	30.7	1.5	GMO	PBS	30	Q_2^P	138.83		
			1.5	GMO	PBS	37	Q_2^P	139.12		
			1.5	GMO	PBS	40	Q_2^P	132.81		
			1.5	GMO	PBS	45	Q_2^P	130.49		
			1.5	GMO	PBS	50	Q_2^P	126.78		
			1.5	GMO	PBS	55	Q_2^P	124.83		
			1.5	GMO	PBS	60	Q_2^P	122.52		
			1.5	GMO	PBS	64	Q_2^P	121.84		
			1.5	GMO	PBS	66	Q_2^P	121.62		
			1.5	GMO	PBS	25	Q_2^P	151.49	200.3	1.71E-03
$P(ODA)_{10}$-*b*-$P(PEGA\text{-}OMe)_{34}$ (Reduced)	**9.9**	33.5	1.5	GMO	PBS	30	Q_2^P	141.11		
			1.5	GMO	PBS	37	Q_2^P	139.10		
			1.5	GMO	PBS	40	Q_2^P	134.14		
			1.5	GMO	PBS	45	Q_2^P	130.58		
			1.5	GMO	PBS	50	Q_2^P	127.87		
			1.5	GMO	PBS	55	Q_2^P	124.69		
			1.5	GMO	PBS	60	Q_2^P	123.42		
			1.5	GMO	PBS	64	Q_2^P	121.47		
			1.5	GMO	PBS	66	Q_2^P	121.20		

Stabilizer					Sol		SAXS		DLS	
P(ODA)-*b*-P(PEGA-OMe)	**ODA (units)**	**PEGA (units)**	**Conc (Mol eq.)**	**Lipid**	**500µl**	**Temp (°C)**	**Phase**	**Lattice Parameter (Å)**	**Z-Ave (nm)**	**PDI**
$P(ODA)_6$-*b*-$P(PEGA\text{-}OMe)_{27}$ (Reduced)	**5.6**	27.1	1.2	GMO	PBS	25	Q_2^P	144.86	159.8	1.10E-03
			1.2	GMO	PBS	30	Q_2^P	145.88		
			1.2	GMO	PBS	37	Q_2^P	146.20		
			1.2	GMO	PBS	40	Q_2^P	133.48		
			1.2	GMO	PBS	45	Q_2^P	131.42		
			1.2	GMO	PBS	50	Q_2^P	128.41		
			1.2	GMO	PBS	55	Q_2^P	125.62		
			1.2	GMO	PBS	60	Q_2^P	123.57		
			1.2	GMO	PBS	64	Q_2^P	122.19		
			1.2	GMO	PBS	66	Q_2^P	121.97		
$P(ODA)_6$-*b*-$P(PEGA\text{-}OMe)_{35}$ (Reduced)	**5.6**	35.1	1.2	GMO	PBS	25	Q_2^P	140.75	207.6	1.29E-03
			1.2	GMO	PBS	30	Q_2^P	143.63		
			1.2	GMO	PBS	37	Q_2^P	144.37		
			1.2	GMO	PBS	40	Q_2^P	132.70		
			1.2	GMO	PBS	45	Q_2^P	129.78		
			1.2	GMO	PBS	50	Q_2^P	126.50		
			1.2	GMO	PBS	55	Q_2^P	123.99		
			1.2	GMO	PBS	60	Q_2^P	122.09		
			1.2	GMO	PBS	64	Q_2^P	120.93		
			1.2	GMO	PBS	66	Q_2^P	120.84		
$P(ODA)_6$-*b*-$P(PEGA\text{-}OMe)_{39}$ (Reduced)	**5.6**	38.7	1.2	GMO	PBS	25	Q_2^P	140.95	148.8	1.60E-03
			1.2	GMO	PBS	30	Q_2^P	137.01		
			1.2	GMO	PBS	37	Q_2^P	136.93		
			1.2	GMO	PBS	40	Q_2^P	131.17		
			1.2	GMO	PBS	45	Q_2^P	128.86		
			1.2	GMO	PBS	50	Q_2^P	125.30		
			1.2	GMO	PBS	55	Q_2^P	123.78		
			1.2	GMO	PBS	60	Q_2^P	121.66		
			1.2	GMO	PBS	64	Q_2^P	121.67		
			1.2	GMO	PBS	66	Q_2^P	121.64		
$P(ODA)_{10}$-*b*-$P(PEGA\text{-}OMe)_{23}$ (Reduced)	**9.9**	23.1	1.2	GMO	PBS	25	Q_2^P	149.20	286.4	1.75E-03
			1.2	GMO	PBS	30	Q_2^P	136.23		
			1.2	GMO	PBS	37	Q_2^P	133.51		
			1.2	GMO	PBS	40	Q_2^P	128.98		
			1.2	GMO	PBS	45	Q_2^P	125.87		
			1.2	GMO	PBS	50	Q_2^P	122.01		
			1.2	GMO	PBS	55	Q_2^P	118.80		
			1.2	GMO	PBS	60	Q_2^P	116.33		
			1.2	GMO	PBS	64	Q_2^P + 1Pk	111.86		
			1.2	GMO	PBS	66	Q_2^P/Q_2^D	111.10/87.37		
$P(ODA)_{10}$-*b*-$P(PEGA\text{-}OMe)_{31}$ (Reduced)	**9.9**	30.7	1.2	GMO	PBS	25	Q_2^P	148.41	296.1	2.07E-03
			1.2	GMO	PBS	30	Q_2^P	136.62		
			1.2	GMO	PBS	37	Q_2^P	136.25		
			1.2	GMO	PBS	40	Q_2^P	130.81		
			1.2	GMO	PBS	45	Q_2^P	128.07		
			1.2	GMO	PBS	50	Q_2^P	125.02		
			1.2	GMO	PBS	55	Q_2^P	122.69		
			1.2	GMO	PBS	60	Q_2^P	120.39		
			1.2	GMO	PBS	64	Q_2^P	119.48		
			1.2	GMO	PBS	66	Q_2^P	119.21		
$P(ODA)_{10}$-*b*-$P(PEGA\text{-}OMe)_{34}$ (Reduced)	**9.9**	33.5	1.2	GMO	PBS	25	Q_2^P	149.23	175.3	1.98E-03
			1.2	GMO	PBS	30	Q_2^P	137.86		
			1.2	GMO	PBS	37	Q_2^P	135.38		
			1.2	GMO	PBS	40	Q_2^P	131.32		
			1.2	GMO	PBS	45	Q_2^P	127.48		
			1.2	GMO	PBS	50	Q_2^P	125.02		
			1.2	GMO	PBS	55	Q_2^P	121.99		
			1.2	GMO	PBS	60	Q_2^P	120.68		
			1.2	GMO	PBS	64	Q_2^P	118.44		
			1.2	GMO	PBS	66	Q_2^P	117.88		

Stabilizer					Sol		SAXS		DLS	
P(ODA)-*b*-P(PEGA-OMe)	**ODA (units)**	**PEGA (units)**	**Conc (Mol eq.)**	**Lipid**	**500µl**	**Temp (°C)**	**Phase**	**Lattice Parameter (Å)**	**Z-Ave (nm)**	**PDI**
			1	GMO	PBS	25	Q_2^P	143.98	204.4	1.60E-03
$P(ODA)_6$-*b*-$P(PEGA\text{-}OMe)_{27}$ (Reduced)	**5.6**	27.1	1	GMO	PBS	30	Q_2^P	145.27		
			1	GMO	PBS	37	Q_2^P	145.38		
			1	GMO	PBS	40	Q_2^P	133.04		
			1	GMO	PBS	45	Q_2^P	130.48		
			1	GMO	PBS	50	Q_2^P	127.56		
			1	GMO	PBS	55	Q_2^P	124.52		
			1	GMO	PBS	60	Q_2^P	122.62		
			1	GMO	PBS	64	Q_2^P	120.91		
			1	GMO	PBS	66	Q_2^P	120.64		
			1	GMO	PBS	25	Q_2^P	139.44	307.8	1.24E-03
$P(ODA)_6$-*b*-$P(PEGA\text{-}OMe)_{35}$ (Reduced)	**5.6**	35.1	1	GMO	PBS	30	Q_2^P	141.96		
			1	GMO	PBS	37	Q_2^P	142.10		
			1	GMO	PBS	40	Q_2^P	131.50		
			1	GMO	PBS	45	Q_2^P	127.59		
			1	GMO	PBS	50	Q_2^P	124.52		
			1	GMO	PBS	55	Q_2^P	121.87		
			1	GMO	PBS	60	Q_2^P	120.28		
			1	GMO	PBS	64	Q_2^P	119.29		
			1	GMO	PBS	66	Q_2^P	119.13		
			1	GMO	PBS	25	Q_2^P	141.23	212.3	1.14E-03
$P(ODA)_6$-*b*-$P(PEGA\text{-}OMe)_{39}$ (Reduced)	**5.6**	38.7	1	GMO	PBS	30	Q_2^P	134.09		
			1	GMO	PBS	37	Q_2^P	133.58		
			1	GMO	PBS	40	Q_2^P	127.92		
			1	GMO	PBS	45	Q_2^P	125.75		
			1	GMO	PBS	50	Q_2^P	122.84		
			1	GMO	PBS	55	Q_2^P	122.28		
			1	GMO	PBS	60	Q_2^P	118.77		
			1	GMO	PBS	64	Q_2^P	118.78		
			1	GMO	PBS	66	Q_2^P	118.75		
			1	GMO	PBS	25	Q_2^P	147.75	305.8	1.72E-03
$P(ODA)_{10}$-*b*-$P(PEGA\text{-}OMe)_{23}$ (Reduced)	**9.9**	23.1	1	GMO	PBS	30	Q_2^P	135.52		
			1	GMO	PBS	37	Q_2^P	132.65		
			1	GMO	PBS	40	Q_2^P	128.40		
			1	GMO	PBS	45	Q_2^P	125.64		
			1	GMO	PBS	50	Q_2^P	121.31		
			1	GMO	PBS	55	Q_2^P	118.26		
			1	GMO	PBS	60	Q_2^P	115.57		
			1	GMO	PBS	64	Q_2^P	111.45		
			1	GMO	PBS	66	Q_2^P/ Q_2^D	110.62/87.14		
			1	GMO	PBS	25	Q_2^P	149.35	397.3	1.35E-03
$P(ODA)_{10}$-*b*-$P(PEGA\text{-}OMe)_{31}$ (Reduced)	**9.9**	30.7	1	GMO	PBS	30	Q_2^P	137.67		
			1	GMO	PBS	37	Q_2^P	137.74		
			1	GMO	PBS	40	Q_2^P	131.85		
			1	GMO	PBS	45	Q_2^P	129.29		
			1	GMO	PBS	50	Q_2^P	125.88		
			1	GMO	PBS	55	Q_2^P	123.77		
			1	GMO	PBS	60	Q_2^P	121.40		
			1	GMO	PBS	64	Q_2^P	120.69		
			1	GMO	PBS	66	Q_2^P	120.43		
			1	GMO	PBS	25	Q_2^P	149.80	204.0	1.10E-03
$P(ODA)_{10}$-*b*-$P(PEGA\text{-}OMe)_{34}$ (Reduced)	**9.9**	33.5	1	GMO	PBS	30	Q_2^P	138.07		
			1	GMO	PBS	37	Q_2^P	135.46		
			1	GMO	PBS	40	Q_2^P	131.50		
			1	GMO	PBS	45	Q_2^P	128.01		
			1	GMO	PBS	50	Q_2^P	124.98		
			1	GMO	PBS	55	Q_2^P	122.07		
			1	GMO	PBS	60	Q_2^P	120.35		
			1	GMO	PBS	64	Q_2^P	116.87		
			1	GMO	PBS	66	Q_2^P	116.07		

Stabilizer					Sol		SAXS		DLS	
P(ODA)-*b*-P(PEGA-OMe)	**ODA (units)**	**PEGA (units)**	**Conc (Mol eq.)**	**Lipid**	**500µl**	**Temp (°C)**	**Phase**	**Lattice Parameter (Å)**	**Z-Ave (nm)**	**PDI**
			0.7	GMO	PBS	25	Q_2^P	147.66	311.0	1.84E-03
$P(ODA)_{6}$-*b*-$P(PEGA\text{-}OMe)_{35}$ (Reduced)	**5.6**	35.1	0.7	GMO	PBS	30	Q_2^P	139.52		
			0.7	GMO	PBS	37	Q_2^P	139.53		
			0.7	GMO	PBS	40	Q_2^P	130.35		
			0.7	GMO	PBS	45	Q_2^P	129.27		
			0.7	GMO	PBS	50	Q_2^P	125.17		
			0.7	GMO	PBS	55	Q_2^P	124.29		
			0.7	GMO	PBS	60	Q_2^P	120.97		
			0.7	GMO	PBS	64	Q_2^P	120.49		
			0.7	GMO	PBS	66	Q_2^P	120.58		
			0.7	GMO	PBS	25	Q_2^P	138.43	179.8	1.77E-03
$P(ODA)_{6}$-*b*-$P(PEGA\text{-}OMe)_{39}$ (Reduced)	**5.6**	38.7	0.7	GMO	PBS	30	Q_2^P	132.82		
			0.7	GMO	PBS	37	Q_2^P	131.78		
			0.7	GMO	PBS	40	Q_2^P	126.68		
			0.7	GMO	PBS	45	Q_2^P	126.28		
			0.7	GMO	PBS	50	Q_2^P	122.81		
			0.7	GMO	PBS	55	Q_2^P	122.81		
			0.7	GMO	PBS	60	Q_2^P	117.94		
			0.7	GMO	PBS	64	Q_2^P	117.79		
			0.7	GMO	PBS	66	Q_2^P	117.28		
			0.7	GMO	PBS	25	Q_2^P	146.58	314.1	2.03E-03
$P(ODA)_{10}$-*b*-$P(PEGA\text{-}OMe)_{31}$ (Reduced)	**9.9**	30.7	0.7	GMO	PBS	30	Q_2^P	132.27		
			0.7	GMO	PBS	37	Q_2^P	131.96		
			0.7	GMO	PBS	40	Q_2^P	127.25		
			0.7	GMO	PBS	45	Q_2^P	124.71		
			0.7	GMO	PBS	50	Q_2^P	121.63		
			0.7	GMO	PBS	55	Q_2^P	118.96		
			0.7	GMO	PBS	60	Q_2^P	116.06		
			0.7	GMO	PBS	64	Q_2^P	114.45		
			0.7	GMO	PBS	66	Q_2^P	113.83		
			0.7	GMO	PBS	25	Q_2^P	144.03	457.9	2.97E-03
$P(ODA)_{10}$-*b*-$P(PEGA\text{-}OMe)_{34}$ (Reduced)	**9.9**	33.5	0.7	GMO	PBS	30	Q_2^P	134.03		
			0.7	GMO	PBS	37	Q_2^P	131.43		
			0.7	GMO	PBS	40	Q_2^P	127.98		
			0.7	GMO	PBS	45	Q_2^P	124.98		
			0.7	GMO	PBS	50	Q_2^P	121.71		
			0.7	GMO	PBS	55	Q_2^P	119.19		
			0.7	GMO	PBS	60	Q_2^P	116.81		
			0.7	GMO	PBS	64	Q_2^P	113.08		
			0.7	GMO	PBS	66	Q_2^P + 1Pk	112.19		

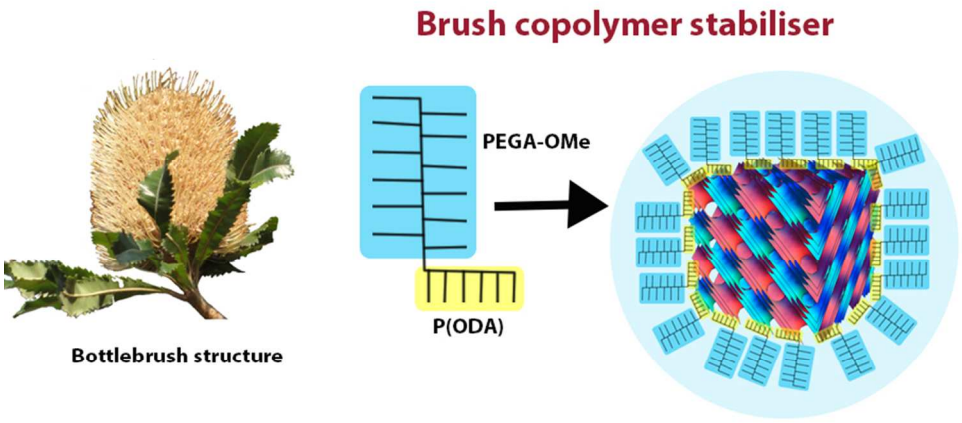

80x39mm (300 x 300 DPI)

Chapter 7

Concluding remarks

Steric stabilisers play a key role in controlling the physical stability as well as other physicochemical properties of lyotropic liquid crystalline nanostructured particles, especially in regard to cubosomes (Chapter 1). This project sets out to investigate the structure-property relationships for stabilisers that dictate steric stabilisation of cubosomes, with a focus on varying the concentration, hydrophilic (PEG) and hydrophobic domain lengths and finally varying the structure design of the steric stabiliser itself. This thesis presents approaches to understand the mechanisms of effective steric stabilisation by studying these structure-function properties, previously listed, for the steric stabilisation of lyotropic liquid crystalline nanostructured particles using cubosomes as a model template. Although cubosome based systems have been previously researched for various biomedical applications (e.g. drug delivery systems), there was still a gap in knowledge with respect to optimising their steric stabilisation. This thesis hopes to reduce that gap by examining the steric stabilisers of cubosome based systems. The overarching hypotheses governing the studies were:

1. That within the poloxamer™ series, the prevailing assumption that Pluronic®F127 is the most effective stabiliser is false, and that other potentially more effective stabilisers for cubosomes exist for both phytantriol and GMO dispersed systems, which are able to retain the internal structure of the native/parent/bulk phase in both systems.
2. That steric stabilisers for cubosomes that are more effective than poloxamers™ exist in other classes of non-ionic surfactants that can be discovered using high throughput approaches and that the effectiveness of a steric stabiliser for cubosomes does not always indicate the retention of the internal structure of the parent/bulk phase.
3. That the design principles for colloidal stabilisers for cubosomes identified from studying existing non-ionic surfactants can be used to design novel effective custom amphiphilic copolymers. Such designer stabilisers will be as effective as small molecule surfactant-based stabilisers and poloxamers™.

On the whole, the hypotheses were well supported by the conclusions reported in this thesis.

Chapter 2 fulfils the first and third hypotheses. Initial investigation of the structure-property relationships affecting cubosome steric stabilisation, was achieved by studying the variation of hydrophilic (PEG) and hydrophobic (PPO) domain lengths of triblock copolymers in the Pluronic® series. The Pluronic® series was investigated because the main steric stabiliser used frequently and extensively in multiple cubosome research/investigations is Pluronic®F127. It was found that Pluronics® with a shorter PEG domain length (i.e. <37 PEG units on average) were internalised within the internal nanostructure of the

phytantriol cubosomes, changing the lyotropic liquid crystalline phase space group from Pn3m (Q^{224}) to Im3m (Q^{229}). It was also discovered that it was possible to retain the Q^{224} cubic phase with the Pn3m space group in GMO dispersions using Pluronic®F108, which has a longer PEG length (i.e. 132 PEG units on average) than Pluronic®F127. Pluronic®F108 was also seen in Chapter 4 to be more effective in sterically stabilising phytantriol and GMO dispersions than Pluronic®F127. In addition to PEG length, stabilisers with the same hydrophilic-lipophilic balance (HLB) value but greater/larger molecular weight were found to be better steric stabilisers, as the quality of their dispersions had fewer aggregates present. Therefore the first hypothesis was proven to be true and structure-properties, such as molecular weight and PEG length of the stabiliser were found to be important design properties of a steric stabiliser.

The second hypothesis was addressed in Chapters 3, 4, 5 and 6. New classes of non-ionic steric stabilisers for lyotropic liquid crystalline nanostructured particles were identified using high throughput approaches. These new classes of steric stabilisers includes: PEG-stearates (Myrj®) identified in Chapter 3, PEGylated-phytanyl copolymers synthesised in Chapter 5 and PEGylated brush copolymers (i.e. P(ODA)-*b*-P(PEGA-OMe)) synthesised in Chapter 6. Their performance and steric stabiliser effectiveness were assessed using an accelerated stability assay, which was a high throughput technique designed in Chapter 4 (described in greater detail below) and implemented to compare known or novel steric stabilisers against gold standard steric stabiliser Pluronic®F127. Myrj®59 was perceived to have better steric stabilisation than Pluronic®F127 in Chapter 3, as it was found to be able to stabilise phytantriol dispersions using a low stabiliser concentration (i.e. 1% w/w relative to lipid), compared to Pluronic®F127, which was unable to retain stable dispersions at the same low concentration. However, when examining Myrj®59 at higher/standard-used concentrations (e.g. 10% w/w relative to lipid) Pluronic®F127 was found to have more effective steric stabilisation (Chapter 4). The second hypothesis was proven to be true when it was identified that the PEGylated-phytanyl copolymers and PEGylated brush copolymers (i.e. P(ODA)-*b*-P(PEGA-OMe)), which were synthesised in Chapter 5 and 6 respectively and are not classified as poloxamers™, were found to have better or equivalent steric stabilisation effectiveness as Pluronic®F127.

Chapter 4 describes the design of a new high throughput technique for the assessment of a steric stabiliser's effectiveness by using an accelerated stability assay (ASA). This methodology was verified using Pluronic®F127 stabilised phytantriol cubosomes at varying concentrations, with low concentrations emulating poorly stabilised samples. There was a reproducible trend occurring whereby the dispersions stabilised with the lowest concentrations displayed the greatest difference in changes of intensity measurements after increased centrifugation. In contrast there was significantly lower occurrence of change in intensity detected for dispersions stabilised at higher stabiliser concentrations which are commonly used (i.e. 10% w/w relative to lipid). Therefore it was deduced that poorly stabilised dispersions produced greater changes in intensity measurements than well stabilised dispersions post-centrifugation, and thus steric stabilisers could be assessed for their effectiveness at stabilising dispersions in this way.

Comparisons of steric stabiliser effectiveness were performed with a few known steric stabilisers that produced well dispersed samples, and confirmed that the class of steric stabilisers that promoted good stabilisation for phytantriol dispersions were poloxamers™, also known as Pluronic® stabilisers. This is an effective screening technique, which is highly applicable to large batch/sample sizes and can be modified for assessing stability in different colloidal systems.

The third and final hypothesis was fulfilled in Chapter 6, whereby design principles which were established from studying steric stabiliser series in Chapters 2, 3 and 5 were utilised. Design principles were especially highlighted by the series of PEGylated-phytanyl copolymers synthesised in Chapter 5, which had various hydrophobic and hydrophilic domain lengths. The implementation of steric stabiliser design principles, such as utilising stabilisers with a longer hydrophilic domain compared to its hydrophobic domain, was considered when synthesizing a mini series of amphiphilic brush copolymer steric stabilisers P(ODA)-*b*-P(PEGA-OMe) in Chapter 6. Although the amphiphilic 'brush' copolymer structure has never been reported for use in the steric stabilisation of lyotropic liquid crystalline nanostructured particles, the polymer structure/design property of increasing the 'branching'/'arms' of PEG by using a 'brush' structure was thought to be an effective design for steric stabilisers because of reports that polyglycerols were just as advantageous as linear PEG polymers for drug delivery systems. Branched polyglycerols were found to have improved antifouling effects[1,2] and protein resistance[3,4] comparable to PEG, while being less susceptible to oxidation or thermal stress[4] than PEG. Their long plasma half-lives of hyperbranched polyglycerols (33 h for 106 kDa and 57 h for 540 kDa)[5] indicate their promises as stealth[6-9] polymers, which was illustrated by their use to prolong liposome circulation[10,11] and prevent protein adsorption to a gold surface[4]. A brush copolymer structure/design was also reported to increase particle stability in micelles.[12] Therefore, with additional ability of functionalisation of the terminal end of the PEG domain via thiol conjugation, there is further opportunity of this brush steric stabiliser to be functionalised with an antibody or antibody fragment for producing active drug delivery systems. This will allow opportunities of active targeting in cubosome systems to be initially/further investigated.

From the summary above, it can be seen that this project has demonstrated that: (i) not all steric stabilisers have universal stabilisation effectiveness on different lipids and that steric stabilisation is heavily dependent on the lipid dispersed; (ii) it is important to have a quantifiable reproducible accelerated stability assay/technique for assessing the performance of steric stabilisers for lyotropic liquid crystalline dispersions, as it is hard to predetermine or assess the performance of steric stabilisers which produce 'good' dispersions against each other – which is valid when resources are limited and determination of which stabiliser is best suited for specific lipids is vital. This technique is powerful/useful because it is also versatile and may be used for other types of colloidal systems with some adjustment; (iii) custom steric stabilisers belonging to new stabiliser classes can be designed with equivalent steric stabilisation effectiveness as standard stabiliser Pluronic®F127; (iv) custom stabilisers allow for flexibility of stabiliser

structure design and permit the possibility of terminal block functionalities, which may shift the drug delivery system from passive to active drug delivery; (v) the structure of the stabiliser also plays a part in the stabilisation in addition the PEG length and stabiliser concentration used.

In addition to drug delivery – cubosomes are also used in the food and agriculture industries, for which the information retained from this project would also be relevant to. As well as ongoing cubosome research, information from this project is also relevant to other lyotropic liquid crystalline particles which required steric stabilisation like hexosomes and their respective applications.

Future Directions

The development of effective drug delivery systems has been an extensive and on-going process, within the pharmaceutical field. To help broaden and improve pharmacological and therapeutic properties of drug delivery systems lipid-based self-assembly systems have been employed. These systems enable the delivery of effective lipophilic and amphiphilic therapeutics, which were previously not amenable to simpler formulation approaches. The application of nanoparticles and nanostructured systems in drug delivery is promising but at present some are still limited by the effectiveness of the steric stabilisers available/used, which are still under development as this field is relatively new. Aspects which need to be investigated in more detail with regards to steric stabilisers for cubosome based systems to reach clinical trial stages include:

i. Investigating different polymer/stabiliser structures (e.g. comb or brush-like structures), especially with specific/different types of lipid based systems for optimisation of steric stabilisation of:

    a. Passive drug delivery systems

    Experimental designs may include utilising different controlled polymerisation methodologies (e.g. RAFT) for new copolymer/stabiliser synthesis. New stabilisers should be assessed for their effectiveness and compared with standard/control stabiliser F127, using various characterisation techniques and the accelerated stability assay (ASA) developed in this thesis.

    b. Active/targeted drug delivery systems

    Experimental designs for developing these systems would be by further functionalisation of the custom-made steric stabiliser, with a functional group on the end (e.g. malemide, thiol), which may enable the attachment of a targeting moiety (e.g. antibody or antibody fragment) for targeting specific antigens. This would allow active/therapeutic payloads within the cubosome based system to be delivered directly to specific sites of interest (e.g. cancer cells), which would subsequently reduce unwanted side-effects caused by strong therapeutics damaging heath cells, and may facilitate uptake of cubosomes into specific cell populations. Control models

with untargeted cubosome based systems should be used to compare the effectiveness of targeted systems in these experiments. Fluorescence markers and MRI imaging agents may be utilised to visualise and track the location of these cubosome based systems during experiments.

ii. Optimising the steric stabiliser concentration of different custom steric stabilisers for the most effective stabilisation of different lipid based cubosome dispersions. This is important for:

a. Passive drug delivery systems

Experimental designs would encompass assessing a range of various steric stabiliser concentrations for each novel steric stabiliser developed for different lipid based systems, using ASA. These results should be compared to results of systems stabilised with control steric stabiliser F127.

b. Active/targeted drug delivery systems

Experimental designs would involve looking at different concentrations and/or mixes of different custom steric stabilisers with functionalised stabilisers for effective/optimal stabilisation of these lipid based systems. Assessment of effective stabilisation (e.g. ASA) of these different concentration and/or mixes of concentrations of various stabilisers should be compared to their non-targeted cubosome based systems, especially those using control stabiliser F127.

iii. Investigate the toxicity and biocompatibility of the stabilised cubosome based systems

Experimental designs to assess the toxicity and biocompatibility of both the passive and/or active/targeted drug delivery systems are required to determine their suitability for clinical trials. These assessments may range from *in vitro* testing, assessing these systems on different cell cultures and cytotoxicity assays, to *in vivo* testing using small animal models (e.g. mouse and rat studies). Experimental samples should be assessed with control lipid based dispersions stabilised using F127. Both loaded (see point v below) and blank cubosome based systems should be assessed.

iv. Investigation of stealth properties provided by the custom steric stabiliser

Experimental designs to investigate stealth properties of the custom steric stabilisers would involve testing these systems in plasma and also within *in vivo* experimentation of their circulation time in small animal models (e.g. mouse, rat). Passive and/or active/targeted drug delivery systems should be assessed against control cubosome models stabilised with F127, and against the well-known long circulating PEG-liposomes as a positive control/gold standard. Further experimentation

involving loaded cubosomes (see point v below) compared to blank cubosome models would also be useful for future developments of these systems.

v. Investigation of loaded cubosome based systems compared to blank/empty cubosome based systems. The incorporation of drugs and other additives of different charges and sizes into self-assembled systems can alter the phase behaviour of the liquid crystal matrix.[13-15] Therefore, it is important to investigate the steric stabilisation of loaded cubosomes compared to their 'unloaded/blank' counterparts.

   Experimental designs on loaded cubosome based systems vs. blank/empty cubsome based systems should involve phase characterisation techniques as well as steric stabilisation assessment (e.g. ASA). Loaded cubosomes systems studied may involve systems encapsulating different types of therapeutics (e.g. amphiphilic, hydrophilic and lipophilic), imaging agents, controlled release agents (e.g. gold nanorods) and/or even fluorescence markers/tags. The number of different types of loads/component encapsulated in the cubosome system and its effect on the overall system stability should also be investigated for the development of more complex/"smart" drug delivery systems. Control cubosome models would be the blank/empty cubosome systems and should also include models stabilised using F127. Both passive and active/targeted cubosome systems should be assessed.

vi. Controlled drug release/delivery studies using the custom stabilised cubosome based systems

   Experimental design for controlled drug release studies for cubosome based systems stabilised with custom steric stabilisers to investigate and developing more complex/"smart" drug delivery systems may explore established controlled release systems using the application of different temperatures, UV/light sensitivity, pH environments and maybe magnetic charges/field. There have been previous studies investigating controlled release of different lyotropic liquid crystalline systems which would complement this area of study.[16-18] Cubosomes based systems with entrapped/encapsulated components and/or additives required for controlling drug release should be assessed (e.g. ASA) for their colloidal stability, in order to determine their practical applicability in practice. Both passive and active/targeted systems should also be assessed for their controlled drug release capabilities.

vii. Investigation of optimal storage environments (e.g. temperature, sensitivity to UV, plastic or glass) for the stabilised cubosome based systems. The type of containment and/or environmental conditions may influence the steric stabilisation of cubosome based systems on a long term basis and should be explored for the optimal performance of these systems in practice.

Experimental design for determining optimal storage environments for stabilised cubosome systems should investigate different storage environments for the cubosome based systems shortly after production to predetermine the shelf life and proper storage of these systems when they get used in practice. As such, all types of cubosome models (e.g. passive, targeted, loaded and/or blank cubosome systems) should be assessed. One possible technique could be to assess the systems using ASA before and after different time lengths, whilst altering one or two variables against a control group. Environmental variables investigated may include temperature, UV sensitivity and storage materials (e.g. glass, polypropylene)

Aspect numbers 3 to 7 will need to be investigated for both passive and active/targeted cubosome based systems, for both blank and loaded cubosomes.

In conclusion, the merging of technologies in the development of custom steric stabilisers for lyotropic liquid crystalline nanostructured particle research for complex drug delivery systems is a rapidly expanding field which may yet revolutionise pharmaceutical treatment. The understanding of these materials and their behaviour on a nano-scale is fundamental for their eventual clinical use. The potential of these 'smart'/complex drug delivery systems has not yet been seen and as such, further research into these systems will be of great fascination to observe, and of great excitement to be a part of.

References

1. Gunkel, G.; Weinhart, M.; Becherer, T.; Haag, R.; Huck, W. T. S. Effect of Polymer Brush Architecture on Antibiofouling Properties, *Biomacromolecules* **2011,** 12, 4169-4172.
2. Banerjee, I.; Pangule, R. C.; Kane, R. S. Antifouling Coatings: Recent Developments in the Design of Surfaces That Prevent Fouling by Proteins, Bacteria, and Marine Organisms, *Adv. Mater.* **2011,** 23, 690-718.
3. Zhuang, Y.; Zhu, Q.; Tu, C.; Wang, D.; Wu, J.; Xia, Y.; Tong, G.; He, L.; Zhu, B.; Yan, D.; Zhu, X. Protein resistant properties of polymers with different branched architecture on a gold surface, *J. Mater. Chem.* **2012,** 22, 23852-23860.
4. Siegers, C.; Biesalski, M.; Haag, R. Self-Assembled Monolayers of Dendritic Polyglycerol Derivatives on Gold That Resist the Adsorption of Proteins, *Chem. Eur. J.* **2004,** 10, 2831-2838.
5. Kainthan, R. K.; Brooks, D. E. In vivo biological evaluation of high molecular weight hyperbranched polyglycerols, *Biomaterials* **2007,** 28, 4779-4787.
6. Knop, K.; Hoogenboom, R.; Fischer, D.; Schubert, U. S. Poly(ethylene glycol) in Drug Delivery: Pros and Cons as Well as Potential Alternatives, *Angew. Chem.-Int. Edit.* **2010,** 49, 6288-6308.
7. Calderón, M.; Quadir, M. A.; Sharma, S. K.; Haag, R. Dendritic Polyglycerols for Biomedical Applications, *Adv. Mater.* **2010,** 22, 190-218.
8. Neoh, K. G.; Kang, E. T. Functionalisation of inorganic nanoparticles with polymers for stealth biomedical applications, *Polym. Chem.* **2011,** 2, 747-759.
9. Amoozgar, Z.; Yeo, Y. Recent advances in stealth coating of nanoparticle drug delivery systems, *Wiley Interdiscip. Rev. Nanomed. Nanobiotechnol.* **2012,** 4, 219-233.
10. Maruyama, K.; Okuizumi, S.; Ishida, O.; Yamauchi, H.; Kikuchi, H.; Iwatsuru, M. Phosphatidyl polyglycerols prolong liposome circulation in vivo, *Int. J. Pharm.* **1994,** 111, 103-107.
11. Hofmann, A. M.; Wurm, F.; Hühn, E.; Nawroth, T.; Langguth, P.; Frey, H. Hyperbranched Polyglycerol-Based Lipids via Oxyanionic Polymerization: Toward Multifunctional Stealth Liposomes, *Biomacromolecules* **2010,** 11, 568-574.

12. Xu, P.; Tang, H.; Li, S.; Ren, J.; Van Kirk, E.; Murdoch, W. J.; Radosz, M.; Shen, Y. Enhanced Stability of Core−Surface Cross-Linked Micelles Fabricated from Amphiphilic Brush Copolymers, *Biomacromolecules* **2004,** 5, 1736-1744.
13. Mulet, X.; Kennedy, D.F.; Conn, C.E.; Hawley, A.; Drummond, C.J. High throughput preparation and characterisation of amphiphilic nanostructured nanoparticulate drug delivery vehicles, *Int. J. Pharm.* **2010,** 395, 1-2, 290-297.
14. Mulet, X.; Boyd, B.J.; Drummond, C.J. Advances in drug delivery and medical imaging using colloidal lyotropic liquid crystalline dispersions. *J. Colloid Interf. Sci.* **2013,** 393, 1-20.
15. Mulet, X.; Conn, C.E; Fong, C.; Kennedy, D.F.; Moghaddam, M.J.; Drummond, C.J. High-Throughput Development of Amphiphile Self-Assembly Materials: Fast-Tracking Synthesis, Characterization, Formulation, Application and Understanding. *Acc. Chem. Res.* **2013,** 46, 7, 1497-1505.
16. Fong, W.-K.; Hanley, T.; Boyd, B. J. Stimuli responsive liquid crystals provide 'on-demand' drug delivery in vitro and in vivo. *J. Control. Release* **2009,** 135, 3, 218-226.
17. Fong, W.-K.; Hanley, T. L.; Thierry, B.; Kirby, N.; Boyd, B. J. Plasmonic Nanorods Provide Reversible Control over Nanostructure of Self-Assembled Drug Delivery Materials. *Langmuir* **2010,** 26, 9, 6136-6139.
18. Fong, W.-K.; Hanley, T. L.; Thierry, B.; Kirby, N.; Waddington, L. J.; Boyd, B. J. Controlling the Nanostructure of Gold Nanorod–Lyotropic Liquid-Crystalline Hybrid Materials Using Near-Infrared Laser Irradiation. *Langmuir* **2012,** 28, 40, 14450-14460.